Data-driven network models to characterize the distribution and spread of tau in the Alzheimer's disease brain

JACOB VOGEL
Integrated Program in Neuroscience
McGill University, Montreal
April 2020

A thesis submitted to McGill University in partial fulfillment of the requirements of the degree of Doctor of Philosophy

Abstract

Alzheimer's disease (AD) is a common and debilitating late-life illness comprising progressive brain damage and slow deterioration of cognitive and functional abilities. The primary neuropathological signature of AD involves accumulation of the β-amyloid (Aβ) and tau proteins into cortical plaques and tangles. While Aβ plaques present diffusely throughout the brain before AD symptoms manifest, fibrillar tau pathology is initially distributed in a very specific part of the brain. As AD symptoms evolve, tau pathology advances through the cerebral cortex in a specific and highly reproducible pattern, perhaps driven by the brain's intrinsic architecture of neuronal connectivity. Most of what we know about tau comes from post-mortem studies and experimental animal models. However, recent advances allow the imaging of tau pathology in the brains of living humans using positron emission tomography (PET). The content of this thesis involves using tau-PET to validate and expand upon the distribution and spread of tau pathology in humans, with a focus on data-driven methodologies. Chapter 1 reviews known aspects of tau biology and pathophysiology – particularly as it relates to the specific pattern of tau accumulation and spread in AD – and critically reviews recent contributions to this literature by tau-PET and other tau biomarkers. Chapter 2 presents a study using hypothesis-free clustering methods to investigate whether regional patterns of tau-PET covariance along the AD spectrum match patterns of tau accumulation expected from postmortem histopathology. These data-driven regions partially matched the expected patterns of tau distribution, but also showed superior performance in tracking variation in cognition, compared to regions derived from post-mortem studies. Chapter 3 tests the hypothesis that the pattern of tau distribution in humans is driven by patterns of neuronal connectivity, by simulating the spread of a pathological agent from an epicenter through the healthy human connectome. This simulated pattern matched well the *in vivo* spatial distribution of tau. Further, regional model error was associated with the magnitude of regional Aβ, suggesting Aβ influences the topography of tau spread. Chapter 4 challenges the notion that tau spreads in a uniform pattern across individuals, by applying a cutting-edge spatiotemporal event-based clustering algorithm to the largest tau-PET dataset described to date. Four different progression

patterns emerged from the data, resembling known subtypes of tau and atypical AD variants, with no single pattern predominating. The subtypes are validated and characterized, and the influence of regional cell-type variation and network spread on subtype expression is explored. The results do not support the notion of a single tau spreading pattern, and suggest atypical AD variants represent early-onset and aggressive variants of typical AD phenotypes. Finally, Chapter 5 considers the novel contributions produced by the original work in this thesis, and discusses how these findings contribute to current dialogues in the field of AD research. Together, the work in this thesis suggests that the *in vivo* and spatially-unbiased nature of tau-PET can provide novel information about the spread of tau through the human brain during AD. In conclusion, current pathological staging systems should be updated to reflect common variation in AD patterns, and models of tau spreading are likely incomplete without incorporating regional vulnerability information and systematic individual variation.

Résumé

La maladie d'Alzheimer (MA) est une maladie qui affecte une grande proportion de personnes âgées et qui cause une dégénération progressive du cerveau ainsi qu'une lente détérioration des capacités cognitives et fonctionnelles. La principale signature neuropathologique de la MA implique l'accumulation des protéines β-amyloïde (Aβ) et tau en plaques corticales et enchevêtrements. Alors que les plaques Aβ sont présentes de manière diffuse à travers le cerveau avant que les symptômes de la MA n'apparaissent, la pathologie tau est initialement distribuée dans une partie très spécifique du cerveau. À mesure que les symptômes de la MA évoluent, la pathologie tau progresse également dans le cortex cérébral de manière spécifique et hautement reproductible, potentiellement déterminée par l'architecture intrinsèque de la connectivité neuronale. La plupart des informations sur la pathologie tau provient d'études post-mortem et de modèles animaux expérimentaux. Cependant, des avancées récentes en imagerie permettent d'évaluer la pathologie tau dans le cerveau d'êtres humains vivants en utilisant la tomographie par émission de positrons (TEP). Le contenu de cette thèse repose sur l'utilisation de la tau-TEP pour valider et mieux comprendre la distribution et la propagation de la pathologie tau chez l'humain, en mettant l'accent sur des méthodologies axées sur les données. Le chapitre 1 détaille la biologie et la physiopathologie du tau - en particulier ce qui peut être lié au patron spécifique selon lequel le tau s'accumule et se propage dans la MA. Il passe également en revue les contributions récentes de la tau-PET et d'autres biomarqueurs de tau à cette littérature. Le chapitre 2 présente une étude utilisant des méthodes de regroupement pour déterminer si la covariance de la tau-PET à travers les régions du cerveau tout au long de la MA correspond au patron d'accumulation du tau attendu selon les études d'histopathologie post-mortem. Ces régions déterminées uniquement sur la base des données correspondaient en partie aux modèles attendus une distribution de tau, mais montraient de meilleure performance pour suivre la variation de la cognition que les régions identifiées sur la base d'études post-mortem. Le chapitre 3 teste l'hypothèse selon laquelle le patron de distribution du tau chez l'humain est déterminé par la connectivité neuronale en simulant la propagation d'un agent pathologique à partir d'un épicentre à travers le connectome du cerveau

humain sain. Ce patron simulé correspondait bien à la distribution spatiale *in vivo* de tau. De plus, l'erreur du modèle par région du cerveau était associée au niveau d'Aβ dans cette région, suggérant que Aβ influence la topographie de la propagation du tau. Le chapitre 4 remet en question la notion selon laquelle le tau se propage de façon uniforme d'un individu à l'autre, en appliquant un algorithme spatio-temporel basé sur les événements pour grouper les participants du plus grand jeu de données tau-PET décrit à ce jour. Quatre profils de progression différents ont émergé des données en utilisant un tel algorithme. Ces profils ressemblent à des sous-types connus de tau et de variantes atypiques de la MA, et aucun motif ne prédominait sur les autres. Les profils ont été validés et caractérisés, et l'influence des différents types de cellules par région du cerveau et de l'étendue de la propagation sur l'expression des différents profils a été explorée. Les résultats ne soutiennent pas la notion d'un modèle de propagation unique de tau et suggèrent que les variantes atypiques de la MA représentent des variantes précoces et agressives de phénotypes typiques de la MA. Enfin, le chapitre 5 examine les contributions nouvelles découlant des travaux originaux de cette thèse et discute de la manière dont ces résultats contribuent aux dialogues actuels dans le domaine de la recherche sur la MA. Les travaux de cette thèse suggèrent que par son accumulation spatiale définie, la tau-PET *in vivo* peut fournir de nouvelles informations sur la propagation du tau à travers le cerveau humain tout au long de la MA. En conclusion, les systèmes de classification des stades pathologiques devraient être mis à jour pour refléter différents modèles connus de la MA. Les modèles de propagation du tau seront probablement incomplets si la vulnérabilité par région et la variation individuelle systématique ne sont pas pris en compte.

Contents

List of Figures

List of Tables

List of Abbreviations

Aβ	**A**myloid β
AD	**A**lzheimer's **D**isease
ADAD	**A**utosomal **D**ominant **A**lzheimer's **D**isease
APOE	**APO**lipoprotein **E**
BASC	**B**ootstrap **A**nalysis of **S**table **C**lusters
EOAD	**E**arly **O**nset **A**lzheimer's **D**isease
ESM	**E**pidemic **S**preading **M**odel
fMRI	**f**unctional **M**agnetic **R**esonance **I**maging
FTLD	**F**rontot**e**mporal **L**obar **D**egeneration
LC	**L**ocus **C**oeruleus
lvPPA	**l**ogopenic **v**ariant **P**rimary **P**rogressive **A**phasia
MAPT	**M**icrotubule-**A**ssociated **P**rotein **Tau**
MCI	**M**ild **C**ognitive **I**mpairment
MRI	**M**agnetic **R**esonance **I**maging
MTL	**M**edial **T**emporal **L**obe
NFT	**N**euro**F**ibrillary **T**angle
NMDAR	**N**-**M**ethyl-**D**-**Aspartate** **R**eceptor
PART	**P**rimary **A**ge-**R**elated **T**auopathy
PCA	**P**osterior **C**ortical **A**trophy
PET	**P**ositron **E**mission **T**omography
PHF	**P**aired **H**elical **F**ilament
ROI	**R**egion **o**f **Interest**
SuStaIn	**Su**btpye and **Sta**ge **In**ference

Acknowledgements

The content of this thesis reflects my progression as a scientist over the five years of my PhD. Much of my personal growth can be attributed to the mentorship and support of a long list of incredible scientists that deserve to be recognized. First and foremost, I would like to thank Alan Evans, my PhD supervisor, for building an environment for me to succeed. Alan supported me at every step, allowing me to grow my network at international conferences every year, realize multiple collaborations with colleagues abroad, pursue many interesting projects, and organize numerous events and workshops. Alan, thank you for always having my back, and for enthusiastically supporting my endeavors, no matter how ambitious, with an infectious light-heartedness and warmth! I would next like to thank Oskar Hansson. Oskar generously provided almost all the data used in my PhD, but he was also always happy to discuss projects, suggest brilliant ideas, and provide kind and supportive feedback throughout. It is difficult to imagine what my thesis would have been like without Oskar's support, and I am very thankful for his presence during my PhD. I would like to thank Sylvia Villeneuve for recruiting me to Montreal, for her steady advisory on both academic and personal matters, and for being the closest thing to family I have in Montreal. I would like to acknowledge and thank Pierre Bellec, Rik Ossenkoppele, Étienne Vachon-Presseau and Yasser Iturria-Medina, each of whom dedicated a great deal of personal time and effort to closely mentoring me during different periods of my PhD. I also want to single out and thank Mallar Chakravarty, Bratislav Misic and Boris Bernhardt for stepping in during crucial periods of my PhD and providing council that that was very valuable to me. Each of these scientists have acted as role models to me, and much of what I take into the future will be lessons I gleaned from watching them work. I want to further acknowledge each of these scientists for helping to promote my scientific career, and supporting my various endeavors. Bratislav, I forgive you for torturing me during my candidacy exam. I also want to acknowledge my mentors and colleagues from my time in Berkeley, who helped mold a raw and scattered kid into a student ready to take on a PhD: Bill Jagust, Gil Rabinovici, Renaud La Joie, Miranka Wirth, Sylvia, Rik and Michael Schöll, among others. I want to acknowledge Cindee Madison for first teaching

me how to code in Python and teaching me the ways of a positive data scientists many years ago, and Greg, Liza, Thomas and Elizabeth DuPre for continuing those lessons, and for holding my hand through the struggles of git, LaTeX and other horrors. I want to thank Theresa Vaughan for building a bridge to neuroscience research for me, by mentoring me during my first lab research experience. I'd like to acknowledge Hampshire College for helping turn my life around and helping me create opportunities to pursue science. I want to thank the Human Amyloid Imaging community for supporting my growth as a scientist and accelerating my understanding of neuroimaging in AD. Finally, I want to thank all of my other co-authors from Sweden, Amsterdam, London, the US, and here in Canada, for being amazing colleagues and friends, and for helping produce the works presented in this thesis.

In addition, the content of this thesis represents an enormous volume of work, which I could never have accomplished without such a vibrant and supportive circle of colleagues, friends and family. I would first like to thank Noor Al-Sharif for being my BFF, sitting next to me for the entirety of my PhD, and making every work day (and many weekends!) so much more fun. I'd also like to acknowledge Liza Levitis, Alex Diaz-Papkovich, Thomas Funck, Konrad Wagstyl, Carolina Makowski, Greg Kiar and others for making the lab environment a more fun place to work, and to poor Seun for tolerating all of our inane conversations. I want to thank Claude for constantly stopping in to say hello, bringing delicious vegetables and sweets, and making silly jokes about the lives of PhD students. I want to acknowledge the MCIN staff, particularly Reza, Terry, Mary, Chris, John Le and Patrick, for supporting me and other students through the numerous administrative hurdles endemic to University life. Similarly, I want to thank Ed Ruthazer, Joe Rochford, Vivian and Katherine, and the IPN office for guiding me through the PhD process, *occasionally* bending some rules here and there, and making the program a charming place to be. Special shout out to Alex DeGuise for his continued delightful visits, and for always keeping it *so* fresh. I also would like to acknowledge Josephine Nalbantoglu for coming to the rescue when McGill was giving me issues about my GPA pre-acceptance. I'd especially like to acknowledge Alexa Pichet Binette, my PhD sister, for constant support and friendship, a lot of favors, and many shared experiences. I also want to thank Julie Gonneaud, Theresa Köbe, PF Meyer, Alexa and everyone in the Villeneuve Lab for making me an honorary member, giving me a lab away from lab, great collaborations, and so many fun times. I would like to say bedankt to Philip Scheltens for hosting me at the Alzheimer's Center, to Rik, Jolanda Lindenberg and Noë Ossenkoppele for giving me a home away from home in Amsterdam, and to Emma Wolters, Tessa Timmers, Colin Groot, Anita van Loenhoud and the whole

Alzheimercentrum crew for making me feel like a (short, scruffy) member of the Dutch family. I want to thank Angela Tam for being my rock, my heart and my partner in crime for much of my PhD, and for so many amazing times that I'll never forget or regret. I want to give a shout out to Liam Crapper, H-Binh Nguyen and Arsenii Foudimov for helping to create the cathartic and degenerate weekly jams that became Horse Doctor, the great and awful shows we played, and all the stress relief that came with. By the same token, I'd like to thank the basketball squad for taking me in, giving me an escape from constant work, and being good old Canadian boys and laughing off my constant shit-talking: Lucas, Wes, Ansh, Brad, Nick, Kash, Tony, Graham, Neil and especially Kev for all dem jawns. I want to thank Parc La Fontaine, Zero Gravité, and all my Montreal and Philly friends for helping me create a positive work-life balance. I want to thank the Philadelphia Eagles for helping me not spend every Sunday working, and for finally rewarding my years of devotion with a Superbowl win. I would especially like to thank Sara Bermudez for being my quarantine partner, for infusing my life with so much fun, joy, beauty and love over the last year, for being so helpful and understanding during the composition of this thesis, and for helping me to keep things light and fun. Finally, I want to thank my family (especially mom, dad and Jess) for supporting me from the start, visiting me, letting me vent, and being so understanding and supportive during this long and stressful process.

I would like to dedicate this thesis
to my parents. I would never
have made it from a ne'er-do-well
kicked out of high-school to a
hopeful PhD candidate without
your love, support, and
occasional guilt and pressure. I
know it wasn't easy, but I hope
my thesis represents a great
reward to all of your dedication
and hardship in raising Jess and I.

"I'd rather have a bottle in front of me than a frontal lobotomy"

Tom Waits

Contribution of authors

The original work in this thesis spans Chapters 2, 3, 4. My role in each of these studies involved study conceptualization and design, data processing, data analysis, development of the methodologies (unless otherwise specified), interpreting the results, drafting of the manuscripts, and generally leading each project. However, each study features a number of co-authors who contributed invaluable support, which will be demarcated below.

Chapter 2

- Niklas Mattsson:Data acquisition, interpretation of results, writing the manuscript
- Yasser Iturria-Medina: provided methodological consultation
- Olof T. Strandberg: data acquisition and processing
- Michael Schöll: data acquisition and processing
- Christian Dansereau: provided methodological consultation
- Sylvia Villeneuve: interpretation of the results
- Wiesje M. van der Flier: drafted the manuscript, interpretation of results
- Philip Scheltens: interpretation of the results
- Pierre Bellec: supervised the study, provided methodological consultation
- Alan C Evans: supervised the study
- Oskar Hansson: supervised the study, provision of study data, interpretation of the results
- Rik Ossenkoppele: Conceptualized the study, supervised the study, interpretation of the results, drafted the manuscript
- All authors: provided critical or conceptual support and revised the manuscript

Chapter 3

- Yasser Iturria-Medina: conceptualized the study, designed the Epidemic Spreading model, designed and developed methodologies, interpreted the findings
- Olof T Strandberg: acquired and processed the data
- Ruben Smith: acquired and processed the data, interpreted the findings
- Elizabeth Levitis: designed and developed methodologies
- Alan C Evans: conceptualized the study, interpreted the findings, supervised the study
- Oskar Hansson: provision of patient data, drafted the manuscript, interpreted the findings, supervised the study
- All authors: revised the manuscript and provided critical feedback

Chapter 4

- Alexandra L Young: developed the SuStaIn methodology, provided methodological consultation, developed the methodologies, interpreted the results
- Neil P Oxtoby: provided methodological consultation, developed the methodologies,
- Ruben Smith: acquired/processed the data
- Rik Ossenkoppele: provided conceptual consultation, interpreted the results
- Olof T. Strandberg: acquired/processed the data
- Renaud La Joie: provided conceptual consultation, interpreted the results
- Leon M Aksman: provided methodological consultation
- Michel J Grothe: provided conceptual consultation, interpreted the results
- Yasser Iturria-Medina: provided methodological consultation
- Gil D Rabinovici: provided patient data, interpreted the results
- Daniel C Alexander: developed the SuStaIn methodology, provided methodological consultation, interpreted the results
- Chul Hyoung Lyoo: provided patient data
- Alan C Evans: conceptualized the study, interpreted the results, supervised the study
- Oskar Hansson: provided patient data, conceptualized the study, interpreted the results, supervised the study
- All authors: provided critical or conceptual support and revised the manuscript

Chronological list of first and co-author publications from PhD

- Pierre Orban, Angela Tam, Sebastian Urchs, Melissa Savard, Amanpreet Badhwar,Christian Dansereau, **Jacob W. Vogel**, Alain Dagher, Sylvia Villeneuve, Judes Poirier, Pedro Rosa-Neto, John Breitner, Pierre Bellec. Subtypes of functional brain connectivity as early markers of neurodegeneration in Alzheimer's disease. *Biorxiv*, pages 1–28, 2017.
- Byoung Seok Ye, Hee Jin Kim, Yeo Jin Kim, Na Yeon Jung, Jin San Lee, Juyoun Lee, Young Kyoung Jang, Jin Ju Yang, Jong Min Lee, **Jacob W. Vogel**, Duk L. Na, and Sang Won Seo. Longitudinal outcomes of amyloid positive versus negative amnestic mild cognitive impairments: A three-year longitudinal study. *Scientific Reports*, 8(1):1–11, 2018.
- **Jacob W. Vogel**, Etienne Vachon-Presseau, Alexa Pichet Binette, Angela Tam, Pierre Orban, Renaud La Joie, Mélissa Savard, Cynthia Picard, Judes Poirier, Pierre Bellec, John C.S. Breitner, and Sylvia Villeneuve. Brain properties predict proximity to symptom onset in sporadic Alzheimer's disease. *Brain*, 141(6):1871–1883, 2018.
- Sylvia Villeneuve, **Jacob W. Vogel**, Julie Gonneaud, Alexa Pichet Binette, Pedro Rosa-Neto, Serge Gauthier, Randall J. Bateman, Anne M. Fagan, John C. Morris, Tammie L.S. Benzinger, Sterling C. Johnson, John C.S. Breitner, and Judes Poirier. Proximity to parental symptom onset and amyloid-

  β burden in sporadic Alzheimer disease. *JAMA Neurology*, 75(5):608–619, 2018.
- Anna Catharina Van Loenhoud, Colin Groot, **Jacob W. Vogel**, Wiesje Maria Van Der Flier, and Rik Ossenkoppele. Is intracranial volume a suitable proxy for brain reserve? Rik Ossenkoppele. Alzheimer's Research and Therapy, 10(1):1–12, 2018.
- **Jacob W. Vogel**, Niklas Mattsson, Yasser Iturria-Medina, Olof T. Strandberg, Michael Schöll, Christian Dansereau, Sylvia Villeneuve, Wiesje M. van der Flier, Philip Scheltens, Pierre Bellec, Alan C. Evans, Oskar Hansson, and Rik Ossenkoppele. Data-driven approaches for tau-PET imaging biomarkers in Alzheimer's disease. Human Brain Mapping, 40(2):638–651, 2019. *
- Niklas Mattsson, Sebastian Palmqvist, Erik Stomrud, **Jacob W. Vogel**, and Oskar Hansson. Staging β-Amyloid Pathology With Amyloid Positron Emission Tomography. *JAMA Neurology*, jul 2019
- Yeo Jin Kim, Seong-Kyoung Cho, Hee Jin Kim, Jin San Lee, Juyoun Lee, Young Kyoung Jang, **Jacob W. Vogel**, Duk L. Na, Changsoo Kim, and Sang Won Seo. Data-driven prognostic features of cognitive trajectories in patients with

amnestic mild cognitive impairments. *Alzheimer's Research & Therapy*, 11(1):1–9, 2019.

- Theresa Köbe, Alexa Pichet Binette, **Jacob W Vogel**, Pierre-François Meyer, John CS Breitner, Judes Poirier, Sylvia Villeneuve. Vascular burden is associated with a decline in default-mode and global resting-state functional connectivity in individuals at risk for Alzheimer's disease. *BioRxiv*, pages 1-20, 2020.
- AmanPreet Badhwar, Yannik Collin-Verreault, Pierre Orban, Sebastian Urchs, Isabelle Chouinard, **Jacob W. Vogel**, Olivier Potvin, Simon Duchesne, and Pierre Bellec. Multivariate consistency of resting-state fMRI connectivity maps acquired on a single individual over 2.5 years, 13 sites and 3 vendors. *NeuroImage*, 205:116210, jan 2020.
- Alexa Pichet Binette, Julie Gonneaud, **Jacob W Vogel**, Renaud La Joie, Pedro Rosa-Neto, D Louis Collins, Judes Poirier, John CS Breitner, Sylvia Villeneuve, Etienne Vachon-Presseau, Alzheimer's Disease Neuroimaging Initiative, PREVENT-AD Research Group. Morphometric network differences in ageing versus Alzheimer's disease dementia. *Brain*, 43(2):635-649, 2020.
- **Jacob W. Vogel**, Renaud La Joie, Michel J. Grothe, Alex Diaz-Papkovich, Andrew Doyle, Etienne Vachon-Presseau, Claude Lepage, Reinder Vos de Wael, Yasser Thomas, Rhalena Iturria-Medina, Boris Bernhardt, Gil D. Rabinovici, and Alan C. Evans. A molecular gradient along the longitudinal axis of the human hippocampus informs large-scale behavioral systems. *Nature Communications*, 11(1):1-17, 2020.
- **Jacob Vogel**, Yasser Iturria-Medina, Olof T Strandberg, Ruben Smith, Elizabeth Levitis, Alan C Evans, Oskar Hansson, Alzheimer's Disease Neuroimaging Initiative and the Swedish BioFINDER study. Spread of pathological tau proteins through communicating neurons in human Alzheimer's disease. *Nature Communications*, In Press. **
- Colin Groot, BT Thomas Yeo, **Jacob W Vogel**, Xiuming Zhang, Nanbo Sun, Elizabeth C Mormino, Yolande AL Pijnenburg, Bruce L Miller, Howard J Rosen, Renaud La Joie, Frederik Barkhof, Philip Scheltens, Wiesje M van der Flier, Gil D Rabinovici, Rik Ossenkoppele. Data-driven detection of latent atrophy factors related to phenotypical variants of posterior cortical atrophy. *Neurology*, In Press.
- **Jacob W. Vogel**, Alexandra L. Young, Neil P. Oxtoby, Ruben Smith, Rik Ossenkoppele, Olof T. Strandberg, Renaud La Joie, Leon M. Aksman, Michel J

Grothe, Yasser Iturria-Medina, Gil D. Rabinovici, Daniel C. Alexander, Chul Hyoung Lyoo, Alan C. Evans, Oskar Hansson. Characterizing the spatiotemporal variability of Alzheimer's disease pathology. In Preparation.***

* Included in Chapter 2 of this thesis
** Included in Chapter 3 of this thesis.
*** Included in Chapter 4 of this thesis.

Summary of novel contributions

Chapter 2

- Unsupervised partitioning of tau-PET covariance leads to Braak-like structures, as well as clusters of non-target signal.
- Isocortical tau accumulation does not appear to be uniform, as suggested by Braak staging – temporo-parietal regions behave differently from frontal regions.
- ROIs from a data-driven parcellation track cognition better than ROIs based on autopsy reports of the spread of tau.
- Tau-PET signal within the hippocampus is heterogenous, including voxels that covary with off-target regions, and voxels that covary with known tau-vulnerable regions.
- Tau-PET covariance clusters stored online as a persistent resource for academic research.

Chapter 3

- A simulated pattern of epidemic spread of tau pathology from the entorhinal cortex through the human connectome correlated strongly with the spatial distribution of tau-PET signal
- Simulations of epidemic spread from the entorhinal cortex also correlated strongly with tau-PET patterns in individuals without Aβ, perhaps indicating synaptic spread in PART.
- Tau levels were underestimated in regions with high Aβ, suggesting Aβ influences the regional spread of tau.
- Modeling spread over macroscale brain connections fits the data better than modeling spread over euclidian distance.

Chapter 4

- In a large dataset of tau-PET images across the AD clinical spectrum, four spatiotemporal patterns fit the data better than a single pattern.
- Well-described limbic-predominant and MTL-sparing phenotypes emerged, as did spatiotemporal patterns resembling atypical clinical variants of AD.
- Across all subtpyes, younger age of onset was associated strongly with more advanced disease stage.

- Including subtype information or individually-tailored information improves sensitivity to detect longitudinal accumulation of tau-PET signal.
- Subtype-specific tau patterns resembled different corticolimbic networks, and implied contribution of distinct cell types.

Chapter 1

Introduction and Literature Review

1.1 General context and rationale

1.1.1 General context

The modern world is threatened by a range of existential challenges, including climate change, overpopulation, pollution, food shortage and disease. The current COVID pandemic is a stark example of the impact of infectious disease, but there are other areas of public health that, while less visible, may have an even greater long-term impact on society than transient eruptions of disease. Specifically, the growing prevalence of dementia in aging populations around the world places a permanent burden on the individual with dementia, the immediate carers and the wider society. Unless direct action is taken to mitigate this burgeoning threat to global brain health, the socioeconomic consequences could be catastrophic. Alzheimer's disease is already the 6th leading cause of death and, without intervention, incidence is expected to more than double in the next thirty years (Association, 2019). The result would of course lead to incredible economic burden. Nearly 300 billion dollars was spent on dementia healthcare in 2019 alone, not to mention the estimated 230 billion lost value of unpaid caregiver support. However, another concern is that the current medical infrastructure is currently not capable of supporting but a fraction of projected dementia cases. It is not totally outrageous to imagine society forced to transform into a caregiver-based economy, with nurses, medical practitioners and aids becoming the generational factory workers, so to speak.

This is not to draw attention away from the enormous emotional and financial cost of dementia to individuals. One in ten people over the age of 65 live with dementia (Association, 2019), meaning many of us experience the direct impact of a family member, friend or loved one losing their quality of life, function and often identity,

to dementia. The lifetime likelihood of AD at age 45 is 10-20% (Association, 2019), meaning anyone reading this may eventually realize one of our worst collective fears in being diagnosed with dementia during life. As disturbing as these realities are, the individual experience with AD will not change or may even improve, and the actual rate of dementia actually may be reducing (Satizabal et al., 2016) . However, the collective, social burden of dementia will continue to rise, and threatens to overcome even our own personal concerns.

The bleak picture painted above is a scenario that assumes no interventions to stop, delay or prepare for the oncoming wave of dementia cases. Preparation would involve building the infrastructure and legal backdrop to accommodate a caregiver-based society. This is a last-case scenario that is not currently underway. In a more ideal circumstance, therapies to halt, cure, ease or delay dementia symptoms could prevent or at least ameliorate the dystopian narrative that introduces this thesis. For example, delaying disease onset by two years now projects to decrease the number of cases in 2050 by over 20% (Brookmeyer et al., 2007). For these and other reasons, funding has been steadily increasing for aging research in United States (Shugart, 2019), even when overall research funding has dipped (Ledford et al., 2019). The hopeful goal is to identify clinical interventions to halt the progression of dementia symptoms.

By now, the urgency of efforts to combat dementia should be clear, and the leading cause of dementia is Alzheimer's disease (AD) (Association, 2019). Unfortunately, despite decades of research and a plethora of clues and valuable insights, the most important questions relating to Alzheimer's disease elude us: what causes it and (how) can it be halted or reversed? Arguably the biggest clues we have are linked in a complicated knot with the disease definition. While Alzheimer's disease *dementia* is a clinical syndrome associated with a constellation of cognitive and functional symptoms, Alzheimer's *disease* is defined by the presence of aggregated extra-cellular plaques of β-amyloid (Aβ), and intracellular neurofibrillary tangles of hyperphosphorylated tau oligomers, in the brain at autopsy (Jack et al., 2018b; Jack, Holtzman, and Sperling, 2019; Jack et al., 2019a). There is a fairly specific cascade of neuronal degeneration, systemic degradation of multiple neural support systems, large-scale brain volume loss, and cognitive and functional decline that is often associated with AD pathology, which is collectively referred to as Alzheimer's disease. However, AD pathology is described exclusively by the abnormal conformation and aggregation of two proteins, Aβ and tau, and the most prominent hypotheses of AD etiology and progression posit these two proteins as central (if not causal) entities. The contents of this thesis focus on the accumulation, spread and clinical biomarker utility of one of these two proteins, tau, in the context of Alzheimer's disease.

1.1.2 Rationale

As will be described in great detail, tau aggregation is associated with progressive clinical decline (Josephs et al., 2008), and regional tau accumulation closely mirrors regional neurodegenerative patterns (Xia et al., 2017). Neither of these two features is true of Aβ accumulation. However, the fact that genetic forms of AD involve mutations to proteins in Aβ processing pathways, and the appearance of Aβ plaques decades prior to symptom onset, lead many to postulate it as the initial catalyzing event in the AD cascade (Hardy and Higgins, 1992; Hardy and Selkoe, 2002; Sperling, Karlawish, and Johnson, 2013; Jack and Holtzman, 2013; Selkoe and Hardy, 2016) While this hypothesis has not been rejected, a slew of failed clinical trials of Aβ-modifying therapies (Schneider et al., 2015) has shifted the focus of many clinical and research groups to other other prominent hypothetical models of AD. Foremost among these are hypotheses relating to tau. Understanding tau physiology, pathology and progression has therefore become a central priority in AD research.

At the time that work toward this thesis began, *in-vivo* measurement of tau in humans using positron emission tomography had only recently begun, and the first major papers on the topic had only just been published (Schöll et al., 2016a; Johnson et al., 2016). This led to a monumental shift in human AD research; while *in-vivo* Aβ-PET imaging had been around for a decade (Klunk et al., 2004), human tau research had only been accessible through fluid measurement lacking spatial information, and autopsy of deceased human brains (Jagust, 2014). Many basic assumptions of tau accumulation that were inferred through autopsy and animal studies now needed to be tested in living humans. Meanwhile, basic questions about the utility and efficacy of tau-PET radiotracers as research or clinical tools were also in need of answers.

Perhaps the most important information afforded by the tau-PET revolution was access to the spatial information relating to tau accumulation. This was a particularly important development given that one of the more prominent enigmas in the study of tau relates to its spatial distribution throughout the brain. Large, serial autopsy studies have demonstrated AD-like neurofibrillary tau tangles are first observed in a very specific strip of cerebral cortex, and appear to spread in a specific and apparently stereotyped sequence throughout the brain (Braak and Braak, 1991). This phenomenon was formalized into a staging system (Braak et al., 2006), referred throughout this document as Braak staging. This particular pattern has great clinical utility, as it provides a pathological progression that evolves alongside clinical progression. The sheer specificity of this pattern may also hold clues as to what makes different neural tissue vulnerable (or resistant) to accumulating and spreading AD pathology. The content of this thesis is specifically focused on using human tau-PET

imaging to probe the spatial distribution of tau in Alzheimer's disease *in vivo*, and its implications for disease biology and clinical utility.

1.1.3 Objectives

The overall objective of the work in this doctoral thesis is to better characterize the *in vivo* distribution of tau in Alzheimer's disease. While large, cross-sectional autopsy studies have provided a model of tau accumulation and spread in AD, it is important to validate (and perhaps build on) this model *in vivo*. Furthermore, little is known about how tau spreads through the cortex, why certain regions are vulnerable and other resistant to tau pathology, how variable tau spreading truly is, or how amyloid and tau interact in AD. Evidence for each of these aspects of tau pathophysiology has accrued over the years from *ex vivo* human research (i.e. autopsy work) and *in vivo* non-human (i.e. animal model) experiments. However, until tau-PET became an available tool, hardly any tau-specific research was possible that was both in humans and *in vivo*. The original work in this thesis seeks to validate and expand upon previous autopsy- and animal-based models of tau distribution and spread using human tau-PET data.

Chapter 1 is composed of an introduction to the topic of tau in AD, as well as a literature review to support the original research in subsequent chapters. The objective of this review is to cover aspects of tau biology and pathophysiology relevant to Alzheimer's disease, to summarize previous work using tau-PET as a research or clinical biomarker, and to illustrate the research context and open questions that motivates the original research contained in this thesis.

One of the first challenges presented by tau-PET was how best to summarize the vast information available in a single tau-PET image for research and clinical purposes. The objectives of (the original work in) Chapter 2 are to present data-driven strategies for identifying regions-of-interest (ROIs) for tau-PET analysis, and to contrast these solutions to other solutions presented in previous literature. A secondary objective was to explore how data-driven strategies specifically treat the hippocampus, a region particularly important in AD but one that shows counterintuitive tau-PET tracer uptake.

How tau spreads through the brain remains and open question, but the leading hypotheses suggest a trans-neuronal spreading model. The objective of (the original work in) Chapter 3 is to test this hypothesis in humans by modeling spread over human brain connections and validating these models using tau-PET data. A secondary objective is to quantify how regional Aβ influences our *in vivo* spreading model.

The existence of several AD "subtypes" and clinical variants with abnormal tau patterns challenges the notion that tau follows a uniform Braak-like progression

throughout the brain in AD. The primary objective of (the original work in) Chapter 4 is to characterize spatiotemporal variation in tau spreading in a massive tau-PET dataset, and to profile the clinical and demographic qualities associated with this variation. A secondary objective of Chapter 4 is to apply knowledge of this variation to individual-tailored biomarkers to capture longitudinal tau accumulation. A final objective is to use transcriptomic and network-spread analyses to explore whether macro- and micro-scale networks can inform variation in tau spreading patterns.

Finally, the objective of Chapter 5 is to summarize the original work contained in this thesis and describe the contribution of the work to the overall field of AD.

1.2 Tau biology

The following section will review known physiological functions of tau and outline the evolution of its pathological expression. This section will also describe known interactions between tau and Aβ, and early abnormal tau processes that may or may not be relevant to AD.

1.2.1 Physiological role of tau in the the non-demented brain

In order to understand tau-related dsyfunction in AD and other tauopathies, it is important to understand its physiological role in the brain. Tau is fairly ubiquitously expressed in neurons throughout the human brain (Binder, Frankfurter, and Rebhun, 1985). The tau protein is encoded by the microtubule-associated protein tau (MAPT) gene, in accordance with its first-discovered role in microtubule assembly (Weingarten et al., 1975). Two haplotypes exist in humans, resulting from a 900mb inversion polymorphism, which affects risk for different tauopathies (Baker et al., 1999). MAPT is subject to alternative splicing involving differential numbers of amino-terminal inserts (zero, one or two) and microtubule binding repeats (three or four), resulting in six different tau isoforms (Goedert et al., 1989) (Fig 1.1A). The number of repeats, discussed below as 3R (3-repeat) and 4R (4-repeat) tau, are important with respect to tauopathy. While the 3R/4R tau ratio in the human brain is fairly even (Spillantini and Goedert, 1998; Goedert and Jakes, 1990), this is not the case for other species (including rodents) (Kosik et al., 1989; Janke et al., 1999), and the ratio differs by brain region (Hara et al., 2013). 3R tau is apparently the primary isoform during fetal development and is substantially downregulated in the adult brain (Drubin, Caput, and Kirschner, 1984; Kosik et al., 1989; Bullmann et al., 2009), whereas, 4R tau binds microtubules with greater affinity (Goedert and Jakes, 1990). Making matters even more complicated, all isoforms of tau undergo postranslational modification, most

notably through phosphorylation, but also through acetylation and cleavage, among other mechanisms (Morris et al., 2015)(Fig 1.1A,B). With nearing 100 phosphosites (Arendt, Stieler, and Holzer, 2016), one starts to realizes the enormous number of possible conformations, making the task of cataloguing the various functional roles of tau a complicated process.

As the MAPT moniker suggests, tau's canonical role involves the assembly, stability and spacing of microtubules (Weingarten et al., 1975; Cleveland, Hwo, and Kirschner, 1977; Drechsel et al., 1992; Chen et al., 1992). Specifically, tau co-assembles with tubulin, promoting polymerization (Cleveland, Hwo, and Kirschner, 1977; Drechsel et al., 1992). This tau-tubulin interaction is apparently a fairly crucial process in morphogenesis and neuronal plasticity (Nunez, 1988; Takei, 2000; Samsonov et al., 2004), perhaps highlighting the role of tau during development. Tau is also involved in transportation of resources along the axon, mainly to pre-synaptic terminals, which occurs through interaction with common molecular motors (Dixit et al., 2010).

Due to its close association with microtubules, tau is most frequently found in axons (Kempf et al., 1996). This is somewhat paradoxical to the finding that tau *pathology* is most frequently localized to the cell soma and apical dendrite (Zempel et al., 2017). More recent research has found evidence for tau being additionally localized within the cell nucleus (Loomis et al., 1990; Sultan et al., 2011; Violet et al., 2014), as well as in dendrites and synapses (Regan, Whitcomb, and Cho, 2017; Tai et al., 2012), with one study finding evidence for tau in most pre- *and* post-synaptic sites (Tai et al., 2012). These findings prompted exploration into other physiological roles of tau outside of microtubule-related functions.

More recent findings have suggested involvement of tau in synaptic plasticity, particularly as it relates to downregulation of N-methyl-D-aspartate receptors (NMDAR, Ittner et al., 2010; Mondragón-Rodríguez et al., 2012; Regan et al., 2015). Hypotheses has been proposed positing tau as an NMDAR regulatory mechanism in the event of over-excitation (Mondragón-Rodríguez et al., 2012; Mondragón-Rodríguez et al., 2018), or during synaptic long-term depression (Kimura et al., 2014; Regan et al., 2015; Regan, Whitcomb, and Cho, 2017). Interestingly, similar tau-related, NMDA-regulated processes appear to be invoked during mammalian hibernation, which involves massive (but reversible) hyperphosphorylation akin to that seen in AD (Arendt et al., 2003). Similar processes may be involved during anesthesia and hypothermia, leading to the proposition that tau may be mobilized as a protection in preparation of hypometabolic shock (Run et al., 2009; Arendt and Bullmann, 2013; Arendt, Stieler, and Holzer, 2016). Tau's role in the nucleus also is not very well understood, though it is notable that tau can bind directly to DNA (Qi et al., 2015).

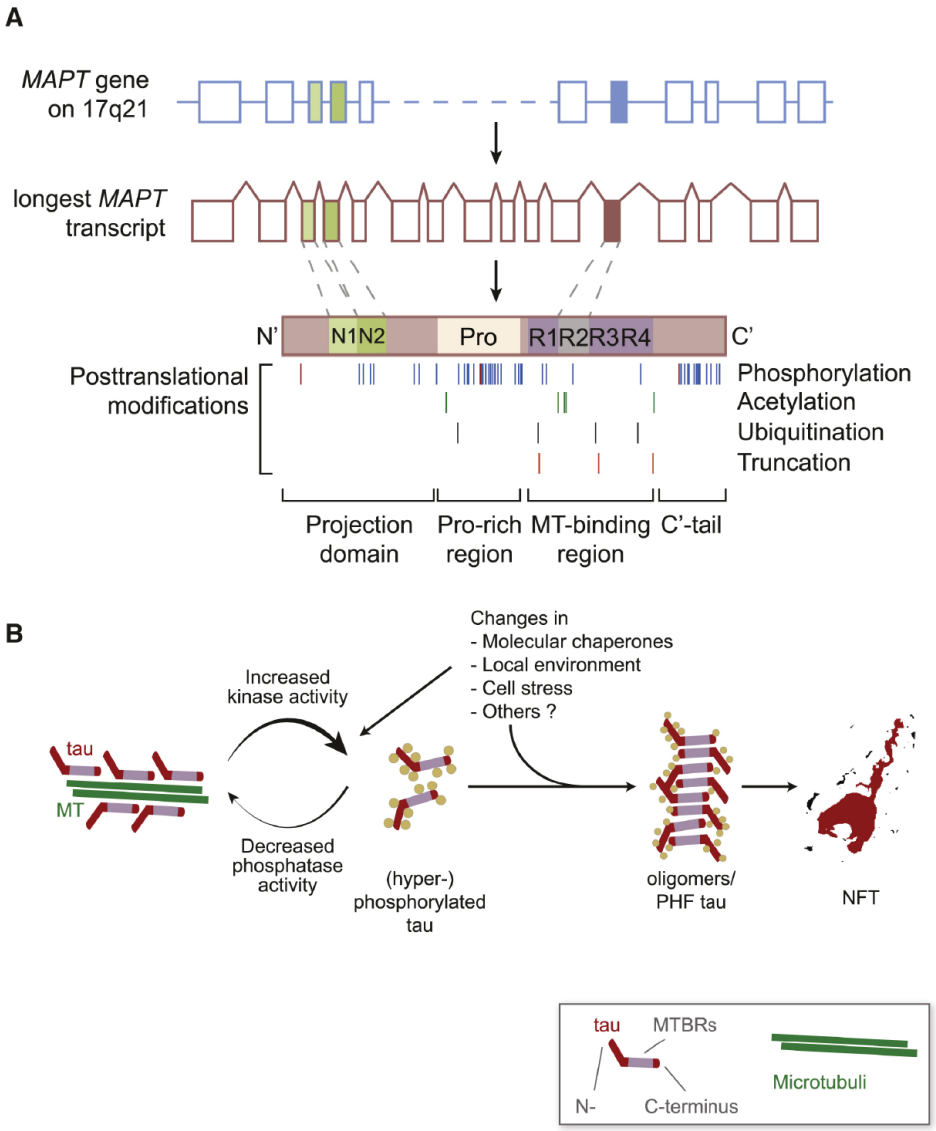

Figure 1.1: Reproduced (with permission from Elsevier) from Ittner and Ittner, 2018. A) The MAPT gene, highlighting exons relating to functional domain and genetic variation, as well as sites of post-translation modification. B) Changes in kinase/phosphotase activity lead to tau hyperphosphorylation, where tau dissociates from microtubules and aggregates into oligomers, which are themselves aggregated into NFTs.

There is evidence for a protective role of tau on DNA (Granic et al., 2010; Sultan et al., 2011; Violet et al., 2014); while knocking out MAPT in mice does not result in an obvious phenotype (Harada et al., 1994), DNA damage in these animals has been observed (Granic et al., 2010), among other factors.

The tau protein clearly has a multitude of functions, many of which remain poorly understood or possibly undiscovered. What is clear, however, is that the different localizations and roles observed in the tau protein are controlled through post-translational events, most notably phosphorylation (Billingsley and Kincaid, 1997; Arendt, Stieler, and Holzer, 2016). Nearly all of these modifications involve a negative regulation of microtubule-associated functions (Lindwall and Cole, 1984;

Drechsel et al., 1992; Bramblett et al., 1993). Differential phosphorylation also controls tau localization and its molecular interactions (Kowall and Kosik, 1987; Jenkins et al., 2000; Arendt, Stieler, and Holzer, 2016; Iwata et al., 2019). Understanding the role of different kinases in tau phosphorylation may hold the key to understanding tau's various conformational states, including those associated with pathological events. As such, this topic is the subject of much research, though literature has not found much consensus, outside of likely roles of GSK-3β and cdk5 (Mandelkow et al., 1992; Baumann et al., 1993).

1.2.2 Pathological role of tau in dementia

Tau is an apparently ubiquitous neuronal protein involved in functions ranging from synaptic development to plasticity to normal neuronal maintenance. It is no surprise then that perturbation to the tau protein can result in an impressive array of different neurodegenerative conditions with distinct expression of pathology, regional vulnerability and clinical expression. Primary tauopathies represent a class of diseases where tau is the sole primary pathology, which includes disorders such as progressive supranuclear palsy, argylophilic grain disease, corticobasal degeneration, Pick's disease, and genetic forms of frontotemporal dementia (Kovacs, 2015; Götz, Halliday, and Nisbet, 2019). Interestingly, these diseases arise sporadically, but tauopathy also occurs as a result of familial genetic mutation to the MAPT gene (Hutton et al., 1998; Van Swieten and Spillantini, 2007; Götz, Halliday, and Nisbet, 2019). Alzheimer's disease is considered a secondary tauopathy (Kovacs, 2015), since AD by definition presents with concurrent Aβ-pathology. While many of the primary tauopathies present specifically with 4R-tau pathology, the pathological profile of AD presents with a mix of 3R- and 4R- tau.

A survey of the pathological and clinical expression of different tauopathies is beyond the scope of this literature review (though see any of Kovacs, 2015; Arendt, Stieler, and Holzer, 2016; Götz, Halliday, and Nisbet, 2019 for a review). However, there are some common feature among most tauopathies. Namely, tauopathies commonly involve hyperphosphorylation of tau, which subsequently co-occurs with aggregation of tau into fibrils and localization of tau into somatodendritic part of the neuron (as opposed to it's native spatial distribution, which is mostly in the axon) (Arendt, Stieler, and Holzer, 2016). These features will be discussed as they relate to AD and putatively to neurodegeneration.

Hyperphosphorylation of tau (or other post-translation modifications) leads to dissociation of tau from microtubules and into its monomeric form (Kopke et al., 1993; Goedert et al., 1996). The monomeric tau then undergoes a process of conformational alteration, leading to aggregation into soluble oligomers, which form

"pretangles" or fibrils, which form insoluble neurofibrillary tangles (NFTs) (Kuret et al., 2005; Grundke-Iqbal, Iqbal, and Tung, 1986)(Fig 1.1B). In AD, 95% of these fibrils are represented by paired-helical filaments (PHF) (Goedert et al., 1992). Hyperphosphorylation is the initial step in this cascade (Kopke et al., 1993; Billingsley and Kincaid, 1997; Buée et al., 2000), prior to aggregation, and dissociated oligomeric tau can therefore be used as an indication of early tau pathology (Maeda and Takashima, 2007). As to how tau escapes the axon, this may be due to phosphorylation-induced breakdown of microtubules composing the barrier that normally keeps tau out of the cell soma (Li et al., 2011; Frandemiche et al., 2014; Zempel et al., 2017). However, as noted earlier, smaller amounts of tau are present outside of the axon physiologically, namely in the post-synaptic areas of dendritic spines (Ittner et al., 2010; Tai et al., 2012). Similarly, others have proposed tau is simply overexpressed in the cell soma and fails to be transported out (Braak and Del Tredici, 2015).

Many aspects of this process remain poorly understood. The cause of systemic hyperphosphorylation is not known. AD tau demonstrates a much larger proportion of phosphorylated sites compared to physiological tau, possibly suggesting an imbalance in tau-related kinases and phosphotases (Ksiezak-Reding, Liu, and Yen, 1992; Kopke et al., 1993). The cause of such an imbalance is still in question (though see subsection 1.2.3 below). Another unanswered question pertains to why disassociated monomeric tau is aggregated into fibrils. The leading hypothesis suggests that the abnormally increased concentration of monomeric tau leads to a programmed physiological aggregative response (Kuret et al., 2005). In addition, caspase cleavage also appears to be an important step in tau fibrilization (Gamblin et al., 2003; De Calignon et al., 2010). Interestingly, injecting soluble tau fractions into the brains of human tau-expressing mice without tau pathology in sufficient to induce aggregation (Clavaguera et al., 2009; Mirbaha et al., 2018). This is discussed in more detail in section 1.3.2 below. A relatively more recent deluge of research has begun to suggest that the soluble oligomeric tau takes on a neurotoxic form (Chung et al., 2001; Fath, Eidenmüller, and Brandt, 2002; Lasagna-Reeves et al., 2010; Flach et al., 2012), and that the process of aggregation may therefore be protective by containing the oligomers into an inert, insoluble form (Santacruz et al., 2005; Götz et al., 2008). However, compromised tau-positive neurons feature extensive PHF formation throughout the somatodendritic compartment, which very likely have a deleterious impact on cellular processes at least in later stages of neuronal degeneration (discussed in Ballatore, Lee, and Trojanowski, 2007).

The notion of a tau gaining neurotoxic function in its oligomeric form represents an interesting addition to the earlier loss-of-function based hypotheses. While dissociation of tau from microtubules may in fact lead to disrupted axonal transportation

(e.g. Ishihara et al., 1999), accumulating evidence suggests this may not be the primary, or at least not the only, threat to neuronal health in AD. For example, in AD brains, PHF concentrations are uncorrelated with microtubule number or length (Paula-Barbosa, Tavares, and Cadete-Leite, 1987; Cash et al., 2003), and axonal transport rates were unaffected by deletion or over-expression of tau in a mouse model (Yuan et al., 2008). Similarly, while MAPT knock-out mice do exhibit some subtle deficits in transport, they do not express any severe developmental or behavioral deficits (Harada et al., 1994; Dawson et al., 2001), suggesting tau is not necessary for microtubule-mediated processes during development or otherwise.

Neither the dissociation of tau from microtubules nor its aggregation into PHF appear to explain it's primary pathogenicity in the neuron. Contemporary ideas point to a disruption or hijcacking of tau's role at the synapse (Spires-Jones and Hyman, 2014; Ittner and Ittner, 2018). Synaptic dysfunction is major component of AD and has been linked to cognitive decline (DeKosky and Scheff, 1990). As noted earlier, tau can be found (Ittner et al., 2010; Tai et al., 2012), and perhaps produced (Kobayashi et al., 2017), in synapses of healthy brains, where it likely plays some physiological role. Overexpression of mutated tau leads to synaptic dysfunction and synapse loss in mice (Crimins et al., 2013; Kopeikina et al., 2013; Hoff et al., 2013; Menkes-Caspi et al., 2015), and neurons with NFT pathology express less synapse-related genes (Callahan, Vaules, and Coleman, 1999; Ginsberg et al., 2000). In a comparison of tissue from unimpaired and impaired humans both expressing tau pathology, AD tissue showed more phosphorylated tau localized to synapses, despite similar NFT numbers to the unimpaired controls (Perez-Nievas et al., 2013).

Interestingly, tau has also been implicated in a number of synaptically-mediated functions in the brain (e.g. Zempel et al., 2010; Decker et al., 2015. For example, tau reduction is associated with decreased seizure risk (Roberson et al., 2007; Holth et al., 2013; DeVos et al., 2013), and markedly decreased excitotoxic neuronal loss after stroke (Bi et al., 2017). Additionally, a number of studies have shown tau reduction in mice to subsequently reduce hippocampal LTD (Kimura et al., 2014; Regan et al., 2015) and long-term potentiation (Ahmed et al., 2014a; Puzzo et al., 2017), important processes for learning and memory. While the mechanisms are not understood, tau has been shown to bind to fyn, a crucial protein for regulation of NMDARs, particularly during excitotoxicity (Ittner et al., 2010; Frandemiche et al., 2014; Miyamoto et al., 2017). Related, tau-related synaptic dysfunction has repeatedly been associated with localized calcium imbalance (e.g. Zempel et al., 2010; Decker et al., 2015). Recent research has also pointed to impairment of presynaptic vesicular functions by mutated tau (Zhou et al., 2017). Finally, a great deal of research has suggested a toxic effect of Aβ at the synapse, though this toxicity appears to be

specifically mediated by tau (reviewed in Section 1.2.4 below). It should be noted that some controversy exists around the effects of tau at the synapse. NFT formation and neurodegeneration in the hippocampus has been seen in the absence of abberant changes to spine density and morphology (Shahani et al., 2006), and the synapses of intact entorhinal cortex neurons of AD patients have been described as undisturbed at autopsy (Scheff and Price, 1993).

Other aspects of tau physiology cannot be ruled out in terms of contributing to pathology. For example, tau binds to f-actin (Griffith and Pollard, 1982) and fruitfly work has suggested a deleterious effect of tau in dendritic spines via this mechanism (Fulga et al., 2007). In addition, their is evidence that tau can induce cell-cycle alteration, aneuploidy and abberant gene expression through its interaction with DNA in the nucleus, and this process can lead quickly to cell death (Nagy et al., 1997; Andorfer et al., 2005; Mosch et al., 2007; Iourov et al., 2009; Frost et al., 2014; Eftekharzadeh et al., 2018). Irrespective of the mechanism by which tau influences neuronal degeneration, accumulating evidence seems to suggest oligomeric tau represents the toxic species, and its appearance is preceded by hypophosphorylation of axonal tau.

The tau pathophysiology literature is confounded by the fact that experiments are conducted in multiple models, animals and settings, involving different perturbations to tau, and reporting inconsistent, varying and sometimes negative results. It is challenging therefore to deduce which mechanisms are relevant to human AD pathophysiology. In light of certain findings (e.g. Harada et al., 1994; Santacruz et al., 2005; Gómez-Isla et al., 1997; Kuchibhotla et al., 2014), one might even question whether tau pathology itself is causal to neurodegeneration. However, this much at least is proven, as mutation of the MAPT gene is sufficient to cause dementing tauopathy and extensive neurodegeneration in humans (Hutton et al., 1998; Spillantini and Goedert, 1998). Recreating these mutations in cell and animal models have shown some mutations to inhibit or improve microtubule assembly, promote fibrillization, impair axonal transport, enhance phosphorylation, impair membrane binding, shift the balance of 3R and 4R tau, or directly affect the expression of tau mRNA (Arendt, Stieler, and Holzer, 2016; Tacik et al., 2016). Importantly, none of these mutations cause Alzheimer's disease (Goedert and Jakes, 2005), and most of them cause tauopathy with pathology distinct from AD. Certain mutations (V337M and R406W) *do* lead to a 3R/4R mixed tau pathology similar to that seen in AD (Spillantini, Crowther, and Goedert, 1996; Reed et al., 1997; Hutton et al., 1998; Smith et al., 2016). However, these patients usually (but not always) present with a different clinical phenotype, with different regions affected, compared to AD. Accordingly, the distinct expression of AD tauopathy is likely due to interactions with other factors, the most well-studied

being Aβ (reviewed in section, 1.2.4).

1.2.3 PART and preclinical AD: The genesis of tau pathology?

The previous two subsections addressed the physiological role of tau in the healthy brain, and aberrant tau activity associated with AD and other tauopathies, respectively. At the intersection of these concepts is a phenomenon called primary age-related tauopathy (PART), which describes the near-ubiquitous appearance of aberrant tau activity in older, non-demented individuals.

This concept was first conceptualized due to observations of older individuals with cognitive impairment that presented with AD-like 3R/4R mixed tau as the primary pathology at autopsy, without any evidence of Aβ (Bouras et al., 1994; Bancher and Jellinger, 1994). These cases were first referred to as tangle-predominant senile dementia, or tangle-only dementia, and were subsumed under the umbrella of FTLD tauopathies (Chartoire et al., 2007). However, numerous studies from autopsy cohorts began describing at least some limited tau pathology in nearly all autopsy cases of older individuals, including those that died in a nondemented state (Crary et al., 2014). These cases consisted of 3R/4R filamentous NFT pathology mostly restricted to the entorhinal cortex and hippocampus (i.e. Braak Stage I and II), occasionally in limbic or temporal association cortex (Stage III or IV), and almost never beyond those regions. The formalization of these cases as a distinct entity called PART by Crary et al. was met with a great deal of controversy (Braak and Del Tredici, 2014; Duyckaerts et al., 2015). Namely, PART individuals presented with pathology apparently identical to that seen in AD, in the same cells and regions and along the same patterns that NFT pathology is observed in AD (Jellinger, 2018), but with little (probable PART) or no (definite PART) measurable Aβ pathology (Braak and Del Tredici, 2014). To this day, controversy persists as to whether PART, as the name suggests, is an inevitable mild tauopathy associated with normal aging, or whether it represents the first step along the sporadic AD continuum (Crary et al., 2014; Braak and Del Tredici, 2014; Duyckaerts et al., 2015; Jellinger, 2018).

Six years later, we know more about the clinical and pathological manifestation of PART, but almost nothing more about its etiology. Compared to individuals with both Aβ and tau pathology, PART individuals tend to be older at death (Crary et al., 2014; Teylan et al., 2020), are less likely to be cognitively impaired, and undergo much slower rate of cognitive decline prior to death (Besser et al., 2017; Bell et al., 2018; Teylan et al., 2020). PART is sufficient to cause clinical cognitive impairment (Besser et al., 2017; Teylan et al., 2020), independently of other co-pathologies, and more advanced pathology (i.e. higher Braak stages) is correlated with worse cognition and advanced age (Josephs et al., 2017; Jefferson-George et al., 2017). PART is also

associated with measurable brain atrophy from antemortem MRI, though this may be partially explained by other age-related copathologies (Josephs et al., 2017; Josephs et al., 2019). Interestingly, compared to AD patients, PART individuals have a lower proportion of carriers of the APOE4 allele, the major genetic risk factor of sporadic AD (Crary et al., 2014; Josephs et al., 2017; Bell et al., 2018).

Despite PART leading to cognitive impairment in old age, to consider it a tauopathy seems unusual given that nearly everyone older than 70 has evidence of NFT pathology in the MTL at autopsy (Braak and Del Tredici, 2014)a. In fact, Braak stage I/II pathology has been seen as early as the second decade of life, and reaches a peak in incidence at the sixth decade, at which point only about 1/3 of such cases show evidence of Aβ (Braak and Del Tredici, 2014)(Fig 1.2D). However, some would suggest that tau pathology occurs even earlier. To understand this, it is necessary to review how tau pathological processes are measured at autopsy.

Braak staging was originally performed using silver-iodide staining, which captures argyrophilic NFT pathology, or "mature tangles" (Uchihara et al., 2001). However, abnormally phosphorylated tau is selectively immuno-responsive to AT8, allowing immunostaining of a tau state that theoretically represents an earlier step in the pathological process (Biernat et al., 1992). These AT8-immunoresponsive inclusions appear to precede tangle formation in AD (Braak and Del Tredici, 2015). As it turns out, AT8-immunoresponsive inclusions are already common in teenagers, specifically in the locus coeruleus (LC) and other specific brainstem nuclei (Simic et al., 2010; Braak et al., 2011; Elobeid, Soininen, and Alafuzoff, 2012; Braak and Del Tredici, 2014; Braak and Del Tredici, 2015; Satoh and Iijima, 2019).(Fig 1.2A,B)

It is tempting to dismiss this observation as either spurious, or unrelated and irrelevant to entorhinal NFT pathology and AD tau pathology. However, there are three rather compelling points that support the notion of AD-like tau pathology beginning in the LC at the second decade of life. First, this subcortical pre-tangle pathology appears to progress in a stereotyped fashion, and this progression increases with age in phasic manner that seems to be in staggered precedence of NFT Braak staging (Fig 1.2), Braak et al., 2011; Braak and Del Tredici, 2014; Braak and Del Tredici, 2015). Second, the early pathological events observed in the midbrain during young adulthood mirror the pathological phases leading to NFTs in other parts of the brain. For example, pretangles are evident in neurons that eventually show NFTs in middle age (Braak and Del Tredici, 2015), and tau seeding similar to that seen in the LC precedes NFT pathology in AD (Kaufman et al., 2018; DeVos et al., 2018b). Finally, not long after NFTs are seen in the entorhinal cortex, NFT pathology appears in the LC, and other structures displaying aberrant behavior in early life (Braak and Del Tredici, 2015; Kaufman et al., 2018) These observations together inform a hypothesis that the

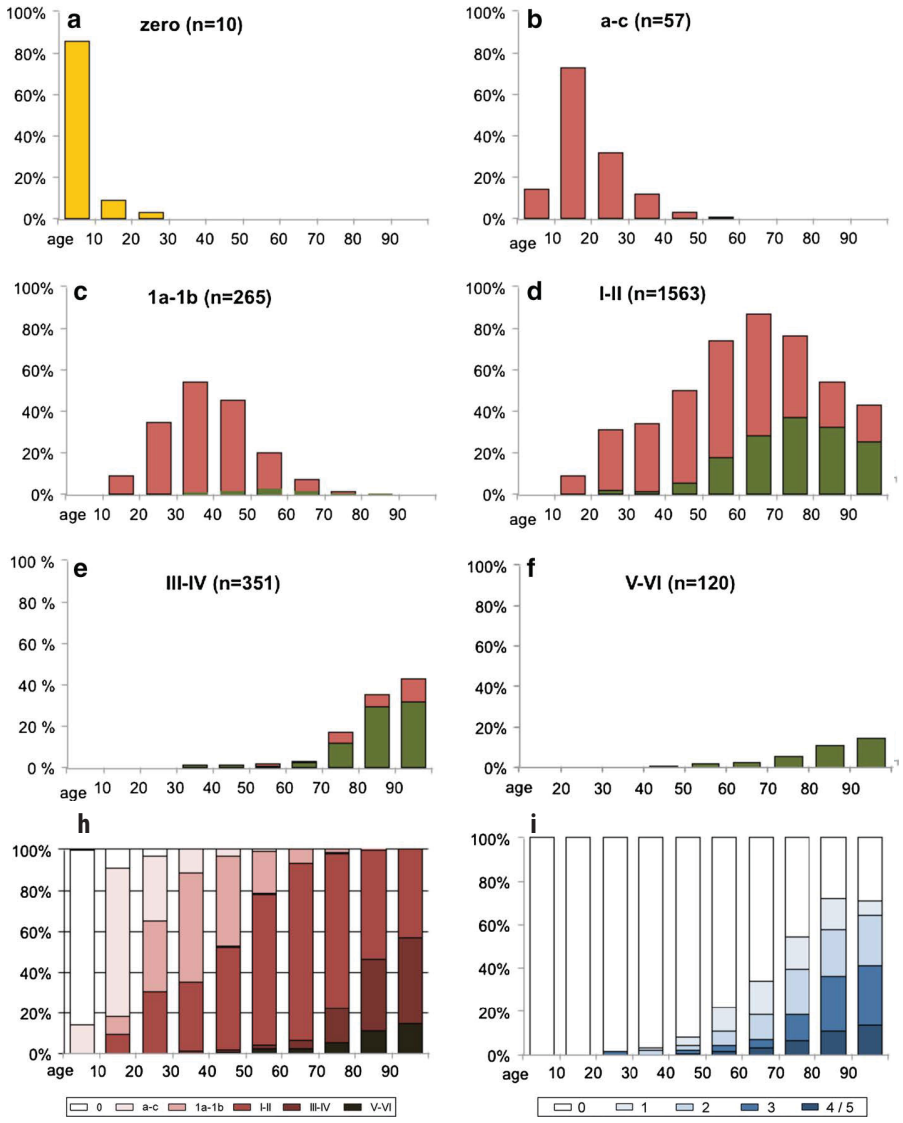

Figure 1.2: Adapted (with permission from Springer Nature) from (Braak and Del Tredici, 2014). For A-F, red bars indicate proportion of individuals showing aberrant tau activity at different ages, green bars indicate aberrant Aβ activity. A) Very few individuals over age 10 lack aberrant AT8-immuno-responsive subcortical tau inclusions. B) Young adulthood is characterized by progression of subcortical aberrant tau activity. C-F) Prevalence of traditional Braak stages across the lifespan, and the proportion of those cases showing Aβ pathology. H) Evolution of Braak stages across the lifespan. Evolution of Thal Aβ phases across lifespan.

AD pathological process evolves very slowly over the lifespan, and is profoundly accelerated by Aβ.

There are of course counter-arguments to this notion. For example, AT8-immunostained lesions appear to negatively affect cortical neurons, and eventually evolving into NFTs, whereas neither of these features are present in early-life LC neurons (Braak and Del Tredici, 2015). This is unlikely to be attributable to different cell types and molecular environments in the LC, as these neurons do show mature tangles at later disease stages. In addition, other more extensive evidence for LC pathology appears only once NFT pathology is already observed in the cortex (Sato et al., 2018). Thus

far, there is no direct evidence that early-life aberrant tau activity in the LC evolves into cortical NFT pathology, PART or AD.

There is, however, indirect evidence linking LC tau and AD. Interestingly, a recent study found mice transgenic for APP and PSEN1 exhibit hypophosphorylated tau in the LC before the entorhinal cortex and hippocampus (Rorabaugh et al., 2017). A different study found that injecting synthetic tau fibrils directly into the LC of transgenic mice overexpressing P301 mutant tau *did* result in spread of NFT pathology, but in a manner that followed LC connectivity rather than a typical AD pattern (Iba et al., 2015). A more recent study involved injection of a viral vector of human tau, phosphorylated at specific sites seen in preclinical human LC tau, into the rat LC. In young rats, hyperphosphorylated human tau and somatodendric misclocalization, but not NFT pathology, was seen in the cortex and brainstem after several weeks, whereas mild cognitive deficits and LC fiber degeneration were seen after several months. The effects were more severe in older rats (Ghosh et al., 2019). These studies unfortunately do not converge on any conclusive evidence. Together, they suggest early life LC tau pathology may be different from AD tau pathology (Ghosh et al., 2019), but that early LC tau pathology is emergent in a pathological Aβ context.

Whether or not early-life aberrant LC tau activity represents the pathogenesis of AD, it could still be a useful model to better understand tau pathophysiology. Relatively little is known about PART processes because there is currently no animal model to use for experimentation (though Ghosh et al., 2019 may be on the right track). [1] A few points of interest stem from human genetics. Along with increasing risk for various types of FTLD syndromes (Dickson, Rademakers, and Hutton, 2007), the H1 haplotype of the MAPT gene (Janocko et al., 2012; Santa-Maria et al., 2012) is related to "tangle-only dementia" – i.e. the most severe instances of PART. Similarly, a SNP near the MAPT locus was found to be associated at genome-wide significance with AD in individuals without an APOE4 allele (Jun et al., 2016). Both of these findings suggest, similarly to primary tauopathies, variation to the MAPT gene can lead to tau dysrgulation in the absence of Aβ.

For the purposes of comparison, it may also be of interest to consider other factors that appear to cause or associate with the accrual of irreversible tau hyperphosphorylation and/or NFT pathology. Other than a heretofore unknown age-related process (PART), MAPT genetic mutation (FTLD), and abnormal proteolytic APP processing (ADAD, trisomy 21, perhaps AD, see section 1.2.4 below), there are other instances of the emergence of tau pathology. Traumatic brain injury (TBI) may cause focal

[1] Several domestic animal species do present with age-related tau hyperphosphorylation, but not NFTs (Youssef et al., 2016). Studies have reported both Aβ accumulation *and* NFT tau pathology in dolphins (Gunn-Moore et al., 2018) and, more conveniently, cats (Chambers et al., 2015; Fiock et al., 2020).

tau phosphorylation and NFT pathology after some delay (Johnson, Stewart, and Smith, 2012; Zanier et al., 2018), and decreases the onset age of AD (Nemetz et al., 1999; LoBue et al., 2017). Meanwhile, sustaining multiple mild or moderate head impacts across a lifespan can lead to chronic traumatic encephalopathy (CTE), a dementing disorder presenting with considerable 3R/4R NFT tau burden similar to AD (McKee et al., 2015; Stern et al., 2019). The cause of tauopathy in these cases is unknown; head impact can stress brain microstructure leading to blood vessel and axonal damage, the latter of which may result in displaced and/or hyperphosphorylated tau (McKee et al., 2015). It is also worth mentioning that focal Aβ frequently appears after TBI in sites proximal to the injury, likely as a mechanism to aid in repairing blood vessel damage (Brothers, Gosztyla, and Robinson, 2018). While CTE does not frequently present with Aβ burden (at least in early stages, McKee et al., 2015), the possibility of focal Aβ-tau relations (see next section) may be sufficient to initiate a more widespread pathological cascade. CTE tau pathology resembles AD tau pathology – it even boasts many of the same (but some different) phosphorylated sites (Katsumoto, Takeuchi, and Tanaka, 2019) – but it presents with a progressive tau spread pattern distinct from AD (McKee et al., 2015). Notably, however, NFT tau pathology is common in the LC in CTE (McKee et al., 2015), while entorhinal and MTL pathology tend not to occur until later stages (Kelley, Perez, and Mufson, 2019). In all, impact-related neuronal injury can cause tau pathology and can sometimes lead to full-blown tauopathy, and the LC is once again highlighted as a region vulnerable to tauopathy.

There are a few more examples of environmental-related tauopathies. On the island of Guadalupe, exposure to annonacin – a selective mitochondrial complex I inhibitor – through frequent consumption of fruit of a specific plant species leads to a high incidence of a specific tauopathy with symptoms that resemble Parkinsons's disease (Lannuzel, Ruberg, and Michel, 2008). A fascinating *in vitro* study showed that annonacin leads to ATP depletion and redistribution of tau to the somatodendritic compartment by retrograde mitochondrial transport. The same study revealed that, in a survey of other neurotoxins, those that reduced ATP lead to a similar pathological redistribution of tau (Escobar-Khondiker et al., 2007). Another study found chronic exposure of mice to the juice of fruit containing annonicin causes not only tauopathy, but also reduces proteins previously associated with tau (Rottscholl et al., 2016).

Another link to environmental exposure and tau comes from data relating to air pollution in Mexico city. One group has published studies showing rather advanced NFT pathology at a very early age in children and adolescents exposed to high levels of air-pollution (Calderón-Garcidueas et al., 2012; Calderón-Garcidueñas et al., 2018).

One study found elevated markers relating to oxidative stress in such cases (Calderón-Garcidueas et al., 2012), though the topic remains understudied and could present interesting information. In addition, a number of studies have reported exaggerated tau pathology, but not other neurodegenerative proteins (Aβ,α-synuclein,TDP-43) in young individuals with ongoing heroin addiction (Ramage et al., 2005; Anthony et al., 2010; Kovacs et al., 2015). Interestingly, these younger individuals showed greater age-related increases in PART regions like the LC and entorhinal cortex, but also showed tau pathology in the frontal lobe that was uncorrelated with age (Kovacs et al., 2015).

Each of the aforementioned environmental factors represents a different pathway of tau hyperphosphorylation and aggregation, and each presents with some similarities and some differences to AD NFT pathology. However, with better-elucidated mechanisms, unifying patterns or pathways may emerge that are common to tau pathology, and which may shed light on what causes ubiquitous tau pathology in aging humans. In nearly all cases, the LC seems to be particularly vulnerable to tau pathology, and further study of this region may provide general insight into regional vulnerability to tau pathology. Together, the literature suggests there are multiple avenues that lead to tau pathology, including simply aging, which may speak to a general human vulnerability to aggregated tau pathology. Further research may also focus on other age-related processes that could be linked with tau pathology; an example perhaps being the finding that iron, which increasingly deposits in the brain with age, also phosphorylates tau and colocalizes with tau-positive neurons (Rao and Adlard, 2018). Another clue might come from genes involved in protein aggregation and supersaturation appear to be upregulated in aging, as well as AD (Ciryam et al., 2016). These threads might prove useful to pursue; even in mice, old age is associated with more aggressive tau pathology and more extensive tau spread (Wegmann et al., 2019).

However, in most cases, this age-related vulnerability appears to be relatively non-threatening until old age, well after human reproductive peak. The threat of PART, an otherwise relatively innocuous aspect of aging, therefore may rest with it's potential to interact with pathological Aβ . This sequence–tau pathology slowly accumulating throughout lifetime and accelerating if contact occurs with Aβ pathology–represents one of the leading hypotheses of AD pathogenesis (Braak and Del Tredici, 2014; Duyckaerts et al., 2015). The next subsection will focus on the interaction between Aβ and tau, and the highly neurotoxic consequences that follow.

1.2.4 Tau and beta-amyloid in Alzheimer's disease

The previous sections went into great detail on what (little) is known about the pathogenic qualities of tau. However, no description of AD pathology is complete without a discussion of Aβ and it's putative interaction(s) with tau. Not only is Aβ necessary for a definition of AD, a leading hypothesis of AD pathogenesis posits Aβ as the initial catalyst in the AD pathological cascade (Hardy and Higgins, 1992; Hardy and Selkoe, 2002; Selkoe and Hardy, 2016; Jack et al., 2010; Jack et al., 2013). This section will discuss this so called "amyloid cascade hypothesis", and will describe in detail known and speculative interactions between Aβ and tau.

Like tau, Aβ is a highly abundant protein in the normal human brain, and shows remarkable conservation across vertebrate species (Tharp and Sarkar, 2013). While it's physiological role is not well understood, it appears to be involved in diverse functions ranging from response to brain injury, to response to microbial pathogens, to blood-brain barrier maintenance, to regulation of long-term potentiation at the synapse (reviewed in Brothers, Gosztyla, and Robinson, 2018). Aβ is generated from the amyloid-β precursor protein (APP), which undergoes a series of cleavage events by β- and γ-secretase, resulting in fragments of 38-43 amino acids (Masters and Selkoe, 2012; Selkoe and Hardy, 2016). Alzhiemer's disease is characteristic of increased levels of Aβ1-42, and in particular, increased ratio of Aβ1-42 to Aβ1-40 (Andreasen et al., 1999; Lewczuk et al., 2014). Interestingly, Aβ is produced by neurons and astrocytes (Sato et al., 2018; Hung et al., 2015) and is released at the synapse upon neuronal stimulation (Cirrito et al., 2005; Sato et al., 2018), after which it is rapidly cleared from the brain and into the CSF (Abramowski et al., 2008). In AD, soluble Aβ oligomers are aggregated into large extracellular plaques (Masters and Selkoe, 2012), which can be imaged *in vivo* using PET tracers (Klunk et al., 2004; Rabinovici and Jagust, 2009).

There is some fairly strong evidence to support the notion that Aβ is a causal, initiating agent in AD pathogenesis, and most of that evidence stems from human genetics. A number of rare autosomal-dominant missense mutations to the APP gene cause an early-onset, often aggressive form of AD with full penetrance (Bateman et al., 2011). Trisomy 21, or Down's syndrome, involves an extra copy of chromosome 21, which contains the APP gene. Affected individuals that live to middle or old age almost always get Alzheimer's disease, and this has been confirmed to be caused by triplicate expression of the APP gene (Prasher et al., 1998; Rovelet-Lecrux et al., 2006). The presenilin 1 and 2 (PSEN1,2) genes are part of the γ-secretase enzyme that cleaves APP into Aβ (De Strooper et al., 1998), and mutations in these genes also cause increased Aβ42/Aβ40 ratio (Takami et al., 2009; Chávez-Gutiérrez et al., 2012)

leading to amyloidosis and AD (Lemere et al., 1996; Bateman et al., 2011). Dementia caused by mutations to these three genes (APP, PSEN1, PSEN2) are collectively referred to as autosomal dominant AD (ADAD), and together account for less than 1% of all AD cases (Bateman et al., 2011). Importantly, these mutations are sufficient to *cause* tauopathy, while as mentioned before, MAPT mutations do not reliably cause amyloidosis.

Amyloidosis also occurs sporadically and, over time, can lead to extensive cortical tauopathy and AD. To be clear, as discussed in the previous section, nearly all elderly individuals eventually develop tau NFT pathology in the medial temporal lobes (Crary et al., 2014; Braak and Del Tredici, 2014; Braak and Del Tredici, 2015). However, while amyloidosis is frequently observed with concurrent cortical NFT pathology, NFT pathology is rarely seen in isocortex, and almost never seen in primary unimodal cortex, in the absence of amyloidosis (Braak et al., 2011). Notably, amyloid plaques are the first (measurable) pathology to develop in genetic forms of AD (Bateman et al., 2012), and precede extra-MTL tau in most cases of sporadic AD (Ossenkoppele et al., 2018). Further evidence comes from cell and animal models. Exposing human tau transgenic (but not wild-type) mice to Aβ (Götz et al., 2001), or crossing such mice with human APP transgenic mice (Lewis et al., 2001), leads to neurofibrillary tau pathology. Meanwhile, in an *in vitro* model using human neuron precursor cells that express mutated APP and PS1, the Aβ 42/40 ratio was tightly correlated with tau accumulation and aggregation (Kwak et al., 2020). This is interesting given that APP processing is upstream of Aβ plaques and pathology, and is dysregulated in most all animal models. Taken together, amyloidosis appears sufficient to cause tauopathy, or otherwise exacerbate existing tau pathology, or perhaps both.

However, there are number of research findings that are somewhat at odds with the amyloid cascade hypothesis, and which add a great deal of complexity to the pathogenesis of AD. A vast number of studies in animal models of AD have reported that removal of amyloid is sufficient to restore cognitive function and halt AD-like processing. However, well over 200 clinical trials in humans with AD, MCI and ADAD have attempted to reduce brain Aβ without achieving clear slowing of cognitive decline or gray matter atrophy (Schneider et al., 2015). [2] Proponents of the amyloid-cascade hypothesis have argued that these interventions have come too far along in the disease progression to be effective, suggesting the Aβ-initiated cascade

[2] A recent Phase III trial of the drug aducanemab failed to meet its pre-specified endpoints relating to slowing of cognitive decline. However, a "re-analysis" of the data suggested one of the two arms of the trial did in fact achieve its endpoint, and that there was a dosage issue in the other arm. At the time of writing, BioGen (the company sponsoring the trial) has made an appeal to the United States Food and Drug Administation to approve of the aducanumab based on this "reanalysis"(Schneider, 2020). Another recent trial in non-demented ADAD mutation carriers also failed to meet its endpoint, but noted a reduction in tau levels (Strobel, 2020)

had already begun. Additional arguments suggest that the drugs may eliminate inert Aβ plaques, but fail to reduce the soluble oligomeric species of Aβ that is thought to be neurotoxic (see below). These and several other counterarguments are discussed at length in Selkoe and Hardy, 2016. However, such hypotheses can only be rejected with further research and additional clinical trials, many of which are currently active or under development (e.g. Sperling et al., 2014), though general enthusiasm for the amyloid-cascade hypothesis wanes further with each failed trial. Interestingly, however, an autopsy follow-up study of deceased AD patients who had participated in Aβ-targeted intervention, found some evidence that regions where Aβ was successfully removed also showed reduced NFT pathology (Nicoll et al., 2019).

Another confound to the amyloid-cascade hypothesis is the question of amyloid toxicity. A voluminous collection of studies in animal models of AD have shown Aβ to be highly neurotoxic, particularly at the synapse (e.g. Lambert et al., 1998; Walsh et al., 2002; Shankar et al., 2008). However, roughly 1/3 of cognitively intact elderly individuals express substantial amyloidosis without obvious signs of cognitive impairment (Jansen et al., 2015). Some studies have suggested such individuals demonstrate subtle cognitive decline (Hedden et al., 2013; Donohue et al., 2017; Vogel et al., 2017), or anomalous neuroimaging signatures (Ch??telat et al., 2010; Sheline et al., 2010; Damoiseaux et al., 2012; Johnson et al., 2014; Mormino et al., 2012a), but these effects do not always reproduce (e.g. Whitwell et al., 2013), and may actually be driven by amyloid-associated tau pathology (Bennett et al., 2004; Fletcher et al., 2018; Gordon et al., 2018). One explanation for this phenomenon is that, like tau, soluble Aβ oligomers represent the toxic species, and Aβ plaques may even represent a neuroprotective sequestration of these oligomers into an inert, insoluble and otherwise innocuous form (Shankar et al., 2008; Esparza et al., 2013; Hong et al., 2014). While this prospect now seems very likely, it should be noted that plaques are often reported to be surrounded by a "halo" of toxic oligomers (Koffie et al., 2009). However, less oligomeric Aβ was visible in human tissue of Aβ-positive non-demented individuals compared to demented individuals (Esparza et al., 2013). Another possibility, which will be discussed in more detail below, is that the toxic effects of Aβ are somehow mediated by tau.

Yet another puzzling aspect of Aβ in AD, which may be related, is described in the so-called "spatial paradox" (Kant, Goldstein, and Ossenkoppele, 2020) (Fig 1.3B. Aβ plaques first emerges fairly uniformly (but see Villeneuve et al., 2015a; Palmqvist et al., 2017; Grothe et al., 2017) and diffusely in the cerebral isocortex, before eventually spreading to the limbic and allocortex, subcortex, certain brainstem nuclei, and to the cerebellum and pons only in very late stages (Thal phases,Thal et al., 2002).

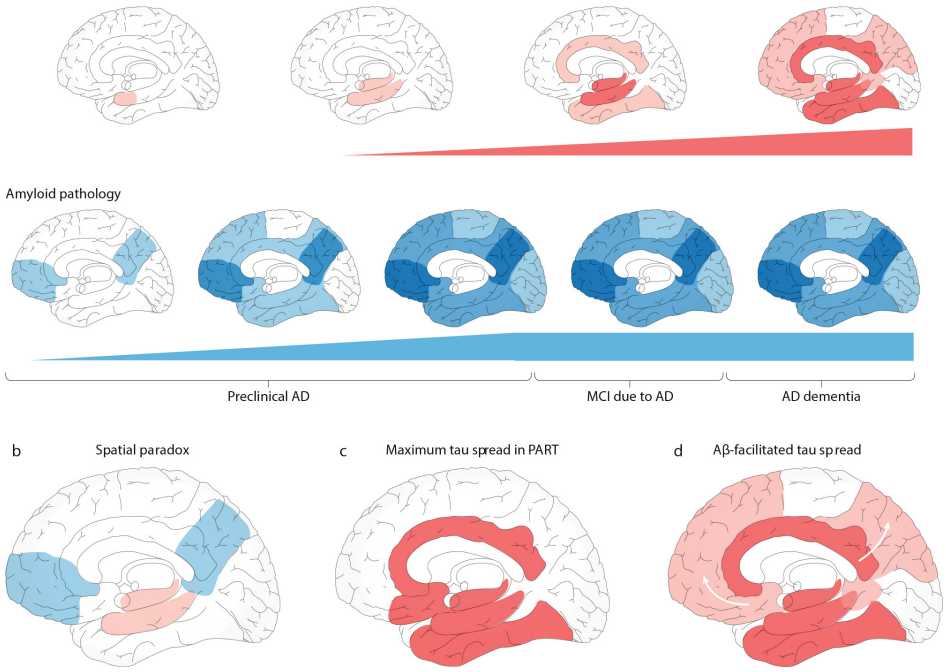

Figure 1.3: Reproduced (with permission from Springer Nature) from (Kant, Goldstein, and Ossenkoppele, 2020). A) Schematic illustrating Braak Stages I, II, IV and V (top) and the evolution of Aβ pathology (bottom), the latter of which extends into the entire isocortex early in the progression of AD. B) These two pathologies start in distinct locations. C) Tau is rarely seen past Braak stage IV unless accompanied by cortical Aβ. D) Aβ may therefore facilitate the rapid progression of tau into isocortical regions.

Meanwhile, in AD, tau NFT pathology shows almost an opposite pattern, germinating in the limbic regions (or possibly the brain stem), before spreading to allocortex and eventually to isocortex (Braak and Braak, 1991; Braak et al., 2006)(Fig 1.3A). How then, if the two pathologies start in different parts of the brain, can one cause the other?

Contemporary hypotheses of AD state that, at least in sporadic AD, Aβ and tau pathology arise independently from one another, and the AD cascade occurs only when these separate pathologies interact (Bloom, 2014; Ittner and Götz, 2011; Braak and Del Tredici, 2014). Notably, extralimbic tau tends not to be observed until Aβ reaches limbic regions at Thal stage 2 (Lockhart et al., 2017a; Kant, Goldstein, and Ossenkoppele, 2020), suggesting this synchrony may initiate due to a spatial interaction. Also of note, neither sporadic amyloidosis absent tau pathology, nor age-related limbic tau pathology absent Aβ, are frequently associated with cognitive impairment (Betthauser et al., 2020). This Aβ/tau synergistic hypothesis of AD suggests either tau somehow mediates the toxic effects of Aβ, or Aβ facilitates tau neurotoxicity, or perhaps both.

No site has been discovered on the tau protein that allows for direct binding with Aβ (Arendt, Stieler, and Holzer, 2016). *In vitro* studies have found Aβ to associate with synapses, which induces translocation of tau into the somatodendritic

compartment (Zempel and Mandelkow, 2012), and microtubule degeneration (Jin et al., 2011). However, while a number of studies have found Aβ to be toxic to synapses (Lambert et al., 1998; Walsh et al., 2002; Shankar et al., 2008), this toxicity appears to require tau. For example, Aβ toxicity is not observed in MAPT knockout mice (Rapoport et al., 2002; Roberson et al., 2007; Ittner et al., 2010; Jin et al., 2011), and is reduced in tau-deficient mice (Vossel et al., 2010; Roberson et al., 2011).

Administration of Aβ leads to tau phosphorylation via GSK3β, in a process dependent on NMDARs (Tackenberg and Brandt, 2009; Shipton et al., 2011; Tackenberg et al., 2013). Other studies have also linked Aβ to neuronal hyperexcitability via NMDARs (Shankar et al., 2008; Roberson et al., 2007). A fair amount of research has pointed to the Fyn protein, a kinase that forms part of a complex that facilitates NMDAR activity. Tau transports Fyn to the NMDAR, and tau phosphorylation not only dissociates Fyn from this complex, but also leads to AMPAR endocytosis . Mice lacking tau cannot recruit this Fyn-mediated functionality of the NMDAR, and this has been theorized to halt Aβ-related excitotoxicity. (Ittner et al., 2010; Roberson et al., 2007; Roberson et al., 2011; Regan et al., 2015). Supporting this idea, a more recent study found that tau-related neural silencing far overshadowed Aβ-related hyperexcitability (Busche et al., 2019). Other interesting work has found Aβ induces neuronal spine loss specifically in regions of the cell where tau had been translocated, also noting microtubule, mitochondrial and calcium dysregulation in these regions (Zempel et al., 2010; Zempel et al., 2013).

On the other side of things, there is some evidence that tau itself can stimulate Aβ production (Leroy et al., 2012; Bright et al., 2015), opening up the possibility that these two proteins engage in a positive feedback loop. One recent study found that reducing tau levels in a mixed APP- and tau-transgenic mouse was less effective at ameliorating AD like pathology, compared to reducing tau in mice that are only tau-transgenic (DeVos et al., 2018b).

So which is the driving pathological force of AD, Aβ or tau? [3] Given the state of the field up to this point, evidence points more to tau. A caveat to the above work is that it is mostly performed *in vitro*, or using mouse models with non-AD tau mutations, and almost always focusing on hippocampal slices only. However, while the mechanisms may still be elusive, the fact that several groups have shown Aβ neurotoxicity to be muted in the absence of tau is quite compelling. Further evidence of tau being the driving force comes from human literature. A simple explanation would be that neurodegeneration closely follows (Ossenkoppele et al., 2015a; Xia et al., 2017), and may even be preceded by (La Joie et al., 2020), tau pathology.

[3] It is of course possible that neither pathology is truly the driving force of AD. Alternative hypotheses of AD are not discussed in the thesis due to space and relevance, though vascular, glial and many other hypotheses have been proposed.

However, Aβ is usually quite widespread by the time tau exits the limbic regions, so atrophying regions actually tend to be regions that demonstrate *both* pathologies. A stronger argument comes from the fact that tau pathology by itself is sufficient to cause neurodegeneration and dementia, including scenarios such as R406W MAPT mutations that present with filamentous, mixed 3R/4R pathology nearly identical to AD tau (Smith et al., 2016). The same cannot be said for amyloidosis, which does not appear sufficient to reliably cause cognitive impairment absent of co-pathologies. [4] Even in ADAD, which is clearly initiated through dysfunctional Aβ processing, measurable neurodegeneration and cognitive impairment occur only in the presence of tau, despite years of measurable Aβ pathology observable beforehand (Bateman et al., 2012; Quiroz et al., 2018). However, it cannot be taken for granted that amyloidosis reliably causes tauopathy in ADAD. Taken together, evidence therefore suggests Aβ almost certainly drives tau pathology (i.e. hyperphosphorylation, fibrillization), and may additionally drive tau toxicity (synaptic silencing, nuclear dysregulation, etc). Tau in turn might promote Aβ toxicity as well. However, the accumulating evidence suggests AD is an "amyloid-induced tauopathy".

In addition to driving tau pathology and toxicity, there is a third way Aβ may facilitate tau in AD: by facilitating it's spread throughout the cortex. This will be one of the foci of the next major section of this thesis.

1.3 AD tau distribution, patterns of accumulation, and hypotheses to explain them

The previous section focused mostly on the function and dysfunction of tau at the molecular and cellular level. In order to appreciate one of the most salient features of tau accumulation in AD, one must integrate a more macroscopic view. Tau has a very specific spatial distribution across the brain, along with stereotyped pattern of progression. In a global sense, the focus of this thesis, and the original work therein, is tau pathology in the context of AD. However, more specifically, the focus is on investigating the spatial distribution of tau. This section will describe the spatial features of tau accumulation, and will discuss theories relating to regional specificity and mechanisms of pathological spread.

[4] An exception would be cerebral amyloid angiopathy, an age-related disease where amyloid builds up around and within the brain's microvascular system. CAA can lead to cognitive impairment through cerebral hemorrhage and other neurovascular damage.(Vinters, 1987; Vonsattel et al., 1991; Knudsen et al., 2001)

1.3.1 The spatial distribution of tau

Unlike Aβ, which in early stages appears diffusely throughout the cerebral cortex (Thal et al., 2002), tau NFT pathology in AD first appears quite focally in the transentorhinal cortex (Braak and Braak, 1991; Braak et al., 2006). In an unselected autopsy case series of over 1000 individuals, agnostic to antemortem clinical status, Braak and Braak described (Braak and Braak, 1991) and eventually formalized (Braak et al., 2006) a progressive pattern of tau accumulation (Fig 1.4). The appearance of NFT pathology in the transentorhinal cortex is Braak Stage I. In Stage II, the superficial pre-α layer (or layer 2) of the entorhinal cortex expresses considerable NFT pathology. Early pathology is also visible in the deep pri-α layer of the entorhinal cortex during Stage II, as well as in the anterior portion of the CA1 and (to a lesser extent) CA2 sections of the hippocampus. Stage III involves advancement of pathology in Stage I and II regions, with encroachment into the parahippocampal, lingual, fusiform and inferior temporal gyri. In Stage IV, the CA3 and 4 regions of the hippocampus become involved, along with deeper layers of the middle temporal neocortex, insula, ventral neocortical regions, and occasionally in peristriate occipital cortex. Stage V is characterized by pathology extending widely into most regions of association cortex, sparing primary somatomotor, visual and auditory cortex. Finally, in Stage VI, extensive pathology is seen throughout the cortex, including primary sensory regions (Braak et al., 2006).

There are further details that are less well described, yet potentially relevant. Braak's 2006 staging formulation (Braak et al., 2006) is conspicuously sparse in its description of associative neocortical (particularly frontal lobe) or subcortical structures. This is most likely due to sufficient information for diagnostic staging present in the temporal lobes. However, Braak's initial work (Braak and Braak, 1991) described the amgydala, basal forebrain and, in particular, anterolateral nucleus of the thalamus, becoming involved early and showing considerable pathology in late stages. The striatum, nucleus reuniens of the thalamus and tuberomamillary nucleus of the hypothalamus become involved later, while the claustrum, reticular thalamic nucleus, lateral tuberal hypothalamic nucleus and substantia nigra are spared of NFT pathology until late disease stages (Braak and Braak, 1991). The earlier description also implicated rather early involvement of the medial orbital frontal lobe, anterior cingulate and retrosplenial cortex, and at later stages, more dorsal and lateral frontoparietal regions becoming more involved. (Braak and Braak, 1991) The cerebellum is spared of NFT pathology (Braak and Braak, 1991; Wegiel et al., 2010). Specific laminar distributions have also been described. The progression of pathology from superficial to deep layers of the entorhinal cortex, and from CA1/2

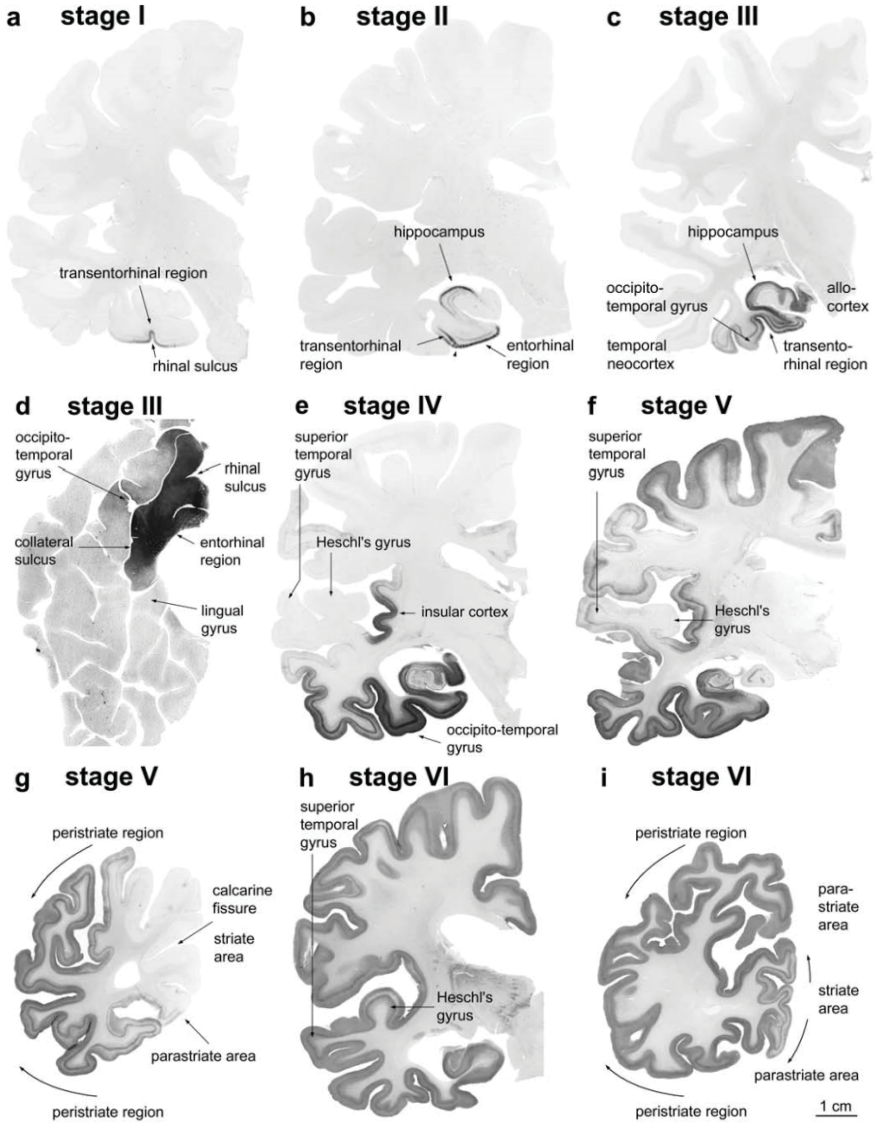

Figure 1.4: The Braak pathological staging scheme using silver-iodide staining of NFT pathology, reproduced from (Braak et al., 2006).

to CA3/4 to the dentate gyrus in the hippocampus, is described in great detail (Braak and Braak, 1991; Braak et al., 2006; Hyman et al., 1984). Meanwhile, layers III and V of the neocortex seem to be preferentially affected early on (Braak and Braak, 1991).

While initial Braak staging was performed with silver staining, addition of AT8 immunolabeling allowed for further labeling of pre-tangle tau pathology, and extension of the Braak staging. Specifically, AT8 immuno-stained tau precedes NFTs in the transentorhinal cortex (Braak Stage 1a and 1b), as well as throughout the rest of the cortex (Braak and Del Tredici, 2015). This technique also allowed a specific staging of early life subcortical phospho-tau activity described as Braak stages a-c (Braak and Del Tredici, 2015). However, these earlier stages are not widely considered to be part of the AD pathologic process and, as described earlier (Section 1.2.3), considerable debate exists as to whether these changes are related in any way to AD or

PART. Finally, a technique has been introduced more recently to label tau "seeds" or phosphorylated oligomers, and this seeding activity has been shown to progress in a Braak-like manner and to precede tangle pathology (Holmes et al., 2014; Furman et al., 2017; Kaufman et al., 2018; DeVos et al., 2018b).

The specificity of tau accumulation may provide clues aiding the pursuit of understanding tau pathology. What is it about that specific sliver of transentorhinal cortex that makes it singularly vulnerable to NFT pathology? Why does tau pathology subsequently advance in such a specific pattern across subjects, targeting certain regions very early while sparing others until much later? There are many unanswered questions pertaining to this topic, but answering them may reveal fundamental insights not only into the genesis of tau pathology, but perhaps also into neurobiology at large. The last decade, in particular, has featured ample exciting research investigating how tau spreads through the brain, what makes certain tissue more vulnerable to its pathological aggregation, and how consistent tau accumulation is across the general population. The remainder of this section will review this literature in order to provide a neurobiological background to the original work in this thesis.

1.3.2 Propagation of tau through the brain

The mechanism by which pathology spreads from one cell or brain region to the next has not been fully elucidated. Theories abound, and include concepts of prion-like propagation of pathology from cell to cell, extracellular or glial spread, spontaneous failure of vulnerable regions, and cascading propagation of pathological states. A scan of Figure 1.4 might suggest tau diffuses non-specifically along the cortical ribbon, moving basally from the MTL to the inferior temporal lobe, then laterally and dorsally along the temporal lobes. Such an observation might suggest tau pathology simply spreads from one neuron to adjacent neurons. However, early observations of tau accumulation quickly noted that i) cells showing minimal pathology could be situated adjacent to those with severe pathology even in late disease stages, and ii) neurons expressing tau pathology shared anatomical, axonal (i.e. synaptic) connections (Braak and Del Tredici, 2015).

Early on, studies noted that the affected regions of the entorhinal cortex projected to the hippocampus, and vulnerable MTL regions themselves projected to cortical and subcortical sites affected in later disease stages (Hyman et al., 1984; Braak and Braak, 1991; Pearson, 1996). These observations are supported by seminal human imaging work showing that sets of vulnerable regions across different dementias resemble macroscale networks of functional connectivity in healthy individuals (Seeley et al., 2009; Lehmann et al., 2013b). Indeed, models allowing neurodegenerative

signal to propagate from a disease epicenter across macroscale human brain connections can recapitulate patterns of neurodegeneration fairly well (Zhou et al., 2012; Raj, Kuceyeski, and Weiner, 2012; Zheng et al., 2019). However, there is clearly some selectivity, as not all regions sharing anatomical connections with tau-positive tissue show NFT pathology themselves in close proximity. Even within the MTL, the propagation of pathology does not perfectly mirror the very well-characterized connectome (Mrdjen et al., 2019). These observations also provide little information about mechanism of spread, nor do they help to differentiate the different hypotheses enumerated to begin this paragraph. However, these observations formed the groundwork for hypotheses of cell-to-cell prion-like propagation of tau, leading to a number of important experiments.

A seminal study showed that taking tau fibrils from a mutated human tau transgenic mouse and injecting it into the brain of a wild-type human tau transgenic mouse induces aggregation and spread of tau pathology (Clavaguera et al., 2009). The same lab found similar results when injecting tau extracted from the brains of patients with various tauopathies, which resulted in expression of disease-specific tau patterns (Clavaguera et al., 2013). These findings have been replicated numerous times by numerous labs, using different types and sources of fibrils (including synthetic varieties) and various flavors of transgenic mice (De Calignon et al., 2012; Liu et al., 2012; Iba et al., 2013; Sanders et al., 2014; Dujardin et al., 2014; Ahmed et al., 2014b; Takeda et al., 2015; Boluda et al., 2015; Guo et al., 2016b; Narasimhan et al., 2017; Dujardin et al., 2018). In many studies, different strains lead to different expression of pathology (Clavaguera et al., 2013; Sanders et al., 2014; Guo et al., 2016a; Dujardin et al., 2018), though one study suggested region of injection (and its connections) were more important for dictating pattern of spread (Narasimhan et al., 2017). Certain studies involved expression of tau specifically in the entorhinal cortex, which lead to an AD-like pattern of regional progression (De Calignon et al., 2012; Liu et al., 2012). There is also evidence that Aβ faciliates the spreading process in these *in vivo* models. Studies have shown the presence of Aβ plaques accelerates propagation, fibrillarization and seeding of tau, along with amplifying tau-induced neuronal loss (Pooler et al., 2015; He et al., 2018). A recent study suggested that Aβ causes neuronal excitability, which in turn facilitates tau production (Rodriguez et al., 2019; more on this below).

Together, these various studies demonstrate two crucial concepts. The first is that tau injected into a single site could propagate to additional sites that were both distal and synaptically connected. Second, many of these studies demonstrate that a pathological tau "seed" can induce a conformational change in native tau species leading to pathologic behavior and subsequent epidemic-like spread. An important prototype

of this concept was demonstrate *in vitro*, showing phosphorylated oligomeric tau was taken up by neurons leading to intracellular tau phosphorylation and subsequent intercellular spread (Frost, Jacks, and Diamond, 2009). The aforementioned studies demonstrated this concept could be applied *in vivo*. Interestingly, even an infusion of exogenous tissue containing NFT pathology could induce the spread of pathology into the native tissue (Ahmed et al., 2014b). These studies lead to the theory that tau spreads through templated misfolding much like a prion. In other words, rather than hyperphosphorylated tau inducing a cascade of events that result in downstream tau phosphorylation, the theory proposes that aberrant tau molecules can directly induce conformational change in other tau molecules.

While the above studies demonstrate rather convincingly that pathological tau states can be induced and spread via synaptic connections, it is important to demonstrate mechanisms of transportation, release and uptake (Fig 1.5). Tau exists in both pre- and post-synaptic sites (Tai et al., 2012), and both anterograde and retrograde axonal transport of tau have been demonstrated (Wu et al., 2013). One interesting study suggested a tau trimer was the largest possible molecule that could be transported in such a manner (Mirbaha et al., 2015). However, the same group showed that even monomers can achieve and induce aberrant conformational states (Mirbaha et al., 2018).

As to how pathological tau can be transported to the post-synapse, a number of studies have shown tau can be released through exosomes, and that exosomal tau is detectable in human CSF (Saman et al., 2012). However, one study showed a tau antibody, which should not have been able to affect exosomal tau, was sufficient to suppress tau spreading (Kfoury et al., 2012). Other studies have shown tau can be secreted "unconventionally", or directly through the cell membrane (Chai, Dage, and Citron, 2012; Katsinelos et al., 2018). Several of the aforementioned studies have also demonstrated the ability of cells to take up exosomal or free tau from media, and at the soma or axon as well as the synapse (Wu et al., 2013). A very recent and elegant study showed the low density lipoprotein receptor-related protein 1 (LRP1) receptor is crucial for the uptake of tau into cells, and that knocking out this receptor blocks tau uptake *in vitro* and halts *in vivo* tau spreading in the rodent brain (Rauch et al., 2020).

Several *in vitro* and *in vivo* studies have now shown that stimulated neurons will release tau into the synapse, and that activation can accelerate spread (Yamada et al., 2014; Wu et al., 2016; Wang et al., 2017; Schultz et al., 2017). These studies are interesting considering findings that Aβ at the synapse leads to neuronal excitability (Roberson et al., 2007; Shankar et al., 2008; Ittner et al., 2010; Busche et al., 2019). Other mechanisms of synaptic exchange of tau have been proposed as well. Microglia,

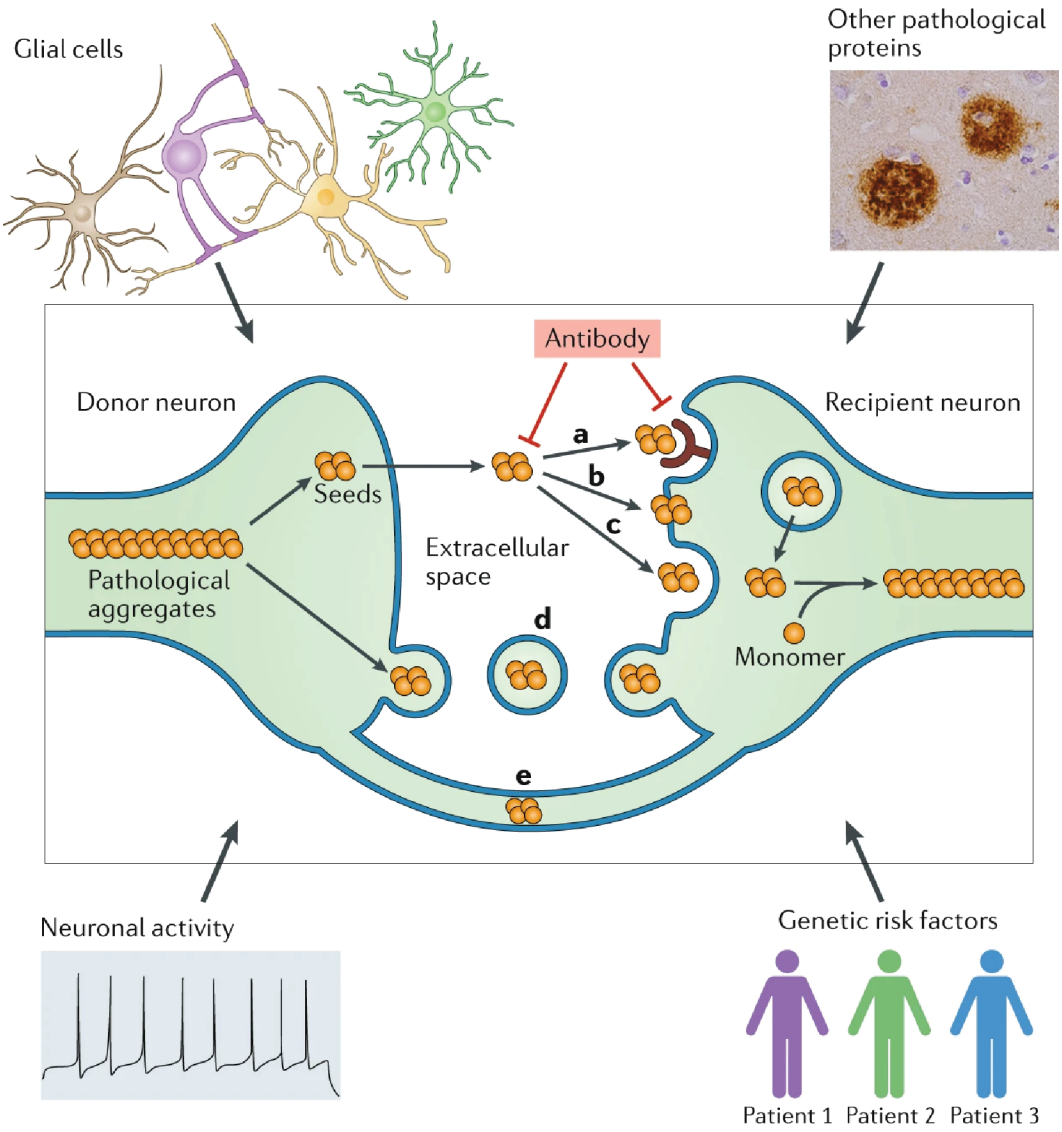

Figure 1.5: Reproduced (with permission from Springer Nature) from (Peng, Trojanowski, and Lee, 2020). In a process possibly initiated through neuronal stimulation or glial cell interaction, pathological seeds (tau molecules or oligomers) from presynaptic NFT pathology are excreted unconventionally into the synapse. These molecules can enter the postsynaptic site through direct penetration or different forms of endocytosis (a-c). Tau can also cross the synaptic cleft via exosomal transportation (d) or tunneling nanotubes (e). Once inside the postsynaptic site, the oligomers can phosphorylate other tau molecules, influencing their conformation and leading to NFT aggregation. This process can be moderated by other co-pathologies and indiviual genetic factors.

but not astroctytes, can take up exosomal tau from medium (Wang et al., 2017), and depleting microglia greatly attenuates tau spreading (Asai et al., 2015). Interestingly, one recent study showed that glia eventually undergo a natural "cellular senescence" that exacerbates the phosphorylation and spread of tau, and that clearance of such cells hinders the spread of tau pathology in MAPT mutant mice (Bussian et al., 2018). In addition, tau appears to be involved in the structure of tunneling nanotubes, and exogenous pathological tau may increase the incidence of these structures at the synapse, providing yet another potential mechanism of synaptic spread (Tardivel

et al., 2016).

This seed-based templated misfolding theory has a great deal of momentum due to strong experimental evidence in animals. The above studies provide enough evidence to prove that tau seeds can be transmitted synaptically. Animal and *in vitro* models have shown multiple mechanisms by which tau can be transported down axons, excreted extracellularly and taken up by other cells. To put all of this together might suggest the following descriptions of cellular propagation of tau: Hyperphosphorylated and aberrantly conformed low molecular weight (e.g. monomeric) tau undergoes antero- or retrograde transport down an axon, where at arrival to the synapse, it can phosphorylate presynaptic tau, which can be exosomally or unconventially released into the synapse through depolarization, where it can be taken up at the postsynaptic sites, leading to further tau phosphorylation, causing a cascade within the postsynaptic neuron. This process is further facilitated by Aβ-induced neuronal excitability and tau seeding, and perhaps by microglial spread. Many things are still unclear, such as the mechanism by which tau exerts conformational change, how (or if) phosphorylated tau reaches and interacts with axonal tau, or why it is then translocated to the somatodendritic compartment.

Whether this process explains the spread of tau in human AD is difficult to prove. If, as the prion hypothesis states, templated tau seeds were sufficient to cause tauopathy, one would surmise tau could be transmitted from human to human similarly to what occurs in iatrogenic Creutzfeldt-Jakob disease. Cadaver-derived human growth hormone has been shown to contain tau, and three of 24 cases of individuals that died of iatrogenic Creutzfeldt-Jakob disease also showed tau accumulation (Duyckaerts et al., 2018). However, given the somewhat low occurrence of tau pathology in this group, and the fact that prion protein itself can interact with tau (Gomes et al., 2019), it is far from conclusive that the tau observed in these cases was iatrogenic in nature. Seeding-competent phosphorylated tau has however been observed in axons of deceased human brains, and appears to precede mature NFT pathology in manner predicted by Braak staging (Holmes et al., 2014; DeVos et al., 2018a). This suggests the presence of hyperphosphorylated tau precedes and predicts the presence of NFTs at later stages. Perhaps the best human evidence of synaptic spread of tau comes from a single case study, in which an individual had a small part of the frontal lobe almost completely disconnected from the rest of the brain during surgery, and died of AD nearly 30 years later. Despite widespread AD pathology in the brain, and considerable Aβ pathology in the disconnected region, the disconnected region nonetheless lacked tau NFT pathology (Duyckaerts et al., 1997). This study provides evidence that tau pathology, but not Aβ, spreads through axonal connections in humans.

Together, these studies suggest synaptic connections are likely necessary (but not

sufficient, see below) for induction of tau into a new region, and that tau itself may be sufficient as an agent of spread. It is still possible that, in humans, other factors that can be synaptically transmitted, and can also influence tau phosphorylation, could be responsible for the spread of tau pathology. For example, tau-related cellular dysfunction might lead to a cellular response that involves transportation or excretion of factors upstream of tau phosphorylation or toxicity, which are transmitted to synaptic partners.

A major unanswered question relating to the prion-like spread hypothesis is why some regions or cells resist tau pathology till later disease stages, despite sharing synaptic connections with infected cells. If tau truly started in the LC, which has afferent connections to nearly the entire isocortex and numerous subcortical locations, why does the entorhinal cortex selectively demonstrate tau pathology in PART and AD? If tau itself can induce tau pathology, why doesn't it do so in all cells? Is it a matter of resistance to conformational change, resistance to aggregation, successful cellular response to aberrant tau, or something else entirely? The next subsection will address cellular and regional resistance and vulnerability to tau pathology.

1.3.3 Regional vulnerability and resistance

Patterns of synaptic connectivity alone cannot perfectly describe the proliferation of tau pathology throughout the brain, indicating that certain regions or cell types may be resistant to tau pathology. Meanwhile, other regions and cells experience very early and rapid tau pathology, indicating a selective vulnerability. Closer inspection of, and quantitative comparisons between, these contrasting cells and regions may reveal clues about tau pathogenesis, as well as potential treatments to ameliorate the spread and toxicity of tau. This subsection will interrogate the regional, cellular and molecular qualities that are associated with resistance and vulnerability to tau pathology in AD.

Many aspects of gross regional vulnerability and resistance have been known for some time based on autopsy studies. The Braak staging framework outlines selective vulnerability of specific entorhinal cell sub-populations and medial temporal lobe structures, and the relative resistance of brain sensory macrostructures (Braak and Braak, 1991). The cerebellum, meanwhile, does not express any tau pathology, though it does express Aβ deposition and atrophy in later disease stages (Wegiel et al., 1999). In general, many hindbrain structures such as the medulla and pons also appear to be mostly resistant to NFTs, and AD pathology does not appear to affect the spine or depart the central nervous system (Braak and Braak, 1991).

Observing this pattern, some have noted an inverse relationship with phylogenetic conservation, where more conserved brain structures are more resistant to AD,

whereas structures that developed more recently are more vulnerable (Rapoport, 1989; Rapoport, 1990; Rapoport and Nelson, 2011). In particular, it was noted that AD vulnerable regions feature long axonal connections, a trait that accelerated during primate and, particularly, hominid evolution (Rapoport, 1990). Along similar lines, it was proposed that the pattern of cortical myelination during human brain development recapitulates the sequence of tau spread, but in reverse order (Braak and Braak, 1996), such that late myelenating structures are vulnerable to early tau pathology. Braak & Del Tredici also noted that the transentorhinal cortex, the first site of NFT tau pathology, is unique to primates and is not present in other mammals (Braak and Del Tredici, 2015). These are all rather compelling points, given that full-on plaque and tangle AD pathology is not seen in other animals (Youssef et al., 2016). The impact of delayed myelination on tau pathology may be worth exploring further.

Autopsy reports also have gone into detail about specific cell populations that appear to be involved early in AD, or which appear to be resistant to tau pathology. Most well characterized are large pyramidal neurons in the hippocampus (CA1 and subiculum specifically), layers III and V of the isocortex (Braak and Braak, 1991), and layer II of the entorhinal cortex (Hyman et al., 1984). Noradrenergic neurons in the LC have also been implicated (Bondareff, Mountjoy, and Roth, 1982), along with cholinergic basal forebrain neurons (Whitehouse et al., 1982; Mesulam et al., 2004), while cerebellar Purkinje cells appear to be immune to NFT pathology (Braak and Braak, 1991; Wegiel et al., 1999). There is also an interesting trend in AD where excitatory (particularly glutamatergic, see Mishizen-Eberz et al., 2004; Lee et al., 2004) neurons tend to be more vulnerable than inhibitory interneurons (Fu et al., 2019). More specifically, excitatory neurons expressing reelin and neurofilament appear to be at increased risk of NFT pathology, whereas inhibitory neurons expressing calcium-binding proteins (e.g. calretinin, somatostatin, parvalbumin) show more resistance (Morrison, Hof, and Morrison, 1998; Fu et al., 2019; Mrdjen et al., 2019). This latter feature might explain why the hippocampal CA2 region, which features a higher densisty of interneurons enriched for calcium binding, is more resistant to NFT pathology compared to CA1 (Mrdjen et al., 2019). An important distinction must be made here: both CA2 interneurons (Solodkin, Veldhuizen, and Van Hoesen, 1996; Wegiel et al., 1999) and Purkinje cells are lost in AD, however this cell loss is likely indirect and almost certainly not due to NFT pathology. Many of these trends match earlier reviewed pathologic processes of tau. For example, calcium regulation appears to be a (perhaps upstream) factor in synaptic tau pathology, and particularly in NDMAR-bearing glutamatergic receptors vulnerable to AD and tau pathology (discussed in Section 1.2.2).

Several more recent studies have investigated systematic molecular qualities of

brain regions that are vulnerable or resistant to AD pathology. One study sampled several brain regions along the AD vulnerability spectrum from healthy rats, and measured relative levels of tau and tau-related genes. The study replicated the finding of absent phosphorylated tau in the rat cerebellum, and also found the cerebellum to feature less tau in general, but increased expression of other microtubule proteins less common in other brain regions. The study did not find any proteins that were expressed in a gradient mirroring Braak stages or AD vulnerability patterns, but did find regions typically resistant to AD had increased 3R/4R tau ratios, and lower expression of tau-modifying enzymes CamK2, cdk5 and PP1 (Hu et al., 2017). A different study using human control and AD tissue found a fairly consistent set of brain changes occurring in a staggered fashion in regions along the Braak stage spectrum, except for the cerebellum, which expressed a completely different pattern of molecular changes (Xu et al., 2019). Together, these studies suggest cerebellar AD resistance might be due to a substantially different molecular environment to AD-affected cortex, and that its resistance to AD may occur by mechanisms distinct to resistant cortical regions. Along the same lines, induced pluropotent stem cells from APP-mutation carrying patients directed to a caudal neuronal fate (as are hindbrain and spinal neurons) have been found to be more resistant to tau pathology compared to those directed to a rostral neuronal fate (as are forebrain neurons) (Muratore et al., 2017).

Similar studies have recently been published examining qualities of AD vulnerable regions using tissue from humans who did not die from neurological causes. One study found that tau- and Aβ-related genes, as well as genes promoting their aggregation, were expressed in higher concentration in early Braak regions compared to late Braak regions, while genes protecting against aggregation were present in lower concentrations in early Braak regions (Freer et al., 2016). Similarly, two different studies in cognitively normal human tissue found tau-associated proteins more highly expressed in regions showing tau-deposition or neurodegeneration in AD (Grothe et al., 2018; Sepulcre et al., 2018).

The advent of single-cell proteomics has resulted in some very interesting studies investigating differences between cell-types specifically vulnerable or resistant to AD. One recent study replicated the finding of excitatory neurons being far more vulnerable to inhibitory neurons in mice, and proceeded to use healthy human single-cell data to compare these two types of neurons. The study found that, compared to healthy inhibitory neurons, healthy excitatory neurons expressed more proteins that promote the aggregation and co-aggregation of tau, and less proteins that protect against tau aggregation. Examining these "protector" proteins, the study isolated

BAG3 as a hub in the aggregation protector network. BAG3 was found to be upregulated in inhibitory neurons and tau-resistant glia, and knocking out this gene *in vitro* lead to tau accumulation in normally resistant cells (Fu et al., 2019).

In another very recent and fascinating study, authors examined various cell subtypes in regions affected early, later and very late in AD. The authors found a specific pair of excitatory neuron subtypes expressed in EC layer II that were especially vulnerable to AD, and which also expressed neuronal differentiation protein RORB. Perhaps most interestingly, they found that the specific vulnerable subpopulations of neurons in more advanced Braak regions were more similar to the vulnerable EC neurons than other neurons, and also expressed RORB (though other RORB-expressing neurons were less vulnerable) (Leng et al., 2020). This intriguing finding suggests that AD pathology may be propagating from region to region primarily in a specific set of regionally homologous neuronal types. Future studies could isolate these neuronal subtypes, along with resistant subtypes, in order to further probe qualities relevant to tau accumulation *in vitro*.

A number of other high-impact, human protemomic studies have recently been published, detailing molecular networks associated with AD vulnerability, often within specific cell subtypes (Mostafavi et al., 2018; Mathys et al., 2019; Grubman et al., 2019; Bai et al., 2020). For example, Mathys et al., 2019 found a number of cell-type specific molecular changes early in the disease process, associated with inflammation, neuronal survival and, in particular, myelination.

There are several convergent themes across these and other studies (Mrdjen et al., 2019; Fu, Hardy, and Duff, 2018), which may themselves be interrelated. For example, many AD-resistant interneurons, for example, feature heavily myelinated axons projecting over short distance, and abundantly express calcium-binding proteins. AD-vulnerable excitatory neurons, on the other hand, often feature long, poorly myelinated axons, and express more proteins associated with synaptic plasticity (like neurofilament) and protein aggregation. Some of these latter features may be better suited to facilitating the specific functions of vulnerable neurons, such as long-range projection and involvement in learning and memory processes, potentially at the expense of longevity. This would be an example of antagonistic pleiotropy (Austad and Hoffman, 2018), and is an interesting complement to the theory that these vulnerable neurons are also phylogenetically less-conserved across mammals.

It is not yet known whether, for example, inducing altered calcium homeostasis in AD-vulnerable neurons would stave off tau pathology, nor whether it would negatively impact wild-type neuronal function. It also remains unclear exactly how these different features might interrelate, or how they facilitate cell-specific functions. The existence of aggregation promoters in AD vulnerable neurons (Freer et al., 2016;

Fu et al., 2019) is a particularly enigmatic observation. These proteins appear to represent an enormous liability to the brain at large, as they are associated not only with aging and AD (Ciryam et al., 2016), but with neurodegenerative diseases at large (Ciryam et al., 2015). Therefore, it is unclear why certain neuronal subtypes might express both supersaturated proteins and aggregation promoters, though a recent study proposed amyloids as a possible substrate for memory (Hervas et al., 2020), perhaps providing a link. However, the last few years have seen enormous advances in understanding selective regional and cellular vulnerability to AD, and this line of research represents a promising avenue for development of tau-based therapies.

Two other more obvious features relating to regional vulnerability to NFT pathology, which have already been discussed but should be mentioned again here, are presence of Aβ and connectivity to tangle-bearing cells. NFT pathology is mostly restricted to the temporal lobes in PART, but in the presence of Aβ, rapidly spreads to isocortical regions. Incidentally, these regions that become inundated with tau in Braak stage V are the very regions that first express Aβ. Therefore, regions prone to Aβ deposition are at increased secondary risk of expressing NFT pathology (though this is not categorically true, since the cerebellum expresses Aβ at late stages, but not tau pathology, Wegiel et al., 1999). A discussion of selective vulnerability to Aβ is beyond the scope of this review, though different groups have pointed out Aβ-vulnerable regions tend to be those under heavy metabolic demands (Buckner et al., 2005; Vlassenko et al., 2010; Arnemann et al., 2018). Further single-cell protemomics work should help ascertain whether or not neuronal subtypes associated with tau are also associated with Aβ.

As indicated earlier, tau can be transmitted from cell to cell through synaptic connections, and so direct connection to NFT-bearing or AD vulnerable cells also puts a cell at risk for developing pathology. Efforts to consolidate regional vulnerability to tau pathology would be quite useful, as it is possible that the combination of synaptic connectivity and regional vulnerability would be sufficient to describe the spatiotemporal evolution of tau pathology in AD – at least on average. Indeed, systematic deviations from the traditional Braak staging of tau pathology are not uncommon. Further investigating such deviations may provide further information about both drivers of synaptic spreading, as well as drivers of regional vulnerability. This will be the focus of the next subsection.

1.3.4 Heterogeneity of tau spreading

Throughout this section, the patterned progression of tau accumulation has been presented as a stereotyped phenomenon that can be described consistently with a

single regime (i.e. Braak staging). In reality, violations of the Braak staging sequence are not uncommon. Some individuals express regional pathology out of sequence, or in far greater regional severity than the Braak staging would anticipate, and these variations seem to occur in a systematic way. This subsection will describe these systematic variations in tau accumulation, and what little is known about them. However, this subsection will differ from the previous section in two ways. First, the research characterizing variations in tau pathology comes almost exclusively from human autopsy and imaging. Second, compared to the other topics covered above, research into variation in tau pathology is fairly sparse and still in its early stages.

Heterogeneity in AD clinical and neurodegenerative presentation has been noted for quite some time (Ritchie and Touchon, 1992). The most extreme cases are represented by the "clinical variants" of AD which, along with non-amnestic cognitive profiles, present with atypical neurodegenerative patterns (Warren, Fletcher, and Golden, 2012). Posterior cortical atrophy (PCA), or the "visual variant" of AD, presents with marked atrophy in occipital, parietal and posterior temporal portions of the cortex, and perhaps with a right-sided lateralization (Crutch et al., 2012). Meanwhile, the logopenic variant of primary progressive aphasia (lvPPA), or "language variant" or AD, features severe lateral temporal atrophy, and a general strong left-sided asymmetry (Mesulam et al., 2008). The behavioral variant of AD (sometimes called frontal variant AD or dysexecutive variant), may or may not feature increased frontal atrophy (Ossenkoppele et al., 2015b). Finally, corticobasal syndrome, which involves deficits in motor function, sometimes presents with AD as the primary underlying pathology and therefore represents yet another atypical clinical variant of AD. In such cases, degeneration and pathology are more frequent in peri-rolandic regions than they are in typical AD (Hassan, Whitwell, and Josephs, 2011; Lam et al., 2017; Sakae et al., 2019).

Recent histological and PET-imaging work has confirmed that, along with distinct atrophy patterns, these clinical variants exhibit matching atypical patterns of NFT pathology (Ossenkoppele et al., 2016a; Petersen et al., 2019). Particularly in the case of PCA and lvPPA, the clinical variants present with marked neurodegeneration in specific regions that defy the Braak staging sequence. The spatiotemporal progression of tau accumulation in these subtypes is unclear; it remains unknown whether pathology begins in AD-typical areas and moves disproportionately to vulnerable regions, or whether pathology spontaneously generates outside of the MTL in such cases (Chan et al., 2015; Ossenkoppele et al., 2015b; Day et al., 2017). In addition, the AD clinical variants all have a much earlier age of onset compared to the more typical amnestic variant of AD (Mendez, 2019), which will be discussed in greater detail below.

Observation of large clinicopathological cohorts has revealed some variation in tau accumulation in typical AD as well. Based on growing recognition of such variability, a seminal study used a semi-quantitative algorithm to define two subtypes of tau accumulation from histological tau staining data. The study defined a limbic-predominant subtype that featured substantial NFT pathology, but restricted mostly to the temporal lobes, and particularly to the medial temporal region. The study also described a hippocampal-sparing subtype (sometimes known has cortical-predominant subtype), which featured marked cortical NFT burden, but relatively sparse pathology in the hippocampus in particular. Individuals demonstrating similar atrophy in both regions were declared as "typical AD" (Murray et al., 2011b). These subtypes have been reproduced by a number of other groups, and the Murray et al. algorithm has been used as the basis of several autopsy and imaging studies exploring characteristics of these subtypes (reviewed in Ferreira, Nordberg, and Westman, 2020).

There have also been a number of MRI imaging studies that have used unsupervised algorithms to uncover natural variations of neurodegenerative patterns among large samples of individuals with MCI or AD (Noh et al., 2014; Dong et al., 2017; Young et al., 2018; Tam et al., 2019; see Habes et al., 2020 for review). While tau pathology and neurodegeneration are spatially associated (Xia et al., 2017), they measure different phenomena and are staggered in time (La Joie et al., 2020). However, unsupervised MRI-based AD subtyping studies mostly converge in describing limbic-predominant and cortical-predominant phenotypes that match those in the pathology literature, and/or posterior or temporal subtypes matching the clinical variants (Badhwar et al., 2019; Habes et al., 2020) . Occasionally, these studies would describe "diffuse atrophy" or "low atrophy" subtypes, but these are hard to interpret without pathological validation. In general, limbic-predominant phenotypes are more likely to present with an amnestic phenotype and a slower disease progression. In contrast, cortical-predominant phenotpyes are more likely to express a non-amnestic clinical phenotype and a faster progression (Murray et al., 2011b; Whitwell et al., 2012; Byun et al., 2015; Risacher et al., 2017; Ferreira, Nordberg, and Westman, 2020).

Little is known about why systematic variation in tau accumulation occurs. However, some salient associations have emerged in association with variation in tau pathology, and perhaps the most well-established is age of symptom onset. Earlier onset AD (EOAD) is generally (and somewhat arbitrarily) characterized as an onset of dementia before age 65. EOAD is associated with atypical clinical presentations, which include the clinical variants described above, but also may involve dysexecutive, non-amnestic or abnormal psychiatric presentation. In addition, EOAD is

generally associated with a more aggressive AD phenotype with a shorter disease duration, faster clinical decline and more extensive pathology (Mendez, 2019). Several studies have associated the hippocampal-sparing (or cortical predominant) subtype of tau pathology with a significantly younger age of onset (Murray et al., 2011b; Ferreira, Nordberg, and Westman, 2020). The observation of EOAD cases frequently defying the expected pathological progression, as well as often presenting with an aggressive and cortical-predominant phenotype, has lead to speculation whether EOAD may be in some way pathologically distinct from typical AD (Tellechea et al., 2018). However, there has thus far been little evidence to distinguish the pathology of EOAD from more late-onset varieties (though see some more recent work discussed below). On the other end of the spectrum, the limbic-predominant subtype of AD has been associated with older age of onset and slower disease progression (Murray et al., 2011b; Ferreira, Nordberg, and Westman, 2020).

In all, age appears to be one of the strongest and most consistent factors in discriminating the various presentations of AD pathology. Further research is needed to determine whether age is directly related to expression of the pathology, or simply a proxy for how aggressive the pathological process is. In other words, are the distinct presentations of early- and late-onset AD due to the same pathology expressing at different biological periods (ages), or are they a result of distinct pathological process producing similar pathology at different ages. For example, it is possible that younger individuals have a healthier brain that is more efficient at accumulating or spreading pathology. Another hypothesis is that processes that differ consistently between middle and old age (for example sex hormone levels) could contribute to the aggressiveness or spatial deposition of NFT pathology. However, evidence against these hypotheses comes from rodent studies showing tau pathology spreads faster in old mice compared to young mice (Wegmann et al., 2019; Ghosh et al., 2019). More likely hypotheses suggest that, either some intrinsic property of the pathology dictates its presentation, or individual deficiencies in protection against aggregative proteins are responsible for an increased vulnerability to pathology. How age relates to the relative vulnerability of certain regions to tau pathology is still quite unclear.

There is also ample evidence to suggest genetic variation can contribute to spatial variation in the expression of tau pathology. The carriage of the E4 allele of the APOE gene engenders a two-four fold increased risk of getting AD (Liu 2013), but it also appears to have some influence on tau patterning. Individuals with a limbic-predominant tau pattern are more likely to carry an APOE4 allele, whereas individuals with a cortical predominant pattern are less likely (Tellechea et al., 2018; Mattsson et al., 2018b; Ferreira, Nordberg, and Westman, 2020). There is therefore an interesting collinearity between ApoE and age, where limbic-predominant

phenotypes are more likely to be older ApoE4 carriers, while cortical-predominant phenotypes are often younger non-carriers. This may appear at odds with the well documented observation that APOE4 allele carriage is associated with an earlier age of AD onset (Blacker et al., 1997; Sando et al., 2008). However, EOAD is relatively uncommon in the population (Mendez, 2019), and younger onset of E4 non-carriers in this groups is overwhelmed by APOE causing earlier age of onset in the much more common late-onset varieties of AD (Flier et al., 2011). With APOE implicated in the pathogenesis of AD, there may be an important link between APOE and the expression of limbic pathology, which has not yet been well characterized.

As for other genetic mutations, there is not enough research to make strong conclusions. The ADAD genetic mutations also cause an aggressive form of ADAD and uniquely feature early Aβ deposition in the striatum (Klunk et al., 2007), but it is not yet known if these individuals feature different patterns of tau accumulation. MAPT haplotype appears to be related in some form to tau patterns; while results have been inconsistent across studies, the H1H1 haplotypes tends to be less common in cortical-predominant phenotypes (Murray et al., 2011a; Janocko et al., 2012; Risacher et al., 2017). One study performed subtyping based on genetic data and found variation was mostly due to presence or absence of APOE4, but also involved CD2AP, SPON1, LOC390956 and PPIAP59. These subtypes exhibited different neurodegenerative patterns, but, perhaps unsurprisingly, mostly differed in limbic and isocortical areas (Varol, Sotiras, and Davatzikos, 2017).

Other contributions to variation in tau pathological progression have been proposed. Limbic-predominant AD has been occasionally associated with female sex, and cortical-predominant AD with male sex (Ferreira, Nordberg, and Westman, 2020). It is certainly possible that biological sex could influence AD pathology given that, for example, the risk of AD afforded by APOE4 is considerably higher in women (Corder, 1995). In addition, a recent study found that cell type-specific transcriptional response to AD pathology differs systematically by sex (Mathys et al., 2019). Another proposed modifier of tau patterning is comorbid pathologies, such as TDP-43, α-synuclein, and neurovascular pathology. In general, cortical-predominant tau profiles are less associated with most copathologies (Josephs et al., 2017; Ferreira et al., 2018; Ferreira, Nordberg, and Westman, 2020), with the possible exceptions of CAA (Ferreira et al., 2018) and Lewy-body pathology (Murray et al., 2011a), the latter being inconsistently reported (Whitwell et al., 2012). However, age-related co-pathology in AD is quite common (e.g. Nelson et al., 2019, and it is unclear if these co-pathologies actually contribute to tau pattern, or whether they are simply both independently age-related. A final consideration is whether Aβ might dictate tau or neurodegenerative patterns, given that tau pathology is exacerbated by Aβ and

colocalizes with it at later disease stages. Aβ is thought to exhibit a diffuse and largely unpatterned presentation that does not differ even in atypical variants (Rabinovici et al., 2010; Lehmann et al., 2013a). Some work has suggested otherwise (Murray et al., 2011b; Whitwell et al., 2018; Firth et al., 2019), but if Aβ pattern contributes to variation in tau patterning, its contribution is subtle. However, while Aβ pattern may not have a strong influence on tau patterning, one study found a distinct structure of Aβ fibrils in "rapidly-progressing AD", as compared to typical AD and PCA (Qiang et al., 2017).

The above observations have lead to a series of models presented to summarize axes of heterogeneity in AD (Fig 1.6). Ritchie & Touchon rejected contemporary notions that heterogeneity in AD is caused by either measurement of individuals at different stages of disease, or idiosyncratic compensatory processes, and instead suggested the existence of AD subtypes (Ritchie and Touchon, 1992). More recent models have considered AD to vary spectrally along quantifiable dimensions. One model emerged recently suggesting heterogeneity in AD can be characterized along three axes: age, APOE4 allele, and comorbitity (Lam et al., 2013)(Fig 1.6A). This model places each of the AD variants within one of the octants in this parameter space. For example, typical AD is characterized as late-onset, APOE4-positive with concurrent vascular pathology, while PCA is characterized as early-onset, APOE4-negative and with concurrent Lewy-body pathology. This model summarizes well the major known sources of variation among AD subtypes, but is perhaps too simple and far from comprehensive. Another model emerged in 2020 based on a comprehensive review of AD subtype literature and position AD heterogeneity along only two orthogonal axes: severity and typicality (Ferreira, Nordberg, and Westman, 2020)(Fig 1.6B). In this model, the typicality axes spanned limbic-predominance on one extreme and cortical-predominance on the other, with "typical AD" situated at the origin. The severity axis describes variation in the aggressiveness of the pathological presentation. This model is better suited at describing the main axes of variation in AD presentation, and does not concern itself with covariates such as age or APOE. However, this two-dimensional model appears not to account for more atypical variants (e.g. PCA, lvPPA), and does not appear to address the fact that the typicality and severity may be somewhat related (e.g. limbic-predominant may be a less aggressive phenotype).

Defining models for heterogeneity in AD may be somewhat premature given what little is known, and this is something acknowledged by Ferreira and colleagues (Ferreira, Nordberg, and Westman, 2020). The above models suffer from oversimplification, though the Ferreira model is perhaps more helpful by attempting to

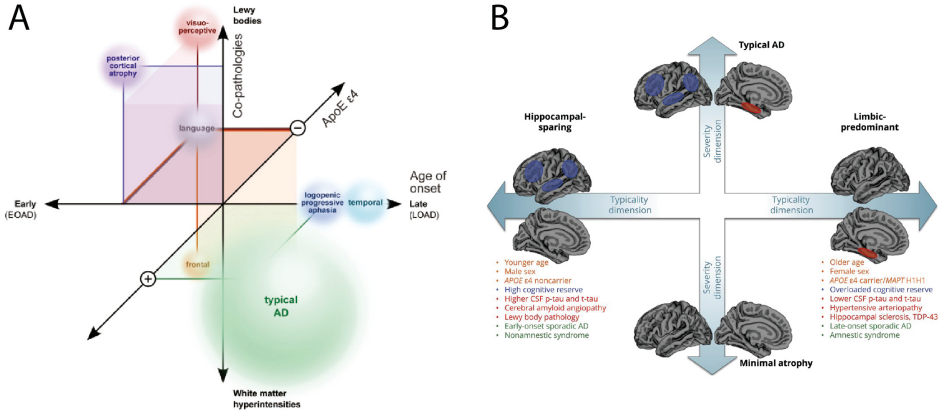

Figure 1.6: Reproduced from (Lam et al., 2013) (with permission from Springer Nature) and (Ferreira, Nordberg, and Westman, 2020) (without permission from Wolters Kluwer, come get me). A) A three-dimensional model summarizing variation along the three best-known factors influencing AD heterogeneity: age (x-axis), co-pathology (y-axis) and APOE genotype (z-axis). B) A two-dimensional model focusing less on factors associated with heterogeneity, and more on characteristics of this heterogeneity. The x-axis represents "typicality", with typical-AD at the origin and limbic- and cortical-predominant AD at the extremes. The y-axis represents "severity", ranging from minimal atrophy subtypes to severely and widespread pathology.

systematize specific qualities with which to compare and quantify pathological variation in AD. However, systematic efforts to truly quantify variation in AD are lacking. The original systematization of limbic-predominant and hippocampal-sparing phenotypes were achieved through a semi-quantitative approach based off of a series of mostly qualitative observations (Murray et al., 2011b). In this case, the quantification was based on only two regions: hippocampus and cortex. This is not unusual as, due to the difficulty in obtaining and processing large quantities of deceased human tissue, few regions are usually sampled, and rarely if ever, from more than one hemisphere. This means that, while histopathological staining is considered the gold standard in AD pathology, it is hardly ground truth. Bihemispheric and whole-brain regional pathological sampling are simply not systematically characterized for AD pathology.

Many of the studies that followed were based directly on the Murray et al. method of subtype definition, even in imaging studies that feature whole-cortex sampling. Those imaging studies that did attempt unbiased and spatially unconstrained characterization of AD neurodegenerative variability have, up to this point, done so using non-specific markers of macroscale brain atrophy. Interestingly, one recent histopathology study attempted an unbiased characterization of regional tau variability, and found that the resulting partition was better at explaining variation in clinical and demographic variation then the Murray et al. model (Petersen et al., 2019). The study, however, only sampled seven regions and featured a highly diverse cohort of different atypical AD variants, very different from the Murray et al. sample. Furthermore, the final partition featured a cortical predominant phenotype, and two "phenotypes" with simply less or more pathology. These latter two phenotypes may

simply be individuals at different stages of tau pathology, as the actual spatial extent of pathology did not differ (this issue is discussed in greater detail in Chapter 4). At this point, variability in tau spread is still not well understood, and further study will be significantly hindered without more extensive efforts to systematically characterize this variability. That being said, at least some things are clear: tau pathology does not always follow the Braak staging schema, and one of the greatest meaningful axes of variation appears to be whether or not tau pathology is specifically concentrated inside of, or outside of, the medial temporal lobe.

The impact of heterogeneity in tau spatiotemporal patterning in AD is perhaps underappreciated. Subtypes might prove meaningful in the clinic as well as clinical trials, as they may prove to be important in determining prognoses and/or treatment response. However, due to being poorly understood or characterized, there is a dearth of studies probing the etiology of AD subtypes, or their biological expression. One interesting lead is the specific contribution of the basal forebrain to cortical predominant and/or early-onset AD. One fascinating study noted increased NFT pathology and neuronal loss in the basal forebrain of deceased patients with a hippocampal-sparing phenotype, and the opposite pattern in limbic-predominant patients. The same study found earlier disease onset was associated with more NFT pathology, but not in limbic-predominant patients (Hanna Al-Shaikh et al., 2020). This is interesting given that cholinergic treatments for AD are less effective in individuals with extensive limbic pathology (Connelly, Prentice, and Fowler, 2005). According to data from Hanna Al Shaikh and colleagues, limbic predominant individuals might be burdened less by cholinergic issues compared to other individuals, and might be burdened more by co-pathologies and other age-related issues. Unfortunately, two other studies using unsupervised imaging-based subtyping approaches found decreased basal forebrain volume in limbic predominant subtypes instead (i.e. the opposite pattern to Hanna Al Shaikh et al.) (Dong et al., 2017; Machado et al., 2020). However, in one of those studies, a targeted basal forebrain treatment appeared more effective for patients with a hippocampal-sparing phenotype (Machado et al., 2020).

A quite young but promising line of evidence with respect to biological qualities of AD pathological subtypes comes from the study of different cell-type specific expression. One study found white matter thorn-shaped astroctyes (argyrophylic thorny astrocytes) clusters, a subtype of aging-related astrogliopathy, was specifically assiciated with lvPPA (Munoz, Woulfe, and Kertesz, 2007). A follow up study in a larger sample did not find this pathology to be specific to atypical AD presentations. However, it did find especially high burden to be associated with language deficits, and that pathology in visual and language regions was associated with visual and

language deficits, respectively. Interestingly, correlation between this astrogliopathy and NFT burden was weak (Resende et al., 2020). Another study investigated the proteomic content of amyloid plaques in late-onset AD (perhaps akin to limbic-predominant) and "rapidly-progressive" AD (perhaps akin to cortical-predominant). The study found plaques from the rapidly-progressive variant to contain more neuron associated proteins, particularly those related to synapse and synaptic vesicles, whereas late-onset AD had more astrocyte-related protein. Importantly, all plaques were taken from the hippocampus. In general, the proteomic content of the plaques was highly distinct, promting the authors to suggest these AD variants represent distinct entities rather than simply differentiated by disease progression (Drummond et al., 2017). None of these studies have strong implications for variation in tau spreading, but larger samples featuring transcriptomic and single-cell data will likely further elucidate biological differences between tau subtypes.

A number of other avenues have been proposed to potentially impact heterogenous tau spread. Particularly suggestive are the rodent studies finding that injecting different strains of tau, and/or injecting tau into different regions, lead to distinct regional patterns of tau accumulation (Clavaguera et al., 2013; Sanders et al., 2014; Iba et al., 2015; Guo et al., 2016a; Dujardin et al., 2018). While different tauopathies feature quite different pathological progressions (Young et al., 2018), a recent study found that tau conformation, rather than tau species, dictated differential regional deposition patterns (He et al., 2020). It is therefore possible that subtypes of tau spread may simply be dictated by distinct tau conformations, perhaps in turn generated by differential kinase or phosphotase expression. This hypothesis can be tested by repeating the Sanders et al. experiment but extracting tau fibrils from the brains of different AD subtypes. However, Sanders et al. found that tau extracted from AD brains results in fairly consistent pathological expression, compared to other tauopathies (Sanders et al., 2014).

Meanwhile, a different study suggested the region of injection dictated the pattern of spread more than the conformational strain of tau injected (Narasimhan et al., 2017). It is therefore possible that different AD subtypes could be due to systematic variation in the human connectome, or perhaps at key synaptic junctures. Perhaps related, some have hypothesized that AD subtypes might stem from premorbid conditions. Perhaps the most well described example comes from the observation of a greater incidence of developmental learning disability in patients with primary progressive aphasia, particularly lvPPA (Rogalski et al., 2008; Miller et al., 2013). Similarly, another study found PCA patients were more likely to have developmental disability in mathematical or visuospatial learning (Miller et al., 2018). The same group recently described developmental abnormalities in three case studies of individuals with

both lvPPA and dyslexia (Miller et al., 2019). These fascinating results suggest developmental factors might predispose individuals to patterns of tau accumulation later in life. Similar developmental factors might contribute to the distribution of tau inside or outside of the medial temporal lobe.

In all, evidence suggests individual deviation from traditional Braak staging is not uncommon, and may be systematically related to factors such as age and genotype. This data presents an interesting compliment to work highlighted earlier in this thesis relating to regional vulnerability and synaptic spreading. Altogether, the work reviewed in this subsection suggests a complete model of tau spatiotemporal accumulation must incorporate additional individual-level information. The mechanisms leading to this variation are still very poorly understood. Therefore we do not yet know whether subtypes of tau spread involve modified regional or cellular vulnerability, modifications in tau spreading dynamics, or as yet characterized factors such as distinct pathological species, genetic variation or developmental differences. However, study of variability in tau spread may lead to important conclusions about AD in general. For example, while AD is so often associated with hippocampal atrophy, it is completely unclear why earlier-onset variants of AD involve relative hippocampal sparing. Further study could lead to advances in personalized treatment, such as the position that cholinergic drugs might be more effective in cortical-predominant phenotypes.

1.4 *In vivo* tau biomarkers as research and clinical tools

Nearly all of the research reviewed up to this point has taken place using either experimental animal models of AD, *in vitro* cell cultures, or *ex vivo* tissue samples. While such approaches have been bountiful in elucidating the functional roles of tau and how they are altered in AD, they come with many caveats. Animal models are mostly performed in animals that do not naturally get AD. While it is possible to recreate AD pathology in these models using genetic mutations, we do not know the degree to which this recapitulates the process that occur in human AD. Differences in the mouse and human transcriptome are enriched for AD-related genes (Miller, Horvath, and Geschwind, 2010), and recent work suggests the transcriptional changes occurring in response to AD pathology differs substantially between humans and mice (Bai et al., 2020). *In vitro* work contains similar caveats related to the fact that an isolated cell culture cannot recreate the complex biological environment of a living human brain. Finally, *ex vivo* work allows only a snapshot of pathological

processes, and one that may be greatly impacted by process related to death. By stitching together results from many sources, it is possible to form conclusions that are relevant to human AD. However, the degree to which our knowledge of AD stems from sources other than human AD is grossly underappreciated. The most obvious indication of this dissonance can be seen by the fact that AD has been multiply cured in animal models, but none of these therapeutics have successfully translated to humans.

There is therefore an imminent need to not only validate previous research in humans, but also to continue to expand the possibilities of directly investigating human AD. Obviously, *in vivo* human work comes with many caveats of its own, the most salient being the relative inaccessibility of cellular and molecular information, and sacred ethical constraints on causal experimentation. However, human tau biomarkers have evolved substantially over the last two decades, and have substantially widened the lens of human AD research. As the original research contained in this thesis is conducted exclusively on human participants, the focus of this section will be to review current tau biomarkers, with a specific focus on tau-PET. PET biomarkers will be discussed with regard to their utility in both clinical and research settings. Tau-PET methods will be critically reviewed and compared to other tau biomarkers.

1.4.1 Tau as a clinical or research biomarker for AD

The original (and for many years, only) method of measuring tau pathology *in vivo* was by detecting it in CSF. This can be achieved by extracting CSF through the spine in a relatively inexpensive procedure known as a lumbar puncture. Total tau (t-tau) can be measured, as well as tau phosphorylated at specific sites (p-tau). Total tau is thought to be a measure of general neuronal or axonal damage, while p-tau is thought to measure tau specifically hyperphosphorylated during the AD process (Blennow et al., 2010). Traditionally, tau phosphorylated at threonine sites 181 and 231 have been associated with AD-specific NFT pathology (Buerger et al., 2006; Blennow et al., 2010). A recent study, however, has described tau phosphorylated at threonine 205 and 217 to be detectable in the CSF and highly related to the progression of AD pathology (Barthélemy et al., 2020a). In addition, a new study finds that tau fragments are present in the CSF, and certain fragments may be more specifically linked to tangle pathology in AD (Blennow et al., 2020).

CSF tau measures have consistently been shown to be elevated in AD (Olsson et al., 2016). In addition, elevated CSF t-tau and p-tau (along with decreased CSF Aβ) can discriminate individuals with MCI that will go on to develop AD (Hansson et al., 2006; Visser et al., 2009; Shaw et al., 2009). Studies in ADAD mutation carriers also indicate elevated CSF tau measures to precede measurable neurodegeneration and

cognitive decline (Bateman et al., 2012; Barthélemy et al., 2020a), and this is generally assumed to be the case in sporadic AD as well (Jack and Holtzman, 2013). There is some work to suggest elevation of CSF p-tau in particular can be used to discriminate AD from other neurodegenerative disorders (Hampel et al., 2004; Koopman et al., 2009; Barthélemy et al., 2020b), but the discrimination is imperfect.

CSF markers of tau have proved to be useful tools to aid clinical and differential diagnosis of AD, and have also been helpful in quantifying the temporal sequencing of different pathological processes. However, there are a number of issues with CSF tau measures that limit their utility in studying tau biology. First, CSF measures can vary by up to an order of magnitude from batch to batch, and from center to center, making standardization tricky and comparison challenging (Mattsson et al., 2011). In addition, tau in the CSF appears to degrade over time, which may contribute to the observation that CSF tau exhibits unusual dynamics when measured longitudinally (Fagan et al., 2014; McDade et al., 2018; Schindler et al., 2019; Lleó et al., 2019). Some studies have concluded that CSF tau levels off around the time of symptom onset, though one recent large study saw no change in CSF p-tau over time, and a *decrease* in total tau (Lleó et al., 2019). However, another recent study in ADAD mutation carriers found rate of change in various CSF tau measures to correlate quite strongly with change in cognition over time (Barthélemy et al., 2020a).

While nearly every biomarker comes with measurement error, CSF tau exhibits two major limitations that are not measurement related. First, it is still unknown exactly how CSF tau relates to tau-related processes in the brain. For example, it is not known at what stage of pathology (e.g. initial phosphorylation, pretangle stage, cell death) tau is concentrated into the CSF, nor whether this occurs uniformly throughout the brain. The lack of substantially elevated t-tau in other neurodegenerative disease calls to question whether it is actually measuring axonal damage. These issues make interpretation rather challenging outside of the general context of clinical use. The other obvious caveat to CSF measures is that they provide absolutely no spatial information. The spatial presentation of tau appears to be incredibly relevant to its pathophysiology, as well the differentiation and progression of different diseases. From a clinical standpoint, one cannot perform Braak staging with CSF measures, and while they appear to be helpful in predicting conversion to dementia, they do not allow for very high resolution tracking along the full disease spectrum. However, the lack of spatial information additionally precludes CSF measures from being used to study the *in vivo* interplay of various neurobiological properties and pathological factors in the pathophysiology of AD.

Given that PET tracers measuring Aβ had been around since 2004 (Klunk et al., 2004), the expectation was that a tau-PET ligand would eventually emerge and

revolutionize the field in a similar fashion. Flortaucipir, the most frequently used and well-characterized tau-PET tracer, was first described in 2013 (Xia et al., 2013), and the first human studies using it emerged in 2016 (Johnson et al., 2016; Schöll et al., 2016b; Ossenkoppele et al., 2016a). [5] The emergence of a viable tau-PET tracer immediately surmounted the spatial limitations that had plagued tau biomarkers up to that point. Early on, tau-PET uptake was seen in patterns highly similar to those described at autopsy, and the pattern varied systematically with advancing disease progression (Johnson et al., 2016; Schöll et al., 2016b; Chiotis et al., 2016; Schwarz et al., 2016; Brier et al., 2016). Furthermore, atypical AD variants exhibited tau-PET patterns that were distinct from one another, and from typical AD (Ossenkoppele et al., 2015b; Ossenkoppele et al., 2016a). Importantly, and unlike Aβ, tau-PET signal co-localized with brain atrophy (Ossenkoppele et al., 2016a; Xia et al., 2017; Iaccarino et al., 2018), advanced with advancing disease stage (Schwarz et al., 2016; Schöll et al., 2016b), correlated well with global cognition (Cho et al., 2016b; Schöll et al., 2016b), and exhibited region-specific effects on various cognitive domains (Bejanin et al., 2017a). Finally, increase in tau-PET signal in the temporal lobes were observed with increasing age, suggesting the possibility that tau-PET could be used to quantify PART (Schöll et al., 2016b; Maass et al., 2018a).

Within two years, tau-PET had proved to be a massive upgrade over CSF. While it has many of its own limitations (outlined below), these limitations do not overlap much with those presented by CSF. Tau-PET, for example, exhibits fairly consistent longitudinal accumulation (Harrison et al., 2018; Pontecorvo et al., 2019; Jack et al., 2018a). This relative longitudinal stability has allowed for more reliable testing of the progression of biomarker sequences in AD (Hanseeuw et al., 2019; La Joie et al., 2020). In addition, partially due to the unintended feature of binding only to mixed 3R/4R (AD-like) tau pathology, tau-PET has proven to be an excellent tool for discriminating AD not only from other dementias, but also from other tauopathies (Ossenkoppele et al., 2018). The most important advantage comes of course from its ability to impart information about spatial location and evolution of tau pathology. This has allowed for a multitude of interesting studies examining spatial interactions between tau and Aβ (Lockhart et al., 2017a; Sepulcre et al., 2017a), glucose metablism (Hanseeuw et al., 2017), functional MRI indices (Sepulcre et al., 2017b; Hansson et al., 2017; Cope et al., 2018) and spatial transcriptomic information (Grothe et al., 2018; Sepulcre et al., 2018).

Perhaps some of the most interesting studies have involved examinations of tau and brain functional changes. For example, a number of studies have shown

[5] The following subsection will describe tau-PET tracers in detail, but they will be discussed here in relation to other *in vivo* tau measures.

dynamic changes in functional networks in response to tau accumulation, perhaps reflecting excitotoxic response (Huijbers et al., 2017; Marks et al., 2017; Harrison et al., 2019) or compensatory reorganization (Schultz et al., 2017; Neitzel et al., 2019). Additional studies have examined fine-grained analyses of medial temporal tau and its association with specific memory and cognitive processes (Marks et al., 2017; Maass et al., 2019). Studies like these can support and extend rodent and *in vitro* findings in ways that were not possible with CSF measures of tau.

Several studies investigated relationships between CSF tau measures and tau-PET measures (Gordon et al., 2016; Chhatwal et al., 2016; Mattsson et al., 2017; La Joie et al., 2018; Meyer et al., 2019; Blennow et al., 2020; Wolters et al., 2020b). Most of these studies found correlations to be rather modest (Gordon et al., 2016; Chhatwal et al., 2016; Mattsson et al., 2017; Meyer et al., 2019; Wolters et al., 2020b), and found correlations between PET and t-tau to be highly similar, or even stronger (Mattsson et al., 2017), than correlations with p-tau. An outlier study, however, found strong correlations between PET and both p-tau and t-tau, found the correlation with p-tau to be stronger, and found the two CSF measures to associate with PET signal in different regions (La Joie et al., 2018). The strenth of the correlation may depend on the sample, as the La Joie et al., sample was composed of many EOAD and atypical AD variants. Another study found a fairly strong correlation between CSF and PET tau measures, but did so using different CSF and PET measures from the other studies mentioned (Blennow et al., 2020). In general, the modest correlation between PET and CSF measures of tau pathology calls to question exactly what processes these tools are measuring.

While tau-PET holds a number of obvious advantages over CSF, there are some alternative perspectives worth considering. While CSF measures may not be as effective as tau-PET in tracking the evolution of AD symptomology, there is some evidence to suggest they may be more sensitive to early changes. Mattsson et al. found that a single tau-PET measure could differentiate AD patients from controls with near perfect accuracy, but that CSF p-tau was slightly better at distinguishing Aβ-positive MCI from controls (Mattsson et al., 2018a). Two recent studies in ADAD participants found several CSF tau measures to become abnormal before tau-PET measures (Barthélemy et al., 2020a; Mattsson-Carlgren et al., 2020). In addition, both CSF and PET measurement are rather invasive. CSF requires lumbar punctures that can cause discomfort and often lead to headaches. PET meanwhile involves intravenous injection of a radioactive tracer, and lying stationary for a period of time. However, lumbar punctures are relatively inexpensive procedures, while a single PET scan can cost a few thousand dollars, making serial PET scanning often prohibitively expensive. In addition, while PET scans provide invaluable spatial

information, this has resulted somewhat in an embarrassment of riches. Tau-PET studies often require the distillation of an image into one or a few measurements, which involves arbitrary decisions that may result in loss of information (reviewed below in section 1.5.1). Finally, tau tracers unfortunately bind to sources other than tangle pathology, making interpretation challenging (review below in section 1.4.2).

One more tau biomarker has recently emerged and represents a major advance. Two independent groups published impressive results showing tau phosphorylated at threonine site 181 is detectable in plasma (Janelidze et al., 2020; Thijssen et al., 2020). The studies together showed plasma p-tau181 could discriminate AD from other neurodegenerative diseases, correlated strongly with tau-PET, advanced with advancing disease stages and with advancing pathology, and distinguished individuals with and without Aβ pathology, using *in vivo* and pathology-confirmed data. Another group also published results showing plasma measures of Aβ and tau could together discriminate AD from controls with high accuracy (Kim et al., 2020). Altogether, plasma tau equals CSF and PET tau in its diagnostic performance, and may exceed CSF in its ability to track disease progression, all while being far less expensive and less invasive than either of the other measures. While further work must be done to characterize this measure, its inexpensive nature should allow fast and easy data collection. If other groups can replicate and extend these results, plasma tau may very well revolutionize clinical AD diagnosis.

Altogether, there is no perfect tool to measure tau *in vivo*. Plasma p-tau may be sufficient in a clinical context, although this may depend on the reliability of plasma Aβ. Longitudinal studies will be necessary to characterize the stability of plasma tau measurements and whether they reliably increase over time. Of course, like CSF, plasma tau does not provide any information pertaining to spatial extent of tau pathology, and so is very limited in a research context. For example, plasma and CSF tau could not identify distinct AD pathological subtypes, nor could they indicate whether tau is spatially advancing. Plasma and CSF tau may still prove useful as complementary research tools to describe the phosphorylation state of brain tau or very early abnormal tau activity, but the ability of PET to localize regional pathology greatly enhances the field of scientific inquiry into tau biology. For example, all of the original research contained in this thesis relies on the spatial properties of tau-PET, and none of it would be possible using fluid markers. The next subsection will go into greater detail regarding the possibilities and limitations of tau-PET.

1.4.2 Tau-PET radiotracers

As with all radiotracers, tau-PET tracers are injected into the bloodstream, where they are transported to the brain, cross the blood-brain barrier, and bind selectively

to a target. The ligand carries elemental isotopes that degrade and emit positrons, which produce gamma rays that are detected and used to approximately localize the source (i.e. the ligand). After an initial wash-in period, the ratio between bound and free tracer increases and concentrates in regions of interest. In order to account for non-specific binding, tracer uptake can be normalized to a reference tissue that should be similar to target tissue, but which is not expected to itself contain the target. In the case of tau and AD, the cerebellum is typically used as a reference region due to the fact that it is neural tissue that does not express tau NFT pathology (Baker, Maass, and Jagust, 2017). All PET tracers suffer from certain measurement limitations, probably the most relevant of which are partial volume effects and off-target binding. Partial volume effects refer to the poor spatial resolution of PET resulting in signal bleeding across regions that are spatially adjacent but functionally distinct. Off-target binding refers to ligand binding to sites other than the target.

Tau-PET tracers have technically been around for decades. [^{18}F]FDDNP was developed to image AD pathology *in vivo*, but demonstrated poor selectivity, specificity and research utility (Thompson et al., 2008; Ossenkoppele et al., 2012). The first set of ostensibly viable tau-PET tracers emerged less than a decade ago, with [^{11}C]PBB3 (Maruyama et al., 2013), [^{18}F]flortaucipir (also known as [^{18}F]T-807 and [^{18}F]AV1451, Chien et al., 2013; Xia et al., 2013), and the [^{18}F]THK tracers (Harada et al., 2015; Harada et al., 2016). Each tracer was shown to bind to PHF tau in NFT inlcusions, ghost tangles and neuritic plaques through post-mortem analysis and autoradiography studies, and have reproduced expected temporo-parietal binding patterns in human AD studies (Leuzy et al., 2019) (Fig 1.7). However, while all of these tracers are still in use today, the vast majority of *in-vivo* human studies to date have been conducted using flortaucipir.

The prominence of flortaucipir is not necessarily because it was initially determined a better tracer. For example, PBB3 (Ono et al., 2017) and the THK tracers (Kikuchi et al., 2016; Ishiki et al., 2018; Jang et al., 2018) bind to 4R tauopathies better than flortaucipir. In addition, flortaucipir shows poor binding kinetics *in vivo*, never quite reaching a steady state in AD patients (Baker et al., 2017). There are four likely reasons that flortaucipir rose to prominence. First, synthesis of PBB3 must be conducted in near total darkness, making it rather inconvenient (Maruyama et al., 2013). Adding to the inconvenience is that the carbon-11 isotope has a short half-life, requiring a cyclotron on-site for synthesis and rapid administration. Second, the first large *in vivo* tau-PET cohort studies, published by some of the most influential laboratories in AD neuroimaging, quantified tau with flortaucipir (Johnson et al., 2016; Schöll et al., 2016b; Ossenkoppele et al., 2016a; Brier et al., 2016), which is likely attributable to successful marketing on the part of AVID Radiopharmaceuticals. In

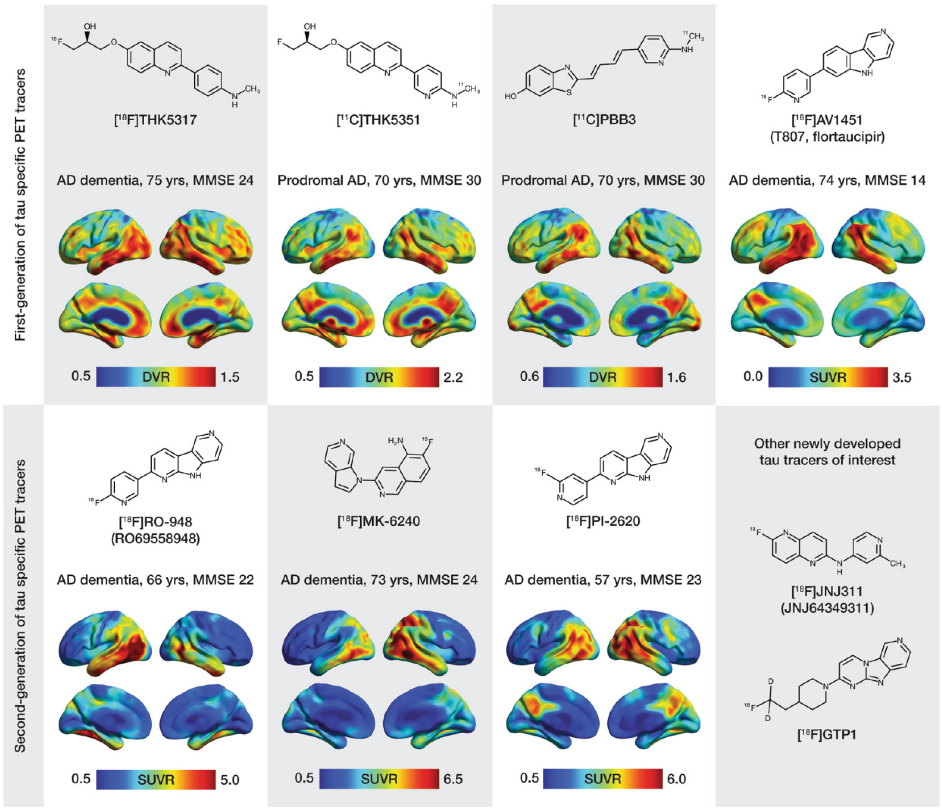

Figure 1.7: Reproduced from (Leuzy et al., 2019). The molecular composition of each tracer is shown, along with the *in vivo* binding pattern in an exemplar subject (different for each tracer). (Top) The first generation tracers, including flortaucipir on the far right. (Bottom) Three "second generation" tracers, which appear to have improved signal-to-noise ratio.

contrast, no large cohort studies using PBB3 exist, whereas studies using THK trailed slightly behind (Chiotis et al., 2016) and were initially less numerous. Third, a highly influential study showed that 60-85% of THK-5351 binding in the human brain was to MAO-B, rather than to tau (Ng et al., 2017). This study was effectively a death sentence for the THK tracers in AD imaging; meanwhile flortaucipir appears not to suffer from the same issue (Hansen, Brooks, and Borghammer, 2018; Baker et al., 2019; Aguero et al., 2019) (though some unpublished studies suggest it may be non-selective MAO inhibitor: Drake et al., 2018; Drake et al., 2019). Finally, a few years separated the first flortaucipir studies from the emergence of the "second-generation" tracers, and during this time, flortaucipir became by far the most well characterized tau-PET radiotracer.

For better or worse, flortaucipir has become the *de facto* tau-PET tracer, at least during the early years of tau-PET. For this reason, and given that it is the tracer used in the original work of this thesis, some of its features will be reviewed. Autoradiography studies show flortaucipir binds with strong affinity to AD-like PHF tau pathology (Marquié et al., 2015; Lowe et al., 2016). This has been confirmed by strong *in vivo* binding not only in AD, but also in patients with other disorders exhibiting AD-like tau pathology, such as R406W MAPT mutation carriers (Smith et al., 2016;

Jones et al., 2018; Tsai et al., 2019) and CTE (Stern et al., 2019; Lesman-Segev et al., 2019). [6]

However, the same autoradiography studies have confirmed flortaucipir does not bind to straight or twist filament 4R tau associated with primary tauopathies (Marquié et al., 2015; Lowe et al., 2016; Marquié et al., 2017). These findings were somewhat distressing, given that weak but significantly elevated *in vivo* binding has been seen in multiple 4R tauopathies, including progressive supranuclear palsy (Smith et al., 2017; Schonhaut et al., 2017), corticobasal degeneration (McMillan et al., 2016; Cho et al., 2017; Niccolini et al., 2018) and frontotemporal dementia (Bevan-Jones et al., 2017; Josephs et al., 2018; Tsai et al., 2019; Smith et al., 2019a). While this may indicate binding to incidental AD-like tau pathology in certain cases (e.g. Tsai et al., 2019), or low-affinity binding to non-AD-like tau pathology, this cannot explain all associations. For example, multiple groups showed semantic variant of primary progressive aphasia, a variant of frontotemporal dementia driven by TDP-43 pathology, expresses elevated flortaucipir-PET binding specifically in regions affected by TDP-43 pathology (Bevan-Jones et al., 2017; Makaretz et al., 2018; Smith et al., 2019a). It is still quite unclear what flortaucipir is binding to in such cases. Autoradiography studies suggest flortaucipir does not bind to TDP-43 pathology (Marquié et al., 2015; Lowe et al., 2016), and this has been confirmed using tissue from cases showing elevated flortaucipir binding (Smith et al., 2019a). The same studies showed flortaucipir also does not bind to Aβ or α-synuclein, though it is possible that binding to these pathologies may occur *in vivo*. A recent study in frontotemporal dementia patients showed strong regional binding correlations between flortaucipir and a PET tracer imaging inflammation, and proceeded to show co-localization between microglia and both TDP-43 and tau pathology at autopsy (Bevan-Jones et al., 2020).

Flortaucipir has also been shown to potentially bind to neuromelanin and iron deposits (particularly in substantia nigra), reactive astrocytes, choroid plexus calcification, and hemorrhagic lesions. Many of these, as well as other binding sites, have been validated *in vivo*. Lockhart et al. described flortaucipir binding to a number of incidental neural insults such as infarctions and meningiomas (Lockhart et al., 2017b). Baker and colleagues performed data-driven analysis of off-target flortaucipir binding using Aβ-negative cognitively normal individuals spanning young to old adulthood. Strong flortaucipir binding was seen in the substantia nigra, striatum, and choroid plexus, even in these healthy, cognitively normal individuals. Furthermore, three separate and orthogonal binding components emerged characterized by striatal

[6] It should be noted that binding to CTE appears quite weak (Lesman-Segev et al., 2019). In addition, a case study with pathologically confirmed CTE and antemortem PET showed that the correlation between regional tau pathology and regional flortaucipir was not significant. (Mantyh et al., 2019)

signal, white matter and thalamic signal, and choroid plexus signal, indicating these off-target binding sites to be independent from one another (Baker et al., 2019). The striatal signal is age-related and correlated with striatal iron accumulation, which is also age-related (Choi et al., 2018; Baker et al., 2019). This may also partially explain elevated binding in tauopathies with striatal pathology, such as progressive supranuclear palsy and corticobasal degeneration. Not much is known about the white matter signal, though using white-matter in a reference region appears to stabilize longitudinal flortaucipir measurement (Southekal et al., 2018; Harrison et al., 2018), inidicating it may be non-specific binding and/or related to poor tracer kinetics (Baker et al., 2017).

The choroid plexus signal is highly problematic, as it may interfere with flortaucipir binding in the adjacent hippocampus (Schöll et al., 2016b; Lee et al., 2018; Wolters et al., 2020a), one of the earliest regions to show tau pathology (Braak and Braak, 1991). Some results suggest regression of choroid plexus signal from the image may at least partially remedy this issue (Lee et al., 2018). However, this ties generally into one of the most enigmatic features of flortaucipir, which is that binding in the hippocampus is much lower that expected. Many studies have abated this issue by combining the hippocampus with other MTL structures (e.g. Schöll et al., 2016b), or removing it from analyses altogether (e.g. Cho et al., 2016a). This is curious given the importance of the hippocampus to the pathogenesis of AD. The unexpected hippocampus signal may actually provide novel insight leading to the nature or specific location of hippocampal pathology, or may simply reflect as yet unknown properties of flortaucipir binding. Finally, isolated age-related flortaucipir binding has been described throughout the cortex even in cognitively normal and unimpaired individuals. While this has been interpreted by some as true signal (Lowe et al., 2018), this must be confirmed by autopsy studies, and more likely reflects some unknown off-target binding source.

The numerous off-target binding sources, sub-optimal properties and false-positives described above combine for a fairly damning report of flortaucipir. Arguments have been made that tau-PET ligands were rushed to research studies without sufficient validation (Klunk, 2018). However, it should not be understated how transformative the first generation of tau-PET tracers have been to the AD field. While interpretation can be challenging at times due to off-target binding, there is no doubt that flortaucipir *is* binding to tau NFT pathology *in vivo*, which makes it enormously useful to the AD research community.

Nonetheless, the imperfections of the first generation of tau tracers motivated the discovery of "second-generation" tau-tracers (Fig 1.7). These include [^{18}F]MK-6240 (Walji et al., 2016), [^{18}F]RO-948 (Gobbi et al., 2017), [^{18}F]JNJ311 (Declercq et al., 2017),

[^{18}F]PI-2620 (Kroth et al., 2019) and [^{18}F]GTP-1 (Sanabria Bohórquez et al., 2019). At present, very few studies have been published characterizing these tracers *in vivo*, and no studies with large samples have been published. However, early *in vivo* works suggests common features across many of these tracers include ostensibly diminished off-target binding in the striatum and choroid plexus, higher affinity to tau pathology, and improved tracer kinetics (Betthauser et al., 2019; Pascoal et al., 2018; Mueller et al., 2019; Teng et al., 2019; Leuzy et al., 2019). Unfortunately, several of the second-generation tracers feature strong meningeal binding in a large subset of individuals. This has been characterized best in RO948, where the meningeal signal was consistent across time and did not interfere with diagnostic distinction between AD and controls (Smith et al., 2020). Further study will be needed to better characterize meningeal binding and its effects, but the binding patterns will likely interfere with analyses involving cortical ROIs.

In all, the second generation tracers were advertised as upgrades over flortaucipir, and this appears to be true in many respects. However, whether the new tracers truly improve upon flortaucipir in practice remains unproven. The second generation tracers may be better suited for study of the medial temporal lobe and for differential diagnosis, whereas flortaucipir may remain the best option for more fine-grained and sophistocated regional analyses involving isocortex. [7] In the end, none of the tau-PET radiotracers are perfect, but most of them are sufficient to measure tau pathology *in vivo*, and therefore represent indispensable tools for the AD research community.

1.5 Distribution and evolution of tau *in vivo*: A selective review of tau-PET studies

Many interesting insights into the pathobiology of AD have emerged from tau-PET studies over the last five years. While such insights are limited by the spatial resolution of PET, and the caveats described at length in the previous subsection, tau-PET has greatly expanded the scope of human AD research. A complete review of the tau-PET literature is beyond the scope of this chapter, but certain topics will be covered in detail. Namely, this section will review literature directly related to the original research presented in this thesis, in order to review the context motivating the goals of each study. The central themes revolve around the spatiotemporal distribution and progression of tau pathology.

[7] While there is not substantial published work to support this statement, these views are a result of the author's own personal experience, personal communications and regular attendance of the Human Amyloid Imaging conference

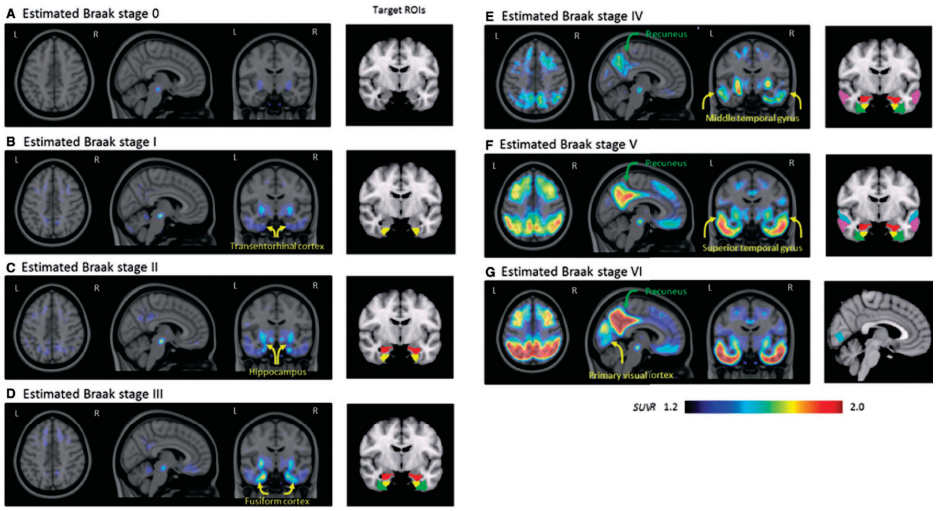

Figure 1.8: ROIs capturing a Braak-like progression of flortaucipir signal *in-vivo*, reproduced from Schwarz et al., 2016 (with permission from Oxford University Press). Each cell represents a Braak stage. Each cell contains (left) a flortaucipir image of an exemplar subject assigned to that Braak stage based on showing abnormal signal in (right) the stage-specific ROI.

1.5.1 *In-vivo* distribution of tau in the human brain

The Braak staging regime was invoked quite early on in the tau-PET era. The first major tau-PET cohort study described a progression from cognitively unimpaired, to MCI to AD to be accompanied by a Braak-like progression of tau-PET signal (Johnson et al., 2016). Not long after, two additional tau-PET studies demonstrated this phenomenon even more directly by creating regions of interest (ROI) mimicking the Braak stages (Fig 1.8). The studies each showed the evolution of cognitive symptoms to associate with progressive advancement of abnormal tau signal into regions from later stages (Schöll et al., 2016b; Schwarz et al., 2016). The general consensus was that the distribution of flortaucipir signal recapitulated the patterns of evolving tau pathology described by Braak and Braak 25 years earlier (Braak and Braak, 1991).

The association was not perfect of course, as unexpected binding in the striatum and choroid plexus, along with unexpectedly low binding in the hippocampus, were described early on (Schöll et al., 2016b). Little by little, additional studies were published further qualifying differences between flortaucipir signal and the expected pattern of tau pathology. One study ranked regions by their rate of abnormally elevated signal in a sample spanning the disease spectrum, and noted regions that became abnormal out of sequence with the expected Braak progression. The study found the insula, lingual gyrus and hippocampus to appear out of sync with the expected Braak-like progression (Cho et al., 2016a). Meanwhile, one of the groups that had originally published data using "Braak stage ROIs" later published a study finding large lobar ROIs to provide a better fit to the flortaucipir data (Schwarz et al., 2018).

Some of these discrepancies be may be attributable to off-target binding or atypical AD variants, though the notion that unbiased and spatially unconstrained quantification of tau pathology could provide new insights into tau spread could not be ruled out. Perhaps one of the most puzzling findings came from one of the first large longitudinal tau-PET studies, which found similar rates of flortaucipir accumulation across most brain regions in Aβ-positive individuals (Jack et al., 2018a). This finding was in stark contrast to the expectation that tau accumulation occurs selectively in certain regions depending on disease stage. However, subsequent longitudinal studies suggested a more progressive longitudinal pattern, with abnormal signal at follow-up extending into regions were not abnormal at baseline (Sepulcre et al., 2018; Harrison et al., 2018; Pontecorvo et al., 2019).

Many of these early studies proceeded under the hypothesis that tau-PET patterns should follow the Braak staging pattern identified through histopathological studies. This was certainly a defensible approach at the time, and most studies to this day support the notion that the Braak stages fit the tau-PET data well – just not perfectly. Indeed, few studies had endeavored to identify discrepancies between tau-PET and tau pathology, or better yet, approach tau-PET data in a hypothesis-free manner. Not only are such analyses important for understanding the structure of tau-PET data, but they may also reveal insights into tau progression that may have eluded autopsy studies.

At the time that the analyses in Chapter 2 had begun (late 2016), no studies invoking data-driven methods to analyze tau-PET had been published. By the time the work was published (Vogel et al., 2019a) and shortly thereafter, quite a few such studies did emerge applying either unsupervised clustering (Sepulcre et al., 2017a; Mishra et al., 2017), factor analysis (Maass et al., 2017) or independent-components analysis (Jones et al., 2017; Hoenig et al., 2018; Pereira et al., 2019; Pereira et al., 2020) to tau-PET data. In summary, the studies found that the tau-PET data naturally partitioned into some structures that resembled Braak stages, but otherwise found a different hierarchical structure to the data. Namely, several studies noted resemblance of tau distribution to functional networks (Jones et al., 2017; Hoenig et al., 2018; Pereira et al., 2019). In addition, while temporal structures tended to frequently covary across the population, other isocortical structures tended to behave fairly independently, particularly frontal lobe structures. This latter finding is worth note given most of the isocortex is uniformly ascribed to Braak stage V, and the details are given little attention in the original descriptions of tau pathology (Braak and Braak, 1991). Some of these findings may be dependent on arbitrary methodological decisions such as the resolution of the partition, or other features idiosyncratic to the methodological approach. However, the results also suggest the advancement of tau

pathology at later stages may be somewhat more nuanced than originally described.

A decade of working with Aβ-PET data (and even longer with FDG-PET) prepared the AD imaging community for tau-PET in many ways, particularly with respect to data pre-processing. However, the spatially dynamic aggregation of tau provided a new challenge, particularly for clinical research. Aβ, for the most part, initially appears diffusely across the extended isocortex (Thal et al., 2002), and *in-vivo* work suggests the pattern of accumulation varies very little across individuals (Grothe et al., 2017). The resulting high covariance of cortical Aβ-PET means that a single measure (i.e. average of several large cortical regions) can be used to summarize the relevant Aβ-PET signal quite effectively. Subsequently, the process of identifying what is an "abnormal" Aβ-PET scan can be reduced to identifying a natural "threshold" separating (effectively sampled) abnormal and normal distributions (Mormino et al., 2012b; Villeneuve et al., 2015b; Jack et al., 2017), perhaps with an estimate of uncertainty. This can be interpreted as a massive oversimplification of data, paired with the potential loss of important information contained in the image. However, such distillations are not only clinician-friendly, but additionally help complex multi-modal analyses by reducing the dimensions of Aβ-PET images, which individually contain hundreds of thousands of data points. In the case of Aβ-PET, even more sophisticated and data-driven distillations suggest the information contained within the cortex is highly homogeneous (Whittington, Sharp, and Gunn, 2018; Whittington and Gunn, 2019).

With tau-PET, spatial information is much more relevant, and constructing a summary measure is not nearly as simple. As AD progresses, abnormal tau-PET signal emerges in more and more cortical areas. While flortaucipir binds to "ghost tangles" – NFT pathology that persists even after neuronal death, longitudinal studies have been mixed as to whether or not tau continues to accumulate in early regions during later disease stages (Jack et al., 2018a; Sepulcre et al., 2018; Harrison et al., 2018; Pontecorvo et al., 2019; Sintini et al., 2019). Therefore, it is unclear whether a single measure can or should be used to summarize tau-PET data. Even if one region or a few regions are chosen, another challenge presents itself, relating to whether and how such a region can be classified as abnormal. Tau accumulates in the medial temporal lobe even in healthy elderly (Crary et al., 2014), obscuring the definition of "abnormal" in this case. In addition, normalizing to a young healthy population is not recommended due to age-related increases in tau-signal (Baker et al., 2019), and may lead to elevated signal that may be spurious (Lowe et al., 2018).

A number of strategies have been imparted in order to optimally summarize tau-PET data. As noted earlier, Braak stage ROIs have been proposed that can track advancing disease progression in a manner resting on a strong hypothesis of

progressive tau spread (Schöll et al., 2016b; Schwarz et al., 2016). Other groups have suggested, mostly on the strength of anecdotal experience, that the bilateral inferior temporal lobe alone can suffice as a summary region for tau-PET (Johnson et al., 2016). The logic behind this selection is that the inferior temporal lobe becomes involved fairly early on (Braak Stage III, Braak et al., 2006), and yet theoretically continues to accumulate more tau in later stages. Still others have elected to use summary measures involving temporal lobe structures implicated in early and/or later Braak stages (Villemagne et al., 2016; Jack et al., 2017), regions previously shown to exhibit neurodegeneration in AD (Wang et al., 2016), or large lobar structures (Schwarz et al., 2018).

Maass et al. performed a comprehensive systematic evaluation of various tau-PET ROIs, including many discussed here, as well as new data-driven approaches, and validated the results in a separate sample. The authors found that the optimal choices of ROI depended on the task: large whole-brain ROIs were best for distinguishing AD from controls, but regional (particular temporal) ROIs had stronger associations with memory, Aβ and other indices. A data-driven approach suggested a large temporoparietal ROI to be the most optimal ROI (Maass et al., 2017). Another study compared several different ROIs in their capacity to discriminate AD from other neurodegenerative disease using tau-PET, also using out-of-sample validation. The results showed similar results across ROIs, with a slight advantage of temporoparietal or temporal aggregate ROIs over large cortical ROIs or specific early Braak regions. In line with Maass et al., the study also found temporal regions to result in better sensitivity, while the larger temporoparietal ROIs provided better specificity. (Ossenkoppele et al., 2018). A pair of longitudinal studies comparing different ROIs produced highly convergent results: larger regions performed better comparing AD to controls, smaller temporal regions for distinguishing early disease progression, and temporal and tempoparietal ROIs performing best overall (Harrison et al., 2018; Jack et al., 2018a). However, neither study included any form of cross-validation. Finally, three different studies found unsupervised data-driven ROIs to outperform more traditional ROIs, and included cross-validation (Maass et al., 2017; Mishra et al., 2017; Vogel et al., 2019a).

The general consensus of these studies recommends against representing tau-PET data using a single ROI. The studies above do suggest temporoparietal areas carry the majority of information relevant to clinical status, though data-driven investigations have noted that there are other sources of covariance in the tau-PET data (Jones et al., 2017; Sepulcre et al., 2017a; Vogel et al., 2019a). More specific research questions might entail use of other types of regions; for example, Bejanin and colleagues showed different cognitive domains to be associated with tau accumulations within

different brain regions (Bejanin et al., 2017a). The field will likely benefit from more sophisticated approaches involving multiple ROIs, though these measures will need to be simplified and/or automated in order to be translated to a clinical setting.

Finally, as mentioned above, even if an ROI has been chosen, identifying whether signal in that region is abnormal presents a challenge. Several approaches have been proposed, but the most common one involves identifying a control sample and finding 2 SDs above the mean of that sample (Jack et al., 2017). This approach assumes non-specific binding in a region with no tau to be normally distributed, which is a reasonable assumption as it turns out (see Chapter 3 below). Across the AD spectrum from unimpaired to dementia, the distribution of tau-PET shows a bivariate distribution (Jack et al., 2019b), and certain studies have taken advantage of this property and have employed data-driven approaches for threshold discovery. Some studies have, for example, used decision-tree methods (Schöll et al., 2016b; Weigand et al., 2020) or mixture models (see Chapter 3 and Chapter 4 below). Another study found that applying a method leveraging sensitivity and specificity between two groups, the Youden index, provides better out-of-sample discrimination accuracy compared to the mean+2SD method (Ossenkoppele et al., 2018).

The issue with all of these approaches here is defining an appropriate "control group" when even Aβ-negative unimpaired elderly still exhibit tau, and young individuals have systematically lower non-specific binding throughout the brain. Jack and co-authors describe the influence of different control groups on different "cut-points", noting they differ widely (Jack et al., 2017). In addition, all of these approaches may err on the side of conservatism in that they may preclude discovery of age-related tau pathology (PART), except using young controls, which may greatly overestimates tau elevation (Lowe et al., 2018). At the very least, using data-driven approaches allow a less biased definition of the control group, even if that group may not be truly "normal".

In all, the studies reviewed above offer a number of practical insights regarding the distribution of tau-PET data. The Braak staging system does seem to generalize well to tau-PET data, but the fit is imperfect, and so far has not emerged as the optimal way of representing tau-PET signal for clinical purposes. Early Braak regions do appear to be elevated near the beginning stages of AD, suggesting tau pathology in the MTL is elevated in the presence of Aβ above and beyond PART. Following with the Braak model, more severe cognitive impairment is marked by pathology moving out of the temporal lobes. However, in particular, tau pathology seems to appear in the medial and lateral parietal lobes far more prominently than frontal regions, suggesting a spatiotemporal dissociation of those structures. Finally, the richness of a tau-PET image cannot be fully exploited using a single summary measure, though

a summary measure may suffice for certain clinical purposes.

1.5.2 Investigating the spread of tau in the human brain using *In-vivo* neuroimaging

The preceding sections have hopefully made a compelling case that the spatiotemporal progression of tau pathology in AD is defined by the intersection of synaptic spreading, cellular vulnerability and individual variability. However, until recently, much of the evidence supporting these three pillars has come from *in vitro*, animal and *ex vivo* studies. Animal studies have proven that tau can spread synaptically, and have provided strong evidence that tau molecules themselves can act as templating mechanisms to induce pathologic conformation in other tau molecules (De Calignon et al., 2012; Liu et al., 2012; Iba et al., 2013; Sanders et al., 2014; Dujardin et al., 2014; Ahmed et al., 2014b; Takeda et al., 2015; Boluda et al., 2015; Guo et al., 2016b; Narasimhan et al., 2017; Dujardin et al., 2018). However, even if this is likely a mechanism of tau propagation in humans, it is quite challenging to actually demonstrate this. The progressive occurrence of tau pathological "seeds" and pretangles in regions of human tissue that typically express NFT pathology in later stages provides one clue (Holmes et al., 2014; Furman et al., 2017; Kaufman et al., 2018; DeVos et al., 2018a). *In vivo* human imaging has the potential to provide another.

If tau is propagated via axonal transport of pathologically conformed tau molecules, this process occurs on a scale far too small to be captured by the current resolution of human neuroimaging. However, if the process of pathological propagation occurs systematically along major neuronal communication pathways, such a process may be detectable. A seminal study has shown that the neurodegenerative patterns of several dementing diseases occur most prominently within specific macroscale brain networks (Seeley et al., 2009), and this finding as been replicated, echoed and advanced extensively (Zhou et al., 2012; Raj, Kuceyeski, and Weiner, 2012; Lehmann et al., 2013b; Iturria-Medina et al., 2014; Crossley et al., 2014; LaJoie et al., 2014; Zeighami et al., 2015; Yau et al., 2018; Acosta et al., 2018; Zheng et al., 2019; Brown et al., 2019). A number of studies have demonstrated this phenomenon in AD, but it is important to note that while neurodegeneration and tau-PET signal correlate strongly, they are not measuring the same thing. Neurodegeneration in AD can be caused by other pathologies (Schneider et al., 2009; Josephs et al., 2017), non-AD age-related degeneration (Bakkour et al., 2013; Pichet Binette et al., 2020), or indirect downstream neurodegeneration. In addition, even in tau-positive regions, measurable neuronal degeneration may not occur immediately (Kuchibhotla et al., 2014; La Joie et al., 2020). Therefore, MRI-measured neurodegeneration is a sub-optimal

proxy for tau pathology, despite occasional statements to the contrary (Torok et al., 2018). The emergence of tau-PET creates an opportunity to more directly investigate whether tau patterns in AD coalesce with the human connectome architecture, which can provide further evidence of synaptic spread of tau.

Several studies have begun to undertake this line of investigation. A number of studies demonstrated that "natural" patterns of tau-PET covariance resemble (Jones et al., 2017) or overlap with (Hoenig et al., 2018; Pereira et al., 2019) resting-state functional networks. Ossenkoppele and colleagues showed tau covariance patterns seeded from certain regions overlapped substantially with functional connectivity patterns seeded from the same region (Ossenkoppele et al., 2019). Similarly, Adams et al. showed a strong spatial overlap between entorhinal cortex functional connectivity and tau-PET signal in cognitively unimpaired elderly, even in those without measurable brain Aβ (Adams et al., 2019). One study further showed that regions with a high degree of connectivity to the rest of the brain show higher tau-PET signal, perhaps implicating these regions as hubs for propagating tau pathology (Cope et al., 2018) (Fig 1.9). Along similar lines, Franzmeier and colleagues found that whole-brain functional connectivity patterns correlate with whole-brain tau-covariance pattern, perhaps suggesting tau distribution is constrained by connectivity (Franzmeier et al., 2019). The same lab went on to show similar results using longitudinal tau-PET data, suggesting regions that accumulate tau at similar rates also tend to be regions that coactivate at rest (Franzmeier et al., 2020).

All of the above studies suggest a strong relationship between macroscale functional connectivity patterns and the spatial distribution of tau-PET signal. On the surface, this certainly provides additional evidence to the notion of tau spreading through synaptic connections even in humans. However, the work of Franzmeier and colleagues in particular highlights another point worth consideration. The authors found that tau-PET distribution and accumulation resembles *global* patterns of functional connectivity (Franzmeier et al., 2019; Franzmeier et al., 2020). In other words, regions more globally connected tend to express more tau pathology, and those regions more isolated tend to express less. Along with findings from Cope et al. (Cope et al., 2018)(Fig 1.9), these results may instead (or in addition) indicate a specific vulnerability of highly connected regions. This is a sentiment echoed by other groups using other imaging modalities and across various brain disorders (Buckner et al., 2009; Crossley et al., 2014). Additionally, distributed association cortex that expresses tau pathology in late stages also shares many other features, including greater variability in individual connectivity, more long-distance connections, and greater evolutionary expansion (Mueller et al., 2013). Therefore, it is difficult to disentangle whether these results reflect tau depositing in synaptically connected regions,

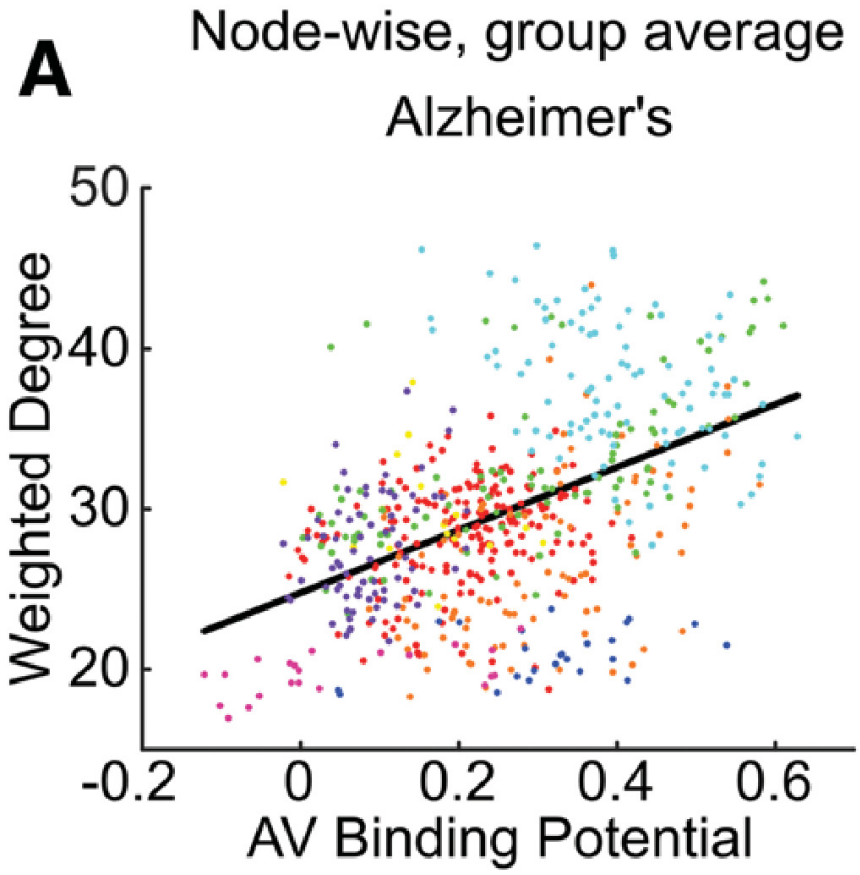

Figure 1.9: Association between flortaucipir signal and whole-brain functional connectivity, reproduced from Cope et al., 2018. Each dot is a reach of interest, and the colors indicate assignment to one of the canonical resting state fMRI networks. The x-axis represents flortaucipir signal, whereas the y-axis represents degree of whole-brain connectivity. Regions with greater connectivity to the rest of the brain (hubs) tend to accumulate more tau-PET tracer binding.

regions that share features (including high connectivity) making them vulnerable to tau, or both.

However, improvements to these approaches can be made in order to further investigate the link between connectivity and tau accumulation. Regions that are functionally connected do not necessarily exhibit direct anatomical connections (Jbabdi et al., 2015; Suárez et al., 2020), and supplementing these results with similar approaches using diffusion imaging tractography would be informative. In addition, these above studies mostly describe correlations or overlap between tau covariance and connectivity, but do not model tau spread. Previous studies have utilized diffusion models to simulate the propagation of signal from an "epicenter" through the human connectome, comparing the results to atrophy patterns in various disease (Raj, Kuceyeski, and Weiner, 2012; Iturria-Medina et al., 2014; Torok et al., 2018; Acosta et al., 2018; Zheng et al., 2019). This approach simulates an epidemic-like

spreading that includes secondary and tertiary seeding events, and therefore may be an excellent model for the hypothetical spread of tau. No studies have thus far extended these models to tau-PET data (but see Chapter 3 below), though Franzmeier et al. applied a simplistic model that explained a considerable amount of tau-PET spatial variance (Franzmeier et al., 2020). Finally, a recent paper showcased prediction of individual-level atrophy patterns in frontotemporal dementia using connectivity information (Brown et al., 2019). This landmark study highlights an eventual goal for tau-PET neuroimaging analyses; ideally, individual-tailored information can be used to sensitively predict and/or track disease progression. The only tau-PET study to examine connectivity and tau-PET correlations at the individual level achieved fairly modest results (Franzmeier et al., 2020).

The study of *in vivo* spread of tau in human AD is still quite young. Future studies should focus on modeling dynamic spread of tau pathology, and ideally should incorporate information relating to other pathologies (namely Aβ, e.g. Iturria-Medina et al., 2017) or *a priori* indices of regional vulnerability (e.g. Zheng et al., 2019). Further effort could also be put toward understanding the individual contributions of connectivity, vulnerability and variability to the progression of tau pathology. Finally, the application of such models to individual-level tau progression would be a welcome complement to the more simplistic and group-average clinical tools currently receiving more attention.

1.5.3 Systematic variation in human *in vivo* tau patterns

As noted earlier, tau progressions distinct from the Braak staging paradigm have been consistently observed, but remain poorly characterized. There are a number of reasons this is the case. Animals used in AD experiments are highly inbred and near genetic clones, making them poor vessels for the study of heterogeneity. Most of the pioneering work to this point has been performed in autopsy studies. The characterization of systematic variation generally requires rather large samples, which are difficult to accumulate. Furthermore atypical and early onset variants of AD are far less common compared to typical cases. Such patients also tend to die in later stages of disease progression, by which time tau can have accumulated throughout the cortex, potentially obliterating signs of distinct progression. In addition, regional tissue sampling tends to be relatively sparse and coarse, and may miss out on important spatial information. This includes the fact that such samples come from only one hemisphere, making the study of asymmetric hemispheric spread challenging.

MRI studies can circumvent some of the aforementioned limitations. Serial MRI can be performed, and amassing larger samples is less challenging. Patients can be

scanned in earlier disease stages with greater frequency, and whole-brain sampling is far easier to achieve. Of course, as noted above, MRI is measuring neurodegeneration, which is a poor proxy for tau pathology. MRI and tau patterns seem to match fairly well in atypical variants (Ossenkoppele et al., 2015c; Ossenkoppele et al., 2016a; Bejanin et al., 2017a), and unbiased clustering using MRI has repeatedly identified cortical- and limbic-predominant phenotypes (Habes et al., 2020) that resemble those described in the autopsy literature (Murray et al., 2011b). However, such studies also frequently described "diffuse", "minimal-atrophy" or subcortical subtypes (Habes et al., 2020), which likely are not reflective of variation in tau pathology. Application of tau-PET to the study of AD heterogeneity is a natural and obvious next-step. Unlike some of the other topics discussed in this literature review, in this case, tau-PET may add more than just *in vivo* validation, but may lead to new discoveries entirely. The challenge, then, is amassing samples large and diverse enough to effectively represent population variation in AD expression, and choosing the right tools to do so.

At the time of writing, very few studies probing individual variability in tau-PET patterns have emerged. As noted earlier, atypical, early onset variants of AD also express atypical tau-PET patterns (Ossenkoppele et al., 2016a; Tetzloff et al., 2018). Early tau-PET work noted individuals that did not fit expected Braak staging patterns, though the numbers were quite low, perhaps due to rather loose staging procedures or choices on abnormality thresholds (Cho et al., 2016a; Schwarz et al., 2018). One of these groups followed up this observation and studied the atypical individuals more formally, but the sample size consisted of only 12 atypical individuals (1/4 of the total sample) (Charil et al., 2019).

Two separate recent studies incorporated semi-supervised approaches to assess tau-PET subtypes, by clustering patients on a highly constrained set of regions. Whitwell et al. clustered individuals based on tau-PET signal in the entorhinal cortex and a cortical composite ROI. This study described a cortical predominant group, a general high tau group and a general low tau group. The study was generally underpowered, but the cortical-predominant group matched other descriptions of this phenotype (younger, less APOE4 carriers, more atypical presentation) (Whitwell et al., 2018). These results did replicate findings from a recent unsupervised pathology study with a similar sample (Petersen et al., 2019), which bodes well for the tracer, but perhaps less well for the choice of methodology and sample sizes used by both studies. Ossenkoppele and colleagues used a large multi-center cohort to cluster based on MRI atrophy in the hippocampus, parietoccipital cortex and frontal cortex, and examined tau-PET patterns of the resulting MRI-derived patient clusters (Fig 1.10). This study replicated commonly observed atrophy-based subtypes and associations,

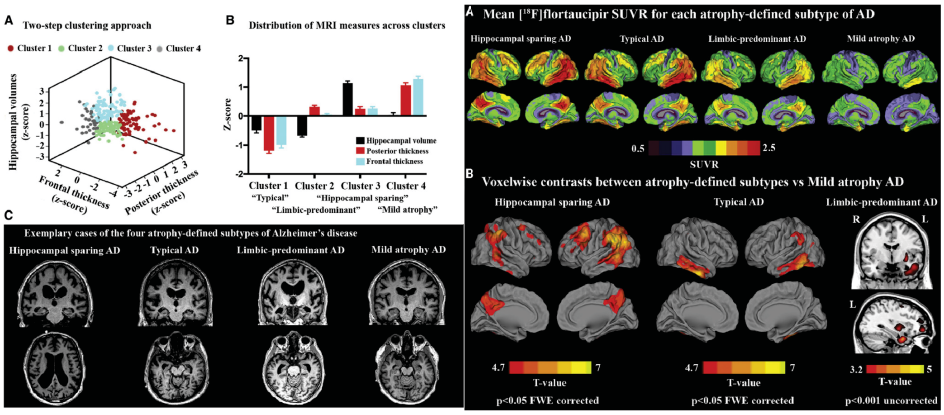

Figure 1.10: Tau-PET patterns in semi-supervised atrophy-based AD subtypes, adapted from (Ossenkoppele et al., 2019). (LEFT) Individuals were clustered based on MRI-derived atrophy in three ROIs, resulting in four subtypes consistent with previous literature. (RIGHT) Flortaucipir signal binding patterns for each subtype.

and found tau-PET patterns to vary in these groups. Limbic-predominant subjects had less tau overall but had the most signal in the MTL, cortical predominant groups had spared MTL binding, and minimal-atrophy subtypes also showed minimal tau (Ossenkoppele et al., 2020).

The studies above represented important steps in validating the existence of pathologiclly-defined subtypes *in-vivo* using tau-PET imaging. However, the studies provide little in the way of novel or exploratory analyses. Two additional studies attempted unsupervised, multi-modal partitioning that incorporated tau-PET data. Jeon et al. clustered vertex-wise tau-PET, Aβ-PET and cortical thickness data from 83 AD patients. The study once again discovered limbic-predominant, cortical-predominant and diffuse atrophy subtypes, and described oft-reported demographic and genetic differences between them. However, this study used the THK-5351 tau tracer, and given the multimodal nature of the results, it is difficult to ascertain the individual contribution of tau (or MAO-B?) to the phenotype(Jeon et al., 2019). Another multi-modal study applied a Bayesian cross-decomposition algorithm to discover canonical associations between neurodegeneration (measured with both tau-PET and atrophy) and cognition. This approach did not involve the clustering of individuals per se, but the latent factors it produced were relevant. Along with an MTL memory factor, the analysis revealed a posterior cortical executive factor and a left temporal language factor, reminiscent of PCA and lvPPA, respectively (Sun et al., 2019) This analysis hints that atypical pathological profiles of AD may be extreme instances of typically occurring latent pathological expression. This notion converges with earlier descriptions (section 1.5.1) of partial independence of tau covariance in various cortical structures, again suggesting the behavior of tau in the association cortex is not well characterized.

In all, these studies continue to affirm the existence of heterogeneous expression of

tau pathology in AD. However, each study has many caveats, and the general sense is that investigation into the details of AD subtypes is just beginning. The most obvious missing piece is a large systematic and unbiased characterization of variability of tau-PET images, somewhat akin to the original Murray et al. study (Murray et al., 2011b). The salient features are known – there is little doubt that limbic-predominant and cortical-predominant subtypes will emerge. However, the spatiotemporal evolution of these subtypes has not been characterized, and it is unclear whether other subtypes may emerge with more unbiased spatial representation. The link between clinical variants in AD and typical AD subtypes is also not understood, and the fact that posterior and highly lateralized subtypes have not emerged in unsupervised studies is puzzling. Once the heterogeneity of tau progression is more firmly established, more concentrated efforts can be undertaken to better understand why this systematic variation occurs. Such analyses might include focused transcriptomic studies, studies of cell-type variation, connectomic variation, and genetic association. As of now, almost nothing is known about the etiology of AD subtypes.

1.6 Summary and conclusions

Tau is a highly conserved protein involved in synaptic plasticity and axonal transport. It's functions appear to be important, if not redundant, in both brain development, maintenance and plasticity. However, tau is also a primary pathology in AD, as well as numerous other dementing syndromes, including various forms of FTLD. Given the prevalence of these disorders, particularly AD, this suggests that tau dysfunction is among the leading causes of death in older humans. Tau dysfunction is also ubiquitously associated with insidious degeneration of noradregenergic and cholinergic nuclei over the lifespan, making it a suspect in age-related cognitive decline. Taken together, tau dysregulation represents one of the biggest threats to cognition known to humans.

The study of tau is obfuscated by the complexity of its post-translational modifications, and the radically disparate behavior apparently encoded by its conformational state. The fact that several different conformations can lead to a multitude of different pathological cascades and diverse dementing syndromes begs the question of what benefits can possibly outweigh tau's risks to the human brain. The fairly unique appearance of NFT pathology among mammals suggests recent phylogenetic shifts may be somewhat incompatible with tau biology. We do not know whether pathological tau results from malfunctioning of an endemic mammalian response system (e.g. hypothermia or hibernation), or from an age-related saturation unfit for human post-reproductive longevity, an example of antagonistic pleiotropy, or something

else entirely. There are also likely many features of tau physiology and function that remain undiscovered. For instance, the potential role of tau in memory-related processes at the synapse of hippocampal neurons remains poorly understood.

After nearly 40 years of steady research, we still do not know by what mechanisms tau confers neurotoxicity, though considerable progress has been made in understanding how tau spreads through the brain. Elucidation of certain aspects of tau biology and spread point to candidates for therapeutic development. However, there are major discrepancies between the expression of murine models of AD and the actual manifestation of AD in humans. For example, many insights have come from mice expressing MAPT mutations, which cause a completely different tauopathy phenotype in humans. In addition, a great deal of work has taken place examining tau at the synapse of hippocampal neurons, when "hippocampal-sparing" phenotypes of AD are not uncommon. There is also no current animal model for PART, which may or may not be a precipitating phase of the AD process. However, there are many avenues for studying the catalysts to tauopathy in AD and other dementia in humans. Traditionally, such approaches were restricted to examination of post-mortem tissue, but recent developments in fluid markers of tau, *in vivo* tau neuroimaging and single-cell transcriptomics will certainly lead to important advances. Over the last five years, these new techniques have been helpful in validating findings from experimental models in living humans. Hopefully, these findings will instigate "human-first" discoveries, that can be further mechanistically probed in experimental models.

In AD, tau pathology advances along a specific spatiotemporal progression. The work reviewed in this chapter suggests this pattern of accumulation is constrained by an interaction between synaptic connectivity and molecular vulnerability, and that systematic individual differences can moderate one or both of these factors. Most of the evidence supporting these claims comes from *ex vivo* tissue and experimental models, but tau-PET now allows tau progression to be tracked in living humans. We are still in the early years of tau-PET imaging, and almost all studies to date have validated and reinforced earlier findings, albeit with an unprecedented field of view, so to speak. As more data is collected for longer periods of time, further opportunity may arise for tau-PET to lead to novel advances in our understanding of AD. Longitudinal imaging will allow tracking of tau spread in real time for the first time, while large datasets and whole-brain spatial sampling may allow for a less biased "cartography" of tau pathology. In addition, tau-PET will be instrumental for studying aspects of tau pathology that are challenging to reproduce with experimental models, such as PART and AD subtypes. Finally, the clinical utility of tau-PET will be challenged by the ascendance of sensitive assays for plasma-derived phospho-tau.

While the spatial component of tau spread makes it indispensable for basic research into AD, only time will tell if spatial information proves relevant enough to disease diagnosis and progress to be utilized in a clinical setting.

The original work in this thesis began in late 2016, shortly after the first large human tau-PET studies were published, and the last project was finished only recently. Therefore, the work described here spans the early, exploratory phases of tau-PET imaging, through to the current period where tau-PET work is edging toward novel discoveries in AD. These studies herein seek to use tau-PET to validate, extend and challenge what we know about tau distribution and progression in AD.

Chapter 2

Data-driven approaches for Tau-PET imaging biomarkers in Alzheimer's disease

[1]

Jacob W. Vogel, Niklas Mattsson, Yasser Iturria-Medina, Olof T. Strandberg, Michael Schöll, Christian Dansereau, Sylvia Villeneuve, Wiesje M. van der Flier, Philip Scheltens, Pierre Bellec, Alan C. Evans, Oskar Hansson, Rik Ossenkoppele

2.1 Preamble

The work contained in this Chapter began in late 2016, less than a year after the first large tau-PET studies had been published. Those early studies quickly showed by various means that Braak stages fit the tau-PET data well (Johnson et al., 2016; Schöll et al., 2016b; Schwarz et al., 2016; Cho et al., 2016a). However, no study at the time had used unsupervised methods to explore the hierarchical structure intrinsic to the tau-PET images. This was a necessary step for two reasons. First, early tau-PET data suggested the presence of considerable off-target binding issues (Marquié et al., 2015; Schöll et al., 2016b). Therefore, an unbiased investigation of the influence of this signal on tau-PET images was needed. Second, to simply fit tau-PET data to a scheme based on neuropathology data undermines the advantages in spatial sampling and *in vivo* nature offered by tau-PET. If tau progresses in a uniform pattern across individuals, an unsupervised analysis on a large enough sample should reveal

[1] This article was reproduced from *Human Brain Mapping* with permissions from John Wiley & Sons

various stages along this progression. [2] The objective of the present analyses was to approach the tau-PET data in a hypothesis-free manner, and try to make sense out of what the data revealed.

Another controversy that was popular around the time this work began was how to effectively summarize the tau-PET data into ROIs without losing important information. As an indication, a few studies were published in 2017 explicitly addressing this concept (Maass et al., 2017; Mishra et al., 2017). A secondary objective of the present study was to test whether data-driven ROIs could prove superior to ROIs from previous studies, which were mostly derived based on findings from the neuropathology literature.

A number of studies with similar objectives were published before the work from this Chapter was officially published (discussed in Sections 1.5.1, 5.1.1). However, the first version of this paper was not far behind, published on *BioRxiv* in January 2018. The final version of the manuscript was published online in *Human Brain Mapping* October 2018, and in print in early 2019 (Vogel et al., 2019a).

2.2 Abstract

Previous positron emission tomography (PET) studies have quantified filamentous tau pathology using regions-of-interest (ROIs) based on observations of the topographical distribution of neurofibrillary tangles in post-mortem tissue. However, such approaches may not take full advantage of information contained in neuroimaging data. The present study employs an unsupervised data-driven method to identify spatial patterns of tau-PET distribution, and to compare these patterns to previously published "pathology-driven" ROIs. Tau-PET patterns were identified from a discovery sample comprised of 123 normal controls and patients with mild cognitive impairment or Alzheimer's disease (AD) dementia from the Swedish BioFINDER cohort, who underwent [18F]AV1451 PET scanning. Associations with cognition were tested in a separate sample of 90 individuals from ADNI. BioFINDER [18F]AV1451 images were entered into a robust voxelwise stable clustering algorithm, which resulted in five clusters. Mean [18F]AV1451 uptake in the data-driven clusters, and in 35 previously published pathology-driven ROIs, was extracted from ADNI [18F]AV1451 scans. We performed linear models comparing [18F]AV1451 signal across all 40 ROIs to tests of global cognition and episodic memory, adjusting for age, sex and education. Two data-driven ROIs consistently demonstrated the strongest or near-strongest effect sizes across all cognitive tests. Inputting all regions plus demographics into

[2] The samples used in this Chapter would probably not qualify as "large enough", but they rival or exceed sample sizes of most papers preceding it.

a feature selection routine resulted in selection of two ROIs (one data-driven, one pathology-driven) and education, which together explained 28% of the variance of a global cognitive composite score. Our findings suggest that [18F]AV1451-PET data naturally clusters into spatial patterns that are biologically meaningful and that may offer advantages as clinical tools.

2.3 Introduction

Alzheimer's disease (AD) is neuropathologically defined by the presence of widespread extracellular plaques containing amyloid-β and intracellular neurofibrillary tangles consisting of aggregated tau proteins (Braak and Braak, 1991; Masters et al., 1985). While amyloid-β may be present decades prior to symptom onset (Jansen et al., 2015), the presence of neocortical tau is temporally more closely related to current cognitive status and degree of neurodegeneration, as convincingly demonstrated by studies utilizing post-mortem tissue, animal models, cerebrospinal fluid and, more recently, the positron emission tomography (PET) tracer [18F]AV1451 (Arriagada et al., 1992; Van Rossum et al., 2012; Nelson et al., 2012; Ossenkoppele et al., 2016a; Bejanin et al., 2017a; Cho et al., 2017). [18F]AV1451 binds paired helical filaments of tau with high affinity and selectivity (Xia et al., 2013; Chien et al., 2013; Marquié et al., 2015; Lowe et al., 2016; Marquié et al., 2017), and can be used to investigate the distribution of tau pathology in the living human brain. Several studies have shown strong spatial resemblance between in vivo tau PET patterns and neuropathological staging of neurofibrillary tangles as proposed by Braak and Braak (Schöll et al., 2016b; Schwarz et al., 2016; Cho et al., 2016a), reflecting prototypical progression from (trans)entorhinal (stage I/II) to limbic (stage III/IV) to isocortical (stage V/VI) regions (Braak and Braak, 1991). Furthermore, regional [18F]AV1451 retention co-localizes with sites of brain atrophy or hypometabolism (Ossenkoppele et al., 2016a; Xia et al., 2017) and has been associated with impairments in specific cognitive domains (Ossenkoppele et al., 2016a; Bejanin et al., 2017a; Cho et al., 2017).

Given this strong regional specificity of tau pathology, it is important to consider how regions-of-interest (ROIs) are defined, as they could potentially impact study outcomes. To date, most studies employing tau-PET tracers involved ROIs constructed based on neuropathological studies. For example, some studies mimicked the Braak stages in vivo (Schöll et al., 2016b; Schwarz et al., 2016; Cho et al., 2016a), while others selected specific regions reflecting early (e.g. entorhinal cortex) or more advanced (e.g. inferior temporal cortex) disease stages (Johnson et al., 2016). These approaches have several advantages as they are supported by fundamental research and enhance generalizability across studies. However, compared to neuroimaging,

neuropathological data typically include only a few slices in a constrained number of brain regions, and brain tissue is affected by death (Scheltens and Rockwood, 2011). Additionally, tau PET signal does not equal presence of tau pathology. There are several sources of [18F]AV1451 signal and noise, including target binding, off-target binding (e.g. Monamine oxidase, neuromelanin, vascular lesions, iron), non-specific binding and imaging related noise (e.g. partial volume effects) (Marquié et al., 2015; Schöll et al., 2016b; Lowe et al., 2016; Lockhart et al., 2017b; Ng et al., 2017; Choi et al., 2018). An alternative approach could therefore be to select ROIs based on data-driven approaches (Dickerson et al., 2011; Landau et al., 2011; Pankov et al., 2016; Grothe et al., 2017), thereby taking full advantage of the abundance of information contained in neuroimaging data, but also accounting for the idiosyncrasies of PET imaging data.

In light of ongoing efforts to define appropriate ROIs and determine tau PET-positivity, it is important to compare data-driven approaches (agnostic, "where is the tau?") with theory-derived ROIs based on post-mortem studies (directed, "is the tau here?"). In the present study, we applied an unsupervised algorithm to identify clusters of [18F]AV1451 signal and compared the spatial patterns of these clusters with neuropathologically derived ROIs described in previous publications. As a secondary analysis, we tested which ROIs best correlated with global cognition in an independent cohort of cognitively normal, mild cognitive impairment and AD dementia subjects. We hypothesized that our data-driven approach would corroborate neuropathological findings, but would also present novel information leading to enhanced associations with cognition.

2.4 Material and Methods

2.4.1 Participants

Two separate cohorts were included in this study. Participants from the Swedish BioFINDER study were used to perform clustering analysis on [18F]AV1451 data, whereas participants from the Alzheimer's Disease Neuroimaging Initiative (ADNI) were used to test associations between the clustering-derived ROIs and cognition. This design allowed us to not only probe the patterns of spatial covariance of [18F]AV1451, but also to assess these utility of these patterns as a general [18F]AV1451 biomarker without concern of overfitting or "double-dipping" (c.f. Kriegeskorte et al., 2009). Demographic, clinical and biomarker information for both cohorts are presented in Table 2.1.

	Controls		MCI		AD		Total	
	BioF	**ADNI**	**BioF**	**ADNI**	**BioF**	**ADNI**	**BioF**	**ADNI**
n	55	43	21	37	47	10	123	90
Age (SD)	**75 (6.2)**	**70.3 (5.9)**	70.8 (10.9)	72 (6.8)	70.1 (8.6)	73.3 (4.3)	72.4 (8.4)	71.3 (6.1)
% Male	50.90%	46.50%	57.10%	67.60%	55.30%	60.00%	53.70%	56.70%
Education	**12 (3.7)**	**16.1 (2.4)**	**11.7 (3.7)**	**16.9 (2.7)**	**12.2 (3.2)**	**15.0 (3.0)**	**12.0 (3.5)**	**16.3 (2.6)**
% Amyloid+	43.60%	33.30%	**100%**	**44%**	100%	100%	**73.30%**	**44.80%**
MMSE	29.1 (1.1)	29.0 (1.3)	**25.7 (2.8)**	**28.4 (2.0)**	**21.2 (5.1)**	**25.5 (5.1)**	**25.5 (4.9)**	**28.3 (2.5)**

Table 2.1: **BOLD** text indicates significant difference (p<0.05) between cohorts, as measured by t-test, or Fisher's Exact Tests.
ADNI = Alzheimer's Disease Neuroimaging Initiative; BioF = BioFINDER, MMSE = Mini-Mental State Examination; SD = Standard Deviation

The BioFINDER cohort is a multi-site study designed for the purpose of developing biomarkers for neurodegenerative diseases. More information can be found at http://biofinder.se. Study participants included 55 subjects with normal cognition, 21 with mild cognitive impairment (MCI), and 47 with Alzheimer's dementia, who had complete MRI and [18F]AV1451 PET data (Table 2.1). Patients with MCI were referred to a memory clinic and demonstrated objective cognitive impairment that could not be explained by another condition. AD dementia patients met criteria for the DSM-V (American Psychiatric Association, 2013) and NINCDS-ADRDA (McKhann et al., 2011) for probable AD, established by clinicians blinded to PET data. To optimize overlap with the ADNI cohort, dementia patients were only included if they presented with an amnestic-predominant phenotype. Both dementia and MCI patients were only included in this study if they demonstrated abnormal Aβ1-42 levels in the CSF (INNOTEST, cut-off: 650 ng/l; Palmqvist et al., 2015). The sample of controls selected for [18F]AV1451 scanning was intentionally enriched for β-amyloid positivity to include people in the preclinical stage of AD (see Table 2.1). This enrichment was achieved by ensuring that 50% of the cognitively normal participants invited for [18F]AV1451 imaging had shown positive PET or CSF β-amyloid measurements at previous visits. PET imaging for the study was approved by the Swedish Medicines and Products Agency and the local Radiation Safety Committee at Skåne University Hospital, Sweden. All participants provided written informed consent according to the Declaration of Helsinki, and ethical approval was given by the Ethics Committee of Lund University, Lund, Sweden.

ADNI is a multi-site open access dataset designed to accelerate the discovery of biomarkers to identify and track AD pathology (adni.loni.usc.edu/). The current study included all ADNI individuals with complete [18F]AV1451 scans that were available in November, 2016. This included 43 cognitively normal elderly controls, 37 patients with MCI, and 10 patients with a recent diagnosis of Alzheimer's dementia (Table 2.1). In addition to imaging data, age, sex, education, diagnosis, amyloid-β status on [18F]florbetapir PET (Landau et al., 2013), and scores from six tests

measuring global cognition or activities of daily living were downloaded from the ADNI-LONI website (adni.loni.usc.edu). The cognitive tests were as follows: Mini-Mental State Examination (MMSE) (Folstein, Folstein, and McHugh, 1975); Clinical Dementia Rating Sum of Boxes (CDRSB) (Hughes et al., 1982); Alzheimer's disease Assessment Scale 11 (ADAS11) (Rosen, Mohs, and Davis, 1984) and 13 (ADAS13) (Mohs et al., 1997); Everyday Cognition (ECog) (Farias et al., 2008); Functional Activities Questionnaire (FAQ) (Pfeffer et al., 1982). We also downloaded the ADNI-MEM score, an episodic memory composite score provided by ADNI (Crane et al., 2012).

2.4.2 Imaging

[18F]AV1451 images were processed using separate but nearly identical pipelines across the two cohorts. Acquisition and processing procedures for [18F]AV1451 processing in the BioFINDER cohort has been described elsewhere (Hansson et al., 2017). Scans were reconstructed into 5-min frames and motion corrected using AFNI's 3dvolreg (https://afni.nimh.nih.gov/). Mean [18F]AV1451 images were created over a time-window of 80-100 minutes post-injection, and these images were coregistered to each subject's T1 image in native space. Mean images were then intensity normalized using a complete cerebellar gray reference region to create standard uptake value ratio (SUVR) images. Coregistered MRI images were normalized to the MNI-ICBM152 template using Advanced Normalization Tools (https://stnava.github.io/ANTs/) and the transformation parameters were applied to the SUVR images. Finally, SUVR images were smoothed with an 8mm FWHM Gaussian filter.

For the ADNI cohort, mean 80-100 min [18F]AV1451 images, as well as MPRAGE images closest to [18F]AV1451 scans, were downloaded from the ADNI-LONI website. Details on acquisition procedures for these [18F]AV1451 and MRI images can be found elsewhere (http://adni.loni.usc.edu/methods/documents/). [18F]AV1451 images were processed in accordance to procedures described in (Schöll et al., 2016b). Briefly, T1 images were processed using Freesurfer v5.3 and [18F]AV1451 images were coregistered to native T1s using Statistical Parametric Mapping 12 (www.fil.ion.ucl.ac.uk/spm/). SUVR images were created using a cerebellar gray reference region and images were normalized to MNI space using the parameters from the coregistered T1. Figure 2.1 shows mean [18F]AV1451 SUVR images stratified by diagnosis and amyloid status for each cohort.

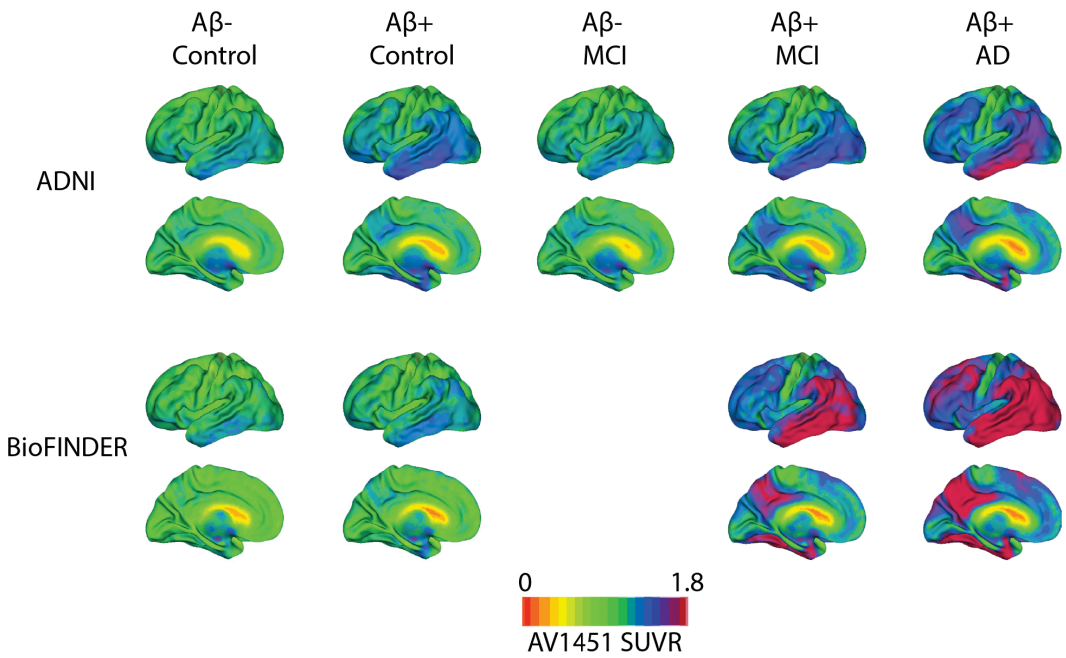

Figure 2.1: Mean [18F]AV1451 SUVR images stratified by amyloid status and disease stage, across both the ADNI (top) and BioFINDER (bottom) cohorts.

2.4.3 Clustering of [18F]AV1451 data

Our primary analysis involved the derivation of data-driven ROIs by using unsupervised machine learning to elucidate stable patterns of [18F]AV1451 signal covariance across a cognitively diverse dataset. Cross-subject [18F]AV1451-PET covariance networks were derived from all 123 BioFINDER [18F]AV1451 images using an open-source unsupervised consensus-clustering algorithm called Bootstrap Analysis of Stable Clusters (BASC; Figure 2.2) (Bellec et al., 2010). BASC is a two-step consensus-clustering algorithm that enhances the stability of the clustering process by repeatedly clustering bootstrapped samples of the input data, and deriving the final partition from this stability matrix, rather than the original data (c.f. Fred and Jain, 2005). This approach offers two advantages in the context of this study. First, the stochastic nature of many clustering algorithms tends to lead to different solutions depending on their initialization state, whereas BASC performs clustering on a stability matrix generated from many solutions (and thus many initializations). This leads to greater reproducibility in the clustering solutions generated by BASC. Second, because the initial set of clustering analyses is performed on bootstrap samples of the input data, the final solution is less dependent on the clinical composition of the input data.

BASC was adapted to 3D [18F]AV1451 data by stacking all 123 BioFINDER [18F]AV1451 images along a fourth (subject) dimension, creating a single 4D image to be submitted as input. BASC first reduces the dimensions of the data with a previously described region-growing algorithm (Bellec et al., 2006), which was set to

extract spatially constrained atoms (small regions of redundant signal) with a size threshold of 1000mm3. In order to reduce computational demands, the Desikan-Killiany atlas (Desikan et al., 2006) was used as a prior for region constraint, and the data was masked with a liberal gray matter mask, which included the subcortex but had the cerebellum manually removed (since this was used as the reference region for [18F]AV1451 images). The region-growing algorithm resulted in a total of 730 atoms, which were included in the BASC algorithm. BASC next performs recursive k-means clustering on bootstrapped samples of the input data. After each clustering iteration, information about cluster membership is stored as a binarized adjacency matrix. The adjacency matrices are averaged resulting in a stability matrix representing probabilities of each pair of atoms clustering together (Figure 2.2). Finally, hierarchical agglomerative clustering with Ward criterion is applied to the stability matrix, resulting in the final clustering solution. The process is repeated over several clustering solutions (k=1 - 50), and the MSTEPs method (Bellec, 2013) was implemented to find the most stable clustering solutions at different resolutions. In the interest of multiple comparisons, and similarity to Braak neuropathological staging (i.e. six ROIs), we chose the lowest resolution solution for subsequent analysis (though the other two solutions are visualized). Note that no size constraints were imposed on clustering solutions (except at the level of atom-size in the region-growing – see above). Cluster-cores were determined as voxels where cluster probability membership exceeded 0.5 (BASC default setting), eliminating unstable voxels from analysis (Bellec et al., 2010; Garcia-Garcia et al., 2017). After determining cluster-cores in the BIOFINDER cohort, we extracted the average [18F]AV1451 SUVR for each cluster core from all ADNI subjects, and these values were used for subsequent analysis investigating associations with cognition.

The choice of the k-means algorithm for the initial clustering and hierarchical clustering with ward criterion for partitioning the stability matrix are somewhat arbitrary. K-means is a particularly fast algorithm and therefore lends itself well to bootstrapping. Meanwhile, the hierarchical clustering routine used in BASC is an appropriate algorithm for the stability matrix, which is a similarity matrix, and it provides solutions at multiple resolutions making it amenable to the BASC framework (Bellec et al., 2010). Both algorithms are standard, well validated, simple and involve few free parameters. This latter point is important, as BASC itself only has a few principle parameters: namely the number of clusters to extract (in this case, determined by MSTEPS), the number of bootstrap samples (in this case, 500), and the size of the bootstrap sample (in this case, the length of the input data – 123 cases) (Bellec et al., 2010; Orban et al., 2015). Other parameters are associated with some of the steps peripheral to the central BASC algorithm, namely the region growing

preprocessing step and MSTEPS algorithm to determine the number of clusters, and these parameters were left to their default settings. Briefly, the region growing includes a threshold parameter limiting the maximum size of "atoms", which is mostly related to computational demand. Meanwhile, MSTEPS works on a sparse grid and includes a parameter specifying the percentage of variance maintained (similar to PCA). In addition, MSTEPS allows the definition of the size of the window within which stable clusters are sought (Bellec, 2013).

2.4.4 Definition of Braak stage ROIs described in other studies

A number of studies have created ROIs mirroring the Braak stages described from pathological studies. To test the utility of our data-driven ROIs vis-à-vis those defined in correspondence to the pathological literature, we recreated the Braak ROIs described in three different studies (Schöll et al., 2016b; Schwarz et al., 2016; Cho et al., 2016a). Schöll, Lockhart et al. and Cho et al. were constructed using regions from the Desikan-Killiany atlas, and we recreated these ROIs in direct correspondence to what has been reported in these two studies. Schwarz et al. instead generated small ROIs designed to mirror the slabs of cerebral cortex extracted during autopsy for Braak staging. These regions were constructed with a script generously provided by the authors. For all analyses, Braak ROIs were included both individually ("single") and cumulatively ("stage"). For example, for Braak Stage III, one ROI was created containing all regions from Braak I, II, and III included ("stage"), as well as a ROI created including only regions in Braak III ("single"). Finally, some studies have chosen to use only the bilateral inferior temporal lobe from the Desikan-Killiany atlas to summarize global tau burden (Johnson et al., 2016), so we included this region in subsequent analysis as well. Studies also frequently used the bilateral entorhinal cortex from this atlas, and it should be noted that this region is also included, namely as Stage I from Cho et al. and Schöll, Lockhart et al. Size-weighted average [18F]AV1451 SUVR was extracted for each ROI (35 in total) for each subject.

2.4.5 Similarity between data-driven clusters, anatomical ROIs and Braak Stage ROIs

We compiled descriptive information about the similarity between our cluster-derived ROIs and the Braak ROIs from the literature. For comparisons to regions from Schöll, Lockhart et al. and Cho et al., we used normalized mutual information. Due to the small size of the Schwarz et al. regions, comparisons involved measuring the percentage of each Schwarz ROI falling inside of each cluster-derived ROI.

2.4.6 Reproducibility of [18F]AV1451 clustering solution

After clustering [18F]AV1451 data using BASC (section 2.4.3), we assessed whether we could reproduce these clusters in a separate dataset. BASC was therefore run on 90 [18F]AV1451 scans from ADNI with the exact same parameters used for the BioFINDER dataset. MSTEPS was again used to define the number of clusters. In order to compare the clustering solution to the solution found in the BioFINDER sample, we matched clusters from the ADNI sample to the most spatially similar clusters from the BioFINDER sample, and harmonized the numeric labels between the two solutions. As a qualitative analysis, we extracted voxels that were part of the same cluster in both clustering solutions. The resulting voxels can be thought to represent regions that demonstrated consistent clustering behavior ([18F]AV1451 signal covariance) across the two samples. For each cluster, we calculated the Dice coefficient representing within-cluster agreement between the two clustering solutions. We also performed the same analyses constrained within the cluster-cores from the BioFINDER solution, assuming the agreement should be higher within the cores. We also calculated both the adjusted Rand index and adjusted mutual information score (passing the BioFINDER solution as the "true labels") as a measurement of overall consistency between the two clustering solutions. To put these measurements into context, we performed five 50% splits of the ADNI data and compared clustering solutions between each split. The purpose of this analysis was to identify whether clustering within the ADNI dataset showed greater or less stability compared to the stability between the ADNI and BioFINDER datasets.

2.4.7 Statistical Analysis

Our secondary analyses were aimed to assess the utility and generalizability of our data-driven covariance networks. We performed linear models between these covariance networks and the scores from six different available test scores assessing global cognition and function (see Table 2.S1). In addition, the scores were summarized using Principal Components Analysis (PCA) using Singular Value Decomposition. The PCA was fit to data from the six cognitive test scores, which were scaled to a 0 mean with unit variance. The first component explained 72% of the total model variance, and was used to transform the cognitive data into a single Global Cognition composite score. For each of the cognitive tests, as well as the composite score, separate general linear models for each ROI (40 in total; our five data-driven clusters and 35 ROIs from the literature) were constructed with cognitive test score as the dependent variable and age, sex and education as covariates. We repeated this analysis for the ADNI-MEM score to test the relationship between [18F]AV1451 and

episodic memory in all 40 ROIs. Tests surviving Bonferroni correction for multiple comparisons are reported.

In order to identify a sparse set of non-redundant covariates that best describe the global cognitive data in ADNI, we submitted all 40 tau ROIs plus age, sex and education to a Least Absolute Shrinkage and Selection Operator (Lasso) regression-based feature selection routine. The Lasso uses L1 regularization (coordinate descent) to penalize regression coefficients based on their maximum likelihood estimates, and is therefore an optimal approach to select a small number of variables from a large number of collinear covariates. In the current implementation, the degree of penalization is optimized using 10-fold cross-validation. All tau ROIs and demographics were scaled to be mean-centered with unit variance, and entered into the Lasso regression model with the Global Cognition composite score as the dependent variable. Features selected by the Lasso (absolute beta > 0.25) were entered together into a general linear model (GLM) with MMSE as the dependent variable. Additionally, to ensure our results were representative of global cognition and not specific to the composite score, the fitted values from this GLM were used to predict scores of each of the six cognitive tests. Finally, the Lasso was repeated separately for each of the individual test as well.

With the exception of BASC, all statistics were implemented using the pandas, numpy, scipy and scikit-learn (Pedregosa et al., 2012) packages in Python 3.5.2 (https://www.python.org/).

2.5 Results

2.5.1 Participant characteristics

Table 2.1 contains demographic information, MMSE scores and amyloid positivity rates for both the ADNI and BioFINDER sample. The sample used for clustering (BioFINDER) demonstrated important differences compared to the sample used for testing (ADNI). BioFINDER subjects were less highly educated across the whole sample, and BioFINDER controls were on average older than ADNI controls. Additionally, the BioFINDER sample demonstrated lower MMSE scores across the whole sample compared to ADNI, including within MCI and dementia groups. Finally, 45% of ADNI subjects were amyloid-positive vs. 73% of BioFINDER subjects, which was primarily related to the fact that only amyloid positive MCI patients were included in the BioFINDER sample.

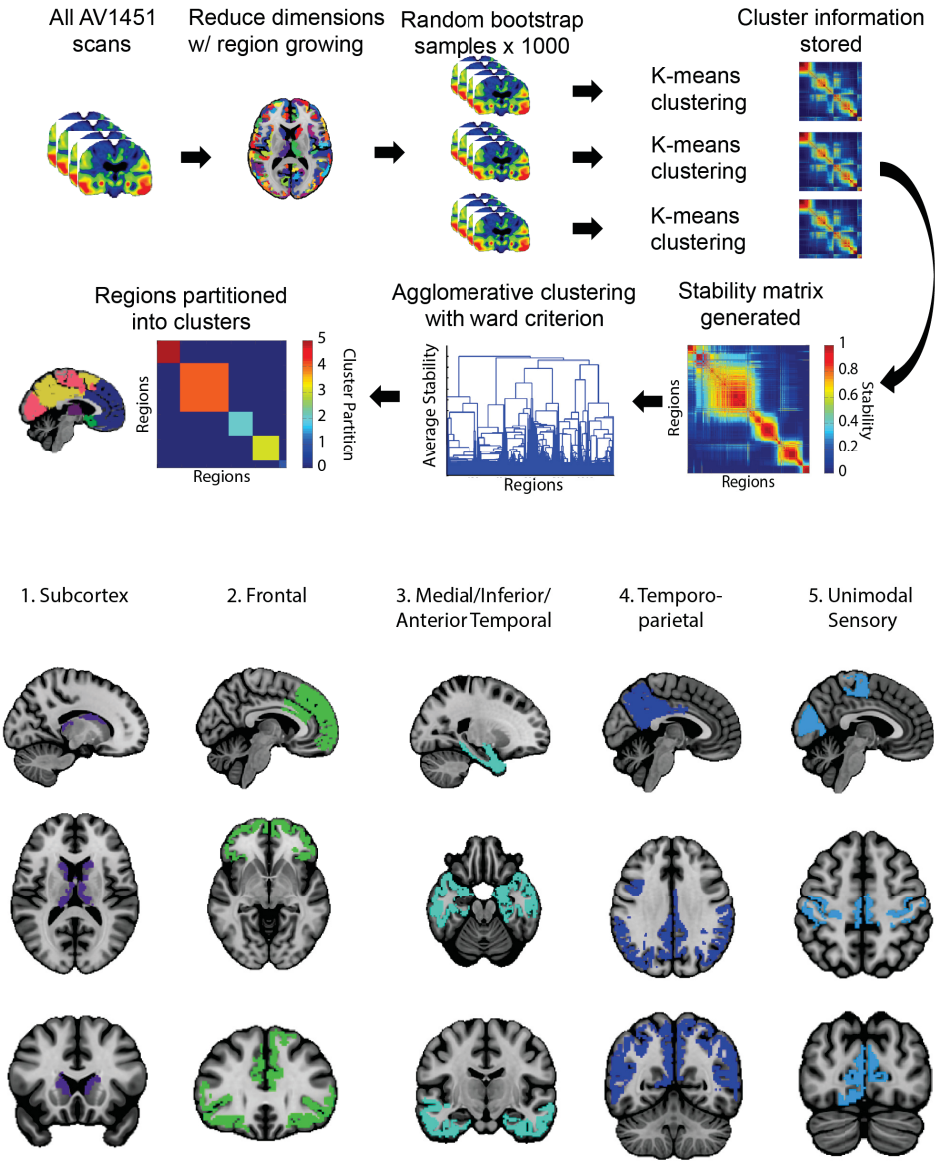

Figure 2.2: [18F]AV1451 scans were entered into a voxelwise clustering algorithm. The optimal solutions were determined using the MSTEPS approach. This resulted in five [18F]AV1451 covariance networks. These networks were masked with a stability threshold of 0.5, and are displayed in the lower half of the figure.

2.5.2 Data-driven Tau-PET covariance networks

123 BioFINDER [18F]AV1451 scans were entered into an advanced clustering algorithm in order to identify networks of regional [18F]AV1451 signal covariance across subjects. The MSTEPS algorithm identified five-, nine- and 32-cluster solutions as optimal solutions. The parcellations generated from the three stable clustering solutions are visualized in Supplementary Figure 2.S1. For the purposes of comparing with Braak stage ROIs, we chose the lowest-resolution solution (k=5) for subsequent analyses, visualized in Figure 2.2. The clusters were interpreted and named as follows: "1: Subcortical", "2: Frontal", "3: Medial/Anterior/Inferior Temporal", "4: Temporo-parietal" and "5: Unimodal Sensory". Cluster 3 bore resemblance to regions

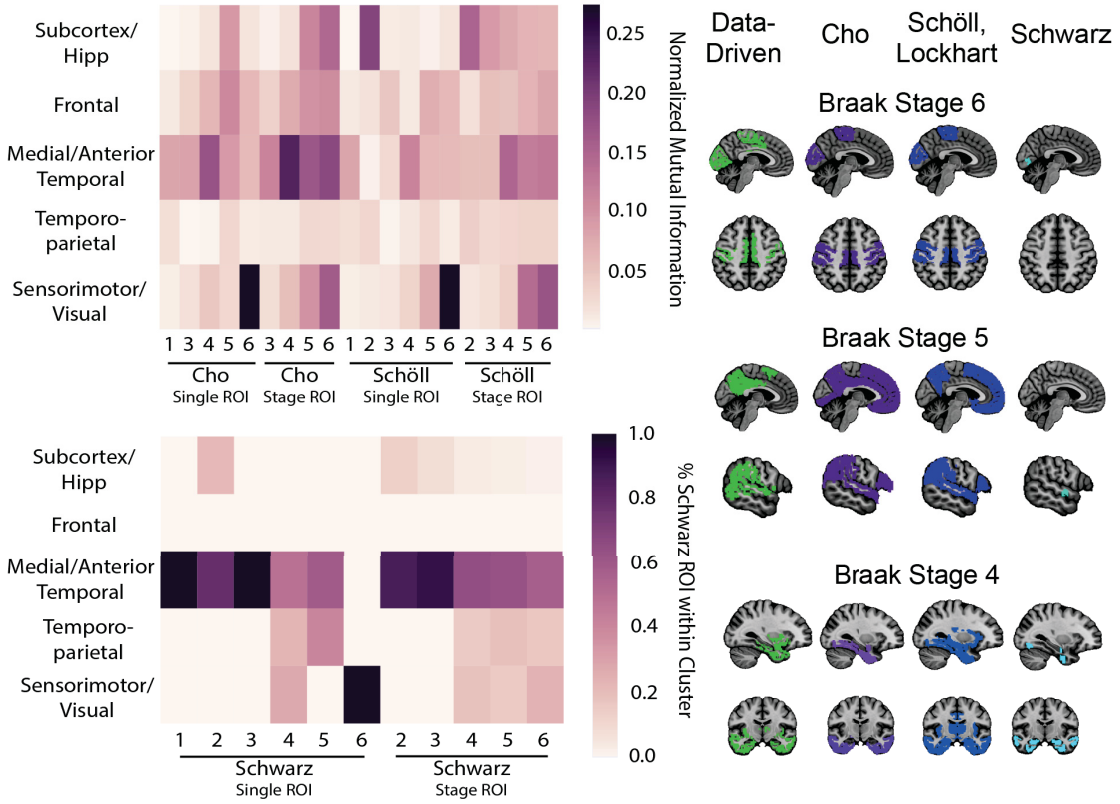

Figure 2.3: [18F]AV1451 covariance networks were compared to previously existing Braak Stage ROIs from the literature using descriptive statistics. The clusters were compared to ROIs from Schöll, Lockhart et al. and Cho et al using Normalized Mutual Information (top left), and were compared to regions from Schwarz et al. using the percentage of Schwarz ROI voxels within each data-driven cluster.

often involved in early tau aggregation and atrophy (Braak and Braak, 1991), while Cluster 4 also appeared similar to regions commonly associated with neurodegeneration in AD (Dickerson et al., 2011; Landau et al., 2011). Of note, the hippocampus was largely unrepresented in any of the cluster-cores, though some voxels in the head of the hippocampus were included in Cluster 3, and a few distributed voxels were included in Cluster 1 (Subcortex). However, using a winner-takes-all clustering approach, the voxels in the hippocampus were almost equally distributed between Cluster 1 and Cluster 3.

2.5.3 Similarity to Braak ROIs

Descriptive metrics were used to quantify the spatial similarity between the data-driven covariance networks and the Braak Stage ROIs introduced in the literature (Figure 2.3). Cluster 5 ("Unimodal Sensory") demonstrated a high degree of overlap with Braak Stage VI across all region sets. Spatial similarity was also evident between

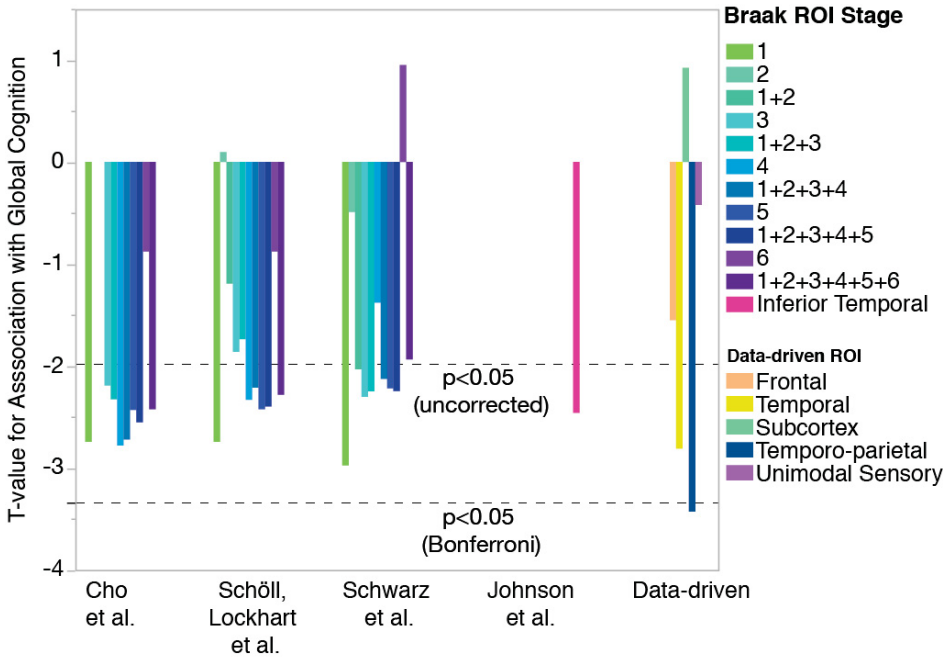

Figure 2.4: General linear models comparing [18F]AV1451 signal to Global Cognition composite scores were run, adjusting for age, sex and education. For each model, a different [18F]AV1451 ROI was used. ROIs included the five clusters identified in our analysis, as well as Braak stage regions taken from three different papers: Schöll et al., 2016b; Schwarz et al., 2016; Cho et al., 2016a. Two versions of each Braak ROI were created, one using regions from that stage only (e.g. Stage 3), and one combining all regions from that stage with all regions from previous stages (e.g. Stage 1+2+3). The effect size (t-value) of each tau ROI is shown. [18F]AV1451 binding in several ROIs demonstrated strong relationships with Global Cognition, though only the data-driven Temporo-parietal region survived multiple comparisons.

Cluster 3 ("Medial/Anterior/Inferior Temporal") and Stage I-IV from Cho et al., and this cluster almost completely circumscribed Stages I-III from Schwarz et al. Cluster 1 ("Subcortex") was most similar to Schöll, Lockhart et al. Stage II, due in part to its inclusion of the hippocampus. Little spatial similarity was evident between Cluster 2 ("Frontal") and any of the Braak Stage ROIs, though some similarity was seen with the Stage V region from Schöll, Lockhart et al. and Cho et al. due to their inclusion of many frontal lobe structures. Similarly, Cluster 4 ("Temporo-parietal") did not demonstrate strong spatial similarity to any of the Braak ROIs, though it did partially overlap with the Braak single IV and V regions from Schwarz et al.

2.5.4 Associations with cognition in ADNI

General linear models were run in the ADNI dataset assessing associations separately between each of 40 tau ROIs (our five data-driven clusters established in the BioFINDER study, and 35 ROIs from the literature) and a Global Cognitive composite score, controlling for age, sex and education (Figure 2.4). [18F]AV1451 signal in several ROIs demonstrated strong associations with global cognition, though only the data-driven Cluster 4 ("Temporo-parietal"; β = -3.24 [SE=0.91], t = -3.43,

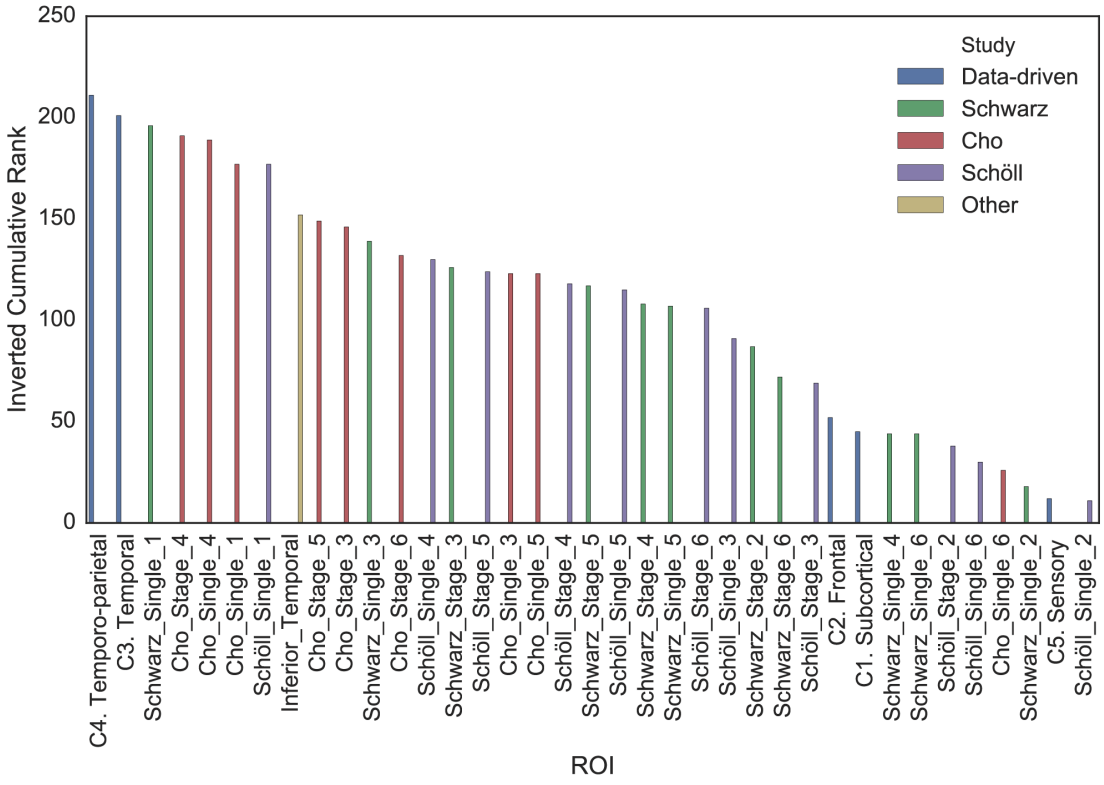

Figure 2.5: For each measure of global cognition, [18F]AV1451 ROIs were ranked from worst to best (such that the worst region would have rank of 1) with respect to the effect size of the association between [18F]AV1451 in that region and the cognitive score. The ranks were then summed across all cognitive measurements and are displayed here. The data-driven Cluster 4 ("Temporo-parietal") ranked the best cumulatively across cognitive tests, with the data-driven Cluster 3 ("Medial/Inferior/Anterior temporal") ranking second best.

$p<0.001$) survived multiple comparisons. To ensure our results were not specific to the Global Cognition composite score, we repeated this analysis using the six individual measures of global cognition and function that composed the composite score (Table 2.S1). The data-driven Cluster 4 ("Temporo-parietal") described global cognition better than all other ROIs using four of the six cognitive measures, and was in the top five for all of them. Across all cognitive measures, Clusters 4 and 3 ("Medial/anterior/inferior temporal") ranked best and second best, respectively, at describing global cognitive data (Figure 2.5). Notably, the Schwarz Stage I ROI also performed well across cognitive measures, except for the MMSE.

Finally, since many ADNI subjects had either MCI or were at early stages of dementia and may not show great variation in tests of global cognition scores, we repeated the above analysis substituting global cognition with a composite measure of episodic memory. (Table 2.S2) shows the top five ROIs with the strongest associations with episodic memory. Although none of the associations survived correction for multiple comparisons, the strongest associations were found with early stage pathological ROIs (resembling (trans)enthorinal cortex), followed by the data-driven temporo-parietal ROI.

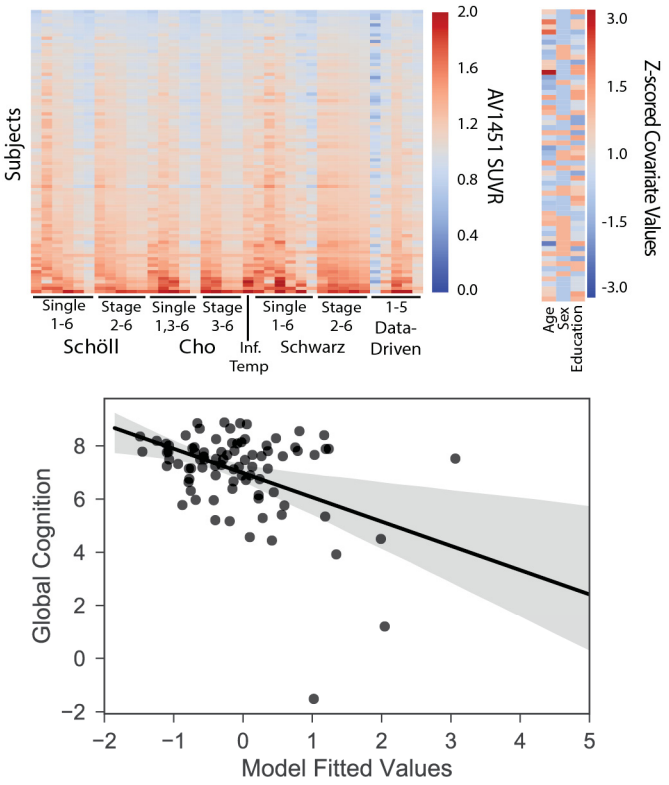

Figure 2.6: [18F]AV1451 ROIs plus age, sex and education were entered into a L1-penalized Lasso regression feature selection routine with the Global Cognitive composite score as the dependent variable. The Lasso selected education and two ROIs: the data-driven Temporo-parietal region, and the Schwarz Single VI region. Together in a general linear model, these features explained 28% of the variance in the Global Cognition score.

2.5.5 Identifying a combinatorial tau-PET biomarker for cognition

Next, all tau ROIs were entered into a Lasso regression model in order to identify a sparse set of covariates that best describe global cognitive data (Figure 2.6). The optimal penalization value was defined through cross-validation as 0.019. The Lasso reduced all coefficients except Cluster 4 ("Temporo-parietal"), Braak Stage VI from Schwarz et al., and education. These three variables were entered together into a general linear model, and together explained a much greater proportion of variance in global cognitive data ($r2[4:81] = 0.28$, $p<0.0001$; Figure 2.6) compared to the individual effect sizes of each covariate (highest $r2 = 0.12$). The earlier negative association between Cluster 4 and Global Cognition was strengthened ($t=-4.98$, $p<0.001$), although positive associations were seen for the other two covariates (Schwarz Single 6: $t = 3.61$, $p = 0.001$; Education: $t = 2.53$, $p = 0.013$). In addition, the fitted values of this GLM explained 18.7 – 26.2% of the variance in the six individual cognitive tests composing the composite score (all $p <0.001$), indicating the model generalizes well to individual cognitive tests (Table 2.S3). Finally, the Lasso feature selection analysis was repeated for the six individual tests of global cognition. The data-driven Cluster 4 was selected across all six analyses, and was the only ROI selected for two analyses

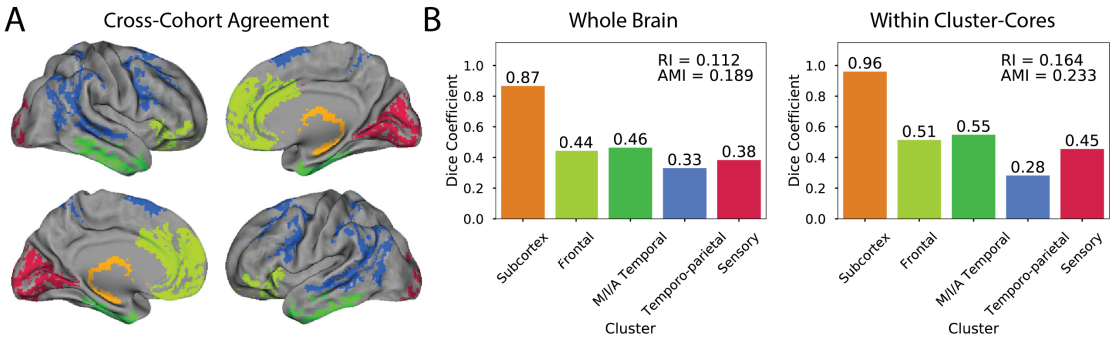

Figure 2.7: BASC clustering was performed on ADNI [18F]AV1451 data and was compared to the original clustering solution from BioFINDER data. Panel A. represents the surface rendering of voxels that shared the same cluster in both BioFINDER and ADNI solutions. Each cluster is represented as a different color. Panel B. shows the dice coefficients representing the correspondence between similar clusters in the BioFINDER and ADNI samples. The left graph represents correspondence across the whole brain, while the right graph represents correspondence between clusters within BioFINDER cluster-core masks. RI = adjusted Rand index; AMI = adjusted mutual information score

(Table 2.S4).

2.5.6 Reproducibility of tau-PET clusters across datasets

BASC analysis was run a second time on the 90 ADNI [18F]AV1451 scans to establish whether patterns of tau-PET covariance are reproducible across different datasets. MSTEPS identified a six-cluster solution as the lowest resolution solution in the ADNI dataset. Five of these clusters demonstrated similar spatial patterns to the five clusters identified in the BioFINDER sample, while a sixth cluster emerged which uniformly encircled the entire cerebral cortex (Figure 2.S2). This sixth cluster labeled 18% of brain voxels, and the average within-cluster [18F]AV1451 SUVR was 0.88 (SD = 0.16). The cluster most likely represents a partial volume or non tau-related atrophy effect, possibly driven by the high proportion of amyloid-negative MCI subjects or the low number of subjects with extensive isocortical tau in the ADNI cohort.

Despite the existence of this sixth cluster and the distinct clinical composition of the two datasets, some agreement between the two clustering solutions could be observed (Figure 2.7). Overall, 35% of brain voxels showed similar clustering patterns between the two datasets (adjusted Rand index = 0.112; adjusted mutual information score = 0.189). Figure 2.7A shows a cortical projection of voxels demonstrating similar clustering behavior across both datasets. Across datasets, [18F]AV1451 spatial covariance was consistent in the medial and inferior temporal lobes, the primary visual cortex, the temporo-parietal cortex, the medial frontal lobe, and most acutely in the subcortex. The subcortex formed its own cluster in both datasets, both including the hippocampus, and overall showed excellent agreement (Dice coefficient = 0.87). The Dice coefficients in the other clusters ranged from 0.33 – 0.46 (Figure 2.7B), indicating

that around one third to one half of voxels within clusters showed agreement between the two datasets. Notable regions of disagreement included the precuneus and posterior cingulate (clustered with the temporal lobes in ADNI), the insula (clustered with the medial frontal lobe in ADNI), the sensorimotor cortex and the lateral frontal lobes (distributed across multiple clusters in ADNI). When restricting the analysis only to voxels contained within the BioFINDER cluster-cores, the agreement between the two datasets improved (Figure 2.7B). This observation was consistent across all clusters except the temporo-parietal cluster, and provides evidence supporting the notion that voxels that covary stably within datasets may also show more stable covariance across datasets.

For the purposes of comparison, BASC was performed on five random 50% splits of the ADNI sample, and the resulting partitions were compared to one another. The average adjusted Rand index across these five within-ADNI train/test splits was 0.166 (SD = 0.031) and the average adjusted mutual information score was 0.225 (SD = 0.021). These within-dataset scores were equivalent to the between-dataset scores when restricted to cluster-cores (adjusted Rand index = 0.164; adjusted mutual information score = 0.233).

2.6 Discussion

In the present study, we applied an advanced unsupervised algorithm to identify clusters of [18F]AV1451 signal in 123 subjects ranging from cognitively normal to AD dementia in the Swedish BioFINDER study. Our approach yielded clusters in the temporoparietal, medial/inferior/anterior temporal, unimodal sensory and frontal cortex, as well as the subcortex. In an independent sample of 90 subjects (ADNI), we performed general linear models between tests of global cognition and each [18F]AV1451 cluster, adjusting for age, sex and education. In addition, we ran similar models using 35 neuropathologically derived ROIs from previous publications (Johnson et al., 2016; Schöll et al., 2016b; Schwarz et al., 2016; Cho et al., 2016a). Several ROIs exhibited strong relationships with cognition, though certain data-driven clusters (temporoparietal and medial/inferior/anterior temporal cortex) appeared to perform slightly but consistently better than other ROIs in ADNI. Supporting this notion, the temporoparietal data-driven cluster was among the three most important features (identified by a Lasso regression model) for predicting global cognition scores. Unsupervised clustering of [18F]AV1451 PET data thus revealed the data to self-assemble into stable ROIs resembling well described vulnerable regions in AD, some of which actually enhanced description of cognitive data in an

independent dataset. This suggests that data-driven approaches to delineate ROIs may improve clinical utility of [18F]AV1451 PET data.

The tau-PET covariance networks derived from our clustering approach exhibited a fair degree of overlap with Braak ROIs derived from autopsy studies, thereby demonstrating biological relevance. Particularly, Cluster 3 ("Medial/Anterior/Inferior Temporal") was reminiscent of regions involved in early tau accumulation, whereas Cluster 5 ("Unimodal Sensory") demonstrated a high degree of similarity to regions involved only in the latest stages of AD. In contrast, Cluster 4 ("Temporo-parietal") did not strongly resemble any of the Braak regions, while its pattern, together with the pattern of Cluster 3, spatially overlapped with cortical regions most vulnerable to neurodegeneration in AD (Dickerson et al., 2011; Landau et al., 2011). Furthermore, signal in the hippocampus was heterogeneous, adding additional evidence that [18F]AV1451 signal in this structure should be interpreted with caution (Cho et al., 2016a; Choi et al., 2018). Similarly, our data-driven approach suggested that most (but not all) frontal lobe structures exhibited [18F]AV1451 signal patterns unique to the rest of the cortex. This is notable considering the original Braak Stage V aggregates frontal lobe structures with many of the temporo-parietal structures captured in our Cluster 4. Part of the successful description of cognitive data by the data-driven ROI may be due to its isolation from many of these frontal lobe structures, which may be contributing signal less informative to AD progression, particularly in early disease stages. Finally, our data-driven ROIs provide information that may reconcile some differences between existing Braak ROIs. For example, in our study, [18F]AV1451 signal in the putamen and insula covaried with other regions involved in early tau accumulation, which was similar to the ROIs described by Schöll, Lockhart et al., but not Cho et al (see Table 2.S5 for a summary). However, this pattern was not fully reproduced within the ADNI sample, and so the staging of different ROIs may require further study with larger samples.

Despite the clusters being derived from a sample with several important and disease-relevant differences compared to the testing sample, these data-driven ROIs described global cognitive data slightly better than regions derived from autopsy studies. While the improvement over the other regions was subtle, the increasing movement toward the development of biomarkers demands optimization of ROIs to summarize [18F]AV1451 signal (Frisoni et al., 2017; Maass et al., 2017; Mishra et al., 2017). As such, even small improvements are important for studies assessing more subtle effects of cortical tau accumulation and studies seeking optimal biomarkers for multimodal classification or disease progression (Ota et al., 2015). The improvement observed is likely due to the data-driven nature of the method used for derivation of the clusters. [18F]AV1451 may be binding to several off-target agents, such as

(neuro)melanin, iron, vascular pathology and MAO-A/B (Marquié et al., 2015; Lowe et al., 2016; Ng et al., 2017; Choi et al., 2018), and as such, [18F]AV1451 signal is likely a mix of true tau pathology and other off-target and non-specific signals. Deriving the clusters from a sample representing a wide breadth of disease stages and additionally including subjects unlikely to have significant cortical tau pathology enhances the likelihood of isolating true tau signal, which covaries strongly and in a regionally specific pattern across disease stages. Additionally, deriving the clusters voxelwise allows freedom from anatomical borders, which may impose unnecessary constraints irrelevant to the spread of tau. Finally, despite its many limitations, multi-subject automatic whole-brain sampling is a distinct advantage of [18F]AV1451-PET over pathological studies. This advantage may further enhance the efficacy of data-driven approaches to ROI generation, which evaluate regions equally that may otherwise be overlooked.

Still, ROIs based on pathology remain important in understanding relationships between tau burden and cognition. In our study, ROIs representing the earliest stages of tau pathology, especially the entorhinal cortex, showed the strongest association with episodic memory in a cohort of individuals with normal cognition, mild cognitive impairment and early AD dementia. This finding supports previous literature highlighting relationships between medial temporal lobe tau pathology and decline in episodic memory (Maass et al., 2017). However, it is noteworthy that the data-driven temporo-parietal ROI was again among the top performing ROIs in describing episodic memory, despite the absence of medial temporal lobe structures within this ROI.

The results of this study thus suggest a possible advantage of data-driven approaches in evaluating [18F]AV1451 PET data as a biomarker for AD. This study adds to a rapidly growing body of data-driven [18F]AV1451-PET studies that have helped to characterize features of this tracer in the context of AD. Sepulcre and colleagues employed a similar unsupervised clustering approach on a set of cognitively intact elderly individuals, which, similar to our study, revealed [18F]AV1451-PET covariance between regions of early- and later- stage tau accumulation (Sepulcre et al., 2017a). This suggests these patterns of signal covariance are stable even in the earliest disease stages, lending credence to the use of data-driven biomarkers in multiple contexts. Meanwhile, Jones et al. used a data-driven Independent Components Analysis approach to summarize [18F]AV1451 data (Jones et al., 2017). While the authors concluded the resulting ROIs represented functional brain networks, three of the ROIs bore a striking similarity to those generated by our clustering approach. Our approach builds on these previous studies by assessing relationships between data-driven ROIs and cognition, and by comparing them with other existing ROIs.

Maass et al. employed a series of a priori and supervised data-driven methods to generate [18F]AV1451 ROIs and found a relative equivalence between these ROIs in their association with cognition and a number of other disease markers (Maass et al., 2017). However, consistent with our study, Maass et al. found [18F]AV1451 signal to covary most strongly within a specific set of AD vulnerable-regions, and conclude that these regional measures may perform better than whole-brain ROIs, particularly regarding associations with cognition.

The consistencies across these studies are also underscored by the consistent patterns of cross-subject [18F]AV1451 spatial covariance found across the two datasets in the current study. Despite the fact that the ADNI cohort had many fewer subjects with extensive tau burden, and despite differences in the demographic and clinical characteristics between the ADNI and BioFINDER cohorts, unsupervised clustering of [18F]AV1451 data revealed a level of consistency between these two datasets that rivaled the consistency of clustering within the ADNI dataset alone. Certain patterns of tau-PET accumulation emerged in key regions across both cohorts. However, the patterns of tau-PET covariance were not entirely consistent between the two datasets, which could reflect true heterogeneity across samples, or could be a matter of instability due to the relatively small sample sizes (particularly in ADNI). However, better consistency between datasets was found within the cluster-cores – regions of greatest clustering stability within the BioFINDER dataset. This finding, alongside the performance of these cluster-cores as biomarkers in ADNI, suggests some degree of cluster stability may be achieved with the BASC approach, even with smaller sample sizes.

We employed a widely used feature selection routine to identify those regions most informative in describing association between [18F]AV1451 signal and cognitive data. The feature most strongly associated with global cognition was the data-driven temporo-parietal cluster, which harbored a strong negative relationship when included with the other selected features ($p<0.001$). The feature selection also resulted in the selection of Schwarz et al. Stage VI and education, both of which associated positively with MMSE in a general linear model. The finding of an association between education and MMSE controlling for tau pathology is consistent with the concept of cognitive reserve (Stern, 2012), and suggests that more highly educated subjects may experience preserved cognition in the face of tau pathology (Hoenig et al., 2017). While the selection of Schwarz Stage VI is less obvious, possible explanations include partial volume effects and age-related off-target or non-specific signal. Because very few ADNI subjects demonstrate strong [18F]AV1451 signal in this ROI, higher [18F]AV1451 signal may be related to the presence of more cortex (and thus more off-target or non-specific binding) rather than increased tau pathology.

Similarly, off-target [18F]AV1451 signal in the cortex and subcortex has been shown to increase with age (Schöll et al., 2016b; Smith et al., 2016; Choi et al., 2018), possibly representing binding to reactive astrocytes (Marquié et al., 2015) or iron deposits (Choi et al., 2018). Since age was not selected by the Lasso and therefore was not included in the multivariate model, this may explain the positive association between these regions and global cognition when accounting for [18F]AV1451 signal in the temporoparietal region. However, the fact that these ROIs were selected instead of age suggests they may carry additional cognition-relevant information, which may demand further exploration. Regardless, the negative relationship between Cluster 4 ("Temporo-parietal") and global cognition was substantially increased after regressing out these other variables. This suggests that [18F]AV1451-cognition relationships may be enhanced by regressing out off-target or non-specific signal sources.

Our study comes with a number of limitations. First, there were several differences in characteristics between the two samples. We decided to use the BioFINDER cohort for clustering given the broad range of both [18F]AV1451 uptake (Figure 2.1) and cognitive scores (Table 2.1). As a consequence, our secondary (cognitive) analysis was performed in subjects from the ADNI cohort with more restricted [18F]AV1451 uptake and cognitive scores. On a related note, our cluster and results could be influenced by the composition of our samples. However, voxels are only included in the clusters derived for our analysis if the clustering occurs across >50% of bootstrap samples, so it is unlikely that the clustering solution would be strongly driven by, for example, the high proportion of late-stage (i.e. AD) subjects in the BioFINDER sample. Third, contrary to other studies, we did not make an attempt to classify individuals according to stages of tau pathology. Finally, we chose not to apply partial volume correction on our data. Investigating the impact of such corrections is certainly important, but we were interested in the natural behavior of tau-PET signal before any corrections.

In order to aid future studies, we have made the [18F]AV1451 clusters from this study available on FigShare (doi = `10.6084/m9.figshare.5758374`).

2.7 Additional manuscript information

[3]

[3]This may seem superfluous, but the thesis requirements state that manuscripts should be reproduced here exactly as they are published or were last submitted, except author contributions, which are moved to the front for whatever reason.

2.7.1 Acknowledgements

The authors would like to thank Emma Wolters, Tessa Timmers, Colin Groot, Angela Tam, Alle Meije Wink, Anita van Loenhoud and Elena Kochova for advice and support. Work at the authors' research centers was supported by the European Research Council, the Swedish Research Council, the Strategic Research Area MultiPark (Multidisciplinary Research in Parkinson's disease) at Lund University, the Swedish Brain Foundation, the Swedish Alzheimer Association, the Marianne and Marcus Wallenberg Foundation, the Skåne University Hospital Foundation, and the Swedish federal government under the ALF agreement. This research was additionally funded by Marie Curie FP7 International Outgoing Fellowship [628812] (to R.O.); The donors of [Alzheimer's Disease Research], a program of BrightFocus Foundation (to R.O.); Author JWV was additionally funded by an Alzheimer Nederland grant and a Vanier Canada Graduate Studies Doctoral award. The authors would additionally like to thank Adam Schwarz for providing scripts to recreate the ROIs from Schwarz et al., 2016, and Chul Hyoung Lyoo for providing information about creating ROIs from Cho et al., 2016. AVID Radiopharmaceutical generously provided the precursor of AV-1451. Data collection and sharing for this project was funded in part by the Alzheimer's Disease Neuroimaging Initiative (ADNI) (National Institutes of Health Grant U01 AG024904) and DOD ADNI (Department of Defense award number W81XWH-12-2-0012). ADNI is funded by the National Institute on Aging, the National Institute of Biomedical Imaging and Bioengineering, and through generous contributions from the following: AbbVie, Alzheimer's Association; Alzheimer's Drug Discovery Foundation; Araclon Biotech; BioClinica, Inc.; Biogen; Bristol-Myers Squibb Company; CereSpir, Inc.; Eisai Inc.; Elan Pharmaceuticals, Inc.; Eli Lilly and Company; EuroImmun; F. Hoffmann-La Roche Ltd and its affiliated company Genentech, Inc.; Fujirebio; GE Healthcare; IXICO Ltd.; Janssen Alzheimer Immunotherapy Research & Development, LLC.; Johnson & Johnson Pharmaceutical Research & Development LLC.; Lumosity; Lundbeck; Merck & Co., Inc.; Meso Scale Diagnostics, LLC.; NeuroRx Research; Neurotrack Technologies; Novartis Pharmaceuticals Corporation; Pfizer Inc.; Piramal Imaging; Servier; Takeda Pharmaceutical Company; and Transition Therapeutics. The Canadian Institutes of Health Research is providing funds to support ADNI clinical sites in Canada. Private sector contributions are facilitated by the Foundation for the National Institutes of Health (www.fnih.org). The grantee organization is the Northern California Institute for Research and Education, and the study is coordinated by the Alzheimer's Disease Cooperative Study at the University of California, San Diego. ADNI data are disseminated by the Laboratory for Neuro Imaging at the University of Southern California

2.7.2 Potential Conflicts of Interest

OH has acquired research support (for the institution) from Roche, GE Healthcare, Biogen, AVID Radiopharmaceuticals, Fujirebio, and Euroimmun. In the past 2 years, he has received consultancy/speaker fees (paid to the institution) from Lilly, Roche, and Fujirebio. Many of these companies are involved in creating tau-PET radioligands, including AVID, who provided the ligands for this study.

2.8 Supplementary Figures

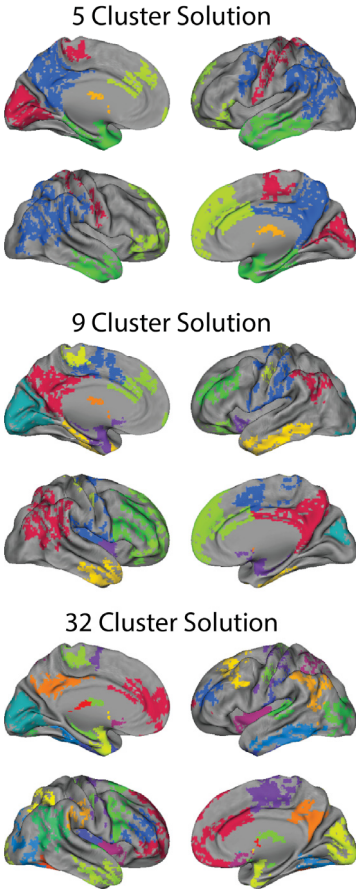

Supplementary Fig. 2.S1: BASC was run on 123 [18F]AV1451 images from the BioFINDER cohort. MSTEPS suggested three different resolutions (k=5, k=9 and k=32) to capture the stable patterns of covariance across multiple resolutions. Cluster-core maps were created by setting voxels with cluster stability <0.5 to 0. The cluster-cores from these three solutions are projected onto a cortical surface.

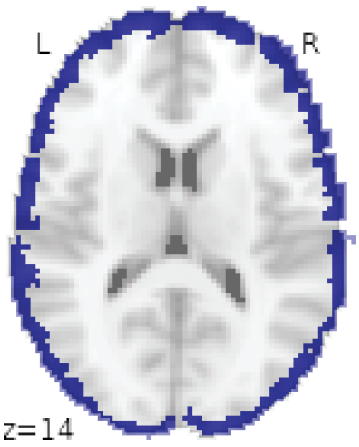

Supplementary Fig. 2.S2: When running BASC in ADNI, a cluster emerged that uniformly surrounded the cerebral cortex, likely representing partial volume effects that could be driven by cortical atrophy in older, amyloid-negative subjects.

2.9 Supplementary Tables

	MMSE			CDRSB		
Rank	**Study**	**ROI**	**t**	**Study**	**ROI**	**t**
1	Data-driven	Temporo-parietal	-2.45*	Schwarz	Stage I	3.60**
2	Data-driven	Temporal	-2.00*	Data-driven	Temporo-parietal	3.49**
3	Cho	Single IV	-1.97	Cho/Scholl	Stage I	3.49**
4	Cho	Stage IV	-1.83	Data-driven	Temporal	3.33**
5	Other	Inferior Temporal	-1.8	Cho	Stage IV	3.18*
	ADAS11			**ADAS13**		
Rank	**Study**	**ROI**	**t**	**Study**	**ROI**	**t**
1	Data-driven	Temporo-parietal	4.10**	Data-driven	Temporo-parietal	3.02*
2	Schwarz	Stage I	3.50**	Schwarz	Stage I	2.57*
3	Cho	Single IV	3.43**	Data-Driven	Temporal	2.35*
4	Data-driven	Temporal	3.39**	Cho/Scholl	Stage I	2.34*
5	Cho	Stage IV	3.33**	Cho	Single IV	2.34*
	ECOG			**FAQ**		
Rank	**Study**	**ROI**	**t**	**Study**	**ROI**	**t**
1	Data-driven	Temporo-parietal	3.68**	Schwarz	Stage I	2.91*
2	Cho	Stage IV	3.48**	Data-driven	Temporal	2.69*
3	Schwarz	Stage I	3.40**	Cho/Scholl	Stage I	2.68*
4	Cho	Single IV	3.40**	Data-driven	Temporo-parietal	2.67*
5	Data-Driven	Temporal	3.40**	Cho	Stage III	2.63*

Supplementary Table 2.S1: * p<0.05 ** p[Bonf.]<0.05
ROI = Region of Interest; MMSE = Mini-Mental State Examination; CDRSB = Clinical Dementia Rating Sum of Boxes; ADAS = Alzheimer's disease Assessment Scale; ECog = Everyday Cognition; FAQ = Functional Activities Questionnaire

	ADNI_MEM		
Rank	**Study**	**ROI**	**t**
1	Schwarz	Stage I	-3.27*
2	Cho/Scholl	Stage I	-2.99*
3	Data-driven	Temporo-parietal	-2.85*
4	Schwarz	Stage II	-2.58*
5	Cho	Stage III	-2.54*

Supplementary Table 2.S2: Best-ranking [18F]AV1451 ROIs at describing episodic memory
* p<0.05

Test	**R2**
CDRSB	0.214
ADAS11	0.261
ADAS13	0.215
FAQ	0.221
ECog	0.196
MMSE	0.219

Supplementary Table 2.S3: Fitted values from the General Linear Model comparing selected [18F]AV1451 ROIs to Global Cognition composite also explains variance in individual cognitive tests.
MMSE = Mini-Mental State Examination; CDRSB = Clinical Dementia Rating Sum of Boxes; ADAS = Alzheimer's disease Assessment Scale; ECog = Everyday Cognition; FAQ = Functional Activities Questionnaire

MMSE		CDRSB		ADAS11	
Study	**ROI**	**Study**	**ROI**	**Study**	**ROI**
Data-driven	Temporo-parietal	Data-driven	Temporo-parietal	Data-driven	Temporo-parietal
Data-driven	Subcortical			Schwarz	Single VI
Schwarz	Stage VI			Schwarz	Stage I
Demographic	Education			Demographic	Education

ADAS13		ECOG		FAQ	
Study	**ROI**	**Study**	**ROI**	**Study**	**ROI**
Data-driven	Temporo-parietal	Data-driven	Temporo-parietal	Data-driven	Temporo-parietal
Schwarz	Single VI			Schwarz	Single VI
Schwarz	Stage I			Schwarz	Stage I
Scholl	Single II			Demographic	Education
Demographic	Education				
Demographic	Age				

Supplementary Table 2.S4: Variables selected by Lasso regression that optimally described global cognition across different cognitive tests
MMSE = Mini-Mental State Examination; CDRSB = Clinical Dementia Rating Sum of Boxes; ADAS = Alzheimer's disease Assessment Scale; ECog = Everyday Cognition; FAQ = Functional Activities Questionnaire

Brain Region	Scholl, Lockhart et al.	Cho et al.	Schwarz et al.	Data-driven
Hippocampus	Included	Not included	Head only	Head only
Lingual Gyrus	Stage 3	Stage 5	Stage 6	TP/US
Thalamus	Stage 4	Not included	Not Included	SCN
Putamen	Stage 5	Not included	Not Included	MAIT
Lateral Occipital	Stage 5	Stage 5	Stage 4	TP/US
PCC	Stage 4	Stage 5	Not Included	TP
Insula	Stage 4	Stage 5	Not Included	MAIT
Frontal Lobe	All stage 5	All stage 5	Not Included	F/TP

Supplementary Table 2.S5: Disparities in Braak stage regions-of-interests across studies
TP = Temporo-parietal; US = Unimodal Sensory; SCN = Subcortical/Noise; MAIT = Medial/Anterior/Inferior Temporal; F = Frontal

2.10 Follow-up analysis: Heterogeneous tau-PET signal in the hippocampus resolves discrepancies between imaging and pathology

2.10.1 Introduction

Neurofibrillary tangles (NFTs) composed of the misfolded tau protein are one of the two pathological hallmarks of Alzheimer's disease (AD), along with amyloid-β (Aβ). Pathology studies suggest that NFTs are first found in the entorhinal cortex (ERC), and next spread into the hippocampus, likely through trans-synaptic mechanisms (Braak and Del Tredici, 2015). The hippocampus is therefore one of the earliest sites of NFT aggregation in AD, and hippocampal NFTs have been associated with increased likelihood of dementia, presence of Aβ and impairment in episodic memory (Reitz

et al., 2009; Robinson et al., 2011). NFTs can now be measured in living humans using positron emission tomography (PET) with the tracer AV14514. However, AV1451 signal in the hippocampus has not corroborated findings from pathology studies (Schöll et al., 2016b; Cho et al., 2016a). While explanations for this discrepancy are often attributed to partial volume effects, it is noteworthy that previous PET studies have often averaged signal across the entire hippocampus. This approach would prove problematic if NFT signal is heterogeneous within the hippocampal formation. In the current study, we examine data-driven patterns of AV1451 signal heterogeneity in the hippocampus to establish whether this may explain the aforementioned discrepancies in this region.

2.10.2 Methods

In a previous study, we used an advanced clustering algorithm in the Swedish BioFINDER cohort (Hansson et al., 2017) to segregate different spatial distribution patterns of AV1451 across the AD spectrum (Figure 2.S2A) (Vogel et al., 2019a). These analyses resulted in an atlas of covariance networks largely reflecting known NFT biology. Here, we created a hippocampal AV1451 atlas by isolating cluster labels in the hippocampus from the rest of the brain. AV1451 images were downloaded from the Alzheimer's Disease Neuroimaging Initiative website (143 older controls, 88 mild cognitive impairment, 27 AD dementia). Average AV1451 signal was extracted across the whole hippocampus, as well as separately across hippocampal voxels belonging to each AV1451 cluster identified in the previous analysis. We then tested whether different AV1451 signal patterns were differentially related to clinical diagnosis, presence of Aβ pathology and episodic memory, using regression models adjusting for age, sex and education. Finally, we used diffusion tractography to measure the number of connections between the ERC and the different hippocampal signal clusters. Diffusion-weighted images for 114 young controls from the BNU1 dataset of the 1000-Functional Connectomes Project study were preprocessed using the ndmg pipeline (Kiar et al., 2017). Data were converted to graphs by fitting streamlines through regions of interest, and all graphs were averaged to create an average healthy connectome.

2.10.3 Results

AV1451 signal in the hippocampus was heterogenous. Signal in the head covaried specifically with other regions involved in early NFT aggregation ("Early NFT"), while signal in the rest of the hippocampus covaried with regions known to be pathology-free but susceptible to off-target AV1451 binding ("Off-Target"; Figure 2.S2B).

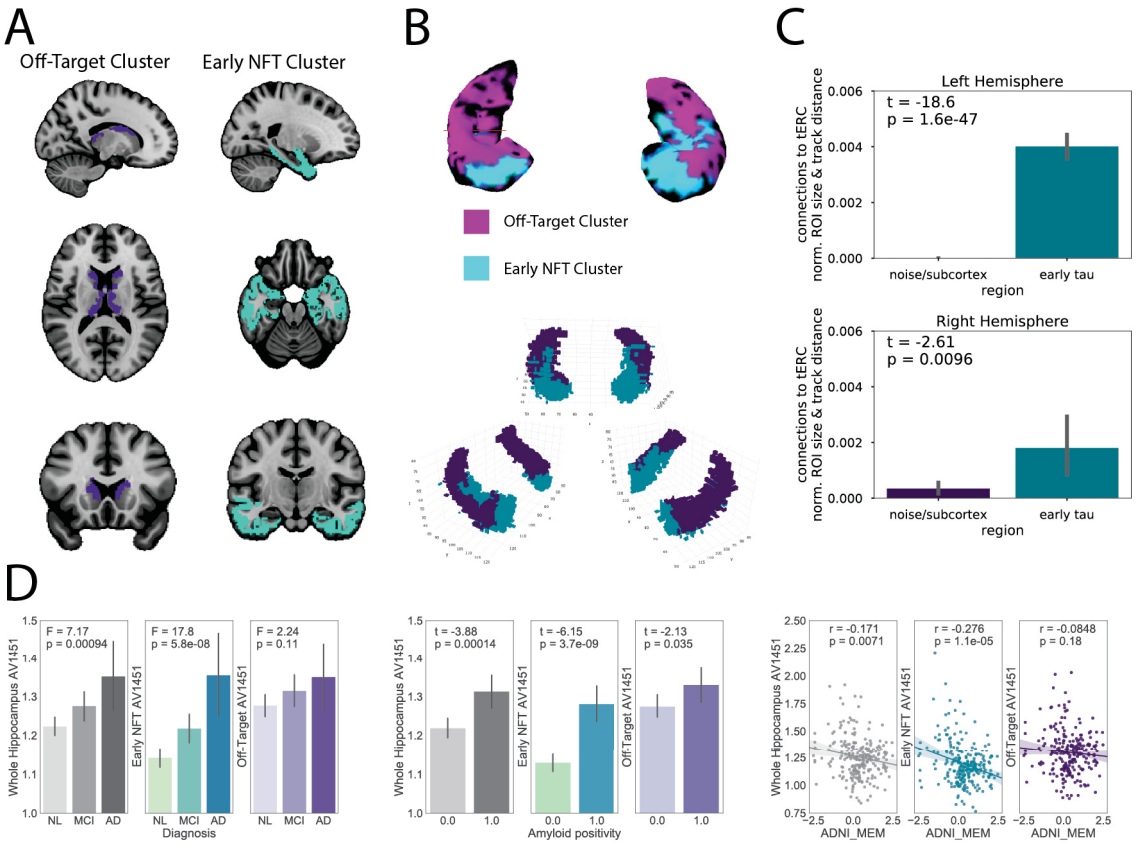

Supplementary Fig. 2.S2: A) Clustering across AV1451 images revealed five spatial covariance networks. B) Two of these networks, were represented inside the hippocampus, indicating signal heterogeneity in this structure. Membership of each hippocampal voxel in the two clusters projected onto a hippocampal surface C) Across both hemispheres, there were significantly more connections from the transentorhinal cortex (tERC) to the Off-Target hippocampal cluster. D) Mean AV1451 signal was extracted from the whole hippocampus (gray), hippocampal voxels falling into the "Early NFT" cluster (teal), and hippocampal voxels falling into the "Off-Target" cluster (Purple). AV1451 signal in the "Early NFT" cluster showed greater effect sizes with relation to Diagnosis (left), frequency of amyloid positivity (middle) and episodic memory (right).

Individuals with higher AV1451 signal in the Early NFT cluster exhibited worse episodic memory ($p < 0.0001$), were more likely to exhibit AB pathology ($p < 0.0001$) and were slightly more likely to have a diagnosis of AD dementia than being cognitively normal ($p < 0.0001$). Relationships were much less pronounced or absent when using the voxels falling into the Off-Target cluster, or when averaging across all hippocampal voxels (Figure 2.S2D). Tractography analysis revealed a greater number of anatomical connections between the ERC and the Early NFT cluster of the hippocampus compared to the Off-Target cluster ($p<0.001$) (Figure 2.S2C).

2.10.4 Discussion

Using data-driven methods, we were able to enhance the associations expected from pathology studies between hippocampal AV1451 signal and other pathological and

cognitive markers. These findings partially resolve discrepancies between previous PET and pathology studies and provide a template for future AV1451 studies

References

American Psychiatric Association, The (2013). *Diagnostic and statistical manual of mental disorders : DSM-5*. Fifth edition. Arlington, VA : American Psychiatric Association, [2013]. URL: https://search.library.wisc.edu/catalog/9910187853902121.

Arriagada, P V et al. (1992). "Neurofibrillary Tangles But Not Senile Plaques Parallel Duration and Severity of Alzheimers-Disease". In: *Neurology* 42.3, pp. 631–639. ISSN: 0028-3878. DOI: 10.1212/WNL.42.3.631.

Bejanin, Alexandre et al. (2017a). "Tau pathology and neurodegeneration contribute to cognitive impairment in Alzheimer ' s disease". In: October, pp. 1–15. DOI: 10.1093/brain/awx243.

Bellec, Pierre (2013). "Mining the hierarchy of resting-state brain networks: Selection of representative clusters in a multiscale structure". In: *Proceedings - 2013 3rd International Workshop on Pattern Recognition in Neuroimaging, PRNI 2013*, pp. 54–57. DOI: 10.1109/PRNI.2013.23.

Bellec, Pierre et al. (2006). "Identification of large-scale networks in the brain using fMRI". In: *NeuroImage* 29.4, pp. 1231–1243. ISSN: 10538119. DOI: 10.1016/j.neuroimage.2005.08.044.

Bellec, Pierre et al. (2010). "Multi-level bootstrap analysis of stable clusters in resting-state fMRI". In: *NeuroImage* 51.3, pp. 1126–1139. ISSN: 10538119. DOI: 10.1016/j.neuroimage.2010.02.082. URL: http://dx.doi.org/10.1016/j.neuroimage.2010.02.082.

Braak, H and E Braak (1991). "Neuropathological stageing of Alzheimer-related changes." In: *Acta neuropathologica* 82.4, pp. 239–59. ISSN: 0001-6322. URL: http://www.ncbi.nlm.nih.gov/pubmed/1759558.

Braak, Heiko and Kelly Del Tredici (2015). "The preclinical phase of the pathological process underlying sporadic Alzheimer's disease". In: *Brain* 138.10, pp. 2814–2833. ISSN: 14602156. DOI: 10.1093/brain/awv236.

Chien, David T. et al. (2013). "Early Clinical PET Imaging Results with the Novel PHF-Tau Radioligand [F-18]-T807". In: *Journal of Alzheimer's Disease* 34.2, pp. 457–468. DOI: 10.3233/JAD-122059.

Cho, Hanna et al. (Aug. 2016a). "In vivo cortical spreading pattern of tau and amyloid in the Alzheimer disease spectrum". In: *Annals of Neurology* 80.2, pp. 247–258. ISSN: 03645134. DOI: 10.1002/ana.24711. URL: http://doi.wiley.com/10.1002/ana.24711.

Cho, Hanna et al. (2017). "18F-AV-1451 binds to motor-related subcortical gray and white matter in corticobasal syndrome". In: *Neurology* 89.11, pp. 1170–1178. ISSN: 1526632X. DOI: 10.1212/WNL.0000000000004364.

Choi, Jae Yong et al. (Jan. 2018). "Off-Target 18 F-AV-1451 Binding in the Basal Ganglia Correlates with Age-Related Iron Accumulation". In: *Journal of Nuclear Medicine* 59.1, pp. 117–120. ISSN: 0161-5505. DOI: 10.2967/jnumed.117.195248. URL: http://jnm.snmjournals.org/lookup/doi/10.2967/jnumed.117.195248.

Crane, Paul K. et al. (2012). "Development and assessment of a composite score for memory in the Alzheimer's Disease Neuroimaging Initiative (ADNI)". In: *Brain Imaging and Behavior* 6.4, pp. 502–516. ISSN: 19317557. DOI: 10.1007/s11682-012-9186-z.

Desikan, Rahul S. et al. (2006). "An automated labeling system for subdividing the human cerebral cortex on MRI scans into gyral based regions of interest". In: *NeuroImage* 31.3, pp. 968–980. ISSN: 10538119. DOI: 10.1016/j.neuroimage.2006.01.021.

Dickerson, B. C. et al. (2011). "Alzheimer-signature MRI biomarker predicts AD dementia in cognitively normal adults". In: *Neurology* 76.16, pp. 1395–1402. ISSN: 00283878. DOI: 10.1212/WNL.0b013e3182166e96.

Farias, Sarah Tomaszewski et al. (July 2008). "The measurement of everyday cognition (ECog): scale development and psychometric properties." In: *Neuropsychology* 22.4, pp. 531–44. ISSN: 0894-4105. DOI: 10.1037/0894-4105.22.4.531. URL: http://www.ncbi.nlm.nih.gov/pubmed/18590364http://www.pubmedcentral.nih.gov/articlerender.fcgi?artid=PMC2877034.

Folstein, M F, Susan E Folstein, and Paul R McHugh (Nov. 1975). ""Mini-mental state". A practical method for grading the cognitive state of patients for the clinician." In: *Journal of psychiatric research* 12.3, pp. 189–98. ISSN: 0022-3956. DOI: 10.1016/0022-3956(75)90026-6. URL: http://dx.doi.org/10.1016/0022-3956(75)90026-6http://www.ncbi.nlm.nih.gov/pubmed/1202204.

Fred, Ana L N and Anil K Jain (2005). "Combining Multiple Clusterings Using Evidence Accumulation". In: *IEEE Trans Pattern Anal Mach Intell* 27.6, pp. 835–850. DOI: 10.1109/TPAMI.2005.113.

Frisoni, Giovanni B et al. (Aug. 2017). "Strategic roadmap for an early diagnosis of Alzheimer's disease based on biomarkers." In: *The Lancet. Neurology* 16.8, pp. 661–676. ISSN: 1474-4465. DOI: 10.1016/S1474-4422(17)30159-X. URL: http://www.ncbi.nlm.nih.gov/pubmed/28721928.

Garcia-Garcia, Manuel et al. (July 2017). "Detecting stable individual differences in the functional organization of the human basal ganglia." In: *NeuroImage* December 2016, pp. 1–15. ISSN: 1095-9572. DOI: 10.1016/j.neuroimage.2017.07.029. URL:

http://linkinghub.elsevier.com/retrieve/pii/S1053811917305979http://www.ncbi.nlm.nih.gov/pubmed/28739120.

Grothe, Michel J et al. (Nov. 2017). "In vivo staging of regional amyloid deposition". In: *Neurology* 89.20, pp. 2031–2038. ISSN: 0028-3878. DOI: 10.1212/WNL.0000000000004643. URL: http://www.ncbi.nlm.nih.gov/pubmed/29046362http://www.neurology.org/lookup/doi/10.1212/WNL.0000000000004643.

Hansson, Oskar et al. (Mar. 2017). "Tau Pathology Distribution in Alzheimer's disease Corresponds Differentially to Cognition-Relevant Functional Brain Networks". In: *Frontiers in Neuroscience* 11.March. ISSN: 1662-453X. DOI: 10.3389/fnins.2017.00167. URL: http://journal.frontiersin.org/article/10.3389/fnins.2017.00167/full.

Hoenig, Merle Christine et al. (2017). "Tau pathology and cognitive reserve in Alzheimer's disease". In: *Neurobiology of Aging* 57, pp. 1–7. ISSN: 15581497. DOI: 10.1016/j.neurobiolaging.2017.05.004. URL: http://dx.doi.org/10.1016/j.neurobiolaging.2017.05.004.

Hughes, C P et al. (June 1982). "A new clinical scale for the staging of dementia." In: *The British journal of psychiatry : the journal of mental science* 140, pp. 566–72. ISSN: 0007-1250. URL: http://www.ncbi.nlm.nih.gov/pubmed/7104545.

Jansen, Willemijn J et al. (May 2015). "Prevalence of cerebral amyloid pathology in persons without dementia: a meta-analysis." In: *JAMA* 313.19, pp. 1924–38. ISSN: 1538-3598. DOI: 10.1001/jama.2015.4668. URL: http://dx.doi.org/10.1001/jama.2015.9719http://www.ncbi.nlm.nih.gov/pubmed/25988462http://www.pubmedcentral.nih.gov/articlerender.fcgi?artid=PMC4486209.

Johnson, Keith A. et al. (2016). "Tau positron emission tomographic imaging in aging and early Alzheimer disease". In: *Annals of Neurology* 79.1, pp. 110–119. ISSN: 15318249. DOI: 10.1002/ana.24546.

Jones, David T. et al. (2017). "Tau, Amyloid, and Cascading Network Failure across the Alzheimer's disease Spectrum". In: *Cortex* October, pp. 1–17. ISSN: 00109452. DOI: 10.1016/j.cortex.2017.09.018. URL: http://linkinghub.elsevier.com/retrieve/pii/S0010945217303246.

Kiar, Gregory et al. (Jan. 2017). "A Comprehensive Cloud Framework for Accurate and Reliable Human Connectome Estimation and Meganalysis". In: *bioRxiv*. URL: http://biorxiv.org/content/early/2017/09/16/188706.abstract.

Kriegeskorte, Nikolaus et al. (2009). "Circular analysis in systems neuroscience – the dangers of double dipping". In: *Nature neuroscience* 12.5, pp. 535–540. DOI: 10.1038/nn.2303.

Landau, Susan M. et al. (2011). "Associations between cognitive, functional, and FDG-PET measures of decline in AD and MCI". In: *Neurobiology of Aging* 32.7, pp. 1207–1218. ISSN: 01974580. DOI: 10.1016/j.neurobiolaging.2009.07.002.

Landau, Susan M. et al. (2013). "Comparing positron emission tomography imaging and cerebrospinal fluid measurements of ??-amyloid". In: *Annals of Neurology* 74.6, pp. 826–836. ISSN: 03645134. DOI: 10.1002/ana.23908.

Lockhart, Samuel N et al. (Mar. 2017b). "Elevated (18)F-AV-1451 PET tracer uptake detected in incidental imaging findings." In: *Neurology* 88.11, pp. 1095–1097. ISSN: 1526-632X. DOI: 10.1212/WNL.0000000000003724. URL: http://www.ncbi.nlm.nih.gov/pubmed/28188303http://www.pubmedcentral.nih.gov/articlerender.fcgi?artid=PMC5384840.

Lowe, Val J. et al. (2016). "An autoradiographic evaluation of AV-1451 Tau PET in dementia". In: *Acta Neuropathologica Communications* 4.1, p. 58. ISSN: 2051-5960. DOI: 10.1186/s40478-016-0315-6. URL: http://actaneurocomms.biomedcentral.com/articles/10.1186/s40478-016-0315-6.

Maass, Anne et al. (2017). "NeuroImage Comparison of multiple tau-PET measures as biomarkers in aging and Alzheimer ' s disease". In: *NeuroImage* 157.December 2016, pp. 448–463. ISSN: 1053-8119. DOI: 10.1016/j.neuroimage.2017.05.058. URL: http://dx.doi.org/10.1016/j.neuroimage.2017.05.058.

Marquié, Marta et al. (Nov. 2015). "Validating novel tau positron emission tomography tracer [F-18]-AV-1451 (T807) on postmortem brain tissue." In: *Annals of neurology* 78.5, pp. 787–800. ISSN: 1531-8249. DOI: 10.1002/ana.24517. URL: http://www.ncbi.nlm.nih.gov/pubmed/26344059http://www.pubmedcentral.nih.gov/articlerender.fcgi?artid=PMC4900162.

Marquié, Marta et al. (Oct. 2017). "[F-18]-AV-1451 binding correlates with postmortem neurofibrillary tangle Braak staging". In: *Acta Neuropathologica* 134.4, pp. 619–628. ISSN: 0001-6322. DOI: 10.1007/s00401-017-1740-8. URL: http://link.springer.com/10.1007/s00401-017-1740-8.

Masters, C L et al. (1985). "Amyloid plaque core protein in Alzheimer disease and Down syndrome." In: *Proceedings of the National Academy of Sciences of the United States of America* 82.12, pp. 4245–9. ISSN: 0027-8424. DOI: 10.1073/pnas.82.12.4245. URL: http://www.ncbi.nlm.nih.gov/pubmed/3159021%5Cnhttp://www.pubmedcentral.nih.gov/articlerender.fcgi?artid=PMC397973.

McKhann, G et al. (2011). "The diagnosis of dementia due to Alzheimer's disease: Recommendations from the National Institute on Aging- Alzheimer's Association workgroups on diagnostic guidelines for Alzheimer's disease". In: *Alzheimers Dementia* 7.3, pp. 263–269. ISSN: 1552-5279. DOI: 10.1016/j.jalz.2011.03.005.The.

Mishra, Shruti et al. (2017). "AV-1451 PET imaging of tau pathology in preclinical Alzheimer disease: Defining a summary measure". In: *NeuroImage* 161.June, pp. 171–178. ISSN: 10959572. DOI: 10.1016/j.neuroimage.2017.07.050.

Mohs, R C et al. (1997). "Development of cognitive instruments for use in clinical trials of antidementia drugs: additions to the Alzheimer's Disease Assessment Scale that broaden its scope. The Alzheimer's Disease Cooperative Study." In: *Alzheimer disease and associated disorders* 11 Suppl 2, pp. 13–21. ISSN: 0893-0341. URL: http://www.ncbi.nlm.nih.gov/pubmed/9236948.

Nelson, Peter T. et al. (May 2012). "Correlation of Alzheimer Disease Neuropathologic Changes With Cognitive Status: A Review of the Literature". In: *Journal of Neuropathology & Experimental Neurology* 71.5, pp. 362–381. ISSN: 0022-3069. DOI: 10.1097/NEN.0b013e31825018f7. URL: https://academic.oup.com/jnen/article-lookup/doi/10.1097/NEN.0b013e31825018f7.

Ng, Kok Pin et al. (2017). "Monoamine oxidase B inhibitor, selegiline, reduces 18 F-THK5351 uptake in the human brain". In: *Alzheimer's Research & Therapy* 9.1, p. 25. ISSN: 0959-4965. DOI: 10.1186/s13195-017-0253-y. URL: http://content.wkhealth.com/linkback/openurl?sid=WKPTLP:landingpage&an=00001756-199808030-00031%5Cnhttp://download.springer.com/static/pdf/689/art%253A10.1186%252Fs13195-017-0253-y.pdf?originUrl=http%3A%2F%2Falzres.biomedcentral.com%2Farticle%2F10.1186%2F.

Orban, Pierre et al. (2015). "Test-retest resting-state fMRI in healthy elderly persons with a family history of Alzheimer's disease." In: *Scientific data* 2, p. 150043. ISSN: 2052-4463. DOI: 10.1038/sdata.2015.43. URL: http://www.nature.com/articles/sdata201543.

Ossenkoppele, Rik et al. (2016a). "Tau PET patterns mirror clinical and neuroanatomical variability in Alzheimer's disease". In: *Brain* 139.5, pp. 1551–1567. ISSN: 14602156. DOI: 10.1093/brain/aww027. URL: http://brain.oxfordjournals.org/.

Ota, Kenichi et al. (2015). "Effects of imaging modalities, brain atlases and feature selection on prediction of Alzheimer's disease". In: *Journal of Neuroscience Methods* 256, pp. 168–183. ISSN: 1872678X. DOI: 10.1016/j.jneumeth.2015.08.020.

Pankov, Aleksandr et al. (2016). "Data-driven regions of interest for longitudinal change in frontotemporal lobar degeneration". In: *NeuroImage: Clinical* 12, pp. 332–340. ISSN: 22131582. DOI: 10.1016/j.nicl.2015.08.002. URL: http://dx.doi.org/10.1016/j.nicl.2015.08.002.

Pedregosa, Fabian et al. (2012). "Scikit-learn: Machine Learning in Python". In: *Journal of Machine Learning Research* 12, pp. 2825–2830. ISSN: 15324435. DOI: 10.1007/s13398-014-0173-7.2. URL: http://arxiv.org/abs/1201.0490.

Pfeffer, R I et al. (May 1982). "Measurement of functional activities in older adults in the community." In: *Journal of gerontology* 37.3, pp. 323–9. ISSN: 0022-1422. URL: http://www.ncbi.nlm.nih.gov/pubmed/7069156.

Reitz, C et al. (2009). "Memory performance is related to amyloid and tau pathology in the hippocampus". In: pp. 715–721. DOI: 10.1136/jnnp.2008.154146.

Robinson, John L et al. (2011). "Neocortical and hippocampal amyloid- b and tau measures associate with dementia in the oldest-old". In: *Brain* 134.12, pp. 3708–3715. DOI: 10.1093/brain/awr308.

Rosen, W. G., R. C. Mohs, and K. L. Davis (1984). "A new rating scale for Alzheimer's disease". In: *American Journal of Psychiatry* 141.11, pp. 1356–1364. ISSN: 0002953X. DOI: 10.1176/ajp.141.11.1356.

Scheltens, Philip and Kenneth Rockwood (2011). "How golden is the gold standard of neuropathology in dementia?" In: *Alzheimer's and Dementia* 7.4, pp. 486–489. ISSN: 15525260. DOI: 10.1016/j.jalz.2011.04.011. URL: http://dx.doi.org/10.1016/j.jalz.2011.04.011.

Schöll, Michael et al. (2016b). "PET Imaging of Tau Deposition in the Aging Human Brain". In: *Neuron* 89.5, pp. 971–982. ISSN: 10974199. DOI: 10.1016/j.neuron.2016.01.028.

Schwarz, Adam J. et al. (2016). "Regional profiles of the candidate tau PET ligand ¹⁸ F-AV-1451 recapitulate key features of Braak histopathological stages". In: *Brain*, aww023. ISSN: 0006-8950. DOI: 10.1093/brain/aww023. URL: http://www.brain.oxfordjournals.org/lookup/doi/10.1093/brain/aww023.

Sepulcre, Jorge et al. (2017a). "Hierarchical Organization of Tau and Amyloid Deposits in the Cerebral Cortex". In: *JAMA Neurology* 74.7, p. 813. ISSN: 2168-6149. DOI: 10.1001/jamaneurol.2017.0263. URL: http://archneur.jamanetwork.com/article.aspx?doi=10.1001/jamaneurol.2017.0263.

Smith, Ruben et al. (2016). "18F-AV-1451 tau PET imaging correlates strongly with tau neuropathology in MAPT mutation carriers". In: *Brain* 139.9, pp. 2372–2379. ISSN: 14602156. DOI: 10.1093/brain/aww163.

Stern, Yaakov (2012). "Cognitive reserve in ageing and Alzheimer's disease". In: *The Lancet Neurology* 11.11, pp. 1006–1012. ISSN: 14744422. DOI: 10.1016/S1474-4422(12)70191-6. URL: http://dx.doi.org/10.1016/S1474-4422(12)70191-6.

Van Rossum, Ineke A. et al. (2012). "Injury markers but not amyloid markers are associated with rapid progression from mild cognitive impairment to dementia in alzheimer's disease". In: *Journal of Alzheimer's Disease* 29.2, pp. 319–327. ISSN: 13872877. DOI: 10.3233/JAD-2011-111694.

Vogel, Jacob W. et al. (Feb. 2019a). "Data-driven approaches for tau-PET imaging biomarkers in Alzheimer's disease". In: *Human Brain Mapping* 40.2, pp. 638–651.

ISSN: 10659471. DOI: 10.1002/hbm.24401. URL: http://doi.wiley.com/10.1002/hbm.24401.

Xia, Chenjie et al. (2017). "Association of In Vivo [¹⁸ F]AV-1451 Tau PET Imaging Results With Cortical Atrophy and Symptoms in Typical and Atypical Alzheimer Disease". In: *JAMA Neurology* 74.4, p. 427. ISSN: 2168-6149. DOI: 10.1001/jamaneurol.2016.5755. URL: http://archneur.jamanetwork.com/article.aspx?doi=10.1001/jamaneurol.2016.5755.

Xia, Chun-Fang et al. (2013). "[18F]T807, a novel tau positron emission tomography imaging agent for Alzheimer's disease". In: *Alzheimer's & Dementia* 9.6, pp. 666–676. ISSN: 15525260. DOI: 10.1016/j.jalz.2012.11.008. URL: http://linkinghub.elsevier.com/retrieve/pii/S1552526012025320.

Chapter 3

Spread of pathological tau proteins through communicating neurons in human Alzheimer's disease

Jacob W. Vogel, Yasser Iturria-Medina, Olof T. Strandberg, Ruben Smith, Elizabeth Levitis, Alan C. Evans, Oskar Hansson

3.1 Preamble

The previous chapter utilized tau-PET to provide an unbiased and spatially-unrestricted view of the *in vivo* distribution of tau in the brain. The findings of this study found even more nuance to an already nuanced progressive pattern, particularly in later stages. However, why tau accumulates in such a specific pattern is still an enigma. Numerous animal experiments have proved tau can spread synaptically from neuron to neuron, suggesting the possibility that tau patterns emerge from brain network organization (reviewed in Section 1.3.2). *In vivo* MRI imaging studies have found links between neurodegenerative patterns and macroscale brain networks, and a few papers using tau-PET have begun to show similar results (reviewed in Section 1.5.2).

However, certain studies found the overall pattern of tau covariance to be correlated with the whole-brain functional connectome, which may indicate a preferential accumulation of tau in brain network hubs and less so in distal nodes (Cope et al., 2018; Franzmeier et al., 2019; Franzmeier et al., 2020). While this could reflect a zoomed-out, gestalt view of synaptic spread, it may also reflect non-causal association between tau accumulation and network "hubness" driven by a shared upstream (e.g. molecular, evolutionary or developmental) cause (discussed in Sections 1.3.3, 5.2.2). Teasing apart these two possibilities is challenging, since the seminal tau-spreading

animal experiments cannot be performed in humans. However, hypotheses of tau spread assume certain properties of tau propagation that resemble constrained diffusion and epidemic spread, lending it to modeling through simulation. While such simulations have been performed in the context of AD neuroimaging (Raj, Kuceyeski, and Weiner, 2012; Iturria-Medina et al., 2014), no such models have thus far been used to simulate tau spread. This type of analysis is superior for testing tau spread, as it tests a specific sequences of events over time, rather than a correlation between two topological patterns.

The work in this chapter involve the application of an Epidemic Spreading Model to simulate the pattern of tau-PET data accumulation. The work also addresses the role of Aβ in influencing tau spread, as well as evidence for synaptic spread in PART, two understudied topics of major interest. Many of the findings in this paper had been conventionally assumed, but not adequately demonstrated in humans. The findings in this chapter are not causal evidence, but they do provide *in vivo* and in-human evidence for concepts that have been conventonally assumed but not convincingly demonstrated in humans. The first version of this data appeared online on *BioRxiv* in February 2019. The current version was recently accepted to *Nature Communications* on March 6th, and should be published online shortly.

3.2 Abstract

Tau is a hallmark pathology of Alzheimer's disease, and animal models have suggested that tau spreads from cell to cell through neuronal connections, facilitated by β-amyloid (Aβ). We test this hypothesis in humans using an epidemic spreading model (ESM) to simulate tau spread, and compare these simulations to observed patterns measured using tau-PET in 312 individuals along Alzheimer's disease continuum. Up to 70% of the variance in the overall spatial pattern of tau can be explained by our model. Surprisingly, the ESM predicts the spatial patterns of tau irrespective of whether brain Aβ is present, but regions with greater Aβ burden show greater tau than predicted by connectivity patterns, suggesting a role of Aβ in accelerating tau spread. Altogether, our results provide evidence in humans that tau spreads through neuronal communication pathways even in normal aging, and that this process is accelerated by the presence of brain Aβ.

3.3 Introduction

Alzheimer's disease is characterized by the presence of β-amyloid plaques and neurofibrillary tangles of hyper-phospohrylated tau at autopsy. Both of these pathological phenomena can now be quantified spatially in the brains of living humans using positron emission tomography (PET), allowing for the study of disease progression before death and, indeed, before symptoms manifest Villemagne et al., 2018. β-amyloid plaques are detectable in the brain many years or even decades before dementia onset Villemagne et al., 2013, but appear to have only subtle effects on cognition and brain health in humans Hedden et al., 2013; Donohue et al., 2017; Palmqvist et al., 2017; Gordon et al., 2018. In contrast, tau neurofibrillary tangles are strongly correlated with local neurodegeneration and, in turn, cognitive impairment Xia et al., 2017; Bejanin et al., 2017b. However, tau tangle aggregation specifically in the medial temporal lobes is a common feature of normative aging Crary et al., 2014; Braak and Del Tredici, 2015; Harrison et al., 2018, itself associated with subtle cognitive effects Maass et al., 2018b; Lowe et al., 2019. Frank cognitive impairment often coincides with the spreading of tau tangles out of the medial temporal lobes and into the surrounding isocortex, a process that animal models have suggested may be potentiated or accelerated by the presence of β-amyloid plaques He et al., 2018; Bennett et al., 2017.

Due to its close link with neurodegeneration and cognitive impairment, tau has received special attention as a potential therapeutic target for Alzheimer's disease Congdon and Sigurdsson, 2018. Perhaps the most compelling features of tau pathophysiology are its rather focal distribution of aggregation and its highly stereotyped pattern of progression through the brain. Specifically, neurofibrillary tangles first appear in the transentorhinal cortex, before spreading to the anterior hippocampus, followed by adjacent limbic and temporal cortex, association isocortex, and finally to primary sensory cortex Braak and Braak, 1991; Braak and Del Tredici, 2015; Cho et al., 2016a; Cho et al., 2018. This very particular pattern has led many to speculate that pathological tau itself, or a pathological process that incurs tau hyper-phosphorylation and toxicity, may spread directly from cell to cell through anatomical connections Goedert, Eisenberg, and Crowther, 2017; Frost and Diamond, 2010. Strong evidence in support of this hypothesis has come from animal models, which have repeatedly demonstrated that human tau injected into the brains of β-amyloid expressing transgenic rodents leads to the aggregation of tau in brain regions anatomically connected to the injection site De Calignon et al., 2012; Liu et al., 2012; Iba et al., 2013; Clavaguera et al., 2013; He et al., 2018. An important caveat to the aforementioned studies is that they involve injection of tau aggregates that

greatly exceed the amount of tau produced naturally in the human brain. In addition, the studies were performed in animals that do not get Alzheimer's disease naturally.

Unfortunately, there are many obstacles to studying the tau-spreading hypothesis in humans. While autopsy studies have provided evidence for tau spreading DeVos et al., 2018a; Brettschneider et al., 2015, this evidence comes in the form of limited snapshots in deceased individuals. Tau-PET allows for the quantification of tau *in vivo*, but the PET signal is contaminated by off-target binding that limit interpretations Choi et al., 2018; Lemoine et al., 2018; Marquié et al., 2017; Lockhart et al., 2017b; Baker et al., 2019. Despite this limitation, circumstantial evidence has emerged supporting the hypothesis that tau spreads through connected neurons in humans. Studies decomposing the spatial distribution of tau-PET signal in the human brain have revealed spatial patterns highly reminiscent of brain functional networks Jones et al., 2017; Vogel et al., 2019a; Hoenig et al., 2018. In addition, brain regions with greater functional connections to the rest of the brain tend to have greater tau accumulation Cope et al., 2018, regional connectivity is associated with longitudinal changes in tau burden Jacobs et al., 2018, and correlations have been found between functional connectivity patterns and tau covariance patterns Franzmeier et al., 2019; Ossenkoppele et al., 2019.

Despite mounting evidence linking brain connectivity and tau expression, the aforementioned studies mostly involve either comparisons between coarse whole-brain measures of tau and brain connectivity, or are limited to only a fraction of brain connections. The initial seeding of tau in the cortex is thought to lead subsequently to secondary seeding events that cascade systematically through the cerebral cortex. Therefore, it is paramount that studies assessing the spread of tau through the brain can effectively model the complex spatio-temporal dynamics of this process. Therefore, we test the tau-spreading hypothesis by placing a "tau seed" in the entorhinal cortex, simulating its diffusion through measured functional and anatomical connections, and comparing the simulated pattern of global tau spread with the actual pattern derived from tau-PET scans of 312 individuals. This method allows for a cascade of secondary tau seeding events to occur along a network over time, more closely simulating proposed models of tau spread in the brain. We then examine how the behavior of our model interacts with brain β-amyloid and what it can tell us about asymmetric tau distribution.

Table 3.1: Demographic information

	CN	MCI	AD	Total	
n	162	89	61	312	
Age (SD)	72.0 (6.4)	70.84 (7.8)	72.0 (7.9)	71.7 (7.1)	
% Women	45.1%	64.0%	58.6%	53.1%	CN =
Education (SD)	14.8 (3.6)	15.3 (3.7)	12.8 (3.9)	14.6 (3.8)	
% *APOE*4	41.9%	58.4%	68.5%	51.7%	
% Amyloid Positive	42.6%	64.0%	100.0%	66.2%	

cognitively normal; MCI = mild cognitive impairment; AD = Alzheimer's disease dementia, SD = Standard Deviation

3.4 Results

3.4.1 Sample information

Flortaucipir (AV1451)-PET scans measuring tau neurofibrillary tangles *in vivo* were available for 312 individuals spanning the Alzheimer's disease spectrum. Demographic information for this sample can be found in Table 3.1.

3.4.2 Tau-positive probabilities enhance fidelity of tau-PET data

We executed a procedure to mitigate off-target binding of Flortaucipir-PET data using mixture modeling. Regional Gaussian mixture modeling of Flortaucipir SUVR data across all subjects suggested a two-component (bimodal) model as a superior fit for all 66 cortical regions-of-interest, including the left and right hippocampi and amygdalae. These 66 regions were converted to tau-positive probabilities (Fig 3.1C) using the Gaussian mixture models. This threshold-free, data-driven transformation yielded a sparse data matrix with a clear pattern suggesting a gradual progression of tau across regions of the brain (Supplementary Figure 1). When sorted from least to most tau (e.g. Cho et al., 2016a), the regional ordering greatly resembled the previously described progression of tau pathology Braak and Braak, 1991 (Fig 3.2).

3.4.3 Neuronal connectivity explains the spatial pattern of tau

An epidemic spreading model (ESM) was fit to the data, simulating the spread of tau from a single epicenter through macro-scale brain connections over time (Fig 3.1). The ESM was fit over several regional tau-PET datasets resulting from combinations of arbitrary data pre-processing decisions (see Methods). All models were fit using the left and right entorhinal cortex as the model epicenter. Models performed best when SUVR data for the 66 cortical regions were converted to tau-positive probabilities as described above, with regression of age, sex, and non-specific choroid-plexus

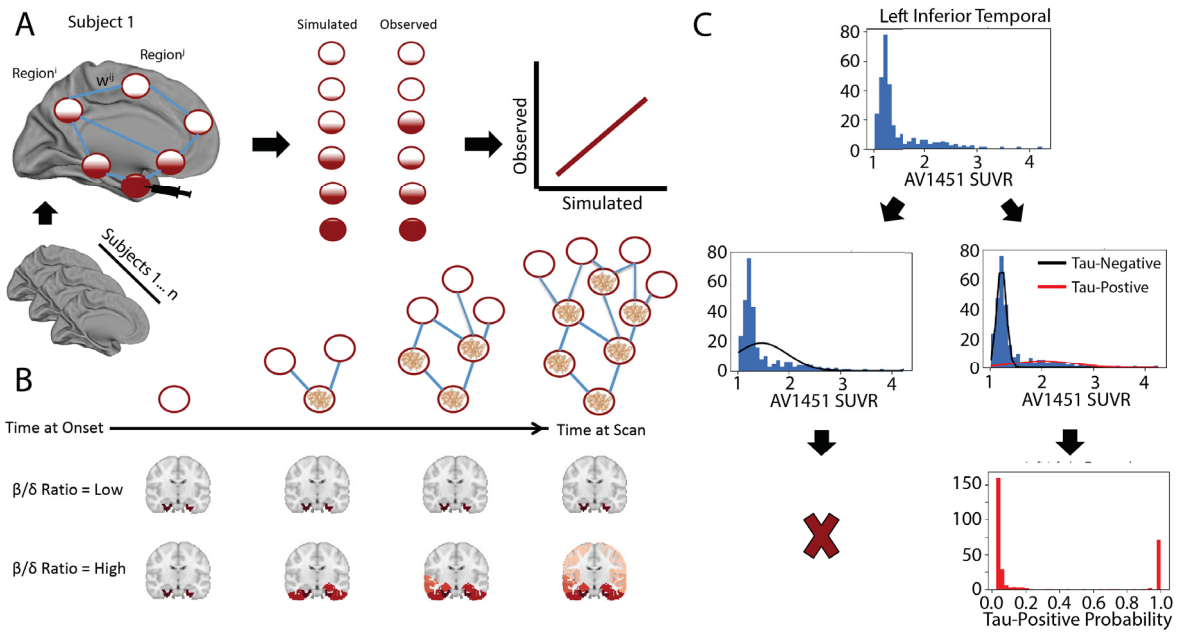

Figure 3.1: A) An artificial system based on a pairwise relationship (e.g. functional connectivity) matrix is created, where the relationship between regions i and j is represented by weight ij. For each subject, a seed is placed at the model epicenter, and the diffusion of this signal over time is simulated through the system, where the inter-regional relationships determine the pattern of spread, and subject-level free parameters determine the velocity of diffusion, until an optimal fit is reached. The simulated tau signal is then compared to the observed tau-PET signal to evaluate the model. B) Advantages of the ESM over traditional approaches includes the initiation of secondary seeding events as the diffusion process reaches new regions (top), and the fitting of subject-level production (β) and clearance (δ) parameters. A balance in these parameters will lead to little to no spreading over time, while increasing imbalance leads to accelerated spread. C) The distribution of all SUVR values in the left inferior temporal ROI are shown. Two Gaussian mixture models are fit to the data. When a one-component model fits the data better, the ROI is discarded. When a two-component model fits better, the probability that each values falls upon the second distribution is calculated.

binding from the data occurring beforehand (Supplementary Figure 2A,B,F). Partial volume correction (PVC) (Supplementary Figure 2C) and exclusion of Aβ- MCI individuals (Supplementary Figure 2E) did not appear to impact model performance, though the best-fitting model did not use PVC and excluded Aβ- MCI individuals (Supplementary Figure 2A).

The best-fitting model was fit over a system of anatomical connections created from a separate sample of young, healthy individuals using DTI tractography. This model explained 70.2% (null model mean r^2 [95% CI] = 0.056 [0.016, 0.135], $p<0.01$) of the overall spatial pattern of tau (Fig 3.3A), and on average, explained 50.9% (SD=21.8%; null model mean r^2 [95% CI] = 0.104 [0.077, 0.147], $p<0.01$) of the spatial pattern within individual subjects (Fig 3.3A). Importantly, across all possible regions of interest, the entorhinal cortex proved to be the epicenter providing the best model fit, corroborating autopsy studies finding neurofibrillary tangles to start in the entorhinal cortex (Fig 3.3B). Model performance was better in ADNI (global

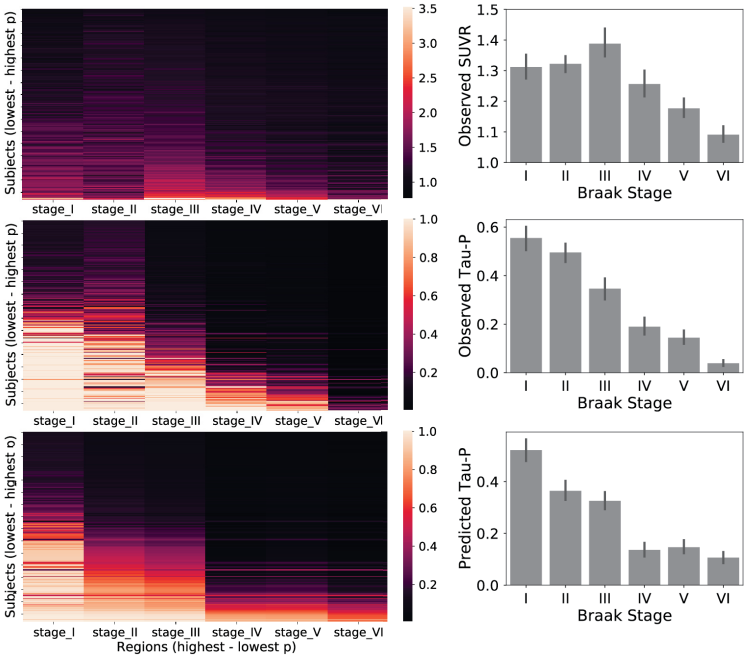

Figure 3.2: Each brain region was divided into one of six "Braak stage" ROIs, based on which Braak stage abnormal tau is first observed in the region (as described in Schöll et al., 2016b). (Left) Each row is a subject sorted top-bottom by least to most overall tau. Each column is an Braak stage ROI, sorted left to right by most to least overall tau. Warmer colors represent higher SUVR values (top), observed tau-positive probabilities (middle) or predicted tau-positive probabilites from the best-fitting ESM (bottom). (Right) The same relationship shown in a barchart format. Error bars represent standard error of the mean. Conversion to tau-positive probabilities creates a sparse distribution of values demonstrating a progression reminiscent of the staging described in the autopsy literature.

pattern r^2 = 0.78) compared to BioFINDER (r^2 = 0.6), though this difference was partially mitigated by subsampling BioFINDER to match ADNI based on demographic variables, and the difference disappeared entirely when subsampling BioFINDER to match ADNI based on mean cortical tau signal (Supplementary Figure 3). Model fit was good across cognitively normal, MCI and AD subjects, and expected increases in mean tau signal were observed as disease severity increased (Supplementary Figure 4). The epidemic spreading model was particularly effective in predicting the early progression of tau, but diverged more from the observed tau pattern over time (Supplementary Figure 5, Fig 3.4).

As a validation, the ESM was fit over a second set of anatomical connections from another non-overlapping dataset consisting of healthy and cognitively impaired older adults. Once again, the ESM demonstrated good model fit, explaining 65.6% (null model mean r^2 [95% CI] = 0.107 [0.052, 0.217], $p<0.01$) of the overall spatial pattern of tau, and explained 44.8% (SD=21.7%; null model mean r^2 [95% CI] = 0.104 [0.077, 0.147], $p<0.01$) of the spatial pattern within individual subjects on average (Supplementary Figure 6).

The ESM was fit once again instead using connectivity matrices composed of functional connections measured in separate samples of young healthy adults, and

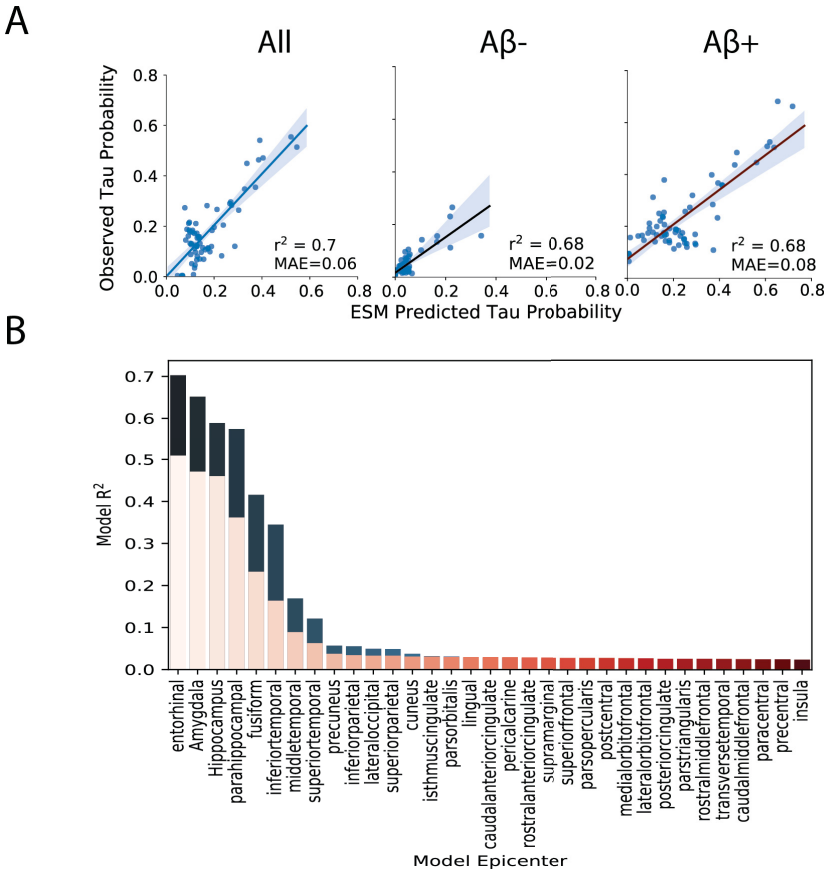

Figure 3.3: A) For each plot, each dot represents a region. The x-axis represents the mean simulated tau-positive probabilities across the population, while the y-axis represents the mean observed tau-positive probability. A value of (say) 0.3 for a given ROI would suggest that an average of 30% of all subjects included were predicted (X) or observed (Y) to have positive abnormal tau signal in that region. The average performance of the four different models are shown separately for (left) all subjects, (center) Aβ- individuals and (right) Aβ+ individuals. B) The ESM was rerun using each left-right pair of ROIs as the model epicenter. The model fit (r^2) is depicted on the y-axis, and each bar represents the fit of model using a given region as model epicenter. Blue bars represents global model fit across all subjects, and red bars represent the mean within-subject model fit. An entorhinal cortex epicenter provided the best model fit.

old healthy and impaired adults, respectively, using resting state functional MRI connectivity (Supplementary Figure 6, Fig 3.4). These analyses test whether the ESM is robust to different measures of macroscale connectivity, but also can be thought to test an alternative hypothesis of tau spread through communication of pathological states, rather than through physical spread of tau oligomers. Models fit over functional connectomes performed quite well, though slightly worse than models using structural connectomes (YOUNG: Global r^2=0.565; null r^2 [95% CI] = 0.089 [0.031 - 0.187]; Individual mean r^2=0.384, SD=0.168, null r^2 [95% CI] = 0.103 [0.069 - 0.156]; OLD: Global r^2=0.586; null r^2 [95% CI] = 0.031 [0.000 - 0.087]; Individual mean r^2=0.451, SD=0.209, null r^2 [95% CI] = 0.063 [0.037 - 0.109]), a trend that was consistent across preprocessing strategies (Supplementary Figure 2D). Additional alternative hypotheses have been proposed suggesting tau may simply spread extracellularly across neighboring regions, rather than through anatomical connections. To test this

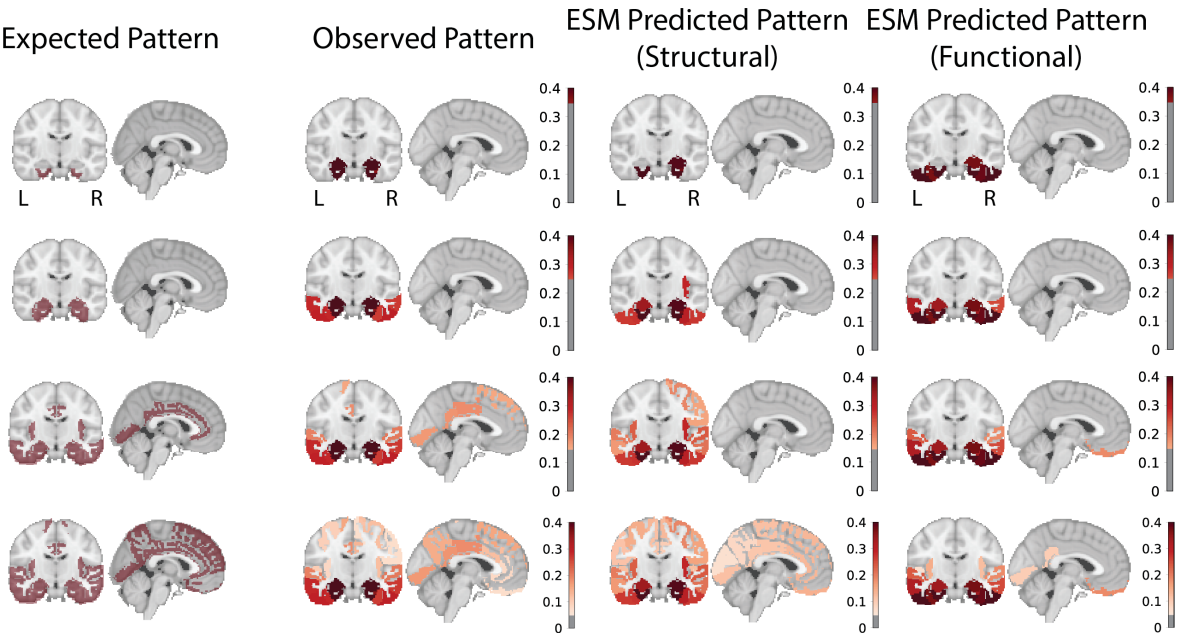

Figure 3.4: (left) Hypothetical spread patterns represented by Braak stages I, II, VI, V and VI as described in Schöll et al., 2016b. (right) Spreading patterns of (from left to right) the observed tau-PET data, the ESM simulated data using a young structural connectome, and using a young functional connectome. Warmer colors represent higher proportion of regional tau-positivity predicted or observed across the population. Each "stage" was achieved by arbitrarily thresholding the population-mean tau-positive probability image at the following thresholds: 0.35, 0.25, 0.15, 0.05

hypothesis, a model was fit over a Euclidean distance matrix instead of a functional or structural connectome (Supplementary Figure 6). As with models using functional connectomes, the euclidan distance matrix performed far greater than chance, but not as well as models using anatomical connectivity.

3.4.4 Low-level tau spreading is evident in amyloid-beta negative individuals

We divided our study sample into groups based on Aβ status and examined model accuracy separately within these groups. Model accuracy remained high even among Aβ- individuals, despite a low overall tau burden (Fig 3.3A). These effects were additionally present when including Aβ- MCI subjects, when summarizing within MCI- subjects alone, and when summarizing results over only cognitively normal Aβ- individuals without marginally elevated CSF Aβ and without any *APOE*4 allele copies (Fig 3.5B). This was validated by examining model fit against the tau pattern of individual Aβ- subjects (Fig 3.5). Model performance was high across most CN- subjects (Fig 3.5A), including those with low or even very low regional tau burden (Fig 3.5C). In many cases, tau levels that would otherwise be considered sub-threshold nonetheless demonstrated a systematic pattern resembling Braak staging, which was also predicted by brain connectivity.

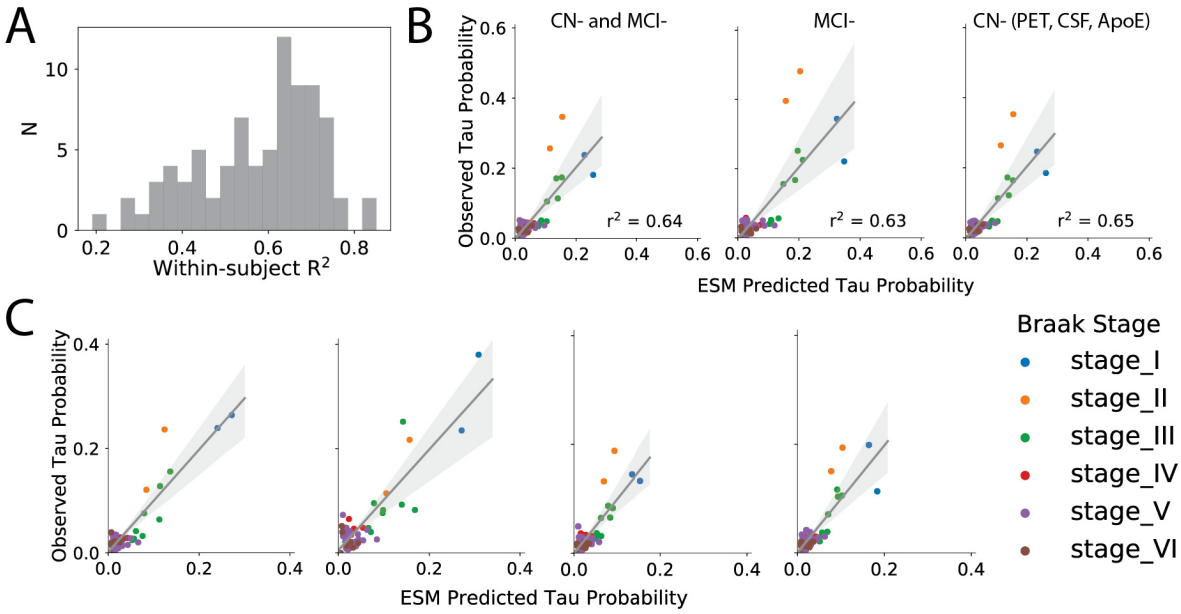

Figure 3.5: All plots are based on the best-fitting ESM model described in the text. (A) The distribution of r^2 values representing the range in individual-level model fit across all CN- subjects. (B) For each plot, each dot represents a region. The x-axis represents the mean simulated tau-positive probabilities across the population, while the y-axis represents the mean observed tau-positive probability. Predicted and observed patterns are plotted for (left) all Aβ- individuals (n=104), (middle) only Aβ- MCI subjects (n=22), and (right) individuals without elevated Aβ-PET or Aβ-CSF, and who carry no *APOE*4 alleles (n=62). (C) Four exemplary subjects spanning both cohorts are plotted. All four subjects are cognitively normal with MMSE 29-30 and do not carry and *APOE*4 allele. Their respective ages are 73, 63, 71 and 78. Even at very low (subthreshold) levels, the distribution of tau follows a pattern similar to Braak staging, and which is predicted by anatomical connectivity patterns.

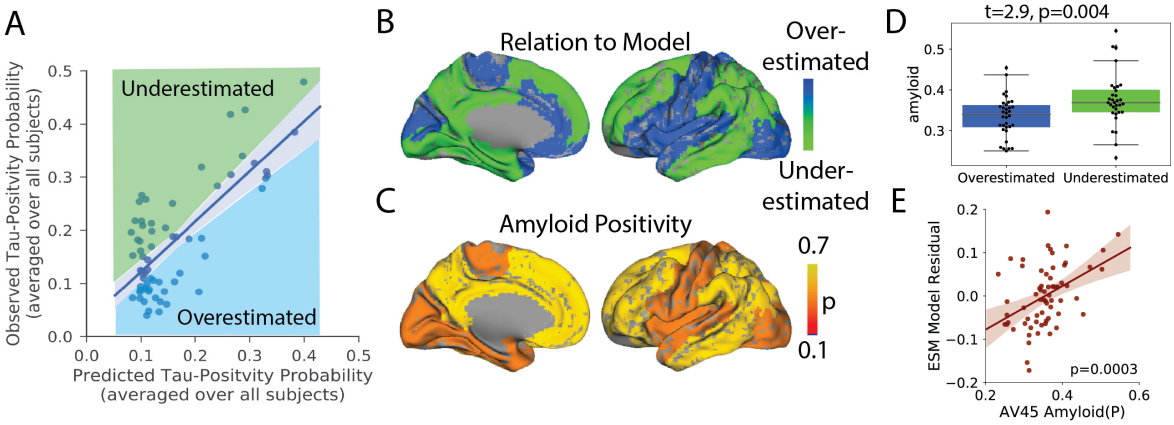

Figure 3.6: A) Regions were classified as overestimated or underestimated based on the sign of the residual in a comparison of predicted vs. observed values. B) A cortical surface render showing the spatial distribution of over- and underestimated regions. C) A surface render showing the spatial distribution of regional amyloid-positive probabilities averaged over all subjects. D) Underestimated regions tended to have significantly greater amyloid burden, suggesting these regions had more tau than would be predicted given their connectivity to the model epicenter. For boxplots, the center line = median, box = inner quartiles, whiskers = extent of data-distribution except * = outliers. E) Correlation between regional model residuals and regional amyloid. Each point is a brain region, and the y-axis summarizes the degree to which a region was underestimated (positive) or overestimated (negative) by the model.

3.4.5 Regional beta-Amyloid affects regional model performance

For each model, regions-of-interest were classified as either overestimated or underestimated by the model based on the sign of the residual (Fig 3.6A,B). Underestimated regions are those demonstrating greater tau burden than would be expected given connectivity to the model epicenter (i.e. observed $>$ predicted), while overestimated regions demonstrate less tau than would be expected given their connectivity profile (i.e. predicted $>$ observed). We compared regional model performance to regional Aβ accumulation as measured from a large dataset of Aβ-PET (^{18}F-florbetapir, or AV45) scans (Fig 3.6C). Compared to overestimated regions, underestimated regions had greater global β-amyloid burden ($t = 2.9$, $p = 0.004$; Fig 3.6D), suggesting the regional presence of Aβ may accelerate the spread or expression of tau tangles. Indeed, we observed a significant correlation ($p<0.001$) between regional model residuals and regional Aβ levels (Fig 3.6E), and this relationship remained significant when adjusting for regional tau.

3.4.6 Evidence for individual asymmetry in tau deposition

Asymmetric lateralization of tau pathology and tau-PET signal is a prominent feature of rare AD variants Ossenkoppele et al., 2016a, and pathology studies have highlighted examples of hemispheric asymmetry in tau spreading Braak and Del Tredici, 2015. We used the ESM to investigate whether a general lateralization of tau deposition could be observed across the population, or whether asymmetric patterns in tau deposition were observable at the individual level. We did not observe a trend of better model performance when using either the left or right entorhinal cortex as the sole epicenter, suggesting tau does not start preferentially in one hemisphere or the other across a population (Fig 3.7A). This effect was only observable when using models fit over DTI connectomes, since rsfMRI connectomes exhibited strong heterotopic (and likely indirect) connectivity in the entorhinal cortex. We next determined the best-fitting epicenter for each individual subject in the study, and categorized subjects accordingly as best described by a left-limbic, right-limbic, or non-limbic epicenter. Epicenter hemisphere was associated with asymmetry in tau deposition ($p<0.001$), and this effect became more prominent ($ps < 0.01$) as disease severity progressed (Fig 3.7D). Specifically, individuals with a left-limbic epicenter exhibited greater left temporoparietal binding, but less right frontal binding, after adjusting for disease status, age and sex. This may point to a differing cortical expression of tau depending on the hemisphere of origin. Right-limbic epicenters were more common, but decreased with disease progression (Fig 3.7B,C). Individuals with a right-limbic

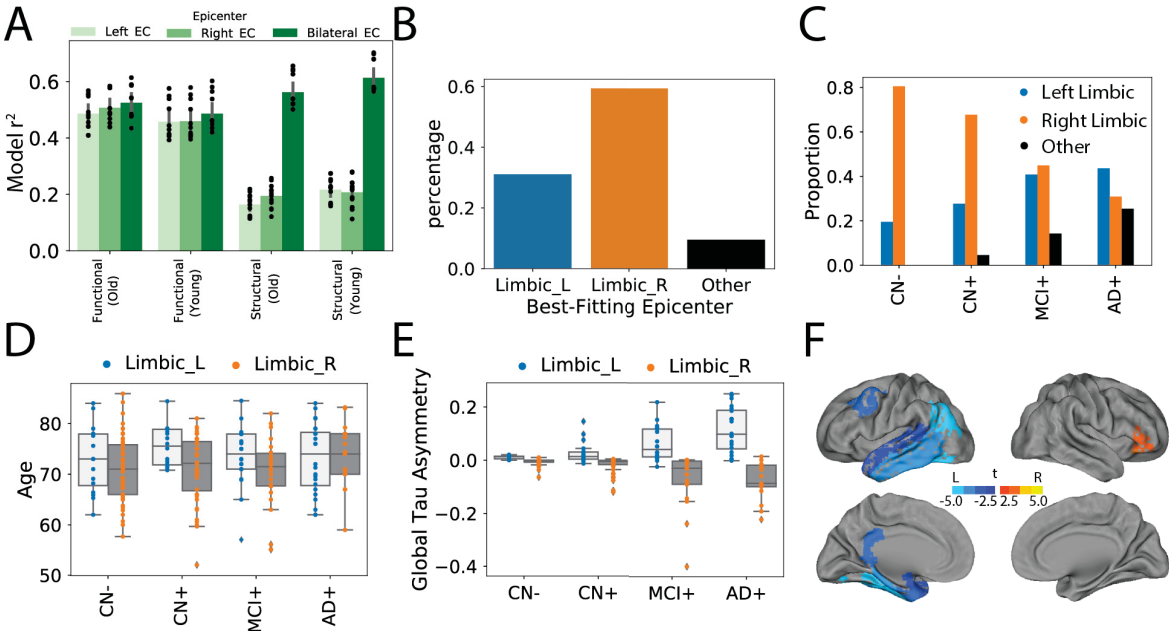

Figure 3.7: (A) Using only left or right entorhinal cortex alone as model epicenter did not result in improvement in model fit. Error bars represent standard error of the mean in variation in model fit depending on PVC strategy, confound-regression strategy, and MCI- inclusion/exclusion. (B) Proportion of individuals for whom a left-limbic, right-limbic or cortical epicenter best fit their individual tau-PET pattern. (C) The same, across disease progression categories. (D) Subjects for whom left-limbic epicenter best fit their data were older, using a two-tailed GLM adjusting for disease status. (E) Epicenter hemisphere was associated with increasing hemispheric asymmetry in tau-PET signal across disease progression, using a two-tailed GLM adjusting for disease status. (F) Regions of higher average tau-PET signal in subjects for whom left-limbic (blue) or right-limbic (orange) epicenters best fit their data; adjusted for age, sex, disease status and multiple comparisons. For boxplots in panels D,E: the center line = median, box = inner quartiles, whiskers = extent of data-distribution except * = outliers.

epicenter tended to be older (p=0.01; (Fig 3.7D)), but did not differ in sex, education, amyloid status, *APOE4* status, or total tau.

3.5 Discussion

Observations in post-mortem human brains Brettschneider et al., 2015; DeVos et al., 2018a and experiments in animal models De Calignon et al., 2012; Liu et al., 2012; Iba et al., 2013; Clavaguera et al., 2013; He et al., 2018 have together provided evidence that tau can be transmitted from cell to cell through neuronal projections. However, post-mortem studies cannot provide direct evidence of cell-to-cell spread, and while animal models have proven tau can spread through neuronal connections under certain unnatural conditions, they cannot prove that this phenomenon occurs naturally in humans. Studies searching for evidence of cell-to-cell transmission of tau in living humans have been limited by small datasets, simplistic models and issues relating to the quantitative measurement of tau. Here, we used a mixture-modeling approach on a large sample of humans on the Alzheimer's disease spectrum to enhance the quantification of tau signal, and we applied to this data a diffusion model based on

theoretical principles of an agent propagating through a network. These simulations explained a majority of the variance in the global spatial distribution of tau-PET signal in the brain, and performed nearly as well in predicting the distribution of tau-PET signal in individual subjects. A similar model testing the hypothesis that tau spreads across neighboring brain regions was less successful at explaining the overall pattern. The models performed well in both Aβ-negative and Aβ-positive individuals, and also systematically underestimated the magnitude of tau in regions classically shown to harbor β-amyloid. Together, these results provides evidence that tau spreads through the limbic network in normal aging, and that the presence of β-amyloid is associated with acceleration of tau tangle expression into isocortical regions.

Brain networks may be key to the evolution of neurodegenerative disease Iturria-Medina and Evans, 2015. The atrophy patterns of many neurodegenerative dementias have been shown to resemble resting-state functional brain networks Seeley et al., 2009; Zhou et al., 2012; Brown et al., 2019, and network "hubs" are especially vulnerable to neurodegeneration across brain disorders Crossley et al., 2014. Studies modeling the diffusion of gray matter degeneration across brain networks have recreated such patterns with impressive accuracy Zhou et al., 2012; Raj, Kuceyeski, and Weiner, 2012; Zheng et al., 2019. However, in many neurodegenerative disorders, brain atrophy is preceded and perhaps caused by the aggregation of pathological agents. In Alzheimer's disease, the presence of tau is closely linked to Xia et al., 2017; Bejanin et al., 2017b, and likely precedes La Joie et al., 2020, gray matter atrophy. However, because gray matter degeneration observed in Alzheimer's dementia may be caused by many sources other than Alzheimer's pathology, gray matter degeneration itself cannot be used as proxy for tau (e.g. Torok et al., 2018). PET studies therefore provide a unique advantage by measuring pathological proteins more directly, and applying network diffusion models to PET data has, for example, led to the successful description of the spatial progression of β-amyloid in Alzheimer's disease Iturria-Medina et al., 2014. Our model uses a similar framework to simulate the spread of tau through the brain and reaches a similar level of success, both within-subject as well as globally across all subjects. The application of network models to other forms of dementia will be needed to conclude whether the spread of pathological proteins through connected neurons is a common thread linking many diseases.

While our model recapitulated the early stages of tau spreading accurately (Braak I-III), later stages (IV-VI) were modeled less accurately, with a systematic underestimation of tau in regions prone to early and high-volume β-amyloid aggregation. While tau, not β-amyloid, is closely associated with atrophy in Alzheimer's disease,

the commonly-observed concurrence of extra-limbic tau and cortical amyloid burden has led to speculation that β-amyloid may accelerate or otherwise facilitate the spread of tau outside the medial temporal lobe. Recent studies in mice have shown that β-amyloid creates an environment facilitating the rapid fibrilization of tau He et al., 2018; Bennett et al., 2017. Our data support this notion, as brain regions harboring more β-amyloid, such as the precuneus and temporoparietal regions, had a higher incidence of abnormal tau than would be predicted simply by their regional connectivity to the medial temporal lobe. A conclusive model of tau spreading may not be complete without incorporating dynamic interaction with Aβ.

Tau tangles are a pathological hallmark of AD, but they are neither specific to AD, nor to neurodegenerative disease in general. The process of aging appears to lead inevitably to the accumulation of tau tangles in the medial temporal lobe and occasionally beyond, a phenomenon known as primary age-related tauopathy (PART) Crary et al., 2014. *In vivo* evidence for the longitudinal accumulation of tangles in healthy elderly has been observed Harrison et al., 2018. While PART may result in subtle insults to cognition and brain health Jefferson-George et al., 2017; Lowe et al., 2019; Maass et al., 2018b, there is still debate as to whether PART and AD are distinct processes Braak and Del Tredici, 2014. We show that even in individuals without significant Aβ burden and low (subthreshold) tau-PET signal, the spatial pattern of tau resembles early Braak staging, and can be predicted by connectivity to the entorhinal cortex. This corroborates a recent study finding tau-PET patterns overlap greater than chance with entorhinal cortex connectivity even in Aβ-negative subjects Adams et al., 2019. The inability of Aβ-PET to identify sparse Aβ burden, especially in cases with predominant diffuse plaques, may lead to the possibility that undetectable levels of Aβ pathology may be driving the observed relationships. However, we demonstrated an early Braak-like pattern of tau in individuals at very low likelihood of having Aβ pathology (cognitively normal, *APOE*4-negative, CSF Aβ negative). These findings suggest that, even in normal aging, tau may spread through communicating neurons. The results also suggest closer scrutiny of subthreshold tau-PET signal in cognitively unimpaired, Aβ-negative individuals. Elevated SUVR values occurring in a consistent pattern in specific limbic regions may be indicative of very low tau pathology, rather than non-specific or off-target ligand binding.

Tau can be directly secreted into extracellular space, and mechanisms have been described for subsequent cellular uptake (c.f. Fuster-Matanzo, Hernández, and Ávila, 2018), leading to the hypothesis that tau may be propagated to neighboring neurons. This idea is not supported by our data, where neuronal connectivity patterns provided a better description of the *in vivo* spatial distribution of tau. Another hypothesis stems from the observation that tau has an excitatory effect on neurons DeVos et al.,

2013, but is also secreted by activated neurons DeVos et al., 2013; Pooler et al., 2013. These two observations have lead to the idea of an excitotoxic cascade, where the presence of tau excites neurons, leading to over-stimulation of connected neurons, which in turn leads to secretion of tau, and so forth. This latter hypothesis cannot be ruled out based on our data, as it is still predicated on the spreading of pathological events across communicating neurons. In our study, we fit the ESM over two different measures of macroscale connectivity, and the choice of modality comes with different sets of assumptions and limitations. DTI tractography endeavors to directly measure white matter connections between brain regions, and may therefore be the most appropriate choice, but also suffers from important methodological limitations such as the gyral bias Jbabdi et al., 2015. On the other hand, rsfMRI connectomes are conflated by indirect connectivity Jbabdi et al., 2015 (e.g. Fig 3.7A), which does not fit with the hypothesis of direct axonal spread. Additionally, one can imagine a scenario where a region may act as way station for tau propagation without itself expressing pathological tau due to (say) its genomic environment. Additionally, alternative hypotheses of tau propagation involving network propagation of a pathological (e.g. excitotoxic or tau overproduction) state would not necessarily require direct connections. fMRI connectivity may be thought of a proxy of some of these hypotheses. In our data, DTI tractography-based connectomes consistently showed superior model fit compared to models fit over other connectomes (Supplementary Figure 6, Supplementary Figure 2D), once again lending support to the cell-to-cell transmission hypothesis, though model fit was ultimately high and reproducible across both connectivity modalities. Next-generation tractography may provide improved models in the future Maier-Hein et al., 2017, but both measures of connectivity appear to be sufficient for fairly high-performing simulations of tau spread.

While our findings lend support to the hypothesis of tau spreading through communicating neurons, connectivity patterns and regional Aβ burden together could not fully explain the observed pattern of tau-PET across the brain. While a portion of this discrepancy may be explained by measurement error, there are likely other factors at play. Recent work has outlined a consistent genomic profile across regions that express tau Grothe et al., 2018, implicating that regional variation in intrinsic molecular environment may mediate the presence and rate of tau tangle formation. This may explain why, for example, many subcortical regions do not show substantial tau burden despite connections to regions expressing neurofibrillary tau tangles. In addition, it is also possible that only certain neuron types can facilitate the transmission of tau, which may be challenging to model using macroscopic neuroimaging-based measures of brain connectivity (though recent advances in single-cell transcriptomic changes in AD may help guide such analyses Mathys et

al., 2019). Heterogeneity in tau patterns Murray et al., 2011b; Ferreira et al., 2019 present yet another difficulty in tau spread modeling. Finally, some studies have suggested the directional flow of neuronal activity may influence the spread of brain pathology Scherr et al., 2019. Future studies incorporating this information, along with dynamics related to regional amyloid burden and regional vulnerability, may achieve a more complete model of tau spreading. However, at present, we show that the spread of tau is predicted by connectivity patterns to a degree that greatly exceeds both chance and other hypotheses of tau spread, and does so in a parsimonious fashion, supporting the notion that connectivity is in some way involved in the spread of tau through the human brain.

The results of the ESM represent an advance on previous human studies testing the spreading hypothesis of tau. Many previous studies addressing this hypothesis have elected to examine covariance between tau patterns and brain networks, usually measured with rsfMRI. Jones et al., Adams et al. and Hoenig et al., described overlap between data-driven tau-PET covariance networks and resting-state functional networks Jones et al., 2017; Hoenig et al., 2018; Adams et al., 2019. Franzemeier et al. and Ossenkoppele et al. each went further to show correlations between rsfMRI connectivity and cross-subject covariance in tau-PET signal, within networks or across the whole brain Franzmeier et al., 2019; Ossenkoppele et al., 2019. Sepulcre et al. instead used longitudinal tau covariance across spatially distributed regions to infer connectivity between those regions Sepulcre et al., 2018. Each of these studies represent clues that tau spreading and connectivity are related in humans. However, they do not construct, test or simulate models of tau spreading. The ESM simulates the spread of tau from the entorhinal cortex through a cascade of secondary seeding events informed by macroscale functional or structural connections, a process that is designed to mimic the hypothetical spreading of tau. This model can explain upwards of 70% of the spatial variation of tau in the human brain, representing a substantial improvement over the aforementioned associational studies, as well as over studies using similar diffusion models on structural MRI measures (e.g. Torok et al., 2018; Acosta et al., 2018). Importantly, our model is unique in finding the entorhinal cortex as the best epicenter, which corroborates autopsy findings. While our simulation explains the tau-PET data to an unprecedented degree, it is imperfect and remains indirect evidence of tau spreading. However, it also provides a first step toward a tau spreading simulation model, which can be improved, perturbed and applied in numerous contexts. In addition, the ESM has potential as a clinical tool by estimating where tau will spread based on individual regional patterns. Knowledge of the expected pattern of tau spread will be helpful in designing regional outcome measures in future treatment trials directed against tau aggregation.

We used the ESM to conduct a preliminary analysis concerning individual variation in asymmetric hemispheric distribution of tau. We observed considerable variation in laterality of tau-PET signal across individuals, particularly in later disease states, and the dominant hemipshere was predicted by the hemisphere of the best-fitting epicenter determined by the ESM. While asymmetric tau deposition is commonly described in rare AD variants Ossenkoppele et al., 2016a, our findings suggest some lateralization even in typical AD, and may be associated with differential cortical patterning of tau accumulation. Subjects with right-side dominant tau patterns tended to be older, but a more thorough analysis is necessary to uncover whether differential hemispheric lateralization of tau deposition leads to distinct phenotypes of clinical expression.

Our study comes with a number of limitations. The premise of testing the hypothesis of tau spread through communicating neurons requires that both neuronal connections and tau burden are accurately measured. We attempt to partially surmount these issues by introducing a data-driven approach for overcoming off-target and non-specific binding in Flortaucipir-PET data, and by validating our findings over different connectomes across different samples and modalities. Our mixture-modeling strategy is sensitive to sample size and composition. While it is unlikely that this phenomenon strongly affected the present findings, it is an important point worth consideration for future studies utilizing this approach to transform tau-PET data. Another limitation is raised by our choice to remove regions that do not demonstrate measurable tau burden, namely subcortical regions, from the model altogether. Certain subnuclei of subcortical structures such as the thalamus do accumulate tau pathology in Alzheimer's disease Aggleton et al., 2016, though we were unable to detect such pathology, perhaps due to the resolution of our measurements. While it is possible that subcortical structures participate in neuronal transmission of pathology without expressing the pathology itself, the current implementation of our model does not support this type of dynamic. However, while incidental measurement of indirect functional connectivity is a common critique of functional MRI, here it may pose an advantage, as functional connectivity mediated by subcortical connections may still be present in functional connectomes used for this study. Finally, we tested the ESM over a number of different pre-processing decisions, and mostly describe results of best-fitting models. It is important to note that a model that best fits our data does not necessarily equate to a model that best fits biology. However, many different pre-processing combinations produced high-performing models (Supplementary Figure 2A), so we are confident that our results are not dependent on our pre-processing decisions.

In conclusion, our data supports the notion that tau pathology itself, or information leading to the the expression of pathology, is transmitted from cell to cell in humans, principally through neuronal connections, and not extracellular space. Our findings further suggest that this phenomenon proceeds fairly ubiquitously in normal aging, and that the process is accelerated in specific brain regions demonstrating β-amyloid burden. While our cross-sectional, *in vivo* results cannot prove that tau spreads through neuronal connections, we show that more highly connected regions have a higher tendency to be affected sooner by tau along a specific network path cascading from the medial temporal lobe. Future models may be able to improve results by incorporating region-specific vulnerability factors, directional flow and Aβ dynamics, though contributing such information in a parsimonious way presents a difficult challenge.

3.6 Methods

3.6.1 Participants

Participants of this study represented a selection of individuals from two large multi-center studies: the Swedish BioFinder Study (BioF; http://biofinder.se/) and the Alzheimer's Disease Neuroimaging Initiative (ADNI;adni.loni.usc.edu). Both studies were designed to accelerate the discovery of biomarkers indicating progression of Alzheimer's disease pathology. Participants were selected based on the following inclusion criteria: participants must i) have a Flortaucipir-PET scan, ii) have either a β-amyloid-PET scan (for ADNI: [^{18}F]-Florbetapir, for BioF: [^{18}F]-Flutemetamol) or lumbar puncture measuring CSF Aβ1-42. In addition, participants were required to be cognitively unimpaired, have a clinical diagnosis of mild cognitive impairment, or have a clinical diagnosis of Alzheimer's dementia with biomarker evidence of β-amyloid positivity. For both cohorts separately, PET-based Aβ1-42 positivity was defined using mixture modeling, as previously described Palmqvist et al., 2017. For BioFINDER, β-amyloid1-42 positivity was defined as an (INNOTEST) level below 650 ng/L All participants fitting the inclusion criteria with Flortaucipir scans acquired (BioFINDER) or that were available for public download (ADNI) in May 2018 were included in this study. In total across both studies, 162 cognitively unimparied individuals, 89 individuals with mild cognitive impairment and 61 amyloid-positive individuals with suspected Alzheimer's dementia were included. Demographic information can be found in Table 1, whereas a detailed comparison of BioFINDER and ADNI cohorts can be found in Table S1. BioFINDER subjects were on average less educated than ADNI subjects, and included a higher

proportion of amyloid-positive individuals. All BioFINDER subjects provided written informed consent to participate in the study according to the Declaration of Helsinki; ethical approval was given by the Ethics Committee of Lund University, Lund, Sweden, and all methods were carried out in accordance with the approved guidelines. Approval for PET imaging was obtained from the Swedish Medicines and Products Agency and the local Radiation Safety Committee at Skåne University Hospital, Sweden. Information related to participant consent in ADNI can be found at (ADNI;adni.loni.usc.edu).

3.6.2 PET Acquisition and Pre-processing

MRI and PET acquisition procedures for ADNI (http://adni.loni.usc.edu/methods/) and BioF Hansson et al., 2017 have both been previously described at length. All Flortaucipir-PET scans across studies were processed using the same pipeline, which has also been previously described Hansson et al., 2017; Vogel et al., 2019a. Briefly, 5-min frames were reconstructed from 80-100 minutes post-injection. These frames were re-aligned using AFNI's 3dvolreg (https://afni.nimh.nih.gov/) and averaged, and the mean image was coregistered to each subject's native space T1 image. The coregistered image was intensity normalized using an inferior cerebellar gray reference region, creating standard uptake value ratios (SUVR). In order to get an independent map of β-amyloid (Aβ) deposition, regional Aβ-PET images were downloaded from a larger cohort of subjects. Baseline ROI-level information for ^{18}F-Florbetapir scans were downloaded from available ADNI subjects (n=974), which had been processed using the whole cerebellum as a reference region.

3.6.3 The Epidemic Spreading Model

The spread of tau through connected brain regions was simulated using the Epidemic Spreading Model (ESM), a previously described diffusion model that has been applied to explain the spread of β-amyloid through the brain Iturria-Medina et al., 2014. The ESM simulates the diffusion of a signal from an epicenter through a set of connected regions over time (Fig 3.1A,B). The dynamics of the spreading pattern are controlled by the weighted connectivity between regions, and by a set of parameters fit within-subject, the latter of which are solved through simulation. Specifically, the parameters represent subject-specific i) global tau production rate, ii) global tau clearance rate and iii) age of onset, which interact with regional-connectivity patterns to determine the velocity of spread. The ESM is simulated over time for each subject across several parameter sets, and the set that produces the closest approximation to observed tau burden for a given subject is selected. Note that these parameters

themselves do not control regional patterning, which is the metric by which the accuracy of the model is evaluated (see below). Instead, the free parameters moderate the overall tau burden (i.e. the stopping point), which allows the ESM to be fit to individuals across the Alzheimer's disease spectrum. For example, an individual with little-to-no tau burden would likely be fit with a balance of production and clearance rates that would preclude the overproduction and spread of tau signal (Fig 3.1C). A detailed and formalized description of the ESM can be found elsewhere Iturria-Medina et al., 2014.

The ESM takes as input a Region x Subject matrix of values ranging from 0 to 1, representing the probability of a pathological burden (in this case, of tau) in a given region for a given subject. The model is fit within-subject and, for each subject, produces an estimate of tau probability for every region-of-interest. In previous applications of the ESM, the model is fit over every possible epicenter as well as combinations of epicenters, and the epicenter providing the best overall fit to the data is selected. In our case, autopsy work provides strong evidence for a consistent "epicenter" of tau neurofibrillary tangles in humans. Tangles first emerge in the trans-entorhinal cortex, before emerging in other parts of the entorhinal cortex as well as the anterior hippocampus Braak and Braak, 1991; Braak and Del Tredici, 2015. We therefore ran models with the left and right entorhinal cortex selected as the model epicenters. In order to validate this choice, we ran the model using the left-right pair of every region of interest (33 pairs in all) and compared the model fit using each regional epicenter. To examine asymmetric spreading, we later fit models using just the left and right entorhinal cortex as separate epicenters. We also found a best-fitting model-derived epicenter for each subject, by fitting the ESM across all possible regions and finding the best within-subject fit.

There are many data pre-processing and model fitting decisions that may affect the performance of the ESM. Some of these decisions include i) what kind of connectivity data to fit the model over, ii) which brain regions to include, iii) what kind of tau measurement to use as input, iv) whether regional tau-PET data should be partial volume corrected, v) whether and how to correct the regional tau-PET data for confounding signals, and vi) whether or not to include amyloid-negative MCI subjects. Rather than arbitrarily choosing these parameters, we fit the ESM over a range of different parameter sets (see subsequent sections) and investigate how these pre-processing decisions affect model performance. We then select the best-fitting models for subsequent analysis. Choices for ii - v are discussed in Section 3.6.4, whereas choices for i are discussed in Section 3.6.5. Across all combinations of methodological choices, a total of 432 models were fit.

3.6.4 Regional tau-PET data pre-processing

Pre-processing of PET data resulted in mean regional tau-PET SUVR values from the FreeSurfer-derived Desikan-Killiany-Tourville (DKT) atlas Desikan et al., 2006, extracted from each individual's native space PET image. Only cortical and sub-cortical regions overlapping with the MindBoggle DKT atlas were used Klein and Tourville, 2012, leaving 78 regions in total. Previous Flortaucipir-PET studies have noted considerable off-target binding of the Flortaucipir signal, leading to signal in regions without pathological tau burden, and likely to pollution of signal in regions accumulating tau Baker et al., 2019; Choi et al., 2018; Lemoine et al., 2018; Lockhart et al., 2017b; Vogel et al., 2019a. While many previous studies have ignored these issues, accounting for off-target binding is essential to the current study, as our model cannot distinguish off-target from target signal, and we are not interested in the propagation of off-target signal. To address this issue, we utilized regional Gaussian mixture modeling under the assumption that the target and off-target signal across the population are distinct and separable Gaussian distributions (Fig 3.1C).

As most individuals do not have tau in most regions, pathological signal should show a skewed distribution across the population, whereas off-target and non-specific signal should be reasonably normally distributed. Such a bimodal distribution has been observed for β-amyloid, and mixture modeling has been used in this context to define global β-amyloid positivity Grothe et al., 2017; Palmqvist et al., 2014. Our approach differs from these previous studies as we do not assume the distribution of target and off-target binding to be homogeneous across cortical areas – we apply Gaussian mixture modeling separately to each region-of-interest (Fig 3.1C). Specifically, for each region, we fit a one-component and a two-component Gaussian mixture model across the entire population. We compare the fit of the two models using Aikake's information criterion. If a two-component model fits the data better, this likely indicates the presence of pathological tau in a proportion of the population, and the Gaussians fit to the data provide a rough estimate of an SUVR threshold, above which Flortaucipir signal has a high probability of being abnormal. If a one-component model fits better, this indicates the Flortaucipir-PET signal within the region is roughly normally distributed across the population, which we do not expect for tau in a population including many cognitively impaired individuals. The ESM receives regional (tau) probabilities as input, and so we calculate the probability that a given subject's ROI SUVR value falls onto the second (i.e. right-most) Gaussian distribution using repeated five-fold cross-validation. Assuming this second distribution represents the subjects with abnormal Flortaucipir signal, this value estimates the proximity of a subject to the pathological distribution. Effectively,

this converts regional SUVRs to regional tau-positive probabilities. This approach defines a fairly conservative, data-driven threshold for SUVR values, above which, one can assume the presence of abnormal signal (perhaps indicating pathological tau accumulation) with a high degree of confidence.

For purposes of comparison, we also use two other preprocessing strategies for regional tau-PET data. First, we apply a regional normalization of SUVR values along a 0-1 scale, which is equivalent to simply using SUVR values as input (the ESM expects values to be between 0 and 1). Second, we reproduce the reference strategy described in the original ESM paper. This approach involves creating a null distribution by obtaining the maximum value of 40,000 bootstrapped samples of the 5-95% largest SUVR values within the reference region. The distribution is used to create an empirical cumulative distribution function, which is applied to each voxel of the PET image, effectively finding the probability that this voxel is greater than values in the reference region (see Iturria-Medina et al., 2014 for details). We also fit the model using different region-sets: i) all cortical and subcortical regions (n=78), ii) cortical regions only (including hippocampus and amygdala, n=66), iii) only regions demonstrating a bimodal distribution (n varies depending on other pre-processing decisions).

As mentioned above, tau-PET signal is confounded by a number of off-target binding sources, some of which are age-related Baker et al., 2019; Choi et al., 2018. Some studies have found that regressing out certain signal sources, such as choroid-plexus binding or age-related subcortical signal, can improve expected relationships between Flortaucipir and other measures (e.g. Lee et al., 2018). In addition, recent studies have found a putative impact of sex on Flortaucipir binding Hohman et al., 2018; Liu et al., 2019. Therefore, we explored the impact of removing confounding signals from tau-PET data on model performance. We tried three different strategies: i) no preprocessing, ii) regressing out age, sex and mean choroid plexus binding from each region separately across all subjects, iii) using a W-score approach La Joie et al., 2012, where regional SUVR values are normalized by Aβ-negative cognitively normal elderly adjusting for age, sex and choroid plexus binding. Native space choroid plexus regions were available for each subject from the Freesurfer parcellation, and the mean Flortaucipir signal was taken between left and right hemispheres. In addition to these processing steps, we experimented with the choice of partial volume correcting (PVC) data before running the model. The geometric transfer matrix Rousset, Ma, and Evans, 1998 method was used for PVC, and models were run with and without PVC.

3.6.5 Connectivity measurements

The overall pattern of spread simulated by the ESM is determined by the relationship matrix, which represents pairwise relationships between each region-of-interest. Indeed, this is the system through which the simulated signal will diffuse. Varying the relationship matrix can, for example, allow for tests of different hypotheses of spread. In addition, replicating model effects over different connectomes can improve confidence that results are robust to different samples or modalities. We fit the ESM over four different connectivity datasets, none of which overlap with one another or with subjects from the tau-PET dataset. We use anatomical connectivity measurements generated using diffusion tensor imaging (DTI) tractography from i) healthy and impaired older adults and ii) young healthy adults. We further validate this procedure using functional connectivity matrix generated from iii) healthy and impaired older adults and iv) young healthy controls to test the hypothesis that tau spreads through communicating neurons. Finally, we additionally test the hypothesis of tau spreading through extra-cellular space by using a Euclidian distance matrix as input.

We created two template structural connectivity matrices using DTI tractography data from two different samples. The first was a dataset of 60 young healthy subjects from the CMU-60 DSI Template Yeh and Tseng, 2011 (http://www.psy.cmu.edu/~coaxlab/data.html). The second was a sample of healthy older and cognitively impaired older adults from ADNI. Demographic information and comparisons to other datasets can be found in Table S1. In total, 204 individuals had one or more DTI scans available, for a total of 540 scans. The two datasets were preprocessed separately with a previously described diffusion tractography pipeline Iturria-Medina et al., 2007, and acquisition and processing information has been described in detail Iturria-Medina et al., 2017. Briefly, orientation distribution functions (ODF) were calculated and in turn used to generate deterministic connections between pairs of brain regions from the Desikan atlas. Specifically, an ACD measure was used, representing the total proportion of regional surface area (across both regions) that contain connecting fibers between the two regions. All images were assessed for quality. Connectomes were averaged across all subjects within each template, resulting in a template structural connectome in aging and in health, respectively.

Functional connectivity measurements were generated separately from two different datasets. The first was a subsample of young healthy controls from the COBRE dataset Bellec, 2016, a publicly available sample which we accessed through the Nilearn python library. All subjects listed as healthy controls under the age of 40 were selected, totaling 74 individuals. The images were already preprocessed using the

NIAK resting-state pipeline (http://niak.simexp-lab.org/pipe$_$preprocessing.html), and additional details can be found elsewhere Bellec, 2016. The second dataset consisted of a subsample of 189 healthy and cognitively impaired older adults from ADNI who passed quality control procedures. Demographic data and comparison to the other datasets can be found in Table S1. These data were processed in-house using NIAK in a manner described previously

Separately for each dataset, correlation matrices were generated by finding the correlation between timeseries' of each pair of regions-of-interest from the Desikan-Killiany atlas, and all available confounds were regressed from the correlation matrices. We took the mean of all correlation matrices to create an average healthy connectome template, and an average older/impaired connectome template. These connectomes were then thresholded so as to only retain the top 10% of connections, and transformed so all values fell between 0 and 1.

To create a Euclidian distance matrix, we calculated the coordinate representing the center of mass for each region of interest, and found the Euclidian distance between it and the center of mass of every other ROI. By using this distance matrix in the epidemic spreading model, we test the hypothesis that tau diffuses radially across adjacent cortex, rather than through connected regions.

3.6.6 Statistical Analysis

The ESM was fit using different relationship matrices and across several different preprocessing choices (see above). Each model was evaluated by mean within-individual fit, as well as global population fit. Individual model fit is calculated as the r^2 between predicted regional tau probabilities and actual regional tau probabilities measured with Flortaucipir-PET, for each individual. The mean r^2 across all individuals was used to represent overall model fit. To evaluate the accuracy of the global pattern, the regional predicted and observed tau probabilities, respectively, were averaged across all subjects, and the r^2 between these group-averaged patterns were calculated. Together, these two accuracy measures represent the degree to which regional connectivity predicts the spatial pattern of tau-PET measured within and across subjects, respectively. To ensure the magnitude of our results were greater than chance given a matrix of similar properties, for select models, we fit the ESM using 100 null matrices with preserved degree and strength distributions using the Brain Connectivity toolbox (https://sites.google.com/site/bctnet/). We use the null distribution to calculate the mean and 95% confidence intervals of the relationship occurring by chance. Since we run only 100 null models per test, the lowest possible p-value is 0.01, which would suggest the observed test value was higher than all values observed by chance.

To examine the global accuracy of the ESM stratified by amyloid status, we first divided all subjects into one of two diagnostic groups: amyloid-negative and amyloid-positive. We then calculated the mean of predicted and observed values across all subjects within each amyloid group, respectively. We performed similar analyses across different diagnoses (CN, MCI, AD). In the same manner, we also examined ESM accuracy stratified by cohort to ensure the model fit was consistent between the ADNI and BioFINDER cohorts. As a follow-up, we implemented a neighborhood search using the ball tree method and Minkowski distance (p=2) to created a subsample of BioFINDER subjects matched to ADNI subjects on either demographics (Age, Sex, Education, *APOE*4 status) or tau load (average cortical tau-PET signal). We then once again compared model fit within this BioFINDER-matched-to-ADNI sample to model fit in ADNI subjects.

Studies in rodents have suggested a role of amyloid in facilitating the rapid fibrillarization of tau oligomers He et al., 2018. This would suggest that amyloid may play a role in explaining tau patterns that is at least partially independent of connectivity patterns. To explore this, we tested the relationship between regional modeling error and regional amyloid depositon. We converted regional amyloid SUVR values to amyloid-positive probabilities using the same regional mixture-modeling approach as described above. Next, we used the sign of the residual to divide regions into those that were overestimated by the ESM, and those that were underestimated by the ESM. An underestimated region, for example, would show more tau than the model predicted given that region's connectivity to the model epicenter. We explored the relationship between model estimation and amyloid by comparing the degree of (group-mean) amyloid between overestimated and underestimated regions using t-tests. We also calculate the correlation between regional model residuals and regional amyloid values. To ensure this relationship is independent of local tau, we fit a model assessing the independent relationship of regional amyloid and tau, respectively, on regional model residuals.

To investigate global asymmetry in tau spreading, we compared the performance of ESM fit with a left entorhinal cortext epicenter to performance of models fit with a right entorhinal cortex epicenter. To explore asymmetry in individual patterning, we fit the ESM over every possible epicenter and stored information pertaining to the best-fitting epicenter for each subject. Epicenters were broadly characterized into left and right hemisphere and limbic or non-limbic. Limbic epicenters included entorhinal cortex, hippocampus, amygdala or parahippocampal gyrus. We stratified subjects by their epicenter hemisphere (Limbic-Left, Limbic-Right, Other) and used ordinary least squares general linear models (GLMs) to examine associations between epicenter hemisphere and other covariates (age, sex, education, *APOE*4

status) covarying for disease status (CN-, CN+, MCI+, AD+). We also compared subjects by their total tau asymmetry (mean of left minus right across all cortical ROIs). Finally, we ran separate GLMs assessing relationships between epicenter hemisphere and tau signal in each region of interest, covarying for disease status, age and sex. These relationships were subsequently FDR corrected using the Benjamini-Hochberg approach.

3.7 Supplementary Information

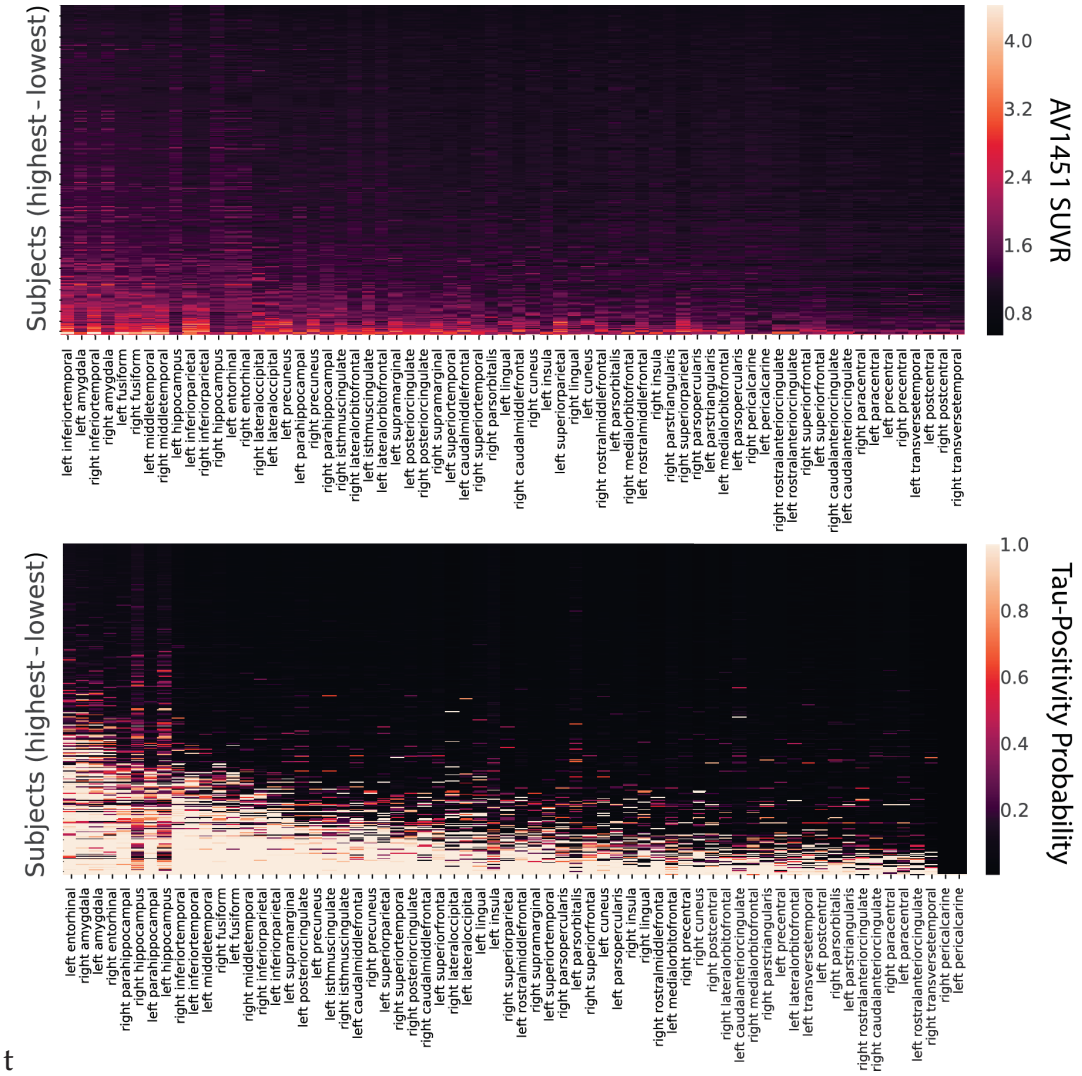

Supplementary Fig. 3.S1: Each row is a subject sorted top-bottom by least to most overall tau. Each column is an ROI, sorted left to right by most to least overall tau. Warmer colors represent higher SUVR values (top) or tau-positive probabilities (bottom). Conversion to tau-positive probabilities creates a sparse distribution of values demonstrating a progression. The order of ROIs resembles those described in the autopsy literature.

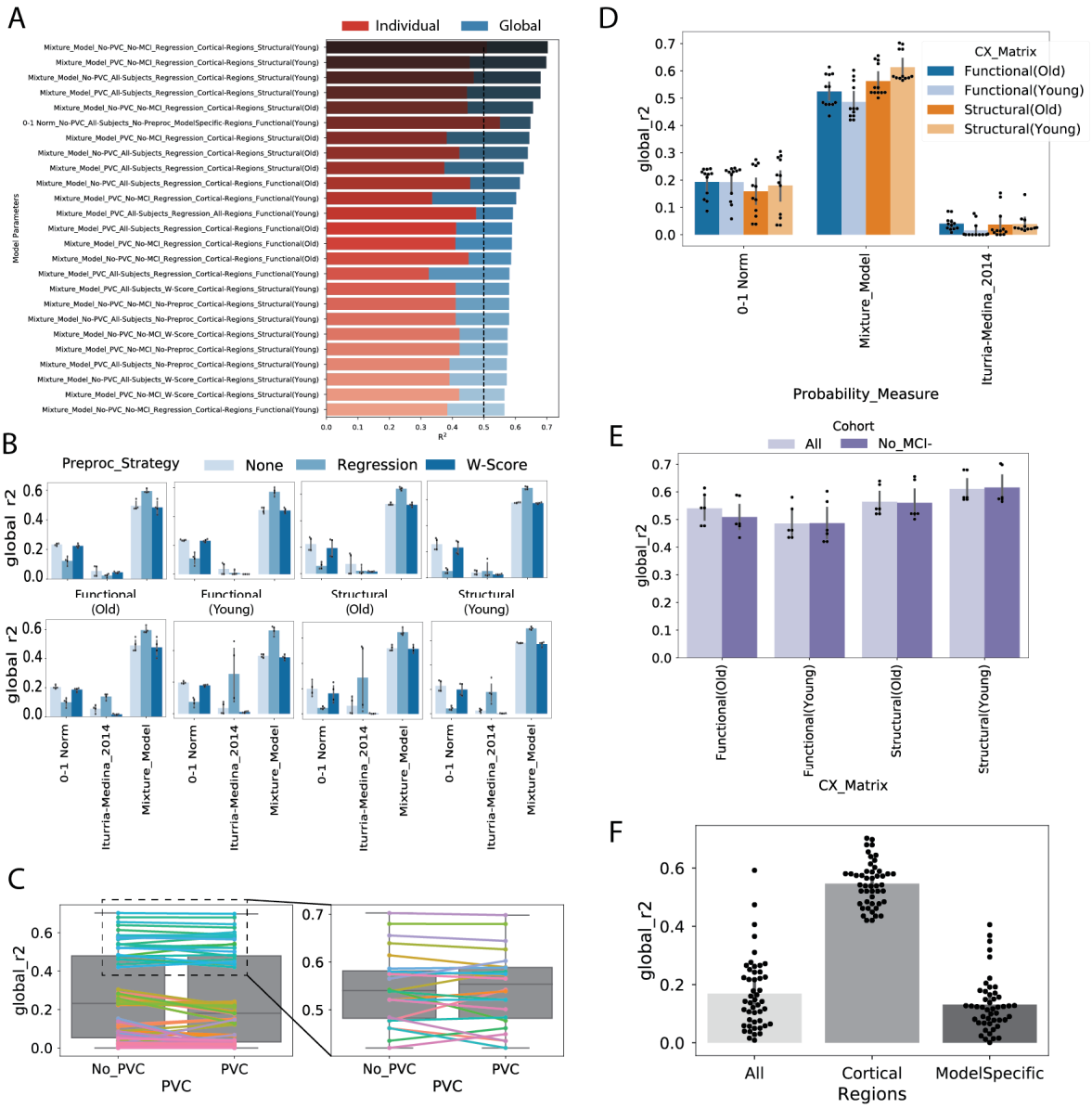

Supplementary Fig. 3.S2: (A) Parameters for the top 25 models. Blue bars represent global model fit, whereas red bars represent average within-subject fit. Models to the right of the black line explain more than half of the total variance in tau spatial pattern. (B) Influence of tau-PET input measure (i.e. tau probability; x-axis) and confound regression strategy (colors) on global model performance (y-axis) across all subjects (top) and Aβ- subjects only (bottom). Error bars represent variation in model fit depending on connectome, PVC strategy, and inclusion/exclusion of MCI- subjects. (C) Impact of PVC on model performance for all models (left) and models using tau-positive probabilities (right). Lines show change in model fit depending on PVC strategy. For boxplots, the center line = median, box = inner quartiles, whiskers = extent of data-distribution. (D) Impact of connectome choice (color) on variation in model performance (y-axis) across different tau input measures (x-axis). Error bars represent variation in model fit depending on PVC strategy, regression strategy and inclusion/exclusion of MCI- subjects. (E) Variation in model performance based on whether MCI- subjects were included or not, across different connectomes. Data are visualized only for models using the mixture modeling approach for tau probabilities. Error bars represent variation in model fit depending on PVC strategy and regression strategy. (F) Model fit variation related to which regions were included. Only models using the mixture-modeling approach for tau probabilities are visualized, and error bars represent variation in model fit depending on PVC strategy, regression strategy, connectome and inclusion/exclusion of MCI- subjects. For all panels, error bars represent standard error of the mean.

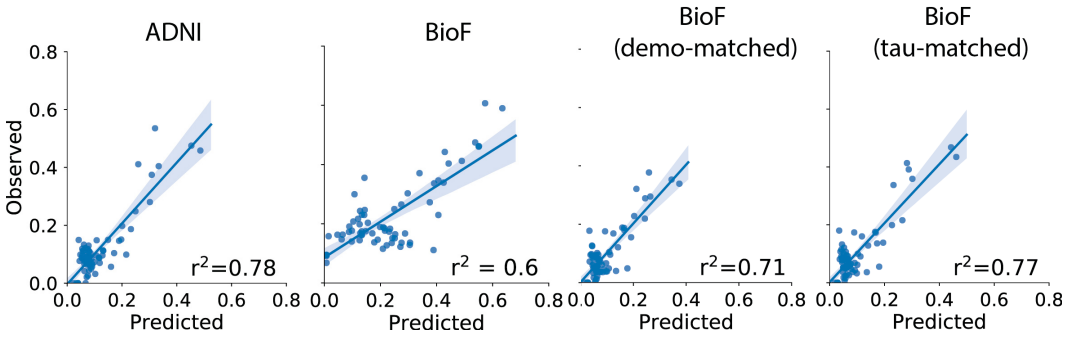

Supplementary Fig. 3.S3: Global model fit for the best-fitting model averaged across (from left to right) ADNI subjects only, BioFINDER subjects only, a subselection of BioFINDER subjects matched to ADNI based on demographics, and a subselection of BioFINDER subjects matched to ADNI based on average cortical tau.

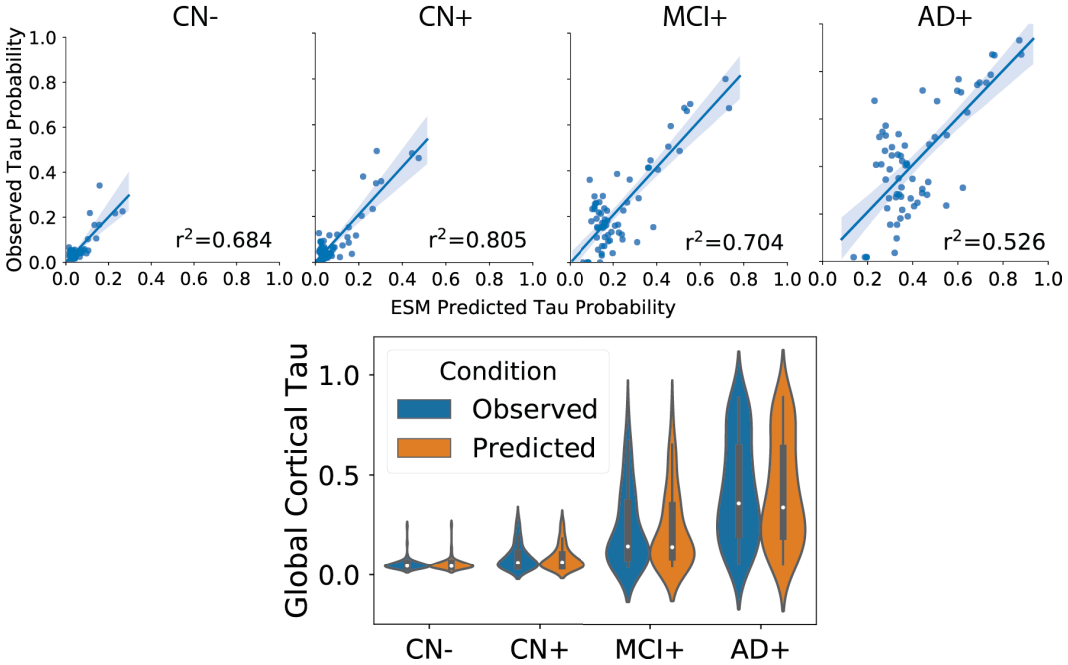

Supplementary Fig. 3.S4: (Top) The ESM predicted the global tau pattern across disease states. (Bottom) Observed tau patterns increased with increased disease severity. By design, the predicted pattern also increases with disease progression, as each model is fit to the individual in terms of magnitude of tau (but not spatial pattern, which is determined by connectivity)

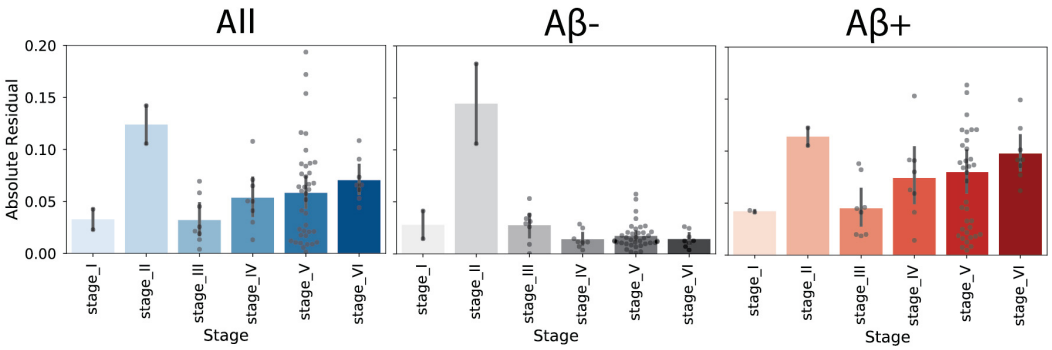

Supplementary Fig. 3.S5: Regions were sorted into Braak Stage as in Main Text Fig 2. The average within-region model fit was calculated as the absolute difference (i.e. residual) between predicted and observed tau-probability in that region. This relationship is depicted across stages for the best-fitting model, across (left) all subjects, (middle) amyloid-negative subjects only and (right) amyloid-positive subjects only. In general, model fit became worse across as in regions belong to later Braak stages, and the hippocamus (Braak Stage II) was generally poorly fit. Error bars represent standard error of the mean.

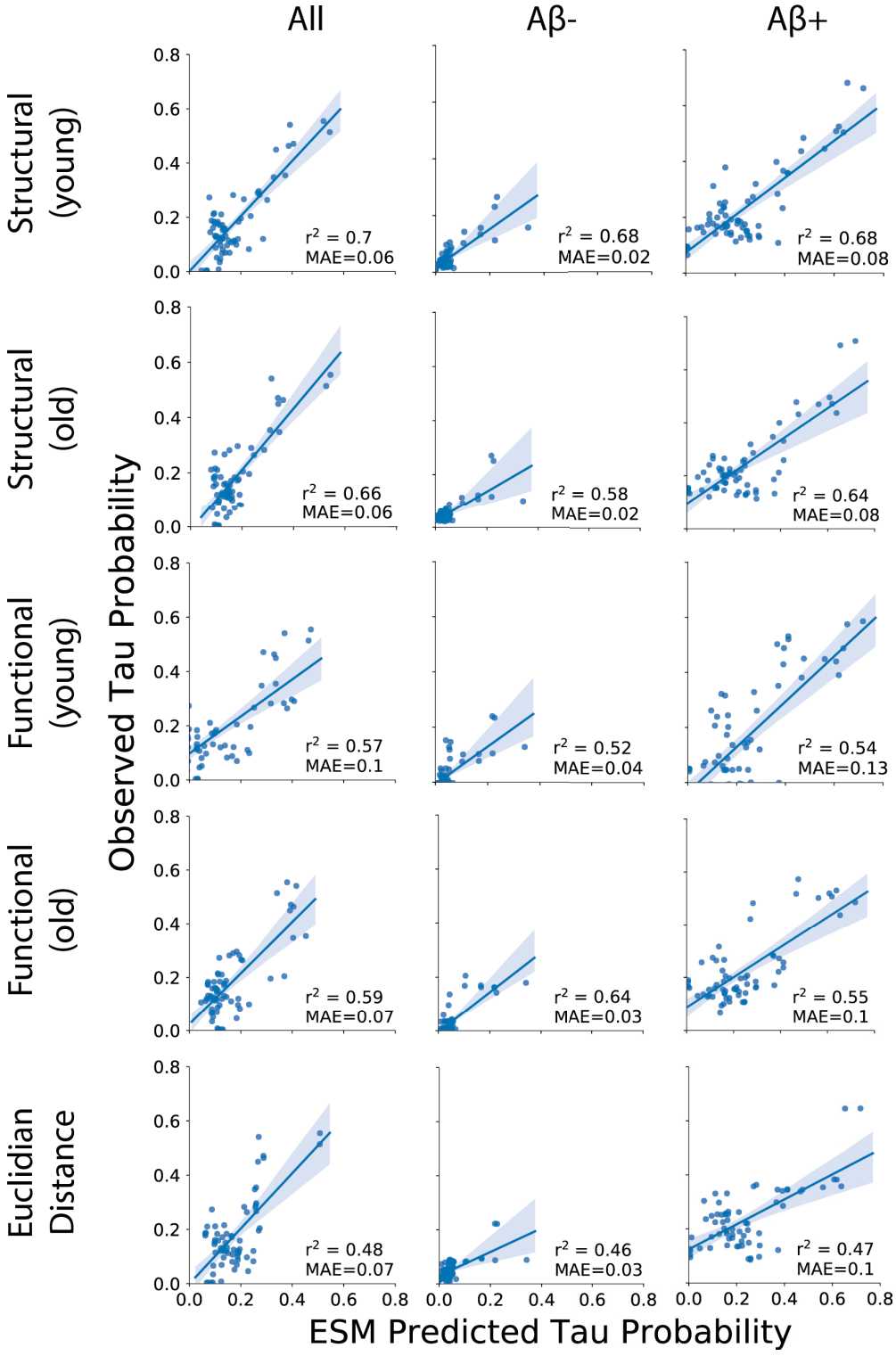

Supplementary Fig. 3.S6: For each plot, each dot represents a region. The x-axis represents the mean simulated tau-positive probabilities across the population, while the y-axis represents the mean observed tau-positive probability. A value of (say) 0.3 for a given ROI would suggest that an average of 30% of all subjects included were predicted (X) or observed (Y) to have positive abnormal tau signal in that region. The results are shown for ESM fit over (from top to bottom) healthy young structural connectome (also selected as best-fitting); aging structural connectome; healthy young functional connectome; aging functional connectome; and a Eucidian distance matrix. B) Breakdown of ESM performance by amyloid status. The average performance of the four different models are shown separately for (left) all subjects, (center) Aβ- individuals and (right) Aβ+ individuals

3.8 Additional information

3.8.1 Acknowledgements

We would like to thank Bratislav Misic, Pierre Bellec, and Mallar Chakravarty for comments and suggestions during the formulation of this work. JWV is supported by the government of Canada through the tri-council Vanier Canada Graduate Doctoral Fellowship. We would also like to acknowledge support from the Ludmer Centre for Neuroinformatics and Mental Health and the Healthy Brains for Healthy Lives initiative. Work at the authors' research center was supported by the European Research Council, the Swedish Research Council, the Knut and Alice Wallenberg foundation, the Marianne and Marcus Wallenberg foundation, the Strategic Research Area MultiPark (Multidisciplinary Research in Parkinson's disease) at Lund University, the Swedish Alzheimer Foundation, the Swedish Brain Foundation, The Parkinson foundation of Sweden, The Parkinson Research Foundation, the Skåne University Hospital Foundation, and the Swedish federal government under the ALF agreement. Doses of 18F-flutemetamol injection were sponsored by GE Healthcare. The precursor of 18F-flortaucipir was provided by AVID radiopharmaceuticals. Data collection and sharing for this project was funded by the Alzheimer's Disease Neuroimaging Initiative (ADNI) (National Institutes of Health Grant U01 AG024904) and DOD ADNI (Department of Defense award number W81XWH-12-2-0012). ADNI is funded by the National Institute on Aging, the National Institute of Biomedical Imaging and Bioengineering, and through generous contributions from the following: AbbVie, Alzheimer's Association; Alzheimer's Drug Discovery Foundation; Araclon Biotech; BioClinica, Inc.; Biogen; Bristol-Myers Squibb Company; CereSpir, Inc.; Cogstate; Eisai Inc.; Elan Pharmaceuticals, Inc.; Eli Lilly and Company; EuroImmun; F. Hoffmann-La Roche Ltd and its affiliated company Genentech, Inc.; Fujirebio; GE Healthcare; IXICO Ltd.;Janssen Alzheimer Immunotherapy Research & Development, LLC.; Johnson & Johnson Pharmaceutical Research & Development LLC.; Lumosity; Lundbeck; Merck & Co., Inc.;Meso Scale Diagnostics, LLC.; NeuroRx Research; Neurotrack Technologies; Novartis Pharmaceuticals Corporation; Pfizer Inc.; Piramal Imaging; Servier; Takeda Pharmaceutical Company; and Transition Therapeutics. The Canadian Institutes of Health Research is providing funds to support ADNI clinical sites in Canada. Private sector contributions are facilitated by the Foundation for the National Institutes of Health (www.fnih.org). The grantee organization is the Northern California Institute for Research and Education, and the study is coordinated by the Alzheimer's Therapeutic Research Institute at the University of Southern California. ADNI data are disseminated by the Laboratory

for Neuro Imaging at the University of Southern California.

3.8.2 Competing Interests

OH has acquired research support (for the institution) from Roche, GE Healthcare, Biogen, AVID Radiopharmaceuticals, Fujirebio, and Euroimmun. In the past 2 years, he has received consultancy/speaker fees (paid to the institution) from Biogen, Roche, and Fujirebio.

3.8.3 Data Availability

Analyses in this manuscript were conducted principally using subjects from the ADNI and BioFINDER cohort. ADNI is a publicly available dataset and can be accessed at http://adni.loni.usc.edu/. BioFINDER data are not publicly available for download, but access requests can be made to the study Principal Investigator, Oskar Hansson. Additionally, data used to create template connectomes are also publicly available. ADNI rsfMRI and DTI data can be downloaded at http://adni.loni.usc.edu/. The COBRE dataset can be accessed at Bellec, 2016, or can be downloaded using the Nilearn python package https://nilearn.github.io/. CMU60 DTI data can be accessed at http://www.psy.cmu.edu/~coaxlab/data.html.

3.8.4 Code Availability Statement

Matlab scripts for the Epidemic Spreading Model will be made available in a forthcoming public software release. Inquiries into acquiring the scripts beforehand can be sent to Yasser Iturria-Medina. Python functions used in part to analyze and plot ESM data can be found at https://github.com/illdopejake/data_driven_pathology/blob/master/esm/ESM_utils.py.

References

Acosta, Diana et al. (June 2018). "Regional vulnerability in Alzheimer's disease: The role of cell-autonomous and transneuronal processes." In: *Alzheimer's & dementia : the journal of the Alzheimer's Association* 14.6, pp. 797–810. ISSN: 1552-5279. DOI: 10.1016/j.jalz.2017.11.014. URL: https://linkinghub.elsevier.com/retrieve/pii/S1552526017338578http://www.ncbi.nlm.nih.gov/pubmed/29306583http://www.pubmedcentral.nih.gov/articlerender.fcgi?artid=PMC5994366.

Adams, Jenna N et al. (2019). "Cortical tau deposition follows patterns of entorhinal functional connectivity in aging". In: *eLife* 8, pp. 1–22. ISSN: 2050084X. DOI: 10.7554/eLife.49132.

Aggleton, John P. et al. (July 2016). "Thalamic pathology and memory loss in early Alzheimer's disease: moving the focus from the medial temporal lobe to Papez circuit". In: *Brain* 139.7, pp. 1877–1890. ISSN: 0006-8950. DOI: 10.1093/brain/aww083. URL: http://www.brain.oxfordjournals.org/lookup/doi/10.1093/brain/aww083https://academic.oup.com/brain/article-lookup/doi/10.1093/brain/aww083.

Baker, Suzanne L et al. (2019). " Effect of off-target binding on 18 F-Flortaucipir variability in healthy controls across the lifespan ". In: *Journal of Nuclear Medicine*, jnumed.118.224113. ISSN: 0161-5505. DOI: 10.2967/jnumed.118.224113.

Bejanin, Alexandre et al. (Dec. 2017b). "Tau pathology and neurodegeneration contribute to cognitive impairment in Alzheimer's disease". In: *Brain* 140.12, pp. 3286–3300. ISSN: 0006-8950. DOI: 10.1093/brain/awx243. URL: https://watermark.silverchair.com/awx243.pdf?token=AQECAHi208BE49Ooan9kkhW_Ercy7Dm3ZL_9Cf3qfKAc485ysgAAAecwggHjBgkqhkiG9w0BBwagggHUMIIB0AIBADCCAckGCSqGSIb3DQEHATAeBgl3OjnBKCYybpS8fEAgEQgIIBmpY9paVgrJr248NQgNg8LAw6UHj7Y8NzZqCqEKPxMOE1DebS.

Bellec, Pierre (Nov. 2016). *COBRE preprocessed with NIAK 0.17 - lightweight release*. DOI: 10.6084/m9.figshare.4197885.v1. URL: https://figshare.com/articles/COBRE_preprocessed_with_NIAK_0_17_-_lightweight_release/4197885/1.

Bennett, Rachel E. et al. (2017). "Enhanced Tau Aggregation in the Presence of Amyloid β". In: *American Journal of Pathology* 187.7, pp. 1601–1612. ISSN: 15252191. DOI: 10.1016/j.ajpath.2017.03.011.

Braak, H and E Braak (1991). "Neuropathological stageing of Alzheimer-related changes." In: *Acta neuropathologica* 82.4, pp. 239–59. ISSN: 0001-6322. URL: http://www.ncbi.nlm.nih.gov/pubmed/1759558.

Braak, Heiko and Kelly Del Tredici (2014). "Are cases with tau pathology occurring in the absence of Aβ deposits part of the AD-related pathological process?" In: *Acta Neuropathologica* 128.6, pp. 767–772. ISSN: 14320533. DOI: 10.1007/s00401-014-1356-1.

Braak, Heiko and Kelly Del Tredici (2015). "The preclinical phase of the pathological process underlying sporadic Alzheimer's disease". In: *Brain* 138.10, pp. 2814–2833. ISSN: 14602156. DOI: 10.1093/brain/awv236.

Brettschneider, Johannes et al. (2015). "Spreading of pathology in neurodegenerative diseases: A focus on human studies". In: *Nature Reviews Neuroscience* 16.2, pp. 109–120. ISSN: 14710048. DOI: 10.1038/nrn3887. URL: http://dx.doi.org/10.1038/nrn3887.

Brown, Jesse A. et al. (2019). "Patient-Tailored, Connectivity-Based Forecasts of Spreading Brain Atrophy". In: *Neuron* 104.5, pp. 856–868. ISSN: 08966273. DOI: 10.1016/j.neuron.2019.08.037. URL: https://doi.org/10.1016/j.neuron.2019.08.037.

Cho, Hanna et al. (Aug. 2016a). "In vivo cortical spreading pattern of tau and amyloid in the Alzheimer disease spectrum". In: *Annals of Neurology* 80.2, pp. 247–258. ISSN: 03645134. DOI: 10.1002/ana.24711. URL: http://doi.wiley.com/10.1002/ana.24711.

Cho, Hanna et al. (Aug. 2018). "Predicted sequence of cortical tau and amyloid-β deposition in Alzheimer disease spectrum". In: *Neurobiology of Aging* 68.January 2015, pp. 76–84. ISSN: 01974580. DOI: 10.1016/j.neurobiolaging.2018.04.007. URL: https://doi.org/10.1016/j.neurobiolaging.2018.04.007https://linkinghub.elsevier.com/retrieve/pii/S0197458018301295.

Choi, Jae Yong et al. (Jan. 2018). "Off-Target 18 F-AV-1451 Binding in the Basal Ganglia Correlates with Age-Related Iron Accumulation". In: *Journal of Nuclear Medicine* 59.1, pp. 117–120. ISSN: 0161-5505. DOI: 10.2967/jnumed.117.195248. URL: http://jnm.snmjournals.org/lookup/doi/10.2967/jnumed.117.195248.

Clavaguera, Florence et al. (2013). "Brain homogenates from human tauopathies induce tau inclusions in mouse brain". In: *Proceedings of the National Academy of Sciences* 110.23, pp. 9535–9540. ISSN: 0027-8424. DOI: 10.1073/pnas.1301175110. URL: http://www.pnas.org/lookup/doi/10.1073/pnas.1301175110.

Congdon, Erin E. and Einar M. Sigurdsson (2018). "Tau-targeting therapies for Alzheimer disease". In: *Nature Reviews Neurology* 14.7, pp. 399–415. ISSN: 17594766. DOI: 10.1038/s41582-018-0013-z. URL: http://dx.doi.org/10.1038/s41582-018-0013-z.

Cope, Thomas E et al. (2018). "Tau burden and the functional connectome in Alzheimer's disease and progressive supranuclear palsy". In: *Brain* 141.2, pp. 550–567. ISSN: 14602156. DOI: 10.1093/brain/awx347.

Crary, John F. et al. (2014). "Primary age-related tauopathy (PART): a common pathology associated with human aging". In: *Acta Neuropathologica* 128.6, pp. 755–766. ISSN: 14320533. DOI: 10.1007/s00401-014-1349-0.

Crossley, Nicolas A. et al. (2014). "The hubs of the human connectome are generally implicated in the anatomy of brain disorders". In: *Brain* 137.8, pp. 2382–2395. ISSN: 14602156. DOI: 10.1093/brain/awu132.

De Calignon, Alix et al. (2012). "Propagation of Tau Pathology in a Model of Early Alzheimer's Disease". In: *Neuron* 73.4, pp. 685–697. ISSN: 08966273. DOI: 10.1016/j.neuron.2011.11.033.

Desikan, Rahul S. et al. (2006). "An automated labeling system for subdividing the human cerebral cortex on MRI scans into gyral based regions of interest". In: *NeuroImage* 31.3, pp. 968–980. ISSN: 10538119. DOI: 10.1016/j.neuroimage.2006.01.021.

DeVos, S. L. et al. (2013). "Antisense Reduction of Tau in Adult Mice Protects against Seizures". In: *Journal of Neuroscience* 33.31, pp. 12887–12897. ISSN: 0270-6474. DOI: 10.1523/JNEUROSCI.2107-13.2013. URL: http://www.jneurosci.org/cgi/doi/10.1523/JNEUROSCI.2107-13.2013.

DeVos, Sarah L. et al. (2018a). "Synaptic tau seeding precedes tau pathology in human Alzheimer's disease brain". In: *Frontiers in Neuroscience* 12.APR, pp. 1–15. ISSN: 1662453X. DOI: 10.3389/fnins.2018.00267.

Donohue, Michael C. et al. (2017). "Association between elevated brain amyloid and subsequent cognitive decline among cognitively normal persons". In: *JAMA - Journal of the American Medical Association* 317.22, pp. 2305–2316. ISSN: 15383598. DOI: 10.1001/jama.2017.6669.

Ferreira, Daniel et al. (2019). "Subtypes of Alzheimer's disease display distinct network abnormalities extending beyond their pattern of brain atrophy". In: *Frontiers in Neurology* 10.MAY. ISSN: 16642295. DOI: 10.3389/fneur.2019.00524.

Franzmeier, Nicolai et al. (Feb. 2019). "Functional connectivity associated with tau levels in ageing, Alzheimer's, and small vessel disease". In: *Brain*, pp. 1–15. ISSN: 0006-8950. DOI: 10.1093/brain/awz026. URL: https://academic.oup.com/brain/advance-article/doi/10.1093/brain/awz026/5321130.

Franzmeier, Nicolai et al. (Dec. 2020). "Functional brain architecture is associated with the rate of tau accumulation in Alzheimer's disease". In: *Nature Communications* 11.1, p. 347. ISSN: 2041-1723. DOI: 10.1038/s41467-019-14159-1. URL: http://www.nature.com/articles/s41467-019-14159-1.

Frost, Bess and Marc I. Diamond (Mar. 2010). "Prion-like mechanisms in neurodegenerative diseases". In: *Nature Reviews Neuroscience* 11.3, pp. 155–159. ISSN: 1471-003X. DOI: 10.1038/nrn2786. URL: http://www.ncbi.nlm.nih.gov/pubmed/20029438http://www.pubmedcentral.nih.gov/articlerender.fcgi?artid=PMC3648341http://www.nature.com/articles/nrn2786.

Fuster-Matanzo, Almudena, Félix Hernández, and Jesús Ávila (Feb. 2018). "Tau Spreading Mechanisms; Implications for Dysfunctional Tauopathies". In: *International Journal of Molecular Sciences* 19.3, p. 645. ISSN: 1422-0067. DOI: 10.3390/ijms19030645. URL: http://www.mdpi.com/1422-0067/19/3/645.

Goedert, Michel, David S. Eisenberg, and R. Anthony Crowther (July 2017). "Propagation of Tau Aggregates and Neurodegeneration". In: *Annual Review of Neuroscience* 40.1, pp. 189–210. ISSN: 0147-006X. DOI: 10.1146/annurev-neuro-072116-031153.

URL: http://www.annualreviews.org/doi/10.1146/annurev-neuro-072116-031153.

Gordon, Brian A. et al. (2018). "Cross-sectional and longitudinal atrophy is preferentially associated with tau rather than amyloid β positron emission tomography pathology". In: *Alzheimer's and Dementia: Diagnosis, Assessment and Disease Monitoring* 10, pp. 245–252. ISSN: 23528729. DOI: 10.1016/j.dadm.2018.02.003.

Grothe, Michel J et al. (Nov. 2017). "In vivo staging of regional amyloid deposition". In: *Neurology* 89.20, pp. 2031–2038. ISSN: 0028-3878. DOI: 10.1212/WNL.0000000000004643. URL: http://www.ncbi.nlm.nih.gov/pubmed/29046362http://www.neurology.org/lookup/doi/10.1212/WNL.0000000000004643.

Grothe, Michel J et al. (2018). "Molecular properties underlying regional vulnerability to Alzheimer's disease pathology". In: *Brain*, pp. 2755–2771. ISSN: 0006-8950. DOI: 10.1093/brain/awy189. URL: https://academic.oup.com/brain/advance-article/doi/10.1093/brain/awy189/5054650.

Hansson, Oskar et al. (Mar. 2017). "Tau Pathology Distribution in Alzheimer's disease Corresponds Differentially to Cognition-Relevant Functional Brain Networks". In: *Frontiers in Neuroscience* 11.March. ISSN: 1662-453X. DOI: 10.3389/fnins.2017.00167. URL: http://journal.frontiersin.org/article/10.3389/fnins.2017.00167/full.

Harrison, Theresa M. et al. (2018). "Longitudinal tau accumulation and atrophy in aging and Alzheimer's disease". In: *Annals of Neurology*, pp. 229–240. ISSN: 00222380. DOI: 10.1002/ana.25406.

He, Zhuohao et al. (2018). "Amyloid-β plaques enhance Alzheimer's brain tau-seeded pathologies by facilitating neuritic plaque tau aggregation". In: *Nature Medicine* 24.1, pp. 29–38. ISSN: 1546170X. DOI: 10.1038/nm.4443. URL: http://dx.doi.org/10.1038/nm.4443.

Hedden, Trey et al. (2013). "Meta-analysis of amyloid-cognition relations in cognitively normal older adults". In: *Neurology* 80.14, pp. 1341–1348. ISSN: 00283878. DOI: 10.1212/WNL.0b013e31828ab35d.

Hoenig, Merle C et al. (2018). "Networks of tau distribution in Alzheimer's disease". In: *Brain* 141.2, pp. 568–581. ISSN: 14602156. DOI: 10.1093/brain/awx353.

Hohman, Timothy J. et al. (Aug. 2018). "Sex-Specific Association of Apolipoprotein E With Cerebrospinal Fluid Levels of Tau". In: *JAMA Neurology* 75.8, p. 989. ISSN: 2168-6149. DOI: 10.1001/jamaneurol.2018.0821. URL: http://archneur.jamanetwork.com/article.aspx?doi=10.1001/jamaneurol.2018.0821.

Iba, M. et al. (2013). "Synthetic Tau Fibrils Mediate Transmission of Neurofibrillary Tangles in a Transgenic Mouse Model of Alzheimer's-Like Tauopathy". In: *Journal of Neuroscience* 33.3, pp. 1024–1037. ISSN: 0270-6474. DOI: 10.1523/JNEUROSCI.

2642-12.2013. URL: http://www.jneurosci.org/cgi/doi/10.1523/JNEUROSCI.2642-12.2013.

Iturria-Medina, Y. et al. (2007). "Characterizing brain anatomical connections using diffusion weighted MRI and graph theory". In: *NeuroImage* 36.3, pp. 645–660. ISSN: 10538119. DOI: 10.1016/j.neuroimage.2007.02.012.

Iturria-Medina, Yasser and Alan C Evans (2015). "On the central role of brain connectivity in neurodegenerative disease progression." In: *Frontiers in aging neuroscience* 7.May, p. 90. ISSN: 1663-4365. DOI: 10.3389/fnagi.2015.00090. URL: http://journal.frontiersin.org/article/10.3389/fnagi.2015.00090/abstract.

Iturria-Medina, Yasser et al. (2014). "Epidemic Spreading Model to Characterize Misfolded Proteins Propagation in Aging and Associated Neurodegenerative Disorders". In: *PLoS Computational Biology* 10.11. ISSN: 15537358. DOI: 10.1371/journal.pcbi.1003956.

Iturria-Medina, Yasser et al. (2017). "Multifactorial causal model of brain (dis)organization and therapeutic intervention: Application to Alzheimer's disease". In: *NeuroImage* 152.February, pp. 60–77. ISSN: 10959572. DOI: 10.1016/j.neuroimage.2017.02.058. URL: http://dx.doi.org/10.1016/j.neuroimage.2017.02.058.

Jacobs, Heidi I.L. et al. (2018). "Structural tract alterations predict downstream tau accumulation in amyloid-positive older individuals". In: *Nature Neuroscience* 21.3, pp. 424–431. ISSN: 15461726. DOI: 10.1038/s41593-018-0070-z. URL: http://dx.doi.org/10.1038/s41593-018-0070-z.

Jbabdi, Saad et al. (Nov. 2015). "Measuring macroscopic brain connections in vivo". In: *Nature Neuroscience* 18.11, pp. 1546–1555. ISSN: 1097-6256. DOI: 10.1038/nn.4134. URL: http://www.ncbi.nlm.nih.gov/pubmed/26505566http://www.nature.com/articles/nn.4134.

Jefferson-George, Kyra S. et al. (2017). "Cognitive decline associated with pathological burden in primary age-related tauopathy". In: *Alzheimer's and Dementia* 13.9, pp. 1048–1053. ISSN: 15525279. DOI: 10.1016/j.jalz.2017.01.028. URL: http://dx.doi.org/10.1016/j.jalz.2017.01.028.

Jones, David T. et al. (2017). "Tau, Amyloid, and Cascading Network Failure across the Alzheimer's disease Spectrum". In: *Cortex* October, pp. 1–17. ISSN: 00109452. DOI: 10.1016/j.cortex.2017.09.018. URL: http://linkinghub.elsevier.com/retrieve/pii/S0010945217303246.

Klein, Arno and Jason Tourville (2012). "101 Labeled Brain Images and a Consistent Human Cortical Labeling Protocol". In: *Frontiers in Neuroscience* 6.DEC, pp. 1–12. ISSN: 16624548. DOI: 10.3389/fnins.2012.00171.

La Joie, R. et al. (2012). "Region-Specific Hierarchy between Atrophy, Hypometabolism, and -Amyloid (A) Load in Alzheimer's Disease Dementia". In: *Journal of Neuroscience* 32.46, pp. 16265–16273. ISSN: 0270-6474. DOI: 10.1523/JNEUROSCI.2170-12.2012. URL: http://www.jneurosci.org/cgi/doi/10.1523/JNEUROSCI.2170-12.2012.

La Joie, Renaud et al. (2020). "Prospective longitudinal atrophy in Alzheimer's disease correlates with the intensity and topography of baseline tau-PET." In: *Science translational medicine* 12.524, pp. 1–13. ISSN: 1946-6242. DOI: 10.1126/scitranslmed.aau5732. URL: http://www.ncbi.nlm.nih.gov/pubmed/31894103.

Lee, Christopher M. et al. (Mar. 2018). "18F-Flortaucipir Binding in Choroid Plexus: Related to Race and Hippocampus Signal". In: *Journal of Alzheimer's Disease* 62.4, pp. 1691–1702. ISSN: 13872877. DOI: 10.3233/JAD-170840. URL: http://www.ncbi.nlm.nih.gov/pubmed/5957532http://www.medra.org/servlet/aliasResolver?alias=iospress&doi=10.3233/JAD-170840.

Lemoine, Laetitia et al. (2018). "Tau positron emission tomography imaging in tauopathies: The added hurdle of off-target binding". In: *Alzheimer's and Dementia: Diagnosis, Assessment and Disease Monitoring* 10, pp. 232–236. ISSN: 23528729. DOI: 10.1016/j.dadm.2018.01.007. URL: https://doi.org/10.1016/j.dadm.2018.01.007.

Liu, Li et al. (2012). "Trans-synaptic spread of tau pathology in vivo". In: *PLoS ONE* 7.2, pp. 1–9. ISSN: 19326203. DOI: 10.1371/journal.pone.0031302.

Liu, Min et al. (2019). " Sex modulates the ApoE ϵ4 effect on brain tau deposition measured by 18 F-AV-1451 PET in individuals with mild cognitive impairment ". In: *Theranostics* 9.17, pp. 4959–4970. DOI: 10.7150/thno.35366.

Lockhart, Samuel N et al. (Mar. 2017b). "Elevated (18)F-AV-1451 PET tracer uptake detected in incidental imaging findings." In: *Neurology* 88.11, pp. 1095–1097. ISSN: 1526-632X. DOI: 10.1212/WNL.0000000000003724. URL: http://www.ncbi.nlm.nih.gov/pubmed/28188303http://www.pubmedcentral.nih.gov/articlerender.fcgi?artid=PMC5384840.

Lowe, Val J. et al. (July 2019). "Cross-sectional associations of tau-PET signal with cognition in cognitively unimpaired adults". In: *Neurology* 93.1, E29–E39. ISSN: 1526632X. DOI: 10.1212/WNL.0000000000007728.

Maass, Anne et al. (2018b). "Entorhinal Tau Pathology , Episodic Memory Decline , and Neurodegeneration in Aging". In: *Journal of Neuroscience* 38.3, pp. 530–543. DOI: 10.1523/JNEUROSCI.2028-17.2017.

Maier-Hein, Klaus H. et al. (Dec. 2017). "The challenge of mapping the human connectome based on diffusion tractography". In: *Nature Communications* 8.1, p. 1349. ISSN: 2041-1723. DOI: 10.1038/s41467-017-01285-x. URL: http://www.

ncbi.nlm.nih.gov/pubmed/29116093http://www.pubmedcentral.nih.gov/articlerender.fcgi?artid=PMC5677006http://www.nature.com/articles/s41467-017-01285-x.

Marquié, Marta et al. (Oct. 2017). "[F-18]-AV-1451 binding correlates with postmortem neurofibrillary tangle Braak staging". In: *Acta Neuropathologica* 134.4, pp. 619–628. ISSN: 0001-6322. DOI: 10.1007/s00401-017-1740-8. URL: http://link.springer.com/10.1007/s00401-017-1740-8.

Mathys, Hansruedi et al. (June 2019). "Single-cell transcriptomic analysis of Alzheimer's disease". In: *Nature* 570.7761, pp. 332–337. ISSN: 0028-0836. DOI: 10.1038/s41586-019-1195-2. URL: http://www.nature.com/articles/s41586-019-1195-2.

Murray, Melissa E. et al. (Sept. 2011b). "Neuropathologically defined subtypes of Alzheimer's disease with distinct clinical characteristics: A retrospective study". In: *The Lancet Neurology* 10.9, pp. 785–796. ISSN: 14744422. DOI: 10.1016/S1474-4422(11)70156-9.

Ossenkoppele, Rik et al. (2016a). "Tau PET patterns mirror clinical and neuroanatomical variability in Alzheimer's disease". In: *Brain* 139.5, pp. 1551–1567. ISSN: 14602156. DOI: 10.1093/brain/aww027. URL: http://brain.oxfordjournals.org/.

Ossenkoppele, Rik et al. (2019). "Tau covariance patterns in Alzheimer's disease patients match intrinsic connectivity networks in the healthy brain". In: *NeuroImage: Clinical* 23.April, p. 101848. ISSN: 22131582. DOI: 10.1016/j.nicl.2019.101848. URL: https://doi.org/10.1016/j.nicl.2019.101848https://linkinghub.elsevier.com/retrieve/pii/S2213158219301986.

Palmqvist, Sebastian et al. (2014). "Accuracy of Brain Amyloid Detection in Clinical Practice Using Cerebrospinal Fluid β-Amyloid 42". In: *JAMA Neurology* 71.10, p. 1282. ISSN: 2168-6149. DOI: 10.1001/jamaneurol.2014.1358. URL: http://archneur.jamanetwork.com/article.aspx?doi=10.1001/jamaneurol.2014.1358.

Palmqvist, Sebastian et al. (Dec. 2017). "Earliest accumulation of β-amyloid occurs within the default-mode network and concurrently affects brain connectivity". In: *Nature Communications* 8.1, p. 1214. ISSN: 2041-1723. DOI: 10.1038/s41467-017-01150-x. URL: http://dx.doi.org/10.1038/s41467-017-01150-xhttp://www.nature.com/articles/s41467-017-01150-x.

Pooler, Amy M et al. (2013). "Physiological release of endogenous tau is stimulated by neuronal activity". In: *EMBO reports* 14.4, pp. 389–394. ISSN: 1469-221X. DOI: 10.1038/embor.2013.15. URL: http://embor.embopress.org/cgi/doi/10.1038/embor.2013.15.

Raj, Ashish, Amy Kuceyeski, and Michael Weiner (2012). "A Network Diffusion Model of Disease Progression in Dementia". In: *Neuron* 73.6, pp. 1204–1215. ISSN: 08966273. DOI: 10.1016/j.neuron.2011.12.040. URL: http://dx.doi.org/10.1016/j.neuron.2011.12.040.

Rousset, O G, Y Ma, and A C Evans (May 1998). "Correction for partial volume effects in PET: principle and validation." In: *Journal of nuclear medicine : official publication, Society of Nuclear Medicine* 39.5, pp. 904–11. ISSN: 0161-5505. URL: http://www.ncbi.nlm.nih.gov/pubmed/9591599.

Scherr, Martin et al. (2019). "Effective connectivity in the default mode network is distinctively disrupted in Alzheimer's disease-A simultaneous resting-state FDG-PET/fMRI study". In: *Human Brain Mapping* June 2018, pp. 1–10. ISSN: 10659471. DOI: 10.1002/hbm.24517. URL: http://doi.wiley.com/10.1002/hbm.24517.

Schöll, Michael et al. (2016b). "PET Imaging of Tau Deposition in the Aging Human Brain". In: *Neuron* 89.5, pp. 971–982. ISSN: 10974199. DOI: 10.1016/j.neuron.2016.01.028.

Seeley, William W. et al. (2009). "Neurodegenerative Diseases Target Large-Scale Human Brain Networks". In: *Neuron* 62.1, pp. 42–52. ISSN: 08966273. DOI: 10.1016/j.neuron.2009.03.024. URL: http://dx.doi.org/10.1016/j.neuron.2009.03.024.

Sepulcre, Jorge et al. (Dec. 2018). "Neurogenetic contributions to amyloid beta and tau spreading in the human cortex." In: *Nature medicine* 24.12, pp. 1910–1918. ISSN: 1546-170X. DOI: 10.1038/s41591-018-0206-4. URL: http://www.nature.com/articles/s41591-018-0206-4http://www.ncbi.nlm.nih.gov/pubmed/30374196http://www.pubmedcentral.nih.gov/articlerender.fcgi?artid=PMC6518398.

Torok, Justin et al. (2018). "A method for inferring regional origins of neurodegeneration". In: *Brain* 141.3, pp. 863–876. ISSN: 14602156. DOI: 10.1093/brain/awx371.

Villemagne, Victor L. et al. (2013). "Amyloid β deposition, neurodegeneration, and cognitive decline in sporadic Alzheimer's disease: A prospective cohort study". In: *The Lancet Neurology* 12.4, pp. 357–367. ISSN: 14744422. DOI: 10.1016/S1474-4422(13)70044-9. URL: http://dx.doi.org/10.1016/S1474-4422(13)70044-9.

Villemagne, Victor L. et al. (Feb. 2018). "Imaging tau and amyloid-β proteinopathies in Alzheimer disease and other conditions". In: *Nature Reviews Neurology* 14.4, pp. 225–236. ISSN: 1759-4758. DOI: 10.1038/nrneurol.2018.9. URL: http://www.nature.com/doifinder/10.1038/nrneurol.2018.9.

Vogel, Jacob W. et al. (Feb. 2019a). "Data-driven approaches for tau-PET imaging biomarkers in Alzheimer's disease". In: *Human Brain Mapping* 40.2, pp. 638–651.

ISSN: 10659471. DOI: 10.1002/hbm.24401. URL: http://doi.wiley.com/10.1002/hbm.24401.

Xia, Chenjie et al. (2017). "Association of In Vivo [¹⁸ F]AV-1451 Tau PET Imaging Results With Cortical Atrophy and Symptoms in Typical and Atypical Alzheimer Disease". In: *JAMA Neurology* 74.4, p. 427. ISSN: 2168-6149. DOI: 10.1001/jamaneurol.2016.5755. URL: http://archneur.jamanetwork.com/article.aspx?doi=10.1001/jamaneurol.2016.5755.

Yeh, Fang Cheng and Wen Yih Isaac Tseng (2011). "NTU-90: A high angular resolution brain atlas constructed by q-space diffeomorphic reconstruction". In: *NeuroImage* 58.1, pp. 91–99. ISSN: 10538119. DOI: 10.1016/j.neuroimage.2011.06.021. URL: http://dx.doi.org/10.1016/j.neuroimage.2011.06.021.

Zheng, Ying Qiu et al. (2019). "Local vulnerability and global connectivity jointly shape neurodegenerative disease propagation". In: *PLoS Biology* 17.11, pp. 1–27. ISSN: 15457885. DOI: 10.1371/journal.pbio.3000495.

Zhou, Juan et al. (2012). "Predicting Regional Neurodegeneration from the Healthy Brain Functional Connectome". In: *Neuron* 73.6, pp. 1216–1227. ISSN: 08966273. DOI: 10.1016/j.neuron.2012.03.004. URL: http://dx.doi.org/10.1016/j.neuron.2012.03.004.

Chapter 4

Characterizing the spatiotemporal variability of Alzheimer's disease pathology

Jacob W. Vogel, Alexandra L. Young, Neil P. Oxtoby, Ruben Smith, Rik Ossenkoppele, Olof T. Strandberg, Renaud La Joie, Leon M. Aksman, Michel J Grothe, Yasser Iturria-Medina, Gil D. Rabinovici, Daniel C. Alexander, Chul Hyoung Lyoo, Alan C. Evans, Oskar Hansson

4.1 Preamble

The previous chapter showed that diffusion of a pathological signal from the entorhinal cortex through the brain connectome produces a pattern resembling tau accumulation, particularly in early disease stages. However, this model did not fit the data perfectly, especially in individuals with AD dementia (Figure 3.S4). Analyses from Chapter 3 suggested regional Aβ contributed to the modeling error, as likely does measurement error and spatial resolution. However, the analyses from Chapter 3 also assumes a homogenous spreading pattern across individuals, which is unlikely given that within-individual model fitting was not as good as fit across individuals (Fig 3.S6). This is also unlikely considering autopsy studies have shown strong evidence for systematic variation in tau spread (reviewed in Section 1.3.4). The latter, however, has not been demonstrated extensively in humans (reviewed in Section 1.5.3).

The existence of atypical variants of tau spreading, and of variation in typical spreading patterns, is a topic that has received relatively little attention compared to other topics in AD research. As medical science slowly inches in the direction

of individualized medicine, understanding individual variation is becoming more of a priority. Investigation of tau spreading variation is not only important for individualized monitoring of disease progression, but may also reflect differing disease biology relevant to the development of therapeutic interventions. Variation in tau spread has been characterized to some degree in large samples of post-mortem data (Murray et al., 2011b), and in imaging data using proxies for tau pathology (Noh et al., 2014; Young et al., 2018; Tam et al., 2019). However, a large-scale investigation of systematic variation in tau distribution *in vivo*, using tau-specific markers, has not been performed.

There are several methodological issues that make examining heterogeneity in AD challenging. One challenge is that enormous sample sizes are necessary for reliable reports. A second challenge is that the spatial pattern of tau varies over time, and therefore time is a confound in any effort to study time-orthogonal spatial variability. An elegant solution to this latter issue was proposed in a recent study, which introduced an algorithm to model both the spatial and temporal aspects of disease progression simultaneously (Young et al., 2018). In this chapter, we apply that algorithm to the largest sample of tau-PET data assembled to date, composed of data from five different centers around the world. This study therefore represents a critical step toward understanding variation in tau spreading patterns in AD. Once again, the spatially unconstrained, tau-specific and *in vivo* features of tau-PET create an opportunity for novel insights.

4.2 Abstract

There has not been a systematic whole-brain characterization of spatiotemporal variation in tau deposition in Alzheimer's disease (AD), despite evidence for heterogeneity across the population. We leverage data-driven disease-progression models to describe four image-based phenotypes of AD with distinct cognitive, genetic and demographic profiles, which remain stable over time, site and methodology. We describe an age-related axis of severity that is orthogonal to phenotype, the extremes of which align with AD clinical variants. Our model allows for individual-tailored prediction of future tau accumulation, and we examine how cortico-limbic networks and neuronal cell-type variation may partially explain AD phenotypes. Our results suggest re-examining the notion of 'typical AD'.

4.3 Introduction

Alzheimer's disease (AD) is the leading cause of dementia worldwide (Prince et al., 2013) and prevalence is expected to double in the next twenty years, which will likely lead to enormous social and economic burden (Hurd et al., 2013). Despite the looming urgency of AD, the cause of of the disease remains unknown. At autopsy, AD presents with diffuse extracellular and neuritic β-amyloid (Aβ) plaques, and intracellular neurofibrillary tangles of hyperphosphorylated tau, along with extensive neurodegeneration (Braak and Braak, 1991). Leading hypotheses have postulated these two hallmark proteins, Aβ and tau, either alone or in combination, are causative agents in disease etiology and progression (Hardy and Selkoe, 2002; Jack and Holtzman, 2013; Sperling, Mormino, and Johnson, 2014). Both proteins have particular preclinical qualities. Around a third of healthy older adults present with cortical Aβ plaques (Jansen et al., 2015) increasing risk for incipient cognitive impairment (Morris et al., 2009; Teipel et al., 2020), which may occur up to two decades later (Villemagne et al., 2013). However, the extent of Aβ burden is poorly correlated with cognitive status (Nelson et al., 2012; Hedden et al., 2013) or local neurodegeneration (Gordon et al., 2018; La Joie et al., 2020), and numerous clinical trials have failed to clearly slow cognitive decline despite successfully reducing brain Aβ (Schneider et al., 2015). Meanwhile, tau tangles in the medial temporal lobe (MTL) is a very common age-related phenomenon (Crary et al., 2014), possibly associated with limited neurodegeneration and/or decrements in episodic memory (Maass et al., 2018b; Jefferson-George et al., 2017). Remarkably, the presence of Aβ is associated with the appearance of tau tangles outside of the MTL, which is itself highly associated with cognitive impairment (Ossenkoppele et al., 2018). Furthermore, cortical tau colocalizes with cortical atrophy and predicts future neurodegeneration (La Joie et al., 2020), while the appearance of tau in specific cognitive networks leads to domain-specific cognitive impairments (Bejanin et al., 2017b). For these reasons and others, the focus of treatment discovery has shifted recently to tau, and numerous therapeutic interventions are currently undergoing research and development (Jadhav et al., 2019). A better understanding of tau pathophysiology is therefore of imminent need in order to aid development of these interventions.

Tau tangles are thought to exhibit a somewhat specific pattern of cortical spread, which has been formalized into the Braak staging system (Braak and Braak, 1991; Braak et al., 2006). The six Braak stages describe the first appearance of cortical tau tangles in the entorhinal cortex, where they spread throughout the medial and basal temporal lobes, then into nearby allocortex, next into isocortical associative regions, and finally into the unimodal sensory cortex (Braak et al., 2006). While this

stereotyped progression was derived from histopathological staining at autopsy, tau can now be measured in vivo in the human brain using positron emission tomography (PET), and early tau-PET imaging studies described spatial patterns that have mostly converged with the Braak staging system (Schöll et al., 2016b; Schwarz et al., 2016; Cho et al., 2016a; Vogel et al., 2019a). However, many examples have emerged of individual tau patterns that violate the sequence of events purported in the Braak staging system. Murray and colleagues described, in a large autopsy sample, a number of individuals showing an MTL-sparing phenotype with extensive cortical tau burden but limited MTL burden, as well as a limbic phenotype with high volume tau pathology that was nonetheless relegated to limbic and temporal cortex (Murray et al., 2011b). The existence of these phenotypes have been routinely replicated (Whitwell et al., 2012; Ossenkoppele et al., 2018; Jeon et al., 2019), and associated with specific patient profiles (see (Ferreira, Nordberg, and Westman, 2020) for a systematic review). Based on these findings, Ferreira and colleagues described a model of AD pathological heterogeneity where individuals vary along an axis of "typicality", but also noted a great deal of variation in AD severity, with patients presenting with more or less aggressive phenotypes (Ferreira, Nordberg, and Westman, 2020). In addition, clinical variants of AD have been described that exhibit specific patterns of pathology that deviate from the Braak stages (Warren et al., 2017). Posterior cortical atrophy (PCA, the "visual variant" of AD) involves marked pathology in the occipitoparietal areas (Crutch et al., 2012), logopenic variant primary progressive aphasia (lvPPA, "language variant") presents with asymmetric left temporal pathology (Mesulam et al., 2008), and frontal/dysecutive and early-onset varieties of AD tend also to have aggressive phenotypes involving frontoparietal regions (Ossenkoppele et al., 2016a).

Taken together, the examples above suggest that, while the Braak staging system appears to be a good description of tau spreading at the population level, it does not account for systematic variability at the individual level. Variation in the pathological spread of AD may have numerous practical repercussions that warrant consideration for both basic research and clinical trials investigating tau. The differing patterns may result from distinct etiological events or vulnerabilities of specific molecular pathways, such as the high proportion of APOE4 carriers with a limbic phenotype (Ferreira, Nordberg, and Westman, 2020), or the vulnerability of specific cell types in certain variants of AD (e.g. (Drummond et al., 2017; Petersen et al., 2019)). Such biological differences could be associated with systematic difference in treatment response. In addition, different AD subtypes may have distinct rates and profiles of cognitive decline (Risacher et al., 2017; Ossenkoppele et al., 2019). Finally, research or clinical samples are likely composed of different mixes of AD phenotypes, which

could result in discrepant findings across studies. The latter issue might be particularly problematic if pathological variants of AD are related to demographic factors such as age, education or research setting, which tend to vary widely across studies.

For the reasons listed above, and many others, a systematic description of variation in AD pathological spread is imminently necessary. Previous studies have provided invaluable information toward this effort (Young et al., 2018; Dong et al., 2017; Zhang et al., 2016; Noh et al., 2014; Murray et al., 2011b; Ferreira, Nordberg, and Westman, 2020; Tam et al., 2019), but suffer from specific limitations. While pathology studies represent an important standard and were responsible for the initial characterization of tau spreading, such studies are typically semi-quantitative in nature, involve limited spatial sampling, and have issues related to inter-rater reliability and working with posthumous human tissue at late stages of the disease (Scheltens and Rockwood, 2011). Application of unsupervised statistical learning methods to neuroimaging data circumvent many of these limitations, but come with limitations of their own. First, nearly all such studies to date have used non-specific measurements of tau pathology—usually structural MRI—meaning pathological information is confounded by non-specific, unrelated or up/downstream sources. In addition, perhaps the most challenging issue relates to the confounding effect of spatiotemporal disease progression: in a set of images sampled from a population along the AD spectrum, the greatest source of variation across images is disease progression, or the variation in space of a pathological entity over time. As such, most unsupervised algorithms will partition images along this "temporal" axis (i.e. less pathology, intermediate pathology, more pathology), which is both uninformative and orthogonal to the axis of interest: spatial variation. Many studies have presented clever solutions to this conundrum, including limiting analyses to a certain window of disease progression (e.g. only in individuals with dementia, (Noh et al., 2014)) or removing or accounting for global tau signal (e.g. (Dong et al., 2017; Tam et al., 2019). These approaches achieve varying levels of success, but often come at the additional cost of reduced sample sizes and/or abstraction to a point of reduced interpretability.

We present a systematic characterization of heterogeneity in tau patterning in AD, which attempts to overcome each of the aforementioned limitations. To accomplish this goal, we have amassed the largest and most diverse sample of tau-PET data to date (n=2324), allowing unprecedented power to detect and characterize AD subtypes. We apply to this data the Subtype and Stage Inference (SuStaIn) model, a paradigm-shifting algorithm that combines disease progression modeling with traditional clustering to achieve probabilistic spatiotemporal partitioning and classification (Young et al., 2018). SuStaIn has previously been used to successfully partition

genetic variants of frontotemporal dementia using imaging data without supervision (Young et al., 2018), and has identified novel variations in chronic obstructive pulmonary disorder biomarkers that demonstrated distinct longitudinal outcomes (Young et al., 2020). We apply SuStaIn to our multi-cohort sample of tau-PET data to discover systematic spatiotemporal variation in tau spreading, and validate our findings over time and across different PET radiotracers. We identify four subtypes that demonstrate impressive stability over time and across cohorts and different PET radiotracers. The subtypes are associated with distinct genetic, cognitive and demographic profiles along with differing cognitive prognoses, and we present certain biological phenomena that may contribute to diversity in tau-PET spreading patterns. Finally, we show we use our model to create individual-tailored predictive tools for tracking disease progression with increased power.

4.4 Results

We compiled a discovery sample of 1143 individuals along the AD spectrum with flortaucipir-PET tau images, spanning five separate cohorts. Demographic information and cross-cohort comparisons can be found in Table 4.S1. Significant cross-cohort differences were observed for all variables assessed.

4.4.1 Spatiotemporal subtypes of Alzheimer's disease

We applied the Subtype and Stage Inference (SuStaIn) algorithm to our large sample of flortaucipir-PET images in order to extract distinct spatiotemporal trajectories of tau spreading. 646 (56.5%) individuals did not demonstrate any abnormal tau-PET signal, and were therefore assigned by SuStaIn to a tau-negative group (S0). Using cross-validation, we determined a four-subtype solution to best represent the data. The four-subtype model was applied to our discovery dataset. These individuals were probabilistically assigned to one of 30 progressive stages along one of the four subtype trajectories (Fig 4.1). Flortaucipir-PET scans are confounded by various sources of off-target tracer retention (Lemoine et al., 2018) that can elevate tau-PET signal in the absence of tau pathology. After post-hoc visual inspection and analysis, we determined one subtype (S2, see below) to contain several individuals with a high-probability of off-target binding (i.e. false-positives). Data-driven approaches were used to identify these individuals and re-label them into the S0 group (see Methods Section 4.6.4,Supplementary Fig 4.S1). After this correction, the S0 class included 78.5% of all cognitively normal individuals, 36.3% of individuals with MCI, and 4.7% of individuals with AD.

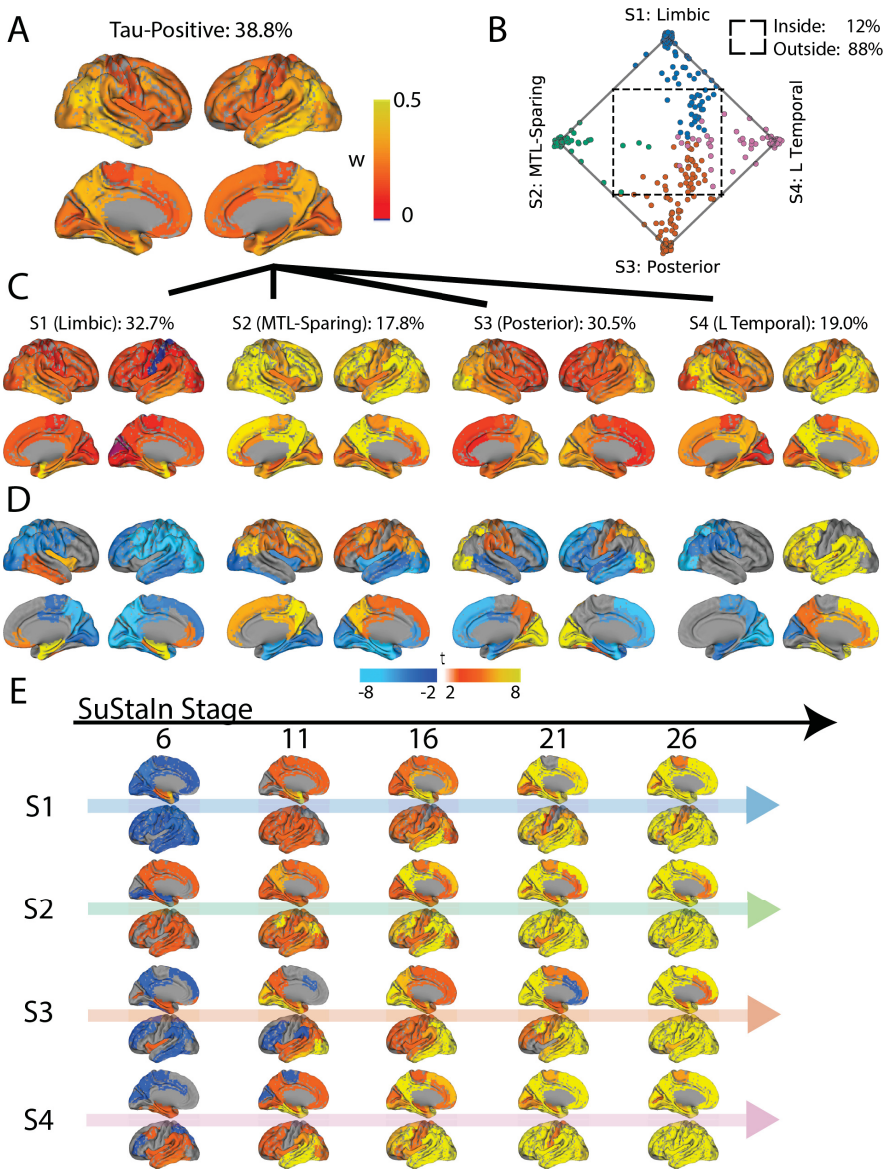

Figure 4.1: A) Tau-PET pattern of tau-positive (subtyped) individuals. B) Quarternary plot showing probability each individual is classified as each subtype. Dots are labeled by final subtype classification: S1 (red), S2 (green), S3 (blue) or S4 (black). Inset box shows individuals that had a probability < 0.5 to be classified as any of the four subtypes (i.e. showing poor fit). C) Average tau-PET pattern for each subtype. The colorbar is the same as Panel A. D) Regions showing significant difference between one subtype and all other subtypes after FDR correction. E) Progression of each subtype through SuStaIn stages. Each image is a mean of individuals classified at the listed stage and up to four stages lower. Only the left hemisphere is shown to conserve space.

The remaining 443 individuals were categorized into one of four tau progression subtypes (Fig 4.1). 145 (32.7%) exhibited a limbic-predominant phenotype, with a highly Braak-like spatial progression across SuStaIn stage (S1: Limbic). These individuals demonstrated higher tau-PET binding in the MTL and right frontotemporal and insular cortex, and relatively lower tau-PET signal in other parts of the cortex, compared to other subtyped (i.e. tau-positive) individuals. An additional 79 individuals (17.8%) expressed a parietal-dominant and MTL-sparing phenotype, where early precuneus binding spread across temporoparietal and frontal cortex, but

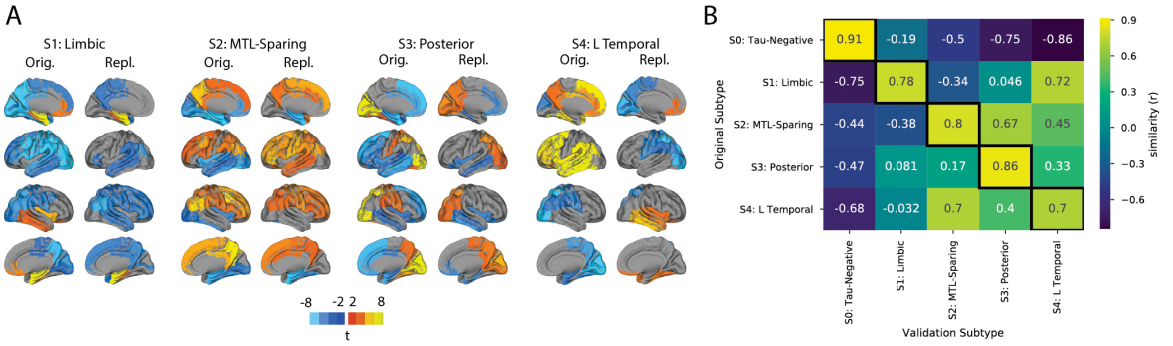

Figure 4.2: A) For both the discovery (Orig) and replication (Repl) cohorts, maps showing regions significantly different between one subtype and all others within the cohort (after FDR correction). Similar spatial patterns were observed, except for a reversed pattern in S4. B) Confusion matrix comparing subtypes identified in the original (discovery) sample (y-axis), and subtypes separately identified in the replication sample (x-axis). Values represent spatial correlation between average regional tau for each subtype. Values along the diagonal indicates similarity between the same subtype across both cohorts.

with relative sparing of the MTL (S2: MTL-Sparing). These individuals expressed significantly higher tau burden in the parietal, dorsal frontal and somatomotor cortex, but exhibited relative sparing in visual, medial frontal, insular, temporal cortex and particularly the MTL (especially the hippocampus). The third subtype composed 135 (30.5%) individuals with a predominant posterior occipitotemporal tau phenotype, involving early occipital lobe binding and gradual anterior progression across SuStaIn stage (S3: Posterior). These individuals demonstrated greater occipital, lingual and dorsal parietal binding compared to other subtypes, but also relatively less binding in frontal, temporal and insular cortex. The remaining 84 (19.0%) individuals showed a temporoparietal phenotype with distinct left-sided asymmetry, characterized by early left-temporal tau eventually spreading to parietal and frontal cortex across disease stage (S4: Lateral [L] Temporal). This subtype was characterized by greater tau signal in left temporal, frontal and parietal cortex compared to other subtypes, but relative sparing of right parietal and occipital cortex. The different subtypes shed light on inconsistencies of tau-PET binding and pathological sequencing of specific brain regions across previous studies (Schöll et al., 2016b; Cho et al., 2016a; Vogel et al., 2019a) (Supplementary Fig 4.S2). Hippocampal binding was high in S1 (limbic individuals) but low in other subtypes, and a similar trend was seen for the lingual gyrus in S3 (Posterior), while the insula showed varied binding across subtypes.

4.4.2 Stability of AD subtypes

While variation in subtype proportion was observed (and expected) across cohorts, all subtypes were represented across all cohorts (Supplementary Fig 4.S3). Most individuals fell neatly into the stereotypical progression of each subtype (Fig 4.1B), allowing a clean stepwise progression across tau abnormality events to be observed

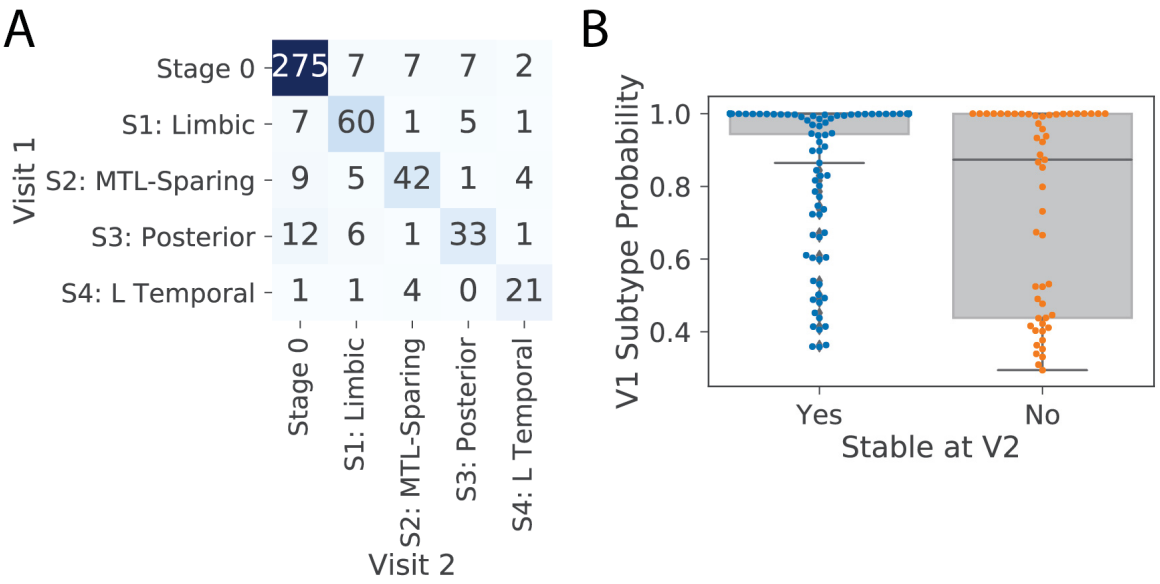

Figure 4.3: A) Confusion matrix showing longitudinal stability of subtypes. Each row shows the number of subjects from a given subtype at Visit 1 that were classified as each subtype at Visit 2. The diagonal represents the number of subjects that were classified as the same subtype at Visit 1 and Visit 2. Overall stability was 84%. B) Individuals with a higher probability of being classified into their subtype were more likely to show a stable subtype over time ($p<0.0001$).

across each subtype population (Supplementary Fig 4.S4). However, 12% of individuals did not fall cleanly into any subtype, demonstrating subtype probabilites below 50% for all subtypes (Fig 4.1B).

We next wished to assess whether the same subtypes could be derived within a separate replication sample of 469 individuals scanned with the RO948 tau-PET tracer. The replication cohort, BioFINDER-II, differed from the discovery sample in all variables assessed, except sex, proportion of AD patients, proportion of homozygous APOE4 carriers and magnitude of inferior temporal lobe tau (Supplementary Table 4.S1). SuStaIn was run separately on these individuals, constraining the analysis to produce four subtypes to match the discovery sample. The four resulting subtypes greatly resembled those derived in the discovery sample (Fig 4.2). The only exception involved the S4: L Temporal subtype, which had a similar overall tau-PET pattern but involved right-sided rather than left-sided asymmetry.

Two possible differences between the discovery and replication datasets that could lead to this discrepancy are tau-PET radiotracer and sample size. To rule out the latter, we split the discovery sample in half (n=571, 572) and reran SuStaIn on each half, constraining the model to four subtypes. While the first three subtypes were once again very similar, a discrepancy was observed once again in the L Temporal phenotype. One half demonstrated a left-lateralized phenotype, while the other half resulted in a right-lateralized phenotype similar to the replication sample (Supplementary Fig 4.S5). These results suggest a consistent overall pattern for the S4: L Temporal phenotype, but that this phenotype has a high propensity for marked

lateralization. The emergence of a more left-predominant or right-predominant phenotype in data-driven analyses such as this one may vary due sample size and composition. The variation in lateralization affected the overall stability of S4 and, to a lesser degree, S1, but S2 and S3 were remarkably stable over the four datasets (original, split 1, split 2, replication; Supplementary Fig 4.S5)

We next evaluated the stability of AD subtypes over time. 519 individuals from the discovery sample also had follow-up flortaucipir-PET scans at least 1 year later. We used the SuStaIn model learnt on the cross-sectional data to subtype and stage follow-up visits from the same subjects. Overall 84% of individuals exhibited the same subtype at both baseline and follow-up (Fig 4.3). Stability remained virtually the same when excluding individuals classified as S0 at baseline and follow-up (83.9%). Stable individuals had a higher subtype probability (i.e. classified with a higher degree of confidence) compared to individuals whose subtype changed at follow-up (stable mean = 0.91, sd = 0.17; change mean = 0.74, sd = 0.27; t = 5.26, $p < 0.0001$; Fig 4.3). Supplementary Table 4.S2 shows longitudinal stability when excluding individuals using various subtype probability thresholds. Using a threshold of 0.5, stability increases to 86.8%, and a threshold of 0.9 increases stability to 88.3%.

4.4.3 AD subtypes characterized by distinct demographic, cognitive and genetic profiles

Various demographic, cognitive and genetic variables were available for all or most of the individuals across all cohorts. We used linear models to assess whether subtypes demonstrated distinct profiles compared to one another, and to S0 individuals. Statistics for these comparisons can be found in Supplementary Tables 4.S3 and 4.S4. All results are reported after multiple-comparisons correction.

Individuals across all four subtypes expressed worse MMSE and cognition across all domains compared to S0 individuals. In addition, individuals across all subtypes except S2 (MTL-Sparing) were more likely to be APOE4 carriers. Compared to S0 individuals, individuals with the S1 (Limbic) subtype were less educated, more likely to be women, and trended at being older. S2 (MTL-Sparing) individuals were younger than S0 individuals, and showed a trend at being more highly educated. S3 (Posterior) individuals showed a trend for being older than S0 individuals, and S4 (L Temporal) individuals showed a trend for being more highly educated (Supplementary Table 4.S3). Some of these relationships were altered after correcting for cohort, clinical diagnosis and various demographics measures (Supplementary Table 4.S3), notably the cognitive domain scores. After corrections, all subtypes still showed memory impairment, and S4 individuals showed impairment in all

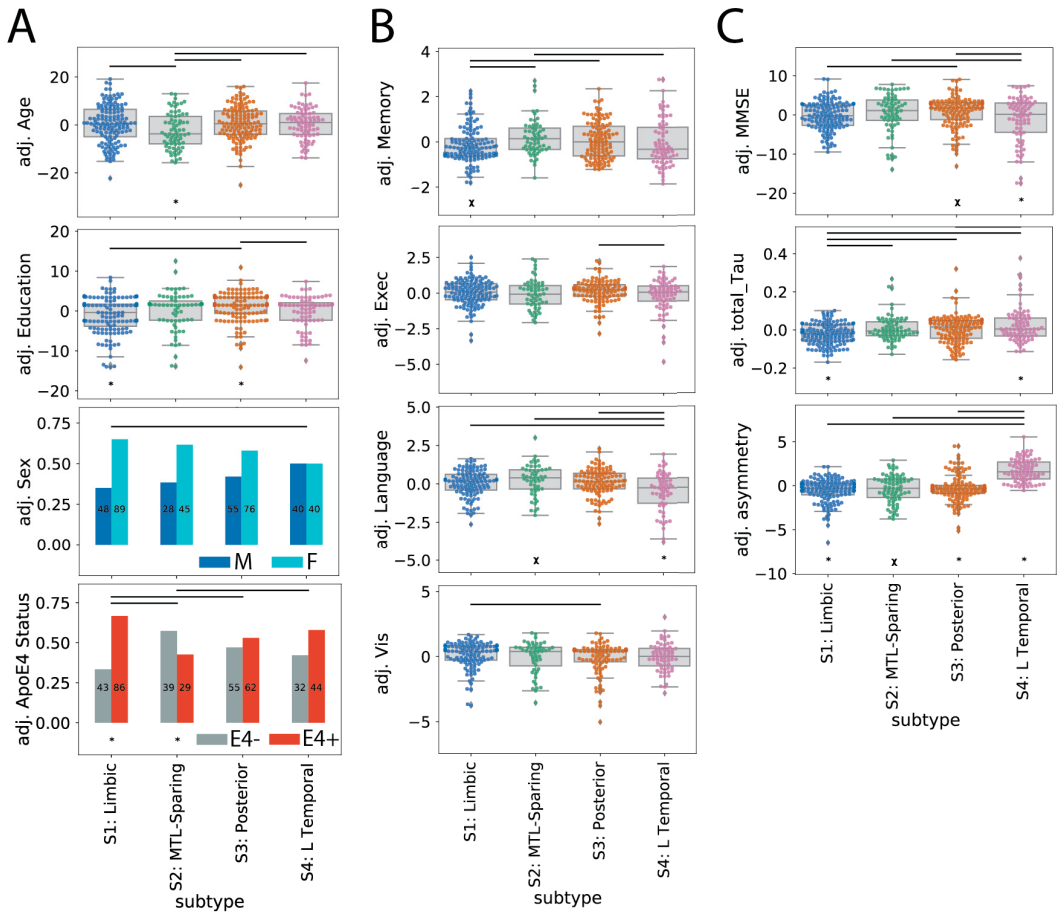

Figure 4.4: For all plots in panels A-C, horizontal lines indicate significant differences between two subtypes. A * below a box indicates the subtype is significantly different ($p<0.05$) from all other subtypes combined, while a χ represents a trend ($p<0.1$). All statistics are adjusted for SuStaIn stage and multiple comparisons. A) Comparisons between subtypes across (from top to bottom) Age, Education, Sex and APOE4 status. b) Comparisons between subtypes across the four cognitive domains: (from top to bottom) Memory, Executive Function, Language and Visuopatial Cognition. c) Comparisons between subtypes on (from top to bottom) MMSE, mean cortical (w-scored) tau-PET signal, and mean cortical tau-PET hemispheric asymmetry (left / right).

domains. However, S1 individuals did not show impairment in the visual domain, S2 individuals did not in the language domain, and S3 did not in the Executive domain, compared to S0 individuals.

Compared to other subtypes (i.e. other tau-positive individuals), individuals with the S1 (Limbic) subtype were older, less educated, were more likely to carry an APOE4 allele, had less overall tau with more right-sided asymmetry, and trended at having spared visuopatial cognition. These relationships did not change after controlling for SuStaIn stage, except relative memory impairment became a trend, and age and visuospatial cognition were no longer significantly different. After additionally controlling for diagnosis, demographics and cohort, only the relationships with APOE4, total tau and asymmetry remained significant. S2 (MTL-Sparing) individuals were younger, less likely to carry an APOE4 allele, had more overall tau burden, worse executive function, and trended at having worse MMSE and more right-sided

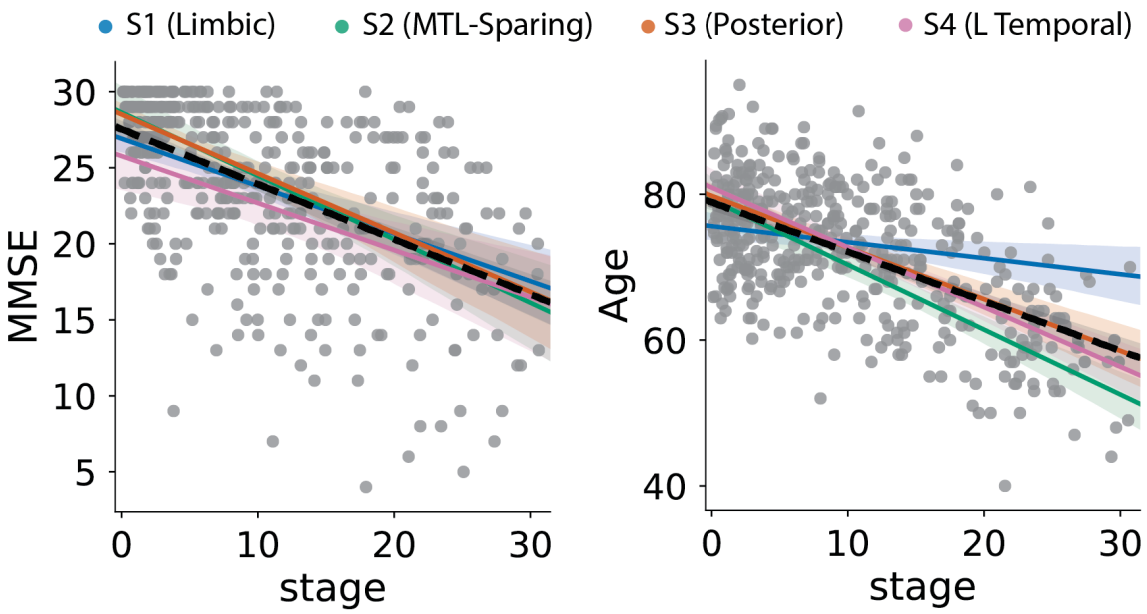

Figure 4.5: Increasing SuStaIn stage is associated with lower age and worse cognition across all subtypes.

tau asymmetry compared to other subtypes. After controlling for SuStaIn stage, the S2 individuals were still younger, less likely to carry an APOE4 allele, and had slightly more right-sided asymmetry, however a trend-level sparing of language function emerged. After controlling for cohort, demographics and clinical diagnosis as well, only the relationships with age and APOE4 and the trend-level asymmetry remained significant. Individuals with the S3 (Posterior) subtype were older, more highly educated, had more right-sided asymmetry, had spared MMSE and executive function scores, and had less overall tau. Controlling for SuStaIn stage abolished most of these relationships, except higher education, more right-sided asymmetry and a trend for spared MMSE scores. Additionally controlling for demographics, clinical disease stage and cohort resulted in no remaining significant relationships. Finally, S4 (L Temporal) individuals had more tau with more left-sided asymmetry, and had worse MMSE, language and executive function. All of these relationships remained after controlling for SuStaIn stage, except executive function. Adjusting for cohort, demographics and clinical diagnosis did not change these relationships, except the relationship with MMSE. These relationships (after adjustment for SuStaIn stage) are visualized in Fig 4.4, and statistics can be found in Supplementary Table 4.S4.

As expected, increasing SuStaIn stage was associated with worse global cognition as measured with MMSE ($r=-0.54$, $p<0.0001$; Fig 4.5). This relationship was consistent across all subtypes (S1: $r = -0.51$, S2: $r = -0.53$, S3: $r = -0.64$, S4: $r = -0.40$, all $ps<0.001$). A strong negative relationship between SuStaIn stage and age was observed, such that individuals at later SuStaIn stages tended to be younger ($r = -0.59$, $p<0.0001$). This relationship was once again consistent across all subtypes, though less prominent

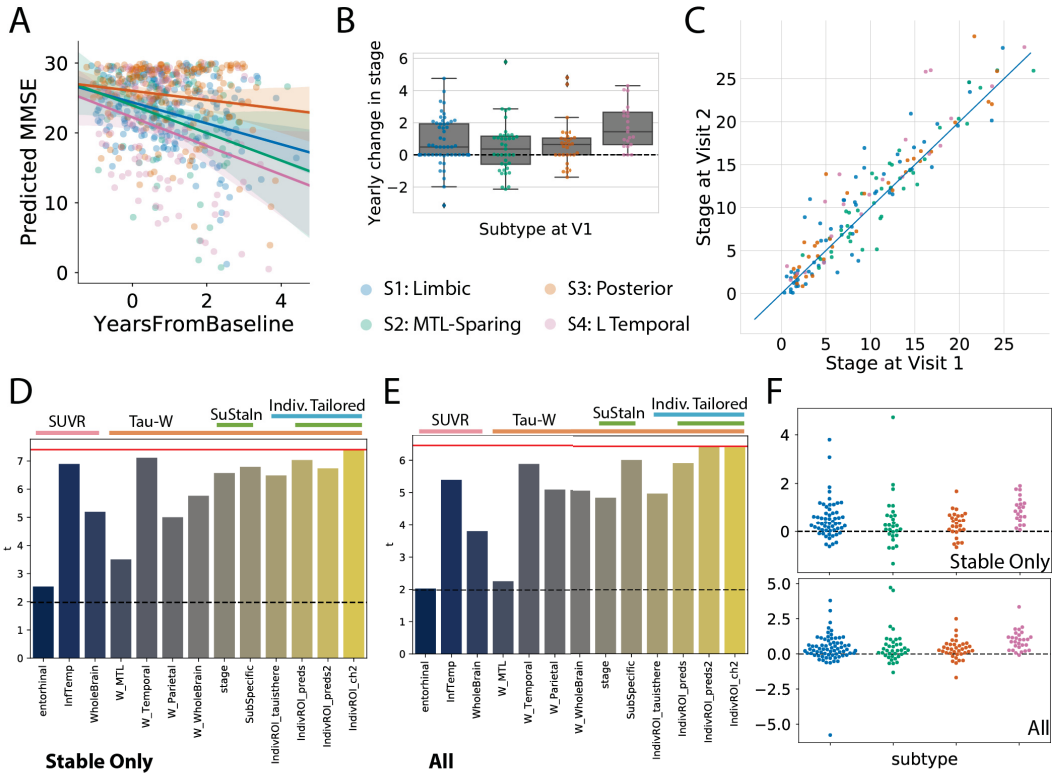

Figure 4.6: A) Rate of longitudinal decline in MMSE for each subtype. The x-axis was jittered for visualization purposes only. The y-axis show MMSE across all observations as predicted by linear mixed models adjusted for age, sex, education and clinical status (CN, MCI, AD). The posterior subtype exhibited significantly slower decline than the other subtypes, while the L Temporal subtype declined faster than the Limbic subtype. B) Annual change in (absolute) SuStaIn stage for each subtype, in individuals with stable subtypes over time. C) Change in SuStaIn stage across two visits independent of time between visit. Individuals above the diagonal advanced in SuStaIn stage. D) Effect-size comparison for annual tau change of different ROIs. The y-axis represents the t-value in a one-sample t-test against 0. The dashed line shows significant ($p<0.05$) difference from 0. The red line indicates the t-value of the highest performing ROI. Lines on top indicate whether the ROI was SUVR based or tau w-score based, and whether the ROI used SuStaIn information and/or was individually tailored based on a longitudinal prediction model. These results are restricted to individuals with a stable subtype over time. E) The same thing but in all individuals (including those who changed subtype over time). F) Annual change in tau W-score in individually-tailored "ch2" ROI for (top) stable individuals only and (bottom) all individuals.

for S1 (S1: r = -0.20, S2: r = -0.68, S3: r = -0.64, S4: r = -0.73, all ps<0.05; Fig 4.5). This negative relationship was also present among individuals younger than 65 (r = -0.17, p = 0.010) and individuals older than 80 (r = -0.14, p = 0.034), but not individuals in between. Asymmetry also increased with increasing SuStaIn stage (Supplementary Fig 4.S6). However, despite trends in asymmetry at higher SuStaIn stage, many individuals were observed with asymmetric tau patterns in the "non-predominant" hemisphere for their subtype (Supplementary Fig 4.S6), suggesting asymmetry to be at least partially orthogonal with subtype.

4.4.4 Longitudinal progression of AD subtypes

Longitudinal MMSE data was available for a subset of 697 individuals. We used linear mixed effects models to test differences between subtypes in the rate of global cognitive decline, adjusting for age, sex, education and disease status (Fig 4.6A). Individuals with the S3 (Posterior) subtype had significantly slower decline compared to all other subtypes. Individuals with the S4 (L Temporal) subtype additionally showed steeper cognitive decline compared to S1 (Limbic) subtype individuals. These relationships were unaltered after additionally controlling for cohort.

We next examined how SuStaIn stage changed over time for each subtype, using the 519 individuals with longitudinal flortaucipir-PET data. For this analysis, we excluded subtype 0 individuals (n=330), and also excluded individuals that were not classified as the same subtype across all measurements (n=36), for a final sample of n=153. Mean change in SuStaIn stage per year was calculated. Across the whole sample, we observed significant yearly increase in SuStaIn stage (mean Δ/year = 0.8, t[148]=6.54, p<0.0001). This relationship was consistent across subtype, though only a trend for S2 (MTL-Sparing) (Fig 4.6B,C; S1: mean = 0.78, t[57]=4.09, p=0.0001; S2: mean = 0.45, t[39]=1.81, p=0.079; S3: mean = 0.64, t[31]=2.61, p=0.014, S4: mean = 1.73, t[21]=5.85, p<0.0001). A significant difference in mean annual rate of SuStaIn stage change was seen across subtypes (F=3.80, p=0.012), and posthoc tests revealed annual SuStaIn stage increased faster in S4 (L Temporal) compared to S2 (MTL-Sparing) and S3 (Posterior) subtypes. Supplementary Table 4.S5 shows the proportion of individuals who progressed, remained stable, or regressed in SuStaIn stage at their second visit, before and after accounting for model uncertainty. Notably, no S4 individuals regressed. No relationship was seen between SuStaIn stage at visit 1 and annual change in stage per year across the whole sample (r = 0.12, p=0.15), nor within any subtype (all ps>0.20).

4.4.5 Individualized prediction of tau progression

We used information from SuStaIn to develop ROIs that are tailored to an individuals baseline tau-PET scan, and we compared these regions to more simpler ROIs using both SUVRs and tau w-scores. The object was to predict which regions would show longitudinal change on an individual basis. The individual-tailored ROIs included: SuStaIn stage ("stage"), selecting a specific lobar ROI depending on subtype ("SubSpecific"), all lobar ROIs with significant within-individual abnormal tau-PET signal ("tauisthere"), all lobar ROIs in regions with abnormal tau and predicted to get tau based on (and weighted by) two types of predictive models ("pred1","pred2"), and all lobar ROIs predicted to increase in tau at next timepoint based on (and weighted

by) a predictive model ("ch2"). The methods by which these ROIs were devised can be found in the Methods. To test the predictive utility of each ROI, we calculate a one-sample t-test against 0 to determine a) if tau is significantly increasing annually with each ROI, and b) the effect size, where higher t-values might indicate increased power to detect tau-PET change.

The results are visualized in Fig 4.6D,E for individuals with a stable subtype over time, and all individuals, respectively. All ROIs showed significant annual increase over time (uncorrected $p<0.05$). SUVR-based ROIs tended to perform worse than W-score-based ROIs, which were themselves improved when incorporating information from SuStaIn and/or individual-specific information. Traditional temporal lobe ROIs had excellent performance, indicating consistent tau accumulation in this region across individuals. Individual-tailored ROIs gave the highest effect sizes, and were particularly helpful when including unstable cases (Fig 4.6E). This is likely due to these measures incorporating probabilistic, rather than absolute, subtype information. Remarkably, the best overall ROI was a weighted composite of regions expected to show tau accumulation at next visit, as predicted by a model combining SuStaIn-based information and individual baseline scans ("ch2"). The individual annualized accumulation rates of tau in this ROI is shown for stable individuals, and all individuals, in Fig 4.6F.

4.4.6 AD subtype patterns associated with distinct corticolimbic networks

The underlying causes of differences in tau spreading patterns are unknown. Leading theories on tau spreading involve network propagation, hypothesizing that tau oligomers spread transneuronally through axonal connections, or that pathological states are propagated through macroscale brain networks (Mudher et al., 2017). We use network diffusion models to examine the possibility that the observed subtype-specific tau spreading patterns may be driven by spread through distinct networks. We previously showed that an epidemic spreading model (ESM) simulating spread of an agent from an epicenter (the entorhinal cortex) through the human connectome predicted the spatial distribution of tau-PET signal in the human brain (Chapter 3). We applied this same simulation separately to tau subtypes defined by SuStaIn, cycling through different possible cortical epicenters. We found that an entorhinal cortex epicenter fit the S1 (Limbic) subtype tau pattern very well (r^2=0.70), but did not fit other subtype patterns nearly as well (S2: r^2=0.04; S3: r^2=0.41; S4: r^2=0.37). However, models using different epicenters substantially improved fit (Fig 4.7A). Best fitting models used the inferior temporal lobe (r^2=0.27) for S2 (MTL-Sparing),

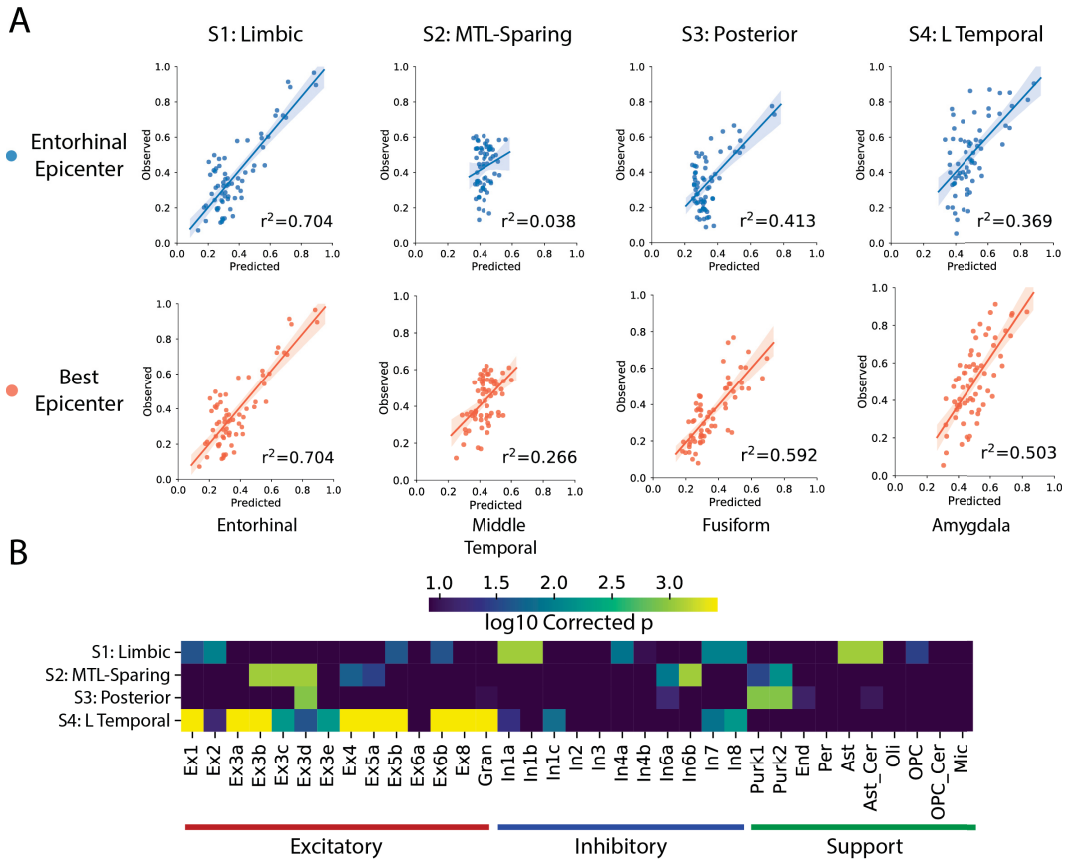

Figure 4.7: A) An epidemic spreading model (Iturria-Medina et al., 2014) was fit separately for each subtype; once using an entorhinal cortex epicenter, and once with a subtype-specific best-fitting epicenter. For each plot, each dot represents a region. The x-axis represents the mean simulated tau-positive probabilities across the population, while the y-axis represents the mean observed tau-positive probability. Each column represents a subtype. The top row shows ESM results when using an entorhinal cortex epicenter. The bottom row shows ESM results when using an epicenter that best fits the subtype pattern. B) The Allen Human Brain Atlas was used to determine genes with expression patterns mirroring subtype-specific tau patterns (top 1%). These gene lists were queried for enrichment of different cell classes using (Lake et al., 2018) as reference data. P-value were determined using permutation tests with 1000 iterations, followed by FDR correction.

the fusiform gyrus (r^2=0.59) for S3 (Posterior) and the amygdala (r^2=0.50) for S4 (L Temporal) (Fig 4.7A; Supp Figure), suggesting a possible predominance of these regions in secondary tau seeding for different subtypes.

4.4.7 AD subtypes associated with distinct transcriptomic signatures

Another possible explanation for heterogeneity in tau spreading patterns may involve vulnerability of region-specific molecular networks. Such vulnerability may be conferred by genetic susceptibility, and may manifest as variability in the expression of different neural cell subtypes, or molecular networks activated in response to AD pathology. We leverage high-resolution transcriptomic data to compare

subtype-specific tau patterns to spatial pattern of gene expression for different cell-subtypes and AD vulnerable networks. We use machine learning to identify sets of genes whose expression patterns match the subtype-specific spatial tau patterns (**Supplementary Data**), and then test whether these lists are enriched for genes known to be expressed in certain cell subtypes (Lake et al., 2018). We found each subtype-specific gene expression pattern to exhibit a unique pattern of cell-type enrichment (Fig 4.7B). For example, the specific pattern of tau associated with the S1 (Limbic) subtype overlapped with a molecular profile enriched for astrocytes and specific inhibitory interneuron markers, among others. The finding of astrocytes is particularly interesting for this subtype, given the high prevalence of APOE4 carriers among S1 individuals, and the fact that APOE is among the top markers for astrocytes. In addition, we found the S4 (L Temporal) pattern to be enriched for excitatory neurons, again interesting given the rapid progression of this subtype compared to other subtypes. We next apply the same approach, except this time to examine enrichment of genes involved in cell-type specific pathological processes in AD (Mathys et al., 2019). Under this framework, we found similar results: The S1 (Limbic) subtype pattern was enriched for genes upgregulated in astrocytes in response to AD pathology, while the S4 (L Temporal) subtype pattern was enriched for genes upregulated in neurons in AD.

4.4.8 A new model for Alzheimer's disease heterogeneity

Ferreira and colleagues presented a working model describing two orthogonal axes explaining heterogeneity in AD presentation: severity and typicality (Ferreira, Nordberg, and Westman, 2020). Based on our findings, we suggest an updated model. Our data support the notion of an axis of disease severity that is orthogonal to the pattern of neurodegeneration, and we find this axis is strongly and inversely related to age (Fig 4.5). However, our data disputes the notion of "typicality" in AD. Rather, the spatial pattern of tau spreading appears to vary along at least four archetypes (Fig 4.1), depending on factors such as age and genotype (Fig 4.4), and without one pattern emerging as "dominant" or "typical". Therefore, we propose heterogeneity in AD is best represented as a plane rather than an axis.

4.5 Discussion

For thirty years, the progression of tau pathology in AD has principally been described by a single model of spatiotemporal evolution (Braak and Braak, 1991; Braak et al., 2006), despite frequent examples of nonconforming cases (Murray et al., 2011b).

We show that the cortical cascade of tau pathology, in a sample of nearly 450 tau-PET-positive individuals, is better described by a model including multiple spatiotemporal patterns. Importantly, this model reconciles atypical AD variants with common variations of typical AD into a single unified model of pathological progression. First, the model reaffirms the existence of oft-observed cortical-predominant and limbic-predominant pathological patterns as distinct subtypes of tau progression, rather than phases along a continuum. In addition, the model also accounts for the most frequently occurring atypical variants of AD, PCA and lvPPA, as the extremes of regularly occurring posterior and lateral-temporal AD subtypes. Together, our data align with a recent model (Ferreira, Nordberg, and Westman, 2020) to suggest variation in the pathological expression of AD along two orthogonal axes: subtype and severity, the latter of which is strongly and inversely correlated with age. Given that no dominant pattern emerged, our data suggest the existence of multiple AD subtypes, confounding the notion that there is such an entity that can be described as "typical" AD.

We found individuals representing each of four subtype patterns in each of the five contributing cohorts, and we reproduced a very similar set of subtypes in a totally separate sample using a different radiotracer. In contrast to the notion of a typical pattern from which all others deviate, no subtype predominated, and most individuals were confidently assigned into one subtype pattern and were consistent over time. The limbic subtype was the most frequent, and presented with many qualities typically associated with AD: older, less educated, greater proportion of APOE4 carriers, strongly amnestic phenotype, and medial temporal pathology with a Braak-like progression of tau spread. However, this subtype represented only a third of all tau-positive cases in our dataset. We suggest instead that, at older onset ages, the subtypes may present with subtle differences that may be difficult to detect in the clinic, while at younger onset ages, the more aggressive phenotype can amplify the distinct subtype expressions. The existence of these phenotypes, if further validated, may necessitate a reform in pathological tau staging where key regions are surveyed to increase sensitivity to detect subtype-specific patterns.

Many pioneering studies have noted variation in AD as deviation from a typical expression pattern. For example, limbic-predominant and MTL-sparing phenotypes are contrasted against "typical" variants that express tau pathology in both the MTL and isocortex (Murray et al., 2011b; Whitwell et al., 2012). In contrast to this notion, we found individuals expressing both cortical and MTL tau to express a more aggressive phenotype with marked asymmetry, the latter feature something that has not been well characterized in histopathological studies of AD. In addition, our model allows the concurrence of MTL and cortical pathology at later stages of several

distinct progressions, perhaps suggesting that solely contrasting cortical and MTL tau (i.e. (Byun et al., 2015; Risacher et al., 2017; Whitwell et al., 2018; Ossenkoppele et al., 2019) may not be sufficient to describe AD heterogeneity. Indeed, while some spatial convergence could be observed in our AD subtypes, particularly at early or late stages, subtle regional variation consistently distinguishes individuals of one subtype from another (Shiino et al., 2006).

Our findings converge with many other supervised and unsupervised AD subtyping studies from the imaging and pathology literature. We characterized limbic-predominant and MTL-sparing phenotypes that demonstrated associations with age, APOE genotype and cognition, converging with previous studies (Murray et al., 2011b; Janocko et al., 2012; Whitwell et al., 2012; Byun et al., 2015; Risacher et al., 2017; Ossenkoppele et al., 2019; Jeon et al., 2019; Ferreira, Nordberg, and Westman, 2020). Notably, these associations were reduced when accounting for disease stage and other covariates, suggesting previously-noted associations may be somewhat confounded. We also characterized two additional subtypes that have been described less frequently. The lateral temporal phenotype resemble "rapid-progressive" AD (Drummond et al., 2017; Qiang et al., 2017) with its steep cognitive decline and rapid tau accumulation, but also lvPPA with its left-lateralized tau pattern and language deficits. The posterior phenotype bore some resemplance to PCA, but generally expressed a more mild phenotype with slower cognitive decline. However, the lack of detection of these subtypes in other studies may be a methodological issue. The occipital lobe is not typically considered to be an AD-vulnerable region and is not frequently sampled in autopsy studies, nor is hemispheric asymmetry consistently assessed in such studies. Several other studies have performed subtyping using a constrained set of regions, usually bilateral cortical and MTL ROIs, which would preclude discovery of posterior or lateralized phenotypes (Murray et al., 2011b; Whitwell et al., 2012; Byun et al., 2015; Risacher et al., 2017; Whitwell et al., 2018; Ossenkoppele et al., 2019). Meanwhile, spatially unbiased studies have described posterior or lateralized phenotypes (Badhwar et al., 2019). Furthermore, a recent study applied a Bayesian cross-decomposition algorithm to discover canonical associations between neurodegeneration (measured with both tau-PET and atrophy) and cognition. Along with an MTL memory factor, the analysis revealed a posterior cortical executive factor and a left temporal language factor, reminiscent of the subtypes described here (Sun et al., 2019). This analysis hints that such subtypes could be exaggerated expressions of latent pathological patterns endemic to AD, and perhaps driven by cognitive networks. The emergence of these phenotypes may also results from our larger samples, or from assessing spatiotemporal dynamics rather than only spatial dynamics.

We show a strong negative correlation between age and tau progression, reproducing previous reports (Marshall et al., 2007; Whitwell et al., 2019). Importantly, this is not to suggest tau is reducing with increased age – in contrast, we show significant advancement of tau pathology is detectable even after a year. Instead, our results suggest a younger age of onset is associated with a more rapid progression of tau pathology. Interestingly, this phenomenon was observable across all subtypes. Previous work has noted that early-onset AD (EOAD) is more likely to present with an atypical phenotype (Koedam et al., 2010). This may be a specific characteristic of EOAD. However, our data suggest that posterior or left-lateralized temporal binding are not uncommon across the age spectrum, but that they are more pronounced at earlier ages. Therefore, atypical variants of AD may represent an accelerated and intensified manifestation of common AD phenotypes, though this will require further validation. Explanations as to why early onset ages result in more aggressive phenotypes are scarce. It is possible that younger individuals have a healthier brain that is more efficient at accumulating or spreading pathology, though it should be noted that older mice exhibit a more aggressive spread of tau pathology than younger mice (Wegmann et al., 2019). Instead, the onset of pathology may be linked to the age-related deterioration of intrinsic properties that protect against pathological protein aggregation (Ciryam et al., 2015; Freer et al., 2016; Kundra et al., 2017). Reducing the efficiency of these (e.g. endosomal/lysosomal) systems through genetic susceptibility, for example, could lead to an earlier and accelerated phenotype as is observed in EOAD.

Other possible subtypes of AD pathology have been described, which we did not reproduce in our study. We did not find any evidence for "diffuse" or "minimal-atrophy" subtypes that have been reported in previous unsupervised subtyping studies (Ferreira, Nordberg, and Westman, 2020). Recent work suggests minimal-atrophy subtypes also display minimal tau pathology (Ossenkoppele et al., 2019), and such individuals would have been labeled S0 in our study. Meanwhile, diffuse subtypes likely represent either catch-all partitions, and/or MRI-specific phenotypes. In addition, variants of AD with prominent dysexecutive and/or behavioral impairments have been described (Dickerson and Wolk, 2011; Ossenkoppele et al., 2015d), sometimes referred to as "frontal AD". A supervised MRI analysis did not find strong evidence for increased frontal atrophy (Ossenkoppele et al., 2015d), nor did a semi-supervised MRI analysis reveal a frontal subtype (Ossenkoppele et al., 2019), though limited evidence may suggest elevated frontal tau-PET binding in such individuals (Ossenkoppele et al., 2016a; Dronse et al., 2017; Li et al., 2020). We did not find evidence for a frontal-predominant phenotype in our study. The MTL-sparing and lateral temporal phenotypes did exhibit elevated frontal binding compared to other

phenotypes. In addition, the lateral temporal subtype showed impaired executive function compared to other subtypes. However, our analysis was based solely on the spatiotemporal characteristics of tau-PET signal, independently of clinical measures. Cognitive subtypes of AD continue to be studied (Crane et al., 2017; Scheltens et al., 2017), though the link between pathological and cognitive subtypes may not be direct.

Our analysis of spatiotemporal variation of tau patterns in AD also produced some unexpected findings worth investigating. Despite the extreme of the posterior subtype being represented by PCA, an aggressive disease variant, the posterior subtype overall demonstrated spared cognition and slower cognitive decline compared to all other subtypes. These individuals exhibited considerable tau pathology in posterior (including occipital) brain regions, but also relatively less MTL and frontal binding. The relatively spared cognition could be due to a chance resistance to tau accumulation in regions important to cognitive maintenance, or perhaps the subtype exhibits a compensatory AD phenotype. Interestingly, the posterior subgroup was more highly educated, perhaps indicating a form of cognitive reserve (Stern, 2012). Future studies will be necessary to validate the existence and qualities of this posterior subtype. We also found that, while certain subtypes exhibited greater overall hemispheric asymmetry of tau-PET binding, aymmetry was common, and the degree of asymmetry increased in all subtypes with disease progression. This corroborates previous findings from both MRI (Derflinger et al., 2011; Sarica et al., 2018) and tau-PET (Chapter 3) studies. A full exploration of the clinical relevance of hemispheric asymmetry is out of scope for this study, though our preliminary findings suggest asymmetry may represent another, possibly orthogonal dimension of tau-PET heterogeneity. This is likely why we found inconsistent lateralization depending on sample composition.

Relatively little is known about subtypes of AD, including why they occur and how much they influence AD research. Different manifestations of AD may represent subtle variations in the spread of pathology, or could signal the influence of highly distinct processes. For example, a recent pathology study found increased NFT pathology and neuronal loss in the basal forebrain specifically in patients with a hippocampal-sparing phenotype, and that earlier disease onset was associated with more NFT pathology in these subjects (Hanna Al-Shaikh et al., 2020). This is interesting given that cholinergic treatments for AD are less effective in individuals with extensive limbic pathology (Connelly, Prentice, and Fowler, 2005). Furthermore, a recent study showed that a targeted basal forebrain treatment appeared most effective for patients with a hippocampal-sparing phenotype (Machado et al., 2020). This research may suggest a unique role of the basal forebrain in certain subtypes of

AD. Meanwhile, APOE has been consistently associated with limbic manifestations of AD (Flier et al., 2011; Murray et al., 2011b; Mattsson et al., 2018b; Therriault et al., 2019; Ferreira, Nordberg, and Westman, 2020), including the present study, and APOE- or hippocampus-based therapies could prove more effective for these individuals. Along similar lines, the proteomic content of hippocampal Aβ plaques differed substantially between rapidly progressive and typical variants of AD. The former expressed more neuron-related genes while the latter more astrocyte-related genes (Drummond et al., 2017), echoing results from our cell-type enrichment analysis. Together, these results point to the possibility that different AD subtypes may be characterized by distinct underlying physiology. Clinical trials may benefit from stratification or enrichment based on AD subtype, or at the very least post-hoc identification of within-subtype effects.

Subtypes can also be very useful in tracking disease progression. The formalization of tau accumulation into distinct stages (Braak et al., 2006) has great utility for tracking the evolution of underlying pathology, independent of clinical manifestation. However, we show that quite some variability in spatiotemporal accumulation exists, and previous tau-PET studies have noted larger lobar ROIs may capture disease progression better than Braak-stage ROIs (Schwarz et al., 2018). In our study, we find that subtype-specific ROIs are more sensitive to capturing longitudinal tau accumulation, and individual-specific ROIs are better still. Individuals appear to reliably accumulate tau along one of several specific subtype trajectories, allowing us to form individual-specific predictions of regions of future tau accumulation. These individual-tailored regions allow for a dynamic tracking based on the subtype and disease stage of an individual, and their superiority over other ROIs further validates the SuStaIn model. However, in terms of "stationary" ROIs, we found temporal lobe ROIs to perform well as sensitive biomarkers for tau accumulation, corroborating other studies (Jack et al., 2018a; Harrison et al., 2018). This may indicate prominence of dynamic tau accumulation in the temporal lobe in many variations and stages of AD. Finally, we found w-scoring to improve sensitivity over traditional SUVR measures, likely due to its region-specific adjustment for non-specific signal (Chapter 3). In all, using individual-tailored ROIs based on disease progression and subtype will likely improve power for clinical trials.

There are currently very few explanations as to why subtypes of AD manifest. Fascinating work has found PCA and lvPPA patients are more likely to exhibit learning disabilities in childhood (Rogalski et al., 2008; Miller et al., 2013; Miller et al., 2018), perhaps mediated by abnormalities during brain development (Miller et al., 2019). While lvPPA and PCA represent extremes along the AD continua, this points to the possibility that distinct subtypes may be influenced by regular variation

in cognitive development or other premorbid factors. Supporting this idea is the finding that the limbic-predominant phenotype in our study was less educated on average. While highly speculative, underdeveloped hippocampal function may be related to both lower likelihood of continuing education and a greater vulnerability to hippocampal dysfunction in late life. AD polygenic risk has been shown to influence hippocampal volume (Mormino et al., 2016; Foley et al., 2017), and individual differences in hippocampal vascular anatomy influence risk for cognitive impairment (Perosa et al., 2020). Another possible explanation for subtypes is interactions between post-translational tau modification and synaptic tau spreading. Several labs have shown that the regional pattern of pathological tau expression in mice is dependent on conformation and injection site of tau seeds (Clavaguera et al., 2013; Sanders et al., 2014; Guo et al., 2016a; Dujardin et al., 2018; He et al., 2020), though one study found the synaptic partners of the injection site to be most important (Narasimhan et al., 2017). It is therefore possible that subtypes of tau spread may simply be dictated by distinct tau conformations and/or systematic variation in the human connectome, perhaps at key synaptic junctures. Supporting the latter hypothesis, we found the tau-PET pattern of AD subtypes resembled macroscale neuronal networks seeded from different brain regions. These findings do not presuppose tau pathology necessarily starts in different regions, but instead that different regions may play a more prominent role in tau propagation across subtypes. This could be mediated by involvement of different neuronal cell subtypes. Recent work has begun to identify specific excitatory neuronal subtypes generally vulnerable to tau pathology (Fu et al., 2019; Peng, Trojanowski, and Lee, 2020), and our results suggest certain neuronal types may also be specifically implicated in different AD subtypes.

This study has a number of limitations that must be addressed. First, while the use of tau-PET imaging is a great improvement over using MRI to measure AD pathology, there is still discrepancy between tau-PET signal and true tau pathology (Lemoine et al., 2018; Leuzy et al., 2019). Other than binding to mature neurfibrillary tangles (Marquié et al., 2015; Lowe et al., 2016), off-target binding is an issue with flortaucipir, particularly in the striatum, white matter and choroid plexus (Baker et al., 2019). We did our best to mitigate this issue by regression of choroid plexus signal, exclusion of subcortical ROIs and non-AD dementia patients, and region-specific normalization against non-specific binding, but it is possible that our results could be influenced by off-target binding. By the same token, while the unbiased spatial sampling of tau-PET data across the brain aided our discovery of these subtype patterns, these subtypes must be validated using histopathology studies. Sample size was an obvious strength of our study, but comes with the caveat of mixing data from multiple cohorts and scanners. We addressed this issue somewhat by examining

subtypes in each cohort separately, replicating our results in a separate sample, and adjusting for cohort in some comparisons. In addition, despite our study boasting the largest tau-PET sample to date, even larger samples would be preferable in order to elucidate the spatiotemporal progression of each subtype in more detail. The unique spatiotemporal modeling approach of SuStaIn is one of the study's greatest strengths. However, there is still a great deal of uncertainty in our model, and large samples will be necessary to reduce that uncertainty.

In conclusion, we describe four distinct but internally stable spatiotemporal phenotypes of AD. These subtypes exhibit different clinical profiles and longitudinal outcomes, and leveraging subtype information improves prediction of future regional tau accumulation at the individual level. Our results call to question whether "typical" and "atypical" AD are quantifiable entities, rather suggesting that several AD subtypes exists, and that their individual differences are exacerbated by more aggressive phenotypes with younger onset ages. Future studies should seek to validate the existence and temporal evolution of these subtypes, as well as identify genetic, cellular and developmental factors that may influence their expression.

4.6 Methods

4.6.1 Sample Characteristics

The total sample for the following analyses comprised of flortaucipir tau-PET scans from 1667 individuals from five different cohorts (BioFINDER I, Seoul, AVID, UCSF, ADNI), and RO948 PET scans from 657 individuals from a sixth cohort (BioFINDER II). Information pertaining to recruitment, diagnostic criteria and β-amyloid positivity assessment for the BioFINDER I (BioF) (Ossenkoppele et al., 2018), ADNI (Vogel et al., 2019a), AVID (Pontecorvo et al., 2019), Seoul (Cho et al., 2018), UCSF (La Joie et al., 2020) and BioFINDER II (BF2) (Berron et al., 2020) cohorts have been previously reported. Informed written consent was provided for all participants or their designated caregiver, and all protocols were approved by each cohort's respective institutional ethical review board.

From this total sample of 1667, a subsample was derived including i) all cognitively unimpaired individuals older than 40 years; and ii) individuals who had both a diagnosis of MCI or AD, AND imaging or fluid evidence of brain β-amyloid pathology. All subjects with a primary diagnosis other than cognitively unimpaired, MCI or AD were excluded. This subsample, used for all subsequent analysis, comprised 1143 individuals. The same screening procedures were used to filter individuals

from BioFINDER II, reducing the samples size from 657 to 469. Characteristics of all samples, including inter-cohort differences, are detailed in Table 4.S1.

4.6.2 Image Acquisition and Preprocessing

Tau-PET data acquisition procedures for each cohort have been previously described (Ossenkoppele et al., 2018; Pontecorvo et al., 2019; Cho et al., 2018; La Joie et al., 2020; Vogel et al., 2019a). All tau-PET data were processed centrally in Lund by analysts blinded to demographic and clinical data, in a manner previously described (Ossenkoppele et al., 2018). Briefly, resampling procedures were used to harmonize image size and voxel dimension across sites. Each image underwent motion correction using AFNI's 3dvolreg (https://afni.nimh.nih.gov/), and individual PET volumes were averaged within-subject. Each subject's mean PET image next underwent rigid coregistration to it's respective skull-stripped native T1 image, and images were intensity normalized using an inferior cerebellar gray reference region, resulting in standardized update value ratio (SUVR) images. T1 images were processed using Freesurfer v6.0 (https://surfer.nmr.mgh.harvard.edu/), resulting in native space parcellations of each subject's brain using the Desikan-Killiany atlas (Desikan et al., 2006). These parcellations were used to extract mean SUVR values within different regions of interest (ROIs) for each subject in native space. For visualization purposes only, each image was spatially normalized to the MNI-ICBM152 template using Advanced Normalization Tools (ANTs; (https://stnava.github.io/ANTs/) and smoothed with an 8 mm FWHM Gaussian filter.

4.6.3 Subtype and Stage Inference

Typical efforts to perform data-driven subtyping of neuroimages in AD are limited by the confound of disease stage. In a sample spanning the AD spectrum from healthy to demented such as ours, disease progression represents the main source of variation in MR and PET images. Therefore, unless disease stage is somehow accounted for, most clustering algorithms will partition individuals based on their disease stage. This is not useful for parsing heterogenous patterns related to progression subtypes, which are theoretically orthogonal to disease progression itslf. The Subtype and Stage Inference (SuStaIn) (Young et al., 2018) algorithm surmounts this limitation by combining clustering with disease progression modeling. SuStaIn uses large cross-sectional imaging datasets to elucidate and model multiple spatiotemporal progression phenotypes. This model can then be used to infer not only the probability a given individual belongs to each spatiotemporal progression, but also where along that progression (i.e. at which stage) that individual is. The given disease "stage"

effectively represents an individual's progression through the unique sequence of abnormal events associated with their given subtype. SuStaIn has been previously used to parse different progression patterns among genetic variants of frontotemporal dementia (Young et al., 2018), as well as distinct longitudinal clinical patterns chronic obstructive pulmonary disorder (Young et al., 2020). Detailed formalization of SuStaIn has been published previously (Young et al., 2018).

SuStaIn models linear transition across discrete points along a progression of indices of severity (typically z-scores), separately across different ROIs. Input requires a subject x feature matrix where, in this case, features represent mean tau-PET signal within different ROIs. In addition, "severity scores", indicating different points along the natural progression of ROI severity, must be provided. Whereas the choice of ROI constrains the spatial dimensions along which individuals may vary, the severity scores instead constrain the temporal dimension of variation. The total number of features is therefore represented by the product of N ROIs by N ROI-specific severity scores. A balance must thus be struck between resolution in the spatial and temporal dimensions, with respect to overall sample size.

Our discovery sample boasts 1143 scans, but even given our inclusion criteria, we expect from previous work (Chapter 3) that the majority of individuals (50-60%) will have minimal tau binding (note that SuStaIn will automatically detect these individuals and exclude them from progression modeling). We therefore expect the modeling to be performed on a sample of closer to N 450-550. We therefore decided on ten different ROIs (spatial features), each with three severity scores (temporal dimension), totalling 30 features. Given an arbitrary rule of 10-20 observations per feature, 300-600 observations should provide sufficient power, and our sample size should therefore be sufficient.

For the ten spatial features, we opted for left and right lobar regions of interest: parietal, frontal, occipital, temporal and medial temporal lobe (MTL). This choice is justified as follows: i) previous imaging and pathology subtyping studies have revealed variation in AD pathology to often occur within specific lobes, e.g. limbic-predominant (MTL), MTL-sparing (parietal) (Murray et al., 2011b; Ferreira, Nordberg, and Westman, 2020), posterior cortical atrophy (occipital), logopenic aphasia (temporal) (Ossenkoppele et al., 2016a) and behavioral variant AD (perhaps frontal) (Ossenkoppele et al., 2015d); ii) hemispheric laterality in AD is understudied, perhaps due to pathological staining often occurring on single hemispheres. However, some laterality has been observed in AD clinical variants (i.e. logopenic aphasia (Ossenkoppele et al., 2016a)) and may point to differing phenotypes in typical AD (e.g. (Vogel et al., 2019b; Braak and Del Tredici, 2015); iii) These lobar regions maintain some orthogonality to disease progression, as multiple lobes are involved in Braak

stages IV - VI (Braak and Braak, 1991).

To define severity score cutoffs, we first sought to normalize SUVR values to account for regional differences in PET signal (due to nonuniformity of off-target binding, perfusion, etc. across the brain) (Chapter 3). Two-component Gaussian mixture models were used to define, for each ROI, a normal (Gaussian-shaped noise) and abnormal distribution. We then created tau W-scores (La Joie et al., 2012) by normalizing all values using the mean of the normal distribution. This procedure centered the w-score values on the normal distribution to allow for more interpretable values (i.e. 2=2 SDs from normal), and also accounted for region-specific differences in normal and abnormal SUVR distributions. Uniform values of w = 2, 5, 10 were arbitrarily chosen as severity score control points for all ROIs.

The number of subtypes (i.e. distinct spatiotemporal progressions) was determined through cross-validation. Separately for each k=1-5 subtypes, 10-fold cross-validation was performed where SuStaIn was fit to 90% of the data, and this model was used to evaluate sample likelihood for the 10% left-out subjects. k was chosen based on the metric of sample likelihood. Finally, SuStaIn was run on the whole sample with the selected k, and all individuals were assigned a subtype and stage. The proportion of individuals classified into each subtype was quantified, stratified by cohort. We additionally quantified the proportion of subjects that did not fall well into any subtype (no subtype probability >50%).

4.6.4 Post-hoc subtype correction

Manual inspection of subtype progressions suggested that the early stages of one subtype (S2: MTL-Sparing; see Results) were composed mostly of cognitively normal individuals with abnormally high off-target binding in the cortex, but little-to-no tau in AD regions, i.e. false (tau) positives. Specifically, these individuals showed binding solely in sensorimotor and frontal regions (regions where tau typically accumulates only in the latest stages of AD (Braak et al., 2006)). We used Gaussian mixture modeling across all individuals as described in (Chapter 3) to define the probability of abnormal tau-positivity in each of the left and right entorhinal cortex and precuneus, respectively. We then marked individuals who had <90% probability of tau in all four regions as low-probability tau individuals (T-). Next, we identified T- individuals in the MTL-Sparing subtype, finding 40.6% of this subtype was composed of this group, and all were classified as stage 5 (of 31) or below. Furthermore these individuals showed many other indications of being false (tau) positives: they had normal MMSE scores, were older, were less likely to be Aβ+ and less likely to be MCI or AD (Supplementary Fig 4.S1). We assume SuStaIn appended this specific group of T- individuals to the MTL-Sparing subtype because the individuals i) had

abnormally high tau in at least one ROI as per our calculations (even if that abnormal signal was not driven by pathology); ii) the abnormal tau was located in the isocortex inclusive of the parietal lobe; iii) these individuals had little-to-no binding in the MTL. As SuStaIn is an unsupervised algorithm, the pathological MTL-sparing phenotype became conflated with this specific profile of T- individuals. To correct this issue, we converted all T- individuals classified as MTL-sparing to Subtype 0 for all further analysis.

4.6.5 Visualization of subtype-specific tau-PET patterns

To visualize tau-PET patterns for each subtype, we calculated the mean tau w-score for each Desikan-Killiany (DKT) atlas ROI. To visualize the progression of the subtype pattern across SuStaIn stages, for each subtype, we created mean images for all individuals falling into the following SuStaIn stage bins: 2-7, 7-11, 12-16, 17-21, 22-26. To deduce regions with relatively greater or less tau signal for each subtype, we created region-wise one-vs-all ordinary least squares (OLS) linear models comparing regional tau in one subtype to all others. This analysis was performed to visualize subtype models inferred by SuStaIn using individual data, and to explore differences between subtypes. Each model included ROI tau w-scores as the dependent variable, a one-hot dummy variable representing membership in the reference subtype, and SuStaIn stage as a covariate. These models were FDR-corrected for the number of comparisons (i.e. number of ROIs).

4.6.6 Subtype Characterization

Several demographic, cognitive and genetic variables were available for nearly all individuals across the five cohorts in our main (discovery) cohort. These variables included clinical diagnosis (100%), age (99.8%), sex (100%), years of education (97.1%), mini-mental state examination (MMSE) score (Folstein, Folstein, and McHugh, 1975) (97.7%) and APOE4 allele carriage (89.5%). In addition, most individuals underwent extensive cohort-specific cognitive batteries assessing multiple domains of cognition. In order to utilize this rich cognitive data, we created cognitive domains scores separately within each cohort by taking the mean of several z-scored tests within the following cognitive domains: memory, executive function, language and visuospatial function. Supplemental Table 4.S6 indicates which cognitive tests were used in each cognitive domain score across each cohort. These z-scored domain scores were then aggregated across all cohorts to maximize the sample size available for cognitive tests: memory (86.6%), language (81.3%), executive function (85.5%), visuospatial function (82.0%). While aggregating scores of different composition across cohorts of

different composition presents a suboptimal solution, we rest on sample sizes and statistical correction helping to overcome these limitations.

Subtypes were statistically compared to one another, and to tau-negative individuals, in order to determine subtype-specific characteristics. These analyses compared age, sex, education, APOE4 carriage, MMSE, the four cognitive domain scores, total tau, and total tau asymmetry. This process involved three steps: 1) Comparison to tau-negative individuals: Tau-negative individuals were those characterized as "Subtype 0" by SuStaIn, i.e. those individuals that did not demonstrate any abnormal tau events. An OLS linear model was fit with each variable described above as the dependent variable, and with dummy-coded subtype entered as the independent variable (with S0 as the reference subtype). Model t and p-values were stored for each model and the latter were FDR-corrected. This process was then repeated covarying for age, sex, education, clinical status (CN, MCI, AD) and cohort. 2) Comparison between subtypes. A one-vs-all approach was applied to subtyped individuals only to assess how different tau-progression subtypes differed from one another. Separately for each subtype, models were fit for each variable with a single dummy variable entered indicating membership to that subtype. T and p values were stored, and the latter was corrected for the number of variables assessed. This process was then repeated, adjusting for SuStaIn stage, and was repeated once again additionally controlling for age, sex, education and clinical status. 3) Finally, each subtype was compared directly to each other subtype (i.e. one-vs-one comparison). OLS models were fit with dummy coded subtype variables as the dependent variable, cycling each subtype as the reference subtype. T and p values for each of these models were stored, and the latter was FDR-corrected for number of comparisons (i.e. number of dependent variables). This process was repeated controlling for SuStaIn stage, and again for demographics, clinical status and cohort. Note that these processes were repeated using different covariates due to the profound differences between cohorts. Controlling for SuStaIn stage effectively corrects for total tau burden. Meanwhile, cohort cannot be used as a covariate without additionally controlling for other variables that differ across cohort, but these models add nine additional parameters to the model, affecting degrees of freedom. We therefore report results form all three models to understand how results change with different covariates.

We also assessed the relationship between SuStaIn stage and two variables: age and global cognition (MMSE). For these analyses, stage was correlated with age and global cognition, and the results were visualized across the whole sample and also stratified by subtype. As a posthoc analysis, we separated individuals into different age groups: 65 or younger, 66-79 and 80 or older. We then reassessed age by SuStaIn stage correlations within each of these age groups.

Longitudinal MMSE data was also available for individuals from all cohorts except UCSF, totalling 697 individuals with at least two timepoints. 188 individuals had an additional third timepoint, 28 had a fourth, and 3 had a fifth. Linear mixed effect models were used to assess difference in longitudinal MMSE change between subtypes. All models were fit using the lme4 library in R, using type-III sum of squares, unstructured covariance matrices, and Satterthwaite's approximation to calculate the demonimator degrees of freedom for p-values. Models featured MMSE measurements as the dependent variable, interactions between time from baseline and dummy coded subtype variables as the independent variables of interest (cycling the reference subtype), subject ID as a random effect (allowing for random intercepts and slopes), and age, sex, education and dummy coded variables for MCI and AD as covariates of no interest. Results were repeated additionally controlling for (dummy coded) cohort.

4.6.7 Replication Analysis

While the five cohorts from the main discovery sample all use flortaucipir as the tau-PET tracer, a sixth cohort (BioFINDER II; BF2) was available that instead used the RO948 radiotracer. While the two tracers have highly similar results, RO948 tends to have less off-target binding in the basal ganglia and better MTL signal, but frequently boasts high meningeal signal that can affect cortical SUVR measurement (Smith et al., 2020). Because of these differences, we opted to leave BF2 out of the discovery sample, and instead use it as a replication cohort. This strategy allowed us to not only evaluate the stability of the subtypes in a new cohort, but also allowed us to evaluate whether the subtypes are robust to tau-PET radiotracer.

We reran SuStaIn *de novo* in the BF2 sample, using identical prodecures to those described above (Section 4.6.3), although using the discovery sample to inform the number of subtypes. The resulting subtypes were compared visually, but quantitative comparisons involved spatial correlations. Specifically, mean within-subtype w-scores were computed for each ROI, and each discovery subtype ROI-vector was correlated to each replication (BF2) subtype ROI-vector. To account for whether different sample sizes contribute to differing results between the discovery and replication datasets, we performed a split-half analysis with the discovery sample. Specifically, we split the discovery sample in half and ran SuStaIn separately on each half, once again using the original discovery sample to inform the number of subtypes. We then compared each half, which had a sample size comparable to that of BF2, to the BF2 samples using spatial correlations.

4.6.8 Assessment of Longitudinal Stability

The SuStaIn framework lends itself to forecasting of future regional tau deposition. Longitudinal PET data was available for individuals across all cohorts except for UCSF, totaling 519 individuals with at least two time points. These longitudinal scans were used to validate the stability of subtypes over time, under the hypothesis that individuals should remain the same subtype, but should advance (or remain stable) in SuStaIn stage over time. ROIs for the longitudinal datasets were w-scored as described above (Section 4.6.3, but using the cross-sectional cohort as the cohort for normalization. The SuStaIn model fitted to the cross-sectional dataset was used to infer subtype and stage of longitudinal data (all timepoints). Confusion matrices were built to assess subtype stability between baseline and first follow-up. Stability was calculated as proportion of individuals classified as the same subtype at follow-up, compared to the total number of individuals. Stability was also calculated excluding individuals at Stage 0 at baseline or follow-up. We also assessed the influence of subtype probability (i.e. the probability a subject falls into their given subtype) on individual subtype stability. Specifically, we compared the subtype probability of stable individuals to unstable individuals. We additionally calculated overall model stability after excluding individuals using various subtype probability thresholds.

Subtype progression was assessed by observing change in SuStaIn stage over time in stable individuals. We calculated the proportion of individuals who advanced, were stable, or regressed in disease stage over time, before and after accounting for model uncertainty. Specifically, while stages are generally characterized by advancing abnormality in a given region, uncertainty leads to certain stages being characterized by probabilities of progressing abnormalities in more than one region. Therefore, individuals who advanced or regressed to a stage with event probabilities overlapping with their previous stage were considered to be stable. We also calculated annual change in SuStaIn stage by dividing total change in SuStaIn stage by number of years between baseline and final available timepoint. We used one-sample t-test against 0 to assess whether significant change over time was observed across the whole sample, and within each subtype. We use ANOVAs and Tukey's posthoc tests to assess differences in annual change in stage across the different subtypes. We also correlate SuStaIn stage with change in stage over time, across the whole sample and within subtypes.

4.6.9 Individual-tailored regions for prediction of longitudinal progression

We tested whether the subtyping and staging information provided by SuStaIn could be used to predict the regions in which tau deposition will increase at follow-up. To do this we sought to generate a composite ROI for each individual that weights each region by the likelihood tau will increase in that area (i.e. each composite ROI is a vector of weights for each region). Four different methods of building this composite ROI were tested:

i) "tauishere": a control ROI that is created by aggregating all lobar regions with substantial tau accumulation (W>2) for a given individual (i.e. an individually tailored ROI that does not use SuStaIn information).

ii) "pred1": an ROI computed by evaluating the SuStaIn-predicted pattern of regional tau deposition at follow-up.

iii) "pred2": an ROI computed by adding the SuStaIn-predicted difference in tau deposition between baseline and follow-up to the pattern of regional tau deposition at baseline, where the SuStaIn-predicted difference is computed by calculating the difference between the SuStaIn-predicted pattern of regional tau deposition at baseline and the SuStaIn-predicted pattern of regional tau deposition at follow-up.

iv) "ch2": an ROI computed by calculating the difference between the SuStaIn-predicted pattern of regional tau deposition at baseline and the SuStaIn-predicted pattern of regional tau deposition at follow-up, i.e. the SuStaIn-predicted difference.

Specifically, we sought to predict an ROI, R, where each entry $r_{i,j}$ gives the weight of biomarker j in subject i, i.e. the likelihood that tau deposition will occur in that region at follow-up for a given individual. To do this we first sought to predict the rate of change of stage for each subtype c and stage k combination, $\delta_{c,k}$. We computed $\delta_{c,k}$ by simply staging each individual at baseline and follow-up and computing the average change in stage per year over each subtype and stage combination at baseline.

Using this average rate of change in SuStaIn stage $\delta_{c,k}$ we were then able to predict an individuals stage at follow-up $k_{i,\text{new}}$ given any stage at baseline k, as $k_{i,\text{new}} = k + \delta_{c,k} t_i$, where t_i is the time between follow-up visits in years.

We can then evaluate the SuStaIn-predicted pattern of regional tau deposition at baseline $Y_{i,j}$ as

$$Y_{i,j} = \sum_{c=1}^{C} \sum_{k=0}^{K} A_{j,c,k} P_{i,c,k},$$

or at follow-up $Z_{i,j}$ as

$$Z_{i,j} = \sum_{c=1}^{C} \sum_{k=0}^{K} A_{j,c,k_{i,\text{new}}} P_{i,c,k},$$

where $A_{j,c,k}$ is an 'archetype' indicating the expected amount of tau deposition for biomarker j at stage k of subtype c and $P_{i,c,k}$ is the probability subject i is at stage k of subtype c. The archetype $A_{j,c,k}$ is estimated probabilistically from the MCMC samples of uncertainty provided by the SuStaIn algorithm, giving an average archetypal pattern accounting for the uncertainty in the progression pattern of each subtype. This means that each SuStaIn-predicted pattern $Y_{i,j}$ accounts for both uncertainty in the progression pattern of each subtype as well as uncertainty in the subtype and stage of each individual.

The weighted vector for each ROI, R, is then computed as

i) "tauishere": $r_{i,j} = (X_{i,j} > 2)$

ii) "pred1": $r_{i,j} = Z_{i,j}$

iii) "pred2": $r_{i,j} = X_{i,j} + (Z_{i,j} - Y_{i,j})$

iv) "ch2": $r_{i,j} = Z_{i,j} - Y_{i,j}$

where $X_{i,j}$ is the w-score for each region in each subject at baseline.

We compare change over time in these individually tailored, weighted composite ROIs compare to change over time some more traditionally used brain regions in tau assessment: entorhinal cortex SUVR, inferior temporal lobe SUVR, whole-cortex SUVR, MTL w-score, temporal lobe w-score, parietal lobe w-score, whole-brain w-score, and SuStaIn stage. Annual change was calculated by finding the difference between first and last timepoint, and dividing by the time between scans. For each ROI, we then used a one-sample t-test to assess a) whether annual accumulation in each ROI was significantly different from 0, and b) the effect size. Higher effect sizes were considered to indicate increased power in detecting change in tau accumulation.

4.6.10 Epidemic spreading model

Perhaps the most prominent hypothesis of tau spread suggests tau oligomers spread directly from neuron to neuron through axonal connections (Mudher et al., 2017). Under this hypothesis, diverse but systematic variations in tau spreading may be driven by variability in macroscale connectivity or network organization. We test this idea by investigating whether a network diffusion model simulating tau spread through the human connectome can recapitulate the various subtype patterns discovered by SuStaIn. We have previously applied the epidemic spreading model (ESM) (Iturria-Medina et al., 2014) to tau-PET data, showing diffusion of an agent through human connectivity data (measured with diffusion imaging-based tractography) can

explain a majority of the variance of spatial tau patterns across a population of individuals along the AD spectrum (Chapter 3). We here conduct the exact same analysis separately for each subtype identified through SuStaIn. We further allow the ESM to identify regional epicenters separately for each subtype, under the hypothesis that different subtype patterns may be driven by prominence of different corticolimbic networks.

As described in (Chapter 3), each tau-PET ROI was converted to tau-positive probabilities using mixture modeling with five-fold cross-validation. These measures represent the probability that a given ROI exhibits tau in the abnormal range. Connectivity was measured from a dataset of 60 young healthy subjects from the CMU-60 DSI Template (Yeh and Tseng, 2011) (http://www.psy.cmu.edu/~coaxlab/data.html). Deterministic tractography was calculated for each individual by finding connections between ROIs using oritentation distribution functions, and connectivity was measured using the ACD metric (Iturria-Medina et al., 2007; Iturria-Medina et al., 2017). Images were assessed for quality and connectomes were averaged across all 60 individuals. For each subtype separately, the ESM was fitted across all individuals, cycling through the average of each left-right pair of cortical ROIs (including hippocampus and amygdala, 33 pairs in total) as the model epicenter. The best fitting epicenter was selected by finding the model with the minimum mean distance between model predicted and observed tau spatial pattern across subjects. Model accuracy was represented as the r^2 between the mean observed ROI-level tau-PET probabilities and mean predicted probabilities across subjects. For each subtype, we compared the r^2 of the model using the best-fitting epicenter to the r^2 of models using an entorhinal epicenter.

4.6.11 Transcriptomic profiling of subtypes

Another possible explanation for variable tau spreading patterns may be explained by variation in genetic vulnerability, expressed as susceptibility of distinct cell-types or gene expression networks. To test this hypothesis, we use transcriptomic data from the Allen Human Brain Atlas (Hawrylycz et al., 2012) to explore whether brain tissue preferentially vulnerable to certain subtypes are enriched for gene expression signals associated with certain cell-types and AD-vulnerable gene networks.

We first create subtype-specific maps representing voxelwise differences in tau-PET signal between each subtype and the average (tau-positive, i.e. subtyped) individual. First, all flortaucipir-PET images were spatially normalized to MNI-ICBM152 template space. Specifically, Advanced Normalization Tools (https://stnava.github.io/ANTs/) was used to normalize matched T1 images to template space, and the transformation

parameters were applied to the SUVR images, and an 8mm isotropic smoothing kernel was applied to all individuals. Next, the same w-scoring procedure as described above (Section 4.6.3) was applied voxelwise across all individuals, within a conservative cortical mask. A mean image was created across all subtyped individuals, and separate mean image were created for each subtype. Subtype-specific maps were created by subtracting each subtype-specific mean image from the global mean image.

The Allen Human Brain Atlas contains 3702 tissue samples extracted from the brains of six adult human donors. Each underwent microarray gene expression analysis using over 58,000 probes, encoding for over 20,000 genes. Acquisition and processing of this data are described in (Hawrylycz et al., 2012), while post-processing specific to these analyses has also been described in (**Vogel2020ASystems**), and using scripts that have been provided online (Vogel, 2019). Corrected MNI-space coordinates for each sample were downloaded from (Devenyi, 2018). Specifically, donor-specific signals were extracted from each probe separately, and tissue samples from all donors were used together. Tissue samples were excluded if falling outside of the conservative cortical mask applied to the subtype-specific tau, resulting in a total of 414 tissue samples. A 7x7x7 window was created around the MNI coordinate of each sample, and mean values within this window were extracted from each subtype-specific image (as in (**Vogel2020ASystems**)). This process resulted in, for each subtype, a vector of values representing subtype-unique tau signal around each tissue sample. Next, we compile ranked gene lists for each subtype by correlating sample-wise expression of each of the 58,692 probes with subtype-specific tau expression around that sample. We then isolated, for each subtype, the top 1% of whole-brain correlations between gene expression and subtype-specific tau expression. These lists were further reduced to only include unique genes (some genes are assessed with multiple probes).

We tested each subtype-specific gene list to see if these lists were enriched for genes associated with specific cell-types or cell-type specific, AD-vulnerable gene networks. For cell-type specific genes, we refer to the lists described in (Lake et al., 2018). The authors performed single-cell RNAseq analysis and identified genes enriched with 35 excitatory and inhibitory neuronal and neural support cell subtypes. For AD-associated gene networks, we refer to the ten genomic modules described in (Mathys et al., 2019). These modules represent gene sets showing altered expression in specific cell types in association with increasing AD pathology and cognitive decline. We assessed whether genes in these various sets (G) were enriched within our subtype-specific gene lists (S) using enrichment analysis. Enrichment was calculated as (b/n) / (B/N), where b is the number of genes in both G and S, n is the number

of genes in S, B is the number of genes in G, and N is the total number of possible genes in the Allen Brain Atlas dataset. Each enrichment analysis was supplemented with permutation testing, where b was represented as a set of random genes of size S. 1000 permutations were used to create a null distribution, which was used to create p-values. Note that, due to the number of permutations, p=0.001 represents the minimum possible p-value. Separately for each category and subtype, p-values were FDR-corrected for multiple comparisons (e.g. for number of cells or modules).

4.7 Supplementary Figures

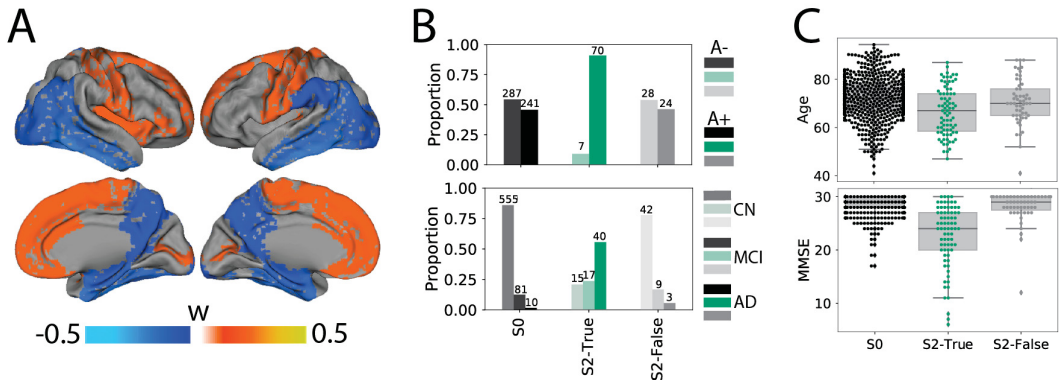

Supplementary Fig. 4.S1: Using methods described in section 4.6.4, several individuals classified as S2 (MTL-Sparing) were found to be tau-negative (i.e. no significant tau in the entorhinal cortex or precuneus). These individuals were classified as S2: False, and compared to other S2 individuals (S2: True) and tau-negative individuals (S0). A) Cortical rendering showing the overall mean tau-PET pattern (using w-scores, see section 4.6.3) of S2: False individuals. Tau-PET signal was observed in regions where pathological tau is not observed until late AD, namely somatomotor cortex, primary visual area, and various frontal lobe regions. Tau-PET signal was conspicuously absent in regions often associated with pathological tau burden, namely the MTL, precuneus, and temporo-parietal regions. B) Comparing the proportion of Aβ+ (top) and cognitively impaired (bottom) individuals in S2: False to S2: True and S0. Using, χ^2-tests with Tukey's posthoc multiple-comparisons correction, a higher proportion of S2: False and S0 individuals were Aβ- and cognitively impaired (ps < 0.0001) than S2: True individuals, but did not differ significantly from one another (ps > 0.05). C) Comparing age and MMSE across S0, S2: False and S2: True groups. Using ANOVAs with Tukey's posthoc correction, S0 and S2: False individuals were older and had higher MMSE scores than S2: True individuals, but did not differ from one another (ps > 0.05)

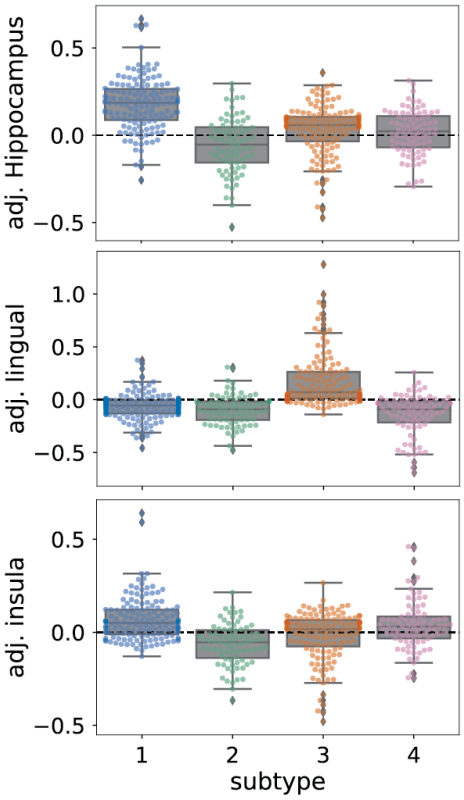

Supplementary Fig. 4.S2: Comparison of the mean tau-PET signal in three regions of contention, after adjustment for total cortical tau.

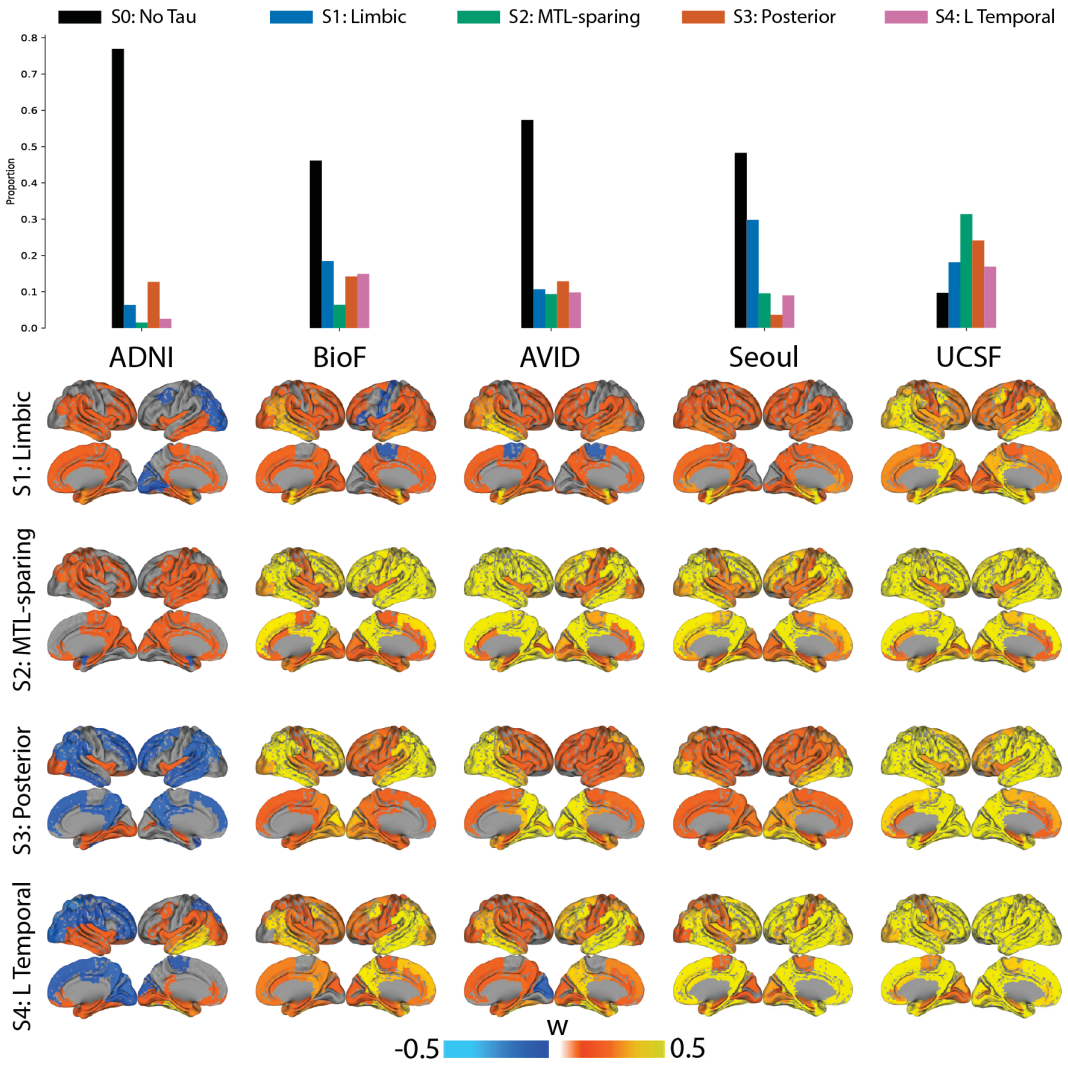

Supplementary Fig. 4.S3: The top Figure shows the proportions of each subtype (plus S0) within each of the five cohorts. All cohorts included individuals from each subtype. The bottom shows the mean tau W image of each subtypes in a given cohort. Variation can be observed across cohorts, particularly regarding phenotypic severity, but patterns are fairly consistent across subtypes.

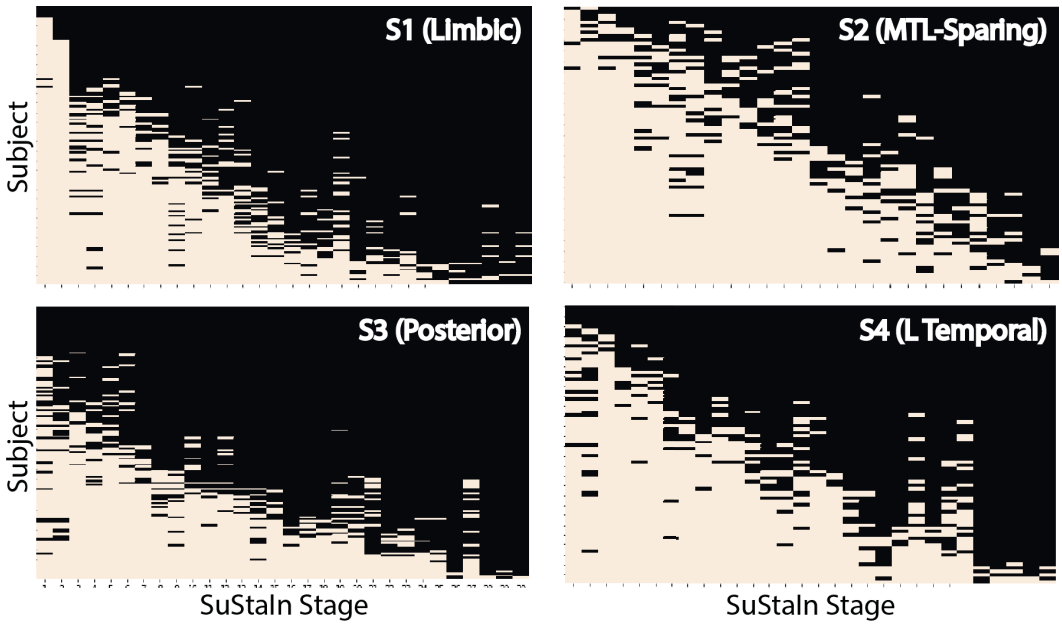

Supplementary Fig. 4.S4: A stepwise progression plot is shown for each subtype. Each row represents an individual, and each column represents a SuStaIn stage. A SuStaIn stage represents tau reaching a given severity (w) score (temporal) at a given region (spatial). Filled boxes indicate an individual fulfills the criteria for that SuStaIn stage. An empty box indicates an individual does not. A perfect fit would be represented by an individual (row) having every box filled before a given stage, and no boxes filled after it. The y-axis (subjects) are sorted from the least (top) to most (bottom) stages fulfilled. Across the population, this would be represented as a stepwise progression. Each subtype demonstrates a stepwise progression indicating good general fit. The average subject fit imperfection was 2.1 boxes.

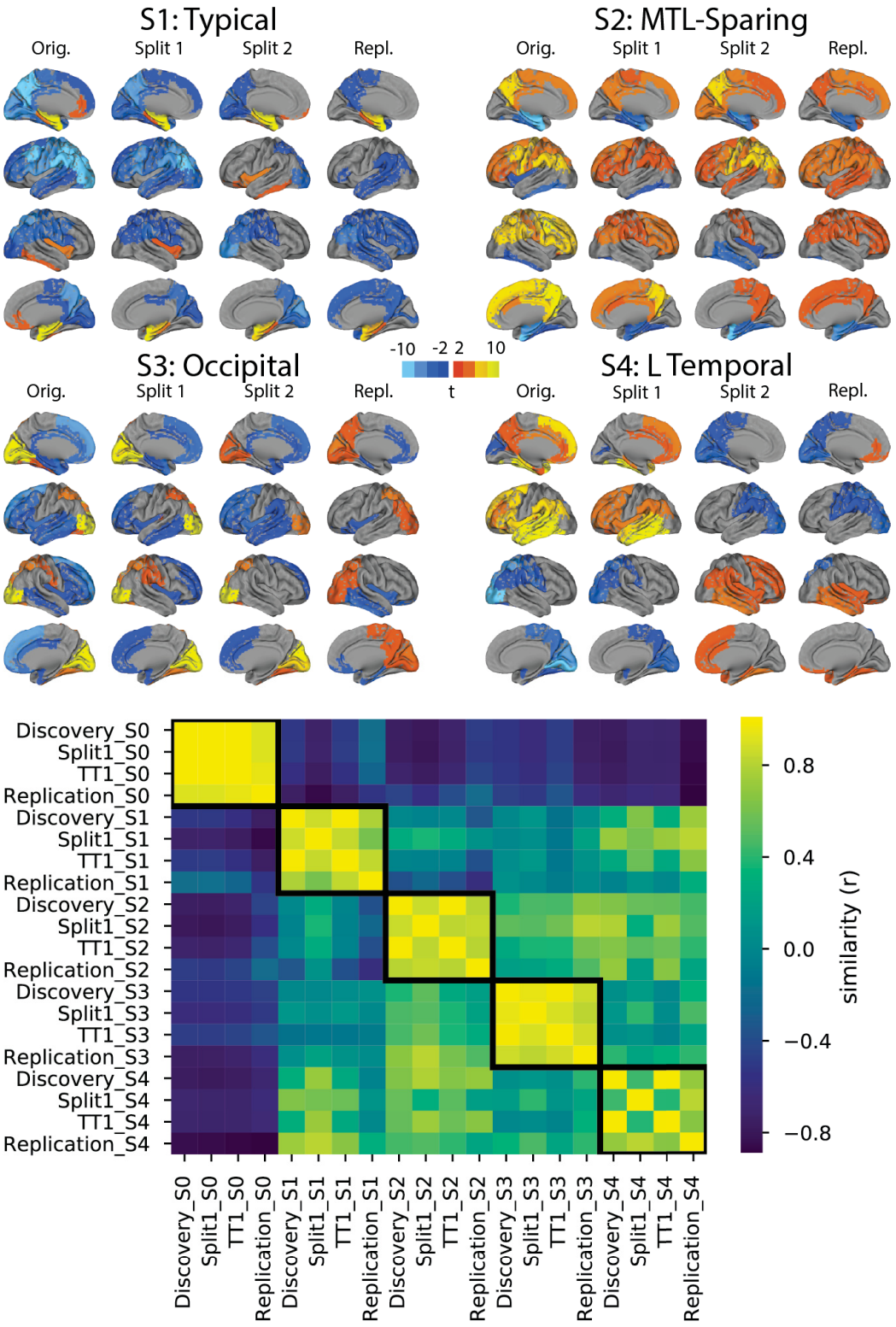

Supplementary Fig. 4.S5: (Top) Cortical renders showing, for each subtype across each dataset, regions with significantly different tau-PET signal compared to other within-dataset subtypes after FDR correction. Hot regions show greater tau-PET whereas cooler regions show lower signal. Remarkable similarity can be observed across subtypes, except S4, where lateralization switches from left to right. (Bottom) A heatmap showing similarity (spatial correlation) between subtypes across all four datasets. The diagonal represents the identity, whereas outlined boxes represent comparisons of the same subtype across cohorts.

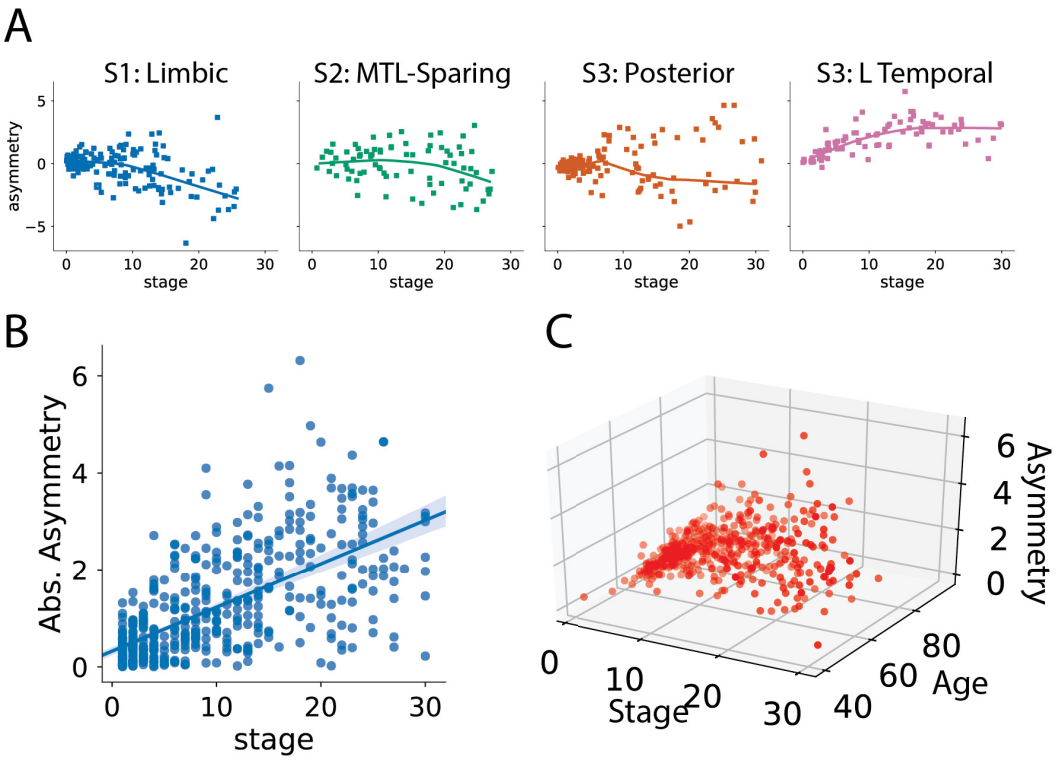

Supplementary Fig. 4.S6: A) Tau asymmetry was measured as the mean left to right ratio of in tau W scores for all ten tau features. Higher positive numbers represent greater left hemisphere tau asymmetry, whereas lower negative numbers represent greater right hemisphere asymmetry. The progression of asymmetry over SuStaIn stage was visualized for each subtype. Asymmetry generally increased with increasing SuStaIn stage. In some subtypes (particularly S2 and S3), strong asymmetry was seen in both hemispheres at later stages. B) The absolute (i.e. agnostic to hemisphere) asymmetry was visualized against SuStaIn stage, indicating a general increase in asymmetry with more severe tau spreading. C) A three-way relationship between Age, SuStaIn stage and absolute asymmetry is visualized, indicating these relationships covary but are independent of one another.

4.8 Supplementary Tables

	Discovery						Validation
	ADNI	**BioF**	**UCSF**	**Seoul**	**AVID**	**Total***	**BF2**
N	486	144	84	188	241	1143	467
Age	74.4 (7.4) [c,d]	72.4 (8.1) [c,d]	63.4 (8.7) [f]	69.2 (9.8) [f]	72.7 (9.1) [c,d]	72.1 (8.9)	69.0 (10.1) [g]
% Female	0.56	0.47 [d]	0.52	0.66 [b,e]	0.49 [d]	0.55	0.5
Education	16.6 (2.5) [b,d,e]	12.2 (3.6) [a,c,e]	17.0 (2.9) [b,d,e]	11.5 (4.9) [a,c,e]	15.4 (2.7) [f]	14.9 (3.8)	12.4 (3.9) [g]
% CN	0.84 [f]	0.46 [a,c,e]	0.05 [f]	0.48 [a,c,e]	0.58 [f]	0.62	0.4 [g]
% MCI	0.16 [e]	0.19	0.18	0.23	0.25	0.2	0.25 [g]
% AD	0.01 [f]	0.35 [a,c,e]	0.77 [f]	0.29 [a,c,e]	0.17 [f]	0.19	0.16
% Aβ+	0.58 [b,c]	0.8 [f]	0.96 [f]	0.57 [b,c]	0.6 [b,c]	0.65	0.56 [g]
% APOE4	0.35 [b,e]	0.59 [a,c,d]	0.42 [b]	0.35 [b,e]	0.48 [a,d]	0.41	0.51 [g]
% APOE4/4	0.05 [b]	0.18 [a,d,e]	0.12	0.08 [b]	0.08 [b]	0.08	0.06
MMSE	28.63 (2.21) [f]	25.67 (4.77) [a,c,e]	22.18 (5.65) [f]	24.75 (5.31) [a,c,e]	27.0 (3.7) [f]	26.85 (4.28)	26.32 (4.29) [g]
Total Tau	1.12 (0.1) [f]	1.27 (0.31) [a,c]	1.68 (0.38) [f]	1.28 (0.26) [a,c,e]	1.22 (0.25) [a,c,d]	1.23 (0.27)	1.16 (0.27) [g]
IT Tau	1.26 (0.2) [f]	1.62 (0.55) [f]	2.11 (0.6) [f]	1.43 (0.48) [a,b,c]	1.42 (0.43) [a,b,c]	1.43 (0.46)	1.44 (0.56)

Supplementary Table 4.S1: Significance testing assessing inter-cohort difference performed with one-way ANOVAs for scalar variables and χ^2 tests for categorical variables. P-values assessed with Tukey's posthoc tests.
* All variables exhibited significant inter-cohort differences.
[a] p<0.05 different from ADNI
[b] p<0.05 different from BioF
[c] p<0.05 different from UCSF
[d] p<0.05 different from Seoul
[e] p<0.05 different from AVID
[f] p<0.05 different from all other cohorts
[g] p<0.05 different from Discovery sample
CN = Cognitively Normal; MCI = Mild Cognitive Impairment; AD = Alzheimer's Disease; MMSE = Mini-mental State Examination; Aβ+ = β-amyloid positive; IT = Inferior temporal lobe

Cutoff	**N**	**Perc. Total**	**Stability**
None	191	100%	83.9
0.5	167	87%	86.8
0.6	163	85%	86.5
0.7	156	82%	86.8
0.8	149	75%	86.6
0.9	137	72%	88.3

Supplementary Table 4.S2: Longitudinal stability at different thresholds

Longitudinal stability of subtypes when only including individuals above different threholds of subtype probability (excluding individuals classified as S0.

	Limbic	MTL-Sparing	Posterior	L Temporal	Limbic	MTL-Sparing	Posterior	L Temporal
Age	0.06^{+}	$4.79E\text{-}06^{-}$	0.036^{+}	0.81	$2.04E\text{-}05^{+}$	0.39	0.00054^{+}	0.1
Education	$8.20E\text{-}07^{-}$	0.072^{+}	0.65	0.049^{-}	0.67	0.8	0.33	0.2
MMSE	$9.60E\text{-}35^{-}$	$9.02E\text{-}36^{-}$	$4.59E\text{-}20^{-}$	$2.54E\text{-}45^{-}$	0.026^{-}	0.00084^{-}	0.0015^{-}	$2.34E\text{-}07^{-}$
Total Tau	$1.02E\text{-}47^{+}$	$8.23E\text{-}89^{+}$	$4.79E\text{-}55^{+}$	$1.01E\text{-}68^{+}$	$5.40E\text{-}21^{+}$	$1.70E\text{-}40^{+}$	$1.79E\text{-}35^{+}$	$1.59E\text{-}34^{+}$
Memory	$3.96E\text{-}37^{-}$	$6.70E\text{-}15^{-}$	$1.82E\text{-}23^{-}$	$5.14E\text{-}24^{-}$	$2.39E\text{-}08^{-}$	0.00011^{-}	$2.54E\text{-}08^{-}$	0.0004^{-}
Language	$7.40E\text{-}14^{-}$	$6.61E\text{-}06^{-}$	$1.49E\text{-}10^{-}$	$1.82E\text{-}25^{-}$	0.083^{-}	0.31	0.021^{-}	$9.61E\text{-}08^{-}$
Exec	$1.20E\text{-}12^{-}$	$4.87E\text{-}17^{-}$	$1.14E\text{-}06^{-}$	$1.11E\text{-}18^{-}$	0.13	$3.09E\text{-}06^{-}$	0.139	0.00032^{-}
Vis	$2.41E\text{-}06^{-}$	$2.36E\text{-}12^{-}$	$7.16E\text{-}10^{-}$	$4.65E\text{-}11^{-}$	0.36	$6.13E\text{-}05^{-}$	0.00013^{-}	0.0043^{-}
asymmetry	0.00035^{R}	0.1	0.3	$8.80E\text{-}61^{L}$	0.0003^{R}	0.081^{R}	0.36	$6.96E\text{-}46^{L}$
Sex	0.004^{F}	0.1	0.17	0.84	$4.63E\text{-}05^{F}$	0.042^{F}	0.0043^{F}	0.156
APOE4	$1.72E\text{-}13^{+}$	0.077^{+}	$1.26E\text{-}05^{+}$	$8.58E\text{-}06^{+}$	$8.03E\text{-}09^{+}$	0.43	0.00094^{+}	0.0063^{+}

Supplementary Table 4.S3: P-values representing significant differences between a subtype and S0 individuals for a given variable, after correction for multiple comparisons. The left table includes the original models, and the right table is adjusted for age (except in the case of age), sex (except in the case of sex), education (except in the case of education), cohort, and clinical diagnosis (i.e. CN, MCI, AD).
MMSE = Mini-Mental State Examination; Exec = Executive Function; Vis = Visuospatial Function; APOE4 = APOE4 carrier status
$^{+}$ Significantly higher in this subtype compared to S0
$^{-}$ Significantly lower in this subtype compared to S0
^{R} Significant right-sided asymmetry in this subtype compared to others
^{L} Significant left-sides asymmetry in this subtype compared to S0.
^{F} Significantly more women compared to S0

	Age	Edu	MMSE	Tot. Tau	Mem	Lang	Exec	Vis	Asym	Sex	APOE4
S1 (Limbic)	0.05^{+}	0.0071^{-}	0.47	0.0011^{-}	0.17	0.49	0.36	0.059^{+}	$5.76E\text{-}05^{R}$	0.17	0.019^{+}
S2 (MTL-Sparing)	$8.41E\text{-}07^{-}$	0.96	0.071^{-}	$3.95E\text{-}06^{+}$	0.43	0.28	0.044^{-}	0.11	0.053^{R}	0.75	0.034^{-}
S3 (Posterior)	0.034^{+}	0.0041^{+}	0.003^{+}	0.045^{-}	0.15	0.13	0.019^{+}	0.88	0.04^{R}	0.77	0.43
S4 (L Temporal)	0.72	0.9	0.0071^{-}	0.044^{+}	0.43	$5.33E\text{-}05^{-}$	0.044^{-}	0.36	$3.29E\text{-}27^{L}$	0.11	0.87
S1 (Limbic)	0.59	0.0065^{-}	0.65	$5.90E\text{-}05^{-}$	0.072^{-}	0.75	0.75	0.18	$5.90E\text{-}05^{R}$	0.19	0.025^{+}
S2 (MTL-Sparing)	0.0065^{-}	0.92	0.59	0.43	0.11	0.085+	0.65	0.75	0.084^{-}	0.81	0.039^{-}
S3 (Posterior)	0.37	0.0065^{+}	0.072^{+}	0.54	0.43	0.37	0.22	0.39	0.04^{R}	0.81	0.5
S4 (L Temporal)	0.75	0.92	0.039^{-}	0.0065^{+}	0.75	0.0002^{-}	0.19	0.81	$1.39E\text{-}27^{L}$	0.13	0.83
S1 (Limbic)	0.58	0.82	0.58	0.00063^{-}	0.46	0.39	0.6	0.148	$1.23E\text{-}06^{R}$	0.39	0.014^{+}
S2 (MTL-Sparing)	0.016^{-}	0.78	0.88	0.88	0.82	0.6	0.32	0.54	0.0641^{R}	0.82	0.034^{-}
S3 (Posterior)	0.39	0.83	0.78	0.95	0.88	0.54	0.39	0.5	0.26	0.9	0.76
S4 (L Temporal)	0.93	0.78	0.15	$7.99E\text{-}06^{+}$	0.46	0.00087^{-}	0.54	0.88	$1.06E\text{-}27^{L}$	0.39	0.88

Supplementary Table 4.S4: P-values representing significant differences between one subtype and all other subtypes for a given variable, after correction for multiple comparisons. The top table includes the original models, the middle table is corrected for SuStaIn stage, and the bottom table is additionally corrected for age (except in the case of age), sex (except in the case of sex), education (except in the case of education), cohort and clinical diagnosis (i.e. CN, MCI, AD).
Edu = Education; MMSE = Mini-Mental State Examination; Tot. Tau = Total Tau; Mem = Memory; Lang = Language; Exec = Executive Function; Vis = Visuospatial Function; Asym = Tau Asymmetry; APOE4 = APOE4 carrier status
$^{+}$ Significantly higher in this subtype compared to other subtypes
$^{-}$ Significantly lower in this subtype compared to other subtypes
^{R} Significant right-sided asymmetry in this subtype compared to others
^{L} Significant left-sides asymmetry in this subtype compared to other subtypes.

Subtype	N	Progressed	Stable	Regressed
All	153	53.8%	27.6%	18.6
S1 (Limbic)	58	50.0%	36.7%	13.3%
S2 (MTL-Sparing)	42	47.6%	19.0%	33.3%
S3 (Posterior)	32	57.6%	21.2%	21.2%
S4 (L Temporal)	21	71.4%	28.6%	0.0%

Subtype	N	Progressed	Stable	Regressed
All	153	37.9%	51.0%	11.1%
S1 (Limbic)	58	36.2%	53.4%	10.3%
S2 (MTL-Sparing)	42	33.3%	47.6%	19.0%
S3 (Posterior)	32	46.9%	43.8%	9.4%
S4 (L Temporal)	21	38.1%	61.9%	0.0%

Supplementary Table 4.S5: Proportion of individuals progressing, regressing and remaining stable in SuStaIn stage, before (top) and after (bottom) accounting for model uncertainty

	Memory	**Executive**	**Language**	**Visuospatial**
ADNI	Logical Memory Total Logical Memory Delayed Recall RAVLT Immediate Recall RAVLT Delayed Recall	DigitSpan Backward DigitSpan Forward Digit Symbol Trails A Trails B	BNT Total Category Fluency: Animals Category Fluency: Vegetables Multilingual Naming Test	Clock Draw Figure Drawing
BioF	ADAS Delayed Recall	AQT Cognitive Speed Letter Fluency: S Trails A Stroop Correct	ADAS Naming Objects Category Fluency: Animals	Clock Drawing Cube
AVID	Clock Draw Recall WMS Immediate Recall WMS Delayed Recall	DigitSpan Backward DigitSpan Forward Digit Symbol Trails A Trails B	ANART BNT Total Category Fluency: Animals	Benton JoLO Clock Draw Copy
Seoul	Modified RFC Delayed Recall SVLT Delay	Digit Symbol Letter Fluency	BNT Total	Modified RFC
UCSF	CVLT Correct Total CVLT Delayed Recall Modified RFC Delayed Recall	Abstract Reasoning Test DigitSpan Backward DigitSpan Forward Letter Fluency Modified Trails Stroop Correct	BNT Total Category Fluency: Animals Repetition test Syntax test Verbal Agility test	Dot Counting Fragmented Letters Modified RFC Number Location Object Decision

Supplementary Table 4.S6: ADAS = Alzheimer's Disease Assessment Scale; ANART = American National Adult Reading Test; AQT = A Quick Test (of); BNT = Boston Naming Test; CVLT = California Verbal Learning Test; JoLO = Judgement of Line Orientation; RAVLT = Rey Auditory Verbal Learning Test; RFC = Rey Figure Copy; SVLT = Seoul Verbal Learning Test; WMS = Wechsler Memory Scale;

References

Badhwar, AmanPreet et al. (2019). "A multiomics approach to heterogeneity in Alzheimer's disease: focused review and roadmap". In: *Brain*, pp. 1–17. ISSN: 0006-8950. DOI: 10.1093/brain/awz384.

Baker, Suzanne L et al. (2019). " Effect of off-target binding on 18 F-Flortaucipir variability in healthy controls across the lifespan ". In: *Journal of Nuclear Medicine*, jnumed.118.224113. ISSN: 0161-5505. DOI: 10.2967/jnumed.118.224113.

Bejanin, Alexandre et al. (Dec. 2017b). "Tau pathology and neurodegeneration contribute to cognitive impairment in Alzheimer's disease". In: *Brain* 140.12, pp. 3286–3300. ISSN: 0006-8950. DOI: 10.1093/brain/awx243. URL: https://watermark.silverchair.com/awx243.pdf?token=AQECAHi208BE49Ooan9kkhW_Ercy7Dm3ZL_9Cf3qfKAc485ysgAAAecwggHjBgkqhkiG9w0BBwagggHUMIIB0AIBADCCAckGCSqGSIb3DQEHATAeBgl3OjnBKCYybpS8fEAgEQgIIBmpY9paVgrJr248NQgNg8LAw6UHj7Y8NzZqCqEKPxMOE1DebS.

Berron, David et al. (Apr. 2020). "Medial temporal lobe connectivity and its associations with cognition in early Alzheimer's disease". In: *Brain*. ISSN: 0006-8950. DOI: 10.1093/brain/awaa068. URL: https://academic.oup.com/brain/advance-article/doi/10.1093/brain/awaa068/5816707.

Braak, H and E Braak (1991). "Neuropathological stageing of Alzheimer-related changes." In: *Acta neuropathologica* 82.4, pp. 239–59. ISSN: 0001-6322. URL: http://www.ncbi.nlm.nih.gov/pubmed/1759558.

Braak, Heiko and Kelly Del Tredici (2015). "The preclinical phase of the pathological process underlying sporadic Alzheimer's disease". In: *Brain* 138.10, pp. 2814–2833. ISSN: 14602156. DOI: 10.1093/brain/awv236.

Braak, Heiko et al. (2006). "Staging of Alzheimer disease-associated neurofibrillary pathology using paraffin sections and immunocytochemistry". In: *Acta Neuropathologica* 112.4, pp. 389–404. ISSN: 00016322. DOI: 10.1007/s00401-006-0127-z.

Byun, Min Soo et al. (2015). "Heterogeneity of regional brain atrophy patterns associated with distinct progression rates in Alzheimer's disease". In: *PLoS ONE* 10.11, pp. 1–16. ISSN: 19326203. DOI: 10.1371/journal.pone.0142756.

Cho, Hanna et al. (Aug. 2016a). "In vivo cortical spreading pattern of tau and amyloid in the Alzheimer disease spectrum". In: *Annals of Neurology* 80.2, pp. 247–258. ISSN: 03645134. DOI: 10.1002/ana.24711. URL: http://doi.wiley.com/10.1002/ana.24711.

Cho, Hanna et al. (Aug. 2018). "Predicted sequence of cortical tau and amyloid-β deposition in Alzheimer disease spectrum". In: *Neurobiology of Aging* 68.January 2015, pp. 76–84. ISSN: 01974580. DOI: 10.1016/j.neurobiolaging.2018.04.007.

URL: https://doi.org/10.1016/j.neurobiolaging.2018.04.007https://linkinghub.elsevier.com/retrieve/pii/S0197458018301295.

Ciryam, Prajwal et al. (Feb. 2015). "Supersaturation is a major driving force for protein aggregation in neurodegenerative diseases". In: *Trends in Pharmacological Sciences* 36.2, pp. 72–77. ISSN: 01656147. DOI: 10.1016/j.tips.2014.12.004. URL: https://linkinghub.elsevier.com/retrieve/pii/S016561471400217X.

Clavaguera, Florence et al. (2013). "Brain homogenates from human tauopathies induce tau inclusions in mouse brain". In: *Proceedings of the National Academy of Sciences* 110.23, pp. 9535–9540. ISSN: 0027-8424. DOI: 10.1073/pnas.1301175110. URL: http://www.pnas.org/lookup/doi/10.1073/pnas.1301175110.

Connelly, P. J., N. P. Prentice, and K. G. Fowler (2005). "Predicting the outcome of cholinesterase inhibitor treatment in Alzheimer's disease". In: *Journal of Neurology, Neurosurgery and Psychiatry* 76.3, pp. 320–324. ISSN: 00223050. DOI: 10.1136/jnnp.2004.043539.

Crane, Paul K. et al. (Dec. 2017). "Incidence of cognitively defined late-onset Alzheimer's dementia subgroups from a prospective cohort study". In: *Alzheimer's & Dementia* 13.12, pp. 1307–1316. ISSN: 15525260. DOI: 10.1016/j.jalz.2017.04.011. URL: http://dx.doi.org/10.1016/j.jalz.2017.04.011http://doi.wiley.com/10.1016/j.jalz.2017.04.011.

Crary, John F. et al. (2014). "Primary age-related tauopathy (PART): a common pathology associated with human aging". In: *Acta Neuropathologica* 128.6, pp. 755–766. ISSN: 14320533. DOI: 10.1007/s00401-014-1349-0.

Crutch, Sebastian J et al. (Feb. 2012). "Posterior cortical atrophy". In: *The Lancet Neurology* 11.2, pp. 170–178. ISSN: 14744422. DOI: 10.1016/S1474-4422(11)70289-7. URL: https://linkinghub.elsevier.com/retrieve/pii/S1474442211702897.

Derflinger, Sabine et al. (2011). "Grey-matter atrophy in Alzheimer's disease is asymmetric but not lateralized". In: *Journal of Alzheimer's Disease* 25.2, pp. 347–357. ISSN: 18758908. DOI: 10.3233/JAD-2011-110041.

Desikan, Rahul S. et al. (2006). "An automated labeling system for subdividing the human cerebral cortex on MRI scans into gyral based regions of interest". In: *NeuroImage* 31.3, pp. 968–980. ISSN: 10538119. DOI: 10.1016/j.neuroimage.2006.01.021.

Devenyi, Gabriel A (2018). "gdevenyi/AllenHumanGeneMNI: Nonlinear registration". In: *Dataset on Zenodo*. DOI: 10.5281/ZENODO.2483290. URL: https://doi.org/10.5281/zenodo.2483290.

Dickerson, B. C. and D. A. Wolk (Jan. 2011). "Dysexecutive versus amnesic phenotypes of very mild Alzheimer's disease are associated with distinct clinical, genetic and cortical thinning characteristics". In: *Journal of Neurology, Neurosurgery*

& Psychiatry 82.1, pp. 45–51. ISSN: 0022-3050. DOI: 10.1136/jnnp.2009.199505. URL: http://jnnp.bmj.com/cgi/doi/10.1136/jnnp.2009.199505.

Dong, Aoyan et al. (2017). "Heterogeneity of neuroanatomical patterns in prodromal Alzheimer's disease: links to cognition, progression and biomarkers". In: *Brain : a journal of neurology* 140.3, pp. 735–747. ISSN: 14602156. DOI: 10.1093/brain/aww319.

Dronse, Julian et al. (2017). "In vivo Patterns of Tau Pathology, Amyloid-β Burden, and Neuronal Dysfunction in Clinical Variants of Alzheimer's Disease". In: *Journal of Alzheimer's Disease* 55.2, pp. 465–471. ISSN: 18758908. DOI: 10.3233/JAD-160316.

Drummond, Eleanor et al. (2017). "Proteomic differences in amyloid plaques in rapidly progressive and sporadic Alzheimer's disease". In: *Acta Neuropathologica* 133.6, pp. 933–954. ISSN: 14320533. DOI: 10.1007/s00401-017-1691-0.

Dujardin, Simon et al. (2018). "Different tau species lead to heterogeneous tau pathology propagation and misfolding". In: *Acta neuropathologica communications* 6.1, p. 132. ISSN: 20515960. DOI: 10.1186/s40478-018-0637-7.

Ferreira, Daniel, Agneta Nordberg, and Eric Westman (2020). "Biological subtypes of Alzheimer's disease: a systematic review and meta-analysis". In: *Neurology* 0, under–review. DOI: 10.1212/WNL.0000000000009058.

Flier, Wiesje M. van der et al. (2011). "Early-onset versus late-onset Alzheimer's disease: The case of the missing APOE ϵ4 allele". In: *The Lancet Neurology* 10.3, pp. 280–288. ISSN: 14744422. DOI: 10.1016/S1474-4422(10)70306-9. URL: http://dx.doi.org/10.1016/S1474-4422(10)70306-9.

Foley, Sonya F. et al. (2017). "Multimodal Brain Imaging Reveals Structural Differences in Alzheimer's Disease Polygenic Risk Carriers: A Study in Healthy Young Adults". In: *Biological Psychiatry* 81.2, pp. 154–161. ISSN: 18732402. DOI: 10.1016/j.biopsych.2016.02.033. URL: http://dx.doi.org/10.1016/j.biopsych.2016.02.033.

Folstein, M F, Susan E Folstein, and Paul R McHugh (Nov. 1975). ""Mini-mental state". A practical method for grading the cognitive state of patients for the clinician." In: *Journal of psychiatric research* 12.3, pp. 189–98. ISSN: 0022-3956. DOI: 10.1016/0022-3956(75)90026-6. URL: http://dx.doi.org/10.1016/0022-3956(75)90026-6http://www.ncbi.nlm.nih.gov/pubmed/1202204.

Freer, Rosie et al. (2016). "A protein homeostasis signature in healthy brains recapitulates tissue vulnerability to Alzheimer ' s disease". In: August, pp. 1–8. ISSN: 2375-2548. DOI: 10.1126/sciadv.1600947.

Fu, Hongjun et al. (2019). "A tau homeostasis signature is linked with the cellular and regional vulnerability of excitatory neurons to tau pathology". In: *Nature*

Neuroscience 22.1, pp. 47–56. ISSN: 15461726. DOI: 10.1038/s41593-018-0298-7. URL: http://dx.doi.org/10.1038/s41593-018-0298-7.

Gordon, Brian A. et al. (2018). "Cross-sectional and longitudinal atrophy is preferentially associated with tau rather than amyloid β positron emission tomography pathology". In: *Alzheimer's and Dementia: Diagnosis, Assessment and Disease Monitoring* 10, pp. 245–252. ISSN: 23528729. DOI: 10.1016/j.dadm.2018.02.003.

Guo, Christine C et al. (May 2016a). "Network-selective vulnerability of the human cerebellum to Alzheimer's disease and frontotemporal dementia". In: *Brain* 139.5, pp. 1527–1538. ISSN: 0006-8950. DOI: 10.1093/brain/aww003. URL: https://academic.oup.com/brain/article-lookup/doi/10.1093/brain/aww003.

Hanna Al-Shaikh, Fadi S. et al. (2020). "Selective Vulnerability of the Nucleus Basalis of Meynert among Neuropathologic Subtypes of Alzheimer Disease". In: *JAMA Neurology* 77.2, pp. 225–233. ISSN: 21686157. DOI: 10.1001/jamaneurol.2019.3606.

Hardy, J. and D.J. Selkoe (July 2002). "The Amyloid Hypothesis of Alzheimer's Disease: Progress and Problems on the Road to Therapeutics". In: *Science* 297.5580, pp. 353–356. ISSN: 00368075. DOI: 10.1126/science.1072994. URL: https://www.sciencemag.org/lookup/doi/10.1126/science.1072994.

Harrison, Theresa M. et al. (2018). "Longitudinal tau accumulation and atrophy in aging and Alzheimer's disease". In: *Annals of Neurology*, pp. 229–240. ISSN: 00222380. DOI: 10.1002/ana.25406.

Hawrylycz, Michael J et al. (2012). "An anatomically comprehensive atlas of the adult human brain transcriptome." In: *Nature* 489.7416, pp. 391–9. ISSN: 1476-4687. DOI: 10.1038/nature11405. URL: http://dx.doi.org/10.1038/nature11405.

He, Zhuohao et al. (2020). "Transmission of tauopathy strains is independent of their isoform composition". In: *Nature Communications* 11.1. ISSN: 20411723. DOI: 10.1038/s41467-019-13787-x. URL: http://dx.doi.org/10.1038/s41467-019-13787-x.

Hedden, Trey et al. (2013). "Meta-analysis of amyloid-cognition relations in cognitively normal older adults". In: *Neurology* 80.14, pp. 1341–1348. ISSN: 00283878. DOI: 10.1212/WNL.0b013e31828ab35d.

Hurd, Michael D. et al. (2013). "Monetary Costs of Dementia in the United States". In: *New England Journal of Medicine* 368.14, pp. 1326–1334. ISSN: 0028-4793. DOI: 10.1056/NEJMsa1204629. URL: http://www.nejm.org/doi/10.1056/NEJMsa1204629.

Iturria-Medina, Y. et al. (2007). "Characterizing brain anatomical connections using diffusion weighted MRI and graph theory". In: *NeuroImage* 36.3, pp. 645–660. ISSN: 10538119. DOI: 10.1016/j.neuroimage.2007.02.012.

Iturria-Medina, Yasser et al. (2014). "Epidemic Spreading Model to Characterize Misfolded Proteins Propagation in Aging and Associated Neurodegenerative Disorders". In: *PLoS Computational Biology* 10.11. ISSN: 15537358. DOI: 10.1371/journal.pcbi.1003956.

Iturria-Medina, Yasser et al. (2017). "Multifactorial causal model of brain (dis)organization and therapeutic intervention: Application to Alzheimer's disease". In: *NeuroImage* 152.February, pp. 60–77. ISSN: 10959572. DOI: 10.1016/j.neuroimage.2017.02.058. URL: http://dx.doi.org/10.1016/j.neuroimage.2017.02.058.

Jack, Clifford R. and David M. Holtzman (2013). "Biomarker modeling of alzheimer's disease". In: *Neuron* 80.6, pp. 1347–1358. ISSN: 10974199. DOI: 10.1016/j.neuron.2013.12.003. URL: http://dx.doi.org/10.1016/j.neuron.2013.12.003.

Jack, Clifford R. et al. (2018a). "Longitudinal tau PET in ageing and Alzheimer's disease". In: *Brain* 141.5, pp. 1517–1528. ISSN: 14602156. DOI: 10.1093/brain/awy059.

Jadhav, Santosh et al. (2019). "A walk through tau therapeutic strategies". In: *Acta neuropathologica communications* 7.1, p. 22. ISSN: 20515960. DOI: 10.1186/s40478-019-0664-z.

Janocko, Nicholas J. et al. (2012). "Neuropathologically defined subtypes of Alzheimer's disease differ significantly from neurofibrillary tangle-predominant dementia". In: *Acta Neuropathologica* 124.5, pp. 681–692. ISSN: 00016322. DOI: 10.1007/s00401-012-1044-y.

Jansen, Willemijn J et al. (May 2015). "Prevalence of cerebral amyloid pathology in persons without dementia: a meta-analysis." In: *JAMA* 313.19, pp. 1924–38. ISSN: 1538-3598. DOI: 10.1001/jama.2015.4668. URL: http://dx.doi.org/10.1001/jama.2015.9719http://www.ncbi.nlm.nih.gov/pubmed/25988462http://www.pubmedcentral.nih.gov/articlerender.fcgi?artid=PMC4486209.

Jefferson-George, Kyra S. et al. (2017). "Cognitive decline associated with pathological burden in primary age-related tauopathy". In: *Alzheimer's and Dementia* 13.9, pp. 1048–1053. ISSN: 15525279. DOI: 10.1016/j.jalz.2017.01.028. URL: http://dx.doi.org/10.1016/j.jalz.2017.01.028.

Jeon, Seun et al. (2019). "Topographical heterogeneity of Alzheimer's disease based on MR imaging, tau PET, and amyloid PET". In: *Frontiers in Aging Neuroscience* 10.JUL, pp. 1–10. ISSN: 16634365. DOI: 10.3389/fnagi.2019.00211.

Koedam, Esther L.G.E. et al. (Mar. 2010). "Early-Versus Late-Onset Alzheimer's Disease: More than Age Alone". In: *Journal of Alzheimer's Disease* 19.4, pp. 1401–1408. ISSN: 18758908. DOI: 10.3233/JAD-2010-1337. URL: https://www.medra.org/servlet/aliasResolver?alias=iospress&doi=10.3233/JAD-2010-1337.

Kundra, Rishika et al. (2017). "Protein homeostasis of a metastable subproteome associated with Alzheimer's disease". In: *Proceedings of the National Academy of Sciences of the United States of America* 114.28, E5703–E5711. ISSN: 10916490. DOI: 10.1073/pnas.1618417114.

La Joie, R. et al. (2012). "Region-Specific Hierarchy between Atrophy, Hypometabolism, and -Amyloid (A) Load in Alzheimer's Disease Dementia". In: *Journal of Neuroscience* 32.46, pp. 16265–16273. ISSN: 0270-6474. DOI: 10.1523/JNEUROSCI.2170-12.2012. URL: http://www.jneurosci.org/cgi/doi/10.1523/JNEUROSCI.2170-12.2012.

La Joie, Renaud et al. (2020). "Prospective longitudinal atrophy in Alzheimer's disease correlates with the intensity and topography of baseline tau-PET." In: *Science translational medicine* 12.524, pp. 1–13. ISSN: 1946-6242. DOI: 10.1126/scitranslmed.aau5732. URL: http://www.ncbi.nlm.nih.gov/pubmed/31894103.

Lake, Blue B. et al. (2018). "Integrative single-cell analysis of transcriptional and epigenetic states in the human adult brain". In: *Nature Biotechnology* 36.1, pp. 70–80. ISSN: 15461696. DOI: 10.1038/nbt.4038. URL: http://dx.doi.org/10.1038/nbt.4038.

Lemoine, Laetitia et al. (2018). "Tau positron emission tomography imaging in tauopathies: The added hurdle of off-target binding". In: *Alzheimer's and Dementia: Diagnosis, Assessment and Disease Monitoring* 10, pp. 232–236. ISSN: 23528729. DOI: 10.1016/j.dadm.2018.01.007. URL: https://doi.org/10.1016/j.dadm.2018.01.007.

Leuzy, Antoine et al. (2019). "Tau PET imaging in neurodegenerative tauopathies—still a challenge". In: *Molecular Psychiatry* 24.8, pp. 1112–1134. ISSN: 14765578. DOI: 10.1038/s41380-018-0342-8.

Li, Cheng Hsuan et al. (2020). "Frontal variant of Alzheimer's disease with asymmetric presentation mimicking frontotemporal dementia: Case report and literature review". In: *Brain and Behavior* 10.3, pp. 1–9. ISSN: 21623279. DOI: 10.1002/brb3.1548.

Lowe, Val J. et al. (2016). "An autoradiographic evaluation of AV-1451 Tau PET in dementia". In: *Acta Neuropathologica Communications* 4.1, p. 58. ISSN: 2051-5960. DOI: 10.1186/s40478-016-0315-6. URL: http://actaneurocomms.biomedcentral.com/articles/10.1186/s40478-016-0315-6.

Maass, Anne et al. (2018b). "Entorhinal Tau Pathology , Episodic Memory Decline , and Neurodegeneration in Aging". In: *Journal of Neuroscience* 38.3, pp. 530–543. DOI: 10.1523/JNEUROSCI.2028-17.2017.

Machado, Alejandra et al. (2020). "The cholinergic system and treatment response in subtypes of Alzheimer's disease". In: *bioRxiv*. DOI: 10.1101/2020.01.23.

20018507. URL: http://adni.loni.usc.edu/wp-content/uploads/how_to_apply/ADNI_Acknowledgement_List.pdf.

Marquié, Marta et al. (Nov. 2015). "Validating novel tau positron emission tomography tracer [F-18]-AV-1451 (T807) on postmortem brain tissue." In: *Annals of neurology* 78.5, pp. 787–800. ISSN: 1531-8249. DOI: 10.1002/ana.24517. URL: http://www.ncbi.nlm.nih.gov/pubmed/26344059http://www.pubmedcentral.nih.gov/articlerender.fcgi?artid=PMC4900162.

Marshall, Gad A. et al. (2007). "Early-onset Alzheimer's disease is associated with greater pathologic burden". In: *Journal of Geriatric Psychiatry and Neurology* 20.1, pp. 29–33. ISSN: 08919887. DOI: 10.1177/0891988706297086.

Mathys, Hansruedi et al. (June 2019). "Single-cell transcriptomic analysis of Alzheimer's disease". In: *Nature* 570.7761, pp. 332–337. ISSN: 0028-0836. DOI: 10.1038/s41586-019-1195-2. URL: http://www.nature.com/articles/s41586-019-1195-2.

Mattsson, Niklas et al. (2018b). "Greater tau load and reduced cortical thickness in APOE ϵ4-negative Alzheimer's disease: a cohort study". In: *Alzheimer's Research and Therapy* 10.1, pp. 1–12. ISSN: 17589193. DOI: 10.1186/s13195-018-0403-x.

Mesulam, Marsel et al. (June 2008). "Alzheimer and frontotemporal pathology in subsets of primary progressive aphasia". In: *Annals of Neurology* 63.6, pp. 709–719. ISSN: 03645134. DOI: 10.1002/ana.21388. URL: https://www.ncbi.nlm.nih.gov/pmc/articles/PMC3624763/pdf/nihms412728.pdfhttp://doi.wiley.com/10.1002/ana.21388.

Miller, Zachary A. et al. (2013). "Handedness and language learning disability differentially distribute in progressive aphasia variants". In: *Brain* 136.11, pp. 3461–3473. ISSN: 14602156. DOI: 10.1093/brain/awt242.

Miller, Zachary A. et al. (2018). "Prevalence of mathematical and visuospatial learning disabilities in patients with posterior cortical atrophy". In: *JAMA Neurology* 75.6, pp. 728–737. ISSN: 21686149. DOI: 10.1001/jamaneurol.2018.0395.

Miller, Zachary A et al. (2019). "Cortical developmental abnormalities in logopenic variant primary progressive aphasia with dyslexia". In: *Brain Communications*, pp. 1–8. DOI: 10.1093/braincomms/fcz027.

Mormino, Elizabeth C. et al. (2016). "Polygenic risk of Alzheimer disease is associated with early- and late-life processes". In: *Neurology*, 10.1212/WNL.0000000000002922. ISSN: 0028-3878. DOI: 10.1212/WNL.0000000000002922.

Morris, John C et al. (2009). "PIB Imaging Predicts Progression from Cognitively Normal to Symptomatic Alzheimer's Disease". In: *Archives of Neurology* 66.12, pp. 1469–1475. DOI: 10.1001/archneurol.2009.269.PIB.

Mudher, Amrit et al. (2017). "What is the evidence that tau pathology spreads through prion-like propagation?" In: *Acta neuropathologica communications* 5.1, p. 99. ISSN: 20515960. DOI: 10.1186/s40478-017-0488-7.

Murray, Melissa E. et al. (Sept. 2011b). "Neuropathologically defined subtypes of Alzheimer's disease with distinct clinical characteristics: A retrospective study". In: *The Lancet Neurology* 10.9, pp. 785–796. ISSN: 14744422. DOI: 10.1016/S1474-4422(11)70156-9.

Narasimhan, Sneha et al. (2017). "Pathological tau strains from human brains recapitulate the diversity of tauopathies in nontransgenic mouse brain". In: *Journal of Neuroscience* 37.47, pp. 11406–11423. ISSN: 15292401. DOI: 10.1523/JNEUROSCI.1230-17.2017.

Nelson, Peter T. et al. (May 2012). "Correlation of Alzheimer Disease Neuropathologic Changes With Cognitive Status: A Review of the Literature". In: *Journal of Neuropathology & Experimental Neurology* 71.5, pp. 362–381. ISSN: 0022-3069. DOI: 10.1097/NEN.0b013e31825018f7. URL: https://academic.oup.com/jnen/article-lookup/doi/10.1097/NEN.0b013e31825018f7.

Noh, Young et al. (2014). "Anatomical heterogeneity of Alzheimer disease: based on cortical thickness on MRIs." In: *Neurology* 83.21, pp. 1936–44. ISSN: 1526-632X. DOI: 10.1212/WNL.0000000000001003. URL: http://www.ncbi.nlm.nih.gov/pubmed/25344382.

Ossenkoppele, Rik et al. (2015d). "The behavioural/dysexecutive variant of Alzheimer's disease: Clinical, neuroimaging and pathological features". In: *Brain* 138.9, pp. 2732–2749. ISSN: 14602156. DOI: 10.1093/brain/awv191.

Ossenkoppele, Rik et al. (2016a). "Tau PET patterns mirror clinical and neuroanatomical variability in Alzheimer's disease". In: *Brain* 139.5, pp. 1551–1567. ISSN: 14602156. DOI: 10.1093/brain/aww027. URL: http://brain.oxfordjournals.org/.

Ossenkoppele, Rik et al. (2018). "Discriminative accuracy of [18F]flortaucipir positron emission tomography for Alzheimer disease vs other neurodegenerative disorders". In: *JAMA - Journal of the American Medical Association* 320.11, pp. 1151–1162. ISSN: 15383598. DOI: 10.1001/jama.2018.12917.

Ossenkoppele, Rik et al. (2019). "Tau covariance patterns in Alzheimer's disease patients match intrinsic connectivity networks in the healthy brain". In: *NeuroImage: Clinical* 23.April, p. 101848. ISSN: 22131582. DOI: 10.1016/j.nicl.2019.101848. URL: https://doi.org/10.1016/j.nicl.2019.101848https://linkinghub.elsevier.com/retrieve/pii/S2213158219301986.

Peng, Chao, John Q Trojanowski, and Virginia M-Y Lee (2020). "Protein transmission in neurodegenerative disease." In: *Nature reviews. Neurology* 16.April, pp. 199–212.

ISSN: 1759-4766. DOI: 10.1038/s41582-020-0333-7. URL: http://www.ncbi.nlm.nih.gov/pubmed/32203399.

Perosa, Valentina et al. (2020). "Hippocampal vascular reserve associated with cognitive performance and hippocampal volume". In: *Brain : a journal of neurology* 143.2, pp. 622–634. ISSN: 14602156. DOI: 10.1093/brain/awz383.

Petersen, Cathrine et al. (2019). "Alzheimer's disease clinical variants show distinct regional patterns of neurofibrillary tangle accumulation". In: *Acta Neuropathologica* 138.4, pp. 597–612. ISSN: 14320533. DOI: 10.1007/s00401-019-02036-6. URL: https://doi.org/10.1007/s00401-019-02036-6.

Pontecorvo, Michael J. et al. (2019). "A multicentre longitudinal study of flortaucipir (18F) in normal ageing, mild cognitive impairment and Alzheimer's disease dementia". In: *Brain* 142.6, pp. 1723–1735. ISSN: 14602156. DOI: 10.1093/brain/awz090.

Prince, Martin et al. (2013). "The global prevalence of dementia: A systematic review and metaanalysis". In: *Alzheimer's and Dementia* 9.1, pp. 63–75. ISSN: 15525260. DOI: 10.1016/j.jalz.2012.11.007. URL: http://dx.doi.org/10.1016/j.jalz.2012.11.007.

Qiang, Wei et al. (2017). "Structural variation in amyloid-β fibrils from Alzheimer's disease clinical subtypes". In: *Nature* 541.7636, pp. 217–221. ISSN: 14764687. DOI: 10.1038/nature20814.

Risacher, Shannon L. et al. (2017). "Alzheimer disease brain atrophy subtypes are associated with cognition and rate of decline". In: *Neurology* 89.21, pp. 2176–2186. ISSN: 1526632X. DOI: 10.1212/WNL.0000000000004670.

Rogalski, Emily et al. (Feb. 2008). "Increased Frequency of Learning Disability in Patients With Primary Progressive Aphasia and Their First-Degree Relatives". In: *Archives of Neurology* 65.2, pp. 1–7. ISSN: 0003-9942. DOI: 10.1001/archneurol.2007.34. URL: http://archneur.jamanetwork.com/article.aspx?doi=10.1001/archneurol.2007.34.

Sanders, David W. et al. (2014). "Distinct tau prion strains propagate in cells and mice and define different tauopathies". In: *Neuron* 82.6, pp. 1271–1288. ISSN: 10974199. DOI: 10.1016/j.neuron.2014.04.047. URL: http://dx.doi.org/10.1016/j.neuron.2014.04.047.

Sarica, Alessia et al. (2018). "MRI asymmetry index of hippocampal subfields increases through the continuum from the mild cognitive impairment to the alzheimer's disease". In: *Frontiers in Neuroscience* 12.AUG, pp. 1–12. ISSN: 1662453X. DOI: 10.3389/fnins.2018.00576.

Scheltens, Nienke M.E. et al. (Nov. 2017). "Cognitive subtypes of probable Alzheimer's disease robustly identified in four cohorts". In: *Alzheimer's & Dementia* 13.11,

pp. 1226–1236. ISSN: 15525260. DOI: 10.1016/j.jalz.2017.03.002. URL: http://doi.wiley.com/10.1016/j.jalz.2017.03.002.

Scheltens, Philip and Kenneth Rockwood (2011). "How golden is the gold standard of neuropathology in dementia?" In: *Alzheimer's and Dementia* 7.4, pp. 486–489. ISSN: 15525260. DOI: 10.1016/j.jalz.2011.04.011. URL: http://dx.doi.org/10.1016/j.jalz.2011.04.011.

Schneider, Lon S et al. (2015). "Disease : an Appraisal From 1984 To 2014". In: 275.3, pp. 251–283. DOI: 10.1111/joim.12191.Clinical.

Schöll, Michael et al. (2016b). "PET Imaging of Tau Deposition in the Aging Human Brain". In: *Neuron* 89.5, pp. 971–982. ISSN: 10974199. DOI: 10.1016/j.neuron.2016.01.028.

Schwarz, Adam J. et al. (2016). "Regional profiles of the candidate tau PET ligand ¹⁸ F-AV-1451 recapitulate key features of Braak histopathological stages". In: *Brain*, aww023. ISSN: 0006-8950. DOI: 10.1093/brain/aww023. URL: http://www.brain.oxfordjournals.org/lookup/doi/10.1093/brain/aww023.

Schwarz, Adam J. et al. (2018). "Topographic staging of tau positron emission tomography images". In: *Alzheimer's and Dementia: Diagnosis, Assessment and Disease Monitoring* 10, pp. 221–231. ISSN: 23528729. DOI: 10.1016/j.dadm.2018.01.006.

Shiino, Akihiko et al. (2006). "Four subgroups of Alzheimer's disease based on patterns of atrophy using VBM and a unique pattern for early onset disease". In: *NeuroImage* 33.1, pp. 17–26. ISSN: 10538119. DOI: 10.1016/j.neuroimage.2006.06.010.

Smith, Ruben et al. (2020). "Head-to-head comparison of tau positron emission tomography tracers [18F]flortaucipir and [18F]RO948". In: *European Journal of Nuclear Medicine and Molecular Imaging* 47.2, pp. 342–354. ISSN: 16197089. DOI: 10.1007/s00259-019-04496-0. URL: http://dx.doi.org/10.1007/s00259-019-04496-0.

Sperling, Reisa A, Elizabeth Mormino, and Keith Johnson (2014). "The evolution of preclinical Alzheimer's disease: Implications for prevention trials". In: *Neuron* 84.3, pp. 608–622. ISSN: 00958301. DOI: 10.1016/j.neuron.2014.10.038.The.

Stern, Yaakov (2012). "Cognitive reserve in ageing and Alzheimer's disease". In: *The Lancet Neurology* 11.11, pp. 1006–1012. ISSN: 14744422. DOI: 10.1016/S1474-4422(12)70191-6. URL: http://dx.doi.org/10.1016/S1474-4422(12)70191-6.

Sun, N. et al. (2019). "Multi-modal latent factor exploration of atrophy, cognitive and tau heterogeneity in Alzheimer's disease". In: *NeuroImage* 201.July. ISSN: 10959572. DOI: 10.1016/j.neuroimage.2019.116043.

Tam, Angela et al. (2019). "A highly predictive signature of cognition and brain atrophy for progression to Alzheimer's dementia". In: *GigaScience* 8.5, pp. 1–16. ISSN: 2047217X. DOI: 10.1093/gigascience/giz055.

Teipel, Stefan J. et al. (2020). "In-vivo staging of regional amyloid deposition predicts functional conversion in the preclinical and prodromal phases of Alzheimer's disease". In: *Neurobiology of Aging*. ISSN: 01974580. DOI: 10.1016/j.neurobiolaging.2020.03.011. URL: http://dx.doi.org/10.1016/j.neurobiolaging.2020.03.011.

Therriault, Joseph et al. (2019). "Association of Apolipoprotein e 4 with Medial Temporal Tau Independent of Amyloid-β". In: *JAMA Neurology* 77.4, pp. 470–479. ISSN: 21686149. DOI: 10.1001/jamaneurol.2019.4421.

Villemagne, Victor L. et al. (2013). "Amyloid β deposition, neurodegeneration, and cognitive decline in sporadic Alzheimer's disease: A prospective cohort study". In: *The Lancet Neurology* 12.4, pp. 357–367. ISSN: 14744422. DOI: 10.1016/S1474-4422(13)70044-9. URL: http://dx.doi.org/10.1016/S1474-4422(13)70044-9.

Vogel, Jacob W. et al. (Feb. 2019a). "Data-driven approaches for tau-PET imaging biomarkers in Alzheimer's disease". In: *Human Brain Mapping* 40.2, pp. 638–651. ISSN: 10659471. DOI: 10.1002/hbm.24401. URL: http://doi.wiley.com/10.1002/hbm.24401.

Vogel, Jacob W et al. (2019b). "Spread of pathological tau proteins through communicating neurons in human Alzheimer's disease". In: *bioRxiv*, p. 555821. DOI: 10.1101/555821. URL: http://biorxiv.org/content/early/2019/05/30/555821.abstract.

Vogel, Jake (Oct. 2019). "illdopejake/Hippocampus_AP_Axis: Hippocampus_LongAxis_NComms". In: *Dataset on Zenodo*. DOI: 10.5281/ZENODO.3483837. URL: https://doi.org/10.5281/zenodo.3483837#.XaTyRzc2_-s.mendeley.

Warren, David E et al. (2017). "Surgically disconnected temporal pole exhibits resting functional connectivity with remote brain regions". In: *Biorxiv*. DOI: 10.1101/127571. URL: http://biorxiv.org/content/biorxiv/early/2017/04/15/127571.full.pdf.

Wegmann, Susanne et al. (2019). "Experimental evidence for the age dependence of tau protein spread in the brain". In: *Science Advances* 5.6. ISSN: 23752548. DOI: 10.1126/sciadv.aaw6404.

Whitwell, Jennifer L. et al. (2012). "Neuroimaging correlates of pathologically defined subtypes of Alzheimer's disease: A case-control study". In: *The Lancet Neurology* 11.10, pp. 868–877. ISSN: 14744422. DOI: 10.1016/S1474-4422(12)70200-4.

Whitwell, Jennifer L. et al. (2018). "[18F]AV-1451 clustering of entorhinal and cortical uptake in Alzheimer's disease". In: *Annals of Neurology* 83.2, pp. 248–257. ISSN: 15318249. DOI: 10.1002/ana.25142.

Whitwell, Jennifer L. et al. (2019). "The role of age on tau PET uptake and gray matter atrophy in atypical Alzheimer's disease". In: *Alzheimer's and Dementia* 15.5, pp. 675–685. ISSN: 15525279. DOI: 10.1016/j.jalz.2018.12.016. URL: https://doi.org/10.1016/j.jalz.2018.12.016.

Yeh, Fang Cheng and Wen Yih Isaac Tseng (2011). "NTU-90: A high angular resolution brain atlas constructed by q-space diffeomorphic reconstruction". In: *NeuroImage* 58.1, pp. 91–99. ISSN: 10538119. DOI: 10.1016/j.neuroimage.2011.06.021. URL: http://dx.doi.org/10.1016/j.neuroimage.2011.06.021.

Young, Alexandra L. et al. (Dec. 2018). "Uncovering the heterogeneity and temporal complexity of neurodegenerative diseases with Subtype and Stage Inference". In: *Nature Communications* 9.1, p. 4273. ISSN: 2041-1723. DOI: 10.1038/s41467-018-05892-0. URL: http://www.nature.com/articles/s41467-018-05892-0.

Young, Alexandra L. et al. (2020). "Disease Progression Modeling in Chronic Obstructive Pulmonary Disease". In: *American journal of respiratory and critical care medicine* 201.3, pp. 294–302. ISSN: 15354970. DOI: 10.1164/rccm.201908-1600OC.

Zhang, Xiuming et al. (2016). "Bayesian model reveals latent atrophy factors with dissociable cognitive trajectories in Alzheimer's disease". In: *Proceedings of the National Academy of Sciences* 113.42, E6535–E6544. ISSN: 0027-8424. DOI: 10.1073/pnas.1611073113. URL: http://www.pnas.org/lookup/doi/10.1073/pnas.1611073113.

Chapter 5

Discussion

5.1 Summary of findings

The main content of this thesis consisted of three studies aimed at better understanding the *in vivo* spatial distribution and accumulation of tau in the human brain. Chapter 2 conducted an unbiased assessment of patterns of tau deposition across the AD spectrum, and investigated whether these patterns were useful as biomarkers. Chapter 3 tested whether the observed distribution of tau-PET signal could be explained by the propagation of pathology from one epicienter through the brain via major neural communication pathways. Finally, Chapter 4 utilized a large and diverse sample to probe whether tau-PET data patterns could be better described by multiple spatiotemporal sequences, rather than a single sequence. Each of these studies used data-driven approaches to explore, explain or dissect the observed pattern of tau NFT pathology in the brain, without imposing assumptions or constraints based on previous literature.

Each of these studies validated previous findings, but each also added novel details and nuances to the overall knowledge-base. The first study found tau-PET data to naturally parse into some Braak-like structures, but noted marked distinctions particularly in isocortical (i.e. Stage V) regions. Specifically, tau-PET signal in temporoparietal regions exhibited distinct patterns from frontal regions across the AD spectrum. These data-driven regions of tau-PET covariance proved superior to regions derived based on Braak staging in tracking global cognition in a separate sample. The second study found that the global pattern of tau-PET distribution could be explained well by the propagation of a pathological agent from the entorhinal cortex through the macroscale brain connectome. The study further found that neither a high degree of tau pathology, nor the presence of Aβ, was necessary for the propagation model to explain the tau patterns. However, when present, regional Aβ

seemed to impact the pattern of spread beyond the constraints of the connectome. Finally, the third study suggested that, rather than a single sequence of regional tau accumulation explaining the observed patterns of tau expression, a model incorporating four spatiotemporal patterns fit the data better. These patterns were robust, and consistent with known variants of tau accumulation, but their expression was most distinct, severe and clinically relevant at younger ages.

5.1.1 Review of novel contributions to the field of AD research

The original work in this thesis began during an explosion of tau-PET literature, where similar analyses were being conducted contemporaneously by different laboratories. As a result, studies with similar aims and designs to the work described here have been published slightly before, alongside, or slightly after. This is beneficial in general to the AD research community, as it can help sort out common and reproducible findings from more idiosyncratic results that may require more scrutiny. The consequences of such a literature boom is that novelty and primacy are somewhat hard to come by, though the relevance of such qualities to scientific progress is debatable. However, in accordance with the regulations dictating the composition of this thesis, novel and original findings will be highlighted.

Analyses in Chapter 2 involved clustering the covariance of tau-PET data across a sample. The publication of this work (Figure 5.1A, Vogel et al., 2019a) was preempted by a study that executed a similar clustering analysis, though in a sample of cognitively unimpaired individuals (Sepulcre et al., 2017a). This study had a smaller sample to begin with (n=88) and, due to a split-half design, only used half of those participants in the clustering. The resulting partition was similar to the one described in Chapter 2, in that it produced, temporal, temporoparietal and primary sensory covariance networks (Figure 5.1B). However, the sensory structures formed separate clusters, and the boundaries of all clusters were fuzzier, less regionally-constrained and less Braak-like. Comparably, the analyses in Chapter 2 incorporated a more sophisticated approach into a dataset composing normal, MCI and AD subjects with considerably more tau-specific binding within the images. However, both studies to different degrees produced hypothesis-free tau covariance clusters that could be said to "look like Braak stages if you squint". The Sepulcre et al. paper also did not examine cognition, though two other studies using different data-driven approaches did, and produced results highly convergent with our own (Mishra et al., 2017; Maass et al., 2017) (Figure 5.1D,E). A number of other papers also examined the structure of tau-PET data in a data-driven fashion using independent-components analysis (e.g. Figure 5.1C), though each of these studies interestingly noted a resemblance

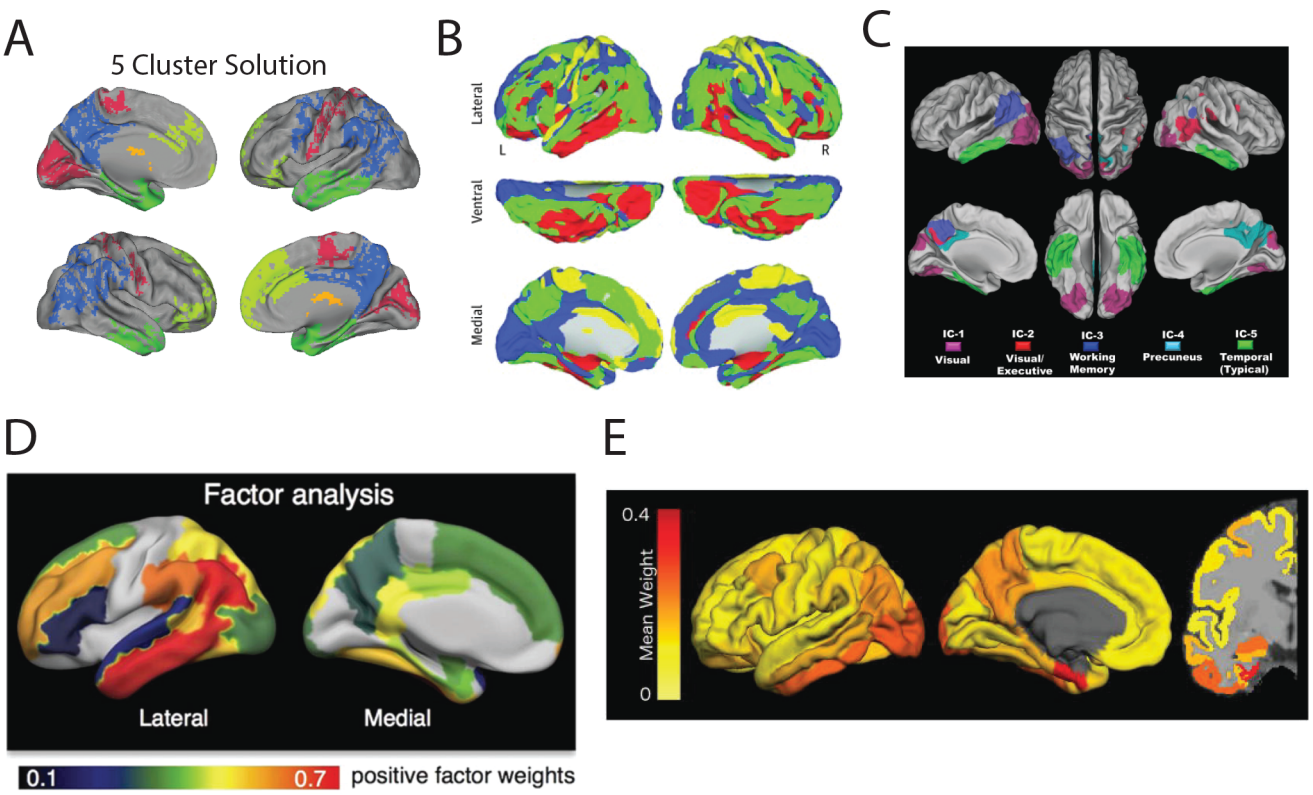

Figure 5.1: A) Parcellation (cluster-cores) of regional tau-PET covariance from Chapter 2 using voxelwise clustering (Vogel et al., 2019a) (with permission from John Wiley and Sons). B) Voxelwise clustering partition of tau-PET data from Sepulcre et al., 2017a (without permission, come and get me). C) Centroids resulting from independent components analysis on tau-PET images from Jones et al., 2017. D) Regional loadings for the first factor of a factor analysis on tau-PET data ROI data (explaining 81% of variance) from Maass et al., 2017 (with permission from Elsevier). E) Regional contribution to cluster that segregated likely tau-positive individuals from likely tau-negative individuals, from (Mishra et al., 2017) (with permission from Elsevier)

between tau-covariance networks and resting-state functional networks (Jones et al., 2017; Hoenig et al., 2018; Pereira et al., 2019).

As related above, few of the findings from Chapter 2 could be considered novel by the time they were published. However, our study was alone in publishing the tau covariance networks we created, to share with other researchers for future use (https://figshare.com/articles/TauRUS_Tau-PET_Atlas_MNI_space_1_mm_/5758374). Additionally, results from Chapter 2 have uniquely suggested that tau-PET signal varies spatially within the hippocampus. Very little work has been done to even acknowledge the discrepant hippocampal flortaucipir signal, much less address it. One study found regressing out choroid plexus signal is beneficial (Lee et al., 2018), while another study tried multiple methods and did not find any method improved associations with clinical measures (Wolters et al., 2020a). Our findings suggest that masking can help to retrieve the hippocampus signal relevant to tau pathology, while eliminating the signal more consistent with off-target binding.

The results from Chapter 3 represent a logical and novel extension to the work that preceded it. Several studies published in the last two years found links between

functional connectivity patterns and tau-PET patterns (Hoenig et al., 2018; Cope et al., 2018; Franzmeier et al., 2019; Adams et al., 2019; Ossenkoppele et al., 2019; Pereira et al., 2019). However, only one of these studies attempted to model or simulate the spread of tau using human connectivity data (Franzmeier et al., 2020), and this model was fairly unsophisticated. Similarly, only the Franzmeier et al. study attempted fitting such a model within-subject, and this attempt did not attain much success. Finally, none of the above studies use white matter tractography to model human synaptic connectivity. In contrast, the original work from Chapter 3 applies a spatial diffusion model across both functional and diffusion-based tractographic human connectivity data to model tau-PET data, both across and within subjects. This distinction is quite important, as it involves modeling of pathology from a single epicenter, through a specific set of paths and secondary seeding events, much like the proposed spread of tau in AD. Other studies have used such diffusion models in the context of AD using MRI (Raj, Kuceyeski, and Weiner, 2012; Acosta et al., 2018; Torok et al., 2018) or Aβ-PET (Iturria-Medina et al., 2014), though no study to date has applied a diffusion model to tau-PET data. The success of the model in explaining variance in tau-PET spatial distribution, especially as compared to previous studies, supports the notion of tau spreading synaptically from the entorhinal cortex, rather than tau simply depositing preferentially in highly connected regions. Of course, these results only add support to ideas that have been previously proposed in humans (Seeley et al., 2009) and demonstrated quite convincingly in rodents (Peng, Trojanowski, and Lee, 2020). The findings from Chapter 3 provide strong evidence for tau spreading in humans, but they are not sufficient to prove this phenomenon occurs, and therefore represent only an incremental advance.

Other results from Chapter 3 may be considered somewhat more novel. The analyses indicated that the pattern of tau spread in PART also occurs through synaptic connections. This provides further evidence that PART and AD tauopathy are similar processes, or different phases of the same process (Braak and Del Tredici, 2014; Duyckaerts et al., 2015). This notion is further supported by the fact that the model underestimated the spread of tau in Aβ-prone regions. One interpretation of this result is that connectivity patterns drive PART-like spread of tau (i.e. in Braak stages I-IV), whereas Aβ somehow potentiates the expression of tau into isocortical (i.e. Braak stage V) regions. This is consistent with recent mouse studies showing an accelerating effect of Aβ on tau spreading (Pooler et al., 2015; He et al., 2018; Rodriguez et al., 2019), and may partially explain the "spatial paradox" of AD (Kant, Goldstein, and Ossenkoppele, 2020) (Figure 1.3).

Another fairly novel contribution of Chapter 3 came from the approach of using region-specific mixture modeling to normalize tau-PET data. The approach was an

invention of necessity, as the ESM would have great difficulty with off-target signal contamination. The strength of the mixture-modeling approach, however, may stem from its region-specific application, which helps account for regional differences in non-specific binding and potential floor and ceiling effects. The approach allows for a data-driven derivation of thresholds for "tau-positivity", which remains a point of contention in the tau-PET literature (Jack et al., 2017; Maass et al., 2017) (see Section 1.3.1 for review).

Chapter 4 provided numerous highly original results, likely because the subject of AD subtypes is difficult to study experimentally. While the findings need further validation, Chapter 4 highlights "typical AD" to be an ill-defined concept. [1] Results from Chapter 4 suggest that the presence of "typical" or "atypical" presentations of tau pathology may be more a factor of aggressive, early onset manifestations exaggerating distinctions between various AD subtypes (Figure 5.2,discussed below). The results in Chapter 4 reproduced subtypes previously described in numerous autopsy and imaging studies (Murray et al., 2011b; Whitwell et al., 2012; Risacher et al., 2017; Ossenkoppele et al., 2020; Ferreira, Nordberg, and Westman, 2020), but did so using fully unsupervised methods, and contrary to previous findings, found no predominant pattern. The approach also revealed estimates of progressive patterns for several different subtypes of AD, something that had only been documented for "typical AD" (Braak and Braak, 1991; Braak et al., 2006) and PCA (Firth et al., 2019). Interestingly, one of the subtypes patterns was a near perfect recapitulation of the Braak stages, though the other patterns appeared quite divergent.

Other findings from Chapter 4 were not themselves novel, but lead to novel interpretations of AD pathological expression. Other studies have reported earlier-onset cases to express greater tau pathology (Marshall et al., 2007; Whitwell et al., 2019), though we show this to be a common feature across AD subtypes. We interpret these results to signify that PCA, lvPPA and perhaps dysexecutive clinical variants are extreme manifestations of typical AD subtypes. This idea suggests, then, that "typical" late-onset varieties of AD include milder posterior and lateralized pathological presentations of AD. This is not inconsistent with the notion that non-amnestic clinical presentations are not uncommon in late-onset AD cohorts (Dickerson and Wolk, 2011; Scheltens et al., 2017; Crane et al., 2017). However, these phenotypes are not well-described, since we may be among the first to describe them. The posterior subtype, for example, exhibited a milder phenotype, whereas the lateralized phenotype was more aggressive.

[1] Here, it may be necessary to once again invoke the distinction between clinical AD dementia, and the pathological phenomenon of AD (Jack, Holtzman, and Sperling, 2019). The definition of "typical" vs. "atypical" clinical presentation of AD is a related but separate debate from "typical" vs "atypical" pathological progression.

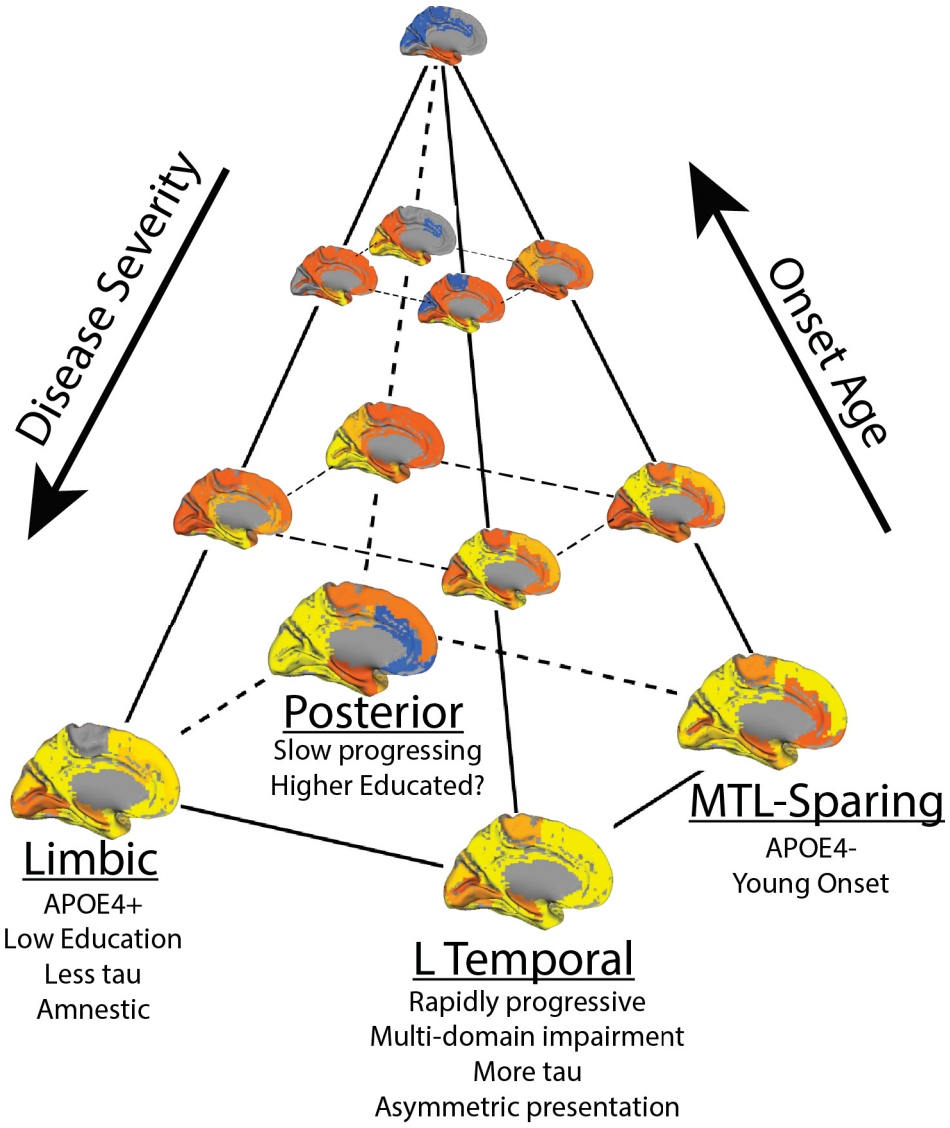

Figure 5.2: Our data support the notion that at least four pathological subtypes of AD exist, with different characteristics. The distinctions between these subtypes is more pronounced in more severe cases, where case severity is proportional to disease onset age.

Finally, while highly preliminary, results from Chapter 4 indicate that different subtypes of AD may arise through individual differences in connectivity patterns, and/or involvement of distinct subtypes. Very little is understood about what make certain regions and cells vulnerable to AD (reviewed in Section 1.3.3), though practically nothing is known about how or whether AD subtypes influences regional or cellular vulnerability (discussed in Section 1.3.4). Our results suggest that the various patterns of tau distribution endemic to each subtype resemble specific network spreading patterns seeded from different limbic or para-limbic regions. This does not necessarily nominate these regions as subtype-specific NFT epicenters, but it may implicate them as central nodes in the subtype-specific spreading of tau pathology. Further, our results found that regions more vulnerable in different subtypes were

enriched for certain neuronal cell-types. While this works needs to be expanded upon and verified, our early results suggest a particular role for astrocytes in the limbic AD subtypes, and several excitatory neurons to be implicated in the rapidly-progressing lateral temporal subtype.

5.2 Placing findings in context

The remainder of this Chapter will cover open questions and controversies in AD research, and how findings presented in this Thesis contribute to the scientific dialogue. In this section, the topics most proximate to the studies in this thesis will be discussed. These topics included the use of tau-PET as a clinical biomarker, updating hypotheses of tau spread, and a challenge to the Braak staging regime.

5.2.1 Considerations of tau-PET as a clinical biomarker

There is a wealth of discussion about what makes a useful biomarker (Humpel, 2011; Califf, 2018). The subsection will not discuss considerations such as invasiveness, reproducibility, safety, cost and so forth, nor will it cover comparison to other tau biomarkers (this is covered in Section 1.4.1). Instead, efforts to utilize tau-PET as a means of diagnosis and prognosis will be covered.

The most frequently mentioned potential uses for a tau-PET biomarker include differential diagnosis, negative/positive tau reads, and monitoring of tau accumulation. Many labs have proposed and evaluated methods for distilling tau-PET images into summary biomarkers, using either *a priori* hypotheses (Schöll et al., 2016b; Schwarz et al., 2016; Cho et al., 2016a; Jack et al., 2017; Ossenkoppele et al., 2018; Schwarz et al., 2018) or data-driven approaches (Jones et al., 2017; Maass et al., 2017; Mishra et al., 2017; Vogel et al., 2019a) (Figure 5.1). These various studies arrived at remarkably similar conclusions: composite temporal or temporo-parietal ROIs perform best for differential diagnosis and separating controls from patients, while limbic ROIs are better for distinguishing early stages of AD from controls. Longitudinal studies found highly similar results (Jack et al., 2018a; Harrison et al., 2018), and the work from Chapter 2 and Chapter 4 are also in agreement. This suggests that different regions of interest can be used depending on the clinical question. For example, a clinical trial in AD patients, or a clinic attempting to differentiate AD from FTD, might prefer to use a larger temporoparietal ROI. Ossenkoppele et al. found accuracy rates consistently around 90% for differential diagnosis of AD from other disorders (Ossenkoppele et al., 2018), which is considerably higher than the 75-85% correct diagnosis in neuropathologically validated AD cases (Fischer et al., 2017; Liesinger

et al., 2018). Notably, the performance of tau-PET in this study was much better than MRI derived biomarkers, indicating tau-PET is a considerable upgrade as a discriminative tool. Meanwhile, a study in cognitively normal individuals such as the A4 trials (Sperling et al., 2014) might do better with an early Braak or inferior temporal ROI. However, this is assuming a static ROI is required. Our work in Chapter 4 utilizes ROIs tailored not only to an individual's tau subtype, but also to their state along the AD spectrum. This appears to be an optimal solution in clinical trials and other situations involving tracking of tau accumulation.

The utility of positive-negative tau reads outside the context of differential diagnosis is not clear. The clinical expression of PART, if any, is not yet known. Given that abnormal tau appears in closer proximity to cognitive impairment (Hanseeuw et al., 2019; Barthélemy et al., 2020a), tau scans may have prognostic value in unimpaired individuals with a positive Aβ read. More longitudinal data is necessary to support more accurate assessments of time from abnormal tau scans to clinical impairment, and the rate of tau accumulation is still debated. However, in such cases, a negative tau read may indicate a patient is not yet proximal to a state of impairment. In such cases, a threshold for abnormality must be attained. Much like the tau ROI debate, the tau threshold work suggests different cutoffs are useful in different contexts (Jack et al., 2017). The mixture modeling approaches described in Chapter 3 and Chapter 4 may be good solutions in this case, as they allow a data-driven decision as to what is "normal". However, applying such an approach requires a large sample to derive the threshold, and all scans to be assessed would have to be processed with the same processing pipeline as the derivation sample. This latter point would be true with any threshold – quantitative values vary quite a bit across different labs and radiotracers. A similar issue with Aβ-PET lead to efforts to harmonize values with a central processing pipeline, though results have been imperfect thus far (La Joie et al., 2019).

Given a standardization in radiotracers and processing pipelines, tau-PET may be useful as a clinical biomarker. However, there is still important work to be done in order to verify this claim. First, very little data has been published as to how well post-mortem tau pathology correlates with tau-PET scans. One study showed high correlations in a single PSEN1 carrier with rapidly progressing AD (Smith et al., 2019b). However, a large and thus far unpublished clinical trial suggested that positive flortaucipir reads, as read manually and raw by a trained clinician, were only reliable for individuals with Braak stage V or VI pathology (Fagan, 2018). Second, there is no data showing how sensitive tau-PET data might be to pharmacological intervention. In addition, tau-PET tracers would be sensitive only to therapies halting the spread of NFT pathology, as current tracers cannot detect oligomeric

tau. This is important, as there is data showing NFTs continue to accumulate even after the suppression of oligomeric tau (Santacruz et al., 2005). Finally, many of the positive features of tau-PET as a biomarker appear to be matched by newly developed phospho-tau plasma assays (Thijssen et al., 2020; Janelidze et al., 2020), which would represent a much cheaper and widely available alternative. Further work needs to be performed on both of these biomarkers to assess whether the spatial component of tau offers any advantage. However, most tau-PET work so far has not made full use of the spatial component of tau-PET. Our work in Chapter 4 suggests incorporating such information can result in performance optimization that may reach a higher ceiling than fluid biomarkers. This may not be enough to offset the cost differential to plasma tau biomarkers for regular clinical use, but it might be sufficient to sway pharmaceutical companies in search of highly sensitive markers for a clinical trial.

5.2.2 Updating hypotheses of tau spread

There is now ample evidence supporting the notion that tau pathology spreads from neuron to neuron through synaptic connections. Numerous animal experiments have demonstrated each stage of this mechanism can occur *in vivo* (reviewed in section 1.3.2). This does not prove tau pathology does spread in humans, but both *in vivo* and post-mortem studies have provided a great deal of support for the hypothesis (Sections 1.3.2, 5.2.2, Chapter 3). Some previous work in humans was perhaps more suggestive of tau preferentially depositing in highly connected regions (Cope et al., 2018; Franzmeier et al., 2019; Franzmeier et al., 2020), though the work in Chapter 3 points more to spread, given that the pattern of tau is best explained by synaptic diffusion from the entorhinal cortex. However, macroscale connectivity patterns fail to fully explain tau-PET patterns in humans. Part of this is likely due to measurement error of the various imaging modalities, and resolution being far too low to image activity at the cellular level. Rodent studies rarely provide results quantitative enough to truly assess the degree to which synaptic connectivity governs spread, and those that do also suggest excellent but imperfect fit (Henderson et al., 2019). However, we know that certain neurons are highly resistant to tau pathology, including those that are adjacent or synaptically connected to NFT-expressing neurons (reviewed in section 1.3.3). Synaptic connectivity cannot explain the entire picture.

Consider three models (Figure 5.3A). In the first model, NFT pathology spreads among all synaptically connected neurons, and no neurons that are not connected. In the second model, NFT pathology spreads exclusively among vulnerable neurons, irrespective of their connectivity patterns. In the third model, NFT pathology spreads only among neurons that are both synaptically connected and vulnerable. While

the first model is the most frequently discussed, it is essentially the only model that has already been falsified. There is ample evidence for neurons that share synaptic connections with NFT-bearing neurons that do not themselves express tau pathology (Mrdjen et al., 2019). In the second model, pathology could be propagated through extracellular means (Yamada et al., 2014; Wu et al., 2016; Wang et al., 2017), or through glial networks (Asai et al., 2015; Wang et al., 2017; Bussian et al., 2018). A singular agent of spread is not even necessary for model 2; a cascading shift in molecular environment (e.g. Aβ) could be sufficient to trigger tau phosphorylation and aggregation specifically in vulnerable neurons (Figure 5.3B). Of course, plenty of evidence supports the notion that tau molecules themselves can instigate conformational change in other molecules (Mirbaha et al., 2018), and that introduction of tau fibrils alone can stimulate the spread of tau pathology (Clavaguera et al., 2009; De Calignon et al., 2012; Ahmed et al., 2014b). However, some have noted that the degree of tau pathology present in the somatodendritic compartment seems excessive in relation to the amount in the axon, suggesting tau-positive neurons accelerate production of tau in the nucleus (Braak and Del Tredici, 2015). Such a process would not require tau seeds to travel from presynaptic sites to the axon, nor would it necessarily require tau seeds at all – another process entirely could stimulate tau production. There is little work to support some of the more radical assertions above, but there is also little work to falsify them.

Model 3 may be the most parsimonious description of tau spread. In such a model, synaptic connectivity could be a binary and relatively stable factor, whereas vulnerability might be both scalar and dynamic. In other words, cells could express different degrees of resistance to oligomeric aggregation, which could itself be modified by external factors (Figure 5.3C), but connectivity does not change (until later stages when the axon is destroyed). Some cells may be entirely invulnerable to formation of NFTs, while others may merely be resistant. A cell's time to NFT expression would then be a function of it's intrinsic vulnerability and connectivity to the disease epicenter. Such a model could even be explored in a single structure such as the hippocampus, where CA1 excitatory neurons are highly vulnerable to NFT aggregation, CA2 interneurons may be entirely or mostly resistant, and dentate gyrus neurons only show pathology at late stages (Braak and Braak, 1991; Braak et al., 2006; Lace et al., 2009; Mrdjen et al., 2019). This would be an interesting structure to study since the instrinsic connectivity of the hippocampus is extremely well documented, and the transcriptomic composition is now undergoing thorough study (**Vogel2020ASystems**; Bienkowski et al., 2018).

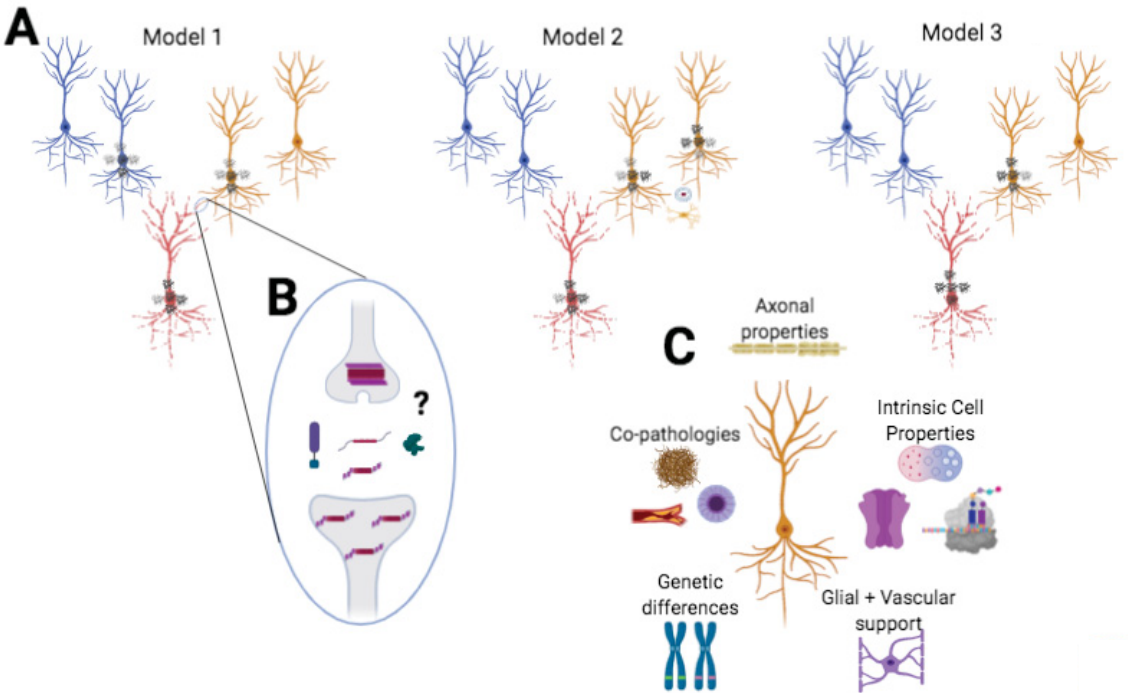

Figure 5.3: A) Three hypothetical models of tau-spread. Red neuron = Tau-positive/compromised, orange neuron = neuronal cell type with increased vulnerability to tau, blue neuron = neuronal cell type with decreased vulnerability to tau. In model 1, tau spreads primarily through synaptically connected neurons, irrespective of neuronal cell type. In model 2, tau spreads primarily to intrinsically vulnerable neurons irrespective of synaptic connection, perhaps through extracellular or glial means, or through agent-absent propagation (i.e. propagation of a pathological state). In model 3, tau spreads primarily to neurons that are both synaptically connected and intrinsically vulnerable to tau. B) In models 1 and 3, an agent is implied that is capable of transynaptic spread. This agent may be tau monomers or oligomers, or could be non-tau agents secreted by the presynaptic neurons. C) Many factors might contribute dynamically to neuronal vulnerability. This includes i. axonal properties such as thin, less-meylinated and later-developing axons; ii. co-pathologies such as Aβ plaques, Lewy bodies, TDP-43 or vascular pathology; iii. intrinsic cell properties such as differing endosomal/lysosomal and calcium homeostatic processes, or distinct synaptic or intracellular proteomes; vi. genetic differences affecting protein expression relevant to tau aggregation; v. degree of trophic, vascular and glial support afforded to an individual neuron. Figure made with BioRender (https://biorender.com/)

As mentioned in previously in Section 1.3.4, even a model incorporating synaptic connectivity and cellular vulnerability would have to somehow reconcile inter-individual differences. Plenty of previous research has demonstrated systematic variability in tau spreading, and the work presented in Chapter 4 elucidated this phenomenon in a large sample using human *in vivo* data. Individual variation in AD could be mitigated by different regions acting as the primary nucleus of spread. For example, the basal forebrain appears to be particularly vulnerable in hippocampal-sparing AD (Hanna Al-Shaikh et al., 2019), and also projects to numerous cortical regions (Bigl, Woolf, and Butcher, 1982; Mesulam et al., 1983). Perhaps basal forebrain projections are responsible for diffuse spreading of pathology above and beyond projections from the entorhinal cortex. Data from Chapter 4 support this concept as a possibility, as do studies showing regional tau injection lead to differential distributions of pathology (Sanders et al., 2014; Narasimhan et al., 2017).

As an alternative, genetic factors could influence cellular vulnerability in a way that modifies which cell types are vulnerable in different subtypes. However, results from Chapter 4 suggests subtypes of AD are not uncommon, and it is unlikely that genetic variation would result in a neat partition of only a few different pathological expressions. Instead, another factor that could influence subtype expression, and which could still fit with Model 3 above, is the existence of distinct conformations of tau. In such a model, certain neuronal subtypes might be resistant to one conformation of tau, but not to another. This is not an unreasonable proposition, given that different tau conformations of various tauopathies lead to distinct regional tau distribution patterns (Kovacs, 2015). Furthermore, numerous studies show distinct tau fibrils lead to different *in vivo* spreading patterns in mice, and a recent study showed this is a product of conformation (Clavaguera et al., 2013; Sanders et al., 2014; Guo et al., 2016a; Dujardin et al., 2018), rather than tau species (He et al., 2020). Conformation could also influence mechanisms of spread. For example, some conformations could lead to exaggerated extracellular or glial spread, further complicating attempts to model pathological spread.

In conclusion, a comprehensive model of tau spread would likely need to incorporate many parameters. This would include synaptic connectivity, as well as regional vulnerability, and numerous factors that can influence vulnerability, such as co-pathologies, internal state and most likely individual genetic information. Furthermore, the model may need to incorporate separate vulnerability states for distinct conformational states of tau pathology. Finally, the model might also need to accommodate the possibility of spread through other mechanisms, such as extracellular or glial spread. Such a model would have numerous parameters, many of which would be very challenging to measure, and likely still would not account for as yet unknown features of tau. However, at the very least, synaptic connectivity alone cannot by itself explain the spread of tau. Further characterization of regional vulnerability can be established through rigorous single-cell transcriptomic analyses, and this may be applicable to macroscale neuroimaging based models (Zheng et al., 2019; Henderson et al., 2019). However, testing a model as comprehensive as the one described above would probably require *in vivo* or *in vitro* experimentation.

5.2.3 Challenging the Braak canon

In the beginning there was darkness. Then, Braak came down and He casteth a light upon six stages, and He doth decreed all who follow these six stages, thou shalt know AD. O Braak, have I walked thine stages, and whilst I seeketh the hippocampus thou promised, I behold only cortex in my wake. – "Relent of the hippocampal-sparing phenotype", author unknown.

No single work influenced this Thesis more than Braak and Braak's seminal 1991 paper, which provided a qualitative description of the spread of tau pathology (Braak and Braak, 1991). The value of this study and long line of studies that followed cannot be overstated. While still incredibly relevant to the study of tau in AD, work in this Thesis suggests the need for amendments to the original staging model. Many of the findings from the original work in this thesis, particularly the work in Chapter 2 and Chapter 4, suggest the Braak staging system is insufficient to describe the pattern of tau NFT spread in AD on an individual basis. While the Braak stages laid the groundwork for modeling tau spread in a way that was extremely beneficial to the AD field, whole-brain sampling of tau *in vivo* has provided novel information. First, results from Chapter 2 suggest regions subsumed under Braak stage V have fairly independent trajectories of tau accumulation, and this appears quite obviously when visualizing a sequence of tau-PET scans. As shown in Figure 1.7, irrespective of radiotracer, tau accumulates in the precuneus and lateral parietal lobes well before pathology is measurable in most frontal areas. Results from Chapter 3 further support his notion, showing some parietal lobe structures to become abnormal shortly after the temporal lobe structures, preceding even the superior temporal lobes that characterize Braak stage V (Braak et al., 2006; Schwarz et al., 2016) Furthermore, certain frontal areas (namely premotor association cortex) appear to express pathology earlier than other frontal areas. If properly validated post-mortem, these findings would suggest a reform to the traditional Braak staging regime. Such a reform would either move the precuneus and angular/supramarginal areas (i.e. the posterior DMN) into Braak stage IV, or would require addition of an intermediary stage including these regions, but preceding other (namely frontal) association cortex.

However, the changes suggested above assume the application of a singular sequence as sufficient to stage all AD cases. Results from Chapter 4 and many other studies (Murray et al., 2011b; Ossenkoppele et al., 2016b; Ossenkoppele et al., 2019; Firth et al., 2019; Ferreira, Nordberg, and Westman, 2020) recommend otherwise. The Braak staging regime may be a perfect fit for certain subtypes of AD, and our results in Chapter 4 suggest as much for the limbic AD subtype. However, cortical-predominant, posterior and lateralized subtypes appear to deviate from the Braak paradigm, fairly radically in some cases. It is possible that tau seeding patterns are indistinguishable across the tau subtypes, and it is the aggregation into NFTs that differs. Similarly, it is possible that tau pathology does proceed in a Braak-like fashion in all cases, but the degree of expression in some subtypes become highly exaggerated in specific parts of the cortex. In either of these two scenarios, discrepancy between tau-PET and histopathology studies may arise, especially given that the latter usually

uses a semi-quantitative approach for measuring the magnitude of NFT expression. However, the subtypes are characterized not only by differential patterns of NFT accumulation, but also matching patterns of neuronal degeneration (Ossenkoppele et al., 2016a; Ossenkoppele et al., 2019). Therefore, the evolution of the disease process appears to follow those regions exhibiting extensive tau pathology, and so an effective staging regime would ultimately aim at capturing this process.

If the findings from Chapter 4 are validated, a new staging procedure might be necessary. The first step would be to more thoroughly define the progression of each subtype. This would require extensive autopsy samples, and/or tau-PET data (and could be assisted using MRI). Our work proposes prototypes for some of these progressions, as do other recent studies, for example Firth et al. who characterized spatiotemporal spread of neurodegeneration in PCA (Firth et al., 2019), but further validation is necessary. Once validated, one possibility would be to derive entirely separate staging paradigms for each subtype. Therefore, an individual patient at autopsy could be assessed based on whichever staging pattern best explained the progression of tau. A second, similar but perhaps more challenging option would be to have a single staging system, which included alternatives within each stage. This is not totally unprecedented; Braak described that occipital NFTs are "occasionally" observed at stage IV (Braak et al., 2006). However, this second option could quickly get out of hand, particularly with subtypes like limbic and hippocampal-sparing, which seem to have progressions nearly reversed from one another. Irrespective of the nature of a reformed staging system, an optimization would be necessary, at least for pathological staging. The smallest number of regions that still offers both subtyping and staging information would need to be identified, and this would be an interesting direction for future work. The original Braak staging cannot reconcile atypical variants of AD, and this was the case even before results from Chapter 4 emerged. However, the results from Chapter 4 calling to question the notion of "typical AD", only make the impetus for reforming Braak staging that much more imperative.

5.3 Main conclusions of thesis work

A few consistent themes emerged across the three studies. Chapter 2 and Chapter 4 both pointed to a reform or extension of the Braak staging regime. Chapter 2 revealed diverse tau behavior among regions subsumed under Braak Stage V, showing that there was more variation *within* Stage V regions then there was *between* regions in Stages I-IV. Meanwhile, Chapter 4 suggested that a single staging regime cannot be used to track the progression of tau pathology in all individuals. These two points

were discussed further in Section 5.2.3, but the consensus across these studies is that the Braak stages, while groundbreaking and useful, may need to be revised. Chapter 2 and Chapter 4 also both pointed to the superiority of unbiased, data-driven models over convention in creating effective biomarkers for tau-PET. Chapter 2 found that data-driven covariance networks were better correlated than other regions with global cognition in a left-out dataset, while Chapter 4 found that a data-driven prediction model was more sensitive to detecting longitudinal tau-PET change than other approaches. This was discussed further in Section 5.2.1. Finally, both Chapter 3 and Chapter 4 provided additional evidence for the spreading of tau through major synaptic pathways, but that macroscale connectivity alone could not fully explain the observed patterns of tau-distribution. This was discussed further in Section 5.2.2.

In all, the original work presented in this thesis composes a thorough investigation of the *in vivo* spatial distribution of tau in the human brain. While most of the tau-PET literature to date has focused on how tau-PET patterns meet the expectations anticipated by post-mortem studies, the work herein rather challenges previous literature, and suggests a more nuanced description of the spread of tau pathology. To distill this work down to just a few points, one can make the following assertions. First, *in vivo* and unbiased spatial sampling of tau in the human brain can provide useful biomarkers and novel information about tau progression in AD, but this is accomplished most effectively using unbiased models and unsupervised models." A more contentions statement might be that Braak staging alone does not capture the full range of individual variability in Braak stage patterns, nor does synaptic connectivity alone appear to fully explain the patterns of tau distribution in human AD. In all, we are only beginning to scratch the surface of tau-PET's utility not just as a tool for clinical use and scientific validation, but as a tool for discovery.

Bibliography

Abramowski, Dorothee et al. (2008). "Dynamics of Aβ turnover and deposition in different β-amyloid precursor protein transgenic mouse models following γ-secretase inhibition". In: *Journal of Pharmacology and Experimental Therapeutics* 327.2, pp. 411–424. ISSN: 00223565. DOI: 10.1124/jpet.108.140327.

Acosta, Diana et al. (June 2018). "Regional vulnerability in Alzheimer's disease: The role of cell-autonomous and transneuronal processes." In: *Alzheimer's & dementia : the journal of the Alzheimer's Association* 14.6, pp. 797–810. ISSN: 1552-5279. DOI: 10.1016/j.jalz.2017.11.014. URL: https://linkinghub.elsevier.com/retrieve/pii/S1552526017338578http://www.ncbi.nlm.nih.gov/pubmed/29306583http://www.pubmedcentral.nih.gov/articlerender.fcgi?artid=PMC5994366.

Adams, Jenna N et al. (2019). "Cortical tau deposition follows patterns of entorhinal functional connectivity in aging". In: *eLife* 8, pp. 1–22. ISSN: 2050084X. DOI: 10.7554/eLife.49132.

Aggleton, John P. et al. (July 2016). "Thalamic pathology and memory loss in early Alzheimer's disease: moving the focus from the medial temporal lobe to Papez circuit". In: *Brain* 139.7, pp. 1877–1890. ISSN: 0006-8950. DOI: 10.1093/brain/aww083. URL: http://www.brain.oxfordjournals.org/lookup/doi/10.1093/brain/aww083https://academic.oup.com/brain/article-lookup/doi/10.1093/brain/aww083.

Aguero, Cinthya et al. (2019). "Autoradiography validation of novel tau PET tracer [F-18]-MK-6240 on human postmortem brain tissue". In: *Acta neuropathologica communications* 7.1, p. 37. ISSN: 20515960. DOI: 10.1186/s40478-019-0686-6.

Ahmed, Tariq et al. (2014a). "Cognition and hippocampal synaptic plasticity in mice with a homozygous tau deletion". In: *Neurobiology of Aging* 35.11, pp. 2474–2478. ISSN: 15581497. DOI: 10.1016/j.neurobiolaging.2014.05.005. URL: http://dx.doi.org/10.1016/j.neurobiolaging.2014.05.005.

Ahmed, Zeshan et al. (2014b). "A novel in vivo model of tau propagation with rapid and progressive neurofibrillary tangle pathology: The pattern of spread

is determined by connectivity, not proximity". In: *Acta Neuropathologica* 127.5, pp. 667–683. ISSN: 14320533. DOI: 10.1007/s00401-014-1254-6.

American Psychiatric Association, The (2013). *Diagnostic and statistical manual of mental disorders : DSM-5*. Fifth edition. Arlington, VA : American Psychiatric Association, [2013]. URL: https://search.library.wisc.edu/catalog/9910187853902121.

Andorfer, Cathy et al. (2005). "Cell-cycle reentry and cell death in transgenic mice expressing nonmutant human tau isoforms". In: *Journal of Neuroscience* 25.22, pp. 5446–5454. ISSN: 02706474. DOI: 10.1523/JNEUROSCI.4637-04.2005.

Andreasen, Niels et al. (June 1999). "Cerebrospinal Fluid β-Amyloid(1-42) in Alzheimer Disease". In: *Archives of Neurology* 56.6, p. 673. ISSN: 0003-9942. DOI: 10.1001/archneur.56.6.673. URL: http://archneur.jamanetwork.com/article.aspx?doi=10.1001/archneur.56.6.673.

Anthony, Iain C. et al. (2010). "Predisposition to accelerated Alzheimer-related changes in the brains of human immunodeficiency virus negative opiate abusers". In: *Brain* 133.12, pp. 3685–3698. ISSN: 00068950. DOI: 10.1093/brain/awq263.

Arendt, Thomas and Torsten Bullmann (2013). "Neuronal plasticity in hibernation and the proposed role of the microtubule-associated protein tau as a "master switch" regulating synaptic gain in neuronal networks". In: *American Journal of Physiology - Regulatory Integrative and Comparative Physiology* 305.5, pp. 478–489. ISSN: 03636119. DOI: 10.1152/ajpregu.00117.2013.

Arendt, Thomas, Jens T. Stieler, and Max Holzer (2016). "Tau and tauopathies". In: *Brain Research Bulletin* 126, pp. 238–292. ISSN: 18732747. DOI: 10.1016/j.brainresbull.2016.08.018.

Arendt, Thomas et al. (2003). "Reversible paired helical filament-like phosphorylation of tau is an adaptive process associated with neuronal plasticity in hibernating animals". In: *Journal of Neuroscience* 23.18, pp. 6972–6981. ISSN: 02706474. DOI: 10.1523/jneurosci.23-18-06972.2003.

Arnemann, Katelyn L. et al. (2018). "Metabolic brain networks in aging and preclinical Alzheimer's disease". In: *NeuroImage: Clinical* 17.December 2017, pp. 987–999. ISSN: 22131582. DOI: 10.1016/j.nicl.2017.12.037. URL: https://doi.org/10.1016/j.nicl.2017.12.037.

Arriagada, P V et al. (1992). "Neurofibrillary Tangles But Not Senile Plaques Parallel Duration and Severity of Alzheimers-Disease". In: *Neurology* 42.3, pp. 631–639. ISSN: 0028-3878. DOI: 10.1212/WNL.42.3.631.

Asai, Hirohide et al. (2015). "Depletion of microglia and inhibition of exosome synthesis halt tau propagation". In: *Nature Neuroscience* 18.11, pp. 1584–1593. ISSN: 15461726. DOI: 10.1038/nn.4132.

Association, Alzheimers (Mar. 2019). "2019 Alzheimer's disease facts and figures". In: *Alzheimer's & Dementia* 15.3, pp. 321–387. ISSN: 15525260. DOI: 10.1016/j.jalz.2019.01.010. URL: https://doi.org/10.1016/j.jalz.2019.01.010http://doi.wiley.com/10.1016/j.jalz.2019.01.010.

Austad, Steven N. and Jessica M. Hoffman (2018). "Is antagonistic pleiotropy ubiquitous in aging biology?" In: *Evolution, Medicine and Public Health* 2018.1, pp. 287–294. ISSN: 20506201. DOI: 10.1093/emph/eoy033.

Badhwar, AmanPreet et al. (2019). "A multiomics approach to heterogeneity in Alzheimer's disease: focused review and roadmap". In: *Brain*, pp. 1–17. ISSN: 0006-8950. DOI: 10.1093/brain/awz384.

Bai, Bing et al. (2020). "Deep Multilayer Brain Proteomics Identifies Molecular Networks in Alzheimer ' s Disease NeuroResource Deep Multilayer Brain Proteomics Identifies Molecular Networks in Alzheimer ' s Disease Progression". In: *Neuron*, pp. 1–17. ISSN: 0896-6273. DOI: 10.1016/j.neuron.2019.12.015. URL: https://doi.org/10.1016/j.neuron.2019.12.015.

Baker, Matt et al. (1999). "Association of an extended haplotype in the tau gene with progressive supranuclear palsy". In: *Human Molecular Genetics* 8.4, pp. 711–715. ISSN: 09646906. DOI: 10.1093/hmg/8.4.711.

Baker, Suzanne L., Anne Maass, and William J. Jagust (2017). "Considerations and code for partial volume correcting [18F]-AV-1451 tau PET data". In: *Data in Brief* 15, pp. 648–657. ISSN: 23523409. DOI: 10.1016/j.dib.2017.10.024. URL: http://dx.doi.org/10.1016/j.dib.2017.10.024.

Baker, Suzanne L. et al. (2017). "Reference tissue-based kinetic evaluation of 18F-AV-1451 for tau imaging". In: *Journal of Nuclear Medicine* 58.2, pp. 332–338. ISSN: 2159662X. DOI: 10.2967/jnumed.116.175273.

Baker, Suzanne L et al. (2019). " Effect of off-target binding on 18 F-Flortaucipir variability in healthy controls across the lifespan ". In: *Journal of Nuclear Medicine*, jnumed.118.224113. ISSN: 0161-5505. DOI: 10.2967/jnumed.118.224113.

Bakkour, Akram et al. (2013). "The effects of aging and Alzheimer's disease on cerebral cortical anatomy: Specificity and differential relationships with cognition". In: *NeuroImage* 76, pp. 332–344. ISSN: 10538119. DOI: 10.1016/j.neuroimage.2013.02.059. URL: http://dx.doi.org/10.1016/j.neuroimage.2013.02.059.

Ballatore, Carlo, Virginia M.Y. Lee, and John Q. Trojanowski (2007). "Tau-mediated neurodegeneration in Alzheimer's disease and related disorders". In: *Nature Reviews Neuroscience* 8.9, pp. 663–672. ISSN: 1471003X. DOI: 10.1038/nrn2194.

Bancher, C. and K. A. Jellinger (1994). "Neurofibrillary tangle predominant form of senile dementia of Alzheimer type: a rare subtype in very old subjects". In: *Acta Neuropathologica* 88.6, pp. 565–570. ISSN: 00016322. DOI: 10.1007/BF00296494.

Barthélemy, Nicolas R. et al. (2020a). "A soluble phosphorylated tau signature links tau, amyloid and the evolution of stages of dominantly inherited Alzheimer's disease". In: *Nature Medicine* 26.3, pp. 398–407. ISSN: 1546170X. DOI: 10.1038/s41591-020-0781-z.

Barthélemy, Nicolas R. et al. (2020b). "Cerebrospinal fluid phospho-tau T217 outperforms T181 as a biomarker for the differential diagnosis of Alzheimer's disease and PET amyloid-positive patient identification". In: *Alzheimer's research & therapy* 12.1, p. 26. ISSN: 17589193. DOI: 10.1186/s13195-020-00596-4.

Bateman, Randall J. et al. (2011). "Autosomal-dominant Alzheimer's disease: A review and proposal for the prevention of Alzheimer's disease". In: *Alzheimer's Research and Therapy* 2.6, pp. 1–13. ISSN: 17589193. DOI: 10.1186/alzrt59.

Bateman, Randall J et al. (2012). "Clinical and biomarker changes in dominantly inherited Alzheimer's disease." In: *The New England journal of medicine* 367.9, pp. 795–804. ISSN: 1533-4406. DOI: 10.1056/NEJMoa1202753.

Baumann, K. et al. (1993). "Abnormal Alzheimer-like phosphorylation of tau-protein by cyclin-dependent kinases cdk2 and cdk5". In: *FEBS Letters* 336.3, pp. 417–424. ISSN: 00145793. DOI: 10.1016/0014-5793(93)80849-P.

Bejanin, Alexandre et al. (2017a). "Tau pathology and neurodegeneration contribute to cognitive impairment in Alzheimer ' s disease". In: October, pp. 1–15. DOI: 10.1093/brain/awx243.

Bejanin, Alexandre et al. (Dec. 2017b). "Tau pathology and neurodegeneration contribute to cognitive impairment in Alzheimer's disease". In: *Brain* 140.12, pp. 3286–3300. ISSN: 0006-8950. DOI: 10.1093/brain/awx243. URL: https://watermark.silverchair.com/awx243.pdf?token=AQECAHi208BE49Ooan9kkhW_Ercy7Dm3ZL_9Cf3qfKAc485ysgAAAecwggHjBgkqhkiG9w0BBwagggHUMIIB0AIBADCCAckGCSqGSIb3DQEHATAeBgl3OjnBKCYybpS8fEAgEQgIIBmpY9paVgrJr248NQgNg8LAw6UHj7Y8NzZqCqEKPxMOE1DebS.

Bell, W Robert et al. (2018). "Neuropathologic , genetic , and longitudinal cognitive profiles in primary age-related tauopathy and Alzheimer ' s disease". In: *Alzheimer's & Dementia* 15.November, pp. 1–9. ISSN: 1552-5260. DOI: 10.1016/j.jalz.2018.07.215. URL: https://doi.org/10.1016/j.jalz.2018.07.215.

Bellec, Pierre (2013). "Mining the hierarchy of resting-state brain networks: Selection of representative clusters in a multiscale structure". In: *Proceedings - 2013 3rd International Workshop on Pattern Recognition in Neuroimaging, PRNI 2013*, pp. 54–57. DOI: 10.1109/PRNI.2013.23.

Bellec, Pierre (Nov. 2016). *COBRE preprocessed with NIAK 0.17 - lightweight release*. DOI: 10.6084/m9.figshare.4197885.v1. URL: https://figshare.com/articles/COBRE_preprocessed_with_NIAK_0_17_-_lightweight_release/4197885/1.

Bellec, Pierre et al. (2006). "Identification of large-scale networks in the brain using fMRI". In: *NeuroImage* 29.4, pp. 1231–1243. ISSN: 10538119. DOI: 10.1016/j.neuroimage.2005.08.044.

Bellec, Pierre et al. (2010). "Multi-level bootstrap analysis of stable clusters in resting-state fMRI". In: *NeuroImage* 51.3, pp. 1126–1139. ISSN: 10538119. DOI: 10.1016/j.neuroimage.2010.02.082. URL: http://dx.doi.org/10.1016/j.neuroimage.2010.02.082.

Bennett, David A. et al. (2004). "Neurofibrillary Tangles Mediate the Association of Amyloid Load with Clinical Alzheimer Disease and Level of Cognitive Function". In: *Archives of Neurology* 61.3, pp. 378–384. ISSN: 00039942. DOI: 10.1001/archneur.61.3.378.

Bennett, Rachel E. et al. (2017). "Enhanced Tau Aggregation in the Presence of Amyloid β". In: *American Journal of Pathology* 187.7, pp. 1601–1612. ISSN: 15252191. DOI: 10.1016/j.ajpath.2017.03.011.

Berron, David et al. (Apr. 2020). "Medial temporal lobe connectivity and its associations with cognition in early Alzheimer's disease". In: *Brain*. ISSN: 0006-8950. DOI: 10.1093/brain/awaa068. URL: https://academic.oup.com/brain/advance-article/doi/10.1093/brain/awaa068/5816707.

Besser, Lilah M. et al. (2017). "Comparison of symptomatic and asymptomatic persons with primary age-related tauopathy". In: *Neurology* 89.16, pp. 1707–1715. ISSN: 1526632X. DOI: 10.1212/WNL.0000000000004521.

Betthauser, Tobey J. et al. (2019). "In vivo characterization and quantification of neurofibrillary tau PET radioligand 18 F-MK-6240 in humans from Alzheimer disease dementia to young controls". In: *Journal of Nuclear Medicine* 60.1, pp. 93–99. ISSN: 2159662X. DOI: 10.2967/jnumed.118.209650.

Betthauser, Tobey J. et al. (2020). "Amyloid and tau imaging biomarkers explain cognitive decline from late middle-age". In: *Brain* 143.1, pp. 320–335. ISSN: 14602156. DOI: 10.1093/brain/awz378.

Bevan-Jones, W R et al. (2017). "[¹⁸ F]AV-1451 binding in vivo mirrors the expected distribution of TDP-43 pathology in the semantic variant of primary progressive aphasia". In: *Journal of Neurology, Neurosurgery & Psychiatry*, pp. 2017–316402. ISSN: 0022-3050. DOI: 10.1136/jnnp-2017-316402. URL: http://jnnp.bmj.com/lookup/doi/10.1136/jnnp-2017-316402.

Bevan-Jones, W. Richard et al. (2020). "Neuroinflammation and protein aggregation co-localize across the frontotemporal dementia spectrum". In: *Brain : a journal of neurology* 143.3, pp. 1010–1026. ISSN: 14602156. DOI: 10.1093/brain/awaa033.

Bi, Mian et al. (2017). "Tau exacerbates excitotoxic brain damage in an animal model of stroke". In: *Nature Communications* 8.1, pp. 1–14. ISSN: 20411723. DOI: 10.1038/s41467-017-00618-0. URL: http://dx.doi.org/10.1038/s41467-017-00618-0.

Bienkowski, Michael S et al. (2018). "Integration of gene expression and brain-wide connectivity reveals the multiscale organization of mouse hippocampal networks". In: *Nature Neuroscience* 21.11, pp. 1628–1643. ISSN: 15461726. DOI: 10.1038/s41593-018-0241-y. URL: http://dx.doi.org/10.1038/s41593-018-0241-y.

Biernat, J. et al. (1992). "The switch of tau protein to an Alzheimer-like state includes the phosphorylation of two serine-proline motifs upstream of the microtubule binding region." In: *The EMBO Journal* 11.4, pp. 1593–1597. ISSN: 0261-4189. DOI: 10.1002/j.1460-2075.1992.tb05204.x.

Bigl, Volker, Nancy J. Woolf, and Larry L. Butcher (1982). "Cholinergic projections from the basal forebrain to frontal, parietal, temporal, occipital, and cingulate cortices: A combined fluorescent tracer and acetylcholinesterase analysis". In: *Brain Research Bulletin* 8.6, pp. 727–749. ISSN: 03619230. DOI: 10.1016/0361-9230(82)90101-0.

Billingsley, Melvin L. and Randall L. Kincaid (1997). "Regulated phosphorylation and dephosphorylation of tau protein: Effects on microtubule interaction, intracellular trafficking and neurodegeneration". In: *Biochemical Journal* 323.3, pp. 577–591. ISSN: 02646021. DOI: 10.1042/bj3230577.

Binder, Lester I., Anthony Frankfurter, and Lionel I. Rebhun (1985). "The distribution of tau in the mammalian central nervous central nervous". In: *Journal of Cell Biology* 101.4, pp. 1371–1378. ISSN: 15408140. DOI: 10.1083/jcb.101.4.1371.

Blacker, D et al. (1997). "ApoE-4 and age at onset of Alzheimer's disease: the NIMH genetics initiative." In: *Neurology* 48.1, pp. 139–147. URL: http://eutils.ncbi.nlm.nih.gov/entrez/eutils/elink.fcgi?dbfrom=pubmed&id=9008509&retmode=ref&cmd=prlinks%0Apapers3://publication/uuid/F9C67A4D-0022-414C-9C69-467762BF9983.

Blennow, Kaj et al. (2010). "Cerebrospinal fluid and plasma biomarkers in Alzheimer disease". In: *Nature Reviews Neurology* 6.3, pp. 131–144. ISSN: 17594758. DOI: 10.1038/nrneurol.2010.4. URL: http://dx.doi.org/10.1038/nrneurol.2010.4.

Blennow, Kaj et al. (2020). "Cerebrospinal fluid tau fragment correlates with tau PET: a candidate biomarker for tangle pathology". In: *Brain : a journal of neurology* 143.2, pp. 650–660. ISSN: 14602156. DOI: 10.1093/brain/awz346.

Bloom, George S. (2014). "Amyloid-β and Tau". In: *JAMA Neurology* 71.4, p. 505. ISSN: 2168-6149. DOI: 10.1001/jamaneurol.2013.5847. URL: http://archneur.jamanetwork.com/article.aspx?doi=10.1001/jamaneurol.2013.5847.

Boluda, Susana et al. (2015). "Differential induction and spread of tau pathology in young PS19 tau transgenic mice following intracerebral injections of pathological tau from Alzheimer's disease or corticobasal degeneration brains". In: *Acta Neuropathologica* 129.2, pp. 221–237. ISSN: 14320533. DOI: 10.1007/s00401-014-1373-0.

Bondareff, W., C. Q. Mountjoy, and M. Roth (Feb. 1982). "Loss of neurons of origin of the adrenergic projection to cerebral cortex (nucleus locus ceruleus) in senile dementia". In: *Neurology* 32.2, pp. 164–164. ISSN: 0028-3878. DOI: 10.1212/WNL.32.2.164. URL: http://www.neurology.org/cgi/doi/10.1212/WNL.32.2.164.

Bouras, Constantin et al. (1994). "Regional distribution of neurofibrillary tangles and senile plaques in the cerebral cortex of elderly patients: A quantitative evaluation of a one-year autopsy population from a geriatric hospital". In: *Cerebral Cortex* 4.2, pp. 138–150. ISSN: 10473211. DOI: 10.1093/cercor/4.2.138.

Braak, H and E Braak (1991). "Neuropathological stageing of Alzheimer-related changes." In: *Acta neuropathologica* 82.4, pp. 239–59. ISSN: 0001-6322. URL: http://www.ncbi.nlm.nih.gov/pubmed/1759558.

Braak, H. and E. Braak (1996). "Development of Alzheimer-related neurofibrillary changes in the neocortex inversely recapitulates cortical myelogenesis". In: *Acta Neuropathologica* 92.2, pp. 197–201. ISSN: 00016322. DOI: 10.1007/s004010050508.

Braak, Heiko and Kelly Del Tredici (2014). "Are cases with tau pathology occurring in the absence of Aβ deposits part of the AD-related pathological process?" In: *Acta Neuropathologica* 128.6, pp. 767–772. ISSN: 14320533. DOI: 10.1007/s00401-014-1356-1.

Braak, Heiko and Kelly Del Tredici (2015). "The preclinical phase of the pathological process underlying sporadic Alzheimer's disease". In: *Brain* 138.10, pp. 2814–2833. ISSN: 14602156. DOI: 10.1093/brain/awv236.

Braak, Heiko et al. (2006). "Staging of Alzheimer disease-associated neurofibrillary pathology using paraffin sections and immunocytochemistry". In: *Acta Neuropathologica* 112.4, pp. 389–404. ISSN: 00016322. DOI: 10.1007/s00401-006-0127-z.

Braak, Heiko et al. (2011). "Stages of the pathologic process in alzheimer disease: Age categories from 1 to 100 years". In: *Journal of Neuropathology and Experimental Neurology* 70.11, pp. 960–969. ISSN: 00223069. DOI: 10.1097/NEN.0b013e318232a379.

Bramblett, Gregory T. et al. (1993). "Abnormal tau phosphorylation at Ser396 in alzheimer's disease recapitulates development and contributes to reduced microtubule binding". In: *Neuron* 10.6, pp. 1089–1099. ISSN: 08966273. DOI: 10.1016/0896-6273(93)90057-X.

Brettschneider, Johannes et al. (2015). "Spreading of pathology in neurodegenerative diseases: A focus on human studies". In: *Nature Reviews Neuroscience* 16.2, pp. 109–

120. ISSN: 14710048. DOI: 10.1038/nrn3887. URL: http://dx.doi.org/10.1038/nrn3887.

Brier, Matthew R et al. (2016). "Tau and A-beta imaging, CSF measures, and cognition in Alzheimer's disease". In: *Science Translational Medicine* 8.338, pp. 1–10. ISSN: 1946-6242. DOI: 10.1126/scitranslmed.aaf2362.

Bright, Jessica et al. (2015). "Human secreted tau increases amyloid-beta production". In: *Neurobiology of Aging* 36.2, pp. 693–709. ISSN: 15581497. DOI: 10.1016/j.neurobiolaging.2014.09.007. URL: http://dx.doi.org/10.1016/j.neurobiolaging.2014.09.007.

Brookmeyer, Ron et al. (2007). "Forecasting the global burden of Alzheimer's disease". In: *Alzheimer's and Dementia* 3.3, pp. 186–191. ISSN: 15525260. DOI: 10.1016/j.jalz.2007.04.381.

Brothers, Holly M., Maya L. Gosztyla, and Stephen R. Robinson (2018). "The physiological roles of amyloid-β peptide hint at new ways to treat Alzheimer's disease". In: *Frontiers in Aging Neuroscience* 10.APR, pp. 1–16. ISSN: 16634365. DOI: 10.3389/fnagi.2018.00118.

Brown, Jesse A. et al. (2019). "Patient-Tailored, Connectivity-Based Forecasts of Spreading Brain Atrophy". In: *Neuron* 104.5, pp. 856–868. ISSN: 08966273. DOI: 10.1016/j.neuron.2019.08.037. URL: https://doi.org/10.1016/j.neuron.2019.08.037.

Buckner, R. L. et al. (2009). "Cortical Hubs Revealed by Intrinsic Functional Connectivity: Mapping, Assessment of Stability, and Relation to Alzheimer's Disease". In: *Journal of Neuroscience* 29.6, pp. 1860–1873. ISSN: 0270-6474. DOI: 10.1523/JNEUROSCI.5062-08.2009. URL: http://www.jneurosci.org/cgi/doi/10.1523/JNEUROSCI.5062-08.2009.

Buckner, Randy L et al. (2005). "Molecular, Structural, and Functional Characterization of Alzheimer's Disease: Evidence for a Relationship between Default Activity, Amyloid, and Memory". In: *Neuroscience* 25.34, pp. 7709 –7717. ISSN: 0270-6474. DOI: 10.1523/JNEUROSCI.2177-05.2005.

Buée, Luc et al. (2000). "Tau protein isoforms, phosphorylation and role in neurodegenerative disorders". In: *Brain Research Reviews* 33.1, pp. 95–130. ISSN: 01650173. DOI: 10.1016/S0165-0173(00)00019-9.

Buerger, Katharina et al. (2006). "CSF phosphorylated tau protein correlates with neocortical neurofibrillary pathology in Alzheimer's disease". In: *Brain* 129.11, pp. 3035–3041. ISSN: 14602156. DOI: 10.1093/brain/awl269.

Bullmann, Torsten et al. (2009). "Pattern of tau isoforms expression during development in vivo". In: *International Journal of Developmental Neuroscience* 27.6, pp. 591–597. ISSN: 07365748. DOI: 10.1016/j.ijdevneu.2009.06.001.

Busche, Marc Aurel et al. (2019). "Alzheimer models in vivo". In: 22.1, pp. 57–64. DOI: 10.1038/s41593-018-0289-8.Tau.

Bussian, Tyler J. et al. (2018). "Clearance of senescent glial cells prevents tau-dependent pathology and cognitive decline". In: *Nature* 562.7728, pp. 578–582. ISSN: 14764687. DOI: 10.1038/s41586-018-0543-y. URL: http://dx.doi.org/10.1038/s41586-018-0543-y.

Byun, Min Soo et al. (2015). "Heterogeneity of regional brain atrophy patterns associated with distinct progression rates in Alzheimer's disease". In: *PLoS ONE* 10.11, pp. 1–16. ISSN: 19326203. DOI: 10.1371/journal.pone.0142756.

Calderón-Garcidueas, Lilian et al. (2012). "Neuroinflammation, hyperphosphorylated tau, diffuse amyloid plaques, and down-regulation of the cellular prion protein in air pollution exposed children and young adults". In: *Journal of Alzheimer's Disease* 28.1, pp. 93–107. ISSN: 18758908. DOI: 10.3233/JAD-2011-110722.

Calderón-Garcidueñas, Lilian et al. (2018). "Hallmarks of Alzheimer disease are evolving relentlessly in Metropolitan Mexico City infants, children and young adults. APOE4 carriers have higher suicide risk and higher odds of reaching NFT stage V at 40 years of age". In: *Environmental Research* 164.December 2017, pp. 475–487. ISSN: 10960953. DOI: 10.1016/j.envres.2018.03.023. URL: https://doi.org/10.1016/j.envres.2018.03.023.

Califf, Robert M. (2018). "Biomarker definitions and their applications". In: *Experimental Biology and Medicine* 243.3, pp. 213–221. ISSN: 15353699. DOI: 10.1177/1535370217750088.

Callahan, Linda M., William A. Vaules, and Paul D. Coleman (Mar. 1999). "Quantitative Decrease in Synaptophysin Message Expression and Increase in Cathepsin D Message Expression in Alzheimer Disease Neurons Containing Neurofibrillary Tangles". In: *Journal of Neuropathology and Experimental Neurology* 58.3, pp. 275–287. ISSN: 0022-3069. DOI: 10.1097/00005072-199903000-00007. URL: https://academic.oup.com/jnen/article-lookup/doi/10.1097/00005072-199903000-00007.

Cash, Adam D. et al. (2003). "Microtubule reduction in Alzheimer's disease and aging is independent of τ filament formation". In: *American Journal of Pathology* 162.5, pp. 1623–1627. ISSN: 00029440. DOI: 10.1016/S0002-9440(10)64296-4.

Chai, Xiyun, Jeffrey L. Dage, and Martin Citron (2012). "Constitutive secretion of tau protein by an unconventional mechanism". In: *Neurobiology of Disease* 48.3, pp. 356–366. ISSN: 09699961. DOI: 10.1016/j.nbd.2012.05.021. URL: http://dx.doi.org/10.1016/j.nbd.2012.05.021.

Chambers, James K. et al. (2015). "The domestic cat as a natural animal model of Alzheimer's disease". In: *Acta neuropathologica communications* 3, p. 78. ISSN:

20515960. DOI: 10.1186/s40478-015-0258-3. URL: http://dx.doi.org/10.1186/s40478-015-0258-3.

Chan, Lung Tat Andrew et al. (2015). "Prodromal posterior cortical atrophy: clinical, neuropsychological, and radiological correlation." In: *Neurocase* 21.1, pp. 44–55. ISSN: 1465-3656. DOI: 10.1080/13554794.2013.860176. URL: http://www.pubmedcentral.nih.gov/articlerender.fcgi?artid=4318700&tool=pmcentrez&rendertype=abstract.

Charil, Arnaud et al. (2019). "Tau Subtypes of Alzheimer's Disease Determined in vivo Using Flortaucipir PET Imaging". In: *Journal of Alzheimer's Disease* 71.3, pp. 1037–1048. ISSN: 18758908. DOI: 10.3233/JAD-190264.

Chartoire, Nathalie et al. (2007). "Resource Systematic Gene Expression Mapping Clusters Nuclear Receptors According to Their Function in the Brain Franc". In: pp. 405–418. DOI: 10.1016/j.cell.2007.09.012.

Chávez-Gutiérrez, Lucía et al. (May 2012). "The mechanism of γ-Secretase dysfunction in familial Alzheimer disease". In: *The EMBO Journal* 31.10, pp. 2261–2274. ISSN: 02614189. DOI: 10.1038/emboj.2012.79. URL: http://emboj.embopress.org/cgi/doi/10.1038/emboj.2012.79.

Chen, J. et al. (1992). "Projection domains of MAP2 and tau determine spacings between microtubules in dendrites and axons". In: *Nature* 360.6405, pp. 674–677. ISSN: 00280836. DOI: 10.1038/360674a0.

Chhatwal, Jasmeer P et al. (2016). "Temporal T807 binding correlates with CSF tau and phospho-tau in normal elderly". In: ISSN: 0028-3878. DOI: 10.1212/WNL.0000000000003050.

Chien, David T. et al. (2013). "Early Clinical PET Imaging Results with the Novel PHF-Tau Radioligand [F-18]-T807". In: *Journal of Alzheimer's Disease* 34.2, pp. 457–468. DOI: 10.3233/JAD-122059.

Chiotis, Konstantinos et al. (2016). "Imaging in-vivo tau pathology in Alzheimer's disease with THK5317 PET in a multimodal paradigm". In: *European Journal of Nuclear Medicine and Molecular Imaging*, pp. 1–14. ISSN: 16197089. DOI: 10.1007/s00259-016-3363-z.

Cho, Hanna et al. (Aug. 2016a). "In vivo cortical spreading pattern of tau and amyloid in the Alzheimer disease spectrum". In: *Annals of Neurology* 80.2, pp. 247–258. ISSN: 03645134. DOI: 10.1002/ana.24711. URL: http://doi.wiley.com/10.1002/ana.24711.

Cho, Hanna et al. (2016b). "Tau PET in Alzheimer disease and mild cognitive impairment." In: *Neurology*, pp. 1–10. ISSN: 1526-632X. DOI: 10.1212/WNL.0000000000002892. URL: http://www.ncbi.nlm.nih.gov/pubmed/27358341.

Cho, Hanna et al. (2017). "18F-AV-1451 binds to motor-related subcortical gray and white matter in corticobasal syndrome". In: *Neurology* 89.11, pp. 1170–1178. ISSN: 1526632X. DOI: 10.1212/WNL.0000000000004364.

Cho, Hanna et al. (Aug. 2018). "Predicted sequence of cortical tau and amyloid-β deposition in Alzheimer disease spectrum". In: *Neurobiology of Aging* 68.January 2015, pp. 76–84. ISSN: 01974580. DOI: 10.1016/j.neurobiolaging.2018.04.007. URL: https://doi.org/10.1016/j.neurobiolaging.2018.04.007https://linkinghub.elsevier.com/retrieve/pii/S0197458018301295.

Choi, Jae Yong et al. (Jan. 2018). "Off-Target 18 F-AV-1451 Binding in the Basal Ganglia Correlates with Age-Related Iron Accumulation". In: *Journal of Nuclear Medicine* 59.1, pp. 117–120. ISSN: 0161-5505. DOI: 10.2967/jnumed.117.195248. URL: http://jnm.snmjournals.org/lookup/doi/10.2967/jnumed.117.195248.

Ch??telat, Ga??l et al. (2010). "Relationship between atrophy and ??-amyloid deposition in Alzheimer disease". In: *Annals of Neurology* 67.3, pp. 317–324. ISSN: 03645134. DOI: 10.1002/ana.21955.

Chung, Chul Woong et al. (2001). "Proapoptotic effects of Tau cleavage product generated by caspase-3". In: *Neurobiology of Disease* 8.1, pp. 162–172. ISSN: 09699961. DOI: 10.1006/nbdi.2000.0335.

Cirrito, John R. et al. (2005). "Synaptic activity regulates interstitial fluid amyloid-β levels in vivo". In: *Neuron* 48.6, pp. 913–922. ISSN: 08966273. DOI: 10.1016/j.neuron.2005.10.028.

Ciryam, Prajwal et al. (Feb. 2015). "Supersaturation is a major driving force for protein aggregation in neurodegenerative diseases". In: *Trends in Pharmacological Sciences* 36.2, pp. 72–77. ISSN: 01656147. DOI: 10.1016/j.tips.2014.12.004. URL: https://linkinghub.elsevier.com/retrieve/pii/S016561471400217X.

Ciryam, Prajwal et al. (2016). "A transcriptional signature of Alzheimer's disease is associated with a metastable subproteome at risk for aggregation". In: *Proceedings of the National Academy of Sciences of the United States of America* 113.17, pp. 4753–4758. ISSN: 10916490. DOI: 10.1073/pnas.1516604113.

Clavaguera, Florence et al. (2009). "Transmission and spreading of tauopathy in transgenic mouse brain". In: *Nature Cell Biology* 11.7, pp. 909–913. ISSN: 14657392. DOI: 10.1038/ncb1901.

Clavaguera, Florence et al. (2013). "Brain homogenates from human tauopathies induce tau inclusions in mouse brain". In: *Proceedings of the National Academy of Sciences* 110.23, pp. 9535–9540. ISSN: 0027-8424. DOI: 10.1073/pnas.1301175110. URL: http://www.pnas.org/lookup/doi/10.1073/pnas.1301175110.

Cleveland, Don W., Shu Ying Hwo, and Marc W. Kirschner (1977). "Purification of tau, a microtubule-associated protein that induces assembly of microtubules

from purified tubulin". In: *Journal of Molecular Biology* 116.2, pp. 207–225. ISSN: 00222836. DOI: 10.1016/0022-2836(77)90213-3.

Congdon, Erin E. and Einar M. Sigurdsson (2018). "Tau-targeting therapies for Alzheimer disease". In: *Nature Reviews Neurology* 14.7, pp. 399–415. ISSN: 17594766. DOI: 10.1038/s41582-018-0013-z. URL: http://dx.doi.org/10.1038/s41582-018-0013-z.

Connelly, P. J., N. P. Prentice, and K. G. Fowler (2005). "Predicting the outcome of cholinesterase inhibitor treatment in Alzheimer's disease". In: *Journal of Neurology, Neurosurgery and Psychiatry* 76.3, pp. 320–324. ISSN: 00223050. DOI: 10.1136/jnnp.2004.043539.

Cope, Thomas E et al. (2018). "Tau burden and the functional connectome in Alzheimer's disease and progressive supranuclear palsy". In: *Brain* 141.2, pp. 550–567. ISSN: 14602156. DOI: 10.1093/brain/awx347.

Corder, Elizabeth H. (Feb. 1995). "The Apolipoprotein E E4 Allele and Sex-Specific Risk of Alzheimer's Disease". In: *JAMA: The Journal of the American Medical Association* 273.5, p. 373. ISSN: 0098-7484. DOI: 10.1001/jama.1995.03520290025013. URL: http://jama.jamanetwork.com/article.aspx?doi=10.1001/jama.1995.03520290025013.

Crane, Paul K. et al. (2012). "Development and assessment of a composite score for memory in the Alzheimer's Disease Neuroimaging Initiative (ADNI)". In: *Brain Imaging and Behavior* 6.4, pp. 502–516. ISSN: 19317557. DOI: 10.1007/s11682-012-9186-z.

Crane, Paul K. et al. (Dec. 2017). "Incidence of cognitively defined late-onset Alzheimer's dementia subgroups from a prospective cohort study". In: *Alzheimer's & Dementia* 13.12, pp. 1307–1316. ISSN: 15525260. DOI: 10.1016/j.jalz.2017.04.011. URL: http://dx.doi.org/10.1016/j.jalz.2017.04.011http://doi.wiley.com/10.1016/j.jalz.2017.04.011.

Crary, John F. et al. (2014). "Primary age-related tauopathy (PART): a common pathology associated with human aging". In: *Acta Neuropathologica* 128.6, pp. 755–766. ISSN: 14320533. DOI: 10.1007/s00401-014-1349-0.

Crimins, Johanna L. et al. (June 2013). "The intersection of amyloid beta and tau in glutamatergic synaptic dysfunction and collapse in Alzheimer's disease". In: *Ageing Research Reviews* 12.3, pp. 757–763. ISSN: 15681637. DOI: 10.1016/j.arr.2013.03.002. URL: https://linkinghub.elsevier.com/retrieve/pii/S1568163713000159.

Crossley, Nicolas A. et al. (2014). "The hubs of the human connectome are generally implicated in the anatomy of brain disorders". In: *Brain* 137.8, pp. 2382–2395. ISSN: 14602156. DOI: 10.1093/brain/awu132.

Crutch, Sebastian J et al. (Feb. 2012). "Posterior cortical atrophy". In: *The Lancet Neurology* 11.2, pp. 170–178. ISSN: 14744422. DOI: 10.1016/S1474-4422(11)70289-7. URL: https://linkinghub.elsevier.com/retrieve/pii/S1474442211702897.

Damoiseaux, Jessica S. et al. (2012). "Functional connectivity tracks clinical deterioration in Alzheimer's disease". In: *Neurobiology of Aging* 33.4, pp. 19–828. ISSN: 01974580. DOI: 10.1016/j.neurobiolaging.2011.06.024. URL: http://dx.doi.org/10.1016/j.neurobiolaging.2011.06.024.

Dawson, Hana N. et al. (2001). "Inhibition of neuronal maturation in primary hippocampal neurons from tau deficient mice". In: *Journal of Cell Science* 114.6, pp. 1179–1187. ISSN: 00219533.

Day, Gregory S. et al. (2017). "Tau-PET Binding Distinguishes Patients With Early-stage Posterior Cortical Atrophy From Amnestic Alzheimer Disease Dementia". In: *Alzheimer Disease and Associated Disorders* 31.2, pp. 87–93. ISSN: 08930341. DOI: 10.1097/WAD.0000000000000196.

De Calignon, Alix et al. (2010). "Caspase activation precedes and leads to tangles". In: *Nature* 464.7292, pp. 1201–1204. ISSN: 00280836. DOI: 10.1038/nature08890. URL: http://dx.doi.org/10.1038/nature08890.

De Calignon, Alix et al. (2012). "Propagation of Tau Pathology in a Model of Early Alzheimer's Disease". In: *Neuron* 73.4, pp. 685–697. ISSN: 08966273. DOI: 10.1016/j.neuron.2011.11.033.

De Strooper, Bart et al. (1998). "deficiency of presenilin 1 inhibits the normal cleavage of APP". In: *Nature* 391.January, pp. 387–390.

Decker, Jochen Martin et al. (2015). "Pro-aggregant Tau impairs mossy fiber plasticity due to structural changes and Ca(++) dysregulation". In: *Acta neuropathologica communications* 3, p. 23. ISSN: 20515960. DOI: 10.1186/s40478-015-0193-3.

Declercq, Lieven et al. (2017). "Preclinical evaluation of 18F-JNJ64349311, a novel PET tracer for tau imaging". In: *Journal of Nuclear Medicine* 58.6, pp. 975–981. ISSN: 2159662X. DOI: 10.2967/jnumed.116.185199.

DeKosky, Steven T. and Stephen W. Scheff (1990). "Synapse loss in frontal cortex biopsies in Alzheimer's disease: Correlation with cognitive severity". In: *Annals of Neurology* 27.5, pp. 457–464. ISSN: 15318249. DOI: 10.1002/ana.410270502.

Derflinger, Sabine et al. (2011). "Grey-matter atrophy in Alzheimer's disease is asymmetric but not lateralized". In: *Journal of Alzheimer's Disease* 25.2, pp. 347–357. ISSN: 18758908. DOI: 10.3233/JAD-2011-110041.

Desikan, Rahul S. et al. (2006). "An automated labeling system for subdividing the human cerebral cortex on MRI scans into gyral based regions of interest". In: *NeuroImage* 31.3, pp. 968–980. ISSN: 10538119. DOI: 10.1016/j.neuroimage.2006.01.021.

Devenyi, Gabriel A (2018). "gdevenyi/AllenHumanGeneMNI: Nonlinear registration". In: *Dataset on Zenodo*. DOI: 10.5281/ZENODO.2483290. URL: https://doi.org/10.5281/zenodo.2483290.

DeVos, S. L. et al. (2013). "Antisense Reduction of Tau in Adult Mice Protects against Seizures". In: *Journal of Neuroscience* 33.31, pp. 12887–12897. ISSN: 0270-6474. DOI: 10.1523/JNEUROSCI.2107-13.2013. URL: http://www.jneurosci.org/cgi/doi/10.1523/JNEUROSCI.2107-13.2013.

DeVos, Sarah L. et al. (2018a). "Synaptic tau seeding precedes tau pathology in human Alzheimer's disease brain". In: *Frontiers in Neuroscience* 12.APR, pp. 1–15. ISSN: 1662453X. DOI: 10.3389/fnins.2018.00267.

DeVos, Sarah L. et al. (2018b). "Tau reduction in the presence of amyloid-β prevents tau pathology and neuronal death in vivo". In: *Brain* 141.7, pp. 2194–2212. ISSN: 14602156. DOI: 10.1093/brain/awy117.

Dickerson, B. C. and D. A. Wolk (Jan. 2011). "Dysexecutive versus amnesic phenotypes of very mild Alzheimer's disease are associated with distinct clinical, genetic and cortical thinning characteristics". In: *Journal of Neurology, Neurosurgery & Psychiatry* 82.1, pp. 45–51. ISSN: 0022-3050. DOI: 10.1136/jnnp.2009.199505. URL: http://jnnp.bmj.com/cgi/doi/10.1136/jnnp.2009.199505.

Dickerson, B. C. et al. (2011). "Alzheimer-signature MRI biomarker predicts AD dementia in cognitively normal adults". In: *Neurology* 76.16, pp. 1395–1402. ISSN: 00283878. DOI: 10.1212/WNL.0b013e3182166e96.

Dickson, Dennis W., Rosa Rademakers, and Michael L. Hutton (2007). "Progressive supranuclear palsy: Pathology and genetics". In: *Brain Pathology* 17.1, pp. 74–82. ISSN: 10156305. DOI: 10.1111/j.1750-3639.2007.00054.x.

Dixit, Ram et al. (2010). "Cultural and social aspects of HIV AIDS sex education in secondary". In: *Journal of Biosocial Science* 319.5866, pp. 1086–1089. ISSN: 00219320. DOI: 10.1126/science.1152993.Differential. URL: http://10.0.3.249/S0021932004006820%0Ahttps://search.ebscohost.com/login.aspx?direct=true&db=a9h&AN=20136870&site=ehost-live.

Dong, Aoyan et al. (2017). "Heterogeneity of neuroanatomical patterns in prodromal Alzheimer's disease: links to cognition, progression and biomarkers". In: *Brain : a journal of neurology* 140.3, pp. 735–747. ISSN: 14602156. DOI: 10.1093/brain/aww319.

Donohue, Michael C. et al. (2017). "Association between elevated brain amyloid and subsequent cognitive decline among cognitively normal persons". In: *JAMA - Journal of the American Medical Association* 317.22, pp. 2305–2316. ISSN: 15383598. DOI: 10.1001/jama.2017.6669.

Drake, Lindsey et al. (May 2018). "[18F]AV1451 is a Weak Inhibitor of Monoamine Oxidase (MAO) A and B". In: *Journal of Nuclear Medicine* 59.supplement 1, p. 549. URL: http://jnm.snmjournals.org/content/59/supplement_1/549.abstract.

Drake, Lindsey et al. (May 2019). "MAO-B Inhibitor Deprenyl Displaces [18F]AV1451 binding on human brain tissue sections and alters uptake in Nonhuman Primate Brain". In: *Journal of Nuclear Medicine* 60.supplement 1, p. 487. URL: http://jnm.snmjournals.org/content/60/supplement_1/487.abstract.

Drechsel, D N et al. (1992). "<Drechsel 1992 Mol Biol Cell_tau prot.pdf>". In: 3.October, pp. 1141–1154.

Dronse, Julian et al. (2017). "In vivo Patterns of Tau Pathology, Amyloid-β Burden, and Neuronal Dysfunction in Clinical Variants of Alzheimer's Disease". In: *Journal of Alzheimer's Disease* 55.2, pp. 465–471. ISSN: 18758908. DOI: 10.3233/JAD-160316.

Drubin, D. G., D. Caput, and M. W. Kirschner (1984). "Studies on the expression of the microtubule-associated protein, tau, during mouse brain development, with newly isolated complementary DNA probes". In: *Journal of Cell Biology* 98.3, pp. 1090–1097. ISSN: 00219525. DOI: 10.1083/jcb.98.3.1090.

Drummond, Eleanor et al. (2017). "Proteomic differences in amyloid plaques in rapidly progressive and sporadic Alzheimer's disease". In: *Acta Neuropathologica* 133.6, pp. 933–954. ISSN: 14320533. DOI: 10.1007/s00401-017-1691-0.

Dujardin, Simon et al. (2014). "Neuron-to-neuron wild-type Tau protein transfer through a trans-synaptic mechanism: Relevance to sporadic tauopathies". In: *Acta Neuropathologica Communications* 2.1, pp. 1–14. ISSN: 20515960. DOI: 10.1186/2051-5960-2-14.

Dujardin, Simon et al. (2018). "Different tau species lead to heterogeneous tau pathology propagation and misfolding". In: *Acta neuropathologica communications* 6.1, p. 132. ISSN: 20515960. DOI: 10.1186/s40478-018-0637-7.

Duyckaerts, Charles et al. (1997). "Dissociation of Alzheimer type pathology in a disconnected piece of cortex". In: *Acta Neuropathologica* 93.5, pp. 501–507. ISSN: 00016322. DOI: 10.1007/s004010050645.

Duyckaerts, Charles et al. (2015). "PART is part of Alzheimer disease". In: *Acta Neuropathologica* 129.5, pp. 749–756. ISSN: 0001-6322. DOI: 10.1007/s00401-015-1390-7. URL: http://link.springer.com/10.1007/s00401-015-1390-7.

Duyckaerts, Charles et al. (2018). "Neuropathology of iatrogenic Creutzfeldt–Jakob disease and immunoassay of French cadaver-sourced growth hormone batches suggest possible transmission of tauopathy and long incubation periods for the transmission of Abeta pathology". In: *Acta Neuropathologica* 135.2, pp. 201–212. ISSN: 14320533. DOI: 10.1007/s00401-017-1791-x. URL: https://doi.org/10.1007/s00401-017-1791-x.

Eftekharzadeh, Bahareh et al. (2018). "Tau Protein Disrupts Nucleocytoplasmic Transport in Alzheimer's Disease". In: *Neuron* 99.5, pp. 925–940. ISSN: 10974199. DOI: 10.1016/j.neuron.2018.07.039. URL: https://doi.org/10.1016/j.neuron.2018.07.039.

Elobeid, Adila, Hilkka Soininen, and Irina Alafuzoff (2012). "Hyperphosphorylated tau in young and middle-aged subjects". In: *Acta Neuropathologica* 123.1, pp. 97–104. ISSN: 00016322. DOI: 10.1007/s00401-011-0906-z.

Escobar-Khondiker, Myriam et al. (2007). "Annonacin, a natural mitochondrial complex I inhibitor, causes tau pathology in cultured neurons". In: *Journal of Neuroscience* 27.29, pp. 7827–7837. ISSN: 02706474. DOI: 10.1523/JNEUROSCI.1644-07.2007.

Esparza, Thomas J. et al. (Jan. 2013). "Amyloid-beta oligomerization in Alzheimer dementia versus high-pathology controls". In: *Annals of Neurology* 73.1, pp. 104–119. ISSN: 03645134. DOI: 10.1002/ana.23748. URL: http://doi.wiley.com/10.1002/ana.23748.

Fagan, Anne M et al. (2014). "Longitudinal change in CSF biomarkers in autosomal-dominant Alzheimer's disease." In: *Science translational medicine* 6.226, 226ra30. ISSN: 1946-6242. DOI: 10.1126/scitranslmed.3007901.

Fagan, Tom (2018). *Flortaucipir Meets Primary Endpoints in Phase 3 Autopsy Trial*.

Farias, Sarah Tomaszewski et al. (July 2008). "The measurement of everyday cognition (ECog): scale development and psychometric properties." In: *Neuropsychology* 22.4, pp. 531–44. ISSN: 0894-4105. DOI: 10.1037/0894-4105.22.4.531. URL: http://www.ncbi.nlm.nih.gov/pubmed/18590364http://www.pubmedcentral.nih.gov/articlerender.fcgi?artid=PMC2877034.

Fath, Thomas, Jochen Eidenmüller, and Roland Brandt (2002). "Tau-mediated cytotoxicity in a pseudohyperphosphorylation model of Alzheimer's disease". In: *Journal of Neuroscience* 22.22, pp. 9733–9741. ISSN: 02706474. DOI: 10.1523/jneurosci.22-22-09733.2002.

Ferreira, Daniel, Agneta Nordberg, and Eric Westman (2020). "Biological subtypes of Alzheimer's disease: a systematic review and meta-analysis". In: *Neurology* 0, under–review. DOI: 10.1212/WNL.0000000000009058.

Ferreira, Daniel et al. (2018). "The contribution of small vessel disease to subtypes of Alzheimer's disease: a study on cerebrospinal fluid and imaging biomarkers". In: *Neurobiology of Aging* 70, pp. 18–29. ISSN: 15581497. DOI: 10.1016/j.neurobiolaging.2018.05.028. URL: https://doi.org/10.1016/j.neurobiolaging.2018.05.028.

Ferreira, Daniel et al. (2019). "Subtypes of Alzheimer's disease display distinct network abnormalities extending beyond their pattern of brain atrophy". In: *Frontiers in Neurology* 10.MAY. ISSN: 16642295. DOI: 10.3389/fneur.2019.00524.

Fiock, Kimberly L. et al. (2020). "B-Amyloid and Tau Pathology in the Aging Feline Brain". In: *Journal of Comparative Neurology* 528.1, pp. 108–113. ISSN: 10969861. DOI: 10.1002/cne.24741.

Firth, Nicholas C. et al. (2019). "Longitudinal neuroanatomical and cognitive progression of posterior cortical atrophy". In: *Brain* 142.7, pp. 2082–2095. ISSN: 14602156. DOI: 10.1093/brain/awz136.

Fischer, Corinne E. et al. (2017). "Determining the impact of psychosis on rates of false-positive and false-negative diagnosis in Alzheimer's disease". In: *Alzheimer's and Dementia: Translational Research and Clinical Interventions* 3.3, pp. 385–392. ISSN: 23528737. DOI: 10.1016/j.trci.2017.06.001. URL: http://dx.doi.org/10.1016/j.trci.2017.06.001.

Flach, Katharina et al. (2012). "Tau oligomers impair artificial membrane integrity and cellular viability". In: *Journal of Biological Chemistry* 287.52, pp. 43223–43233. ISSN: 00219258. DOI: 10.1074/jbc.M112.396176.

Fletcher, Evan et al. (2018). "Staging of amyloid β, t-tau, regional atrophy rates, and cognitive change in a nondemented cohort: Results of serial mediation analyses". In: *Alzheimer's and Dementia: Diagnosis, Assessment and Disease Monitoring* 10, pp. 382–393. ISSN: 23528729. DOI: 10.1016/j.dadm.2018.04.001.

Flier, Wiesje M. van der et al. (2011). "Early-onset versus late-onset Alzheimer's disease: The case of the missing APOE ϵ4 allele". In: *The Lancet Neurology* 10.3, pp. 280–288. ISSN: 14744422. DOI: 10.1016/S1474-4422(10)70306-9. URL: http://dx.doi.org/10.1016/S1474-4422(10)70306-9.

Foley, Sonya F. et al. (2017). "Multimodal Brain Imaging Reveals Structural Differences in Alzheimer's Disease Polygenic Risk Carriers: A Study in Healthy Young Adults". In: *Biological Psychiatry* 81.2, pp. 154–161. ISSN: 18732402. DOI: 10.1016/j.biopsych.2016.02.033. URL: http://dx.doi.org/10.1016/j.biopsych.2016.02.033.

Folstein, M F, Susan E Folstein, and Paul R McHugh (Nov. 1975). ""Mini-mental state". A practical method for grading the cognitive state of patients for the clinician." In: *Journal of psychiatric research* 12.3, pp. 189–98. ISSN: 0022-3956. DOI: 10.1016/0022-3956(75)90026-6. URL: http://dx.doi.org/10.1016/0022-3956(75)90026-6http://www.ncbi.nlm.nih.gov/pubmed/1202204.

Frandemiche, Marie Lise et al. (2014). "Activity-dependent tau protein translocation to excitatory synapse is disrupted by exposure to amyloid-beta oligomers".

In: *Journal of Neuroscience* 34.17, pp. 6084–6097. ISSN: 15292401. DOI: 10.1523/JNEUROSCI.4261-13.2014.

Franzmeier, Nicolai et al. (Feb. 2019). "Functional connectivity associated with tau levels in ageing, Alzheimer's, and small vessel disease". In: *Brain*, pp. 1–15. ISSN: 0006-8950. DOI: 10.1093/brain/awz026. URL: https://academic.oup.com/brain/advance-article/doi/10.1093/brain/awz026/5321130.

Franzmeier, Nicolai et al. (Dec. 2020). "Functional brain architecture is associated with the rate of tau accumulation in Alzheimer's disease". In: *Nature Communications* 11.1, p. 347. ISSN: 2041-1723. DOI: 10.1038/s41467-019-14159-1. URL: http://www.nature.com/articles/s41467-019-14159-1.

Fred, Ana L N and Anil K Jain (2005). "Combining Multiple Clusterings Using Evidence Accumulation". In: *IEEE Trans Pattern Anal Mach Intell* 27.6, pp. 835–850. DOI: 10.1109/TPAMI.2005.113.

Freer, Rosie et al. (2016). "A protein homeostasis signature in healthy brains recapitulates tissue vulnerability to Alzheimer ' s disease". In: August, pp. 1–8. ISSN: 2375-2548. DOI: 10.1126/sciadv.1600947.

Frisoni, Giovanni B et al. (Aug. 2017). "Strategic roadmap for an early diagnosis of Alzheimer's disease based on biomarkers." In: *The Lancet. Neurology* 16.8, pp. 661–676. ISSN: 1474-4465. DOI: 10.1016/S1474-4422(17)30159-X. URL: http://www.ncbi.nlm.nih.gov/pubmed/28721928.

Frost, Bess and Marc I. Diamond (Mar. 2010). "Prion-like mechanisms in neurodegenerative diseases". In: *Nature Reviews Neuroscience* 11.3, pp. 155–159. ISSN: 1471-003X. DOI: 10.1038/nrn2786. URL: http://www.ncbi.nlm.nih.gov/pubmed/20029438http://www.pubmedcentral.nih.gov/articlerender.fcgi?artid=PMC3648341http://www.nature.com/articles/nrn2786.

Frost, Bess, Rachel L. Jacks, and Marc I. Diamond (2009). "Propagation of Tau misfolding from the outside to the inside of a cell". In: *Journal of Biological Chemistry* 284.19, pp. 12845–12852. ISSN: 00219258. DOI: 10.1074/jbc.M808759200.

Frost, Bess et al. (Mar. 2014). "Tau promotes neurodegeneration through global chromatin relaxation". In: *Nature Neuroscience* 17.3, pp. 357–366. ISSN: 1097-6256. DOI: 10.1038/nn.3639. URL: http://www.nature.com/articles/nn.3639.

Fu, Hongjun, John Hardy, and Karen E. Duff (2018). "Selective vulnerability in neurodegenerative diseases". In: *Nature Neuroscience* 21.10, pp. 1350–1358. ISSN: 15461726. DOI: 10.1038/s41593-018-0221-2.

Fu, Hongjun et al. (2019). "A tau homeostasis signature is linked with the cellular and regional vulnerability of excitatory neurons to tau pathology". In: *Nature Neuroscience* 22.1, pp. 47–56. ISSN: 15461726. DOI: 10.1038/s41593-018-0298-7. URL: http://dx.doi.org/10.1038/s41593-018-0298-7.

Fulga, Tudor A. et al. (2007). "Abnormal bundling and accumulation of F-actin mediates tau-induced neuronal degeneration in vivo". In: *Nature Cell Biology* 9.2, pp. 139–148. ISSN: 14657392. DOI: 10.1038/ncb1528.

Furman, Jennifer L et al. (2017). "Widespread Tau Seeding Activity at Early Braak Stages HHS Public Access Author manuscript". In: *Acta Neuropathol* 133.1, pp. 91–100. DOI: 10.1007/s00401-016-1644-z. URL: https://www.ncbi.nlm.nih.gov/pmc/articles/PMC5833300/pdf/nihms916392.pdf.

Fuster-Matanzo, Almudena, Félix Hernández, and Jesús Ávila (Feb. 2018). "Tau Spreading Mechanisms; Implications for Dysfunctional Tauopathies". In: *International Journal of Molecular Sciences* 19.3, p. 645. ISSN: 1422-0067. DOI: 10.3390/ijms19030645. URL: http://www.mdpi.com/1422-0067/19/3/645.

Gamblin, T. Chris et al. (2003). "Caspase cleavage of tau: Linking amyloid and neurofibrillary tangles in Alzheimer's disease". In: *Proceedings of the National Academy of Sciences of the United States of America* 100.17, pp. 10032–10037. ISSN: 00278424. DOI: 10.1073/pnas.1630428100.

Garcia-Garcia, Manuel et al. (July 2017). "Detecting stable individual differences in the functional organization of the human basal ganglia." In: *NeuroImage* December 2016, pp. 1–15. ISSN: 1095-9572. DOI: 10.1016/j.neuroimage.2017.07.029. URL: http://linkinghub.elsevier.com/retrieve/pii/S1053811917305979http://www.ncbi.nlm.nih.gov/pubmed/28739120.

Ghosh, Abhinaba et al. (2019). "An experimental model of Braak's pretangle proposal for the origin of Alzheimer's disease: The role of locus coeruleus in early symptom development". In: *Alzheimer's Research and Therapy* 11.1, pp. 1–17. ISSN: 17589193. DOI: 10.1186/s13195-019-0511-2.

Ginsberg, Stephen D. et al. (2000). "Expression profile of transcripts in Alzheimer's disease tangle-bearing CA1 neurons". In: *Annals of Neurology* 48.1, pp. 77–87. ISSN: 03645134. DOI: 10.1002/1531-8249(200007)48:1<77::AID-ANA12>3.0.CO;2-A.

Gobbi, Luca C. et al. (2017). "Identification of Three Novel Radiotracers for Imaging Aggregated Tau in Alzheimer's Disease with Positron Emission Tomography". In: *Journal of Medicinal Chemistry* 60.17, pp. 7350–7370. ISSN: 15204804. DOI: 10.1021/acs.jmedchem.7b00632.

Goedert, M. and R. Jakes (1990). "Expression of separate isoforms of human tau protein: correlation with the tau pattern in brain and effects on tubulin polymerization." In: *The EMBO Journal* 9.13, pp. 4225–4230. ISSN: 0261-4189. DOI: 10.1002/j.1460-2075.1990.tb07870.x.

Goedert, M. et al. (1989). "Multiple isoforms of human microtubule-associated protein tau: sequences and localization in neurofibrillary tangles of Alzheimer's disease". In: *Neuron* 3.4, pp. 519–526. ISSN: 08966273. DOI: 10.1016/0896-6273(89)90210-9.

Goedert, M. et al. (1992). "Tau proteins of alzheimer paired helical filaments: Abnormal phosphorylation of all six brain isoforms". In: *Neuron* 8.1, pp. 159–168. ISSN: 08966273. DOI: 10.1016/0896-6273(92)90117-V.

Goedert, M. et al. (1996). *Assembly of microtubule-associated protein tau into Alzheimer-like filaments induced by sulphated glycosaminoglycans*. DOI: 10.1038/383550a0.

Goedert, Michel, David S. Eisenberg, and R. Anthony Crowther (July 2017). "Propagation of Tau Aggregates and Neurodegeneration". In: *Annual Review of Neuroscience* 40.1, pp. 189–210. ISSN: 0147-006X. DOI: 10.1146/annurev-neuro-072116-031153. URL: http://www.annualreviews.org/doi/10.1146/annurev-neuro-072116-031153.

Goedert, Michel and Ross Jakes (2005). "Mutations causing neurodegenerative tauopathies". In: *Biochimica et Biophysica Acta - Molecular Basis of Disease* 1739.2, pp. 240–250. ISSN: 09254439. DOI: 10.1016/j.bbadis.2004.08.007.

Gomes, Luis Aragão et al. (2019). "Aβ-induced acceleration of Alzheimer-related τ-pathology spreading and its association with prion protein". In: *Acta Neuropathologica* 138.6, pp. 913–941. ISSN: 14320533. DOI: 10.1007/s00401-019-02053-5. URL: https://doi.org/10.1007/s00401-019-02053-5.

Gómez-Isla, Teresa et al. (Jan. 1997). "Neuronal loss correlates with but exceeds neurofibrillary tangles in Alzheimer's disease". In: *Annals of Neurology* 41.1, pp. 17–24. ISSN: 03645134. DOI: 10.1002/ana.410410106. URL: http://doi.wiley.com/10.1002/ana.410410106.

Gordon, Brian A. et al. (2016). "The relationship between cerebrospinal fluid markers of Alzheimer pathology and positron emission tomography tau imaging". In: *Brain*, aww139. ISSN: 0006-8950. DOI: 10.1093/brain/aww139. URL: http://www.brain.oxfordjournals.org/lookup/doi/10.1093/brain/aww139.

Gordon, Brian A. et al. (2018). "Cross-sectional and longitudinal atrophy is preferentially associated with tau rather than amyloid β positron emission tomography pathology". In: *Alzheimer's and Dementia: Diagnosis, Assessment and Disease Monitoring* 10, pp. 245–252. ISSN: 23528729. DOI: 10.1016/j.dadm.2018.02.003.

Götz, J. et al. (2001). "Formation of neurofibrillary tangles in P301L tau transgenic mice induced by Aβ42 fibrils". In: *Science* 293.5534, pp. 1491–1495. ISSN: 00368075. DOI: 10.1126/science.1062097.

Götz, Jürgen, Glenda Halliday, and Rebecca M. Nisbet (2019). "Molecular Pathogenesis of the Tauopathies". In: *Annual Review of Pathology: Mechanisms of Disease* 14.1, pp. 239–261. ISSN: 1553-4006. DOI: 10.1146/annurev-pathmechdis-012418-012936.

Götz, Jürgen et al. (2008). "Is tau aggregation toxic or protective: A sensible question in the absence of sensitive methods?" In: *Journal of Alzheimer's Disease* 14.4, pp. 423–429. ISSN: 13872877. DOI: 10.3233/JAD-2008-14410.

Granic, Antoneta et al. (Feb. 2010). "Alzheimer Aβ Peptide Induces Chromosome Mis-Segregation and Aneuploidy, Including Trisomy 21: Requirement for Tau and APP". In: *Molecular Biology of the Cell* 21.4. Ed. by Yixian Zheng, pp. 511–520. ISSN: 1059-1524. DOI: 10.1091/mbc.e09-10-0850. URL: https://www.molbiolcell.org/doi/10.1091/mbc.e09-10-0850.

Griffith, L. M. and T. D. Pollard (1982). "The interaction of actin filaments with microtubules and microtubule-associated proteins". In: *Journal of Biological Chemistry* 257.15, pp. 9143–9151. ISSN: 00219258.

Grothe, Michel J et al. (Nov. 2017). "In vivo staging of regional amyloid deposition". In: *Neurology* 89.20, pp. 2031–2038. ISSN: 0028-3878. DOI: 10.1212/WNL.0000000000004643. URL: http://www.ncbi.nlm.nih.gov/pubmed/29046362http://www.neurology.org/lookup/doi/10.1212/WNL.0000000000004643.

Grothe, Michel J et al. (2018). "Molecular properties underlying regional vulnerability to Alzheimer's disease pathology". In: *Brain*, pp. 2755–2771. ISSN: 0006-8950. DOI: 10.1093/brain/awy189. URL: https://academic.oup.com/brain/advance-article/doi/10.1093/brain/awy189/5054650.

Grubman, Alexandra et al. (2019). "A single cell brain atlas in human Alzheimer's disease". In: *bioRxiv*, p. 628347. DOI: 10.1101/628347. URL: https://www.biorxiv.org/content/10.1101/628347v1.

Grundke-Iqbal, I., K. Iqbal, and Y. C. Tung (1986). "Abnormal phosphorylation of the microtubule-associated protein τ (tau) in Alzheimer cytoskeletal pathology". In: *Proceedings of the National Academy of Sciences of the United States of America* 83.13, pp. 44913–44917. ISSN: 00278424. DOI: 10.1097/00002093-198701030-00020.

Gunn-Moore, Danièlle et al. (2018). "Alzheimer's disease in humans and other animals: A consequence of postreproductive life span and longevity rather than aging". In: *Alzheimer's and Dementia* 14.2, pp. 195–204. ISSN: 15525279. DOI: 10.1016/j.jalz.2017.08.014.

Guo, Christine C et al. (May 2016a). "Network-selective vulnerability of the human cerebellum to Alzheimer's disease and frontotemporal dementia". In: *Brain* 139.5, pp. 1527–1538. ISSN: 0006-8950. DOI: 10.1093/brain/aww003. URL: https://academic.oup.com/brain/article-lookup/doi/10.1093/brain/aww003.

Guo, Jing L. et al. (2016b). "Unique pathological tau conformers from alzheimer's brains transmit tau pathology in nontransgenic mice". In: *Journal of Experimental Medicine* 213.12, pp. 2635–2654. ISSN: 15409538. DOI: 10.1084/jem.20160833.

Habes, Mohamad et al. (2020). "Disentangling Heterogeneity in Alzheimer's Disease and Related Dementias Using Data-Driven Methods". In: *Biological Psychiatry*. ISSN: 18732402. DOI: 10.1016/j.biopsych.2020.01.016. URL: https://doi.org/10.1016/j.biopsych.2020.01.016.

Hampel, Harald et al. (2004). "Measurement of Phosphorylated Tau Epitopes in the Differential Diagnosis of Alzheimer Disease: A Comparative Cerebrospinal Fluid Study". In: *Archives of General Psychiatry* 61.1, pp. 95–102. ISSN: 0003990X. DOI: 10.1001/archpsyc.61.1.95.

Hanna Al-Shaikh, Fadi S. et al. (2019). "Selective Vulnerability of the Nucleus Basalis of Meynert among Neuropathologic Subtypes of Alzheimer Disease". In: *JAMA Neurology* 32224, pp. 225–233. ISSN: 21686149. DOI: 10.1001/jamaneurol.2019.3606.

Hanna Al-Shaikh, Fadi S. et al. (2020). "Selective Vulnerability of the Nucleus Basalis of Meynert among Neuropathologic Subtypes of Alzheimer Disease". In: *JAMA Neurology* 77.2, pp. 225–233. ISSN: 21686157. DOI: 10.1001/jamaneurol.2019.3606.

Hanseeuw, Bernard J. et al. (Apr. 2017). "Fluorodeoxyglucose metabolism associated with tau-amyloid interaction predicts memory decline". In: *Annals of Neurology* 81.4, pp. 583–596. ISSN: 03645134. DOI: 10.1002/ana.24910. URL: http://doi.wiley.com/10.1002/ana.24910.

Hanseeuw, Bernard J. et al. (2019). "Association of Amyloid and Tau with Cognition in Preclinical Alzheimer Disease: A Longitudinal Study". In: *JAMA Neurology* 76.8, pp. 915–924. ISSN: 21686157. DOI: 10.1001/jamaneurol.2019.1424.

Hansen, Allan K., David J. Brooks, and Per Borghammer (2018). "MAO-B Inhibitors Do Not Block In Vivo Flortaucipir([18F]-AV-1451) Binding". In: *Molecular Imaging and Biology* 20.3, pp. 356–360. ISSN: 18602002. DOI: 10.1007/s11307-017-1143-1.

Hansson, Oskar et al. (2006). "Association between CSF biomarkers and incipient Alzheimer's disease in patients with mild cognitive impairment: A follow-up study". In: *Lancet Neurology* 5.3, pp. 228–234. ISSN: 14744422. DOI: 10.1016/S1474-4422(06)70355-6.

Hansson, Oskar et al. (Mar. 2017). "Tau Pathology Distribution in Alzheimer's disease Corresponds Differentially to Cognition-Relevant Functional Brain Networks". In: *Frontiers in Neuroscience* 11.March. ISSN: 1662-453X. DOI: 10.3389/fnins.2017.00167. URL: http://journal.frontiersin.org/article/10.3389/fnins.2017.00167/full.

Hara, Makoto et al. (2013). "Isoform transition from four-repeat to three-repeat tau underlies dendrosomatic and regional progression of neurofibrillary pathology".

In: *Acta Neuropathologica* 125.4, pp. 565–579. ISSN: 00016322. DOI: 10.1007/s00401-013-1097-6.

Harada, A. et al. (1994). "Altered microtubule organization in small-calibre axons of mice lacking tau protein". In: *Nature* 369.6480, pp. 488–491. ISSN: 00280836. DOI: 10.1038/369488a0.

Harada, Ryuichi et al. (2015). "18F-THK5351: A Novel PET Radiotracer for Imaging Neurofibrillary Pathology in Alzheimer's Disease." In: *Journal of nuclear medicine : official publication, Society of Nuclear Medicine*, pp. 1–43. ISSN: 1535-5667. DOI: 10.2967/jnumed.115.164848. URL: http://www.ncbi.nlm.nih.gov/pubmed/26541774.

Harada, Ryuichi et al. (2016). "Characteristics of Tau and Its Ligands in PET Imaging". In: *Biomolecules* 6.1, p. 7. ISSN: 2218-273X. DOI: 10.3390/biom6010007. URL: http://www.mdpi.com/2218-273X/6/1/7.

Hardy, J. and G. Higgins (Apr. 1992). "Alzheimer's disease: the amyloid cascade hypothesis". In: *Science* 256.5054, pp. 184–185. ISSN: 0036-8075. DOI: 10.1126/science.1566067. URL: https://www.sciencemag.org/lookup/doi/10.1126/science.1566067.

Hardy, J. and D.J. Selkoe (July 2002). "The Amyloid Hypothesis of Alzheimer's Disease: Progress and Problems on the Road to Therapeutics". In: *Science* 297.5580, pp. 353–356. ISSN: 00368075. DOI: 10.1126/science.1072994. URL: https://www.sciencemag.org/lookup/doi/10.1126/science.1072994.

Harrison, Theresa M. et al. (2018). "Longitudinal tau accumulation and atrophy in aging and Alzheimer's disease". In: *Annals of Neurology*, pp. 229–240. ISSN: 00222380. DOI: 10.1002/ana.25406.

Harrison, Theresa M. et al. (2019). "Tau deposition is associated with functional isolation of the hippocampus in aging". In: *Nature Communications* 10.1. ISSN: 20411723. DOI: 10.1038/s41467-019-12921-z. URL: http://dx.doi.org/10.1038/s41467-019-12921-z.

Hassan, Anhar, Jennifer L. Whitwell, and Keith A. Josephs (2011). "The corticobasal syndrome-Alzheimer's disease conundrum". In: *Expert Review of Neurotherapeutics* 11.11, pp. 1569–1578. ISSN: 14737175. DOI: 10.1586/ern.11.153.

Hawrylycz, Michael J et al. (2012). "An anatomically comprehensive atlas of the adult human brain transcriptome." In: *Nature* 489.7416, pp. 391–9. ISSN: 1476-4687. DOI: 10.1038/nature11405. URL: http://dx.doi.org/10.1038/nature11405.

He, Zhuohao et al. (2018). "Amyloid-β plaques enhance Alzheimer's brain tau-seeded pathologies by facilitating neuritic plaque tau aggregation". In: *Nature Medicine* 24.1, pp. 29–38. ISSN: 1546170X. DOI: 10.1038/nm.4443. URL: http://dx.doi.org/10.1038/nm.4443.

He, Zhuohao et al. (2020). "Transmission of tauopathy strains is independent of their isoform composition". In: *Nature Communications* 11.1. ISSN: 20411723. DOI: 10.1038/s41467-019-13787-x. URL: http://dx.doi.org/10.1038/s41467-019-13787-x.

Hedden, Trey et al. (2013). "Meta-analysis of amyloid-cognition relations in cognitively normal older adults". In: *Neurology* 80.14, pp. 1341–1348. ISSN: 00283878. DOI: 10.1212/WNL.0b013e31828ab35d.

Henderson, Michael X. et al. (2019). "Spread of α-synuclein pathology through the brain connectome is modulated by selective vulnerability and predicted by network analysis". In: *Nature Neuroscience* 22.8, pp. 1248–1257. ISSN: 15461726. DOI: 10.1038/s41593-019-0457-5. URL: http://dx.doi.org/10.1038/s41593-019-0457-5.

Hervas, Ruben et al. (2020). "Cryo-EM structure of a neuronal functional amyloid implicated in memory persistence in Drosophila". In: *Science* 367.6483, pp. 1230–1234. ISSN: 10959203. DOI: 10.1126/science.aaw1114.

Hoenig, Merle C et al. (2018). "Networks of tau distribution in Alzheimer's disease". In: *Brain* 141.2, pp. 568–581. ISSN: 14602156. DOI: 10.1093/brain/awx353.

Hoenig, Merle Christine et al. (2017). "Tau pathology and cognitive reserve in Alzheimer's disease". In: *Neurobiology of Aging* 57, pp. 1–7. ISSN: 15581497. DOI: 10.1016/j.neurobiolaging.2017.05.004. URL: http://dx.doi.org/10.1016/j.neurobiolaging.2017.05.004.

Hoff, G E Anna-Jasmijn et al. (2013). "On development of functional brain connectivity in the young brain." In: *Frontiers in human neuroscience* 7.October, p. 650. ISSN: 1662-5161. DOI: 10.3389/fnhum.2013.00650. URL: http://www.pubmedcentral.nih.gov/articlerender.fcgi?artid=3792361&tool=pmcentrez&rendertype=abstract.

Hohman, Timothy J. et al. (Aug. 2018). "Sex-Specific Association of Apolipoprotein E With Cerebrospinal Fluid Levels of Tau". In: *JAMA Neurology* 75.8, p. 989. ISSN: 2168-6149. DOI: 10.1001/jamaneurol.2018.0821. URL: http://archneur.jamanetwork.com/article.aspx?doi=10.1001/jamaneurol.2018.0821.

Holmes, Brandon B. et al. (2014). "Proteopathic tau seeding predicts tauopathy in vivo". In: *Proceedings of the National Academy of Sciences of the United States of America* 111.41, E4376–E4385. ISSN: 10916490. DOI: 10.1073/pnas.1411649111.

Holth, Jerrah K. et al. (2013). "Tau loss attenuates neuronal network hyperexcitability in mouse and drosophila genetic models of epilepsy". In: *Journal of Neuroscience* 33.4, pp. 1651–1659. ISSN: 02706474. DOI: 10.1523/JNEUROSCI.3191-12.2013.

Hong, Soyon et al. (2014). "Soluble Aβ oligomers are rapidly sequestered from brain ISF in vivo and bind GM1 ganglioside on cellular membranes". In: *Neuron*

82.2, pp. 308–319. ISSN: 10974199. DOI: 10.1016/j.neuron.2014.02.027. URL: http://dx.doi.org/10.1016/j.neuron.2014.02.027.

Hu, Wen et al. (2017). "Expression of tau pathology-related proteins in different brain regions: A molecular basis of tau pathogenesis". In: *Frontiers in Aging Neuroscience* 9.SEP, pp. 1–14. ISSN: 16634365. DOI: 10.3389/fnagi.2017.00311.

Hughes, C P et al. (June 1982). "A new clinical scale for the staging of dementia." In: *The British journal of psychiatry : the journal of mental science* 140, pp. 566–72. ISSN: 0007-1250. URL: http://www.ncbi.nlm.nih.gov/pubmed/7104545.

Huijbers, Willem et al. (2017). "Tau Accumulation in Clinically Normal Older Adults Is Associated With Increases in Hippocampal Fmri Activity". In: *Alzheimer's & Dementia* 13.7, P1215. ISSN: 15525260. DOI: 10.1016/j.jalz.2017.07.388.

Humpel, Christian (2011). "Identifying and validating biomarkers for Alzheimer's disease". In: *Trends in Biotechnology* 29.1, pp. 26–32. ISSN: 01677799. DOI: 10.1016/j.tibtech.2010.09.007. URL: http://dx.doi.org/10.1016/j.tibtech.2010.09.007.

Hung, Victor K.L. et al. (2015). "Selective astrocytic endothelin-1 overexpression contributes to dementia associated with ischemic stroke by exaggerating astrocyte-derived amyloid secretion". In: *Journal of Cerebral Blood Flow and Metabolism* 35.10, pp. 1687–1696. ISSN: 15597016. DOI: 10.1038/jcbfm.2015.109.

Hurd, Michael D. et al. (2013). "Monetary Costs of Dementia in the United States". In: *New England Journal of Medicine* 368.14, pp. 1326–1334. ISSN: 0028-4793. DOI: 10.1056/NEJMsa1204629. URL: http://www.nejm.org/doi/10.1056/NEJMsa1204629.

Hutton, M. et al. (1998). "Association of missense and 5'-splice-site mutations in tau with the inherited dementia FTDP-17". In: *Nature* 393.6686, pp. 702–704. ISSN: 00280836. DOI: 10.1038/31508.

Hyman, Bradley et al. (Sept. 1984). "Alzheimer's disease: cell-specific pathology isolates the hippocampal formation". In: *Science* 225.4667, pp. 1168–1170. ISSN: 0036-8075. DOI: 10.1126/science.6474172. URL: https://www.sciencemag.org/lookup/doi/10.1126/science.6474172.

Iaccarino, Leonardo et al. (2018). "Local and distant relationships between amyloid, tau and neurodegeneration in Alzheimer's Disease". In: *NeuroImage: Clinical* 17.February 2017, pp. 452–464. ISSN: 22131582. DOI: 10.1016/j.nicl.2017.09.016. URL: http://dx.doi.org/10.1016/j.nicl.2017.09.016.

Iba, M. et al. (2013). "Synthetic Tau Fibrils Mediate Transmission of Neurofibrillary Tangles in a Transgenic Mouse Model of Alzheimer's-Like Tauopathy". In: *Journal of Neuroscience* 33.3, pp. 1024–1037. ISSN: 0270-6474. DOI: 10.1523/JNEUROSCI.2642-12.2013. URL: http://www.jneurosci.org/cgi/doi/10.1523/JNEUROSCI.2642-12.2013.

Iba, Michiyo et al. (2015). "Tau pathology spread in PS19 tau transgenic mice following locus coeruleus (LC) injections of synthetic tau fibrils is determined by the LC's afferent and efferent connections". In: *Acta Neuropathologica* 130.3, pp. 349–362. ISSN: 14320533. DOI: 10.1007/s00401-015-1458-4.

Iourov, Ivan Y. et al. (2009). "Aneuploidy in the normal, Alzheimer's disease and ataxia-telangiectasia brain: Differential expression and pathological meaning". In: *Neurobiology of Disease* 34.2, pp. 212–220. ISSN: 09699961. DOI: 10.1016/j.nbd.2009.01.003. URL: http://dx.doi.org/10.1016/j.nbd.2009.01.003.

Ishihara, Takeshi et al. (1999). "Age-dependent emergence and progression of a tauopathy in transgenic mice overexpressing the shortest human tau isoform". In: *Neuron* 24.3, pp. 751–762. ISSN: 08966273. DOI: 10.1016/S0896-6273(00)81127-7.

Ishiki, Aiko et al. (2018). "Neuroimaging-pathological correlations of [18F]THK5351 PET in progressive supranuclear palsy". In: *Acta neuropathologica communications* 6.1, p. 53. ISSN: 20515960. DOI: 10.1186/s40478-018-0556-7.

Ittner, Arne and Lars M. Ittner (2018). "Dendritic Tau in Alzheimer's Disease". In: *Neuron* 99.1, pp. 13–27. ISSN: 10974199. DOI: 10.1016/j.neuron.2018.06.003. URL: https://doi.org/10.1016/j.neuron.2018.06.003.

Ittner, Lars M. and Jörgen Götz (2011). "Amyloid-β and tau - A toxic pas de deux in Alzheimer's disease". In: *Nature Reviews Neuroscience* 12.2, pp. 67–72. ISSN: 1471003X. DOI: 10.1038/nrn2967. URL: http://dx.doi.org/10.1038/nrn2967.

Ittner, Lars M. et al. (2010). "Dendritic function of tau mediates amyloid-β toxicity in alzheimer's disease mouse models". In: *Cell* 142.3, pp. 387–397. ISSN: 00928674. DOI: 10.1016/j.cell.2010.06.036.

Iturria-Medina, Y. et al. (2007). "Characterizing brain anatomical connections using diffusion weighted MRI and graph theory". In: *NeuroImage* 36.3, pp. 645–660. ISSN: 10538119. DOI: 10.1016/j.neuroimage.2007.02.012.

Iturria-Medina, Yasser and Alan C Evans (2015). "On the central role of brain connectivity in neurodegenerative disease progression." In: *Frontiers in aging neuroscience* 7.May, p. 90. ISSN: 1663-4365. DOI: 10.3389/fnagi.2015.00090. URL: http://journal.frontiersin.org/article/10.3389/fnagi.2015.00090/abstract.

Iturria-Medina, Yasser et al. (2014). "Epidemic Spreading Model to Characterize Misfolded Proteins Propagation in Aging and Associated Neurodegenerative Disorders". In: *PLoS Computational Biology* 10.11. ISSN: 15537358. DOI: 10.1371/journal.pcbi.1003956.

Iturria-Medina, Yasser et al. (2017). "Multifactorial causal model of brain (dis)organization and therapeutic intervention: Application to Alzheimer's disease". In: *NeuroImage* 152.February, pp. 60–77. ISSN: 10959572. DOI: 10.1016/j.neuroimage.2017.02.058. URL: http://dx.doi.org/10.1016/j.neuroimage.2017.02.058.

Iwata, Minori et al. (2019). "Regulatory mechanisms for the axonal localization of tau protein in neurons". In: *Molecular Biology of the Cell* 30.19, pp. 2441–2457. ISSN: 19394586. DOI: 10.1091/mbc.E19-03-0183.

Jack, Clifford, David Holtzman, and Reisa Sperling (2019). "Dementia is not synonymous with Alzheimer's disease". In: *Science Translational Medicine* 11.522, pp. 2–4. ISSN: 19466242. DOI: 10.1126/scitranslmed.aav0511.

Jack, Clifford R. and David M. Holtzman (2013). "Biomarker modeling of alzheimer's disease". In: *Neuron* 80.6, pp. 1347–1358. ISSN: 10974199. DOI: 10.1016/j.neuron.2013.12.003. URL: http://dx.doi.org/10.1016/j.neuron.2013.12.003.

Jack, Clifford R et al. (2010). "Hypothetical Pathological Cascade in Alheimer's Disease". In: *Lancet Neurology* 9.1, pp. 1–20. ISSN: 1474-4465. DOI: 10.1016/S1474-4422(09)70299-6.Hypothetical.

Jack, Clifford R. et al. (2013). "Tracking pathophysiological processes in Alzheimer's disease: An updated hypothetical model of dynamic biomarkers". In: *The Lancet Neurology* 12.2, pp. 207–216. ISSN: 14744422. DOI: 10.1016/S1474-4422(12)70291-0.

Jack, Clifford R. et al. (2017). "Defining imaging biomarker cut points for brain aging and Alzheimer's disease". In: *Alzheimer's and Dementia* 13.3, pp. 205–216. ISSN: 15525279. DOI: 10.1016/j.jalz.2016.08.005. URL: http://dx.doi.org/10.1016/j.jalz.2016.08.005.

Jack, Clifford R. et al. (2018a). "Longitudinal tau PET in ageing and Alzheimer's disease". In: *Brain* 141.5, pp. 1517–1528. ISSN: 14602156. DOI: 10.1093/brain/awy059.

Jack, Clifford R. et al. (2018b). "NIA-AA Research Framework: Toward a biological definition of Alzheimer's disease". In: *Alzheimer's and Dementia* 14.4, pp. 535–562. ISSN: 15525279. DOI: 10.1016/j.jalz.2018.02.018. URL: https://doi.org/10.1016/j.jalz.2018.02.018.

Jack, Clifford R. et al. (2019a). "Prevalence of Biologically vs Clinically Defined Alzheimer Spectrum Entities Using the National Institute on Aging-Alzheimer's Association Research Framework". In: *JAMA Neurology* 76.10, pp. 1174–1183. ISSN: 21686149. DOI: 10.1001/jamaneurol.2019.1971.

Jack, Clifford R et al. (2019b). "The bivariate distribution of amyloid- b and tau : relationship with established neurocognitive clinical syndromes". In: pp. 3230–3242. DOI: 10.1093/brain/awz268.

Jacobs, Heidi I.L. et al. (2018). "Structural tract alterations predict downstream tau accumulation in amyloid-positive older individuals". In: *Nature Neuroscience* 21.3, pp. 424–431. ISSN: 15461726. DOI: 10.1038/s41593-018-0070-z. URL: http://dx.doi.org/10.1038/s41593-018-0070-z.

Jadhav, Santosh et al. (2019). "A walk through tau therapeutic strategies". In: *Acta neuropathologica communications* 7.1, p. 22. ISSN: 20515960. DOI: 10.1186/s40478-019-0664-z.

Jagust, William (2014). "Time for tau". In: *Brain* 137.6, pp. 1570–1571. ISSN: 14602156. DOI: 10.1093/brain/awu093.

Janelidze, Shorena et al. (2020). "Plasma P-tau181 in Alzheimer's disease: relationship to other biomarkers, differential diagnosis, neuropathology and longitudinal progression to Alzheimer's dementia". In: *Nature Medicine* 26.3, pp. 379–386. ISSN: 1546170X. DOI: 10.1038/s41591-020-0755-1. URL: http://dx.doi.org/10.1038/s41591-020-0755-1.

Jang, Young Kyoung et al. (2018). "Head to head comparison of [18F] AV-1451 and [18F] THK5351 for tau imaging in Alzheimer's disease and frontotemporal dementia". In: *European Journal of Nuclear Medicine and Molecular Imaging* 45.3, pp. 432–442. ISSN: 16197089. DOI: 10.1007/s00259-017-3876-0.

Janke, Carsten et al. (1999). "Phylogenetic diversity of the expression of the microtubule-associated protein tau: Implications for neurodegenerative disorders". In: *Molecular Brain Research* 68.1-2, pp. 119–128. ISSN: 0169328X. DOI: 10.1016/S0169-328X(99)00079-0.

Janocko, Nicholas J. et al. (2012). "Neuropathologically defined subtypes of Alzheimer's disease differ significantly from neurofibrillary tangle-predominant dementia". In: *Acta Neuropathologica* 124.5, pp. 681–692. ISSN: 00016322. DOI: 10.1007/s00401-012-1044-y.

Jansen, Willemijn J et al. (May 2015). "Prevalence of cerebral amyloid pathology in persons without dementia: a meta-analysis." In: *JAMA* 313.19, pp. 1924–38. ISSN: 1538-3598. DOI: 10.1001/jama.2015.4668. URL: http://dx.doi.org/10.1001/jama.2015.9719http://www.ncbi.nlm.nih.gov/pubmed/25988462http://www.pubmedcentral.nih.gov/articlerender.fcgi?artid=PMC4486209.

Jbabdi, Saad et al. (Nov. 2015). "Measuring macroscopic brain connections in vivo". In: *Nature Neuroscience* 18.11, pp. 1546–1555. ISSN: 1097-6256. DOI: 10.1038/nn.4134. URL: http://www.ncbi.nlm.nih.gov/pubmed/26505566http://www.nature.com/articles/nn.4134.

Jefferson-George, Kyra S. et al. (2017). "Cognitive decline associated with pathological burden in primary age-related tauopathy". In: *Alzheimer's and Dementia* 13.9, pp. 1048–1053. ISSN: 15525279. DOI: 10.1016/j.jalz.2017.01.028. URL: http://dx.doi.org/10.1016/j.jalz.2017.01.028.

Jellinger, Kurt A. (2018). "Different patterns of hippocampal tau pathology in Alzheimer's disease and PART". In: *Acta Neuropathologica* 136.5, pp. 811–813. ISSN: 14320533.

DOI: 10.1007/s00401-018-1894-z. URL: https://doi.org/10.1007/s00401-018-1894-z.

Jenkins, Scott M. et al. (2000). "Modulation of tau phosphorylation and intracellular localization by cellular stress". In: *Biochemical Journal* 345.2, pp. 263–270. ISSN: 02646021. DOI: 10.1042/0264-6021:3450263.

Jeon, Seun et al. (2019). "Topographical heterogeneity of Alzheimer's disease based on MR imaging, tau PET, and amyloid PET". In: *Frontiers in Aging Neuroscience* 10.JUL, pp. 1–10. ISSN: 16634365. DOI: 10.3389/fnagi.2019.00211.

Jin, Ming et al. (2011). "Soluble amyloid β-protein dimers isolated from Alzheimer cortex directly induce Tau hyperphosphorylation and neuritic degeneration". In: *Proceedings of the National Academy of Sciences of the United States of America* 108.14, pp. 5819–5824. ISSN: 10916490. DOI: 10.1073/pnas.1017033108.

Johnson, Keith A. et al. (2016). "Tau positron emission tomographic imaging in aging and early Alzheimer disease". In: *Annals of Neurology* 79.1, pp. 110–119. ISSN: 15318249. DOI: 10.1002/ana.24546.

Johnson, Sterling C. et al. (2014). "Amyloid burden and neural function in people at risk for Alzheimer's Disease". In: *Neurobiology of Aging* 35.3, pp. 576–584. ISSN: 01974580. DOI: 10.1016/j.neurobiolaging.2013.09.028. URL: http://dx.doi.org/10.1016/j.neurobiolaging.2013.09.028.

Johnson, Victoria E., William Stewart, and Douglas H. Smith (Mar. 2012). "Widespread Tau and Amyloid-Beta Pathology Many Years After a Single Traumatic Brain Injury in Humans". In: *Brain Pathology* 22.2, pp. 142–149. ISSN: 10156305. DOI: 10.1111/j.1750-3639.2011.00513.x. URL: http://doi.wiley.com/10.1111/j.1750-3639.2011.00513.x.

Jones, David T. et al. (2017). "Tau, Amyloid, and Cascading Network Failure across the Alzheimer's disease Spectrum". In: *Cortex* October, pp. 1–17. ISSN: 00109452. DOI: 10.1016/j.cortex.2017.09.018. URL: http://linkinghub.elsevier.com/retrieve/pii/S0010945217303246.

Jones, David T. et al. (2018). "In vivo 18 F-AV-1451 tau PET signal in MAPT mutation carriers varies by expected tau isoforms". In: *Neurology* 90.11, e947–e954. ISSN: 1526632X. DOI: 10.1212/WNL.0000000000005117.

Josephs, Keith A. et al. (2008). "B-Amyloid Burden Is Not Associated With Rates of Brain Atrophy". In: *Annals of Neurology* 63.2, pp. 204–212. ISSN: 03645134. DOI: 10.1002/ana.21223.

Josephs, Keith A. et al. (2017). "Tau aggregation influences cognition and hippocampal atrophy in the absence of beta-amyloid: a clinico-imaging-pathological study of primary age-related tauopathy (PART)". In: *Acta Neuropathologica* 133.5, pp. 705–715. ISSN: 14320533. DOI: 10.1007/s00401-017-1681-2.

Josephs, Keith A et al. (Mar. 2018). "[18 F]AV-1451 tau-PET and primary progressive aphasia". In: *Annals of Neurology* 83.3, pp. 599–611. ISSN: 03645134. DOI: 10.1002/ana.25183. URL: http://doi.wiley.com/10.1002/ana.25183.

Josephs, Keith A. et al. (2019). "Brain atrophy in primary age-related tauopathy is linked to transactive response DNA-binding protein of 43 kDa". In: *Alzheimer's and Dementia* 15.6, pp. 799–806. ISSN: 15525279. DOI: 10.1016/j.jalz.2019.03.003. URL: https://doi.org/10.1016/j.jalz.2019.03.003.

Jun, G. et al. (2016). "A novel Alzheimer disease locus located near the gene encoding tau protein". In: *Molecular Psychiatry* 21.1, pp. 108–117. ISSN: 14765578. DOI: 10.1038/mp.2015.23.

Kant, Rik van der, Lawrence S.B. Goldstein, and Rik Ossenkoppele (2020). "Amyloid-β-independent regulators of tau pathology in Alzheimer disease". In: *Nature Reviews Neuroscience* 21.1, pp. 21–35. ISSN: 14710048. DOI: 10.1038/s41583-019-0240-3. URL: http://dx.doi.org/10.1038/s41583-019-0240-3.

Katsinelos, Taxiarchis et al. (2018). "Unconventional Secretion Mediates the Trans-cellular Spreading of Tau". In: *Cell Reports* 23.7, pp. 2039–2055. ISSN: 22111247. DOI: 10.1016/j.celrep.2018.04.056.

Katsumoto, Atsuko, Hideyuki Takeuchi, and Fumiaki Tanaka (2019). "Tau Pathology in Chronic Traumatic Encephalopathy and Alzheimer's Disease: Similarities and Differences". In: *Frontiers in Neurology* 10.September, pp. 1–9. ISSN: 16642295. DOI: 10.3389/fneur.2019.00980.

Kaufman, Sarah K. et al. (2018). "Tau seeding activity begins in the transentorhinal/entorhinal regions and anticipates phospho-tau pathology in Alzheimer's disease and PART". In: *Acta Neuropathologica* 136.1, pp. 57–67. ISSN: 14320533. DOI: 10.1007/s00401-018-1855-6. URL: https://doi.org/10.1007/s00401-018-1855-6.

Kelley, Christy M., Sylvia E. Perez, and Elliott J. Mufson (2019). "Tau pathology in the medial temporal lobe of athletes with chronic traumatic encephalopathy: A chronic effects of neurotrauma consortium study". In: *Acta Neuropathologica Communications* 7.1, pp. 1–18. ISSN: 20515960. DOI: 10.1186/s40478-019-0861-9.

Kempf, Martina et al. (1996). "Tau binds to the distal axon early in development of polarity in a microtubule- and microfilament-dependent manner". In: *Journal of Neuroscience* 16.18, pp. 5583–5592. ISSN: 02706474. DOI: 10.1523/jneurosci.16-18-05583.1996.

Kfoury, Najla et al. (2012). "Trans-cellular propagation of Tau aggregation by fibrillar species". In: *Journal of Biological Chemistry* 287.23, pp. 19440–19451. ISSN: 00219258. DOI: 10.1074/jbc.M112.346072.

Kiar, Gregory et al. (Jan. 2017). "A Comprehensive Cloud Framework for Accurate and Reliable Human Connectome Estimation and Meganalysis". In: *bioRxiv*. URL: http://biorxiv.org/content/early/2017/09/16/188706.abstract.

Kikuchi, Akio et al. (2016). "In vivo visualization of tau deposits in corticobasal syndrome by 18 F-THK5351". In:

Kim, Kayoung et al. (2020). "Clinically accurate diagnosis of Alzheimer's disease via multiplexed sensing of core biomarkers in human plasma". In: *Nature Communications* 11.1, pp. 1–9. ISSN: 20411723. DOI: 10.1038/s41467-019-13901-z. URL: http://dx.doi.org/10.1038/s41467-019-13901-z.

Kimura, Tetsuya et al. (2014). "Microtubule-associated protein tau is essential for long-term depression in the hippocampus". In: *Philosophical Transactions of the Royal Society B: Biological Sciences* 369.1633. ISSN: 14712970. DOI: 10.1098/rstb.2013.0144.

Klein, Arno and Jason Tourville (2012). "101 Labeled Brain Images and a Consistent Human Cortical Labeling Protocol". In: *Frontiers in Neuroscience* 6.DEC, pp. 1–12. ISSN: 16624548. DOI: 10.3389/fnins.2012.00171.

Klunk, William E. (2018). "Molecular imaging: What is right and what is an illusion?" In: *Alzheimer's and Dementia: Diagnosis, Assessment and Disease Monitoring* 10, pp. 217–220. ISSN: 23528729. DOI: 10.1016/j.dadm.2018.01.004. URL: https://doi.org/10.1016/j.dadm.2018.01.004.

Klunk, William E et al. (Mar. 2004). "Imaging brain amyloid in Alzheimer's disease with Pittsburgh Compound-B." In: *Annals of neurology* 55.3, pp. 306–19. ISSN: 0364-5134. DOI: 10.1002/ana.20009. URL: http://www.ncbi.nlm.nih.gov/pubmed/14991808.

Klunk, William E. et al. (2007). "Amyloid deposition begins in the striatum of presenilin-1 mutation carriers from two unrelated pedigrees". In: *Journal of Neuroscience* 27.23, pp. 6174–6184. ISSN: 02706474. DOI: 10.1523/JNEUROSCI.0730-07.2007.

Knudsen, Katherine A. et al. (2001). "Clinical diagnosis of cerebral amyloid angiopathy: Validation of the boston criteria". In: *Neurology* 56.4, pp. 537–539. ISSN: 00283878. DOI: 10.1212/WNL.56.4.537.

Kobayashi, Shunsuke et al. (2017). "Local Somatodendritic Translation and Hyperphosphorylation of Tau Protein Triggered by AMPA and NMDA Receptor Stimulation". In: *EBioMedicine* 20, pp. 120–126. ISSN: 23523964. DOI: 10.1016/j.ebiom.2017.05.012. URL: http://dx.doi.org/10.1016/j.ebiom.2017.05.012.

Koedam, Esther L.G.E. et al. (Mar. 2010). "Early-Versus Late-Onset Alzheimer's Disease: More than Age Alone". In: *Journal of Alzheimer's Disease* 19.4, pp. 1401–

1408. ISSN: 18758908. DOI: 10.3233/JAD-2010-1337. URL: https://www.medra.org/servlet/aliasResolver?alias=iospress&doi=10.3233/JAD-2010-1337.

Koffie, Robert M. et al. (2009). "Oligomeric amyloid β associates with postsynaptic densities and correlates with excitatory synapse loss near senile plaques". In: *Proceedings of the National Academy of Sciences of the United States of America* 106.10, pp. 4012–4017. ISSN: 00278424. DOI: 10.1073/pnas.0811698106.

Koopman, Karen et al. (2009). "Improved discrimination of autopsy-confirmed Alzheimer's disease (AD) from non-AD dementias using CSF P-tau181P". In: *Neurochemistry International* 55.4, pp. 214–218. ISSN: 01970186. DOI: 10.1016/j.neuint.2009.02.017.

Kopeikina, Katherine J. et al. (2013). "Synaptic alterations in the rTg4510 mouse model of tauopathy". In: *Journal of Comparative Neurology* 521.6, pp. 1334–1353. ISSN: 00219967. DOI: 10.1002/cne.23234.

Kopke, E. et al. (1993). "Microtubule-associated protein tau. Abnormal phosphorylation of a non- paired helical filament pool in Alzheimer disease". In: *Journal of Biological Chemistry* 268.32, pp. 24374–24384. ISSN: 00219258.

Kosik, Kenneth S. et al. (1989). "Developmentally regulated expression of specific tau sequences". In: *Neuron* 2.4, pp. 1389–1397. ISSN: 08966273. DOI: 10.1016/0896-6273(89)90077-9.

Kovacs, Gabor G. (2015). "Invited review: Neuropathology of tauopathies: Principles and practice". In: *Neuropathology and Applied Neurobiology* 41.1, pp. 3–23. ISSN: 13652990. DOI: 10.1111/nan.12208.

Kovacs, Gabor G. et al. (Nov. 2015). "Heroin abuse exaggerates age-related deposition of hyperphosphorylated tau and p62-positive inclusions". In: *Neurobiology of Aging* 36.11, pp. 3100–3107. ISSN: 01974580. DOI: 10.1016/j.neurobiolaging.2015.07.018. URL: https://linkinghub.elsevier.com/retrieve/pii/S0197458015003784.

Kowall, Neil W. and Kenneth S. Kosik (Nov. 1987). "Axonal disruption and aberrant localization of tau protein characterize the neuropil pathology of Alzheimer's disease". In: *Annals of Neurology* 22.5, pp. 639–643. ISSN: 0364-5134. DOI: 10.1002/ana.410220514. URL: http://doi.wiley.com/10.1002/ana.410220514.

Kriegeskorte, Nikolaus et al. (2009). "Circular analysis in systems neuroscience – the dangers of double dipping". In: *Nature neuroscience* 12.5, pp. 535–540. DOI: 10.1038/nn.2303.

Kroth, Heiko et al. (2019). "Discovery and preclinical characterization of [18F]PI-2620, a next-generation tau PET tracer for the assessment of tau pathology in Alzheimer's disease and other tauopathies". In: *European Journal of Nuclear*

Medicine and Molecular Imaging 46.10, pp. 2178–2189. ISSN: 16197089. DOI: 10.1007/s00259-019-04397-2.

Ksiezak-Reding, Hanna, Wan Kyng Liu, and Shu Hui Yen (1992). "Phosphate analysis and dephosphorylation of modified tau associated with paired helical filaments". In: *Brain Research* 597.2, pp. 209–219. ISSN: 00068993. DOI: 10.1016/0006-8993(92)91476-U.

Kuchibhotla, Kishore V. et al. (2014). "Neurofibrillary tangle-bearing neurons are functionally integrated in cortical circuits in vivo". In: *Proceedings of the National Academy of Sciences of the United States of America* 111.1, pp. 510–514. ISSN: 00278424. DOI: 10.1073/pnas.1318807111.

Kundra, Rishika et al. (2017). "Protein homeostasis of a metastable subproteome associated with Alzheimer's disease". In: *Proceedings of the National Academy of Sciences of the United States of America* 114.28, E5703–E5711. ISSN: 10916490. DOI: 10.1073/pnas.1618417114.

Kuret, Jeff et al. (2005). "Evaluating triggers and enhancers of tau fibrillization". In: *Microscopy Research and Technique* 67.3-4, pp. 141–155. ISSN: 1059910X. DOI: 10.1002/jemt.20187.

Kwak, Sang Su et al. (2020). "Amyloid-β42/40 ratio drives tau pathology in 3D human neural cell culture models of Alzheimer's disease". In: *Nature Communications* 11.1, pp. 1–14. ISSN: 20411723. DOI: 10.1038/s41467-020-15120-3. URL: http://dx.doi.org/10.1038/s41467-020-15120-3.

La Joie, R. et al. (2012). "Region-Specific Hierarchy between Atrophy, Hypometabolism, and -Amyloid (A) Load in Alzheimer's Disease Dementia". In: *Journal of Neuroscience* 32.46, pp. 16265–16273. ISSN: 0270-6474. DOI: 10.1523/JNEUROSCI.2170-12.2012. URL: http://www.jneurosci.org/cgi/doi/10.1523/JNEUROSCI.2170-12.2012.

La Joie, Renaud et al. (2018). "Associations between [18F]AV1451 tau PET and CSF measures of tau pathology in a clinical sample". In: *Neurology* 90.4, E282–E290. ISSN: 1526632X. DOI: 10.1212/WNL.0000000000004860.

La Joie, Renaud et al. (Feb. 2019). "Multisite study of the relationships between antemortem [11 C]PIB-PET Centiloid values and postmortem measures of Alzheimer's disease neuropathology". In: *Alzheimer's & Dementia* 15.2, pp. 205–216. ISSN: 15525260. DOI: 10.1016/j.jalz.2018.09.001. URL: http://doi.wiley.com/10.1016/j.jalz.2018.09.001.

La Joie, Renaud et al. (2020). "Prospective longitudinal atrophy in Alzheimer's disease correlates with the intensity and topography of baseline tau-PET." In: *Science translational medicine* 12.524, pp. 1–13. ISSN: 1946-6242. DOI: 10.1126/scitranslmed.aau5732. URL: http://www.ncbi.nlm.nih.gov/pubmed/31894103.

Lace, G. et al. (2009). "Hippocampal tau pathology is related to neuroanatomical connections: An ageing population-based study". In: *Brain* 132.5, pp. 1324–1334. ISSN: 14602156. DOI: 10.1093/brain/awp059.

LaJoie, Renaud et al. (2014). "Intrinsic connectivity identifies the hippocampus as a main crossroad between alzheimer's and semantic dementia-targeted networks". In: *Neuron* 81.6, pp. 1417–1428. ISSN: 10974199. DOI: 10.1016/j.neuron.2014.01.026.

Lake, Blue B. et al. (2018). "Integrative single-cell analysis of transcriptional and epigenetic states in the human adult brain". In: *Nature Biotechnology* 36.1, pp. 70–80. ISSN: 15461696. DOI: 10.1038/nbt.4038. URL: http://dx.doi.org/10.1038/nbt.4038.

Lam, Benjamin et al. (2013). "Clinical, imaging, and pathological heterogeneity of the Alzheimer's disease syndrome". In: *Alzheimer's Research and Therapy* 5.1, pp. 1–14. ISSN: 17589193. DOI: 10.1186/alzrt155.

Lam, Benjamin et al. (2017). "Characterizing familial corticobasal syndrome due to Alzheimer's disease pathology and PSEN1 mutations". In: *Alzheimer's and Dementia* 13.5, pp. 520–530. ISSN: 15525279. DOI: 10.1016/j.jalz.2016.08.014.

Lambert, M. P. et al. (1998). "Diffusible, nonfibrillar ligands derived from Aβ1-42 are potent central nervous system neurotoxins". In: *Proceedings of the National Academy of Sciences of the United States of America* 95.11, pp. 6448–6453. ISSN: 00278424. DOI: 10.1073/pnas.95.11.6448.

Landau, Susan M. et al. (2011). "Associations between cognitive, functional, and FDG-PET measures of decline in AD and MCI". In: *Neurobiology of Aging* 32.7, pp. 1207–1218. ISSN: 01974580. DOI: 10.1016/j.neurobiolaging.2009.07.002.

Landau, Susan M. et al. (2013). "Comparing positron emission tomography imaging and cerebrospinal fluid measurements of ??-amyloid". In: *Annals of Neurology* 74.6, pp. 826–836. ISSN: 03645134. DOI: 10.1002/ana.23908.

Lannuzel, Annie, Merle Ruberg, and Patrick P. Michel (2008). "Atypical parkinsonism in the Caribbean island of Guadeloupe: Etiological role of the mitochondrial complex I inhibitor annonacin". In: *Movement Disorders* 23.15, pp. 2122–2128. ISSN: 08853185. DOI: 10.1002/mds.22300.

Lasagna-Reeves, Cristian A. et al. (2010). "Preparation and characterization of neurotoxic tau oligomers". In: *Biochemistry* 49.47, pp. 10039–10041. ISSN: 00062960. DOI: 10.1021/bi1016233.

Ledford, Heidi et al. (Mar. 2019). "Trump seeks big cuts to science funding — again". In: *Nature*. ISSN: 0028-0836. DOI: 10.1038/d41586-019-00719-4. URL: http://www.nature.com/articles/d41586-019-00719-4.

Lee, Christopher M. et al. (Mar. 2018). "18F-Flortaucipir Binding in Choroid Plexus: Related to Race and Hippocampus Signal". In: *Journal of Alzheimer's Disease* 62.4, pp. 1691–1702. ISSN: 13872877. DOI: 10.3233/JAD-170840. URL: http://www.ncbi.nlm.nih.gov/pubmed/5957532http://www.medra.org/servlet/aliasResolver?alias=iospress&doi=10.3233/JAD-170840.

Lee, Hyoung Gon et al. (2004). "Aberrant expression of metabotropic glutamate receptor 2 in the vulnerable neurons of Alzheimer's disease". In: *Acta Neuropathologica* 107.4, pp. 365–371. ISSN: 00016322. DOI: 10.1007/s00401-004-0820-8.

Lehmann, Manja et al. (2013a). "Diverging patterns of amyloid deposition and hypometabolism in clinical variants of probable Alzheimer's disease". In: *Brain* 136.3, pp. 844–858. ISSN: 14602156. DOI: 10.1093/brain/aws327.

Lehmann, Manja et al. (July 2013b). "Intrinsic connectivity networks in healthy subjects explain clinical variability in Alzheimer's disease". In: *Proceedings of the National Academy of Sciences* 110.28, pp. 11606–11611. ISSN: 0027-8424. DOI: 10.1073/pnas.1221536110. URL: http://www.pnas.org/cgi/doi/10.1073/pnas.1221536110%5Cnpapers3://publication/doi/10.1073/pnas.1221536110http://www.pnas.org/cgi/doi/10.1073/pnas.1221536110.

Lemere, C. A. et al. (1996). "Sequence of deposition of heterogeneous amyloid β-peptides and APO E in down syndrome: Implications for initial events in amyloid plaque formation". In: *Neurobiology of Disease* 3.1, pp. 16–32. ISSN: 09699961. DOI: 10.1006/nbdi.1996.0003.

Lemoine, Laetitia et al. (2018). "Tau positron emission tomography imaging in tauopathies: The added hurdle of off-target binding". In: *Alzheimer's and Dementia: Diagnosis, Assessment and Disease Monitoring* 10, pp. 232–236. ISSN: 23528729. DOI: 10.1016/j.dadm.2018.01.007. URL: https://doi.org/10.1016/j.dadm.2018.01.007.

Leng, Kun et al. (2020). "Molecular characterization of selectively vulnerable neurons in Alzheimer's Disease". In:

Leroy, Karelle et al. (2012). "Lack of tau proteins rescues neuronal cell death and decreases amyloidogenic processing of APP in APP/PS1 mice". In: *American Journal of Pathology* 181.6, pp. 1928–1940. ISSN: 00029440. DOI: 10.1016/j.ajpath.2012.08.012. URL: http://dx.doi.org/10.1016/j.ajpath.2012.08.012.

Lesman-Segev, Orit H. et al. (2019). "Tau PET and multimodal brain imaging in patients at risk for chronic traumatic encephalopathy". In: *NeuroImage: Clinical* 24.May, p. 102025. ISSN: 22131582. DOI: 10.1016/j.nicl.2019.102025. URL: https://doi.org/10.1016/j.nicl.2019.102025.

Leuzy, Antoine et al. (2019). "Tau PET imaging in neurodegenerative tauopathies—still a challenge". In: *Molecular Psychiatry* 24.8, pp. 1112–1134. ISSN: 14765578. DOI: 10.1038/s41380-018-0342-8.

Lewczuk, Piotr et al. (2014). "Amyloid-β 42/40 cerebrospinal fluid concentration ratio in the diagnostics of Alzheimer's disease: Validation of two novel assays". In: *Journal of Alzheimer's Disease* 43.1, pp. 183–191. ISSN: 18758908. DOI: 10.3233/JAD-140771.

Lewis, J. et al. (2001). "Enhanced neurofibrillary degeneration in transgenic mice expressing mutant tau and APP". In: *Science* 293.5534, pp. 1487–1491. ISSN: 00368075. DOI: 10.1126/science.1058189.

Li, Cheng Hsuan et al. (2020). "Frontal variant of Alzheimer's disease with asymmetric presentation mimicking frontotemporal dementia: Case report and literature review". In: *Brain and Behavior* 10.3, pp. 1–9. ISSN: 21623279. DOI: 10.1002/brb3.1548.

Li, Xiaoyu et al. (2011). "Novel diffusion barrier for axonal retention of Tau in neurons and its failure in neurodegeneration". In: *EMBO Journal* 30.23, pp. 4825–4837. ISSN: 02614189. DOI: 10.1038/emboj.2011.376. URL: http://dx.doi.org/10.1038/emboj.2011.376.

Liesinger, Amanda M. et al. (2018). "Sex and age interact to determine clinicopathologic differences in Alzheimer's disease". In: *Acta Neuropathologica* 136.6, pp. 873–885. ISSN: 14320533. DOI: 10.1007/s00401-018-1908-x. URL: https://doi.org/10.1007/s00401-018-1908-x.

Lindwall, G. and R. D. Cole (1984). "Phosphorylation affects the ability of tau protein to promote microtubule assembly". In: *Journal of Biological Chemistry* 259.8, pp. 5301–5305. ISSN: 00219258.

Liu, Li et al. (2012). "Trans-synaptic spread of tau pathology in vivo". In: *PLoS ONE* 7.2, pp. 1–9. ISSN: 19326203. DOI: 10.1371/journal.pone.0031302.

Liu, Min et al. (2019). " Sex modulates the ApoE ϵ4 effect on brain tau deposition measured by 18 F-AV-1451 PET in individuals with mild cognitive impairment ". In: *Theranostics* 9.17, pp. 4959–4970. DOI: 10.7150/thno.35366.

Lleó, Alberto et al. (2019). "Longitudinal cerebrospinal fluid biomarker trajectories along the Alzheimer's disease continuum in the BIOMARKAPD study". In: *Alzheimer's and Dementia* 15.6, pp. 742–753. ISSN: 15525279. DOI: 10.1016/j.jalz.2019.01.015.

LoBue, Christian et al. (2017). "Traumatic brain injury history is associated with earlier age of onset of Alzheimer disease". In: *Clinical Neuropsychologist* 31.1, pp. 85–98. ISSN: 17444144. DOI: 10.1080/13854046.2016.1257069.

Lockhart, Samuel N. et al. (2017a). "Amyloid and tau PET demonstrate region-specific associations in normal older people". In: *NeuroImage* 150.February, pp. 191–199. ISSN: 10959572. DOI: 10.1016/j.neuroimage.2017.02.051. URL: http://dx.doi.org/10.1016/j.neuroimage.2017.02.051.

Lockhart, Samuel N et al. (Mar. 2017b). "Elevated (18)F-AV-1451 PET tracer uptake detected in incidental imaging findings." In: *Neurology* 88.11, pp. 1095–1097. ISSN: 1526-632X. DOI: 10.1212/WNL.0000000000003724. URL: http://www.ncbi.nlm.nih.gov/pubmed/28188303http://www.pubmedcentral.nih.gov/articlerender.fcgi?artid=PMC5384840.

Loomis, P. A. et al. (1990). "Identification of nuclear T isoforms in human neuroblastoma cells". In: *Proceedings of the National Academy of Sciences of the United States of America* 87.21, pp. 8422–8426. ISSN: 00278424. DOI: 10.1073/pnas.87.21.8422.

Lowe, Val J. et al. (2016). "An autoradiographic evaluation of AV-1451 Tau PET in dementia". In: *Acta Neuropathologica Communications* 4.1, p. 58. ISSN: 2051-5960. DOI: 10.1186/s40478-016-0315-6. URL: http://actaneurocomms.biomedcentral.com/articles/10.1186/s40478-016-0315-6.

Lowe, Val J. et al. (2018). "Widespread brain tau and its association with ageing, Braak stage and Alzheimer's dementia". In: *Brain* 141.1, pp. 271–287. ISSN: 14602156. DOI: 10.1093/brain/awx320.

Lowe, Val J. et al. (July 2019). "Cross-sectional associations of tau-PET signal with cognition in cognitively unimpaired adults". In: *Neurology* 93.1, E29–E39. ISSN: 1526632X. DOI: 10.1212/WNL.0000000000007728.

Maass, Anne et al. (2017). "NeuroImage Comparison of multiple tau-PET measures as biomarkers in aging and Alzheimer ' s disease". In: *NeuroImage* 157.December 2016, pp. 448–463. ISSN: 1053-8119. DOI: 10.1016/j.neuroimage.2017.05.058. URL: http://dx.doi.org/10.1016/j.neuroimage.2017.05.058.

Maass, Anne et al. (2018a). "Entorhinal Tau Pathology , Episodic Memory Decline , and Neurodegeneration in Aging". In: 38.3, pp. 530–543. DOI: 10.1523/JNEUROSCI.2028-17.2017.

Maass, Anne et al. (2018b). "Entorhinal Tau Pathology , Episodic Memory Decline , and Neurodegeneration in Aging". In: *Journal of Neuroscience* 38.3, pp. 530–543. DOI: 10.1523/JNEUROSCI.2028-17.2017.

Maass, Anne et al. (2019). "Alzheimer's pathology targets distinct memory networks in the ageing brain". In: *Brain : a journal of neurology* 142.8, pp. 2492–2509. ISSN: 14602156. DOI: 10.1093/brain/awz154.

Machado, Alejandra et al. (2020). "The cholinergic system and treatment response in subtypes of Alzheimer's disease". In: *bioRxiv*. DOI: 10.1101/2020.01.23.

20018507. URL: http://adni.loni.usc.edu/wp-content/uploads/how_to_apply/ADNI_Acknowledgement_List.pdf.

Maeda, Sumihiro and Akihiko Takashima (2007). "Granular Tau Oligomers as Intermediates of Tau Filaments Supporting information". In: 000023, pp. 2–5.

Maier-Hein, Klaus H. et al. (Dec. 2017). "The challenge of mapping the human connectome based on diffusion tractography". In: *Nature Communications* 8.1, p. 1349. ISSN: 2041-1723. DOI: 10.1038/s41467-017-01285-x. URL: http://www.ncbi.nlm.nih.gov/pubmed/29116093http://www.pubmedcentral.nih.gov/articlerender.fcgi?artid=PMC5677006http://www.nature.com/articles/s41467-017-01285-x.

Makaretz, Sara J. et al. (2018). "Flortaucipir tau PET imaging in semantic variant primary progressive aphasia". In: *Journal of Neurology, Neurosurgery and Psychiatry* 89.10, pp. 1024–1031. ISSN: 1468330X. DOI: 10.1136/jnnp-2017-316409.

Mandelkow, E. M. et al. (1992). "Glycogen synthase kinase-3 and the Alzheimer-like state of microtubule-associated protein tau". In: *FEBS Letters* 314.3, pp. 315–321. ISSN: 00145793. DOI: 10.1016/0014-5793(92)81496-9.

Mantyh, William G. et al. (2019). "Tau Positron Emission Tomographic Findings in a Former US Football Player with Pathologically Confirmed Chronic Traumatic Encephalopathy". In: *JAMA Neurology* 94158.4, pp. 517–521. ISSN: 21686157. DOI: 10.1001/jamaneurol.2019.4509.

Marks, Shawn M. et al. (2017). "Tau and β-amyloid are associated with medial temporal lobe structure, function, and memory encoding in normal aging". In: *Journal of Neuroscience* 37.12, pp. 3192–3201. ISSN: 15292401. DOI: 10.1523/JNEUROSCI.3769-16.2017.

Marquié, Marta et al. (Nov. 2015). "Validating novel tau positron emission tomography tracer [F-18]-AV-1451 (T807) on postmortem brain tissue." In: *Annals of neurology* 78.5, pp. 787–800. ISSN: 1531-8249. DOI: 10.1002/ana.24517. URL: http://www.ncbi.nlm.nih.gov/pubmed/26344059http://www.pubmedcentral.nih.gov/articlerender.fcgi?artid=PMC4900162.

Marquié, Marta et al. (Oct. 2017). "[F-18]-AV-1451 binding correlates with postmortem neurofibrillary tangle Braak staging". In: *Acta Neuropathologica* 134.4, pp. 619–628. ISSN: 0001-6322. DOI: 10.1007/s00401-017-1740-8. URL: http://link.springer.com/10.1007/s00401-017-1740-8.

Marshall, Gad A. et al. (2007). "Early-onset Alzheimer's disease is associated with greater pathologic burden". In: *Journal of Geriatric Psychiatry and Neurology* 20.1, pp. 29–33. ISSN: 08919887. DOI: 10.1177/0891988706297086.

Maruyama, Masahiro et al. (2013). "Imaging of tau pathology in a tauopathy mouse model and in alzheimer patients compared to normal controls". In: *Neuron* 79.6,

pp. 1094–1108. ISSN: 08966273. DOI: 10.1016/j.neuron.2013.07.037. URL: http://dx.doi.org/10.1016/j.neuron.2013.07.037.

Masters, C L et al. (1985). "Amyloid plaque core protein in Alzheimer disease and Down syndrome." In: *Proceedings of the National Academy of Sciences of the United States of America* 82.12, pp. 4245–9. ISSN: 0027-8424. DOI: 10.1073/pnas.82.12.4245. URL: http://www.ncbi.nlm.nih.gov/pubmed/3159021%5Cnhttp://www.pubmedcentral.nih.gov/articlerender.fcgi?artid=PMC397973.

Masters, Colin L. and Dennis J. Selkoe (2012). "Biochemistry of amyloid β-protein and amyloid deposits in Alzheimer disease". In: *Cold Spring Harbor Perspectives in Medicine* 2.6. ISSN: 21571422. DOI: 10.1101/cshperspect.a006262.

Mathys, Hansruedi et al. (June 2019). "Single-cell transcriptomic analysis of Alzheimer's disease". In: *Nature* 570.7761, pp. 332–337. ISSN: 0028-0836. DOI: 10.1038/s41586-019-1195-2. URL: http://www.nature.com/articles/s41586-019-1195-2.

Mattsson, Niklas et al. (July 2011). "The Alzheimer's Association external quality control program for cerebrospinal fluid biomarkers". In: *Alzheimer's & Dementia* 7.4, pp. 386–395. ISSN: 15525260. DOI: 10.1016/j.jalz.2011.05.2243. URL: http://doi.wiley.com/10.1016/j.jalz.2011.05.2243.

Mattsson, Niklas et al. (2017). " 18 F-AV-1451 and CSF T-tau and P-tau as biomarkers in Alzheimer's disease ". In: *EMBO Molecular Medicine* 9.9, pp. 1212–1223. ISSN: 1757-4676. DOI: 10.15252/emmm.201707809.

Mattsson, Niklas et al. (2018a). "Comparing 18 F-AV-1451 with CSF t-tau and p-tau for diagnosis of Alzheimer disease". In: *Neurology* 90.5, e388–e395. ISSN: 1526632X. DOI: 10.1212/WNL.0000000000004887.

Mattsson, Niklas et al. (2018b). "Greater tau load and reduced cortical thickness in APOE ϵ4-negative Alzheimer's disease: a cohort study". In: *Alzheimer's Research and Therapy* 10.1, pp. 1–12. ISSN: 17589193. DOI: 10.1186/s13195-018-0403-x.

Mattsson-Carlgren, Niklas et al. (Apr. 2020). "Aβ deposition is associated with increases in soluble and phosphorylated tau that precede a positive Tau PET in Alzheimer's disease". In: *Science Advances* 6.16, eaaz2387. ISSN: 2375-2548. DOI: 10.1126/sciadv.aaz2387. URL: https://advances.sciencemag.org/lookup/doi/10.1126/sciadv.aaz2387.

McDade, Eric et al. (2018). "Longitudinal cognitive and biomarker changes in dominantly inherited Alzheimer disease". In: *Neurology* 91.14, E1295–E1306. ISSN: 1526632X. DOI: 10.1212/WNL.0000000000006277.

McKee, Ann C. et al. (2015). "The neuropathology of chronic traumatic encephalopathy". In: *Brain Pathology* 25.3, pp. 350–364. ISSN: 17503639. DOI: 10.1111/bpa.12248.

McKhann, G et al. (2011). "The diagnosis of dementia due to Alzheimer's disease: Recommendations from the National Institute on Aging- Alzheimer's Association workgroups on diagnostic guidelines for Alzheimer's disease". In: *Alzheimers Dementia* 7.3, pp. 263–269. ISSN: 1552-5279. DOI: 10.1016/j.jalz.2011.03.005.The.

McMillan, Corey T. et al. (Dec. 2016). "Multimodal evaluation demonstrates in vivo 18F-AV-1451 uptake in autopsy-confirmed corticobasal degeneration". In: *Acta Neuropathologica* 132.6, pp. 935–937. ISSN: 0001-6322. DOI: 10.1007/s00401-016-1640-3. URL: http://link.springer.com/10.1007/s00401-016-1640-3.

Mendez, Mario F. (Feb. 2019). "Early-onset Alzheimer Disease and Its Variants". In: *CONTINUUM: Lifelong Learning in Neurology* 25.1, pp. 34–51. ISSN: 1080-2371. DOI: 10.1212/CON.0000000000000687. URL: http://journals.lww.com/00132979-201902000-00005.

Menkes-Caspi, Noa et al. (2015). "Pathological tau disrupts ongoing network activity". In: *Neuron* 85.5, pp. 959–966. ISSN: 10974199. DOI: 10.1016/j.neuron.2015.01.025. URL: http://dx.doi.org/10.1016/j.neuron.2015.01.025.

Mesulam, M. -Marsel et al. (1983). "Cholinergic innervation of cortex by the basal forebrain: Cytochemistry and cortical connections of the septal area, diagonal band nuclei, nucleus basalis (Substantia innominata), and hypothalamus in the rhesus monkey". In: *Journal of Comparative Neurology* 214.2, pp. 170–197. ISSN: 10969861. DOI: 10.1002/cne.902140206.

Mesulam, Marsel et al. (2004). "Cholinergic nucleus basalis tauopathy emerges early in the aging-MCI-AD continuum". In: *Annals of Neurology* 55.6, pp. 815–828. ISSN: 03645134. DOI: 10.1002/ana.20100.

Mesulam, Marsel et al. (June 2008). "Alzheimer and frontotemporal pathology in subsets of primary progressive aphasia". In: *Annals of Neurology* 63.6, pp. 709–719. ISSN: 03645134. DOI: 10.1002/ana.21388. URL: https://www.ncbi.nlm.nih.gov/pmc/articles/PMC3624763/pdf/nihms412728.pdfhttp://doi.wiley.com/10.1002/ana.21388.

Meyer, Pierre François et al. (2019). "Characterization of Alzheimer Disease Biomarker Discrepancies Using Cerebrospinal Fluid Phosphorylated Tau and AV1451 Positron Emission Tomography". In: *JAMA Neurology*, pp. 1–9. ISSN: 21686157. DOI: 10.1001/jamaneurol.2019.4749.

Miller, Jeremy A, Steve Horvath, and Daniel H Geschwind (2010). "Divergence of human and mouse brain transcriptome highlights Alzheimer disease pathways". In: *Proceedings of the National Academy of Sciences* 107.28, pp. 12698–12703. ISSN: 0027-8424. DOI: 10.1073/pnas.0914257107. URL: http://www.pnas.org/lookup/doi/10.1073/pnas.0914257107.

Miller, Zachary A. et al. (2013). "Handedness and language learning disability differentially distribute in progressive aphasia variants". In: *Brain* 136.11, pp. 3461–3473. ISSN: 14602156. DOI: 10.1093/brain/awt242.

Miller, Zachary A. et al. (2018). "Prevalence of mathematical and visuospatial learning disabilities in patients with posterior cortical atrophy". In: *JAMA Neurology* 75.6, pp. 728–737. ISSN: 21686149. DOI: 10.1001/jamaneurol.2018.0395.

Miller, Zachary A et al. (2019). "Cortical developmental abnormalities in logopenic variant primary progressive aphasia with dyslexia". In: *Brain Communications*, pp. 1–8. DOI: 10.1093/braincomms/fcz027.

Mirbaha, Hilda et al. (2015). "Tau trimers are the minimal propagation unit spontaneously internalized to seed intracellular aggregation". In: *Journal of Biological Chemistry* 290.24, pp. 14893–14903. ISSN: 1083351X. DOI: 10.1074/jbc.M115.652693.

Mirbaha, Hilda et al. (2018). "Inert and seed-competent tau monomers suggest structural origins of aggregation". In: *eLife* 7, pp. 1–29. ISSN: 2050084X. DOI: 10.7554/eLife.36584.

Mishizen-Eberz, Amanda J. et al. (2004). "Biochemical and molecular studies of NMDA receptor subunits NR1/2A/2B in hippocampal subregions throughout progression of Alzheimer's disease pathology". In: *Neurobiology of Disease* 15.1, pp. 80–92. ISSN: 09699961. DOI: 10.1016/j.nbd.2003.09.016.

Mishra, Shruti et al. (2017). "AV-1451 PET imaging of tau pathology in preclinical Alzheimer disease: Defining a summary measure". In: *NeuroImage* 161.June, pp. 171–178. ISSN: 10959572. DOI: 10.1016/j.neuroimage.2017.07.050.

Miyamoto, Takashi et al. (2017). "Phosphorylation of tau at Y18, but not tau-fyn binding, is required for tau to modulate NMDA receptor-dependent excitotoxicity in primary neuronal culture". In: *Molecular Neurodegeneration* 12.1, pp. 1–19. ISSN: 17501326. DOI: 10.1186/s13024-017-0176-x.

Mohs, R C et al. (1997). "Development of cognitive instruments for use in clinical trials of antidementia drugs: additions to the Alzheimer's Disease Assessment Scale that broaden its scope. The Alzheimer's Disease Cooperative Study." In: *Alzheimer disease and associated disorders* 11 Suppl 2, pp. 13–21. ISSN: 0893-0341. URL: http://www.ncbi.nlm.nih.gov/pubmed/9236948.

Mondragón-Rodríguez, Siddhartha et al. (2012). "Interaction of endogenous tau protein with synaptic proteins is regulated by N-methyl-D-aspartate receptor-dependent tau phosphorylation". In: *Journal of Biological Chemistry* 287.38, pp. 32040–32053. ISSN: 00219258. DOI: 10.1074/jbc.M112.401240.

Mondragón-Rodríguez, Siddhartha et al. (June 2018). "Phosphorylation of Tau protein correlates with changes in hippocampal theta oscillations and reduces hippocampal excitability in Alzheimer's model". In: *Journal of Biological Chemistry* 293.22, pp. 8462–8472. ISSN: 0021-9258. DOI: 10.1074/jbc.RA117.001187. URL: http://www.jbc.org/lookup/doi/10.1074/jbc.RA117.001187.

Mormino, Elizabeth C. et al. (2012a). "Aβ Deposition in aging is associated with increases in brain activation during successful memory encoding". In: *Cerebral Cortex* 22.8, pp. 1813–1823. ISSN: 10473211. DOI: 10.1093/cercor/bhr255.

Mormino, Elizabeth C. et al. (2012b). "Not quite PIB-positive, not quite PIB-negative: Slight PIB elevations in elderly normal control subjects are biologically relevant". In: *NeuroImage* 59.2, pp. 1152–1160. ISSN: 10538119. DOI: 10.1016/j.neuroimage.2011.07.098. URL: http://dx.doi.org/10.1016/j.neuroimage.2011.07.098.

Mormino, Elizabeth C. et al. (2016). "Polygenic risk of Alzheimer disease is associated with early- and late-life processes". In: *Neurology*, 10.1212/WNL.0000000000002922. ISSN: 0028-3878. DOI: 10.1212/WNL.0000000000002922.

Morris, John C et al. (2009). "PIB Imaging Predicts Progression from Cognitively Normal to Symptomatic Alzheimer's Disease". In: *Archives of Neurology* 66.12, pp. 1469–1475. DOI: 10.1001/archneurol.2009.269.PIB.

Morris, Meaghan et al. (2015). "Tau post-translational modifications in wild-type and human amyloid precursor protein transgenic mice". In: *Nature Neuroscience* 18.8, pp. 1183–1189. ISSN: 15461726. DOI: 10.1038/nn.4067.

Morrison, Brett M., Patrick R. Hof, and John H. Morrison (1998). "Determinants of neuronal vulnerability in neurodegenerative diseases". In: *Annals of Neurology* 44.S1, S32–S44. ISSN: 0364-5134. DOI: 10.1002/ana.410440706.

Mosch, Birgit et al. (2007). "Aneuploidy and DNA replication in the normal human brain and Alzheimer's disease". In: *Journal of Neuroscience* 27.26, pp. 6859–6867. ISSN: 02706474. DOI: 10.1523/JNEUROSCI.0379-07.2007.

Mostafavi, Sara et al. (2018). "A molecular network of the aging human brain provides insights into the pathology and cognitive decline of Alzheimer's disease". In: *Nature Neuroscience* 21.6, pp. 811–819. ISSN: 15461726. DOI: 10.1038/s41593-018-0154-9. URL: http://dx.doi.org/10.1038/s41593-018-0154-9.

Mrdjen, Dunja et al. (2019). "The basis of cellular and regional vulnerability in Alzheimer's disease". In: *Acta Neuropathologica* 138.5, pp. 729–749. ISSN: 14320533. DOI: 10.1007/s00401-019-02054-4. URL: https://doi.org/10.1007/s00401-019-02054-4.

Mudher, Amrit et al. (2017). "What is the evidence that tau pathology spreads through prion-like propagation?" In: *Acta neuropathologica communications* 5.1, p. 99. ISSN: 20515960. DOI: 10.1186/s40478-017-0488-7.

Mueller, Andre et al. (2019). " Tau PET imaging with 18 F-PI-2620 in patients with Alzheimer's disease and healthy controls: a first-in-human study ". In: *Journal of Nuclear Medicine*, jnumed.119.236224. ISSN: 0161-5505. DOI: 10.2967/jnumed.119.236224.

Mueller, Sophia et al. (2013). "Individual Variability in Functional Connectivity Architecture of the Human Brain". In: *Neuron* 77.3, pp. 586–595. ISSN: 08966273. DOI: 10.1016/j.neuron.2012.12.028. URL: http://dx.doi.org/10.1016/j.neuron.2012.12.028.

Munoz, David G., John Woulfe, and Andrew Kertesz (2007). "Argyrophilic thorny astrocyte clusters in association with Alzheimer's disease pathology in possible primary progressive aphasia". In: *Acta Neuropathologica* 114.4, pp. 347–357. ISSN: 00016322. DOI: 10.1007/s00401-007-0266-x.

Muratore, Christina R. et al. (2017). "Cell-type Dependent Alzheimer's Disease Phenotypes: Probing the Biology of Selective Neuronal Vulnerability". In: *Stem Cell Reports* 9.6, pp. 1868–1884. ISSN: 22136711. DOI: 10.1016/j.stemcr.2017.10.015. URL: https://doi.org/10.1016/j.stemcr.2017.10.015.

Murray, Alison D. et al. (2011a). "The balance between cognitive reserve and brain imaging biomarkers of cerebrovascular and Alzheimer's diseases". In: *Brain* 134.12, pp. 3684–3693. ISSN: 14602156. DOI: 10.1093/brain/awr259.

Murray, Melissa E. et al. (Sept. 2011b). "Neuropathologically defined subtypes of Alzheimer's disease with distinct clinical characteristics: A retrospective study". In: *The Lancet Neurology* 10.9, pp. 785–796. ISSN: 14744422. DOI: 10.1016/S1474-4422(11)70156-9.

Nagy, Zs et al. (1997). "Cell cycle markers in the hippocampus in Alzheimer's disease". In: *Acta Neuropathologica* 94.1, pp. 6–15. ISSN: 00016322. DOI: 10.1007/s004010050665.

Narasimhan, Sneha et al. (2017). "Pathological tau strains from human brains recapitulate the diversity of tauopathies in nontransgenic mouse brain". In: *Journal of Neuroscience* 37.47, pp. 11406–11423. ISSN: 15292401. DOI: 10.1523/JNEUROSCI.1230-17.2017.

Neitzel, Julia et al. (July 2019). "Left frontal connectivity attenuates the adverse effect of entorhinal tau pathology on memory". In: *Neurology* 93.4, e347–e357. ISSN: 0028-3878. DOI: 10.1212/WNL.0000000000007822. URL: http://www.neurology.org/lookup/doi/10.1212/WNL.0000000000007822.

Nelson, Peter T. et al. (May 2012). "Correlation of Alzheimer Disease Neuropathologic Changes With Cognitive Status: A Review of the Literature". In: *Journal of Neuropathology & Experimental Neurology* 71.5, pp. 362–381. ISSN: 0022-3069.

DOI: 10.1097/NEN.0b013e31825018f7. URL: https://academic.oup.com/jnen/article-lookup/doi/10.1097/NEN.0b013e31825018f7.

Nelson, Peter T. et al. (2019). "Limbic-predominant age-related TDP-43 encephalopathy (LATE): Consensus working group report". In: *Brain* 142.6, pp. 1503–1527. ISSN: 14602156. DOI: 10.1093/brain/awz099.

Nemetz, P. N. et al. (Jan. 1999). "Traumatic Brain Injury and Time to Onset of Alzheimer's Disease: A Population-based Study". In: *American Journal of Epidemiology* 149.1, pp. 32–40. ISSN: 0002-9262. DOI: 10.1093/oxfordjournals.aje.a009724. URL: https://academic.oup.com/aje/article-lookup/doi/10.1093/oxfordjournals.aje.a009724.

Ng, Kok Pin et al. (2017). "Monoamine oxidase B inhibitor, selegiline, reduces 18 F-THK5351 uptake in the human brain". In: *Alzheimer's Research & Therapy* 9.1, p. 25. ISSN: 0959-4965. DOI: 10.1186/s13195-017-0253-y. URL: http://content.wkhealth.com/linkback/openurl?sid=WKPTLP:landingpage&an=00001756-199808030-00031%5Cnhttp://download.springer.com/static/pdf/689/art%253A10.1186%252Fs13195-017-0253-y.pdf?originUrl=http%3A%2F%2Falzres.biomedcentral.com%2Farticle%2F10.1186%2F.

Niccolini, Flavia et al. (2018). "Disease-related patterns of in vivo pathology in Corticobasal syndrome". In: *European Journal of Nuclear Medicine and Molecular Imaging* 45.13, pp. 2413–2425. ISSN: 16197089. DOI: 10.1007/s00259-018-4104-2.

Nicoll, James A.R. et al. (2019). "Persistent neuropathological effects 14 years following amyloid-β immunization in Alzheimer's disease". In: *Brain* 142.7, pp. 2113–2126. ISSN: 14602156. DOI: 10.1093/brain/awz142.

Noh, Young et al. (2014). "Anatomical heterogeneity of Alzheimer disease: based on cortical thickness on MRIs." In: *Neurology* 83.21, pp. 1936–44. ISSN: 1526-632X. DOI: 10.1212/WNL.0000000000001003. URL: http://www.ncbi.nlm.nih.gov/pubmed/25344382.

Nunez, J. (1988). "Immature and mature variants of MAP2 and tau proteins and neuronal plasticity". In: *Trends in Neurosciences* 11.11, pp. 477–479. ISSN: 01662236. DOI: 10.1016/0166-2236(88)90004-5.

Olsson, Bob et al. (2016). "CSF and blood biomarkers for the diagnosis of Alzheimer's disease: a systematic review and meta-analysis". In: *The Lancet Neurology* 15.7, pp. 673–684. ISSN: 14744465. DOI: 10.1016/S1474-4422(16)00070-3.

Ono, Maiko et al. (2017). "Distinct binding of PET ligands PBB3 and AV-1451 to tau fibril strains in neurodegenerative tauopathies". In: *Brain* 140.3, pp. 764–780. ISSN: 14602156. DOI: 10.1093/brain/aww339.

Orban, Pierre et al. (2015). "Test-retest resting-state fMRI in healthy elderly persons with a family history of Alzheimer's disease." In: *Scientific data* 2, p. 150043.

ISSN: 2052-4463. DOI: 10.1038/sdata.2015.43. URL: http://www.nature.com/articles/sdata201543.

Ossenkoppele, Rik et al. (2012). "Longitudinal imaging of Alzheimer pathology using [11C]PIB, [18F]FDDNP and [18F]FDG PET". In: *European Journal of Nuclear Medicine and Molecular Imaging* 39.6, pp. 990–1000. ISSN: 16197070. DOI: 10.1007/s00259-012-2102-3.

Ossenkoppele, Rik et al. (2015a). "Atrophy patterns in early clinical stages across distinct phenotypes of Alzheimer's disease". In: *Human Brain Mapping* 36.11, pp. 4421–4437. ISSN: 10970193. DOI: 10.1002/hbm.22927.

Ossenkoppele, Rik et al. (2015b). "Atrophy patterns in early clinical stages across distinct phenotypes of Alzheimer's disease". In: *Human Brain Mapping* 36.11, pp. 4421–4437. ISSN: 10970193. DOI: 10.1002/hbm.22927.

Ossenkoppele, Rik et al. (Feb. 2015c). "Tau, amyloid, and hypometabolism in a patient with posterior cortical atrophy". In: *Annals of Neurology* 77.2, pp. 338–342. ISSN: 03645134. DOI: 10.1002/ana.24321. URL: http://doi.wiley.com/10.1002/ana.24321.

Ossenkoppele, Rik et al. (2015d). "The behavioural/dysexecutive variant of Alzheimer's disease: Clinical, neuroimaging and pathological features". In: *Brain* 138.9, pp. 2732–2749. ISSN: 14602156. DOI: 10.1093/brain/awv191.

Ossenkoppele, Rik et al. (2016a). "Tau PET patterns mirror clinical and neuroanatomical variability in Alzheimer's disease". In: *Brain* 139.5, pp. 1551–1567. ISSN: 14602156. DOI: 10.1093/brain/aww027. URL: http://brain.oxfordjournals.org/.

Ossenkoppele, Rik et al. (2016b). "Tau PET patterns mirror clinical and neuroanatomical variability in Alzheimer's disease". In: *Brain* 139.5, pp. 1551–1567. ISSN: 14602156. DOI: 10.1093/brain/aww027.

Ossenkoppele, Rik et al. (2018). "Discriminative accuracy of [18F]flortaucipir positron emission tomography for Alzheimer disease vs other neurodegenerative disorders". In: *JAMA - Journal of the American Medical Association* 320.11, pp. 1151–1162. ISSN: 15383598. DOI: 10.1001/jama.2018.12917.

Ossenkoppele, Rik et al. (2019). "Tau covariance patterns in Alzheimer's disease patients match intrinsic connectivity networks in the healthy brain". In: *NeuroImage: Clinical* 23.April, p. 101848. ISSN: 22131582. DOI: 10.1016/j.nicl.2019.101848. URL: https://doi.org/10.1016/j.nicl.2019.101848https://linkinghub.elsevier.com/retrieve/pii/S2213158219301986.

Ossenkoppele, Rik et al. (Feb. 2020). "Distinct tau PET patterns in atrophy-defined subtypes of Alzheimer's disease". In: *Alzheimer's & Dementia* 16.2, pp. 335–344. ISSN: 1552-5260. DOI: 10.1016/j.jalz.2019.08.201. URL: https://doi.org/

10.1016/j.jalz.2019.08.201https://onlinelibrary.wiley.com/doi/abs/10.1016/j.jalz.2019.08.201.

Ota, Kenichi et al. (2015). "Effects of imaging modalities, brain atlases and feature selection on prediction of Alzheimer's disease". In: *Journal of Neuroscience Methods* 256, pp. 168–183. ISSN: 1872678X. DOI: 10.1016/j.jneumeth.2015.08.020.

Palmqvist, Sebastian et al. (2014). "Accuracy of Brain Amyloid Detection in Clinical Practice Using Cerebrospinal Fluid β-Amyloid 42". In: *JAMA Neurology* 71.10, p. 1282. ISSN: 2168-6149. DOI: 10.1001/jamaneurol.2014.1358. URL: http://archneur.jamanetwork.com/article.aspx?doi=10.1001/jamaneurol.2014.1358.

Palmqvist, Sebastian et al. (Dec. 2017). "Earliest accumulation of β-amyloid occurs within the default-mode network and concurrently affects brain connectivity". In: *Nature Communications* 8.1, p. 1214. ISSN: 2041-1723. DOI: 10.1038/s41467-017-01150-x. URL: http://dx.doi.org/10.1038/s41467-017-01150-xhttp://www.nature.com/articles/s41467-017-01150-x.

Pankov, Aleksandr et al. (2016). "Data-driven regions of interest for longitudinal change in frontotemporal lobar degeneration". In: *NeuroImage: Clinical* 12, pp. 332–340. ISSN: 22131582. DOI: 10.1016/j.nicl.2015.08.002. URL: http://dx.doi.org/10.1016/j.nicl.2015.08.002.

Pascoal, Tharick A. et al. (2018). "In vivo quantification of neurofibrillary tangles with [18 F]MK-6240". In: *Alzheimer's Research and Therapy* 10.1, pp. 1–14. ISSN: 17589193. DOI: 10.1186/s13195-018-0402-y.

Paula-Barbosa, Manuel, Maria Amélia Tavares, and António Cadete-Leite (1987). "A quantitative study of frontal cortex dendritic microtubules in patients with Alzheimer's disease". In: *Brain Research* 417.1, pp. 139–142. ISSN: 00068993. DOI: 10.1016/0006-8993(87)90188-0.

Pearson, R. C.A. (1996). "Cortical connections and the pathology of Alzheimer's disease". In: *Neurodegeneration* 5.4, pp. 429–434. ISSN: 10558330. DOI: 10.1006/neur.1996.0058.

Pedregosa, Fabian et al. (2012). "Scikit-learn: Machine Learning in Python". In: *Journal of Machine Learning Research* 12, pp. 2825–2830. ISSN: 15324435. DOI: 10.1007/s13398-014-0173-7.2. URL: http://arxiv.org/abs/1201.0490.

Peng, Chao, John Q Trojanowski, and Virginia M-Y Lee (2020). "Protein transmission in neurodegenerative disease." In: *Nature reviews. Neurology* 16.April, pp. 199–212. ISSN: 1759-4766. DOI: 10.1038/s41582-020-0333-7. URL: http://www.ncbi.nlm.nih.gov/pubmed/32203399.

Pereira, Joana B. et al. (2019). "Amyloid and tau accumulate across distinct spatial networks and are differentially associated with brain connectivity". In: *eLife* 8, pp. 1–25. ISSN: 2050084X. DOI: 10.7554/eLife.50830.

Pereira, Joana B. et al. (2020). "Spatial patterns of tau deposition are associated with amyloid, ApoE, sex, and cognitive decline in older adults". In: *European Journal of Nuclear Medicine and Molecular Imaging*. ISSN: 16197089. DOI: 10.1007/s00259-019-04669-x.

Perez-Nievas, Beatriz G. et al. (2013). "Dissecting phenotypic traits linked to human resilience to Alzheimer's pathology". In: *Brain* 136.8, pp. 2510–2526. ISSN: 14602156. DOI: 10.1093/brain/awt171.

Perosa, Valentina et al. (2020). "Hippocampal vascular reserve associated with cognitive performance and hippocampal volume". In: *Brain : a journal of neurology* 143.2, pp. 622–634. ISSN: 14602156. DOI: 10.1093/brain/awz383.

Petersen, Cathrine et al. (2019). "Alzheimer's disease clinical variants show distinct regional patterns of neurofibrillary tangle accumulation". In: *Acta Neuropathologica* 138.4, pp. 597–612. ISSN: 14320533. DOI: 10.1007/s00401-019-02036-6. URL: https://doi.org/10.1007/s00401-019-02036-6.

Pfeffer, R I et al. (May 1982). "Measurement of functional activities in older adults in the community." In: *Journal of gerontology* 37.3, pp. 323–9. ISSN: 0022-1422. URL: http://www.ncbi.nlm.nih.gov/pubmed/7069156.

Pichet Binette, Alexa et al. (2020). "Morphometric network differences in ageing versus Alzheimer's disease dementia". In: *Brain : a journal of neurology* 143.2, pp. 635–649. ISSN: 14602156. DOI: 10.1093/brain/awz414.

Pontecorvo, Michael J. et al. (2019). "A multicentre longitudinal study of flortaucipir (18F) in normal ageing, mild cognitive impairment and Alzheimer's disease dementia". In: *Brain* 142.6, pp. 1723–1735. ISSN: 14602156. DOI: 10.1093/brain/awz090.

Pooler, Amy M et al. (2013). "Physiological release of endogenous tau is stimulated by neuronal activity". In: *EMBO reports* 14.4, pp. 389–394. ISSN: 1469-221X. DOI: 10.1038/embor.2013.15. URL: http://embor.embopress.org/cgi/doi/10.1038/embor.2013.15.

Pooler, Amy M. et al. (2015). "Amyloid accelerates tau propagation and toxicity in a model of early Alzheimer's disease". In: *Acta neuropathologica communications* 3, p. 14. ISSN: 20515960. DOI: 10.1186/s40478-015-0199-x.

Prasher, V. P. et al. (1998). "Molecular mapping of Alzheimer-type dementia in Down's syndrome". In: *Annals of Neurology* 43.3, pp. 380–383. ISSN: 03645134. DOI: 10.1002/ana.410430316.

Prince, Martin et al. (2013). "The global prevalence of dementia: A systematic review and metaanalysis". In: *Alzheimer's and Dementia* 9.1, pp. 63–75. ISSN: 15525260. DOI: 10.1016/j.jalz.2012.11.007. URL: http://dx.doi.org/10.1016/j.jalz.2012.11.007.

Puzzo, Daniela et al. (2017). "LTP and memory impairment caused by extracellular Aβ and Tau oligomers is APP-dependent". In: *eLife* 6, pp. 1–21. ISSN: 2050-084X. DOI: 10.7554/elife.26991.

Qi, Haoling et al. (2015). "Nuclear magnetic resonance spectroscopy characterization of interaction of Tau with DNA and its regulation by phosphorylation". In: *Biochemistry* 54.7, pp. 1525–1533. ISSN: 15204995. DOI: 10.1021/bi5014613.

Qiang, Wei et al. (2017). "Structural variation in amyloid-β fibrils from Alzheimer's disease clinical subtypes". In: *Nature* 541.7636, pp. 217–221. ISSN: 14764687. DOI: 10.1038/nature20814.

Quiroz, Yakeel T. et al. (2018). "Association between amyloid and tau accumulation in young adults with autosomal dominant Alzheimer disease". In: *JAMA Neurology* 75.5, pp. 548–556. ISSN: 21686149. DOI: 10.1001/jamaneurol.2017.4907.

Rabinovici, G. D. and W. J. Jagust (2009). "Amyloid imaging in aging and dementia: Testing the amyloid hypothesis in vivo". In: *Behavioural Neurology* 21.1-2, pp. 117–128. ISSN: 09534180. DOI: 10.3233/BEN-2009-0232.

Rabinovici, Gil D et al. (Feb. 2010). "Increased metabolic vulnerability in early-onset Alzheimer's disease is not related to amyloid burden." In: *Brain : a journal of neurology* 133.Pt 2, pp. 512–28. ISSN: 1460-2156. DOI: 10.1093/brain/awp326. URL: http://www.ncbi.nlm.nih.gov/pubmed/20080878http://www.pubmedcentral.nih.gov/articlerender.fcgi?artid=PMC2858015.

Raj, Ashish, Amy Kuceyeski, and Michael Weiner (2012). "A Network Diffusion Model of Disease Progression in Dementia". In: *Neuron* 73.6, pp. 1204–1215. ISSN: 08966273. DOI: 10.1016/j.neuron.2011.12.040. URL: http://dx.doi.org/10.1016/j.neuron.2011.12.040.

Ramage, S. N. et al. (2005). "Hyperphosphorylated tau and amyloid precursor protein deposition is increased in the brains of young drug abusers". In: *Neuropathology and Applied Neurobiology* 31.4, pp. 439–448. ISSN: 03051846. DOI: 10.1111/j.1365-2990.2005.00670.x.

Rao, Shalini S. and Paul Anthony Adlard (2018). "Untangling Tau and Iron: Exploring the Interaction Between Iron and Tau in Neurodegeneration". In: *Frontiers in Molecular Neuroscience* 11.August, pp. 1–13. ISSN: 16625099. DOI: 10.3389/fnmol.2018.00276.

Rapoport, Mark et al. (2002). "Tau is essential to β-amyloid-induced neurotoxicity". In: *Proceedings of the National Academy of Sciences of the United States of America* 99.9, pp. 6364–6369. ISSN: 00278424. DOI: 10.1073/pnas.092136199.

Rapoport, S. I. (1989). "Hypothesis: Alzheimer's disease is a phylogenetic disease". In: *Medical Hypotheses* 29.3, pp. 147–150. ISSN: 03069877. DOI: 10.1016/0306-9877(89)90185-0.

Rapoport, Stanley I. (1990). "Integrated phylogeny of the primate brain, with special reference to humans and their diseases". In: *Brain Research Reviews* 15.3, pp. 267–294. ISSN: 01650173. DOI: 10.1016/0165-0173(90)90004-8.

Rapoport, Stanley I. and Peter T. Nelson (Dec. 2011). "Biomarkers and evolution in Alzheimer disease". In: *Progress in Neurobiology* 95.4, pp. 510–513. ISSN: 03010082. DOI: 10.1016/j.pneurobio.2011.07.006. URL: https://linkinghub.elsevier.com/retrieve/pii/S0031938416312148https://linkinghub.elsevier.com/retrieve/pii/S0301008211001171.

Rauch, Jennifer N. et al. (2020). "LRP1 is a master regulator of tau uptake and spread". In: *Nature* 1.October 2019, pp. 1–5. ISSN: 0028-0836. DOI: 10.1038/s41586-020-2156-5. URL: http://www.nature.com/articles/s41586-020-2156-5.

Reed, Lee A. et al. (1997). "Autosomal dominant dementia with widespread neurofibrillary tangles". In: *Annals of Neurology* 42.4, pp. 564–572. ISSN: 03645134. DOI: 10.1002/ana.410420406.

Regan, Philip, Daniel J. Whitcomb, and Kwangwook Cho (2017). "Physiological and pathophysiological implications of synaptic tau". In: *Neuroscientist* 23.2, pp. 137–151. ISSN: 10894098. DOI: 10.1177/1073858416633439.

Regan, Philip et al. (2015). "Tau phosphorylation at serine 396 residue is required for hippocampal LTD". In: *Journal of Neuroscience* 35.12, pp. 4804–4812. ISSN: 15292401. DOI: 10.1523/JNEUROSCI.2842-14.2015.

Reitz, C et al. (2009). "Memory performance is related to amyloid and tau pathology in the hippocampus". In: pp. 715–721. DOI: 10.1136/jnnp.2008.154146.

Resende, Elisa de Paula França et al. (2020). "Language and spatial dysfunction in Alzheimer disease with white matter thorn-shaped astrocytes". In: *Neurology*, 10.1212/WNL.0000000000008937. ISSN: 0028-3878. DOI: 10.1212/wnl.0000000000008937.

Risacher, Shannon L. et al. (2017). "Alzheimer disease brain atrophy subtypes are associated with cognition and rate of decline". In: *Neurology* 89.21, pp. 2176–2186. ISSN: 1526632X. DOI: 10.1212/WNL.0000000000004670.

Ritchie, Karen and Jacques Touchon (1992). "Heterogeneity in senile dementia of the Alzheimer type: Individual differences, progressive deterioration or clinical sub-types?" In: *Journal of Clinical Epidemiology* 45.12, pp. 1391–1398. ISSN: 08954356. DOI: 10.1016/0895-4356(92)90201-W.

Roberson, Erik D. et al. (2007). "Reducing endogenous tau ameliorates amyloid β-induced deficits in an Alzheimer's disease mouse model". In: *Science* 316.5825, pp. 750–754. ISSN: 00368075. DOI: 10.1126/science.1141736.

Roberson, Erik D. et al. (2011). "Amyloid-β/fyn-induced synaptic, network, and cognitive impairments depend on tau levels in multiple mouse models of alzheimer's disease". In: *Journal of Neuroscience* 31.2, pp. 700–711. ISSN: 02706474. DOI: 10.1523/JNEUROSCI.4152-10.2011.

Robinson, John L et al. (2011). "Neocortical and hippocampal amyloid- b and tau measures associate with dementia in the oldest-old". In: *Brain* 134.12, pp. 3708–3715. DOI: 10.1093/brain/awr308.

Rodriguez, Gustavo A et al. (2019). "Attenuation of entorhinal cortex hyperactivity reduces Aβ and tau pathology". In: *bioRxiv*, p. 487405. DOI: 10.1101/487405. URL: http://biorxiv.org/content/early/2019/03/21/487405.abstract.

Rogalski, Emily et al. (Feb. 2008). "Increased Frequency of Learning Disability in Patients With Primary Progressive Aphasia and Their First-Degree Relatives". In: *Archives of Neurology* 65.2, pp. 1–7. ISSN: 0003-9942. DOI: 10.1001/archneurol.2007.34. URL: http://archneur.jamanetwork.com/article.aspx?doi=10.1001/archneurol.2007.34.

Rorabaugh, Jacki M. et al. (2017). "Chemogenetic locus coeruleus activation restores reversal learning in a rat model of Alzheimer's disease". In: *Brain* 140.11, pp. 3023–3038. ISSN: 14602156. DOI: 10.1093/brain/awx232.

Rosen, W. G., R. C. Mohs, and K. L. Davis (1984). "A new rating scale for Alzheimer's disease". In: *American Journal of Psychiatry* 141.11, pp. 1356–1364. ISSN: 0002953X. DOI: 10.1176/ajp.141.11.1356.

Rottscholl, Robert et al. (2016). "Chronic consumption of Annona muricata juice triggers and aggravates cerebral tau phosphorylation in wild-type and MAPT transgenic mice". In: *Journal of Neurochemistry* 139.4, pp. 624–639. ISSN: 14714159. DOI: 10.1111/jnc.13835.

Rousset, O G, Y Ma, and A C Evans (May 1998). "Correction for partial volume effects in PET: principle and validation." In: *Journal of nuclear medicine : official publication, Society of Nuclear Medicine* 39.5, pp. 904–11. ISSN: 0161-5505. URL: http://www.ncbi.nlm.nih.gov/pubmed/9591599.

Rovelet-Lecrux, Anne et al. (2006). "APP locus duplication causes autosomal dominant early-onset Alzheimer disease with cerebral amyloid angiopathy". In: *Nature Genetics* 38.1, pp. 24–26. ISSN: 10614036. DOI: 10.1038/ng1718.

Run, Xiaoqin et al. (Mar. 2009). "Anesthesia Induces Phosphorylation of Tau". In: *Journal of Alzheimer's Disease* 16.3, pp. 619–626. ISSN: 18758908. DOI: 10.3233/JAD-

2009-1003. URL: https://www.medra.org/servlet/aliasResolver?alias=iospress&doi=10.3233/JAD-2009-1003.

Sakae, Nobutaka et al. (2019). "Clinicopathologic subtype of Alzheimer's disease presenting as corticobasal syndrome". In: *Alzheimer's and Dementia* 15.9, pp. 1218–1228. ISSN: 15525279. DOI: 10.1016/j.jalz.2019.04.011.

Saman, Sudad et al. (2012). "Exosome-associated tau is secreted in tauopathy models and is selectively phosphorylated in cerebrospinal fluid in early Alzheimer disease". In: *Journal of Biological Chemistry* 287.6, pp. 3842–3849. ISSN: 00219258. DOI: 10.1074/jbc.M111.277061.

Samsonov, Andrey et al. (2004). "Tau interaction with microtubules in vivo". In: *Journal of Cell Science* 117.25, pp. 6129–6141. ISSN: 00219533. DOI: 10.1242/jcs.01531.

Sanabria Bohórquez, Sandra et al. (2019). "[18F]GTP1 (Genentech Tau Probe 1), a radioligand for detecting neurofibrillary tangle tau pathology in Alzheimer's disease". In: *European Journal of Nuclear Medicine and Molecular Imaging* 46.10, pp. 2077–2089. ISSN: 16197089. DOI: 10.1007/s00259-019-04399-0.

Sanders, David W. et al. (2014). "Distinct tau prion strains propagate in cells and mice and define different tauopathies". In: *Neuron* 82.6, pp. 1271–1288. ISSN: 10974199. DOI: 10.1016/j.neuron.2014.04.047. URL: http://dx.doi.org/10.1016/j.neuron.2014.04.047.

Sando, Sigrid B. et al. (2008). "APOE ϵ4 lowers age at onset and is a high risk factor for Alzheimer's disease; A case control study from central Norway". In: *BMC Neurology* 8, pp. 1–7. ISSN: 14712377. DOI: 10.1186/1471-2377-8-9.

Santa-Maria, Ismael et al. (2012). "The MAPT H1 haplotype is associated with tangle-predominant dementia". In: *Acta Neuropathologica* 124.5, pp. 693–704. ISSN: 00016322. DOI: 10.1007/s00401-012-1017-1.

Santacruz, K. et al. (2005). "Medicine: Tau suppression in a neurodegenerative mouse model improves memory function". In: *Science* 309.5733, pp. 476–481. ISSN: 00368075. DOI: 10.1126/science.1113694.

Sarica, Alessia et al. (2018). "MRI asymmetry index of hippocampal subfields increases through the continuum from the mild cognitive impairment to the alzheimer's disease". In: *Frontiers in Neuroscience* 12.AUG, pp. 1–12. ISSN: 1662453X. DOI: 10.3389/fnins.2018.00576.

Satizabal, Claudia L et al. (2016). "Incidence of dementia over three decades in the Framingham heart study." In: *New England Journal of Medicine* 374, pp. 523–532. ISSN: 0028-4793. DOI: 10.1056/NEJMoa1504327.

Sato, Chihiro et al. (2018). "Tau Kinetics in Neurons and the Human Central Nervous System". In: *Neuron* 97.6, pp. 1284–1298. ISSN: 10974199. DOI: 10.1016/j.neuron.2018.02.015.

Satoh, Akiko and Koichi M. Iijima (2019). "Roles of tau pathology in the locus coeruleus (LC) in age-associated pathophysiology and Alzheimer's disease pathogenesis: Potential strategies to protect the LC against aging". In: *Brain Research* 1702.Lc, pp. 17–28. ISSN: 18726240. DOI: 10.1016/j.brainres.2017.12.027. URL: https://doi.org/10.1016/j.brainres.2017.12.027.

Scheff, Scheff W. and Douglas A. Price (1993). "Synapse loss in the temporal lobe in Alzheimer's disease". In: *Annals of Neurology* 33.2, pp. 190–199. ISSN: 15318249. DOI: 10.1002/ana.410330209.

Scheltens, Nienke M.E. et al. (Nov. 2017). "Cognitive subtypes of probable Alzheimer's disease robustly identified in four cohorts". In: *Alzheimer's & Dementia* 13.11, pp. 1226–1236. ISSN: 15525260. DOI: 10.1016/j.jalz.2017.03.002. URL: http://doi.wiley.com/10.1016/j.jalz.2017.03.002.

Scheltens, Philip and Kenneth Rockwood (2011). "How golden is the gold standard of neuropathology in dementia?" In: *Alzheimer's and Dementia* 7.4, pp. 486–489. ISSN: 15525260. DOI: 10.1016/j.jalz.2011.04.011. URL: http://dx.doi.org/10.1016/j.jalz.2011.04.011.

Scherr, Martin et al. (2019). "Effective connectivity in the default mode network is distinctively disrupted in Alzheimer's disease-A simultaneous resting-state FDG-PET/fMRI study". In: *Human Brain Mapping* June 2018, pp. 1–10. ISSN: 10659471. DOI: 10.1002/hbm.24517. URL: http://doi.wiley.com/10.1002/hbm.24517.

Schindler, Suzanne E. et al. (2019). "Emerging cerebrospinal fluid biomarkers in autosomal dominant Alzheimer's disease". In: *Alzheimer's and Dementia* 15.5, pp. 655–665. ISSN: 15525279. DOI: 10.1016/j.jalz.2018.12.019.

Schneider, Julie A. et al. (Aug. 2009). "The neuropathology of probable Alzheimer disease and mild cognitive impairment". In: *Annals of Neurology* 66.2, pp. 200–208. ISSN: 03645134. DOI: 10.1002/ana.21706. URL: https://www.ncbi.nlm.nih.gov/pmc/articles/PMC3624763/pdf/nihms412728.pdfhttp://doi.wiley.com/10.1002/ana.21706.

Schneider, Lon (2020). "A resurrection of aducanumab for Alzheimer's disease". In: *The Lancet Neurology* 19.2, pp. 111–112. ISSN: 14744465. DOI: 10.1016/S1474-4422(19)30480-6. URL: http://dx.doi.org/10.1016/S1474-4422(19)30480-6.

Schneider, Lon S et al. (2015). "Disease : an Appraisal From 1984 To 2014". In: 275.3, pp. 251–283. DOI: 10.1111/joim.12191.Clinical.

Schöll, Michael et al. (2016a). "PET Imaging of Tau Deposition in the Aging Human Brain". In: *Neuron*. ISSN: 10974199. DOI: 10.1016/j.neuron.2016.01.028.

Schöll, Michael et al. (2016b). "PET Imaging of Tau Deposition in the Aging Human Brain". In: *Neuron* 89.5, pp. 971–982. ISSN: 10974199. DOI: 10.1016/j.neuron.2016.01.028.

Schonhaut, Daniel R et al. (Oct. 2017). "18 F-flortaucipir tau positron emission tomography distinguishes established progressive supranuclear palsy from controls and Parkinson disease: A multicenter study". In: *Annals of Neurology* 82.4, pp. 622–634. ISSN: 03645134. DOI: 10.1002/ana.25060. URL: http://doi.wiley.com/10.1002/ana.25060.

Schultz, Aaron P. et al. (2017). "Phases of Hyperconnectivity and Hypoconnectivity in the Default Mode and Salience Networks Track with Amyloid and Tau in Clinically Normal Individuals". In: *The Journal of Neuroscience* 37.16, pp. 4323–4331. ISSN: 0270-6474. DOI: 10.1523/JNEUROSCI.3263-16.2017. URL: http://www.jneurosci.org/lookup/doi/10.1523/JNEUROSCI.3263-16.2017.

Schwarz, Adam J. et al. (2016). "Regional profiles of the candidate tau PET ligand ¹⁸ F-AV-1451 recapitulate key features of Braak histopathological stages". In: *Brain*, aww023. ISSN: 0006-8950. DOI: 10.1093/brain/aww023. URL: http://www.brain.oxfordjournals.org/lookup/doi/10.1093/brain/aww023.

Schwarz, Adam J. et al. (2018). "Topographic staging of tau positron emission tomography images". In: *Alzheimer's and Dementia: Diagnosis, Assessment and Disease Monitoring* 10, pp. 221–231. ISSN: 23528729. DOI: 10.1016/j.dadm.2018.01.006.

Seeley, William W. et al. (2009). "Neurodegenerative Diseases Target Large-Scale Human Brain Networks". In: *Neuron* 62.1, pp. 42–52. ISSN: 08966273. DOI: 10.1016/j.neuron.2009.03.024. URL: http://dx.doi.org/10.1016/j.neuron.2009.03.024.

Selkoe, Dennis J and John Hardy (2016). "The amyloid hypothesis of Alzheimer's disease at 25 years." In: *EMBO molecular medicine*, pp. 1–14. ISSN: 1757-4684. DOI: 10.15252/emmm.201606210. URL: http://www.ncbi.nlm.nih.gov/pubmed/27025652.

Sepulcre, Jorge et al. (2017a). "Hierarchical Organization of Tau and Amyloid Deposits in the Cerebral Cortex". In: *JAMA Neurology* 74.7, p. 813. ISSN: 2168-6149. DOI: 10.1001/jamaneurol.2017.0263. URL: http://archneur.jamanetwork.com/article.aspx?doi=10.1001/jamaneurol.2017.0263.

Sepulcre, Jorge et al. (2017b). "Tau and amyloid β proteins distinctively associate to functional network changes in the aging brain". In: *Alzheimer's and Dementia* 13.11, pp. 1261–1269. ISSN: 15525279. DOI: 10.1016/j.jalz.2017.02.011. URL: http://dx.doi.org/10.1016/j.jalz.2017.02.011.

Sepulcre, Jorge et al. (Dec. 2018). "Neurogenetic contributions to amyloid beta and tau spreading in the human cortex." In: *Nature medicine* 24.12, pp. 1910–1918.

ISSN: 1546-170X. DOI: 10.1038/s41591-018-0206-4. URL: http://www.nature.com/articles/s41591-018-0206-4http://www.ncbi.nlm.nih.gov/pubmed/30374196http://www.pubmedcentral.nih.gov/articlerender.fcgi?artid=PMC6518398.

Shahani, Neelam et al. (2006). "Tau aggregation and progressive neuronal degeneration in the absence of changes in spine density and morphology after targeted expression of Alzheimer's disease-relevant tau constructs in organotypic hippocampal slices". In: *Journal of Neuroscience* 26.22, pp. 6103–6114. ISSN: 02706474. DOI: 10.1523/JNEUROSCI.4245-05.2006.

Shankar, Ganesh M. et al. (2008). "Amyloid-β protein dimers isolated directly from Alzheimer's brains impair synaptic plasticity and memory". In: *Nature Medicine* 14.8, pp. 837–842. ISSN: 10788956. DOI: 10.1038/nm1782.

Shaw, Leslie M. et al. (2009). "Cerebrospinal fluid biomarker signature in alzheimer's disease neuroimaging initiative subjects". In: *Annals of Neurology* 65.4, pp. 403–413. ISSN: 03645134. DOI: 10.1002/ana.21610.

Sheline, Yvette I. et al. (2010). "Amyloid Plaques Disrupt Resting State Default Mode Network Connectivity in Cognitively Normal Elderly". In: *Biological Psychiatry* 67.6, pp. 584–587. ISSN: 00063223. DOI: 10.1016/j.biopsych.2009.08.024. URL: http://dx.doi.org/10.1016/j.biopsych.2009.08.024.

Shiino, Akihiko et al. (2006). "Four subgroups of Alzheimer's disease based on patterns of atrophy using VBM and a unique pattern for early onset disease". In: *NeuroImage* 33.1, pp. 17–26. ISSN: 10538119. DOI: 10.1016/j.neuroimage.2006.06.010.

Shipton, Olivia A. et al. (2011). "Tau protein is required for amyloid β-induced impairment of hippocampal long-term potentiation". In: *Journal of Neuroscience* 31.5, pp. 1688–1692. ISSN: 02706474. DOI: 10.1523/JNEUROSCI.2610-10.2011.

Shugart, Jessica (2019). *Senate ups funding for Alzheimer's research by 350 million for 2020*. URL: https://www.alzforum.org/news/community-news/senate-ups-funding-alzheimers-research-350-million-2020.

Simic, Goran et al. (2010). "Does Alzheimer's disease begin in the brainstem". In: *Neuropathology and applied neurobiology* 35.6, pp. 532–554. DOI: 10.1111/j.1365-2990.2009.01038.x.Annotation.

Sintini, Irene et al. (2019). "Longitudinal tau-PET uptake and atrophy in atypical Alzheimer's disease". In: *NeuroImage: Clinical* 23.March, pp. 1–12. ISSN: 22131582. DOI: 10.1016/j.nicl.2019.101823.

Smith, R. et al. (2019a). "18 F-Flortaucipir in TDP-43 associated frontotemporal dementia". In: *Scientific Reports* 9.1, pp. 1–10. ISSN: 20452322. DOI: 10.1038/s41598-019-42625-9.

Smith, Ruben et al. (2016). "18F-AV-1451 tau PET imaging correlates strongly with tau neuropathology in MAPT mutation carriers". In: *Brain* 139.9, pp. 2372–2379. ISSN: 14602156. DOI: 10.1093/brain/aww163.

Smith, Ruben et al. (2017). "Increased basal ganglia binding of 18F-AV-1451 in patients with progressive supranuclear palsy". In: *Movement Disorders* 32.1, pp. 108–114. ISSN: 15318257. DOI: 10.1002/mds.26813.

Smith, Ruben et al. (2019b). "Correlation of in Vivo [18 F]Flortaucipir with Postmortem Alzheimer Disease Tau Pathology". In: *JAMA Neurology* 76.3, pp. 310–317. ISSN: 21686149. DOI: 10.1001/jamaneurol.2018.3692.

Smith, Ruben et al. (2020). "Head-to-head comparison of tau positron emission tomography tracers [18F]flortaucipir and [18F]RO948". In: *European Journal of Nuclear Medicine and Molecular Imaging* 47.2, pp. 342–354. ISSN: 16197089. DOI: 10.1007/s00259-019-04496-0. URL: http://dx.doi.org/10.1007/s00259-019-04496-0.

Solodkin, Ana, Stacy D. Veldhuizen, and Gary W. Van Hoesen (1996). "Contingent vulnerability of entorhinal parvalbumin-containing neurons in Alzheimer's disease". In: *Journal of Neuroscience* 16.10, pp. 3311–3321. ISSN: 02706474. DOI: 10.1523/jneurosci.16-10-03311.1996.

Southekal, Sudeepti et al. (2018). "Flortaucipir F 18 quantitation using parametric estimation of reference signal intensity". In: *Journal of Nuclear Medicine* 59.6, pp. 944–951. ISSN: 2159662X. DOI: 10.2967/jnumed.117.200006.

Sperling, Reisa a, Jason Karlawish, and Keith a Johnson (2013). "Preclinical Alzheimer disease-the challenges ahead." In: *Nature reviews. Neurology* 9.1, pp. 54–8. ISSN: 1759-4766. DOI: 10.1038/nrneurol.2012.241. URL: http://www.pubmedcentral.nih.gov/articlerender.fcgi?artid=3643203&tool=pmcentrez&rendertype=abstract.

Sperling, Reisa A, Elizabeth Mormino, and Keith Johnson (2014). "The evolution of preclinical Alzheimer's disease: Implications for prevention trials". In: *Neuron* 84.3, pp. 608–622. ISSN: 00958301. DOI: 10.1016/j.neuron.2014.10.038.The.

Sperling, Reisa a et al. (2014). "The A4 study: stopping AD before symptoms begin?" In: *Science translational medicine* 6.228, 228fs13. ISSN: 1946-6242. DOI: 10.1126/scitranslmed.3007941. URL: http://www.pubmedcentral.nih.gov/articlerender.fcgi?artid=4049292&tool=pmcentrez&rendertype=abstract.

Spillantini, M. G., R. A. Crowther, and M. Goedert (June 1996). "Comparison of the neurofibrillary pathology in Alzheimer's disease and familial presenile dementia with tangles". In: *Acta Neuropathologica* 92.1, pp. 42–48. ISSN: 0001-6322. DOI: 10.1007/s004010050487. URL: http://link.springer.com/10.1007/s004010050487.

Spillantini, Maria Grazia and Michel Goedert (1998). "Tau protein pathology in neurodegenerative diseases". In: *Trends in Neurosciences* 21.10, pp. 428–433. ISSN: 01662236. DOI: 10.1016/S0166-2236(98)01337-X.

Spires-Jones, Tara L. and BradleyT Hyman (2014). "The Intersection of Amyloid Beta and Tau at Synapses in Alzheimer's Disease". In: *Neuron* 82.4, pp. 756–771. ISSN: 10974199. DOI: 10.1016/j.neuron.2014.05.004. URL: http://dx.doi.org/10.1016/j.neuron.2014.05.004.

Stern, Robert A. et al. (2019). "Tau positron-emission tomography in former national football league players". In: *New England Journal of Medicine* 380.18, pp. 1716–1725. ISSN: 15334406. DOI: 10.1056/NEJMoa1900757.

Stern, Yaakov (2012). "Cognitive reserve in ageing and Alzheimer's disease". In: *The Lancet Neurology* 11.11, pp. 1006–1012. ISSN: 14744422. DOI: 10.1016/S1474-4422(12)70191-6. URL: http://dx.doi.org/10.1016/S1474-4422(12)70191-6.

Strobel, Gabrielle (2020). *In DIAN-TU, Gantenerumab Brings Down Tau. By a Lot. Open Extension Planned*.

Suárez, Laura E. et al. (2020). "Linking Structure and Function in Macroscale Brain Networks". In: *Trends in Cognitive Sciences* 24.4, pp. 302–315. ISSN: 1879307X. DOI: 10.1016/j.tics.2020.01.008. URL: https://doi.org/10.1016/j.tics.2020.01.008.

Sultan, Audrey et al. (2011). "Nuclear Tau, a key player in neuronal DNA protection". In: *Journal of Biological Chemistry* 286.6, pp. 4566–4575. ISSN: 1083351X. DOI: 10.1074/jbc.M110.199976.

Sun, N. et al. (2019). "Multi-modal latent factor exploration of atrophy, cognitive and tau heterogeneity in Alzheimer's disease". In: *NeuroImage* 201.July. ISSN: 10959572. DOI: 10.1016/j.neuroimage.2019.116043.

Tacik, Pawel et al. (2016). "Genetic disorders with tau pathology: A review of the literature and report of two patients with tauopathy and positive family histories". In: *Neurodegenerative Diseases* 16.1-2, pp. 12–21. ISSN: 16602862. DOI: 10.1159/000440840.

Tackenberg, C. et al. (2013). "NMDA receptor subunit composition determines beta-amyloid-induced neurodegeneration and synaptic loss". In: *Cell Death and Disease* 4.4, pp. 608–10. ISSN: 20414889. DOI: 10.1038/cddis.2013.129. URL: http://dx.doi.org/10.1038/cddis.2013.129.

Tackenberg, Christian and Roland Brandt (2009). "Divergent pathways mediate spine alterations and cell death induced by amyloid-β, wild-type tau, and R406W tau". In: *Journal of Neuroscience* 29.46, pp. 14439–14450. ISSN: 02706474. DOI: 10.1523/JNEUROSCI.3590-09.2009.

Tai, Hwan Ching et al. (2012). "The synaptic accumulation of hyperphosphorylated tau oligomers in alzheimer disease is associated with dysfunction of the ubiquitin-proteasome system". In: *American Journal of Pathology* 181.4, pp. 1426–1435. ISSN: 00029440. DOI: 10.1016/j.ajpath.2012.06.033. URL: http://dx.doi.org/10.1016/j.ajpath.2012.06.033.

Takami, Mako et al. (2009). "γ-Secretase: Successive tripeptide and tetrapeptide release from the transmembrane domain of β-carboxyl terminal fragment". In: *Journal of Neuroscience* 29.41, pp. 13042–13052. ISSN: 02706474. DOI: 10.1523/JNEUROSCI.2362-09.2009.

Takeda, Shuko et al. (Dec. 2015). "Neuronal uptake and propagation of a rare phosphorylated high-molecular-weight tau derived from Alzheimer's disease brain". In: *Nature Communications* 6.1, p. 8490. ISSN: 2041-1723. DOI: 10.1038/ncomms9490. URL: http://www.nature.com/articles/ncomms9490.

Takei, Y (2000). "Defects in axonal elongation and neuronal migration in mice with disrupted tau and map1b genes". In: *Neuroscience Research* 38.5, S105. ISSN: 01680102. DOI: 10.1016/S0168-0102(00)81476-5. URL: https://linkinghub.elsevier.com/retrieve/pii/S0168010200814765.

Tam, Angela et al. (2019). "A highly predictive signature of cognition and brain atrophy for progression to Alzheimer's dementia". In: *GigaScience* 8.5, pp. 1–16. ISSN: 2047217X. DOI: 10.1093/gigascience/giz055.

Tardivel, Meryem et al. (2016). "Tunneling nanotube (TNT)-mediated neuron-to neuron transfer of pathological Tau protein assemblies". In: *Acta neuropathologica communications* 4.1, p. 117. ISSN: 20515960. DOI: 10.1186/s40478-016-0386-4. URL: http://dx.doi.org/10.1186/s40478-016-0386-4.

Teipel, Stefan J. et al. (2020). "In-vivo staging of regional amyloid deposition predicts functional conversion in the preclinical and prodromal phases of Alzheimer's disease". In: *Neurobiology of Aging*. ISSN: 01974580. DOI: 10.1016/j.neurobiolaging.2020.03.011. URL: http://dx.doi.org/10.1016/j.neurobiolaging.2020.03.011.

Tellechea, P. et al. (2018). "Early- and late-onset Alzheimer disease: Are they the same entity?" In: *Neurología (English Edition)* 33.4, pp. 244–253. ISSN: 21735808. DOI: 10.1016/j.nrleng.2015.08.009. URL: http://dx.doi.org/10.1016/j.nrleng.2015.08.009.

Teng, Edmond et al. (Sept. 2019). "Cross-sectional associations between [18F]GTP1 tau PET and cognition in Alzheimer's disease". In: *Neurobiology of Aging* 81, pp. 138–145. ISSN: 01974580. DOI: 10.1016/j.neurobiolaging.2019.05.026. URL: https://doi.org/10.1016/j.neurobiolaging.2019.05.026https://linkinghub.elsevier.com/retrieve/pii/S0197458019301824.

Tetzloff, Katerina A. et al. (Mar. 2018). "Regional Distribution, Asymmetry, and Clinical Correlates of Tau Uptake on [18F]AV-1451 PET in Atypical Alzheimer's Disease". In: *Journal of Alzheimer's Disease* 62.4, pp. 1713–1724. ISSN: 13872877. DOI: 10.3233/JAD-170740. URL: https://www.medra.org/servlet/aliasResolver?alias=iospress&doi=10.3233/JAD-170740.

Teylan, Merilee et al. (2020). "Cognitive trajectory in mild cognitive impairment due to primary age-related tauopathy". In: *Brain : a journal of neurology* 143.2, pp. 611–621. ISSN: 14602156. DOI: 10.1093/brain/awz403.

Thal, Dietmar R et al. (June 2002). "Phases of Aβ-deposition in the human brain and its relevance for the development of AD". In: *Neurology* 58.12, pp. 1791–1800. ISSN: 0028-3878. DOI: 10.1212/WNL.58.12.1791. URL: http://www.neurology.org/lookup/doi/10.1212/WNL.58.12.1791.

Tharp, William G. and Indra Neil Sarkar (2013). "Origins of amyloid-β". In: *BMC Genomics* 14.1. ISSN: 14712164. DOI: 10.1186/1471-2164-14-290.

Therriault, Joseph et al. (2019). "Association of Apolipoprotein e 4 with Medial Temporal Tau Independent of Amyloid-β". In: *JAMA Neurology* 77.4, pp. 470–479. ISSN: 21686149. DOI: 10.1001/jamaneurol.2019.4421.

Thijssen, Elisabeth H. et al. (2020). "Diagnostic value of plasma phosphorylated tau181 in Alzheimer's disease and frontotemporal lobar degeneration". In: *Nature Medicine* 26.3, pp. 387–397. ISSN: 1546170X. DOI: 10.1038/s41591-020-0762-2.

Thompson, Carol L et al. (2008). "Article Genomic Anatomy of the Hippocampus". In: *Neuron* 60.6, pp. 1010–1021. ISSN: 0896-6273. DOI: 10.1016/j.neuron.2008.12.008. URL: http://dx.doi.org/10.1016/j.neuron.2008.12.008.

Torok, Justin et al. (2018). "A method for inferring regional origins of neurodegeneration". In: *Brain* 141.3, pp. 863–876. ISSN: 14602156. DOI: 10.1093/brain/awx371.

Tsai, Richard M. et al. (2019). "18F-flortaucipir (AV-1451) tau PET in frontotemporal dementia syndromes". In: *Alzheimer's Research and Therapy* 11.1, pp. 1–18. ISSN: 17589193. DOI: 10.1186/s13195-019-0470-7.

Uchihara, T. et al. (2001). "Evolution from pretangle neurons to neurofibrillary tangles monitored by thiazin red combined with Gallyas method and double immunofluorescence". In: *Acta Neuropathologica* 101.6, pp. 535–539. ISSN: 00016322. DOI: 10.1007/s004010000306.

Van Rossum, Ineke A. et al. (2012). "Injury markers but not amyloid markers are associated with rapid progression from mild cognitive impairment to dementia in alzheimer's disease". In: *Journal of Alzheimer's Disease* 29.2, pp. 319–327. ISSN: 13872877. DOI: 10.3233/JAD-2011-111694.

Van Swieten, John and Maria Grazia Spillantini (2007). "Hereditary frontotemporal dementia caused by Tau gene mutations". In: *Brain Pathology* 17.1, pp. 63–73. ISSN: 10156305. DOI: 10.1111/j.1750-3639.2007.00052.x.

Varol, Erdem, Aristeidis Sotiras, and Christos Davatzikos (2017). "HYDRA: Revealing heterogeneity of imaging and genetic patterns through a multiple max-margin discriminative analysis framework". In: *NeuroImage* 145, pp. 346–364. ISSN: 10959572. DOI: 10.1016/j.neuroimage.2016.02.041. URL: http://dx.doi.org/10.1016/j.neuroimage.2016.02.041.

Villemagne, Victor et al. (May 2016). "Generating continuous and categorical measures from tau imaging studies with 18F-AV1451 and 18F-THK5351: The Tau MeTeR scale". In: *Journal of Nuclear Medicine* 57.supplement 2, p. 128. URL: http://jnm.snmjournals.org/content/57/supplement_2/128.abstract.

Villemagne, Victor L. et al. (2013). "Amyloid β deposition, neurodegeneration, and cognitive decline in sporadic Alzheimer's disease: A prospective cohort study". In: *The Lancet Neurology* 12.4, pp. 357–367. ISSN: 14744422. DOI: 10.1016/S1474-4422(13)70044-9. URL: http://dx.doi.org/10.1016/S1474-4422(13)70044-9.

Villemagne, Victor L. et al. (Feb. 2018). "Imaging tau and amyloid-β proteinopathies in Alzheimer disease and other conditions". In: *Nature Reviews Neurology* 14.4, pp. 225–236. ISSN: 1759-4758. DOI: 10.1038/nrneurol.2018.9. URL: http://www.nature.com/doifinder/10.1038/nrneurol.2018.9.

Villeneuve, Sylvia et al. (2015a). "Existing Pittsburgh Compound-B positron emission tomography thresholds are too high: Statistical and pathological evaluation". In: *Brain* 138.7, pp. 2020–2033. ISSN: 14602156. DOI: 10.1093/brain/awv112.

Villeneuve, Sylvia et al. (2015b). "Existing Pittsburgh Compound-B positron emission tomography thresholds are too high: Statistical and pathological evaluation". In: *Brain* 138.7, pp. 2020–2033. ISSN: 14602156. DOI: 10.1093/brain/awv112.

Vinters, Harry V. (1987). "Cerebral amyloid angiopathy a critical review". In: *Stroke* 18.2, pp. 311–324. ISSN: 15244628. DOI: 10.1161/01.STR.18.2.311.

Violet, Marie et al. (2014). "A major role for Tau in neuronal DNA and RNA protection in vivo under physiological and hyperthermic conditions". In: *Frontiers in Cellular Neuroscience* 8.MAR, pp. 1–11. ISSN: 16625102. DOI: 10.3389/fncel.2014.00084.

Visser, Pieter Jelle et al. (2009). "Prevalence and prognostic value of CSF markers of Alzheimer's disease pathology in patients with subjective cognitive impairment or mild cognitive impairment in the DESCRIPA study: a prospective cohort study". In: *The Lancet Neurology* 8.7, pp. 619–627. ISSN: 14744422. DOI: 10.1016/S1474-4422(09)70139-5. URL: http://dx.doi.org/10.1016/S1474-4422(09)70139-5.

Vlassenko, Andrei G et al. (2010). "Spatial correlation between brain aerobic glycolysis and amyloid-β (Aβ) deposition." In: *Proceedings of the National Academy of Sciences*

of the United States of America 107.41, pp. 17763–7. ISSN: 1091-6490. DOI: 10.1073/pnas.1010461107. URL: http://www.pubmedcentral.nih.gov/articlerender.fcgi?artid=2955133&tool=pmcentrez&rendertype=abstract.

Vogel, Jacob W. et al. (Nov. 2017). "Subjective cognitive decline and β-amyloid burden predict cognitive change in healthy elderly". In: *Neurology* 89.19, pp. 2002–2009. ISSN: 0028-3878. DOI: 10.1212/WNL.0000000000004627. URL: http://www.neurology.org/lookup/doi/10.1212/WNL.0000000000004627.

Vogel, Jacob W. et al. (Feb. 2019a). "Data-driven approaches for tau-PET imaging biomarkers in Alzheimer's disease". In: *Human Brain Mapping* 40.2, pp. 638–651. ISSN: 10659471. DOI: 10.1002/hbm.24401. URL: http://doi.wiley.com/10.1002/hbm.24401.

Vogel, Jacob W et al. (2019b). "Spread of pathological tau proteins through communicating neurons in human Alzheimer's disease". In: *bioRxiv*, p. 555821. DOI: 10.1101/555821. URL: http://biorxiv.org/content/early/2019/05/30/555821.abstract.

Vogel, Jake (Oct. 2019). "illdopejake/Hippocampus_AP_Axis: Hippocampus_LongAxis_NComms". In: *Dataset on Zenodo*. DOI: 10.5281/ZENODO.3483837. URL: https://doi.org/10.5281/zenodo.3483837#.XaTyRzc2_-s.mendeley.

Vonsattel, Jean Paul G. et al. (1991). "Cerebral amyloid angiopathy without and with cerebral hemorrhages: A comparative histological study". In: *Annals of Neurology* 30.5, pp. 637–649. ISSN: 15318249. DOI: 10.1002/ana.410300503.

Vossel, Keith A. et al. (2010). "Tau reduction prevents Aβ-induced defects in axonal transport". In: *Science* 330.6001, pp. 8–10. ISSN: 00368075. DOI: 10.1126/science.1194653.

Walji, Abbas M. et al. (2016). "Discovery of 6-(Fluoro-18F)-3-(1H-pyrrolo[2,3-c]pyridin-1-yl)isoquinolin-5-amine ([18F]-MK-6240): A Positron Emission Tomography (PET) Imaging Agent for Quantification of Neurofibrillary Tangles (NFTs)". In: *Journal of Medicinal Chemistry* 59.10, pp. 4778–4789. ISSN: 15204804. DOI: 10.1021/acs.jmedchem.6b00166.

Walsh, Dominic M. et al. (2002). "Naturally secreted oligomers of amyloid β protein potently inhibit hippocampal long-term potentiation in vivo". In: *Nature* 416.6880, pp. 535–539. ISSN: 00280836. DOI: 10.1038/416535a.

Wang, Liang et al. (2016). "Evaluation of Tau Imaging in Staging Alzheimer Disease and Revealing Interactions Between β-Amyloid and Tauopathy". In: *JAMA Neurology* 63110, pp. 1–8. ISSN: 2168-6149. DOI: 10.1001/jamaneurol.2016.2078. URL: http://archneur.jamanetwork.com/article.aspx?doi=10.1001/jamaneurol.2016.2078.

Wang, Yipeng et al. (2017). "The release and trans-synaptic transmission of Tau via exosomes". In: *Molecular Neurodegeneration* 12.1, pp. 1–25. ISSN: 17501326. DOI: 10.1186/s13024-016-0143-y. URL: http://dx.doi.org/10.1186/s13024-016-0143-y.

Warren, David E et al. (2017). "Surgically disconnected temporal pole exhibits resting functional connectivity with remote brain regions". In: *Biorxiv*. DOI: 10.1101/127571. URL: http://biorxiv.org/content/biorxiv/early/2017/04/15/127571.full.pdf.

Warren, Jason D., Phillip D. Fletcher, and Hannah L. Golden (2012). "The paradox of syndromic diversity in Alzheimer disease". In: *Nature Reviews Neurology* 8.8, pp. 451–464. ISSN: 17594758. DOI: 10.1038/nrneurol.2012.135. URL: http://dx.doi.org/10.1038/nrneurol.2012.135.

Wegiel, Jerzy et al. (1999). "Cerebellar atrophy in Alzheimer's disease - Clinico-pathological correlations". In: *Brain Research* 818.1, pp. 41–50. ISSN: 00068993. DOI: 10.1016/S0006-8993(98)01279-7.

Wegiel, Jerzy et al. (2010). "The neuropathology of autism: Defects of neurogenesis and neuronal migration, and dysplastic changes". In: *Acta Neuropathologica* 119.6, pp. 755–770. ISSN: 00016322. DOI: 10.1007/s00401-010-0655-4.

Wegmann, Susanne et al. (2019). "Experimental evidence for the age dependence of tau protein spread in the brain". In: *Science Advances* 5.6. ISSN: 23752548. DOI: 10.1126/sciadv.aaw6404.

Weigand, Alexandra J et al. (2020). "Is tau in the absence of amyloid on the Alzheimer's continuum?: A study of discordant PET positivity". In: *Brain Communications* 2.1, pp. 1–18. DOI: 10.1093/braincomms/fcz046.

Weingarten, M. D. et al. (1975). "A protein factor essential for microtubule assembly". In: *Proceedings of the National Academy of Sciences of the United States of America* 72.5, pp. 1858–1862. ISSN: 00278424. DOI: 10.1073/pnas.72.5.1858.

Whitehouse, P. et al. (Mar. 1982). "Alzheimer's disease and senile dementia: loss of neurons in the basal forebrain". In: *Science* 215.4537, pp. 1237–1239. ISSN: 0036-8075. DOI: 10.1126/science.7058341. URL: https://www.sciencemag.org/lookup/doi/10.1126/science.7058341.

Whittington, Alex and Roger N. Gunn (2019). "Amyloid load: A more sensitive biomarker for amyloid imaging". In: *Journal of Nuclear Medicine* 60.4, pp. 536–540. ISSN: 2159662X. DOI: 10.2967/jnumed.118.210518.

Whittington, Alex, David J. Sharp, and Roger N. Gunn (2018). "Spatiotemporal distribution of B-Amyloid in Alzheimer disease is the result of heterogeneous regional carrying capacities". In: *Journal of Nuclear Medicine* 59.5, pp. 822–827. ISSN: 2159662X. DOI: 10.2967/jnumed.117.194720.

Whitwell, Jennifer L. et al. (2012). "Neuroimaging correlates of pathologically defined subtypes of Alzheimer's disease: A case-control study". In: *The Lancet Neurology* 11.10, pp. 868–877. ISSN: 14744422. DOI: 10.1016/S1474-4422(12)70200-4.

Whitwell, Jennifer L. et al. (2013). "Does amyloid deposition produce a specific atrophic signature in cognitively normal subjects?" In: *NeuroImage: Clinical* 2.1, pp. 249–257. ISSN: 22131582. DOI: 10.1016/j.nicl.2013.01.006. URL: http://dx.doi.org/10.1016/j.nicl.2013.01.006.

Whitwell, Jennifer L. et al. (2018). "[18F]AV-1451 clustering of entorhinal and cortical uptake in Alzheimer's disease". In: *Annals of Neurology* 83.2, pp. 248–257. ISSN: 15318249. DOI: 10.1002/ana.25142.

Whitwell, Jennifer L. et al. (2019). "The role of age on tau PET uptake and gray matter atrophy in atypical Alzheimer's disease". In: *Alzheimer's and Dementia* 15.5, pp. 675–685. ISSN: 15525279. DOI: 10.1016/j.jalz.2018.12.016. URL: https://doi.org/10.1016/j.jalz.2018.12.016.

Wolters, Emma E. et al. (2020a). "Hippocampal [18F]flortaucipir BPND corrected for possible spill-in of the choroid plexus retains strong clinico-pathological relationships". In: *NeuroImage: Clinical* 25.December 2019, p. 102113. ISSN: 22131582. DOI: 10.1016/j.nicl.2019.102113. URL: https://doi.org/10.1016/j.nicl.2019.102113.

Wolters, Emma E et al. (2020b). "Regional [18 F] flortaucipir PET is more closely associated with disease severity than CSF p-tau in Alzheimer ' s disease". In:

Wu, Jessica W. et al. (2013). "Small misfolded tau species are internalized via bulk endocytosis and anterogradely and retrogradely transported in neurons". In: *Journal of Biological Chemistry* 288.3, pp. 1856–1870. ISSN: 00219258. DOI: 10.1074/jbc.M112.394528.

Wu, Jessica W. et al. (2016). "Neuronal activity enhances tau propagation and tau pathology in vivo". In: *Nature Neuroscience* 19.8, pp. 1085–1092. ISSN: 15461726. DOI: 10.1038/nn.4328.

Xia, Chenjie et al. (2017). "Association of In Vivo [¹⁸ F]AV-1451 Tau PET Imaging Results With Cortical Atrophy and Symptoms in Typical and Atypical Alzheimer Disease". In: *JAMA Neurology* 74.4, p. 427. ISSN: 2168-6149. DOI: 10.1001/jamaneurol.2016.5755. URL: http://archneur.jamanetwork.com/article.aspx?doi=10.1001/jamaneurol.2016.5755.

Xia, Chun-Fang et al. (2013). "[18F]T807, a novel tau positron emission tomography imaging agent for Alzheimer's disease". In: *Alzheimer's & Dementia* 9.6, pp. 666–676. ISSN: 15525260. DOI: 10.1016/j.jalz.2012.11.008. URL: http://linkinghub.elsevier.com/retrieve/pii/S1552526012025320.

Xu, Jingshu et al. (2019). "Regional protein expression in human Alzheimer's brain correlates with disease severity". In: *Communications Biology* 2.1. ISSN: 23993642. DOI: 10.1038/s42003-018-0254-9. URL: http://dx.doi.org/10.1038/s42003-018-0254-9.

Yamada, Kaoru et al. (2014). "Neuronal activity regulates extracellular tau in vivo". In: *The Journal of Experimental Medicine* 211.3, pp. 387–393. ISSN: 0022-1007. DOI: 10.1084/jem.20131685. URL: http://www.jem.org/lookup/doi/10.1084/jem.20131685.

Yau, Y. et al. (2018). "Network connectivity determines cortical thinning in early Parkinson's disease progression". In: *Nature Communications* 9.1, pp. 1–10. ISSN: 20411723. DOI: 10.1038/s41467-017-02416-0.

Yeh, Fang Cheng and Wen Yih Isaac Tseng (2011). "NTU-90: A high angular resolution brain atlas constructed by q-space diffeomorphic reconstruction". In: *NeuroImage* 58.1, pp. 91–99. ISSN: 10538119. DOI: 10.1016/j.neuroimage.2011.06.021. URL: http://dx.doi.org/10.1016/j.neuroimage.2011.06.021.

Young, Alexandra L. et al. (Dec. 2018). "Uncovering the heterogeneity and temporal complexity of neurodegenerative diseases with Subtype and Stage Inference". In: *Nature Communications* 9.1, p. 4273. ISSN: 2041-1723. DOI: 10.1038/s41467-018-05892-0. URL: http://www.nature.com/articles/s41467-018-05892-0.

Young, Alexandra L. et al. (2020). "Disease Progression Modeling in Chronic Obstructive Pulmonary Disease". In: *American journal of respiratory and critical care medicine* 201.3, pp. 294–302. ISSN: 15354970. DOI: 10.1164/rccm.201908-1600OC.

Youssef, S. A. et al. (2016). "Pathology of the Aging Brain in Domestic and Laboratory Animals, and Animal Models of Human Neurodegenerative Diseases". In: *Veterinary Pathology* 53.2, pp. 327–348. ISSN: 15442217. DOI: 10.1177/0300985815623997.

Yuan, Aidong et al. (2008). "Axonal transport rates in vivo are unaffected by tau deletion or overexpression in mice". In: *Journal of Neuroscience* 28.7, pp. 1682–1687. ISSN: 02706474. DOI: 10.1523/JNEUROSCI.5242-07.2008.

Zanier, Elisa R. et al. (2018). "Induction of a transmissible tau pathology by traumatic brain injury". In: *Brain* 141.9, pp. 2685–2699. ISSN: 14602156. DOI: 10.1093/brain/awy193.

Zeighami, Yashar et al. (2015). "Network structure of brain atrophy in de novo parkinson???s disease". In: *eLife* 4.September 2015, pp. 1–20. ISSN: 2050084X. DOI: 10.7554/eLife.08440.

Zempel, Hans and Eva Maria Mandelkow (2012). "Linking amyloid-β and tau: Amyloid-β induced synaptic dysfunction via local wreckage of the neuronal cytoskeleton". In: *Neurodegenerative Diseases* 10.1-4, pp. 64–72. ISSN: 16602854. DOI: 10.1159/000332816.

Zempel, Hans et al. (2010). "Aβ oligomers cause localized Ca2+ elevation, missorting of endogenous Tau into dendrites, Tau phosphorylation, and destruction of microtubules and spines". In: *Journal of Neuroscience* 30.36, pp. 11938–11950. ISSN: 02706474. DOI: 10.1523/JNEUROSCI.2357-10.2010.

Zempel, Hans et al. (2013). "Amyloid-β oligomers induce synaptic damage via Tau-dependent microtubule severing by TTLL6 and spastin". In: *EMBO Journal* 32.22, pp. 2920–2937. ISSN: 02614189. DOI: 10.1038/emboj.2013.207. URL: http://dx.doi.org/10.1038/emboj.2013.207.

Zempel, Hans et al. (2017). "Axodendritic sorting and pathological missorting of Tau are isoform-specific and determined by axon initial segment architecture". In: *Journal of Biological Chemistry* 292.29, pp. 12192–12207. ISSN: 1083351X. DOI: 10.1074/jbc.M117.784702.

Zhang, Xiuming et al. (2016). "Bayesian model reveals latent atrophy factors with dissociable cognitive trajectories in Alzheimer's disease". In: *Proceedings of the National Academy of Sciences* 113.42, E6535–E6544. ISSN: 0027-8424. DOI: 10.1073/pnas.1611073113. URL: http://www.pnas.org/lookup/doi/10.1073/pnas.1611073113.

Zheng, Ying Qiu et al. (2019). "Local vulnerability and global connectivity jointly shape neurodegenerative disease propagation". In: *PLoS Biology* 17.11, pp. 1–27. ISSN: 15457885. DOI: 10.1371/journal.pbio.3000495.

Zhou, Juan et al. (2012). "Predicting Regional Neurodegeneration from the Healthy Brain Functional Connectome". In: *Neuron* 73.6, pp. 1216–1227. ISSN: 08966273. DOI: 10.1016/j.neuron.2012.03.004. URL: http://dx.doi.org/10.1016/j.neuron.2012.03.004.

Zhou, Lujia et al. (2017). "Tau association with synaptic vesicles causes presynaptic dysfunction". In: *Nature Communications* 8.May, pp. 1–13. ISSN: 20411723. DOI: 10.1038/ncomms15295. URL: http://dx.doi.org/10.1038/ncomms15295.